# Epitranscriptomic determinants of aggressive breast and prostate cancers

**Jennifer Lothion-Roy**

BVM BVS BVMedSci

**Thesis submitted to the University of Nottingham for the degree of Doctor of Philosophy**

**June 2023**

# Abstract

Prostate (PCa) and breast cancer (BCa) continue to pose huge global clinical challenges, being among the most commonly diagnosed and deadly cancer types in men and women, respectively. The androgen and estrogen hormones that drive their growth, together with their specific receptors, play a fundamental role in carcinogenesis and disease progression, and the targeting of these hormone signalling pathways forms an integral part of cancer treatment plans. However, in BCa, some tumours lack the estrogen receptor and thus the therapeutic target, and in PCa, resistance to androgen deprivation therapy is common. In these cases, few treatment options remain, and prognosis is poor.

Methylation of the $N^6$ position of adenosine on mRNA, known as $N^6$-methyladenosine ($m^6A$), is the most common internal mRNA modification. The $m^6A$ RNA modification plays a vital role in regulating many vital physiological processes such embryogenesis, response to DNA damage, and cell differentiation, as well as the regulation of alternative splicing. However, recent studies into the regulators of the $m^6A$ RNA modification have implicated them in the development and progression of a number of types of cancer. Indeed, small molecule inhibitors of METTL3, the catalytic subunit of the $m^6A$ methyltransferase complex, have demonstrated potential in treating haematological cancers in preclinical models, and also show promise in the treatment of solid tumours.

CBLL1, one of the components of the $m^6A$ methyltransferase complex, was originally implicated in cancer through its function as a ubiquitin E3 ligase that

targets E-cadherin for degradation, however its more recently discovered role in the RNA $m^6A$ methyltransferase complex remains poorly understood. Whilst increased expression of CBLL1 has been associated with many cancer types, little is known about the role and function of CBLL1 in PCa and BCa.

To test the hypothesis that dysregulated CBLL1 promotes aggressive cancer development and progression, the expression and clinical relevance of CBLL1 in both PCa and BCa cell lines and patient specimens were assessed. Furthermore, siRNA-mediated knockdown of *CBLL1* in PCa and BCa cell lines allowed analysis of the function of CBLL1 in differential gene expression and alternative splicing.

In PCa cell lines and patient specimens, CBLL1 expression was linked with carcinogenesis and associated with poorer prognostic factors. In functional studies CBLL1 was demonstrated to have a key role in maintaining normal androgen regulation of a number of pivotal cancer-related genes and their pathways in PCa cells. It was also found that enzalutamide resistance causes PCa cells to become independent of the influence of CBLL1 on gene regulation. Moreover, CBLL1 was demonstrated to play a role in selective regulation of splicing in PCa.

In BCa cell lines, CBLL1 expression was linked with carcinogenesis, however, in patient specimens, nuclear CBLL1 expression was found to be an independent positive prognostic factor for survival, whereas cytoplasmic CBLL1 expression was associated primarily with negative clinicopathological parameters. Similar to PCa, in functional studies in BCa cells, CBLL1 was

demonstrated to play a role in maintaining normal estrogen regulation of many oncogenes and tumour suppressor genes and their associated pathways.

Collectively these results support a role for CBLL1 in PCa and BCa, including in androgen deprivation therapy resistance in PCa, and highlight CBLL1 as a potential new specific therapeutic target, particularly in advanced hormone-independent PCa.

# Peer-reviewed publications

**Arising from this study:**

**Lothion-Roy J**, Haigh DB, Harris AE, Metzler VM, Alsaleem M, Toss M.S, Kariri Y, Ntekim A, Robinson BD, Khani F, Gudas LJ, Allegrucci C, James VH, Madhusudan S, Mather M, Emes RD, Archer N, Fray RG, Rakha E, Jeyapalan JN, Rutland CS, Mongan NP and Woodcock CL (2023). Clinical and molecular significance of the RNA m6A methyltransferase complex in prostate cancer. *Frontiers in Genetics* 13:1096071. doi: 10.3389/fgene.2022.109607114, 5148.

**Contributions to other studies:**

Metzler VM, de Brot, S, Haigh DB, Woodcock CL, **Lothion-Roy J**, Harris AE, Nilsson EM, Ntekim A, Persson JL, Robinson BD, Khani F, Laursen KB, Gudas LJ, Toss MS, Madhusudan S, Rakha E, Heery DM, Rutland CS, Mongan NP, Jeyapalan JN (2023). The KDM5B and KDM1A lysine demethylases cooperate in regulating androgen receptor expression and signalling in prostate cancer. *Frontiers in Cell and Developmental Biology*, 19;11:1116424. doi: 10.3389/fcell.2023.1116424.

Haigh DB, Woodcock CL, **Lothion-Roy J**, Harris AE, Metzler VM, Persson, JL, Robinson BD, Khani F, Alsaleem M, Ntekim A, Madhusudan S, Davis MB, Laursen KB, Gudas LJ, Rutland CS, Toss MS, Archer N, Bodi Z, Rakha EA, Fray RG, Jeyapalan JN, Mongan NP (2022). The METTL3 RNA Methyltransferase Regulates Transcriptional Networks in Prostate Cancer. *Cancers*, 14, 5148. doi: 10.3390/ cancers14205148.

Harris AE, Metzler VM, **Lothion-Roy J**, Varun D, Woodcock CL, Haigh DB, Endeley C, Haque M, Toss MS, Alsaleem M, Persson JL, Gudas LJ, Rakha E, Robinson BD, Khani F, Martin LM, Moyer JE, Brownlie J, Madhusudan S, Allegrucci C, James VH, Rutland CS, Fray RG, Ntekim A, de Brot S, Mongan NP and Jeyapalan JN (2022). Exploring antiandrogen therapies in hormone dependent prostate cancer and new therapeutic routes for castration resistant prostate cancer. *Frontiers in Endocrinology*, 13:1006101. doi: 10.3389/fendo.2022.1006101.

Jeyapalan JN, James V, Gardner DS, **Lothion-Roy J**, Mongan NP, & Rutland CS (2022). Impact of COVID-19 on student attainment and pedagogical needs when undertaking independent scientific research. *Anatomia, Histologia, Embryologia*, 00, 1– 8. doi: 10.1111/ahe. 12842.

Ryman-Tubb T, **Lothion-Roy J**, Metzler VM, Harris AE, Robinson BD, Rizvanov A, Jeyapalan JN, James VH, England GCW, Rutland CS, Persson

JL, Kenner L, Rubin MA, Mongan NP, & de Brot S (2021). Comparative pathology of dog and human prostate cancer, *Veterinary Medicine and Science*, 1-11. doi: 10.1002/vms3.642.

Rutland CS, Cockroft JM, **Lothion-Roy J**, Harris AE, Jeyapalan JN, Simpson S, Alibhai A, Bailey C, Ballard-Reisch AC, Rizvanov AA, Dunning MD, de Brot S, & Mongan NP (2021). Immunohistochemical Characterisation of GLUT1, MMP3 and NRF2 in Osteosarcoma, *Frontiers in Veterinary Science*, 8:704598. doi: 10.3389/fvets.2021.704598.

de Brot S, **Lothion-Roy J**, Grau-Roma L, White E, Guscetti F, Rubin MA, & Mongan NP (2021). Histological and immunohistochemical investigation of canine prostate carcinoma with identification of common intraductal carcinoma component, *Veterinary and Comparative Oncology*, 1-12. doi: 10.1111/vco.12704.

Simpson S, Dunning MD, de Brot S, Alibhai A, Bailey C, Woodcock CL, Mestas M, Akhtar S, Jeyapalan JN, **Lothion-Roy J**, Emes RD, Allegrucci C, Rizvanov AA, Mongan NP, & Rutland CS (2020). Molecular Characterisation of Canine Osteosarcoma in High Risk Breeds, *Cancers*, 12, 2405. doi: 10.3390/cancers12092405.

Dhiman A, Srivastava N, Goyal M, Rakha E, **Lothion-Roy J**, Mongan NP, Miftakhova RR, Khaiboullina SF, Rizvanov A, Baranwal M (2019) Metadherin: a therapeutic target in multiple cancers, *Frontiers in Oncology,* 9:349. doi: 10.3389/fonc.2019.00349.

# Acknowledgements

The completion of thesis would not have been possible without the wonderful team of supervisors, lab group colleagues, friends and family who have supported me throughout this journey.

It is only right that my primary supervisor, Professor Nigel Mongan should be first on my list of people to thank. I will be forever indebted to him for his guidance, his sharing of his vast scientific knowledge, and his kind and enthusiastic support of me, both personally and professionally, throughout my PhD. Having a baby in the middle of a PhD, and in the middle of a global pandemic no less, I am sure is never easy and I will always be profoundly grateful for Nigel's support in helping to make it as stress-free as possible and for giving me the precious time that I needed in order to balance motherhood and a productive return to work. I would also like to extend my heartfelt thanks to the rest of my supervisors, Dr Catrin Rutland, Professor Rupert Fray, and Dr Jennie Jeyapalan for their wonderful support and insightful conversations over the past four and a half years. Thank you so much to all of my supervisors for being my cheerleaders and I look forward to continuing to work with you all over the coming years.

I would also like to thank our collaborators at Nottingham City Hospital, to Professor Emad Rakha for access to his precious archive of patient samples, and to Dr Mansour Alsaleem and Dr Michael Shawky Toss for their kindness and support in helping to navigate me through the analysis. Many thanks also to Chris Nolan, Dr Chitra Joseph, Holly Nicholls and Alex Dean for all their practical support and warm welcome to City Hospital.

Special thanks also go to our international collaborators, Dr Brian Robinson and Professor Lorraine Gudas at Weill Cornell Medicine, New York, both for access to their valuable patient samples and for the wonderful welcome that was extended to me when I was lucky enough to visit WCM in 2019. Further thanks also go to Dr Akira Funahashi and Dr Sasagu Kurozumi for their machine learning and pathology expertise and for the unforgettable experience of visiting them both in Tokyo in 2019.

I must also say an enormous thank you to the cancer patients that have entrusted their tumour samples and confidential medical information to researchers like myself over the years, so that we may be able to try to further our understanding of cancer and ultimately improve patient outcomes.

I must express my immense gratitude to my lab group colleagues, both past and present, who I feel lucky to also call my friends. Veronika, Daisy, Nataliya, Corinne, Anna, Rodhan, Dhruvika and Maria, it has been my absolute pleasure to work with you over these past few years. Thank you so much for your good humour, kindness and support. In particular I don't know how I could have survived this past year without the current group members. Thank you for always answering my questions, for the chats that made the four-hour cell culture sessions bearable, and for helping me finish up at the end of the day so I could dash off for nursery pick up before they closed the doors. A huge thank you also goes to Rodhan for all his help and Inkscape mastery.

I am also very thankful to the technical and administrative teams at the Vet School and the Biodiscovery Institute, and to the BBSRC and University of Nottingham for the scholarship that has allowed me to complete this PhD.

Finally, I must thank my amazing family and friends who have lived and breathed my PhD with me. I would not be where I am today without my dear friend Charlotte and my godmother ‘Auntie’ Brenda, who both very sadly lost their battles with cancer in 2012-2013, and who were the inspiration to begin my journey in cancer research.

An enormous thank you goes to my parents, who made me what I am and who I love dearly. Mum, you don’t need to worry, I promise I am done with trying to get any more letters after my name for the time being!

To my wonderful husband Thibaut- thank you for your unwavering love and support, and for taking care of me, our home and our family when I have been too busy working to be of any use to man or beast. As the late, great, Tina Turner said, you are simply the best. And to my darling son George, my raison d’être, thank you for bringing me joy every day, your laughter is a tonic to all the world’s ills. Thank you for being so understanding of all the times Mummy had to work and couldn’t play. At some point in the future I hope you will understand what it was all for but, for now, let’s play.

# Table of Contents


Chapter 1. General introduction ..... 2

1.1 Importance of cancer ..... 2

1.2 Hormonal cancers ..... 3

1.2.1 Steroid hormone signalling in cancer ..... 3

1.3 Prostate cancer ..... 8

1.3.1 Prostate anatomy and physiology ..... 8

1.3.2 Incidence and risk factors ..... 10

1.3.3 Diagnosis and treatment ..... 11

1.3.4 Androgen deprivation therapy resistance ..... 16

1.4 Breast cancer ..... 19

1.4.1 Breast anatomy and physiology ..... 19

1.4.2 Incidence and risk factors ..... 21

1.4.3 Diagnosis and molecular subtypes of BCa ..... 23

1.4.4 Treatment of breast cancer ..... 26

1.5 E-cadherin ..... 28

1.5.1 Biological function ..... 28

1.5.2 E-cadherin in cancer ..... 30

1.6 The epitranscriptome ..... 36

1.7 *N*$^6$-methyladenosine (m$^6$A) ..... 37

1.7.1 Biological function ..... 37

1.7.2 m$^6$A in cancer ..... 41

1.8 CBLL1 ..... 45

1.8.1 Biological function ..... 45

1.8.2 CBLL1 in cancer ..... 50

1.9 Aims of study ..... 55

Chapter 2. Materials and methods ..... 57
2.1 Bioinformatic analysis of publicly available data ..... 57
2.2 Cell culture ..... 58
2.2.1 Cell lines ..... 58
2.2.2 Cell culture conditions ..... 62
2.2.3 Hormone treatment of cells ..... 63
2.2.4 siRNA-mediated functional depletion of *CBLL1* ..... 64
2.3 RNA analysis ..... 66
2.3.1 RNA isolation using TRI Reagent ..... 66
2.3.2 RNA isolation using GenElute™ Mammalian Total RNA Miniprep Kit ..... 67
2.3.3 Reverse transcription cDNA synthesis ..... 68
2.3.4 Quantitative real-time polymerase chain reaction analysis ..... 68
2.4 Protein analysis ..... 69
2.4.1 Total protein extraction ..... 69
2.4.2 Fractionation of protein by subcellular location ..... 70
2.4.3 Protein quantification ..... 71
2.5 Western blot ..... 71
2.5.1 Protein loading and separation ..... 71
2.5.2 Protein transfer ..... 73
2.5.3 Antibody incubation and imaging ..... 74
2.5.4 Antibody optimisation with blocking peptide ..... 75
2.5.5 Western blot quantification ..... 77
2.6 Cell phenotyping ..... 77
2.6.1 Proliferation assay ..... 77
2.7 RNA sequencing ..... 78
2.8 Immunohistochemistry analysis of patient specimens ..... 79

2.8.1 Nottingham prostate cancer tissue microarray ..... 79
2.8.2 Nottingham breast cancer tissue microarray ..... 80
2.8.3 Nottingham TMAs and immunohistochemistry staining ..... 80
2.8.4 Weill Cornell Medicine prostate cancer tissue microarray and immunohistochemistry staining ..... 83
2.8.5 H-scoring analysis ..... 84
2.9 Statistical analysis ..... 85
2.9.1 Cell line experiment analysis ..... 85
2.9.2 Immunohistochemistry analysis ..... 86
Chapter 3. Expression of CBLL1 in prostate cancer patient samples and cell lines ..... 88
3.1 Introduction ..... 88
3.2 Results ..... 89
3.2.1 CBLL1 expression and copy number alterations in prostate cancer patients ..... 89
3.2.2 CBLL1 expression in prostate cancer cell lines ..... 96
3.2.3 Androgen regulation of CBLL1 expression in prostate cancer cell lines ..... 98
3.2.4 CBLL1 expression in prostate tissue specimens from Nottingham patient cohort ..... 105
3.2.5 CBLL1 expression in prostate tissue specimens from Weill Cornell Medicine patient cohorts ..... 114
3.3 Discussion ..... 126
Chapter 4. Functional role of CBLL1 in prostate cancer cell lines ..... 136
4.1 Introduction ..... 136
4.2 Results ..... 139
4.2.1 siRNA depletion of *CBLL1* in prostate cancer cell lines ..... 139

4.2.2 Phenotypic effect of siRNA depletion of *CBLL1* in prostate cancer cell lines ..... 147

4.2.3 Effect of siRNA depletion of *CBLL1* on differential gene expression in control and androgen-treated LNCaP:C4-2 and LNCaP:C4-$2_{enzR}$ cells .. 148

4.2.4 Effect of siRNA depletion of *CBLL1* on significantly enriched KEGG pathways associated with differential gene expression in basal and androgen-treated LNCaP:C4-2 and LNCaP:C4-$2_{enzR}$ cells..... 163

4.2.5 Effect of siRNA depletion of *CBLL1* on alternative splicing in control and androgen-treated LNCaP:C4-2 and LNCaP:C4-$2_{enzR}$ cells ..... 167

4.3 Discussion ..... 173

Chapter 5. Expression of CBLL1 in breast cancer patient samples and cell lines ..... 198

5.1 Introduction..... 198

5.2 Results ..... 200

5.2.1 CBLL1 expression and copy number alterations in breast cancer patients ..... 200

5.2.2 CBLL1 expression in breast cancer cell lines ..... 209

5.2.3 Estrogen regulation of CBLL1 expression in breast cancer cell lines ..... 211

5.2.4 CBLL1 expression in breast tissue specimens from Nottingham patient cohorts..... 218

5.3 Discussion ..... 232

Chapter 6. Functional role of CBLL1 in breast cancer cell lines ..... 245

6.1 Introduction..... 245

6.2 Results ..... 248

6.2.1 siRNA depletion of *CBLL1* in breast cancer cell lines ..... 248

6.2.2 Phenotypic effect of siRNA depletion of *CBLL1* in breast cancer cell lines ..... 256

6.2.3 Effect of siRNA depletion of *CBLL1* on differential gene expression in basal and estrogen-treated MCF7 cells ..... 258

6.2.4 Effect of siRNA depletion of *CBLL1* on differential gene expression in basal and estrogen-treated T-47D cells ..... 266

6.2.5 Effect of siRNA depletion of *CBLL1* on alternative splicing in basal and estrogen-treated MCF7 and T-47D cells ..... 273

6.3 Discussion ..... 280

Chapter 7. Conclusions and future work ..... 308

# List of Figures

Figure 1.1 Structure of the androgen receptor and estrogen receptor..... 6

Figure 1.2 Therapeutic targets in androgen deprivation therapy in prostate cancer ..... 16

Figure 1.3 Intrinsic and molecular subtypes of breastcancer ..... 25

Figure 1.4 The structure and location of E-cadherin on epithelial cells..... 30

Figure 1.5. The cycle of epithelial to mesenchymal cell transition and mesenchymal to epithelial transition ..... 32

Figure 1.6 Transcription factors that activate mesenchymal marker genes and repress epithelial marker genes during EMT..... 34

Figure 1.7 The components of the $m^6A$ methyltransferase complex, as well as $m^6A$ binding proteins and demethylases involved in dynamic $m^6A$ mRNA modification ..... 38

Figure 1.8 Structure of the CBLL1 and c-Cbl proteins..... 47

Figure 1.9 Post-translational regulation of E-cadherin expression. ..... 49

Figure 2.1 CBLL1 protein expression in prostate cancer cell lines with and without CBLL1-specific blocking peptide..... 76

Figure 3.1 *CBLL1* alteration frequency in prostate cancer ..... 91

Figure 3.2 *CBLL1* putative copy number alterations in prostate cancer ..... 93

Figure 3.3 *CBLL1* mRNA expression and correlation with clinicopathological parameters ..... 95

Figure 3.4 CBLL1 expression in non-malignant and prostate cancer cell lines ..... 97

Figure 3.5 *CBLL1* expression in non-malignant and prostate cancer cell lines in response to androgen treatment ..... 99

Figure 3.6 CBLL1 expression in non-malignant and prostate cancer cell lines in response to androgen treatment ..... 101
Figure 3.7 CBLL1 protein localisation expression in prostate cancer cell lines in response to androgen treatment ..... 103
Figure 3.8 Chromatin binding profile of AR within the *CBLL1* gene..... 104
Figure 3.9 Representative images of CBLL1 IHC staining of Nottingham cohort TMA of prostate cancer tissue ..... 106
Figure 3.10 CBLL1 expression in non-malignant prostate and tumour patient tissue samples in Nottingham cohort TMA..... 107
Figure 3.11 Significant correlations of clinicopathological parameters with CBLL1 expression in prostate cancer patient tissue samples in Nottingham cohort TMA..... 109
Figure 3.12 CBLL1 expression correlated with biochemical recurrence-free survival in prostate cancer patients in Nottingham cohort TMA..... 110
Figure 3.13 Correlation of nuclear and cytoplasmic expression of CBLL1 in prostate cancer patient tissue samples in Nottingham cohort TMA..... 111
Figure 3.14 Correlation of CBLL1 and AR expression in prostate cancer patient tissue samples in Nottingham cohort TMA..... 113
Figure 3.15 Representative images of CBLL1 IHC staining of WCM cohort 1 TMA of prostate cancer tissue ..... 115
Figure 3.16 CBLL1 expression in non-malignant prostate and tumour patient tissue samples in WCM cohort 1 TMA ..... 116
Figure 3.17 Correlations of clinicopathological parameters with CBLL1 expression in prostate cancer patient specimens in WCM cohort 1 TMA... 118

Figure 3.18 Representative images of CBLL1 IHC staining of WCM cohort 2 TMA of prostate cancer tissue ..... 120
Figure 3.19 CBLL1 expression in non-malignant prostate and tumour patient tissue samples in WCM cohort 2 TMA ..... 122
Figure 3.20 Correlation of nuclear and cytoplasmic expression of CBLL1 in prostate cancer patient tissue samples in WCM cohorts 1 and 2 TMA ..... 123
Figure 4.1 Effect of siRNA-mediated CBLL1 knockdown and R1881 treatment on protein expression in LNCaP:C4-2, LNCaP:C4-$2_{enzR}$ and 22Rv1 cells .. 141
Figure 4.2 Effect of siRNA-mediated *CBLL1* knockdown and R1881 treatment on *CBLL1* mRNA expression in LNCaP:C4-2, LNCaP:C4-$2_{enzR}$ and 22Rv1 cells ..... 144
Figure 4.3 Effect of siRNA-mediated *CBLL1* knockdown and R1881 treatment on mRNA expression in LNCaP:C4-2 and LNCaP:C4-$2_{enzR}$ cells..... 146
Figure 4.4 Phenotypic effect of siRNA-mediated *CBLL1* knockdown and R1881 treatment in LNCaP:C4-2 and LNCaP:C4-$2_{enzR}$ cells ..... 148
Figure 4.5 Comparison of differential gene expression and associated over-represented KEGG pathways in scrambled control LNCaP:C4-2 and LNCaP:C4-$2_{enzR}$ cells in response to R1881 ..... 151
Figure 4.6 Differential gene expression and associated over-represented KEGG pathways in vehicle-treated LNCaP:C4-2 and LNCaP:C4-$2_{enzR}$ cells in response to siRNA-mediated *CBLL1* knockdown ..... 154
Figure 4.7 Differential gene expression and associated over-represented KEGG pathways in scrambled control LNCaP:C4-2 and LNCaP:C4-$2_{enzR}$ cells in response to R1881 treatment..... 158

Figure 4.8 Differential gene expression and associated over-represented KEGG pathways in *CBLL1*-depleted LNCaP:C4-2 and LNCaP:C4-$2_{enzR}$ cells in response to R1881 treatment ..... 161

Figure 4.9 Summary of over-represented pathways associated with differentially expressed genes in LNCaP:C4-2 and LNCaP:C4-$2_{enzR}$ cells in response to siRNA-mediated *CBLL1* knockdown and R1881 treatment .... 166

Figure 4.10 Significant alternative splicing event types in LNCaP:C4-2 and LNCaP:C4-$2_{enzR}$ cells in response to siRNA-mediated CBLL1 knockdown and R1881 treatment..... 171

Figure 5.1 *CBLL1* and *CDH1* alteration frequency in breast cancer..... 202

Figure 5.2 *CBLL1* and *CDH1* copy number alterations in breast cancer .... 204

Figure 5.3 *CBLL1* and *CDH1* mRNA expression and correlation with clinicopathological parameters..... 205

Figure 5.4 *CBLL1* and *CDH1* expression and correlation with different survival types..... 207

Figure 5.5 *CBLL1* and *CDH1* expression and correlation with overall survival ..... 208

Figure 5.6 CBLL1 and E-cadherin expression in non-malignant and breast cancer cell lines..... 210

Figure 5.7 *CBLL1* and *CDH1* expression in breast cancer cell lines in response to estradiol treatment..... 212

Figure 5.8 CBLL1 expression in breast cancer cell lines in response to estradiol treatment..... 213

Figure 5.9 CBLL1 and E-cadherin protein localisation expression in breast cancer cell lines in response to estradiol treatment..... 215

Figure 5.10 Chromatin binding profile of ERα within the *CBLL1* gene..... 217
Figure 5.11 Representative images of CBLL1 IHC staining of Nottingham cohort TMA of breast cancer tissue ..... 219
Figure 5.12 Significant correlations of clinicopathological parameters with CBLL1 expression in breast cancer patient tissue samples ..... 222
Figure 5.13 CBLL1 expression correlated with survival in breast cancer patients..... 224
Figure 5.14 Correlation of nuclear and cytoplasmic expression of CBLL1 in breast cancer patient tissue samples..... 226
Figure 5.15 Multivariant Cox regression analysis of CBLL1 and E-cadherin expression and survival in BCa patients ..... 227
Figure 5.16 of CBLL1 and E-cadherin expression in breast cancer patient tissue samples..... 229
Figure 6.1 Effect of siRNA-mediated *CBLL1* knockdown and $\beta E_2$ treatment on protein expression in MCF7 and T47D cells ..... 250
Figure 6.2 Effect of siRNA-mediated *CBLL1* knockdown and $\beta E_2$ treatment on mRNA expression in MCF7 cells ..... 252
Figure 6.3 Effect of siRNA-mediated *CBLL1* knockdown and $\beta E_2$ treatment on mRNA expression in T-47D cells..... 255
Figure 6.4 Phenotypic effect of siRNA-mediated *CBLL1* knockdown and $\beta E_2$ treatment in MCF7 and T-47D cells..... 257
Figure 6.5 Differential gene expression in MCF7 cells in response to siRNA-mediated *CBLL1* knockdown and $\beta E_2$ treatment..... 259

Figure 6.6 Summary of differentially expressed genes and over-represented KEGG pathways in MCF7 cells in response to siRNA-mediated *CBLL1* knockdown and $\beta E_2$ treatment ..... 261
Figure 6.7 Ten most significantly enriched KEGG pathways in MCF7 cells in response to siRNA-mediated *CBLL1* knockdown and $\beta E_2$ treatment ..... 263
Figure 6.8 Pathways in cancer KEGG pathway with commonly differentially expressed genes in scrambled control and *CBLL1*-depleted MCF7 and T47D cells in response to estrogen. ..... 265
Figure 6.9 Differential gene expression in T-47D cells in response to siRNA-mediated *CBLL1* knockdown and $\beta E_2$ treatment..... 267
Figure 6.10 Summary of differentially expressed genes and over-represented pathways in T-47D cells in response to siRNA-mediated *CBLL1* knockdown and $\beta E_2$ treatment..... 269
Figure 6.11 Ten most significantly enriched KEGG pathways in T-47D cells in response to siRNA-mediated *CBLL1* knockdown and $\beta E_2$ treatment ..... 271
Figure 6.12 Significant alternative splicing event types in MCF7 cells in response to siRNA-mediated *CBLL1* knockdown and $\beta E_2$ treatment ..... 275
Figure 6.13 Significant alternative splicing event types in T-47D cells in response to siRNA-mediated *CBLL1* knockdown and $\beta E_2$ treatment ..... 278
Figure i Representative images of E-cadherin IHC staining of Nottingham cohort TMA of breast cancer tissue ..... 414

# List of Tables

Table 1.1 Modified Gleason prognostic grading system ..... 13

Table 2.1 Key characteristics of the prostate cell lines used in this study .... 60

Table 2.2 Key characteristics of the breast cell lines used in this study ..... 62

Table 2.3 Preparation of the gel for SDS-PAGE ..... 72

Table 2.4 Primary antibodies used in this study ..... 74

Table 3.1 CBLL1 IHC staining summary ..... 125

Table 5.1 Correlations of CBLL1 expression with other breast cancer-related proteins ..... 231

Table i Patient demographics and clinicopathological parameters examined in Nottingham PCa TMA. ..... 386

Table ii Correlation of CBLL1 staining with clinicopathological parameters in Nottingham cohort. ..... 387

Table iii Patient demographics and clinicopathological parameters examined in WCM cohort 1 PCa TMA. ..... 388

Table iv Correlation of CBLL1 staining with clinicopathological parameters in WCM cohort 1. ..... 389

Table v Analysis of significantly enriched KEGG pathways associated with differentially expressed genes (DEGs) upon R1881 treatment in LNCaP:C4-2 scrambled control cells (si*Scr* Vehicle vs si*Scr* R1881) (FDR<0.05). ..... 390

Table vi Analysis of significantly enriched KEGG pathways associated with differentially expressed genes (DEGs) upon R1881 treatment in LNCaP:C4-2 *CBLL1* knockdown cells (si*CBLL1* Vehicle vs si*CBLL1* R1881) (FDR<0.05). ..... 391

Table vii Summary of KEGG pathways associated with differentially expressed genes in LNCaP:C4-2 cells grouped by R1881 treatment and *CBLL1* knockdown (FDR<0.05). ..... 392
Table viii Analysis of significantly enriched KEGG pathways associated with differentially expressed genes (DEGs) upon *CBLL1* knockdown in vehicle-treated LNCaP:C4-2 cells (si*Scr* Vehicle vs si*CBLL1* Vehicle) (FDR<0.05). ..... 393
Table ix Analysis of significantly enriched KEGG pathways associated with differentially expressed genes (DEGs) upon *CBLL1* knockdown in vehicle-treated LNCaP:C4-2 cells (si*Scr* R1881 vs si*CBLL1* R1881) (FDR<0.05).. 394
Table x Summary of KEGG pathways associated with differentially expressed genes in LNCaP:C4-2 cells grouped by R1881 treatment and *CBLL1* knockdown (FDR<0.05). ..... 395
Table xi Analysis of significantly enriched KEGG pathways associated with differentially expressed genes (DEGs) upon R1881 treatment in LNCaP:C4-$2_{enzR}$ scrambled control cells (si*Scr* Vehicle vs si*Scr* R1881) (FDR<0.05).. 396
Table xii Analysis of significantly enriched KEGG pathways associated with differentially expressed genes (DEGs) upon R1881 treatment in LNCaP:C4-$2_{enzR}$ *CBLL1* knockdown cells (si*CBLL1* Vehicle vs si*CBLL1* R1881) (FDR<0.05). ..... 397
Table xiii Summary of KEGG pathways associated with differentially expressed genes in LNCaP:C4-$2_{enzR}$ cells grouped by R1881 treatment and *CBLL1* knockdown (FDR<0.05). ..... 398

Table xiv Analysis of KEGG pathways associated with differentially spliced genes in LNCaP:C4-2 cells (dPSI ≥5%, FDR<0.05). Pathways listed in grey are not statistically significant. ..... 399
Table xv Analysis of KEGG pathways associated with differentially spliced genes in LNCaP:C4-$2_{enzR}$ cells (dPSI ≥5%, FDR<0.05). All pathways marked in grey are not statistically significant. ..... 406
Table xvi Patient demographics and clinicopathological parameters examined in Nottingham BCa TMA with CBLL1 staining. ..... 411
Table xvii Correlation of CBLL1 staining with clinicopathological parameters in Nottingham cohort. ..... 412
Table xviii Patient demographics and clinicopathological parameters examined in Nottingham BCa TMA with E-cadherin staining. ..... 415
Table xix Correlation of E-cadherin staining with clinicopathological parameters in Nottingham cohort. ..... 416
Table xx Analysis of significantly enriched KEGG pathways associated with differentially expressed genes (DEGs) upon $\beta E_2$ treatment in MCF7 scrambled control cells (si*Scr* Vehicle vs si*Scr* $\beta E_2$) (FDR<0.05). ..... 418
Table xxi Analysis of KEGG pathways associated with differentially expressed genes upon $\beta E_2$ treatment in MCF7 *CBLL1* knockdown cells (si*CBLL1* Vehicle vs si*CBLL1* $\beta E_2$) (FDR<0.05). ..... 420
Table xxii Summary of KEGG pathways associated with differentially expressed genes in MCF7 cells grouped by $\beta E_2$ treatment and *CBLL1* knockdown (FDR<0.05). ..... 421

Table xxiii Analysis of KEGG pathways associated with differentially expressed genes upon $\beta E_2$ treatment in T-47D scrambled control cells (si*Scr* Vehicle vs si*Scr* $\beta E_2$) (FDR<0.05). ..... 422
Table xxiv Analysis of KEGG pathways related to differentially expressed genes upon $\beta E_2$ treatment in T-47D *CBLL1* knockdown cells (si*CBLL1* Vehicle vs si*CBLL1* $\beta E_2$) (FDR<0.05). ..... 423
Table xxv Summary of KEGG pathways related to differentially expressed genes in T-47D cells grouped by $\beta E_2$ treatment and *CBLL1* knockdown (FDR<0.05). ..... 424
Table xxvi Analysis of KEGG pathways associated with differentially spliced genes in MCF7 cells (dPSI ≥5%, FDR<0.05). ..... 426
Table xxvii Analysis of KEGG pathways associated with differentially spliced genes in T-47D cells (dPSI ≥5%, FDR<0.05). ..... 427

# Abbreviations and acronyms

A5SS Alternative 5' splice site

A3SS Alternative 3' splice site

ADT Androgen deprivation therapy

AF-1 Activation Function 1

AF-2 Activation Function 2

Akt AK strain transforming

AKT3 AKT Serine/Threonine Kinase 3

ALDH1A1 Aldehyde dehydrogenase 1 family member A1

ALKBH3 Human AlkB homolog H3

ALKBH5 Human AlkB homolog H5

AMH Anti-Mullerian hormone

AML Acute myeloid leukaemia

ANOVA Analysis of variance

APS Ammonium persulphate

AR Androgen receptor

ARE Androgen response element

ARSI AR signalling inhibitors

ARv7 Androgen receptor variant 7

ARvs Androgen receptor variants

ASCL1 Achaete-Scute family basic helix-loop-helix transcription factor

ATM ATM serine/threonine kinase

ATR ATR serine/threonine kinase

BCa Breast Cancer

BCEI Breast cancer estrogen-inducible protein

BCLAF1 BCL2-associated transcription factor 1

BCR Biochemical recurrence

BCSS Breast cancer specific survival

βE2 Beta-estradiol

BioGRID The Biological General Repository for Interaction Datasets

BMI Body mass index

bp Base pair

BRCA1 Breast Cancer Associated gene 1

BRCA2 Breast Cancer Gene 2

BSA Bovine serum albumin

CA9 Carbonic anhydrase 9

cAMP 3'-5'-cyclic adenosine monophosphate

Cbl Casitas B-lineage lymphoma

CBLL1 Cbl proto-oncogene like 1

CCNB2- Cyclin B2

cDNA complementary DNA

CDH1 E-cadherin

CER Cytoplasmic extraction reagent

ChIP-seq Chromatin immunoprecipitation sequencing

CNA copy number alteration

CRC Colorectal cancer

CRPC Castration-resistant prostate cancer

CSC Cancer stem cell

CTD C terminal domain

DAB 3,3'-diaminobenzidine tetrahydrochloride

DBD DNA binding domain

DC Detergent compatible

DCIS Ductal Carcinoma in situ

DEG Differentially expressed gene

DFI Disease free interval

DHT 5-α- dihydrotestosterone

DMEM Dulbecco's modified eagle's medium

DMFS Distant metastasis free survival

DMSO Dimethyl sulfoxide

DNA Deoxyribonucleic acid

DNase Deoxyribonuclease

DOK1 Docking Protein 1

dPSI Difference in percentage spliced in

DPX Distyrene, plasticiser and xylene

DSG Differentially spliced gene

DST Differentially spliced transcript

DTT DL-dithiothreitol

E3 Enzyme 3

ECL Enhanced chemiluminescence

ECM Extracellular matrix

EDTA Ethylenediamine tetraacetic acid

EGF Epidermal growth factor

EIF4A1 Eukaryotic translation initiation factor 4A1

EMT Epithelial to mesenchymal transition

ER Estrogen Receptor alpha

ERα Estrogen Receptor alpha

ERβ Estrogen Receptor beta

ErbB Erythroblastic leukaemia viral oncogene

ERBB2 Erb-B2 receptor tyrosine kinase

ERG ETS transcription factor ERG

ESR1 Estrogen Receptor alpha

ESR2 Estrogen Receptor beta

ETS Erythroblast transformation-specific

FAS Fas cell surface death receptor

FBS Foetal bovine serum

FC Fold change

FDR False discovery rate

FFPE Formalin-fixed paraffin wax-embedded

FGFR Fibroblast growth factor receptor

FGFR3 Fibroblast growth factor receptor 3

FOXA1 Forkhead Box A1

FSB Final sample buffer

FSH Follicle stimulating hormone

FTO Fat mass and obesity related

GAPDH Glyceraldehyde-3-phosphate dehydrogenase

GATA3 GATA binding protein 3

GC Gastric cancer

GH Growth hormone

GHR Growth hormone receptor

GISTIC Genomic identification of significant targets in cancer

GnRH Gonadotropin-releasing hormone

GNRHR  Gonadotropin releasing hormone receptor

H&E Haematoxylin & eosin

H19 Long non-coding RNA gene

HCC Hepatocellular carcinoma

HDAC1 Histone deacetylase 1

HER2 human epidermal growth factor receptor 2

HIF1α Hypoxia-inducible factor 1-alpha

HIFs Hypoxia-inducible factors

HNRNP Heterogeneous nuclear ribonucleoprotein

HRE Hormone response element

HRP Horse radish peroxidase

HYB Hakai phosphotyrosine-binding

ICC Intraclass correlation coefficient

IDC Invasive ductal carcinoma

IDC-NST Invasive ductal carcinoma of no special type

IGF Insulin like growth factor

IGF1 Insulin like growth factor 1

IGF2BP insulin-like growth factor 2 mRNA-binding protein

IHC Immunohistochemistry

ILC Invasive lobular carcinoma

IMS Industrial methylated spirit

INHA Inhibin α subunit

kb Kilobase

KD Knockdown

kDa Kilodalton

KEGG Kyoto encyclopaedia of genes and genomes

KLK3 Kallikrein related peptidase 3

KM Kaplan-Meier

LBD Ligand binding domain

LCIS Lobular Carcinoma in situ

LH Luteinising hormone

LHRH Luteinising hormone-releasing hormone

lncRNA Long non-coding RNA

m⁶A N6-methyladenosine

MAP3K1 Mitogen-activated protein kinase kinase kinase 1

MAPK Mitogen-activated protein kinase

MDCK Madin-Darby canine kidney

MET Mesenchymal to epithelial transition

METABRIC Molecular taxonomy of breast cancer international consortium

METTL14 Methyltransferase 14

METTL3 Methyltransferase 3

ml Millilitre

mm Millimetre

MR Mineralocorticoid receptor

MRI Magnetic resonance imaging

mRNA Messenger RNA

MTOR Mechanistic Target of Rapamycin Kinase

MXE Mutually exclusive exons

MYC MYC proto-oncogene, bHLH transcription factor

NCBI National Center for Biotechnology Information

NCOA1 Nuclear receptor coactivator 1

ncRNA Non-coding RNA

NEPC Neuroendocrine prostate cancer

NER Nuclear extraction reagent

NFKB1 Nuclear factor kappa B subunit 1

NKX3-1 NK3 homeobox 1

nM Nanomolar

NPI Nottingham Prognostic Index

ns Not significant

NSCLC Non-small cell lung cancer

NST No special type

NTD N-terminal domain

OS Overall survival

P53 Tumour protein P53

PAGE Polyacrylamide gel electrophoresis

PARP Poly-ADP ribose polymerase

PBS Phosphate buffered saline

PCa Prostate cancer

PCR Polymerase chain reaction

PGR Progesterone Receptor

PI3K Phosphatidylinositol-4,5-bisphosphate 3-kinase

PI3K-Akt Phosphatidylinositol-4,5-bisphosphate 3-kinase/protein kinase B

PIK3CA Phosphatidylinositol-4,5-bisphosphate 3-kinase catalytic subunit alpha

PIK3CB Phosphatidylinositol-4,5-bisphosphate 3-kinase catalytic subunit beta

PIK3R3 Phosphatidylinositol-4,5-bisphosphate 3-kinase regulatory subunit 3

PIN Prostatic intraepithelial neoplasia

PPL Periplakin protein

PR Progesterone Receptor

PRC2 Polycomb repressive complex 2

pre-mRNA Precursor mRNA

PRKCA Protein kinase C alpha

PS2 Trefoil factor 1 *(alias)*

PSA Prostate-specific antigen

PSF Polypyrimidine tract-binding protein associated splicing factor

PTB Polypyrimidine tract-binding protein

PTBP1 Polypyrimidine tract-binding protein 1

PTEN Phosphatase and tensin homolog

PVDF Polyvinylidene difluoride

qRT-PCR Quantitative real-time polymerase chain reaction

R1881 Methyltrienolone

Rack1 Receptor for activated C kinase 1

Rap1 Ras-associated protein 2

RBM15 RNA-binding motif protein 15

RBM15B RNA-binding motif protein 15 beta

RFS Recurrence free survival

RI Retained intron

RING Really interesting new gene

rMATs Replicate multivariate analysis of transcript splicing

RNA Ribonucleic acid

RNA-Seq RNA sequencing

rpm Rotations per minute

rRNA Ribosomal RNA

RTK Receptor tyrosine kinase

SCLC Small cell lung cancer

Scr Scrambled control

SDS Sodium dodecyl sulphate

SE Skipped exon

SERM Selective estrogen receptor modulator

siRNA Short interference RNA

SNP Single nucleotide polymorphism

SPSS Statistical Package for Social Sciences

Src Steroid receptor coactivator

SRC-1 Steroid receptor coactivator-1

Sxl Sex lethal

TCGA The Cancer Genome Atlas

TDLU Terminal duct lobular unit

TEMED Tetramethylethylenediamine

TERT Telomerase reverse transcriptase

TFEB Transcription factor EB

TFF1 Trefoil factor 1 *(also known as PS2)*

TGF-β1 Transforming growth factor beta 1

TGF-β2 Transforming growth factor beta 2

THRAP3 Thyroid hormone receptor associated protein 3

TMA Tissue microarray

TMPRSS2 Transmembrane serine protease 2

TNBC Triple negative breast cancer

TNM Tumour node metastasis

TP53 Tumour protein P53

tRNA Transfer RNA

UCSC University of California Santa Cruz

UK United Kingdom

USA United States of America

UTR Untranslated region

VEGF Vascular endothelial growth factor

VEGFA Vascular endothelial growth factor alpha

VEGFR Vascular endothelial growth factor receptor

Veh Vehicle

VIRMA Vir like m6A methyltransferase

WCM Weill Cornell Medicine

WebGestalt WEB-based Gene SeT AnaLysis Toolkit

Wnt Wingless and Int-1

WT1 Wilms tumour suppressor gene

WTAP Wilms tumour 1-associating protein

XRCC3 X-ray repair cross complementing 3

YTHDC1 YTH domain containing 1

YTHDC2 YTH domain containing 2

YTHDF1 YTH $N^6$-methyladenosine RNA binding protein 1

YTHDF2 YTH $N^6$-methyladenosine RNA binding protein 2

YTHDF3 YTH $N^6$-methyladenosine RNA binding protein 3

ZC3H13 Zinc finger CCCH-type containing 13

ZEB2 Zinc finger E-box binding homeobox 1

ZFP217 Zinc-finger protein 217

µl Microlitre

µm Micrometre

$\chi 2$ Chi-squared

# Chapter 1

General introduction

# 1 General introduction

## 1.1 Importance of cancer

Cancer poses one of the greatest threats to global human health as the leading cause of death in high-income countries, and second only to cardiovascular disease worldwide (Dagenais et al., 2020, Sung et al., 2021). The global incidence of cancer continues to increase, with new cancer diagnoses increasing by 43% from 2008 to 2018, with ~19.3 million new cases and ~10 million estimated deaths in 2020 (Ferlay et al., 2015, Ferlay et al., 2019, Sung et al., 2021).

Cancer describes the disease state where aberrant cell growth disrupts normal physiological processes, usually manifesting as abnormal tissue masses, otherwise known as malignant tumours or neoplasms (Knowles and Selby, 2005). Normal tissue architecture and function is maintained by a number of homeostatic mechanisms that ensure cell growth and proliferation only occur as new cells are required to replace those that have reached the end of their natural lifespan, or to repair regions of damage (Hanahan and Weinberg, 2011). Malignant cells undergo genetic and epigenetic changes that enable them to circumvent these tightly regulated processes and proliferate in an uncontrolled manner (Hanahan and Weinberg, 2000). These hallmark capabilities include the autonomous generation of growth signals and stimulation of blood supply, the evasion of anti-growth signals and programmed cell death, unlimited replicative potential, and the ability to invade normal tissue and travel to distant sites in the body (Hanahan and Weinberg, 2000). Invasive cancer is defined once this abnormal proliferation of cells penetrates the

basement membrane and invades different tissue types (Flug and Köpf-Maier, 1995).

The ability of malignant cells to spread, or metastasise, is characteristic of the deadliest cancers. Lethality results from either the establishment of secondary tumours in vital organs, subsequently impairing their function, or a number of paraneoplastic syndromes such as thrombosis or cachexia caused by over-production of cytokines and tumour-derived catabolic factors (Loberg et al., 2007).

## 1.2 Hormonal cancers

In a distinct group of endocrine-related cancers, hormones are responsible for driving the process of carcinogenesis, stimulating cell proliferation and therefore the opportunity to acquire genetic mutations during cell division (Hahn et al., 1999, Henderson and Feigelson, 2000). Cancers stimulated by estrogen hormones include breast, cervical, uterine and ovarian (Henderson et al., 1988), which feature among the eight most commonly diagnosed cancers in women worldwide (Sung et al., 2021). Notable male hormonal cancers include prostate, (the second most commonly diagnosed in men globally (Sung et al., 2021)), and testicular cancer, where both are stimulated by androgen hormones such as testosterone and 5-α- dihydrotestosterone (DHT) (Huggins and Hodges, 1941).

### 1.2.1 Steroid hormone signalling in cancer

#### 1.2.1.1 Steroid hormones

Steroid hormones comprise five main classes: androgens, estrogens, glucocorticoids, mineralocorticoids and progestin (Payne and Hales, 2004). Androgens and estrogens are cholesterol-derived sex steroid or gonadal

hormones, so-called due to their production primarily in gonads, but also in the adrenal glands (Payne and Hales, 2004). Both androgens and estrogens are produced by males and females to varying degrees, and are vital for normal embryonic development, pubertal maturation, and function of sexual organs, characteristics and behaviour (Lek et al., 2018, Mongan et al., 2015, Mueller and Korach, 2001). The most abundant male androgen hormone is testosterone, which is metabolised to the more potent DHT and is responsible for normal prostate development and function (Imperato-McGinley et al., 1974). In females the most important estrogen hormone is β-estradiol ($\beta E_2$), again key to maintaining normal reproductive development and function (Mueller and Korach, 2001). The production of both androgens and estrogens is regulated by the hypothalamic-pituitary-gonadal axis, through gonadotropin-releasing hormone (GnRH) release from the hypothalamus stimulating the release of follicle stimulating hormone (FSH) and luteinising hormone (LH) into circulation, which, in turn, stimulates sex hormone production in the gonads (Payne and Hales, 2004). The androgen:estrogen ratio changes throughout life, and this may play a role in promoting prostate and breast carcinogenesis.

#### 1.2.1.2 Nuclear receptors

Steroid hormones function through binding with ligand-dependent transcription factors known as nuclear receptors (Mangelsdorf et al., 1995). There are three groups of nuclear receptors, comprising the steroid receptor family, the non-steroid receptor family and the orphan receptor, each of which bind steroid hormones, non-steroid hormones and unknown ligands, respectively, and together are responsible for regulating a wide range of physiological processes (Olefsky, 2001).

The structure of the majority of nuclear receptors comprises three distinct domains, the N-terminal domain (NTD), DNA-binding domain (DBD) and ligand-binding domain (LBD) (Beato, 1989, Claessens et al., 2008). The NTD, the most variable domain between different nuclear receptors, is the site of the transcriptional activation function-1 (AF-1) region, which functions in a ligand-independent manner (Bocquel et al., 1989, Germain et al., 2006, Moras and Gronemeyer, 1998). The DBD is the site of selective binding to specific hormone response elements on target genes to mediate transcription (Moras and Gronemeyer, 1998). Finally, a flexible hinge region attaches the DBD to the LBD, the site of coregulator and ligand binding (Bocquel et al., 1989). The LBD is also the site of the transcriptional activation function-2 (AF-2) region which is dependent on ligand binding (Moras and Gronemeyer, 1998). Full transcriptional activation of target genes is then seen when both of the transcriptional activation function regions in the NTD and LBD are simultaneously activated (Wärnmark et al., 2003).

#### 1.2.1.3 The androgen receptor

The androgen receptor (AR) is a transcription factor encoded by the *AR* gene, belonging to the steroid receptor family of nuclear receptors, whose specific ligands are androgen hormones (Olefsky, 2001). The AR is essential for normal developmental processes in males and plays a fundamental role in the development and progression of prostate cancer (PCa) (Heinlein and Chang, 2004, Imperato-McGinley et al., 1974). Coregulators and corepressors can also interact with the activation function regions in the AR and influence its transactivation (Bevan and Parker, 1999, Gritsina et al., 2019). The AR is also known to exert its influence on gene expression through influencing alternative

splicing (Auboeuf et al., 2002). Alternative splicing is the process of differential excising of introns from precursor mRNA, whereby different transcripts and ultimately different proteins result from the same gene (Ast, 2004, Berget et al., 1977). The structure of the AR, which is largely the same as the rest of the nuclear receptors except for some specialised differences in the length and amino acid sequence in the NTD, is illustrated in **Figure 1.1.**

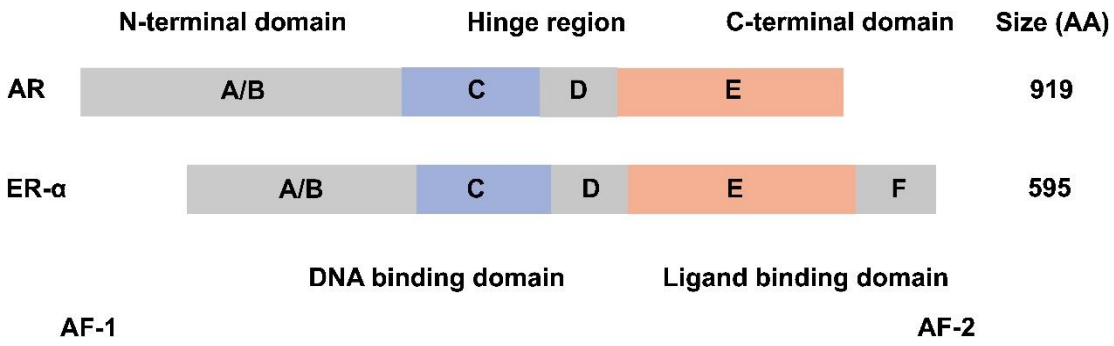


**Figure 1.1 Structure of the androgen receptor and estrogen receptor**

Schematic of the structure and domains of the AR and ERα proteins.

### 1.2.1.4 The estrogen receptor

Like the AR, the two distinct types of estrogen receptor, ERα and ERβ, are also steroid receptors that function as ligand-inducible transcription factors to regulate target gene expression (Mueller and Korach, 2001). Estrogen receptors are the key mediators of the actions of estrogen hormones and play a fundamental role in female development and reproduction, as well as in breast cancer (BCa) development and progression (Henderson and Feigelson, 2000, Mueller and Korach, 2001). ERα and ERβ, encoded by *ESR1* and *ESR2*, respectively, are structurally similar, yet expressed in different tissue types

(Paterni et al., 2014). ERα expression is higher and is known to play a much more prominent role in breast tissue than ERβ, so therefore ERα (also known simply as ER) is the focus of this study. As with the AR, the ERα also interacts with numerous coregulators and corepressors that influence its transactivation functions (Paterni et al., 2014). Steroid hormones are known to influence alternative splicing, with estrogen having been demonstrated to significantly alter splicing events in target genes in ERα-expressing BCa cells (Auboeuf et al., 2002, Auboeuf et al., 2004). The structure of the ERα is illustrated in **Figure 1.1** alongside the AR.

#### 1.2.1.5 Steroid hormone signalling

Steroid hormones enter cells in target tissues via diffusion and bind with their specific receptors in the cytoplasm, where they tend to be located in the absence of their ligand, bound by heat shock proteins in an inactive state (Allan et al., 1991, Mooradian et al., 1987, Veldscholte et al., 1990). Once the steroid hormone binds, its receptor undergoes conformational change that causes it to dissociate from these inactivating heat shock proteins, undergo receptor dimerisation and translocation to the nucleus (Cutress et al., 2008, Ni et al., 2013). Once inside the nucleus, the steroid receptor is guided to its specific hormone response element in either the promoter or enhancer region of target genes by pioneer factors such as FOXA1 (Bennett et al., 2010). The activated steroid receptor then recruits coregulators that either induce or suppress transcription of hormone-regulated genes (Bennett et al., 2010).

Hormone signalling is responsible for a mediating a great number of vital physiological process, and therefore any aberration in these pathways can result in pathology, including cancer (Caldon, 2014, Dhiman et al., 2018, Zhou

et al., 2015). The AR and ERα, together with their respective sex hormone ligands androgen and estrogen, are widely reported to play key roles in altering cellular proliferation and survival, thereby contributing to carcinogenesis and disease progression in both PCa and BCa, respectively (Huggins and Hodges, 1941, Williams and Lin, 2013, Zhou et al., 2015).

## 1.3 Prostate cancer

### 1.3.1 Prostate anatomy and physiology

The prostate is the largest accessory sex gland in males and is situated below the bladder surrounding the urethra (Motrich et al., 2018). Its glandular tissue can be split into three zones, namely the peripheral zone, which accounts for ~70% of the prostate's mass, the central zone (~25%) and the transitional zone (~5%) (McNeal, 1988). The peripheral zone is the most common site of both tumours and prostatitis, whilst the transitional zone is most commonly where benign prostate hyperplasia (BPH) arises (McNeal, 1988).

The glandular tissue of the prostate comprises ducts and acini which are lined by luminal, basal and neuroendocrine cells, contained within a basement membrane (Ittmann, 2018). Columnar luminal cells are the secretory cells that surround the lumen of glands and acini and express high levels of AR, whereas cuboidal basal cells sit beneath the luminal cells, adjacent to the basement membrane and express low to negative levels of AR (Kwon et al., 2014, Shen and Abate-Shen, 2010). Neuroendocrine cells are found occasionally at the level of basal cells, have neuronal characteristics, and do not express AR (Shen and Abate-Shen, 2010).

The main function of the prostate is to secrete the seminal fluid which comprises one third of the volume of semen and is essential to maintain

spermatozoan health and motility during and following ejaculation (Huggins and Neal, 1942, Sørensen et al., 1999, Yoshida et al., 2008). A key component of this seminal fluid is the prostate-specific antigen (PSA) protein, encoded by the gene *KLK3*, as well as a number of enzymes, zinc and citrate (Verze et al., 2016).

Luminal cells of the acini are widely considered to be the most common cell of origin for PCa, with acinar adenocarcinoma with enhanced AR expression accounting for ~95% of PCa cases (Orihuela and Green, 2008, Zhang et al., 2018). High-grade prostatic intraepithelial neoplasia (PIN) is widely considered to be a precursor to PCa and is defined by increased proliferation of luminal cells, usually with enlarged and atypical nuclei and nucleoli, with a simultaneous reduction in basal cells (Bostwick and Brawer, 1987, Bostwick et al., 2004, Davidson et al., 1995).

PCa arising in neuroendocrine cells is rare (observed in <2% of patients), however neuroendocrine PCa (NEPC) more commonly develops following androgen deprivation therapy of adenocarcinoma, and is seen in ~25% of patients with metastatic PCa (Humphrey, 2012, Mucci et al., 2000). The true origin of NEPC cells is still not fully understood, however NEPC cells are known to lack AR or PSA expression and are associated with loss of key tumour suppressor proteins including p53 and PTEN (Beltran et al., 2011, Beltran et al., 2014, Krausch et al., 2011). NEPC represents a key clinical challenge due to its highly aggressive phenotype, and because androgen deprivation therapy (ADT) is not effective (Beltran et al., 2014, Hu et al., 2012).

### 1.3.2 Incidence and risk factors

PCa is the second most commonly diagnosed male cancer type globally and in 2020 was responsible for ~375,000 deaths (Sung et al., 2021). A number of risk factors for PCa have been identified, including age, ethnicity, and family history (Gann, 2002), as well as environmental and lifestyle factors such as diet and smoking (Kenfield et al., 2011, Malik et al., 2018, Peisch et al., 2017).

PCa is most commonly a disease seen in men over 65 years of age, however where PCa develops before the age of 55, a more aggressive phenotype is usually seen, resulting in poorer patient outcomes (Salinas et al., 2014).

There are significant differences in PCa incidence rates between ethnic groups, with incidence twice as high in men of African ethnicity compared to their age-matched Caucasian counterparts (Giovannucci et al., 2007, Lloyd et al., 2015). This increased incidence in men self-identifying as black remains significant after adjusting for differing access to healthcare institutions, socioeconomic and environmental adversity, and associated stress (Kantor et al., 2019, Nettey et al., 2018).

When considering family history, almost a three-fold increase is seen in PCa incidence in men with an affected brother, increasing further as more first-degree relatives are affected (Bratt et al., 2016, Hemminki, 2012). The world's largest study of cancer in twins estimated overall PCa heritability at 57%, second only to melanoma at 58% when compared with 15 other common cancer types (Hjelmborg et al., 2014, Mucci et al., 2016). Indeed, men with a dizygotic twin diagnosed with PCa experience almost twice the lifetime risk of developing PCa as the general population (Hjelmborg et al., 2014). Taken

together, the increased risks of developing PCa associated with family history and ethnicity suggest a strong genetic influence on PCa aetiology.

Other non-genetic risk factors for PCa include smoking (Kenfield et al., 2011, Malik et al., 2018, Peisch et al., 2017) and obesity (Cao and Ma, 2011, Peisch et al., 2017). Dietary components have also been linked to increased risk of PCa, including high consumption of processed red meat and saturated fat (Gann, 2002). In contrast, diets high in lycopene, a carotenoid compound commonly found in tomatoes, have been associated with a reduced risk of PCa (Gann et al., 1999, Gann, 2002).

### 1.3.3 Diagnosis and treatment

PCa diagnoses increased markedly from the late 1980s following the introduction of the prostate specific antigen (PSA) blood screening test (Salinas et al., 2014). Routine screening using PSA has been controversial, as it may have contributed to overdiagnosis and thus overtreatment of PCa, both by detecting false positives and clinically insignificant PCa (Heidenreich et al., 2013). In a systematic review of five large randomised controlled trials, it was found that routine screening saved approximately one life per 1000 men, but that the resulting over-treatment caused life-changing side effects in up to 25 times as many patients (Ilic et al., 2018).

PCa diagnosis is usually achieved following routine screening by digital rectal examination and serum concentration of PSA, followed by transrectal ultrasound-guided biopsy and, increasingly, MRI (de Rooij et al., 2016, Heidenreich et al., 2014). Prostatic malignancies are characteristically diffuse and heterogeneous, therefore histopathological examination of biopsy specimens is required to confirm PCa diagnosis and subsequently grade and

stage the disease, aided by the Gleason scoring system (Gleason, 1966, Mottet et al., 2017). The Gleason score remains the most effective prognostic predictor of prostate cancer and aids in directing therapy (Gordetsky and Epstein, 2016). The Gleason scoring system comprises five histological patterns, with patterns 1-2 containing well-delineated malignant glands, progressing through moderately- to poorly-differentiated tumour cells growing either singularly, in cords or solid fields, through to evidence of comedonecrosis in pattern 5 (Gleason, 1966, Gleason and Mellinger, 1974). The characteristic heterogeneity of prostate tumours is accounted for by adding together the two most common histological patterns to give the Gleason composite score (Epstein et al., 2005, Gleason, 1966, Gleason and Mellinger, 1974).

The Gleason scoring system has been revised over time, however this has increased its complexity, leading to some confusion for both patients and clinicians (Gordetsky and Epstein, 2016). For example, despite the Gleason scoring scale ranging from 2-10, it is now recommended that the minimum score given following biopsy is 6, as it has been found that scores lower than this are rarely representative of the true extent of disease when examined following radical prostatectomy (Epstein, 2000). More recently, a new prognostic five-point grading system has been recommended for use in conjunction the Gleason grading system by the World Health Organization (**Table 1.1**) (Epstein et al., 2016, Pierorazio et al., 2013). This new grading system is based on the modified Gleason score groups and has been validated as simpler to use and a more accurate representation of prostate cancer biology (Gordetsky and Epstein, 2016).

| Grade group | Gleason score | 5 year biochemical recurrence- free survival |
|---|---|---|
| 1 | ≤ 6 | 96% |
| 2 | 3 + 4 = 7 | 88% |
| 3 | 4 + 3 = 7 | 63% |
| 4 | 4 + 4 = 8 | 48% |
| 5 | 9 and 10 | 26% |

**Table 1.1 Modified Gleason prognostic grading system**

New PCa prognostic grading system based on the modified Gleason scoring system (Pierorazio et al., 2013).

Once PCa has been diagnosed, its progression is monitored by serial serum PSA measurements and follow up imaging. It has been demonstrated that there is a directly proportional relationship between PSA levels and tumour size, with each 3.5ng/ml elevation in serum PSA representing a 1ml increase in tumour volume (Stamey et al., 1987, Stamey and Kabalin, 1989).

PCa is unusual as a malignancy in that it generally progresses so slowly in most affected men that it remains clinically insignificant and does not cause death (Stamey et al., 1993). PCa has been shown to be present in more than 30% of men aged over 50 years, only found incidentally at post-mortem examination, having never caused clinical disease (Franks, 1954, Scardino et al., 1992). However, the lifetime risk of being clinically diagnosed with PCa is ~13% in the UK, with risk of dying of PCa around 4% (Lloyd et al., 2015, Smittenaar et al., 2016). Given the morbidity associated with treatment and the

minimal impact on survival rates, it has been accepted since the late 2000s that routine PSA screening of men outside of the highest risk groups is not justified (Andriole et al., 2009, Ilic et al., 2007).

A number of treatment options are currently available for PCa patients, although many come with marked side effects that must be considered carefully when devising a therapeutic plan (Evans, 2018, Teo et al., 2019). Available treatments include radical prostatectomy and radiotherapy for organ-confined disease, and systemic cytotoxic chemotherapy and hormone deprivation therapy for more advanced PCa (Cornford et al., 2017, Mottet et al., 2017). Associated side effects include nausea, fatigue, urinary and faecal incontinence, sexual dysfunction, loss of bone density and sarcopenia (Boukovala et al., 2019). Therefore, in men over 55 years old with low grade PCa (Gleason score of 6/10 or less), conservative management, or 'watchful waiting', is the recommended approach, given the impact on quality of life that treatment side effects have, and that risk of death within 15 years of diagnosis is below 7% (Albertsen et al., 1998, Chen et al., 2016).

Identifying the subset of men who will develop clinically significant PCa, and those that will progress to lethal PCa, therefore remains a key clinical challenge. Current guidelines advise that active treatment should be considered in men with the following presentations: those with tumours with a Gleason score ≥7 or that extend beyond one side of the prostate, serum PSA concentration over 10ng/ml, or evidence of lymphovascular invasion (Mottet et al., 2017).

In PCa that is advanced at diagnosis, or following metastasis, the first line treatment is androgen deprivation therapy (ADT), using anti-androgen drugs to deprive the PCa cells of the hormones that stimulate their growth (Cornford et al., 2017, Hussain et al., 2018, Semenas et al., 2012) (**Figure 1.2**). A number of therapeutic agents are available and can be used in combination to block the stimulating effects of the androgen hormones testosterone and DHT (de Brot et al., 2015). 'Chemical castration' via luteinising hormone-releasing hormone (LHRH) agonists (such as buserelin acetate and leuprorelin) and antagonists (such as degarelix), together with steroid synthesis inhibitors (such as abiraterone acetate) serve to reduce circulating androgen levels, whilst anti-androgen drugs (such as enzalutamide) work at the level of the androgen receptor, blocking its ability to bind and respond to any remaining androgen hormone (Attar et al., 2009, Beer et al., 2014, Fizazi et al., 2017).

Enzalutamide was the first second generation anti-androgen drug approved for use in metastatic CRPC, after having demonstrated in clinical trials that it increased overall survival in relapsed PCa patients following chemotherapy (Scher et al., 2012), and progression-free survival in chemotherapy-naïve patients (Beer et al., 2014). More recently it has also been approved for use in non-metastatic CRPC as it has been proven to improve metastasis-free survival in these patients too (Tombal, 2019).

Chemotherapy drugs such as docetaxel, in combination with the corticosteroid prednisone or radiotherapy, have been demonstrated to improve survival rates when used alongside ADT (Cornford et al., 2017, Fizazi et al., 2017).

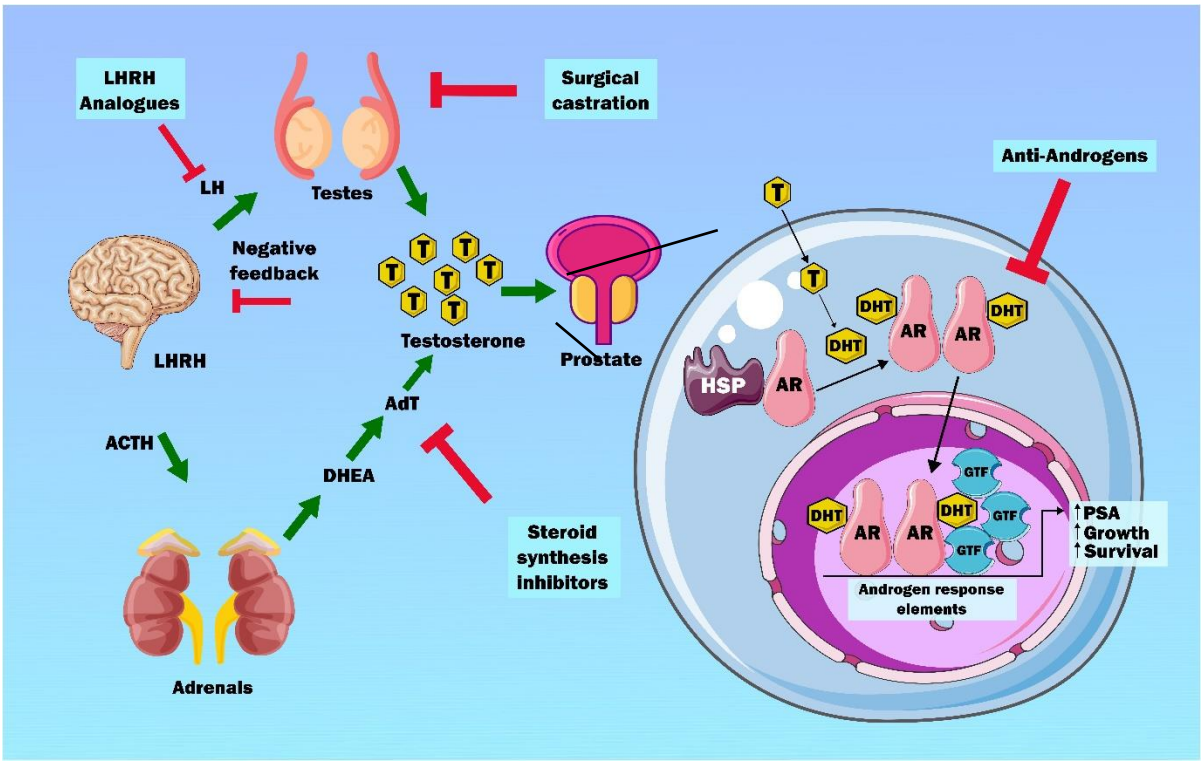


**Figure 1.2 Therapeutic targets in androgen deprivation therapy in prostate cancer**

Schematic of the therapeutic targets and agents used in androgen deprivation therapy in PCa (adapted from Attar et al., (2009)).

More recent innovations in PCa treatment include immunotherapeutics such as Sipuleucel-T, which uses a patient's own antigen presenting cells and activates them against prostatic acid phosphatase (PAP) (Kantoff et al., 2010), although its cost is inhibitory outside of the USA, and the monoclonal antibody pembrolizumab (Hansen et al., 2018). However, to date these have shown limited patient benefit.

### 1.3.4 Androgen deprivation therapy resistance

ADT is effective initially, with ~80% of patients seeing tumour regression, however in the majority of these patients ADT will fail after approximately two

years when their PCa progresses to an androgen-independent or castrate-resistant disease state (Gravis et al., 2013, Sweeney et al., 2015).

This tumour progression, despite androgen blockade, is known as the development of castration-resistant prostate cancer (CRPC) (Longo, 2010). The initial positive effect of ADT occurs via either reducing the levels of circulating hormones (abiraterone, LH-targeting therapies), together with antagonism of the androgen receptor (AR) (flutamide, bicalutamide, enzalutamide, apalutamide, darolutamide), preventing androgen from binding its receptor and the downstream signalling that occurs (Attar et al., 2009, Knudsen and Penning, 2010). Formerly known as hormone-refractory or androgen-independent PCa, it is now known that the castrate-resistant state still exploits AR transcriptional activity and androgen signalling (Longo, 2010). PCa cells use a number of mechanisms to reactivate AR signalling in low level androgen conditions (Attar et al., 2009). These include increased expression of the AR protein (Linja et al., 2001, Visakorpi et al., 1995), AR gene mutation, expression of AR splice variants (Hara et al., 2003, Li et al., 2013), altered androgen biosynthesis and sensitivity (Chandrasekar et al., 2015, Jernberg et al., 2017), and altered expression of transcriptional co-regulators such as the p160/SRC family (Groner et al., 2016).

ADT has been associated with both upregulated expression of AR and increased frequency of *AR* gain-of-function mutations (Chen et al., 2004, Grasso et al., 2012, Taplin et al., 1995). These mutations can cause the AR to lose its ligand specificity, allowing activation to occur secondary to binding of other steroid hormones, so-called ligand promiscuity (Gottlieb et al., 2012, Taplin et al., 1995, Veldscholte et al., 1990), and even enable enzalutamide

and bicalutamide to activate, rather than inhibit, transcription once bound to the AR (Bohl et al., 2005, Korpal et al., 2013) .

No curative treatment options exist for PCa once metastasis has occurred, most commonly to the bones of the pelvis and lumbar spine, as well as the regional lymph nodes, abdominal viscera and lungs (Loberg et al., 2005, Shah et al., 2004), with a subsequent median survival time of approximately three years (Afshar et al., 2015, Sweeney et al., 2015). There is increasing focus now on personalised precision medicine, to examine the underlying mechanisms of cancer progression in individual patients, and to identify markers that will predict efficacy of drugs and facilitate selection of the most appropriate treatment plans to optimise outcomes (Prekovic et al., 2018).

#### 1.3.4.1 Alternative splicing in prostate cancer

The AR exerts its influence on gene expression not only through regulation of target gene transcription, but also through influencing alternative splicing (Auboeuf et al., 2002). Alternative splicing of genes in cellular proliferation and survival-associated pathways and dysregulation of alternative splicing has been associated with disease progression and resistance to therapy in PCa (Kahles et al., 2018, Paschalis et al., 2018, Zhang et al., 2020a).

Alternative splicing of the AR itself giving rise to pathogenic AR variants is something that is commonly seen in castrate-resistant metastatic PCa and in response to ADT (Antonarakis et al., 2014, Antonarakis et al., 2017, Armstrong et al., 2019, Scher et al., 2016, Sharp et al., 2019). Out of the more than 20 AR variants that have been identified, only two, namely ARv7 and ARv567es, have been demonstrated to be clinically relevant in PCa (Dehm and Tindall, 2011,

Gjyrezi et al., 2021, Guo et al., 2009, Kim et al., 2022, Sun et al., 2010, Thadani-Mulero et al., 2014). These truncated AR variants contribute to the development of CRPC through their loss of the C-terminal ligand-binding domain, the binding site of anti-androgen drugs such as enzalutamide, rendering them incapable of fulfilling their intended effect (Antonarakis et al., 2014, Cao et al., 2014, Dehm and Tindall, 2011). It has been reported that ARv7 is more abundantly expressed in CRPC compared with androgen-sensitive tumours and, whilst rare in primary tumours, is expressed in over 75% of metastatic tumours, evidencing the selective pressure of ADT (Guo et al., 2009, Hu et al., 2009, Sharp et al., 2019). It is unsurprising, therefore, that a number of studies have reported increased expression of ARv7 to be associated with ADT resistance, CRPC development and poorer patient survival (Antonarakis et al., 2014, Antonarakis et al., 2017, Armstrong et al., 2019, Scher et al., 2016).

## 1.4 Breast cancer

### 1.4.1 Breast anatomy and physiology

The breasts are two mammary glands that cover the pectoral muscle at the top of the anterior rib cage and comprise both glandular and adipose tissue, and stroma (Jesinger, 2014). Each mammary gland comprises between 12 and 20 lobes that are, in turn, subdivided into thousands of lobules, which each contain ~200 acini (Jesinger, 2014). A terminal duct is formed from the joining together of many acinar ducts, and this, together with its associated lobule, comprises the terminal duct lobular unit (TDLU) (Hassiotou and Geddes, 2013).

Luminal epithelial cells are the secretory cells that surround the lumen of each gland (Jesinger, 2014). These are enclosed by a layer of myoepithelial cells,

that appear and function similarly to smooth muscle cells, and the basement membrane (Hassiotou and Geddes, 2013).

The function of the mammary gland, unique to mammals (including the platypus), is to synthesise, secrete and deliver milk for the feeding of neonates (Hassiotou and Geddes, 2013). The TDLU is the functional unit of the breast responsible for milk production, which then drains through a number of ducts and sinuses to the nipple, where it reaches the suckling baby (Jesinger, 2014).

BCa most commonly originates in the epithelial cells of the TDLU (Weigelt et al., 2010b). Invasive ductal carcinoma (IDC) is the most common histological subtype of BCa, accounting for ~75-80% of all BCa diagnoses (Feng et al., 2018, Tavassoli, 2003). IDC is then further morphologically classified as either tubular, medullary, mucinous papillary, cribriform carcinoma, or the most common form, known as 'no special type' (NST) (Feng et al., 2018, Tavassoli, 2003). The second most commonly diagnosed histological subtype is invasive lobular carcinoma (ILC), which is responsible for ~15% of diagnoses (Feng et al., 2018).

Precursors of invasive carcinoma are ductal carcinoma *in situ* (DCIS), and the less common lobular carcinoma *in situ* (LCIS), characterised by epithelial cell proliferation whilst still being contained within the basement membrane (Sgroi, 2010). As BCa progresses, it tends to have a distinctive metastatic pattern, spreading to local structures such as the soft tissues of the thorax and regional lymph nodes, then most commonly to the lungs, liver and bone marrow (Müller et al., 2001).

### 1.4.2 Incidence and risk factors

BCa is the most commonly diagnosed cancer in women, with disease incidence continuing to increase, and the leading cause of female cancer-related deaths worldwide (Nolan et al., 2023, Sung et al., 2021). BCa is a collection of over 20 different sub-types of disease, each with their own distinct morphology, genetic profile and clinical presentation (Lakhani et al., 2012).

BCa is largely a disease of post-menopausal women, with the majority of patients aged over 50 years at diagnosis (DeSantis et al., 2011). However, it should be noted that when diagnosed in younger women, BCa is likely to be more aggressive and lethal (McGuire et al., 2015). This is evidenced by the differences in survival rates between age groups in British women, with five-year post-diagnosis survival in women aged under 40 years 5% lower than their counterparts aged 60-69 years, and with ten-year survival rates over 8% lower (Magadi et al., 2016). Whilst mortality rates are higher still in patients over 70 years old, this is most likely associated with age-related co-morbidities rather than a more aggressive BCa phenotype (Aaldriks et al., 2013, Magadi et al., 2016).

Genetic risk factors for BCa have garnered many headlines in recent years, in particular following the discovery of a hereditary mutation in the Breast Cancer 1 (BRCA1) gene that conferred BCa susceptibility (Hall et al., 1990, Miki et al., 1994). A number of studies have found that lifetime risk of developing BCa in north-western European women with *BRCA1* or *BRCA2* mutations ranges from ~30-80% (Antoniou et al., 2008, Brohet et al., 2014, Kuchenbaecker et al., 2017), compared with 16% among the general population (CRUK, 2017). Interestingly, it has also been found that women with a family history of PCa

have an increased risk of developing BCa (Barber et al., 2018). However, family history and inherited genetic mutations account for only 5 -10% of BCa cases (De Greve et al., 2008). Indeed, it has been demonstrated through observing migrating populations that it is non-hereditary factors that appear to be the major drivers of BCa (Tyczynski et al., 1994, Ziegler et al., 1993).

Decades of epidemiological studies have identified a number of lifestyle and environmental BCa risk factors (Maas et al., 2016). Increased exposure to estrogen (through early menarche, late menopause and consumption of exogenous hormones in oral contraceptives and post-menopausal therapies) has long been known to increase BCa risk (Henderson, 1989, Hsieh et al., 1990). Reproductive history such as older age at first birth, reduced parity, and lack of breast-feeding are also known risk factors (CGHFBC, 2002, Kelsey et al., 1993, Lambertini et al., 2016, Victora et al., 2016). Alcohol consumption is likewise considered to increase risk of BCa, exerting its effect via elevating endogenous estrogen levels (Hamajima et al., 2002, Hartman et al., 2016). Such increased estrogen levels have also been implicated in the association of obesity with increased risk of BCa, through the conversion of circulating androgen hormones into estrogens in adipose tissue, with the chronic inflammatory state induced by obesity also a contributing factor (Cleary and Grossmann, 2009, Morris et al., 2011, Neuhouser et al., 2015).

Interestingly, a link between smoking and increased BCa risk has been more difficult to clearly demonstrate, despite smoking being associated with a number of other cancer types (Hamajima et al., 2002, Miller et al., 2007, National Center for Chronic Disease et al., 2014), although recent large studies have reported increasing evidence for a modest increase in BCa risk in women

who smoke, particularly in those with a family history of BCa (Jones et al., 2017, Macacu et al., 2015).

### 1.4.3 Diagnosis and molecular subtypes of BCa

From the late 1980s, the concept of assessing women at high level of BCa risk and applying preventative strategies was introduced (Claus et al., 1993, Gail et al., 1989). Current screening guidelines in the UK include mammography every three years in women aged 50-70 years, with annual imaging offered to women aged from as young as 30 where a high risk of BCa due to family history or where a gene mutation such as in *BRCA1/BRCA2* has been identified (NICE, 2020). Whilst a small proportion of BCa cases are diagnosed following patient self-presentation due to symptoms, the majority of tumours are found during routine mammography screening, with BCa being diagnosed in ~7-9% of screened patients (Bevers et al., 2018, Marmot et al., 2013).

Abnormal findings on mammogram are followed up with additional imaging and biopsy where indicated (NICE, 2016). Biopsied tumour samples are then assessed to determine histological subtype, grade, and specific marker expression (Kooistra et al., 2010). BCa tumours are classified as to histological grade, from I to III based on the level of cellular differentiation and indicators of aggressiveness (Ellis et al., 1992, Elston and Ellis, 1991, Tavassoli, 2003). Three factors are examined in order to grade tumour samples: i) the percentage of tubules present (T; scored from 1 for >75% to 3 for <10%); ii) nuclear pleomorphism (P; scored from 1 for small, regular nuclei to 3 for pronounced nuclear variation); and iii) the mitotic count (M; scored from 1 for <9 mitotic figures visible per 10 high powered fields to 3 for >20). The TNM scores are added to give the grade, with a TNM score of 3-5 resulting in a

grade I classification with a good prognosis, through to >8 designated grade III with poor prognosis (Elston and Ellis, 1991, Rakha et al., 2008).

This information is then inputted into the Nottingham Prognostic Index (NPI), the standard of care method recommended by the World Health Organisation for stratifying BCa patients for therapeutic purposes (Elston and Ellis, 2002, Galea et al., 1992, Haybittle et al., 1982, Tavassoli, 2003). The NPI provides a relatively quick, inexpensive and easy method of reaching a prognostic score (good, moderate or poor) based on tumour size, degree of lymph node involvement, and histological grade (Blamey et al., 2007).

At present BCa treatment is largely guided by these clinical and histopathological features, together with hormone receptor and tyrosine-protein kinase receptor human epidermal growth factor receptor 2 (HER2) positivity determined by immunohistochemistry (Lakhani et al., 2012, Sachs et al., 2018).

Microarray-based gene expression profiling became available at the turn of the new millennium and has provided an additional layer of stratification for BCa patients, determining the intrinsic molecular characteristics and their likely effect on tumour cellular responses to therapy (Weigelt et al., 2010a). This allowed for the compilation of an ‘intrinsic gene’ list (of those genes that vary most between tumour and normal tissues) to allow for grouping of BCa tumours into molecular subtypes (Perou et al., 2000). Ongoing studies have further highlighted the heterogeneity of BCa, with over 90 genes found to be associated with BCa to date, and the identification of over 1600 likely mutations driving BCa carcinogenesis (Sachs et al., 2018).

BCa tumours can be broadly grouped into four main categories based on their intrinsic and molecular subtypes (**Figure 1.3**), the most common and diverse being the hormone receptor-positive luminal cancers, accounting for approximately 70-80% of all BCa diagnoses (Eroles et al., 2012, McGuire et al., 2015).

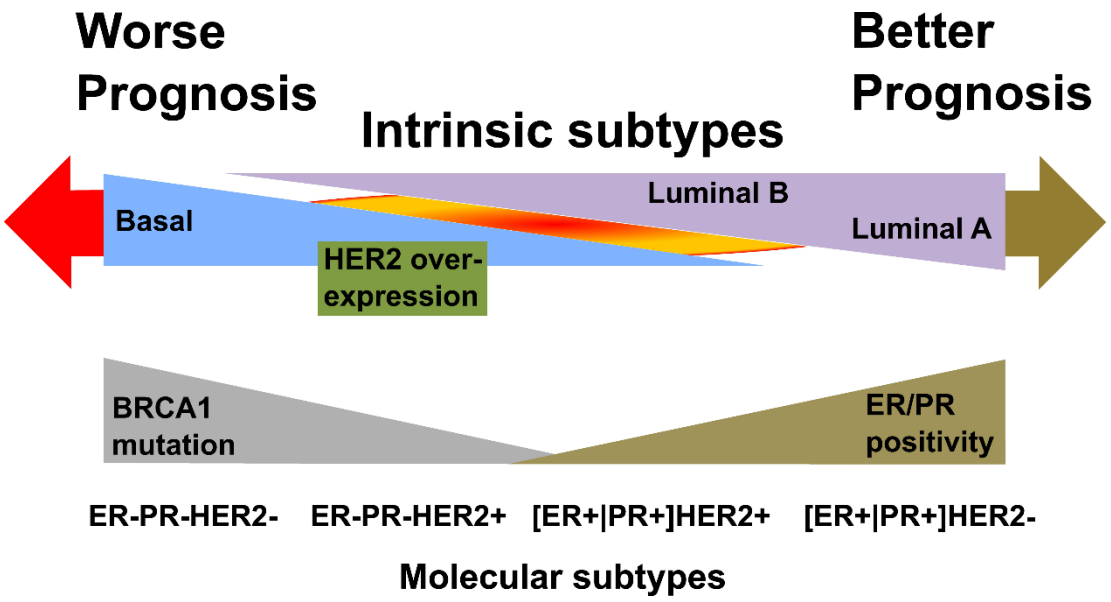


**Figure 1.3 Intrinsic and molecular subtypes of breast cancer**

Schematic of the intrinsic and molecular subtypes of BCa, together with their associated features and prognoses (adapted from Dai et al., (2015).

Luminal A tumours express the estrogen receptor (ER) and the progesterone receptor (PR), but do not express HER2, whilst Luminal B tumours are positive for ER, PR and HER2 (Goldhirsch et al., 2011). In contrast, HER2-overexpressing tumours represent 10-20% of BCa cases, and whilst expressing HER2, do not express ER or PR, and triple negative breast cancer (TNBC), or basal-like, tumours, found in around 10% of BCa patients, lack ER,

PR and HER2 (Dai et al., 2015, Perou et al., 2000, Sweeney et al., 2014). Luminal and HER2-overexpressing BCa occurs most commonly in post-menopausal women, whereas TNBC incidence is higher in younger women, typically pre-menopausal, and is more likely to be associated with genetic mutations such as in *BRCA1/BRCA2* (Calza et al., 2006, Sweeney et al., 2014). It is these TNBC tumours that pose one of the greatest clinical challenges, as they lack the therapeutic targets that these hormone receptors provide, as well displaying the most aggressive BCa phenotype, and are thus associated with a poor prognosis (Dai et al., 2015, Onitilo et al., 2009, Perou, 2011).

### 1.4.4 Treatment of breast cancer

Once diagnosed, the overwhelming majority of BCa patients undergo surgery. In smaller or less aggressive tumours, this can be a lumpectomy (also known as breast-conserving surgery), or a full mastectomy, commonly followed by chemo- or radiotherapy (Bray et al., 2018). Women with more advanced disease at diagnosis will often proceed straight to radiation or chemotherapy protocols including drugs such as cyclophosphamide or fluorouracil (Miller et al., 2016).

Around 80% of BCa patients with hormone or HER2 receptor positivity will receive targeted therapy, regardless of cancer stage (ACS, 2015). In hormone receptor-positive BCa, the cornerstones of treatment are reduction of circulating estrogen levels and blockade of the ER, either in isolation or concurrently (ATAC, 2002). The first-line selective ER modulator is tamoxifen, used in both early stage and advanced BCa, in pre- and post-menopausal women (Francis et al., 2014). This can be used alongside GnRH agonists such

as goserelin in pre-menopausal women to inhibit ovarian production of estrogen, or aromatase inhibitors such as anastrozole in post-menopausal women to prevent aromatisation of endogenous androgens into estrogen (Forward et al., 2004). In the event of resistance to hormone therapy and disease progression, a PR agonist such as megestrol acetate can be added. (Mohammed et al., 2015). The PR has been found to modulate the ER in BCa, and synthetic progesterones have demonstrated an anti-proliferative effect in breast tissue (Mohammed et al., 2015).

In HER2-overexpressing BCa, anti-HER2 monoclonal antibody treatments such as pertuzumab or trastuzumab (also known as Herceptin™) are used alongside chemotherapy drugs to boost clinical benefit, either prior to or post-surgery (Slamon et al., 2001).

Given the lack of specific therapeutic targets in TNBC, systemic chemotherapy such as docetaxel represents the primary treatment option, which is effective in some patients, however other patients fail to respond, with rapid metastasis ensuing (Denkert et al., 2017). More recent studies have investigated the utility of platinum-based compounds in these patients, with some potentially promising results (Isakoff et al., 2015, Minckwitz et al., 2013).

Many mechanisms of therapeutic resistance have been reported, including gain-of-function mutations in the *ESR1* gene that results in hormone-independent activity treatment selection for a tumourigenic sub-population of tumour cells that exhibit stem cell-like characteristics, and oncogenic signalling from extracellular vesicles to dormant cancer stem-like cells (Al-Hajj et al., 2003, Jeselsohn et al., 2015, Sansone et al., 2017).

Recent developments in BCa treatments particularly aimed at TNBC patients include poly(ADP-ribose) polymerase (PARP) inhibitors such as olaparib and talazoparib, which have been shown to improve survival rates compared with standard chemotherapy (Litton et al., 2018, Robson et al., 2017). PARP inhibitors act by targeting the specific DNA repair defect seen in patients with germline mutations in either *BRCA1* or *BRCA2* (Lord and Ashworth, 2017). However, development of resistance to PARP inhibitors can be common, leading to the need for combination therapies, in particular immunotherapies, designed to resensitise tumour cells (Lord and Ashworth, 2017, Pantelidou et al., 2019).

Despite the range of therapies available for use in BCa, it is clear that further work is needed to understand the heterogeneity of BCa, and to be able to adequately tailor treatments to the individual needs of patients (Sachs et al., 2018).

## 1.5 E-cadherin

### 1.5.1 Biological function

As invasion beyond the basement membrane is a key feature of malignant tumours, the mechanisms of metastasis are a key feature of cancer cells. Epithelial cadherin (E-cadherin) is a member of the cadherin superfamily of proteins found in animals (metazoans), whose main function is to provide calcium-dependent adhesion between epithelial cells (Brasch et al., 2011). Also known as cadherin-1, E-cadherin is encoded by the *CDH1* gene which sits on chromosome 16 (Natt et al., 1989). Cadherin activity occurs in the majority of tissue types, and subclasses of cadherins have been defined based on their distinct immunological specificities in different tissues (Takeichi et al.,

1988). Interestingly, cadherin proteins are not found in non-metazoan multicellular organisms such as plants (Abedin and King, 2008).

E-cadherin is a transmembrane glycoprotein that is found at adherens junctions on the plasma membrane of epithelial cells (Riethmacher et al., 1995). E-cadherin functions as an adhesive between cells through the binding of its extracellular domain with $Ca^{2+}$ and the extracellular E-cadherin extending from the surface of neighbouring cells (Takeichi, 1991). Meanwhile, the cytoplasmic domain of E-cadherin interacts with an additional group of proteins, the catenins, which mediate contact with the intracellular actin cytoskeleton to stabilise intercellular connections (Riethmacher et al., 1995). β-catenin and α-catenin, together with p120-catenin, form a cytoplasmic bridge between the transmembrane E-cadherin molecule and the actin cytoskeleton (**Figure 1.4**) (Baranwal and Alahari, 2009, Davis et al., 2003).

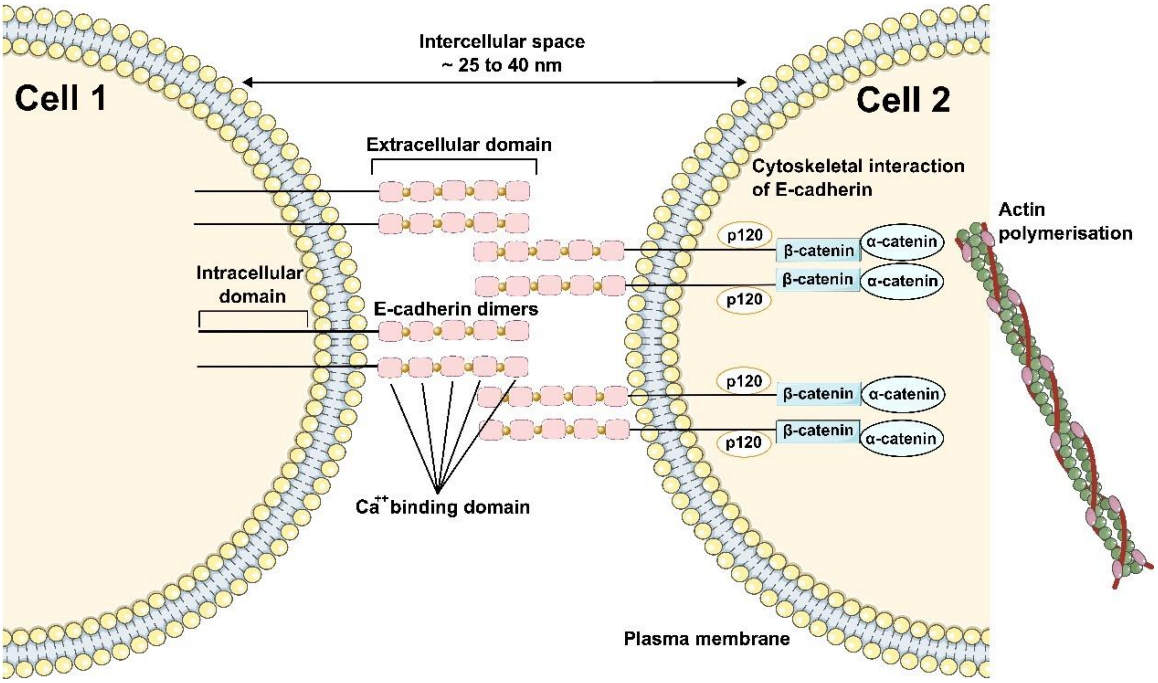


**Figure 1.4 The structure and location of E-cadherin on epithelial cells**

Schematic of the interaction of the extracellular domain of E-cadherin with that of neighbouring cells, and of its cytoplasmic domain with catenin proteins (adapted from Baranwal and Alahari, (2009)).

E-cadherin has been found to be essential during embryogenesis, with *CDH1* knock-out mouse embryos unable to develop beyond the blastocyst stage (Riethmacher et al., 1995). E-cadherin is expressed on the surface of oocytes and all early embryonic cells, and is an essential mediator of the cellular compaction required for an embryo to progress from loosely attached blastomeres to the morula stage (Larue et al., 1994). In adult epithelial tissues E-cadherin plays a vital role in tissue architecture homeostasis, repair following trauma, immune response, tumour invasion and metastasis (Berx et al., 1995).

### 1.5.2 E-cadherin in cancer

Epithelial cells are the site of origin for over 90% of human cancers, forming epithelial tumours known as carcinomas (Christofori and Semb, 1999, Nollet et

al., 1999). E-cadherin expression is tightly regulated in adult cells, and its downregulation or loss is a key feature of carcinoma progression, and is associated with a more invasive phenotype in a large number of cancer types, including BCa (Pokutta and Weis, 2007). Considering its function, it is intuitive that loss of E-cadherin and its resultant cell-to-cell adhesion can contribute to metastasis, enabling cells to break away from a primary tumour and travel to distant sites in the body where they can invade normal tissues (Christofori and Semb, 1999).

However, this loss of cell-to-cell adhesion is only one of a number of mechanisms that contribute to carcinogenesis. E-cadherin loss feeds into a key carcinogenic pathway, that of epithelial to mesenchymal cell transition (EMT) (Aparicio et al., 2012). In normal development, EMT (and its reverse process of mesenchymal to epithelial transition) is an essential part of tissue differentiation and development in embryogenesis, and tissue maintenance and repair in adults (Schöck and Perrimon, 2002). There are a number of differences in function and form between epithelial and mesenchymal cells (Kalluri and Weinberg, 2009). For example, epithelial cells are held in close association in distinct layers by specialised junctions, organised by their apical-basolateral and actin cytoskeleton polarity, with a basal lamina at their deep surface (Thiery et al., 2009). In contrast, mesenchymal cells have a spindle-shaped, fibroblast-like appearance, are not organised by polarity, are not associated with a basal lamina, only have focal contacts with neighbouring cells, and tend to be highly motile (Thiery et al., 2009). In addition, whilst all epithelial cells express E-cadherin, this expression is silenced in mesenchymal cells (Peinado et al., 2004).

EMT encompasses a series of events where epithelial cells take on the form and characteristics of mesenchymal cells, of which transcriptional suppression of E-cadherin is a key step (**Figure 1.5**) (Lamouille et al., 2014).

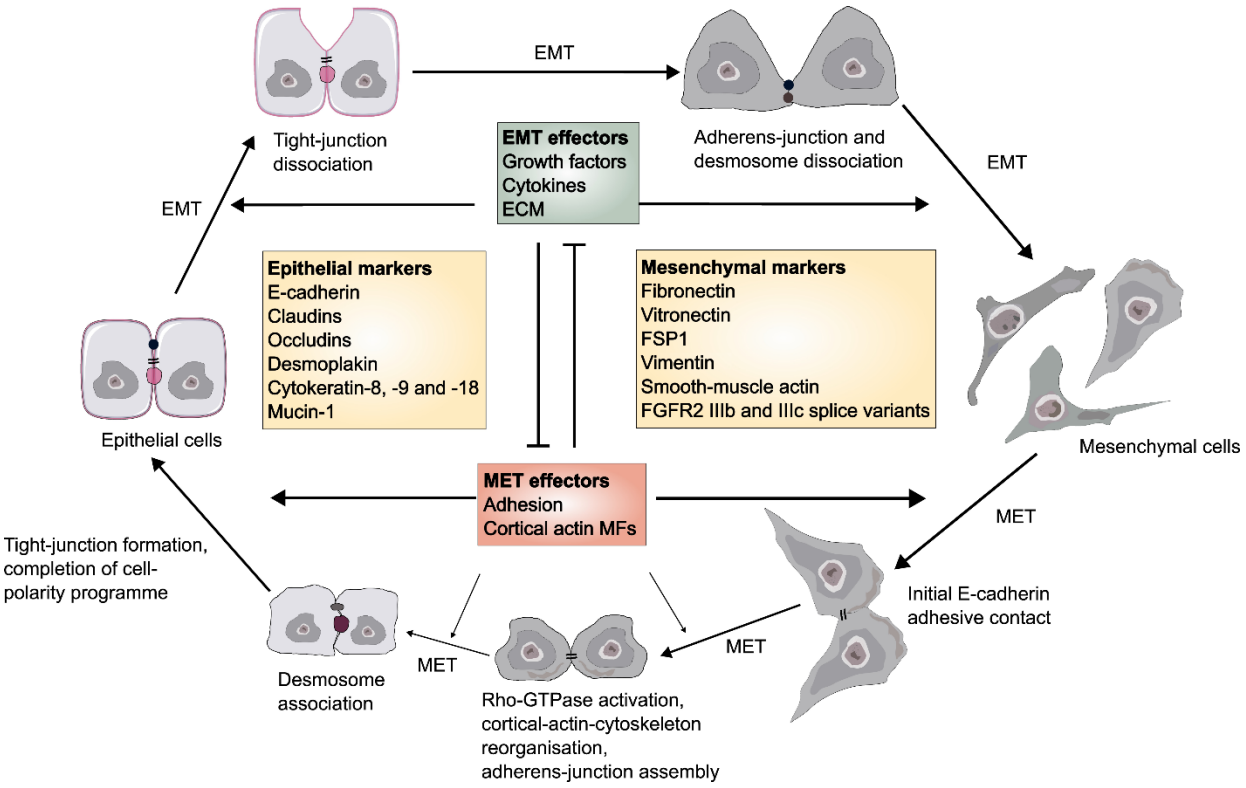


**Figure 1.5. The cycle of epithelial to mesenchymal cell transition and mesenchymal to epithelial transition**

Schematic of the steps in the cycle of the transition of epithelial cells to mesenchymal cells (EMT) and the reverse process of mesenchymal to epithelial transition (MET), with the effectors and markers of these processes. ECM= extracellular matrix, FSP1= fibroblast, specific protein-1, FGFR2= fibroblast growth factor receptor-2, MFs= microfilaments (adapted from Thiery et al., (2009)).

A number of mechanisms have been suggested to contribute to the downregulation of E-cadherin expression. These include genetic mutations, both within the *CDH1* gene, but also, more commonly, in *TP53* and *PI3K3CA* (Koboldt et al., 2012), two genes discussed in greater detail in later chapters. Other mechanisms of E-cadherin downregulation include modulation of transcription through promoter region hypermethylation, and post-transcriptional modification through the activation of factors promoting mesenchymal differentiation (**Figure 1.6**) (Berx et al., 1995, Lamouille et al., 2014, Paredes et al., 2012). EMT is driven by a number of transcription factors that activate mesenchymal marker genes and repress genes associated with the epithelial phenotype. The activity, localisation and stability of these transcription factors is regulated by post-translational modifications. For example SNAIL is activated via a number of mechanisms; following MAPK-mediated phosphorylation, TWIST is imported to the nucleus where it carries out its EMT-related functions; ZEB2 is sumoylated by PRC2 and exported from the nucleus, where its activity as a transcription factor is reduced (Lamouille et al., 2014)

Downregulation of E-cadherin expression on the cell surface can occur through it being ubiquitinated and subsequently degraded following binding by its specific ubiquitin E3 ligase CBLL1 (Aparicio et al., 2012). This is discussed further in section 1.8. More recent work has also found that downregulation of *CDH1* expression is associated with increased expression of E-cadherin transcription suppressors such as TWIST2, ZEB2, and NFKB1 (Alsaleem et al., 2019).

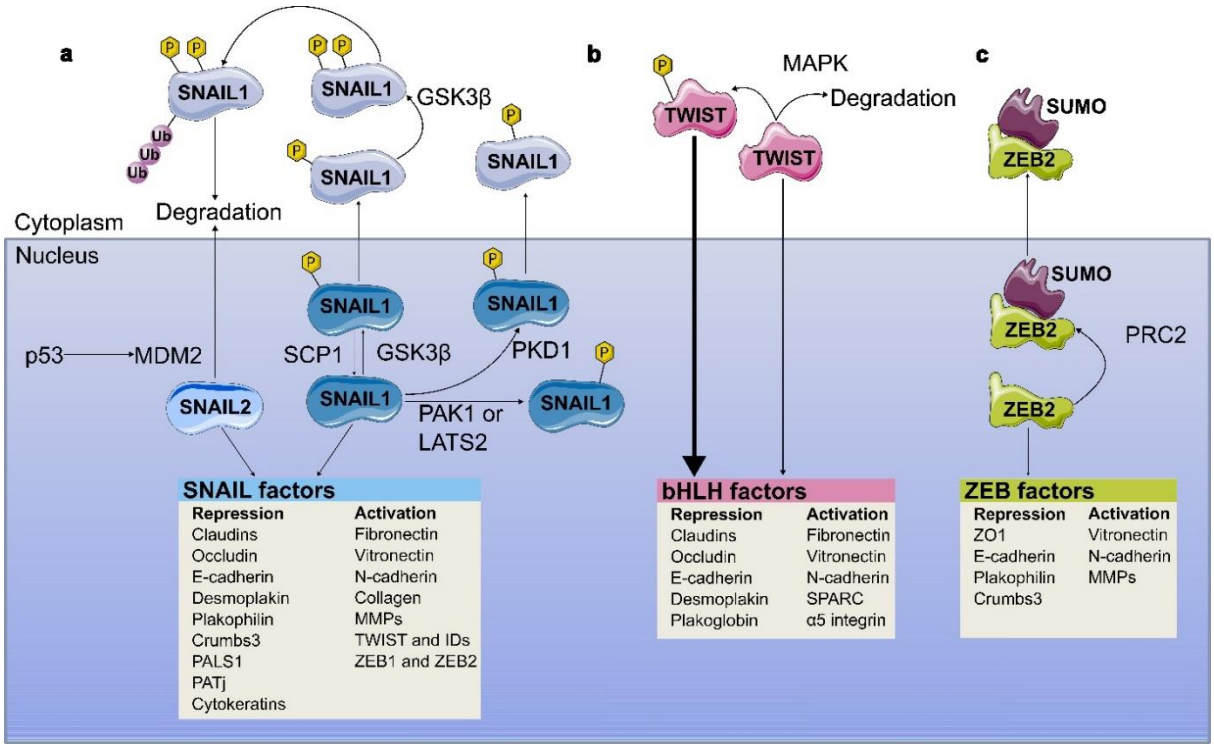


**Figure 1.6 Transcription factors that activate mesenchymal marker genes and repress epithelial marker genes during EMT**

Schematic of a number of transcription factors that activate mesenchymal marker genes and repress genes associated with the epithelial phenotype during EMT (adapted from Lamouille et al., (2014)).

Since *CDH1* gene knockout mice demonstrate that a lack of E-cadherin is incompatible with life during development, it is unsurprising that downregulated expression of E-cadherin in adult tissues results in serious pathology (Paredes et al., 2012). *CDH1* is considered to be a tumour- and invasion-suppressor gene, with loss of its expression or function observed in most carcinomas, together with an inverse relationship between level of E-cadherin expression and malignancy (Berx et al., 1995). Equally, it has been shown that restoring E-cadherin expression reduces invasiveness of cancer cells *in vitro*, and produces differentiated non-invasive tissue structures in *in vivo,* in contrast to

the invasive, poorly-differentiated phenotype of those tumours lacking E-cadherin (Vleminckx et al., 1991).

In particular, genetic mutations in *CDH1* have been linked to diffuse gastric carcinoma, where downregulation of E-cadherin occurs in the majority of cases (Becker et al., 1994). Moreover, in familial gastric carcinoma, germline mutations in *CDH1* have been shown to be causative in hereditary diffuse gastric cancer syndrome (Guilford et al., 1998). Likewise, somatic mutations resulting in downregulated E-cadherin expression have been associated with carcinomas of the ovary, endometrium and breast (Berx et al., 1996, Risinger et al., 1994) .

In BCa downregulated E-cadherin expression is a hallmark feature of invasive lobular carcinomas and is also associated with a number of other breast tumour types (Becker et al., 1994, Berx et al., 1996). The importance of E-cadherin in BCa is evidenced by the efficacy of the drug tamoxifen which, in addition to its anti-estrogen properties, also exerts a therapeutic effect through restoring the function of inactive cell surface E-cadherin in ER-positive BCa cells (Bracke et al., 1994). Furthermore, downregulation of E-cadherin and the process of EMT is thought to be one of the mechanisms for tamoxifen resistance in recurrent BCa (Ward et al., 2012). E-cadherin expression in BCa has been demonstrated to be a robust prognostic indicator and is now a key target for a precision medicine approach (Bajrami et al., 2018, Li et al., 2017d, Rakha et al., 2005).

The role of E-cadherin in prostate cancer (PCa) is more ambiguous. Some studies have demonstrated that E-cadherin expression is reduced in around half of all prostate tumours (Umbas et al., 1992, Umbas et al., 1994). However,

other studies have found E-cadherin to be normally expressed across all stages of PCa, even in the most advanced metastatic cases (Rubin et al., 2001), or indeed that low levels of E-cadherin may actually be associated with better outcomes (Barber et al., 2015). Interestingly, one study found that upregulated E-cadherin in PCa was associated with metastasis as it facilitated tumour cell adhesion to bone (Voss et al., 2020).

Other studies have suggested that rather than downregulation of E-cadherin expression, perhaps it is cadherin switching that is occurring (Tomita et al., 2000). It has been suggested that E-cadherin expression can switch to that of mesenchymal N-cadherin (nerve tissue cadherin) or cadherin-11, with significant differences in expression seen between E-cadherin-poor and N-cadherin-rich areas of tumour versus E-cadherin-rich, N-cadherin-poor normal tissue (Bussemakers et al., 2000). Other prognostic markers have been put forward for PCa, such as MiR-22 which is known to affect E-cadherin expression, however it is unclear if the changes in PCa progression are being driven by downregulation of E-cadherin or these other markers (Dhar et al., 2017). Further work is needed to understand the role of E-cadherin in PCa and whether it may have any utility as a potential biomarker or precision medicine target in PCa.

## 1.6 The epitranscriptome

The complex process of gene expression begins with accessing the sequence information encoded in DNA, subsequent transcription of the nucleotides in the genetic code into RNA, followed by translation of the mRNA into a protein (Schaefer et al., 2017). Translation and protein synthesis are tightly regulated by a number of mechanisms, including regulatory proteins and non-coding

RNAs, and post-transcriptional covalent modifications of the nucleotides in RNA molecules (Hoernes and Erlacher, 2017). There are over 150 post-transcriptional modifications of RNAs, serving to affect their stability and function, ultimately affecting gene expression (Boccaletto et al., 2017, Meyer et al., 2012). These modifications of messenger RNA (mRNA) are collectively known as the epitranscriptome (Fray and Simpson, 2015). Despite their initial discovery decades ago (Amos and Korn, 1958, Desrosiers et al., 1974), it is only in recent years that technological advances have made these RNA modifications accessible to molecular investigation, therefore enabling us to begin to understand their significance in gene regulation (Dominissini et al., 2012, Meyer et al., 2012).

## 1.7 *N*$^6$-methyladenosine (m$^6$A)

### 1.7.1 Biological function

The most common internal modification of messenger RNA (mRNA) in eukaryotes is the methylation of the N$^6$ position of adenosine on cellular mRNA, also known as *N*$^6$-methyladenosine (m$^6$A), (Desrosiers et al., 1974, Jia et al., 2011). m$^6$A is thought to be found at between three and five sites per mRNA molecule (Rottman et al., 1974, Wei et al., 1975). The m$^6$A mRNA modification is conserved across species, from viruses, yeast and plants through to animals, including humans (Bokar, 2005, Pan, 2013). m$^6$A has been shown to influence key areas of mRNA metabolism, such as translation and degradation (Zhao et al., 2016).

The effects of m$^6$A on RNA are controlled by its interacting methyltransferases (“writers”), binding proteins (“readers”), and demethylases (“erasers”) (Yang et al., 2018) (**Figure 1.7**). If the role of the “writers” and “erasers” is to regulate

the dynamic and reversible m$^6$A modification of mRNA, then it is the “readers” that detect these modifications and initiate their downstream effects (Sun et al., 2019). The YTH domain family of proteins are the best characterised, performing a number of distinct functions in both the nucleus and cytoplasm of cells (Du et al., 2016, Li et al., 2017a). Recently the HNRNP and IGF2BP families of proteins have been found to serve as m$^6$A readers, regulating the secondary structure and stability of mRNA respectively (Huang et al., 2018, Liu et al., 2017).

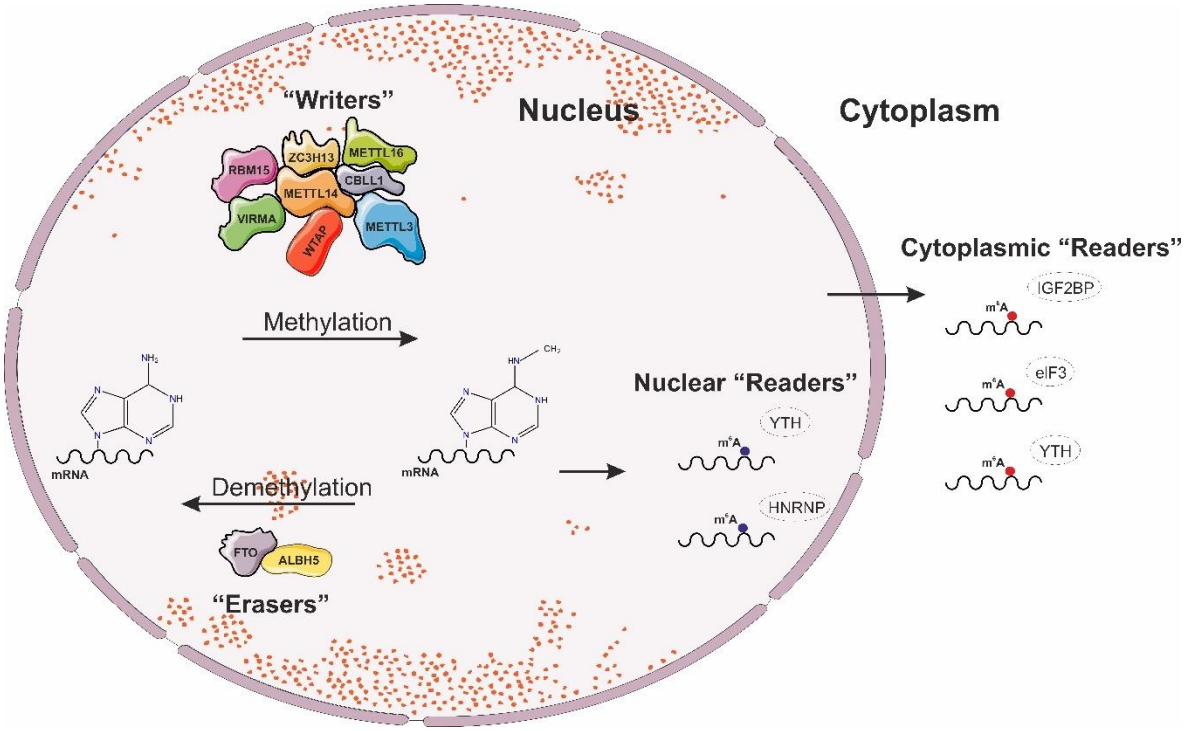


**Figure 1.7 The components of the m$^6$A methyltransferase complex, as well as m$^6$A binding proteins and demethylases involved in dynamic m$^6$A mRNA modification**

Schematic of the “writer” proteins that make up the m$^6$A methyltransferase complex, the “reader” binding proteins that operate both within the nucleus and cytoplasm of cells, and the m$^6$A demethlyase “eraser” proteins.

The addition of m$^6$A occurs co-transcriptionally in the nucleus (Horiuchi et al., 2013, Ping et al., 2014) and is mediated by the RNA m$^6$A methyltransferase complex, also known as the m$^6$A “writers” (Desrosiers et al., 1974, Jia et al., 2021). This complex includes the methyltransferase-like 3 (METTL3) catalytic subunit bound in a stable complex with methyltransferase-like 14 (METTL14) (Liu et al., 2014). Wilms tumour-1 associated protein (WTAP) binds to and stabilises the METTL3-METTL14 heterodimer (Ping et al., 2014, Selberg et al., 2019). *WTAP* was originally discovered in association with the Wilms tumour suppressor gene (*WT1*) (Little et al., 2000), where it was found to partner with WT1 and regulate cell proliferation and quiescence (Penalva et al., 2000, Small et al., 2007). WTAP is thought to recruit RNA that has been targeted for m$^6$A modification, facilitates binding by the METTL3-METTL14 complex, and is implicated in the regulation of splicing (Liu et al., 2014, Ping et al., 2014, Su et al., 2022). WTAP has been found to recruit a number of adaptor proteins to the complex to facilitate mRNA processing including VIRMA (KIAA1429), the RBM15 and RBM15B RNA binding proteins, and the ZC3H13 zinc finger protein (Liu et al., 2014, Patil et al., 2016, Schwartz et al., 2014, Wen et al., 2018). Further adaptor proteins are associated with this methyltransferase complex of proteins, including Cbl proto-oncogene like 1 (CBLL1), also known as HAKAI, which is believed to be required for full m$^6$A methylation activity, although its role is not yet fully understood (Horiuchi et al., 2013, Ruzicka et al., 2017, Sun et al., 2019, Wen et al., 2018, Yue et al., 2018). CBLL1 is a ubiquitin E3 ligase that regulates E-cadherin levels (Fujita et al., 2002) that was later found to be involved in m$^6$A regulation as part of the METTL3-METTL14-

WTAP complex (Horiuchi et al., 2013, Ruzicka et al., 2017). CBLL1 will be discussed in greater detail later in this chapter.

The discovery of the demethylase FTO in 2011 demonstrated that $m^6A$ was a reversible modification of RNA, and was likely therefore, to be involved in dynamic gene regulation and RNA processing (Jia et al., 2011). A second demethylase, or “eraser”, of $m^6A$ is ALKBH5, discovered in 2013 (Zheng et al., 2013). A number of other ALKB-homolog proteins are known of, and some of these are suspected to have demethylase activity, although to date only ALKBH3 in transfer RNA has been well described (Sun et al., 2019, Ueda et al., 2017).

It has been demonstrated that $m^6A$ modification of mRNA is essential for normal development and function across a wide range of species (Dai et al., 2018, Fray and Simpson, 2015, Geula et al., 2015, Haussmann et al., 2016, Zhang et al., 2022a), suggesting evolutionary conservation of mechanisms involving $m^6A$. The $m^6A$ modification has been shown to play a vital role in regulating a number of key physiological processes such as embryogenesis, circadian rhythms, response to DNA damage, and cell differentiation (Fustin et al., 2013, Geula et al., 2015, Lin et al., 2017, Wang et al., 2014, Xiang et al., 2017). Although the precise contribution of $m^6A$ to alternative splicing, exon selection and transcript stability has been debated (Darnell et al., 2018, Ke et al., 2015, Ke et al., 2017, Zhao et al., 2018), there is evidence to support a role for $m^6A$ in regulating context-dependent splicing *in vivo* (Haussmann et al., 2016, Lence et al., 2016).

### 1.7.2 m$^6$A in cancer

Dysregulation of the “writers”, “readers” and “erasers” of m$^6$A has been linked to a number of diseases, including cancer, and linked to therapy resistance through a variety of mechanisms (Cai et al., 2018, Jia et al., 2011, Li et al., 2020a, Wang et al., 2020c, Zhang et al., 2016a).

METTL3 has been reported to have both oncogenic and tumour suppressor roles in a number of cancer types. An oncogenic role for METTL3 has been suggested in several cancers, with high levels of METTL3 expression reported in acute myeloid leukaemia (AML), gastric cancer and hepatocellular carcinoma (Barbieri et al., 2017, Chen et al., 2018, Vu et al., 2017, Wei et al., 2022). In addition to its m$^6$A methyltransferase function, METTL3 has also been shown to promote the translation of oncogenes, such as epidermal growth factor receptor (*EGFR*) in lung cancer, via interaction with ribosomes and the translation initiation complex (Lin et al., 2016). In contrast, *METTL3* has demonstrated a tumour suppressive role in other cancer types such as renal cell carcinoma and colorectal cancer (Deng et al., 2019, Li et al., 2017b).

A number of recent studies have revealed that METTL3 is upregulated in PCa, and that this increased expression promotes migration and invasion of PCa cells, tumour growth, and is associated with higher tumour stage and poorer prognosis (Cai et al., 2019, Ma et al., 2020, Yuan et al., 2020). Indeed, our research group have recently reported consistent findings, that higher METTL3 expression is associated with PCa compared with non-malignant cell lines, and that METTL3 expression in patient PCa specimens was positively associated with PCa, disease progression and poorer patient outcomes (Haigh et al., 2022, Lothion-Roy et al., 2022). We also found that METTL3 was both

androgen-regulated and influenced AR expression, and that it regulated *FTO* expression, however no effect on *WTAP* expression was observed (Lothion-Roy et al., 2022), as has been previously reported (Sorci et al., 2018).

METTL3 expression has also been reported to be upregulated in BCa, with *METTL3* knockdown resulting in reduced cellular proliferation and tumour growth (Wang et al., 2020c).

Like METTL3, METTL14 has been shown to act both as a tumour suppressor and an oncogene in regulating the development of a number of different tumour types (Guan et al., 2022). It functions as a tumour suppressor gene in many types of cancer, including liver, kidney, bladder, endometrial and glioblastoma, gastric, colorectal and rectal cancer (Cai et al., 2021, Fan et al., 2022, Yang et al., 2020, Zhou et al., 2021a). Oncogenic functions for *METTL14* have been suggested in several cancer types, including pancreatic, breast and AML (Kong et al., 2020, Paris et al., 2019, Wang et al., 2020b, Weng et al., 2018, Yi et al., 2020). In PCa, higher METTL14 expression has been correlated with poor prognosis in PCa patients, with knockdown of *METTL14* attenuating tumour proliferation both *in vitro* and *in vivo* (Wang et al., 2022c). Furthermore, upregulation of *METTL14* has been demonstrated to enhance the invasion and metastatic potential of PCa cells (Liu et al., 2022a). Consistent with this, recently reported results from our research group included METTL14 expression being associated with PCa compared to non-malignant cell lines, although no significant correlation with clinicopathological parameters was observed in patient PCa specimens (Lothion-Roy et al., 2022).

An oncogenic function has been described for *WTAP*, though it has not yet been fully established whether this is through its association with WT1 or the METTL3-METTL14 $m^6A$ methyltransferase complex (Knuckles et al., 2018, Zhang et al., 2016b). *WTAP* expression is regulated by METTL3, with its oncogenic function in some cancer types found to be related to its $m^6A$ methyltransferase complex function (Sorci et al., 2018). Recent studies have reported an overexpression of *WTAP* in bladder cancer (Chen and Wang, 2018) and AML (Bansal et al., 2014). However conflicting findings have been reported in BCa, where *WTAP* expression has been reported to be both increased and decreased, as well as not significantly changed, across different stages and molecular subtypes (Christgen et al., 2007, Wu et al., 2019). The relevance of *WTAP* in PCa remains poorly understood. Two recent studies of distinct publicly available PCa patient genomic data sets reported no significant difference in *WTAP* expression between normal prostate and tumour tissue (Liu et al., 2022a, Wu et al., 2021). Ji and colleagues reported that *WTAP* expression was significantly higher in PCa (Ji et al., 2020) and that lower *WTAP* expression was associated with elevated Gleason score, suggesting complex roles for WTAP in tumour initiation and progression (Ji et al., 2020). Recently published results from our research group included higher WTAP expression being observed in PCa compared to non-malignant cell lines, although no significant correlation with clinicopathological parameters was observed in patient PCa specimens (Lothion-Roy et al., 2022).

Whilst CBLL1 is known to regulate E-cadherin, a protein with a key role in the development of cancer (Alsaleem et al., 2019), little is known about the role of CBLL1 in carcinogenesis. CBLL1 expression is markedly elevated in in gastric,

colon and non-small cell lung cancers (NSCLC), suggesting a pro-oncogenic role (Castosa et al., 2018, Figueroa et al., 2009b, Hui et al., 2019). However, the relative importance of the E-cadherin and m$^6$A methyltransferase complex functions of CBLL1 in cancer remains poorly understood.

#### 1.7.2.1 Therapeutic targeting of m$^6$A

Altered METTL3 expression and, by inference, altered m$^6$A expression, has been associated with therapy resistance in PCa (Cotter et al., 2021). Given the implication of METTL3 in the development and progression of numerous cancer types, there has been considerable interest in small molecule METTL3 inhibitors, which are currently being developed by several companies. The METTL3 inhibitor STM2457 has been demonstrated to reduce cancer cell growth in AML and to improve survival (Yankova et al., 2021). Such METTL3 inhibitors may also have utility in solid tumours (Sun et al., 2023, Wang et al., 2023, Zhang et al., 2022c), having been shown to inhibit cellular proliferation in PCa (Haigh et al., 2022).

A number of inhibitors of the m$^6$A demethylase FTO have also been developed or have subsequently been discovered to function as FTO inhibitors during the study of previously developed drugs (Aik et al., 2013, Huang et al., 2015, Peng et al., 2019, Su et al., 2020, Zhou et al., 2021b). Such repurposed therapeutics now being used in trials to treat AML include the Parkinson's disease drug entacapone, immunosuppressant drug brequinar, and the anti-neoplastic drug bisantrene (Peng et al., 2019, Su et al., 2020, Zhou et al., 2021b).

To date only one CBLL1-specific small molecule inhibitor, called Hakin-1, has been reported (Martinez-Iglesias et al., 2020), however it is interesting that no

follow-up studies or commercial development of this compound have subsequently been reported. Closer inspection of the initial study revealed a questionable clinical effect of the inhibitor, in that no inhibition of CBLL1 expression was observed, only a reduction in its E3 ligase ubiquitination capacity, and even then only when CBLL1 was ectopically overexpressed (Martinez-Iglesias et al., 2020).

These studies highlight the therapeutic potential of specifically targeting m$^6$A regulators in cancer, both as standalone and combination therapies.

## 1.8 CBLL1

### 1.8.1 Biological function

Discovered in 2002, Cbl proto-oncogene like 1 *(CBLL1)* was first given the name *HAKAI*, meaning 'destruction' in Japanese (Fujita et al., 2002). It was so-called due to its reported function as a ubiquitin E3 ligase, resulting in degradation of its target protein, E-cadherin (Fujita et al., 2002). In 2013 it was found to have an additional function, as a component of the m$^6$A methyltransferase complex, assisting in the application of the m$^6$A modification to mRNA (Horiuchi et al., 2013). New insights into the functionality of CBLL1 were revealed in 2013 with the discovery of CBLL1 in the novel WTAP complex of proteins that binds to the METTL3-METTL14 heterodimer and is responsible for supporting the writing of m$^6$A in mRNAs (Horiuchi et al., 2013). Alongside CBLL1 and WTAP, the complex was found to comprise Virilizer homolog (also known as VIRMA or KIAA1429), KIAA0853, RBM15, BCLAF1 and THRAP3, as well as a number of other splicing regulators (Horiuchi et al., 2013). Knockdown of CBLL1, as well as each of the other components individually, results in lower levels of m$^6$A (Yue et al., 2018), and ultimately cell cycle arrest

and significantly reduced cell proliferation (Horiuchi et al., 2013). Thus, normal CBLL1 expression is essential for normal function of the $m^6A$ methyltransferase complex.

Cbl (Casitas B-lineage lymphoma) proto-oncogene was first identified in the retrovirus Cas NS-1 and found to induce lymphomas of B-cell origin in mice (Langdon et al., 1989a, Langdon et al., 1989b). *c-Cbl*, one of the key cellular isoforms of *Cbl*, is ubiquitously expressed and is encoded on chromosome 11 in humans (Langdon et al., 1989b). Initially, many studies focussed on its expression in a range of haematopoietic cell lines, and it was found that mutations in this region of the genome in humans are associated with acute lymphocytic leukaemias (Yunis and Brunning, 1986). Later work found other roles for the multi-domain Cbl protein, including the discovery that Cbl possesses E3 ubiquitin-ligase activity for receptor tyrosine kinases such as active platelet-derived growth factor (PDGF) and epidermal growth factor (EGF) (Miyake et al., 1998, Waterman et al., 1999).

*CBLL1* is located on chromosome 7 and encodes a protein of 492 amino acids that comprise a RING (Really Interesting New Gene) finger domain, a phosphotyrosine recognition domain, and a proline-rich sequence (Fujita et al., 2002). It is these RING finger and phosphotyrosine domains, similar to those found in c-Cbl, that gave rise to the naming of CBLL1 as being Cbl-like, although there are also notable structural differences between the two proteins, including the much larger protein size and reverse order of the RING finger and phosphotyrosine binding domains in c-Cbl compared to CBLL1 (**Figure 1.8**).

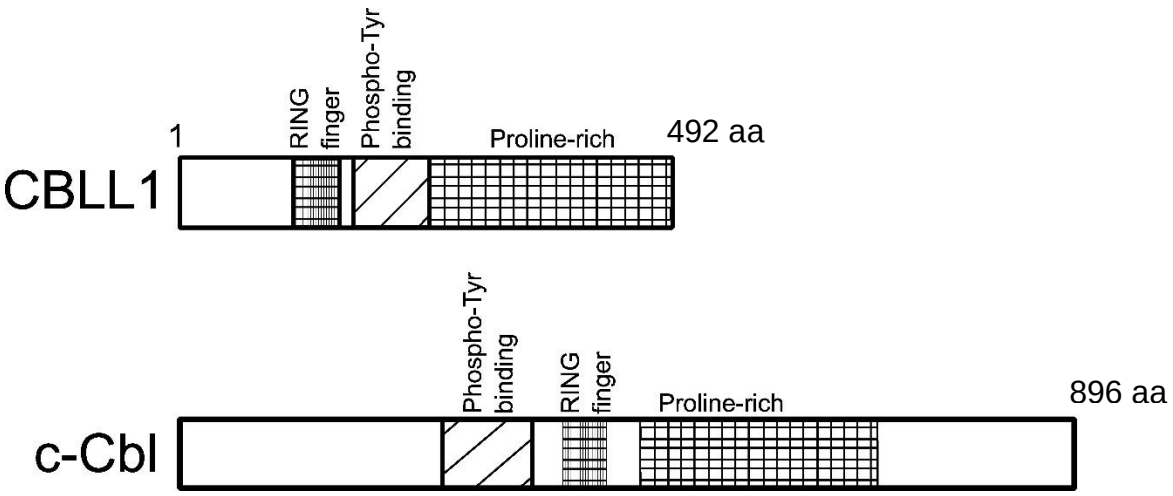


**Figure 1.8 Structure of the CBLL1 and c-Cbl proteins**

Schematic of the structure and domains of the CBLL1 and c-Cbl proteins (adapted from Fujita et al., (2002)). aa= amino acids.

The crystal structure of the CBLL1 protein's first two domains was published in 2012, which characterised a novel and specific phosphotyrosine binding site structure (the HYB domain), leading to the proposal of a new potential drug target (Mukherjee et al., 2012). Substrates known to interact with the HYB domain and be regulated by CBLL1 include Cortactin and DOK1 (Mukherjee et al., 2012, Mukherjee et al., 2014). Cortactin is a protein of the cytoskeleton that regulates actin assembly during cell movement and, when upregulated, is associated with cancer progression and poorer patient outcomes (Noh et al., 2013). DOK1 regulates assembly of signalling complexes (Mashima et al., 2009) and has a tumour suppressor function, with downregulation of expression resulting in a higher incidence of multiple cancer types (Siouda et al., 2012, Lee et al., 2004).

CBLL1 has been found to be vital in early embryonic development in *Drosophila melanogaster* (the common fruit fly), with *CBLL1* mutants displaying

a number of epithelial cell defects and becoming non-viable at the larval stage (Kaido et al., 2009). To date no *CBLL1* knockout mouse model has been published. The CBLL1 homolog has also been identified in the $m^6A$ writer complex in plants (termed HAKAI), although interestingly, HAKAI knockdown did not result in lethality when knockdown of the plant homologs of *METTL3* and *WTAP* proved embryo-lethal (Ruzicka et al., 2017). Indeed, whilst knockdown of HAKAI resulted in a 35% reduction of $m^6A$ writing, very little difference was observed phenotypically in *HAKAI* mutant plants compared to wild type (Ruzicka et al., 2017).

CBLL1 is expressed ubiquitously in normal human tissues, with protein expression highest in the brain and endocrine organs such as the thyroid and adrenal glands, uterus and placenta (Uhlen, 2015). Interestingly, CBLL1 is even found in tissues that do not express E-cadherin (Figueroa et al., 2009a, Kaido et al., 2009). The Human Protein Atlas details a medium level of CBLL1 expression in normal breast and prostate tissue, with CBLL1 expressed in 100% of breast and prostate tumour tissues (Uhlen, 2015).

The first key function attributed to CBLL1 was as a ubiquitin E3 ligase of E-cadherin (Fujita et al., 2002), as illustrated in **Figure 1.9**. Ubiquitination is a eukaryotic post-translational protein modification that occurs through the conjugation of ubiquitin (a small, regulatory protein) to other intracellular proteins (Pickart, 2001). Once tagged with ubiquitin, many proteins are then endocytosed and transported to proteasomes for degradation (Pece and Gutkind, 2002).

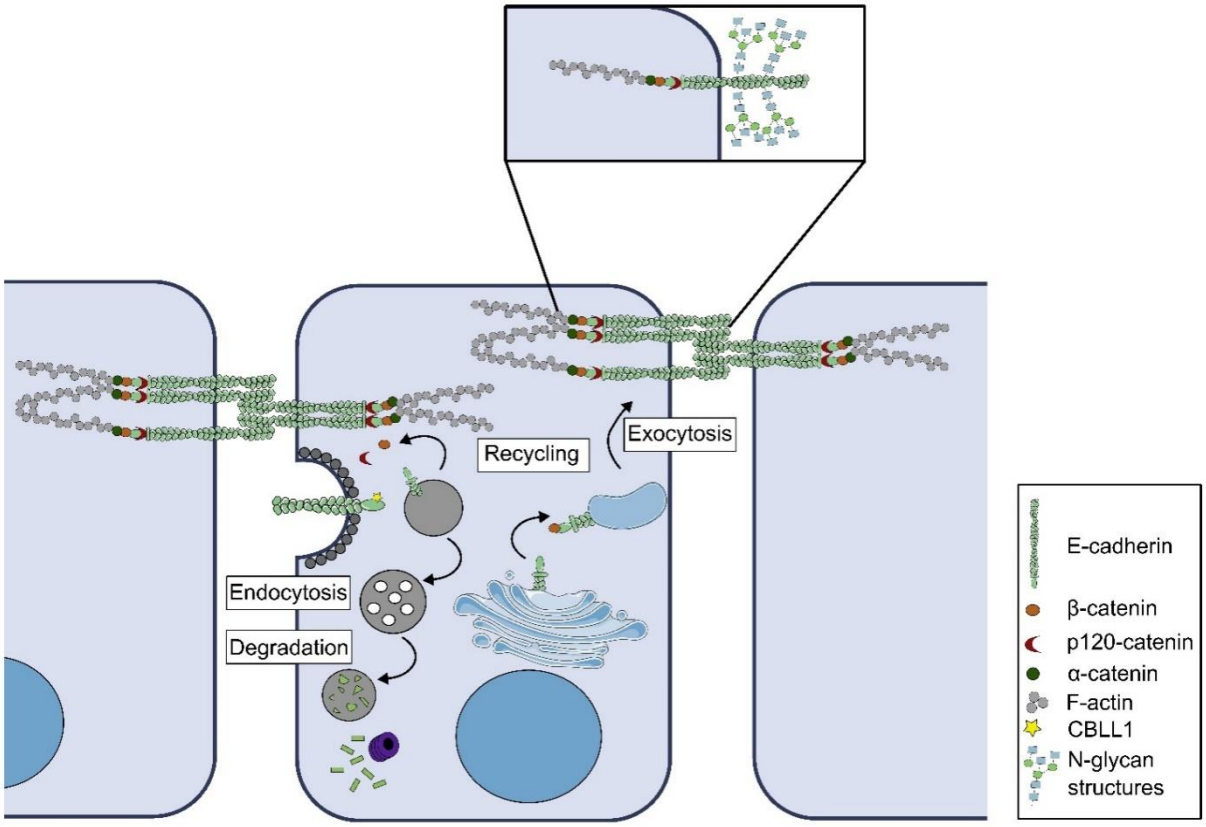


**Figure 1.9 Post-translational regulation of E-cadherin expression.**

Schematic of the processes that regulate post-translational expression of E-cadherin at the surface of epithelial cells, including ubiquitination by CBLL1 (adapted from Paredes et al., (2012)).

A series of three enzymes are required for protein ubiquitination: E1 activating enzymes prepare the ubiquitin for binding, E2 conjugating enzymes carry the activated ubiquitin, and E3 ligase enzymes bring the E2/ubiquitin complex to the target protein and catalyse the transfer of ubiquitin from the E2 enzyme to its target protein (Pickart, 2001). It is the E3 ligase enzymes that confer specificity to this process, and it has been suggested that E3 ligases could make excellent drug targets (Koepp, 2014).

CBLL1 was the first post-translational regulator of E-cadherin stability to be discovered, and was proposed to exert this effect by binding with the E-cadherin complex following its phosphorylation by the fibroblast growth factor receptor (Src), subsequently catalysing its ubiquitination and resultant endocytosis, leading to a reduction in the amount of E-cadherin at the cell surface, and reduced adhesion between cells (Fujita et al., 2002). More recent work has gone on to elucidate some of the additional players in this process, particularly during carcinogenesis. For example, Slit-Robo signalling has been found to play a role in recruiting CBLL1 to E-cadherin (Zhou et al., 2011a). Slit-Robo signalling stimulates angiogenesis and lymphangiogenesis via tumour cell secretion of Slit proteins that bind with Robo1 proteins expressed on endothelial cells lining blood and lymphatic vessels (Wang et al., 2003). Likewise, Tumour growth factor β (TGFβ) induces CBLL1 transcription, resulting in downregulated E-cadherin expression, EMT and cancer progression (Janda et al., 2006, Xu et al., 2009). In contrast, the tumour suppressor Rack1 has been found to downregulate CBLL1 by inhibiting Src signalling, therefore preventing CBLL1 from binding and ubiquitinating E-cadherin and thus promoting cell-cell adhesion (Aparicio et al., 2012, Swaminathan and Cartwright, 2012).

### 1.8.2 CBLL1 in cancer

Ubiquitination affects the function of intracellular proteins, including master regulatory proteins, and therefore regulates a wide range of vital cellular processes, including cell cycle progression and immune function (Koepp, 2014, Pickart, 2001, Rock and Goldberg, 1999). Therefore, unsurprisingly, dysregulation of protein ubiquitination has been associated with a number of

cancer types (Bignell et al., 2000, Loda et al., 1997, Scheffner et al., 1990), and hereditary diseases (Kishino et al., 1997, Shimura et al., 2000).

CBLL1 has been implicated to have a pro-oncogenic role, with its expression markedly upregulated in gastric and colon tumours compared with normal tissues, and CBLL1 expression increasing further with colon carcinoma of advancing stage (Castosa et al., 2018, Figueroa et al., 2009b). Moreover, higher CBLL1 expression has been reported in non-small cell lung cancer (NSCLC) cell lines compared with normal bronchial epithelial cells (Liu et al., 2018c), and in NSCLC tumour tissue compared with adjacent non-malignant tissue (Hui et al., 2019). It also been reported that *CBLL1* knockdown resulted in reduced growth, migration and invasion of NSCLC cells, whilst also significantly increasing chemosensitivity to cisplatin, most likely through its effect on E-cadherin expression (Liu et al., 2018c). Similarly, overexpression of *CBLL1* resulted in increased tumour cell growth in hepatocellular carcinoma, whereas *CBLL1* depletion produced significantly reduced growth (Liu et al., 2018b). Likewise, MDCK cells over-expressing CBLL1 formed epithelial tumours in all inoculated nude mice, whereas inoculated parental MDCK cells did not form tumours (Castosa et al., 2018).

It has been suggested that CBLL1 has a number of E-cadherin- and $m^6A$-independent roles in normal cellular processes and tumourigenesis (Figueroa et al., 2009b, Rodriguez-Rigueiro et al., 2011). In addition to endocytosis of E-cadherin and the resulting destruction of adherens junctions, it has also been demonstrated that cell-to-cell adhesion is decreased in cells over-expressing CBLL1 through downregulation of Paxillin, a key protein component of cell-matrix adhesion (Rodriguez-Rigueiro et al., 2011). Other work has found that

CBLL1 also upregulates proliferation in fibroblasts and epithelial cells (Figueroa et al., 2009b), and can regulate proteins responsible for actin-cytoskeleton dynamics, affecting cell plasticity and motility (Diaz-Diaz et al., 2017). It should be noted however, that despite growing in vitro evidence, it remains unclear if CBLL1 regulates EMT in vivo (Cooper et al., 2015).

Many studies have reported a role for the $m^6A$ RNA modification in alternative splicing (Alarcón et al., 2015, Dominissini et al., 2012, Haigh et al., 2022, Haussmann et al., 2016, Horiuchi et al., 2013, Lence et al., 2016, Lothion-Roy et al., 2022, Ping et al., 2014, Su et al., 2022, Yang et al., 2018, Zhao et al., 2014), however, little is known about the role of CBLL1 in alternative splicing. It has been reported that CBLL1 interacts with polypyrimidine tract-binding protein (PTB)-associated splicing factor (PSF) in the nucleus and is crucial to the ability of PSF to bind RNA (Figueroa et al., 2009a, Figueroa et al., 2009b). PSF regulates a number of cellular process, including transcription, pre-MRNA splicing and retention of edited RNA in the nucleus (Patton et al., 1993, Shav-Tal and Zipori, 2002), and has been associated with tumourigenesis in both colon and prostate cancer (Takayama et al., 2017, Tsukahara et al., 2013). More recently, PSF has been implicated in BCa, and associated with a poorer prognosis in patients with ER-positive BCa (Mitobe et al., 2020).

Very few studies have reported on CBLL1 expression in PCa. There is some evidence that *CBLL1* expression may be androgen-regulated in prostate cancer cell lines (Jin et al., 2013). Whilst it has been found that CBLL1 cannot repress transcriptional activity of the androgen receptor (AR), interestingly, it has been suggested that it may act as a co-repressor of the estrogen receptor (ERα) in breast cancer (Gong et al., 2010). In one study it was found that

CBLL1 competitively binds the ERα and interferes with recruitment of coactivators (Gong et al., 2010). One prior study focussed on E-cadherin expression described a decrease in CBLL1 expression in response to silibinin treatment in the PCa cell lines PC3, PC3MM2 and LNCaP:C4-2B (Deep et al., 2011). Another recent study reported *CBLL1* mRNA expression only in a publicly available PCa patient database without independent protein validation in other cohorts (Su et al., 2021). Interestingly, in contrast to the many studies in other cancer types who universally reported pro-oncogenic roles for CBLL1 (Castosa et al., 2018, Figueroa et al., 2009b, Hui et al., 2019, Liu et al., 2018b, Liu et al., 2018c), Su and colleagues (2021) found CBLL1 to be a crucial $m^6A$ regulator in PCa, reporting that lower *CBLL1* expression was associated with PCa development and progression.

The role of CBLL1 in BCa is also not yet clear. Consistent with reports of higher CBLL1 expression being associated with a pro-oncogenic features in other cancer types (Castosa et al., 2018, Liu et al., 2018b, Liu et al., 2018c), it has been reported that CBLL1 expression is positively associated with oncogenic features in BCa cells, including increased invasive potential and metastasis (Liu et al., 2022b, Ma et al., 2023). However, another study, specifically in ER-positive BCa cells, found that CBLL1 inhibited cellular proliferation and migration (Gong et al., 2010). Gong and colleagues (2010) also reported a direct interaction between CBLL1 and the ERα, and moreover reported reduced CBLL1 expression in response to estrogen treatment (Gong et al., 2010).

In the two studies that have examined CBLL1 expression in BCa patient samples, one failed to find any significant associations with E-cadherin

expression, malignancy or prognostic factors in their small patient cohort (n=30) (Makdissi et al., 2009). The other study had a slightly larger patient cohort (n=134) and reported conflicting findings, of lower CBLL1 expression in normal breast tissue compared with BCa, yet found higher expression to be associated with better relapse-free and overall survival in BCa patients (Zheng et al., 2021).

Further work, including in a larger cohort of patient specimens, is now indicated to further understand the role of CBLL1 in PCa and BCa, and some of the mechanisms underpinning this.

## 1.9 Aims of study

The involvement of $m^6A$ “writer” proteins in the development and progression of numerous cancer types has been well-documented. The relatively recent discovery that CBLL1 was also a component of the $m^6A$ methyltransferase protein complex, together with evidence for its oncogenic role through its interaction with E-cadherin and negative effect on cell-cell adhesion, warrants further investigation into the role of CBLL1 in cancer. This study aimed to further the understanding of the expression, function and clinical relevance of CBLL1 in PCa and BCa specimens and cell lines and to test the hypothesis that dysregulated CBLL1 promotes aggressive cancer development and progression. To this end, experiments were carried out that examined the expression and clinical relevance of CBLL1 in both PCa and BCa patient specimens, the expression and mechanistic role of CBLL1 in both BCa and PCa cell lines, the role of CBLL1 in AR signalling, alternative splicing and treatment resistance in PCa, and the role of CBLL1 in ER signalling and alternative splicing in BCa. This thesis therefore reports the role and clinical relevance of CBLL1 in PCa and BCa and the function of CBLL1 in hormone signalling, alternative splicing and therapy resistance in PCa and BCa.

# Chapter 2

Materials and methods

# 2 Materials and methods

## 2.1 Bioinformatic analysis of publicly available data

A number of bioinformatic tools were used to study *CBLL1* and *CDH1* expression in cancer. The cBioPortal for Cancer Genomics was consulted to examine genetic mutations, copy number alterations and mRNA expression in *CBLL1* in PCa patients (Cerami et al., 2012, Gao et al., 2013). PCa patient data was sourced from the primary adenocarcinoma TCGA Firehose Legacy cohort (Liu et al., 2018a), the metastatic adenocarcinoma SU2C/PCF Dream Team cohort (Abida et al., 2019), and the Neuroendocrine Prostate Cancer Multi-Institute study (Beltran et al., 2016).

The UCSC Xena browser (Goldman et al., 2020) was used to further investigate *CBLL1* expression in the primary adenocarcinoma TCGA Firehose Legacy patient cohort (Liu et al., 2018a) in association with clinicopathological parameters including malignancy, response to primary therapy, and biochemical recurrence.

In BCa patients the expression of *CBLL1* and *CDH1* was analysed in publicly available datasets using the cBioPortal for Cancer Genomics (Cerami et al., 2012, Gao et al., 2013). BCa patient data was sourced from the TCGA Firehose Legacy breast invasive carcinoma study (Liu et al., 2018a) and the Molecular Taxonomy of Breast Cancer International Consortium (METABRIC) (Curtis et al., 2012, Pereira et al., 2016).

The UCSC Xena Functional Genomics Browser (Goldman et al., 2020) was used to analyse alterations in *CBLL1* and *CDH1* expression in primary and

metastatic breast carcinoma compared with non-malignant tissue, using the GDC TCGA Breast Cancer patient cohort (Liu et al., 2018a).

The Kaplan-Meier Plotter online tool (Győrffy, 2021) and the Genome to Outcome web server (Pongor et al., 2015) were used to further investigate the prognostic value of *CBLL1* and *CDH1* in BCa with respect to overall survival (OS), relapse-free survival (RFS), and distant metastasis-free survival (DMFS).

The Integrative Genomics Viewer (Robinson et al., 2011) was used to analyse gene regulation datasets from both PCa and BCa from the NCBI Gene Expression Omnibus (GEO) database (Barrett et al., 2013). Androgen-regulated activation of *CBLL1* in PCa had been assessed genome-wide by self-transcribing active regulatory region sequencing (STARR-Seq) and then downloaded from the NCBI GEO database (Barrett et al., 2013), under accession number GSE154633 (Huang et al., 2021). Similarly, chromatin modifications in *CBLL1* in BCa had been assessed genome-wide by ChIP-Seq and then downloaded from the NCBI GEO database (Barrett et al., 2013), under accession number GSM1003709 (Jansen et al., 2013, Nevedomskaya et al., 2014).

## 2.2 Cell culture

### 2.2.1 Cell lines

Six human prostatic epithelial cell lines were used in this study, comprising one non-malignant cell line (PNT1A) and five prostate carcinoma cell lines (LNCaP, LNCaP:C4-2, 22Rv1, PC3, and DU145) representing progressive stages of PCa. The non-malignant PNT1A cells were kindly provided by Dr Jenny Persson (Lund University, Sweden). The malignant cell lines LNCaP (ATCC CRL-1740$^{TM}$) and PC3 (ATCC CRL-1435$^{TM}$) were purchased from the

American Type Culture Collection (Manassas, VA, USA). The LNCaP:C4-2 cells (Thalmann et al., 1994) were generously gifted by Dr Doug Scherr, and the DU145 and 22Rv1 cell lines were generously gifted by Professor Lorraine Gudas, both of Weill Cornell Medicine (NY USA). **Table 2.1** summarises the key characteristics of the prostatic cell lines used.

PNT1A cells are immortalised luminal epithelial cells that were used as a non-malignant model, and which rapidly lose AR expression in culture. LNCaP cells represent a primary prostatic adenocarcinoma which is androgen-dependent and androgen-sensitive. LNCaP:C4-2 cells were derived from the LNCaP cell lines and represent castrate-resistant metastatic PCa. Whilst they will still respond to androgen, they are not dependent upon it. Similarly, 22Rv1 cells are sensitive to androgen but can grow independently of it and are therefore also castrate-resistant. LNCaP, LNCaP:C4-2 and 22Rv1 express the androgen receptor (AR), with 22Rv1 also expressing AR variant splice forms including ARv7, hence their ability to respond to androgen. However, PC3 and DU145 do not express AR and are not, therefore, responsive to androgen.

| Cell line | Representative disease state | AR expression | Androgen responsive | References |
|---|---|---|---|---|
| PNT1A | Non-malignant | No | No | (Cussenot et al., 1991) |
| LNCaP | Localised PCa | Yes | Yes | (Horoszewicz et al., 1983) |
| LNCaP: C4-2 | Hormone refractory, recurrent PCa | Yes | Yes | (Thalmann et al., 1994) |
| 22Rv1 | Hormone refractory, recurrent PCa | Yes<br>plus ARvs | Yes | (Marcias et al., 2010, Sramkoski et al., 1999) |
| PC3 | Hormone refractory, recurrent PCa | No | No | (Kaighn et al., 1979) |
| DU145 | Hormone refractory, recurrent PCa | No | No | (Stone et al., 1978) |

**Table 2.1 Key characteristics of the prostate cell lines used in this study**

Six human breast epithelial cell lines were used in this study, comprising a primary normal human mammary epithelial cell line (HMEC), a non-malignant immortalised cell line (MCF10A) and four breast carcinoma cell lines (MCF7, T-47D, MDA-MB-453, and MDA-MB-231) representing progressive stages of BCa. HMEC cells were purchased from Lonza Group (Switzerland), and all other cell lines were generously gifted by Professor Lorraine Gudas (Weill

Cornell Medical College, USA) and Dr Cinzia Allegrucci (University of Nottingham, UK).

**Table 2.2** summarises the key characteristics of the breast cell lines used.

HMEC are cells taken from normal human breast epithelium and MCF10A are immortalised cells from fibrocystic breast tissue. Both cell lines represent non-malignant models but rapidly lose their ER expression in culture and thus do not respond to estrogen treatment. MCF7 and T-47D cells represent luminal BCa and are ER and PR positive, and therefore respond to estrogen, but are HER2 negative. The MDA-MB-453 and MDA-MB-231 cell lines represent metastatic BCa and are triple negative, although MDA-MB-453 may express HER2 at a low level. Neither MDA-MB-453 nor MDA-MB-231 respond to estrogen. The MDA-MB-231 cell line is a model for highly aggressive BCa. All cells except MDA-MB-453 and MDA-MB-231 express E-cadherin.

| Cell line | Representative disease state | ER expression | Estrogen-responsive | References |
|---|---|---|---|---|
| HMEC | Normal | No | No | (Ades et al., 1992) |
| MCF10A | Non-malignant | No | No | (Soule et al., 1990) |
| MCF7 | Luminal carcinoma | Yes | Yes | (Soule et al., 1973) |
| T-47D | Luminal carcinoma | Yes | Yes | (Keydar et al., 1979) |
| MDA-MB-453 | Triple negative carcinoma (low HER2 expression) | No | No | (Cailleau et al., 1978) |
| MDA-MB-231 | Triple negative, highly aggressive BCa with *BRCA1* mutation | No | No | (Cailleau et al., 1974, Elstrodt et al., 2006) |

**Table 2.2 Key characteristics of the breast cell lines used in this study**

### 2.2.2 Cell culture conditions

The BCa cell lines MCF7, T-47D, MDA-MB-453 and MDA-MB-231 cells were maintained in 'RPMI complete medium' comprising phenol red-containing RPMI-1640 medium plus 2mM L-glutamine, 1% penicillin-streptomycin-glutamine, and 1mM sodium pyruvate (all Gibco® by Life Technologies, USA), supplemented with 10% foetal bovine serum (FBS) (Sigma-Aldrich®, USA).

Cell culture of the HMEC and MCF10A cell lines was carried out by a colleague (Dr Corinne Woodcock; CW). They were maintained in HuMEC Basal Serum-Free Medium with addition of the HuMEC Supplement Kit (Gibco® by Life Technologies, USA). Cholera toxin was added to the MCF10A cell lines at a concentration of 100ng/ml (Sigma-Aldrich®, USA). All cell lines were incubated at 37°C in 5% $CO_2$.

Enzalutamide-resistant LNCaP:C4-$2_{enzR}$ and the parental LNCaP:C4-$2_{LT}$ (long-term) cell lines were isolated following long-term culture (~6 months) by a colleague (CW). The LNCaP:C4-$2_{enzR}$ line was maintained in the presence of 20μM enzalutamide (MedChemExpress®, USA).

Basal expression experiments were carried out in collaboration with colleagues (Dr Daisy Haigh; DH, Dr Veronika Metzler; VM, and CW). All cell lines were grown in their respective medium and plated in 6 well plates. Cells were then incubated for 72 hours before being harvested for RNA or protein extraction.

### 2.2.3 Hormone treatment of cells

MCF7 and T-47D BCa cells, and LNCaP, LNCaP:C4-2, 22Rv1 and LNCaP:C4-$2_{enzR}$ prostate cell lines were cultured in 6 well plates (Greiner Bio-one) with 2ml complete medium per well until ~30-40% confluency was reached. The RPMI complete medium was then removed and 2ml of phenol red-free RPMI-1640 (Gibco® by Life Technologies, USA), supplemented with charcoal-stripped FBS, was added. Charcoal-stripped serum was prepared using 1% activated charcoal in heat-inactivated FBS and Dextran T-70 to a final concentration of 0.1% (all Sigma-Aldrich®, USA). This was agitated at room temperature for one hour, then centrifuged at 12,000 x g for 15 minutes.

Vacuum filtration of the supernatant was then carried out through 110mm Whatman paper then through a 0.2µm filter.

In the prostate cell lines, each well was then treated with either 1nM R1881 synthetic androgen (Sigma-Aldrich®, USA) dissolved in 100% ethanol, or 0.1% ethanol as vehicle control. A non-metabolisable androgen (R1881) was selected in preference to a physiological androgen such as testosterone to prevent off-target effects due to aromatisation to estrogen. Treatment of the breast cell lines was carried out by colleagues (CW and Prof. Nigel P. Mongan; NPM) and following the change of medium to 2ml of charcoal-depleted serum phenol red-free RPMI-1640, either 10nM physiological estrogen (β-oestradiol) dissolved in dimethyl sulfoxide (DMSO), or 0.1% DMSO as vehicle control was added. All cell lines were then incubated for 72 hours before being harvested for RNA or protein extraction.

### 2.2.4 siRNA-mediated functional depletion of *CBLL1*

The small interfering RNA (siRNA) technique was used to functionally deplete *CBLL1*. SMARTpool ON-TARGETplus siRNA targeting human *CBLL1* (L-007069-00-0005; GE Dharmacon™, USA) was used to knock down *CBLL1*, whilst ON-TARGETplus non-targeting scrambled control siRNA (D-001810-10-05; GE Dharmacon, USA) was used as a negative control in the BCa cell lines MCF7 and T-47D, and PCa cell lines LNCaP:C4-$2_{LT}$ and LNCaP:C4-$2_{enzR}$.

Transfection of the cell lines was carried out as per the manufacturer's protocol using DharmaFECT 1 Transfection Reagent (GE Dharmacon™, USA) for the BCa cell lines and DharmaFECT 2 Transfection Reagent (GE Dharmacon™, USA) for the PCa cell lines. Briefly, BCa and PCa cell lines were plated in a 6

well plate in 2ml RPMI complete medium 24 hours prior to transfection in order to achieve ~30-40% confluency on the day of transfection.

The day following plating, the RPMI complete medium was withdrawn and replaced with 2ml of charcoal-stripped FBS supplemented phenol red-free RPMI-1640. In preparation for transfection, a mixture of the appropriate DharmaFECT Transfection Reagent (GE Dharmacon™, USA) and either the SMARTpool ON-TARGETplus siRNA targeting human *CBLL1* or ON-TARGETplus non-targeting scrambled control siRNA was created. Briefly, four tubes were prepared, two containing 2.08µl DharmaFECT Transfection reagent mixed gently with 83.34µl of phenol red-free RPMI-1640 medium (not containing charcoal-stripped FBS) per well, and two containing 2.08µl *siScr* or *siCBLL1* mixed gently with 83.34µl of phenol red free RPMI-1640 medium (not containing charcoal stripped serum) per well. The tubes were incubated at room temperature for five minutes, and then each pair of tubes containing DharmaFECT Transfection reagent and the siRNA were carefully combined and incubated for a further 15 minutes at room temperature. Each siRNA/DharmaFECT combination (170µl) was pipetted dropwise in each well. Each plate was gently mixed then incubated for 48 hours at 37°C in 5% $CO_2$ before a second transfection was carried out.

The siRNA-containing media was drawn off each well and the above steps were repeated. Following the addition of fresh medium and 170µl of each siRNA/DharmaFECT combination, 2.17µl of either 10nM β-oestradiol dissolved in DMSO, or 0.1% DMSO as vehicle control was added to the BCa cell line wells. In the PCa cell lines, 2.17µl of either 1nM R1881 (Sigma-Aldrich®, USA) dissolved in 100% ethanol, or 0.1% ethanol as vehicle control

was added to each well. Each plate was gently mixed then incubated for a further 72 hours at 37°C in 5% $CO_2$. siRNA treatment was conducted for 120 hours in total before harvesting for RNA or protein.

## 2.3 RNA analysis

### 2.3.1 RNA isolation using TRI Reagent

Isolation of RNA using TRI Reagent (Sigma-Aldrich®, USA) was carried out in all PCa cell lines by colleagues (Veronika Metzler; VM, and Daisy Haigh; DH) using phenol-chloroform extraction as per the manufacturer's protocol. Briefly, following cell lysis with 750µl TRI Reagent per well and transfer of the lysate to a new 1.5ml microcentrifuge tube, 200µl chloroform was added to each sample, vortexed, then incubated at room temperature for two-three minutes. Samples were subsequently centrifuged at 12,000 x g at 4°C for 15 minutes. The colourless upper aqueous phase was transferred to a new tube and one volume of 100% isopropanol was added to precipitate the RNA. Following incubation for 10 minutes at room temperature each sample was centrifuged at 13,000 x g at 4°C for 10 minutes. Following removal of the supernatant, the RNA pellet was washed with 500µl 70% ethanol. The samples were then vortexed and centrifuged at 9,000 x g at 4°C for five minutes. The supernatant was subsequently removed, and the RNA pellet resuspended in 20-30µl RNase free water. The Nanodrop™ 8000 spectrophotometer (Thermo Fisher Scientific™, USA) was then used to assess the RNA concentration and purity, before storing at -80°.

### 2.3.2 RNA isolation using GenElute™ Mammalian Total RNA Miniprep Kit

In all BCa cell lines, RNA was extracted using the GenElute™ Mammalian Total RNA Miniprep Kit (Sigma-Aldrich®, USA) as per the manufacturer's protocol. RNA isolation in basal MCF7 cells was carried out by a colleague (CW). Briefly, cells were lysed in the well of their 6 well plate using 250µl of Lysis Solution/2-ME and the lysis solution subsequently transferred to a sterile 1.5ml microcentrifuge tube. 250µl of 70% ethanol was added to each sample and then vortexed. Each sample was then loaded on to a GenElute binding column within a 2ml collection tube and centrifuged at 13,000 x g at room temperature for 15 seconds. The binding column and collection tube were retained, with the flow through discarded. In order to wash the RNA retained within the column, 250µl of Wash Solution 1 was pipetted on to the column and centrifuged again at 13,000 x g at room temperature for 15 seconds. Again, the flow through was discarded. DNA digestion was performed by pipetting a mix of 10µl DNase I (Sigma-Aldrich®, USA) and 70µl DNase Digest Buffer (Sigma-Aldrich®, USA) on to the membrane within the binding column, followed by a 15 minute incubation at room temperature. Following this an additional 250µl of Wash Solution 1 was pipetted on to the column and centrifuged again at 13,000 x g at room temperature for 15 seconds. Again, the flow through was discarded. The column was transferred to a fresh collection tube, where 500µl of Wash Solution 2 was pipetted on to the column and centrifuged again at 13,000 x g at room temperature for 15 seconds. The flow through was discarded and another 500µl of Wash Solution 2 was added to the column with centrifugation repeated at 13,000 x g, this time for two minutes. Following discarding of the flow through, the column was replaced in the collection tube

and centrifuged for a further one minute at 13,000 x g at room temperature for removal of any residual wash solution. For elution of the RNA, the column was transferred to a fresh microcentrifuge tube and 30µl of Elution Solution was pipetted on to the filter of the column and left to incubate for two minutes at room temperature before centrifuging at 13,000 x g at room temperature for one minute. The Nanodrop™ 8000 spectrophotometer was then used to assess the RNA concentration and purity, before storing at -80°.

### 2.3.3 Reverse transcription cDNA synthesis

Complementary DNA (cDNA) synthesis was carried out using 0.5-1µg of total RNA, reverse transcribed with the qScript™ cDNA Synthesis Kit (Quanta Biosciences™, USA) as per the manufacturer's protocol. 1.5µl qScript buffer and 0.5µl reverse transcriptase were added to 0.5 or 1µg of RNA template, made up to a total volume of 10µl with RNase free water. The solution was then incubated in a water bath (Grant SUB Aqua Pro, Grant Instruments) at 42°C for 60 minutes. The cDNA was diluted using deionised double distilled water ($ddH_2O$) to a final concentration of 10ng/µl and then stored at -20 °C.

### 2.3.4 Quantitative real-time polymerase chain reaction analysis

Analysis of mRNA expression was carried out using quantitative real time polymerase chain reaction (qRT-PCR). A master mix of 0.65µl TaqMan™ Real-Time PCR probe (Thermo Fisher Scientific™, USA), 7.5µl TaqMan™ Fast Advanced Master Mix (Thermo Fisher Scientific™, USA) and 5.85µl RT-PCR grade water (Roche Diagnostics, Switzerland), was combined with 1µl of cDNA. The following TaqMan™ probes were used: *CBLL1* (Hs00227265_m1), *CDH1* (E-cadherin) (Hs01023895_m1), *TFF1* (PS2) (Hs00907239_m1), *ESR1* (ERα) (Hs01046816_m1), *KLK3* (PSA) (Hs02576345_m1), *AR*

(Hs00171172_m1), and *β-actin* (Hs01060665_g1) (all Thermo Fisher Scientific™, USA).

All qRT-PCR reactions in the basal prostate cell lines were carried out on a LightCycler 480 II instrument (Roche Diagnostics, Switzerland). The qRT-PCR programme comprised heating to 95°C for 10 minutes followed by 45 cycles of denaturation at 95°C for 10 seconds, annealing at 60°C for 30 seconds, then amplification at 72°C for 1 second. The programme concluded with a 30 second cooling phase at 40°C. All qRT-PCR reactions in all other cell lines were carried out on a CFX Connect Real-Time PCR Detection System (Bio-Rad Laboratories, USA) using the same programme as described above. mRNA expression was analysed relative to the *β-actin* housekeeping gene and was calculated using the Pfaffl method (Pfaffl, 2001).

## 2.4 Protein analysis

### 2.4.1 Total protein extraction

Cells were collected for protein extraction and subsequent analysis following removal of growth medium from the plate wells and washing with 1X phosphate-buffered saline (PBS). Final sample buffer (FSB; 100 mM Tris-HCl pH 6.8, 4% SDS and 20% glycerol) was added to each well in order to lyse the cells. The cell lysate was then scraped from the bottom of each well and transferred into a 1.5ml microcentrifuge tube. In order to maximise cell lysis, each tube was sonicated by running along a tube rack 20 times, then boiled at 95°C for five minutes and put through a freeze-thaw cycle. Protein was then stored at -80°C.

### 2.4.2 Fractionation of protein by subcellular location

The NE-PER™ Nuclear and Cytoplasmic Extraction Reagents (Thermo Fisher Scientific™, USA) were used to separate and prepare cytoplasmic and nuclear extracts from cultured cells as per the manufacturer's protocol. Briefly, cells (at an estimated packed cell volume of 10µl) were harvested from plate wells through trypsinisation and washed with PBS. Cells were transferred to a 1.5ml microcentrifuge tube and centrifuged at 500 x g at 4°C for two minutes 30 seconds. Halt™ Protease Inhibitor Cocktail (Thermo Fisher Scientific™, USA) at 10µl/ml was added to cytoplasmic extraction reagent (CER) I and nuclear extraction reagent (NER) reagents. Once centrifuged, the supernatant was carefully drawn off from the cell pellet, in order to leave the cell pellet as dry as possible. 100µl ice cold CER I reagent was added to the cell pellet, and the tube then vortexed vigorously for 15 seconds to fully resuspend the cells. The tube was then incubated on ice for 10 minutes. 5.5µl ice cold CER II reagent was added to the microcentrifuge tube, and the tube then vortexed vigorously for five seconds followed by incubation on ice for one minute. The tube was vortexed again for five seconds, followed by centrifugation at maximum speed (~16,000 x g) at 4°C for five minutes. The supernatant, containing the cytoplasmic extract, was immediately transferred to a clean pre-chilled microcentrifuge tube and placed on ice. The remaining cell pellet (containing nuclei) was re-suspended in 50µl ice-cold NER reagent and vortexed vigorously for 15 seconds every 10 minutes for a total of 40 minutes. The tube was then centrifuged at maximum speed (~16,000 x g) at 4°C for 10 minutes. The supernatant, containing the nuclear extract, was immediately transferred to a clean pre-chilled microcentrifuge tube and placed on ice. All protein fractions were stored at -80°C.

### 2.4.3 Protein quantification

Quantification of protein was carried out in a 96-well plate using the DC™ (detergent compatible) Protein Assay (Bio-Rad Laboratories, USA) as per the manufacturer's protocol.

A standard curve using bovine serum albumin (BSA) diluted in FSB was prepared at concentrations of 0, 200, 400, 600, 800, 1000, 1500 and 2000µg/µl. To perform the assay, the following reagents were added to each well: 5µl of either BSA standard or protein sample, 25µl of Reagent AS (from a master mix comprising 1ml of Reagent A and 20µl of Reagent S), followed by 200µl of Reagent B. The reagents were mixed through gentle agitation of the plate, which was then incubated at room temperature in the dark for 15 minutes. Protein quantification was then carried out by measurement of the absorbance at 750nm of the colour generated in the reaction using the Varioskan® LUX Multimode Microplate Reader (Thermo Fisher Scientific™, USA). Following quantification, proteins were then diluted with FSB to a concentration of 10µg in 20µl and stored at -80°C

## 2.5 Western blot

### 2.5.1 Protein loading and separation

For analysis using western blot, 20µl FSB-diluted protein samples were combined with 5X Laemmli loading buffer (250mM Tris HCl pH 6.8, 10% SDS, 30% Glycerol, 5% β-Mercaptoethanol, and 0.02 % Bromophenol Blue) and 10mM DL-dithiothreitol (DTT). This mixture was then boiled at 95°C for five minutes ready for loading into the sodium dodecyl sulphate-polyacrylamide gel electrophoresis (SDS-PAGE) gel. Briefly, 1.00mm 10% SDS-PAGE gels were cast using the Mini-PROTEAN® Tetra cell casting modules, Mini-PROTEAN®

short plates and spacer plates with 1.00mm integrated spacers (all Bio-Rad Laboratories, USA). The resolving gel was prepared and poured first (**Table 2.3**), covered with a thin layer of isopropanol and left to set for ~30 minutes in a fume cupboard at room temperature. The isopropanol was subsequently rinsed with dd$H_2O$, dried with Whatman® paper, and the stacking gel prepared (**Table 2.3**) and poured, a 10 or 15 well 1.0mm Mini-PROTEAN® comb (Bio-Rad Laboratories, USA) was inserted as required, and the gel was left to set for a further ~30 minutes.

| **Reagent** | **10% Resolving Gel** | **4% Stacking Gel** |
|---|---|---|
| | Volume (ml) *(unless otherwise stated)* | Volume (ml) *(unless otherwise stated)* |
| 30% acrylamide and bis-acrylamide solution, 29:1 (Bio-Rad Laboratories, USA) | 3.3 | 3 |
| ddH2O | 4 | 3 |
| 1.5M Tris HCL, pH 8.8 | 2.5 | - |
| 1.25M Tris HCL, pH 6.8 | - | 1.3 |
| 10% SDS | 0.1 | 50µl |
| TEMED (added shortly before casting) | 5µl | 5µl |
| 10% APS (added shortly before casting) | 50µl | 25µl |

**Table 2.3 Preparation of the gel for SDS-PAGE**

The gels were subsequently assembled into the Mini-PROTEAN® Tetra unit (Bio-Rad Laboratories, USA), the tank filled with 1X electrophoresis buffer (25mM Tris, 192mM glycine, 0.1% SDS), and the combs removed. 10µl of the molecular weight marker Spectra™ Multicolor Broad Range Protein Ladder (Thermo Fisher Scientific, USA) was loaded in the first well of each gel, followed by 20µl of the protein/Laemmli buffer/DTT mixture into each subsequent well and run at 180 volts for ~60 minutes using the PowerPac™ Basic (Bio-Rad Laboratories, USA).

### 2.5.2 Protein transfer

Proteins were transferred using a semi-dry blotting technique on to a polyvinylidene difluoride (PVDF) membrane (Immobilon-P membrane, 0.45µm; Merck, USA). The membrane was activated through immersion in 100% methanol for ten seconds, then soaked in transfer buffer for ten minutes (25mM Tris, 190mM glycine, 10% methanol, 0.1% SDS) together with two sets of four sheets of Whatman® paper pre-cut to match the size of the PVDF membrane. Following SDS-PAGE completion, the resolving gel was extracted and soaked in transfer buffer for ten minutes. The blotting sandwich was then assembled within a cassette of the Trans-Blot® Turbo™ Transfer System (Bio-Rad Laboratories, USA) from the bottom up, starting with four sheets of soaked Whatman® paper, followed by the PVDF membrane, topped with the SDS-PAGE gel and finished with four more sheets of soaked Whatman® paper on top. Any air bubbles within the sandwich were removed with a roller before the cassette was closed and run within the Trans-Blot® System at 25 volts for 30 minutes.

### 2.5.3 Antibody incubation and imaging

Following protein transfer from the gel to the PVDF membrane, the blotting sandwich was disassembled, and the membrane blocked in either 5% bovine serum albumin (BSA) or 5% milk in Tris-buffered saline with Tween 20 (TBS-T; 25mM Tris, pH 7.5 150mM NaCI, 0.1% Tween 20), to match the diluent required by the primary antibody in the manufacturer's protocol. Blocking was carried out on a rocker at room temperature for one hour. Following blocking, the membrane was incubated with primary antibody diluted as appropriate (

**Table 2.4**) on a rocker at 4°C overnight.

| Target protein | Predicted molecular weight (kDa) | Host and clonality | Source and catalogue number | Blocking agent & diluent | Western blot dilution |
|---|---|---|---|---|---|
| CBLL1 | 55 | Rabbit polyclonal | Novus Biologicals, USA NBP1-83589 | 5% milk | 1:1000 |
| E-cadherin | 110 | Mouse monoclonal | Invitrogen, USA 4A2C7 | 5% milk | 1:1000 |
| AR | 110 | Rabbit polyclonal | Santa Cruz Biotechnology, USA sc-816 | 5% milk | 1:5000 |
| ERα | 65 | Rabbit monoclonal | Dako, Denmark M3634 | 5% milk | 1:250 |
| β-Actin | 42 | Mouse monoclonal | Invitrogen, USA MA5-15739 | 5% milk | 1:10,000 |
| HDAC1 | 62 | Mouse monoclonal | Cell Signalling Technology, USA 5356 | 5% milk | 1:1000 |
| GAPDH | 36 | Mouse monoclonal | Abcam, UK ab9484 | 5% BSA | 1:5000 |

**Table 2.4 Primary antibodies used in this study**

The following morning, the PVDF membrane was removed from the primary antibody solution and washed three times for five minutes in 1X TBS-T with a fourth longer wash of 15 minutes on a rocker at room temperature. The secondary antibody was dependent upon the host the primary antibody was generated in, and either horseradish peroxidase conjugated goat anti-rabbit (sc-2003) or goat anti-mouse (c-2004) (both Santa Cruz, USA) was used at a dilution of 1:10,000. Following incubation of the PVDF membrane for one hour on a rocker at room temperature, the PVDF membrane was removed and washed again three times for five minutes in 1x TBS-T with a fourth longer wash of 30 minutes on a rocker at room temperature. The membrane was then incubated with 1ml Amersham™ ECL™ Prime Western Blotting Detection Reagent (comprising 500µl of Solution A and 500µl of Solution B) (GE Healthcare, USA), for ~30 seconds at room temperature before imaging was carried out using the ChemiDoc™ MP Imaging System (Bio-Rad Laboratories, USA).

### 2.5.4 Antibody optimisation with blocking peptide

In order to determine that all of the bands being detected on western blot were specific to the CBLL1 protein, a specific CBLL1 blocking peptide mimicking the antigen used to raise the antibody was used alongside incubation of the CBLL1 primary antibody. The aim of the blocking peptide is to bind all of the CBLL1 antibody so that this is unable to bind with any CBLL1 protein on the membrane. Any bands that remain visible on the blot following incubation would thus be as a result of non-specific binding. A standard western blot protocol was then carried out using PCa cell line proteins as described in sections 2.5.1 to 2.5.2. After blocking the PVDF membrane, and prior to

primary antibody incubation, the membrane was cut in half lengthways, leaving each half containing four lanes of protein. One half was incubated in 5% milk and CBLL1 primary antibody with 1.5µl of 0.4mg/µl CBLL1 Recombinant Protein Antigen at 0.4mg/µl (NBP1-83589PEP; Novus Biologicals, USA), and the other half in 5% milk and CBLL1 primary antibody with 1.5µl of PBS added as a control. Both blots were subsequently incubated and imaged as described in section 2.5.3. A lack of CBLL1 signal from the blot incubated with the blocking peptide confirmed specificity of the CBLL1 antibody (**Figure 2.1**).

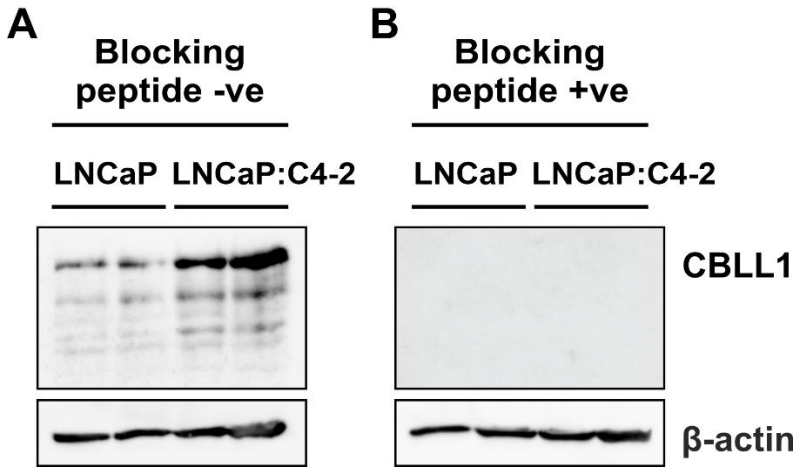


**Figure 2.1 CBLL1 protein expression in prostate cancer cell lines with and without CBLL1-specific blocking peptide**

CBLL1 protein expression was analysed by western blot in LNCaP and LNCaP:C4-2 cell lines both with and without CBLL1-specific blocking peptide incubation. β-actin was used as a loading control. (A) LNCaP and LNCaP:C4-2 protein probed with CBLL1 antibody (n=2). (B) LNCaP and LNCaP:C4-2 protein probed with CBLL1 antibody and its specific blocking peptide (n=2).

### 2.5.5 Western blot quantification

Western blots were analysed using Image Studio Lite version 5.2 (LI-COR Biosciences, USA). The software was utilised to generate intensity values from protein bands of interest and of the β-actin housekeeping control from raw western blot images. Relative expression was then calculated by comparing intensity of expression of the protein of interest with the β-actin housekeeping control, and then comparing relative expression between the control and other cell lines or conditions.

## 2.6 Cell phenotyping

### 2.6.1 Proliferation assay

To determine the effect of functional depletion of *CBLL1* on cellular proliferation, MCF7 and T-47D, and LNCaP:C4-$2_{LT}$ and LNCaP:C4-$2_{enzR}$ cells were plated in a 96 well plate in phenol-red free RPMI supplemented with 10% charcoal-stripped FBS. Cells were treated with either *siScr* or *siCBLL1*, and with the appropriate hormone or vehicle control over 6 days as described in section 2.2.4. Subsequent quantification of DNA content was performed using the CyQUANT™ Direct Cell Proliferation Assay (Invitrogen, USA) as per the manufacturer's instructions. Briefly, on day 6 a master mix of 2X detection reagent was prepared comprising 11.7ml PBS and 48µl of CyQUANT™ Direct nucleic acid stain (Invitrogen, USA) per 96 well plate. 100µl of this 2X detection reagent was added to each well and then incubated at 37°C and 5% $CO_2$ for one hour. Fluorescence of samples was then read at 480/535nm using the Varioskan Flash plate reader (Thermo Fisher Scientific, USA), and the relative DNA content calculated.

## 2.7 RNA sequencing

Illumina paired-end RNA sequencing (RNA-Seq) of vehicle and hormone-treated *siScr* control and *CBLL1*-depleted MCF7, T-47D, LNCaP:C4-2 and LNCaP:C4-$2_{enzR}$ cells (as described in section 2.2.4) was completed using an Illumina NovoSeq instrument (Novogene, UK). Raw data was analysed using standard approaches (NPM). Briefly, the TrimGalore wrapper (GitHub, Inc., USA, https://github.com/FelixKrueger/TrimGalore) for FastQC and Cutadapt (Martin, 2011) was used to remove contaminating adaptor sequences and reads with phred <30 were discarded. Retained fastq reads were aligned to the Ensembl annotated human reference genome (GRCh38.83) using the STAR aligner (Dobin et al., 2013), and gene level expression quantified by FeatureCounts (Liao et al., 2014). Statistically significant differential expression (fold change ≤±1.5 and adjusted p value <0.05) was determined using DESeq2 (Love et al., 2014). The VolcaNoseR ShinyApp (https://huygens.science.uva.nl/VolcaNoseR/) was used to prepare volcano plots of differentially expressed genes.

The replicate multivariate analysis of transcript splicing (rMATS) tool version 3.2.5 (Shen et al., 2014) was used to identify differential canonical and *de novo* splicing. Briefly, reads were trimmed to a uniform length (145bp) using the rMATS trimFastq python script (Shen et al., 2014) and the resultant reads aligned to the Ensembl reference genome (GRCh38.83) using the rMATS implementation of STAR to align reads. Differential splicing was considered biologically and statistically significant based on percent spliced in (dPSI ≥5%) and false discovery rate (FDR) <0.05. Pathway analysis was completed using the Web-Based Gene Set AnaLysis Toolkit (WebGestalt) to identify

significantly enriched Kyoto Encyclopaedia of Genes and Genomes (KEGG) pathways (Liao et al., 2019). Genes that were significantly differentially expressed were compared using Venny 2.1.0 (https://bioinfogp.cnb.csic.es/tools/venny/).

## 2.8 Immunohistochemistry analysis of patient specimens

### 2.8.1 Nottingham prostate cancer tissue microarray

Immunohistochemistry (IHC) staining was carried out on human prostate tissues following ethics approval by the Nottingham University Hospitals NHS Trust (NUH) Biobank (ACP0000184) and the University of Nottingham (1533 150901). Tissue microarray (TMA) approval was granted under ethics approval number 1861 161001. The TMA was constructed by a colleague (VM) in collaboration with histopathologist Michael Shawky Toss (MST) and the NUH at Nottingham City Hospital. The tissue was taken from a well-characterised cohort of PCa patients who underwent radical prostatectomy from 2003-2007, and a database constructed from the accompanying deidentified clinical records. Cores measuring 0.6mm were punched from the prostate tissue and the TMA was assembled 0.8mm apart using a TMA Grand Master 2.4-UG-EN Machine (3DHISTECH, Hungary). Non-malignant prostate tissue from the same patient cohort was also used alongside the neoplastic tissue as a control. The TMA comprised 160 tissue cores, of which 104 in the top half of the TMA were malignant, and 56 in the bottom half were non-malignant. Orientation of the TMA was facilitated by the application of three cores of liver and tonsil tissue in the first and last rows, respectively. Formalin fixed paraffin wax embedded (FFPE) TMA sections of 4µm were cut with a tissue microtome for slide preparation and subsequent IHC.

### 2.8.2 Nottingham breast cancer tissue microarray

Immunohistochemistry staining was carried out on human breast tumour tissue from two patient cohorts that were then combined. The first cohort (PS series) TMA comprised specimens from over 1800 early stage (I-III) BCa patients who underwent surgical removal of their tumour tissue at Nottingham City Hospital without receiving neoadjuvant treatment between 1987 and 1998. The PS series TMA was constructed following ethics approval by the Nottingham Research Ethics Committee 2 (Reference title: Development of a molecular genetic classification of breast cancer).

The second cohort (PB series) comprised specimens from over 1000 Nottingham City Hospital BCa patients who underwent surgical tumour removal without neoadjuvant treatment between 1998 and 2006. The PB series TMA was constructed following ethics approval by the North West Greater Manchester Central Research Ethics Committee (Reference title: Nottingham Health Science Biobank; reference number: 15/NW/0685). Patient data regarding clinical history, tumour characteristics, therapy and response were maintained prospectively (**Appendix 5** and **Appendix 8**)

The TMAs comprised 150 x 0.6mm cores per slide, spaced 0.8mm apart in FFPE blocks. FFPE TMA sections of 4μm were cut with a tissue microtome for slide preparation and subsequent IHC, carried out as detailed in section 2.8.3.

### 2.8.3 Nottingham TMAs and immunohistochemistry staining

Optimal antibody dilution was validated on TMA slides cut from special optimisation blocks, first using the Sequenza (Thermo Fisher Scientific™, USA) immunostaining system, followed by optimisation on TMA slides lay flat (flatbed method). Optimal antibody dilution was determined with the help of a

histopathologist (MST) and based on that which afforded a wide range of staining intensity across the samples, together with minimal background staining. The optimal IHC dilution for the CBLL1 antibody (NBP1-83589; Novus Biologicals, USA) in prostate tissue was found to be 1:250, and 1:100 in breast tissue. The optimal IHC dilution for the E-cadherin antibody (4A2C7; Invitrogen, USA) in breast tissue was found to be 1:50.

The final TMA IHC staining was carried out using the flatbed method using the Novolink™ Max Polymer Detection System (RE7280-K; Leica Biosystems, Germany) following the manufacturer's protocol, with a Leica ST5010 Autostainer XL (Leica Biosystems, Germany). Briefly, the slide was labelled and then heated on a hotplate at 60˚C for 10 minutes then placed in a Leica Autostainer slide rack (Leica Biosystems, Germany) following cooling to room temperature. The rack was loaded into the Autostainer for dewaxing and rehydrating of the TMA slide and 'Program 1' was selected. Program 1 comprised: two xylene immersions for five minutes each; three 100% Industrial Methylated Spirit (IMS) immersions for two minutes each, followed by a single immersion in water for five minutes. The rack was then transferred to a water bath for antigen retrieval. This was carried out using 1X citrate buffer at pH 6.0 (adjusted with 1M sodium hydroxide solution as required) heated for 20 minutes in a Whirlpool Sixth Sense microwave oven (Whirlpool Corporation, USA). The rack was subsequently cooled for five minutes in a water bath using running cold tap water. The slide was then removed from the rack, marked with an Immedge hydrophobic pen (Vector Laboratories, UK) to create a barrier ~5mm around the tissue cores ~5mm from the outer edge of the tissue and laid flat on a flatbed humidity chamber (Sigma-Aldrich®, USA).

Staining of the slide was then carried out using the Novolink™ Max Polymer Detection System as per the manufacturer's protocol. All incubations were at room temperature and all wash steps carried out with TBS-Tween (TBS-T; TBS containing 0.1% Tween 20) for five minutes each. Briefly the Novolink™ protocol comprised two washes, followed by the addition of 300µl Peroxidase Block and a five minute incubation. Three washes were then performed, and 300µl Protein Block was added and left to incubate for five minutes. Another three washes followed, then 300µl of primary antibody, diluted in Leica antibody diluent to a concentration of 1:250) was added to the slide and incubated for one hour. Following incubation, three washes were performed and 300µl post-primary solution was applied to the slide and incubated for 30 minutes. Three more washes were performed followed by application of 300µl polymer and incubation for a further 30 minutes. Three washes were carried out and 300µl freshly made DAB working solution (1:20 diaminobenzidine chromogen in diaminobenzidine substrate buffer) was applied and incubated for five minutes. Following three more washes, 300µl haematoxylin was applied and incubated for six minutes. The slide was then transferred back into a Leica autostainer rack, placed in water and loaded into the Autostainer for dehydrating and clearing of the TMA slide, for which 'Program 2' was used. Program 2 comprised: three 100% Industrial Methylated Spirit (IMS) immersions for two minutes each, and two xylene immersions for five minutes each. Finally, DPX mounting media (a mixture of distyrene, plasticiser and xylene) was applied to the slide and a coverslip placed. The slides were left in a fume cupboard for 24 hours for drying at room temperature, and

subsequently scanned using the NanoZoomer scanner (Hamamatsu Photonics, UK) at the Queens Medical Centre, Nottingham.

Due to restricted laboratory access at the Nottingham City Hospital site during the COVID-19 pandemic, IHC staining of the BCa TMAs was carried out by a colleague with approved access for City Hospital, Dr Yousif Kariri (YK).

### 2.8.4 Weill Cornell Medicine prostate cancer tissue microarray and immunohistochemistry staining

Immunohistochemistry staining was carried out on human prostate tissues following ethics approval by the University of Nottingham School of Veterinary Medicine & Science (1578 151019; 2809 190819) and the Weill Cornell Medicine (WCM) Institutional Review Board. The cohort 1 and 2 TMAs were kindly provided by Dr Brian Robinson (WCM). Patient clinicopathological data were only available for cohort 1 (**Appendix 3** and **Appendix 4**). In the cohort 1 TMA, tissue was taken from radical prostatectomy specimens from PCa patients, and a database constructed from the accompanying deidentified clinical records. Triplicate 0.6mm cores of both primary adenocarcinoma and non-malignant control tissue were punched from the prostate specimens and mounted in FFPE blocks. In the cohort 2 TMA, tissue was taken from prostate specimens at rapid autopsy, with no clinical records available for analysis. Triplicate 1mm cores of primary adenocarcinoma, metastatic, CRPC and NEPC specimens, as well as non-malignant control tissue were punched from the prostate specimens and mounted in FFPE blocks. FFPE TMA sections of 5µm were cut with a tissue microtome for slide preparation and subsequent IHC.

The final IHC staining of the TMA was carried out manually at WCM by a colleague (CW) using the flatbed method. Briefly, the slides were labelled and then baked at 60˚C for 5 minutes and then cooled to room temperature. The slides were subsequently manually dewaxed and rehydrated: one xylene immersion for five minutes; two xylene immersions for five minutes each; two 100% ethanol immersions for two minutes each; two 70% ethanol immersions for two minutes each; two immersions in double distilled water (dd$H_2O$) for two minutes each. Antigen retrieval was performed using a pressure cooker to boil slides for four minutes in 15ml citrate-based antigen unmasking solution (Vector) in 1.6L dd$H_2O$. The slide holder was subsequently cooled for five minutes in a water bath using running cold tap water.

Staining of the slide was then carried out using the Novolink™ Max Polymer Detection System (RE7280-K; Leica Biosystems, Germany) as per the manufacturer's protocol and as described in section 2.8.3, with the CBLL1 primary antibody (as detailed in **Table 2.4**) diluted in PBS. Following staining, the slides were manually dehydrated and cleared: two 70% ethanol immersions for two minutes each; two 95% ethanol immersions for two minutes each; two 100% ethanol immersions for two minutes each; two xylene immersions for five minutes each. Finally, DPX mounting media was applied to the slide and a coverslip placed. The slides were left in a fume cupboard for 24 hours for drying at room temperature, and subsequently scanned.

### 2.8.5 H-scoring analysis

Following scanning, Nottingham cohort TMA images were uploaded to Xplore computational pathology software (Philips Electronics, Netherlands) for viewing and scoring. WCM cohort TMA images were viewed and scored using

Aperio Imagescope v 12.4 (Leica Biosystems, USA). The histo-scoring (H-scoring) system is a semi-quantitative method of assessing the IHC staining intensity and thus the immunoreactivity of a tissue (Goulding et al., 1995). The H-score was determined by calculating the sum of the percentage of cells at four intensity levels denoted as: 0= no staining, 1= mild staining, 2= moderate staining, 3= strong staining, with a final H-score ranging between 0 and 300. The following formula was used for this calculation:

% strongly stained cells x 3 + % moderately stained cells x 2 + % mildly stained cells x 1 =Final H-score (0-300)

A second observer (CW and Anna Harris (AH)) independently scored 10-20% of all cores across all cohorts. Concordance between scorers was evaluated via the intraclass correlation coefficient (ICC) using IBM® SPSS® Statistics 26 (IBM®, UK). ICC concordance across all cohorts was >0.8 and therefore validated the H-scores given.

## 2.9 Statistical analysis

### 2.9.1 Cell line experiment analysis

P values <0.05 were considered statistically significant with a confidence interval of 95%. Generally, a minimum of a two-fold difference and an adjusted p value <0.05 in gene expression was considered biologically significant. All *in vitro* experiments were performed using a minimum of three biologically independent repeats analysed in technical triplicates. All data generated from these experiments were statistically analysed and subsequent graphs created using GraphPad Prism 9 (GraphPad Software, USA). Data were expressed as mean ± standard error of the mean. Comparison of the means of different sample groups was carried out using either a Student's t-test or a one-way

analysis of variance (ANOVA) with Bonferroni's post hoc test correction as appropriate.

### 2.9.2 Immunohistochemistry analysis

TMA clinical correlations were analysed using IBM® SPSS® Statistics 26 (IBM®, UK). Statistical p values were determined by $\chi^2$ test (asymptotic significance, 2-sided) using both IBM® SPSS® Statistics (version 26) and the VassarStats Statistical Computation Website (http://vassarstats.net/; ©Richard Lowry). In the BCa TMAs, correlation of clinicopathological parameters with H-scores was carried out by a colleague (MST) to maintain confidentiality of potentially identifiable patient data. Statistical significance of Kaplan Meier estimates was calculated using the log-rank (Mantel-Cox) test. H-scoring reliability between two independent scorers was analysed by Spearman's rank order correlation in Microsoft Excel (Microsoft Corporation, USA) and GraphPad Prism 9 (GraphPad Software, USA). Association of expression between markers of interest was analysed using Pearson's correlation coefficient in Microsoft Excel (Microsoft Corporation, USA) and GraphPad Prism 9 (GraphPad Software, USA). Cox's proportional hazard model was utilised to assess the prognostic independence of a marker from established prognostic factors of stage, grade and tumour size using IBM® SPSS® Statistics (version 26).

# Chapter 3

## Molecular and clinical significance of CBLL1 expression in prostate cancer patient samples and cell lines

# 3 Expression of CBLL1 in prostate cancer patient samples and cell lines

## 3.1 Introduction

CBLL1 was originally reported to function as a ubiquitin E3 ligase that regulates E-cadherin expression (Fujita et al., 2002), a protein with an important role in the development of cancer (Alsaleem et al., 2019). CBLL1 was later found to also act as an adaptor protein associated with the METTL3-methyltransferase protein complex responsible for $m^6A$ regulation, and is understood to be necessary for full $m^6A$ methylation activity (Horiuchi et al., 2013, Ruzicka et al., 2017, Sun et al., 2019, Wen et al., 2018, Yue et al., 2018).

The $m^6A$ modification of mRNA plays a vital role in regulating many key physiological processes including cell differentiation and DNA damage repair (Fustin et al., 2013, Geula et al., 2015, Lin et al., 2017, Wang et al., 2014, Xiang et al., 2017). Dysregulation of the mRNA $m^6A$ modification is associated with a number of cancer types and has been implicated in therapy resistance (Li et al., 2020a, Wang et al., 2020c)

CBLL1 expression has been found to be upregulated in a number of lung and gastrointestinal tract cancers, suggesting a pro-oncogenic role (Castosa et al., 2018, Figueroa et al., 2009b, Hui et al., 2019, Liu et al., 2018c). However, little is known about the relative importance of the functions of CBLL1 with respect to E-cadherin and the $m^6A$ methyltransferase protein complex in PCa. Given the involvement of dysregulated E-cadherin and $m^6A$ in the development of many different cancer types, this chapter aimed to further elucidate the expression and clinical relevance of CBLL1 in PCa.

The diverse roles of CBLL1 in the regulation of cell-to-cell adhesion and as a component of the $m^6A$ methyltransferase complex supports the hypothesis that increased CBLL1 expression promotes carcinogenesis and cancer progression through convergent mechanisms and is associated with malignancy and poorer outcomes. To test this hypothesis, bioinformatic analysis of alterations in *CBLL1* expression in PCa patients in publicly available data sets was completed. Expression of CBLL1 was subsequently investigated in both PCa cell lines and in PCa patient specimens, and the effect of androgen on CBLL1 mRNA and protein expression examined. These results provide novel insights into the regulation, expression and clinical significance of CBLL1 in PCa.

## 3.2 Results

### 3.2.1 CBLL1 expression and copy number alterations in prostate cancer patients

The expression of *CBLL1* was analysed in publicly-available datasets of PCa patients using the cBioPortal for Cancer Genomics (Cerami et al., 2012, Gao et al., 2013). Three patient cohorts were examined: the primary adenocarcinoma TCGA Firehose Legacy cohort (n=492) (Liu et al., 2018a), the metastatic adenocarcinoma SU2C/PCF Dream Team cohort (n=444) (Abida et al., 2019), and the Neuroendocrine Prostate Cancer Multi-Institute study (including castrate-resistant PCa cases) (n=114) (Beltran et al., 2016) (retrieved 28 March 2023).

Comparative analysis of mutations and putative copy number alterations from GISTIC was carried out to determine the frequency of genetic alterations affecting *CBLL1* in patients with different types of PCa. Altered *CBLL1*

expression was found to be rare in prostate adenocarcinoma patients, with amplification, mutation and deep deletion of the gene occurring in only 0.2%, 0.4% and 0.6% of cases, respectively (**Figure 3.1A**). In cases of metastatic adenocarcinoma, gene amplification was the most commonly observed alteration (3.15%), followed by deep deletion (1.13%) and mutation (0.23%) (**Figure 3.1A**). No copy number alterations or mutations were reported in the Neuroendocrine PCa (NEPC) and castrate-resistant PCa (CRPC) patient cohort (**Figure 3.1A**).

To evaluate the clinical relevance of the CBLL1 protein in PCa, mRNA expression of *CBLL1* in the three patient cohorts was then assessed (**Figure 3.1B**). Expression of *CBLL1* mRNA was most commonly altered in patients in the prostate adenocarcinoma cohort, with high expression (relative to the median) in 13.03% of cases, and low expression in 3.26% of cases (**Figure 3.1B**). In patients with NEPC, only elevated *CBLL1* mRNA expression was observed in 11.43% of cases (**Figure 3.1B**). Of the CRPC cases, 7.14% harboured high mRNA expression, and 2.27% low expression (**Figure 3.1B**). Altered mRNA expression was only seen in 3.83 % of patients with metastatic PCa, with high expression in 3.6% of cases and low expression in just 0.23% of cases (**Figure 3.1B**).

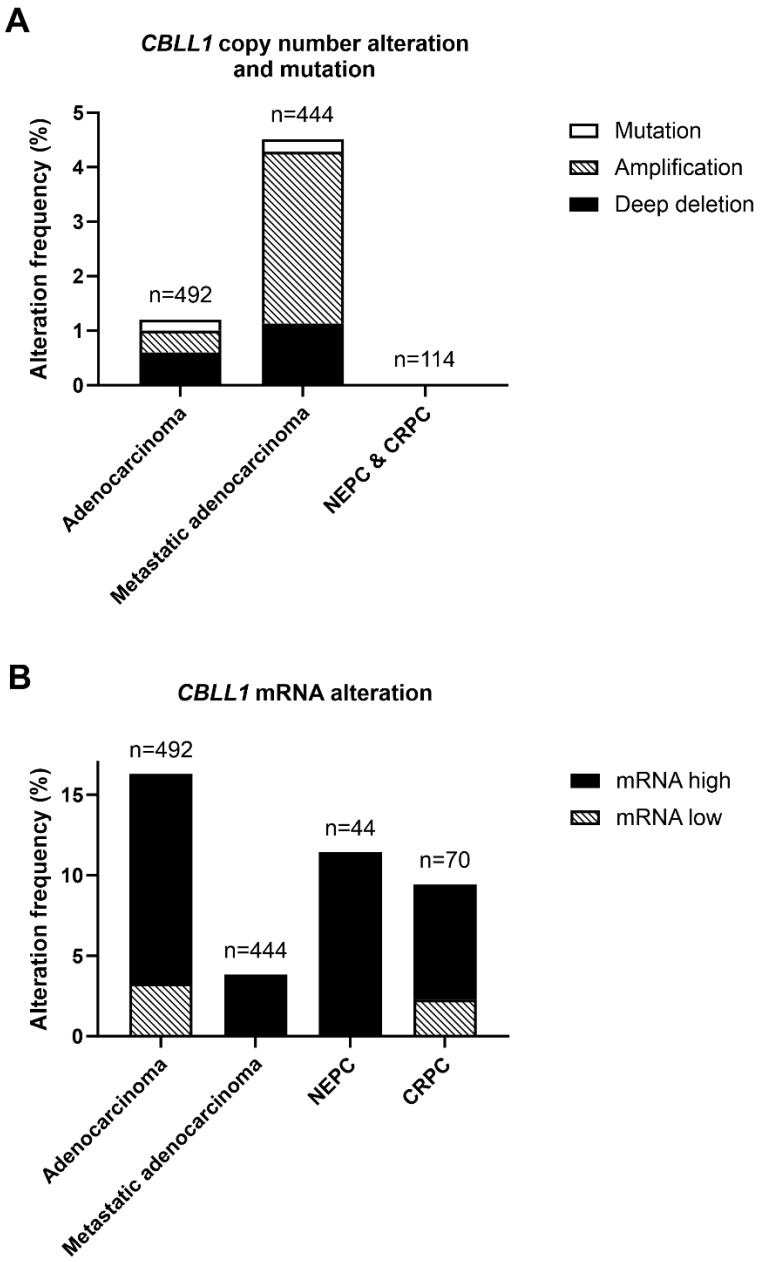


**Figure 3.1 *CBLL1* alteration frequency in prostate cancer**

The cBioPortal for Cancer Genomics (Cerami et al., 2012, Gao et al., 2013) was utilised to assess the incidence of *CBLL1* amplification, deep deletion and mutation, together with its mRNA expression in patients with prostatic adenocarcinoma (Liu et al., 2018a), metastatic adenocarcinoma (Abida et al., 2019), neuroendocrine PCa (NEPC) and castrate-resistant PCa (CRPC) (Beltran et al., 2016). (**A**) Copy number alterations and mutations in *CBLL1* in patients with the four types of PCa. (**B**) Alterations in mRNA expression of *CBLL1* in the four types of PCa patients (z score threshold ± 1).

The effect of copy number alterations on *CBLL1* mRNA expression in the prostate adenocarcinoma and metastatic adenocarcinoma patient cohorts was assessed (**Figure 3.2**). No *CBLL1* copy number alterations were reported for NEPC and CRPC cases (Beltran et al., 2016). Whilst the majority of cases are diploid, with two alleles at the *CBLL1* locus, a similar trend was observed between *CBLL1* expression and copy number, with higher mRNA expression in cases with copy number gain and amplification, and lower mRNA expression seen with copy number shallow and deep deletion (**Figure 3.2**).

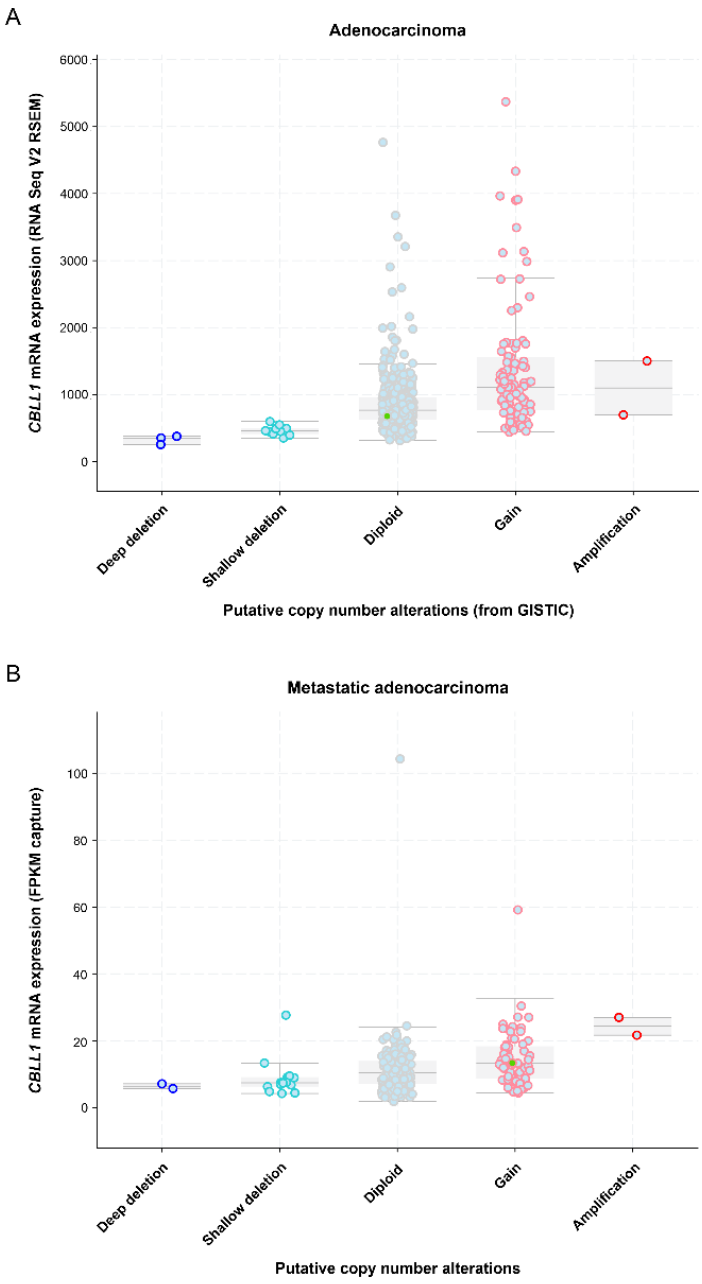


**Figure 3.2 *CBLL1* putative copy number alterations in prostate cancer**

The cBioPortal for Cancer Genomics (Cerami et al., 2012, Gao et al., 2013) was utilised to assess *CBLL1* putative copy number alterations in patients with different prostate cancer types and their association with mRNA expression. (**A**) *CBLL1* putative copy number alterations in prostate adenocarcinoma patients (n=492) (Liu et al., 2018a). (**B**) *CBLL1* putative copy number alterations in metastatic adenocarcinoma patients (n=444) (Abida et al., 2019).

The UCSC Xena browser (Goldman et al., 2020) was used to further investigate *CBLL1* expression in the primary adenocarcinoma TCGA Firehose Legacy patient cohort (Liu et al., 2018a) in association with clinicopathological parameters (retrieved 28 March 2023) Figure **3.3**). No significant difference was seen in *CBLL1* expression between normal prostate (n=52) and primary tumour tissue (n=498) ($p>0.05$; **Figure 3.3A**). Similarly, no significant association was observed between *CBLL1* expression and response to primary therapy ($p>0.05$; **Figure 3.3B**), or biochemical recurrence ($p>0.05$; **Figure 3.3C**).

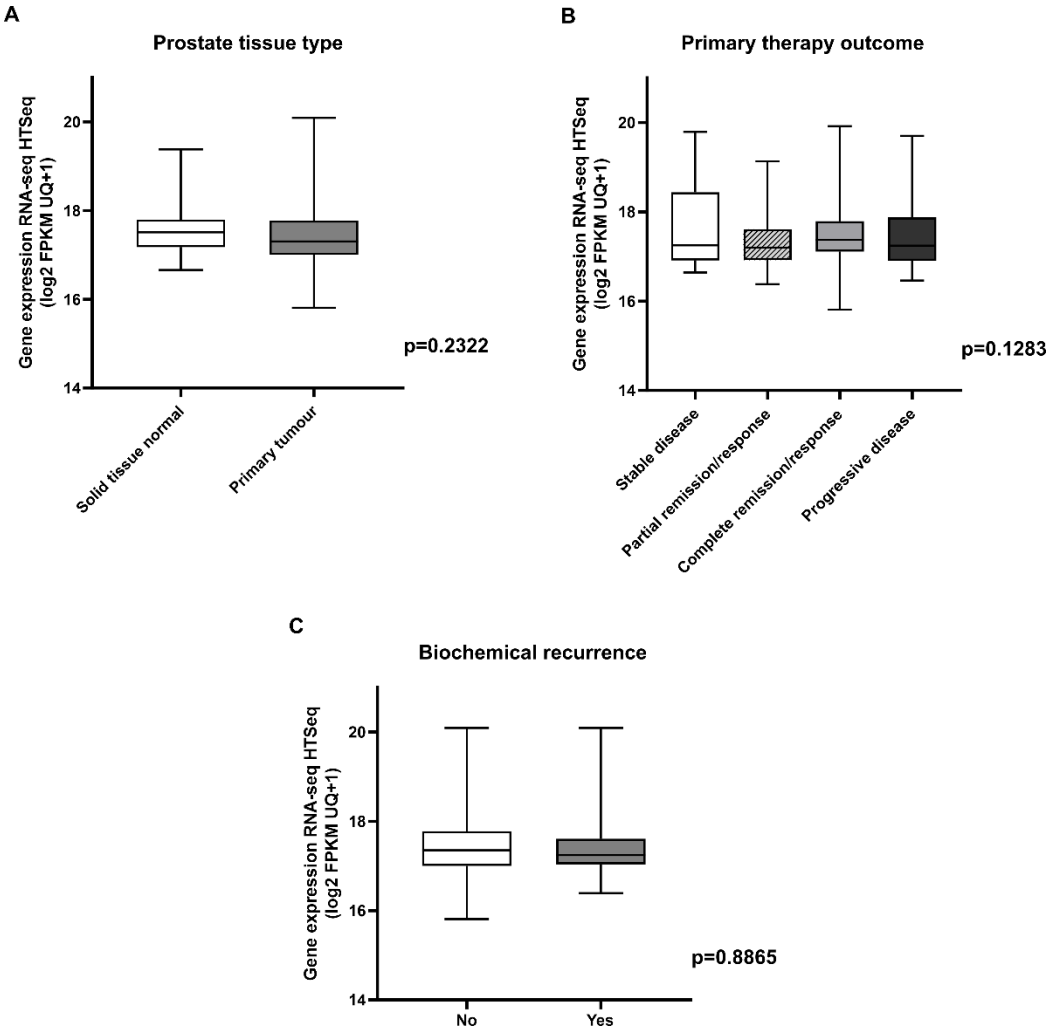


**Figure 3.3 *CBLL1* mRNA expression and correlation with clinicopathological parameters**

The UCSC Xena browser (Goldman et al., 2020) was utilised to assess *CBLL1* expression and its correlation with clinicopathological parameters in the TCGA adenocarcinoma patient cohort (Liu et al., 2018a). (**A**) *CBLL1* mRNA expression in primary tumour (n=498) compared with normal prostate tissue (n=52). (**B**) *CBLL1* mRNA expression in association with primary therapy outcome; stable disease (n=26), partial remission/response (n=36), complete remission/ response (n=358) and progressive disease (n=29). (**C**) *CBLL1* mRNA expression in association with biochemical recurrence; No (n=412), Yes (n=61). Analysed by unpaired t-test (**A**), (**C**); and one-way Anova (**B**).

### 3.2.2 CBLL1 expression in prostate cancer cell lines

Basal expression of CBLL1 mRNA and protein was analysed in the PCa cell lines LNCaP, LNCaP:C4-2, 22Rv1, PC3, DU145, a long-term culture of LNCaP:C4-$2_{LT}$ and enzalutamide-resistant LNCaP:C4-$2_{enzR}$ relative to the non-malignant PNT1A control cell line (**Figure 3.4**). *CBLL1* mRNA was expressed in all cell lines and was significantly higher in all PCa cell lines except PC3 compared with PNT1A ($p<0.01$; **Figure 3.4A**). *CBLL1* was expressed at the highest level in those cell lines expressing AR and thus androgen-responsive (**Figure 3.4A**).

CBLL1 protein was expressed in all cell lines examined (**Figure 3.4B**). CBLL1 protein expression was consistent with *CBLL1* mRNA, again with the highest expression observed in the AR-expressing PCa cell lines (**Figure 3.4B**).

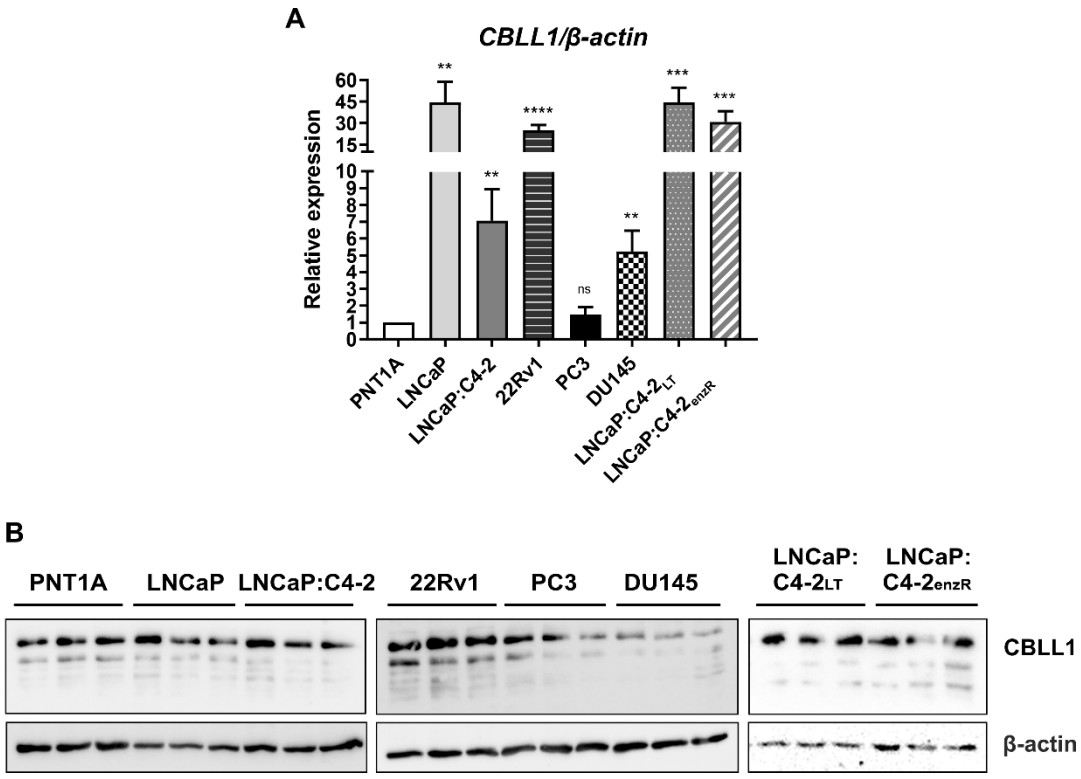


**Figure 3.4 CBLL1 expression in non-malignant and prostate cancer cell lines**

*CBLL1* mRNA expression was analysed by qRT-PCR relative to *β-actin* and CBLL1 protein expression was analysed by western blot with β-actin loading control. (**A**) *CBLL1* mRNA expression in PCa cell lines LNCaP, LNCaP:C4-2, 22Rv1, PC3, DU145, LNCaP:C4-$2_{LT}$ and LNCaP:C4-$2_{enzR}$ compared with the non-malignant control cell line PNT1A (n=6). (**B**) CBLL1 protein expression in the non-malignant PNT1A control cell line and PCa cell lines LNCaP, LNCaP:C4-2, 22Rv1, PC3, DU145, LNCaP:C4-$2_{LT}$ and LNCaP:C4-$2_{enzR}$ (n=3). $_{LT}$= Long-term parental; $_{enzR}$= Enzalutamide-resistant. * = p ≤0.05, ** = p ≤0.01, *** = p ≤0.001, **** = p ≤0.0001 by unpaired t-test.

### 3.2.3 Androgen regulation of CBLL1 expression in prostate cancer cell lines

As *CBLL1* expression was highest in the AR-expressing PCa cell lines, the effect of androgen (R1881) treatment on *CBLL1* mRNA expression was next examined (**Figure 3.5**). The androgen-responsive cell lines LNCaP, LNCaP:C4-2, 22Rv1 and LNCaP:C4-$2_{enzR}$ were treated for 72 hours with either vehicle (100% ethanol) or R1881 (1nM) before harvesting. *CBLL1* expression was upregulated in LNCaP ($p<0.01$; **Figure 3.5A**), LNCaP:C4-2 ($p<0.05$; **Figure 3.5B**) and LNCaP:C4-$2_{enzR}$ ($p<0.01$; **Figure 3.5D**) cells in response to androgen treatment, but downregulated in 22Rv1 cells ($p<0.0001$; **Figure 3.5C**).

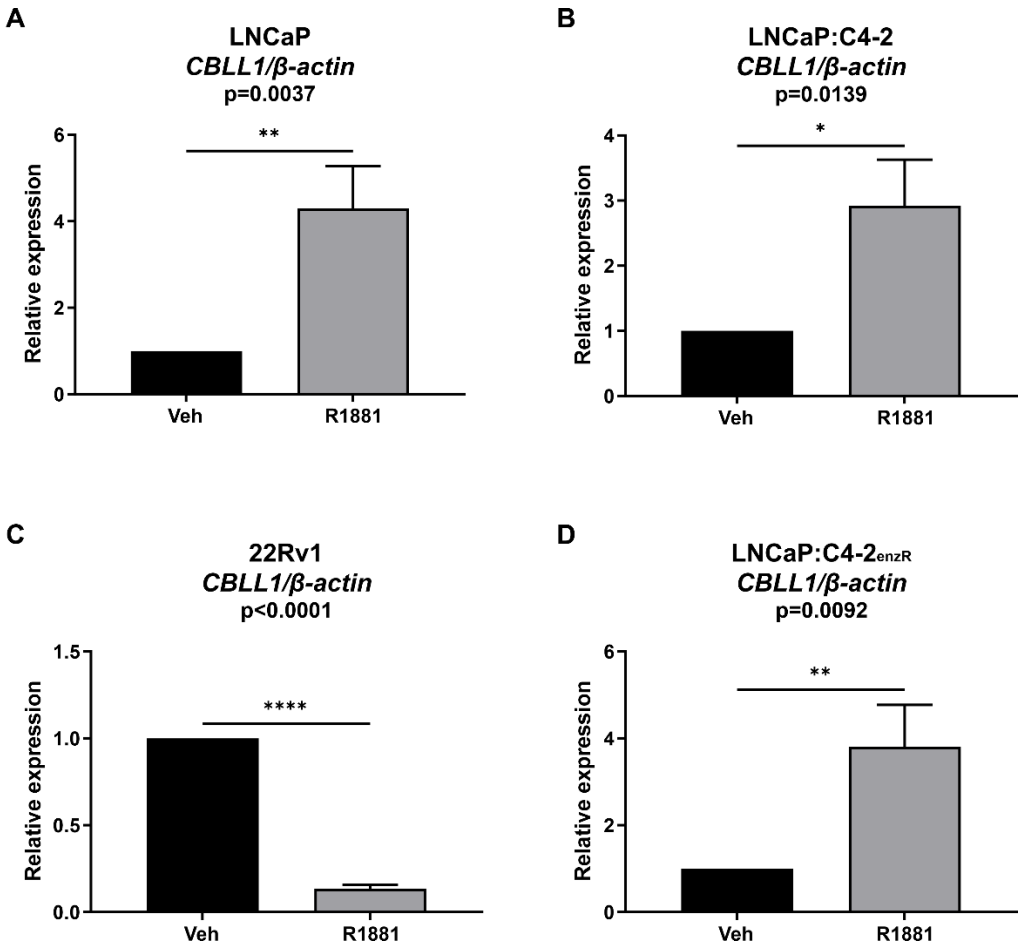


**Figure 3.5 *CBLL1* expression in prostate cancer cell lines in response to androgen treatment**

*CBLL1* mRNA expression was analysed by qRT-PCR relative to *β-actin* following vehicle or R1881 (1nM) treatment for 72 hours in PCa cell lines. (**A**) *CBLL1* mRNA expression in LNCaP (n=6). (**B**) *CBLL1* mRNA expression in LNCaP:C4-2 (n=6). (**C**) *CBLL1* mRNA expression in 22Rv1 (n=6). (**D**) *CBLL1* mRNA expression in LNCaP:C4-$2_{enzR}$ (n=6). $_{enzR}$ = Enzalutamide-resistant. Veh= Vehicle. * = p ≤0.05, ** = p ≤0.01, *** = p ≤0.001, **** = p ≤0.0001 by paired t-test.

The expression of CBLL1 and AR protein in response to androgen (R1881) treatment was subsequently investigated (**Figure 3.6**). The androgen-responsive cell lines LNCaP, LNCaP:C4-2, 22Rv1 and LNCaP:C4-$2_{enzR}$ were treated for 72 hours with either 100% ethanol vehicle or 1nM R1881 before harvesting. No significant changes in CBLL1 expression were observed in response to androgen treatment in any cell line (**Figure 3.6**). AR expression was upregulated in all cell lines following androgen treatment (**Figure 3.6**). AR variants were observed in the 22Rv1 cell line, and their expression was also upregulated in response to androgen treatment (**Figure 3.6C**). Interestingly, AR variants were observed in the LNCaP:C4-$2_{enzR}$ cell line following androgen treatment (**Figure 3.6D**).

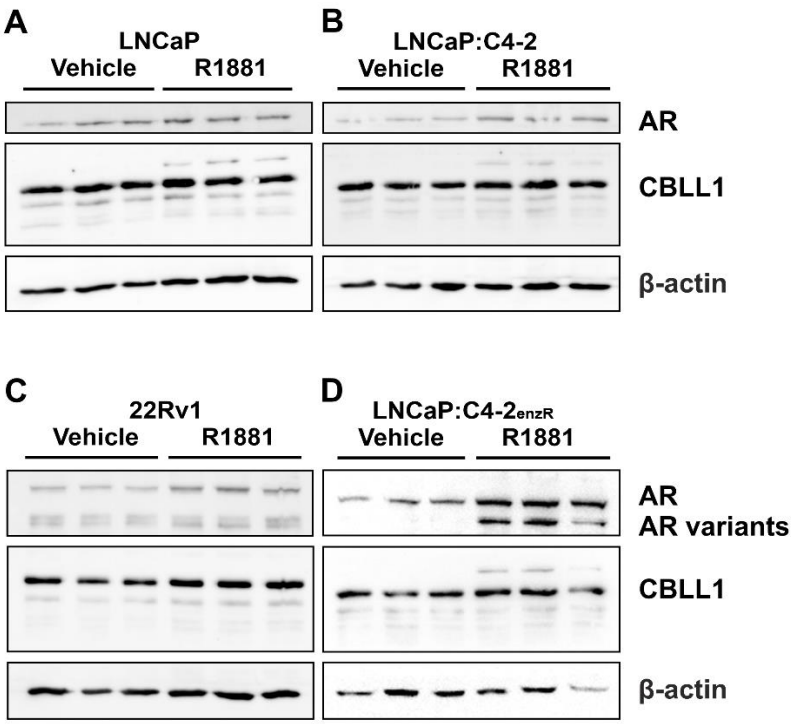


**Figure 3.6 CBLL1 expression in prostate cancer cell lines in response to androgen treatment**

CBLL1 and AR protein expression was analysed by western blot with β-actin loading control following vehicle or R1881 (1nM) treatment for 72 hours in PCa cell lines. (**A**) CBLL1 and AR protein expression in LNCaP (n=3). (**B**) CBLL1 and AR protein expression in LNCaP:C4-2 (n=3). (**C**) CBLL1 and AR protein expression in 22Rv1 (n=3). (**D**) CBLL1 and AR protein expression in LNCaP:C4-$2_{enzR}$ (n=3). $_{enzR}$ = Enzalutamide-resistant.

Given the dual roles of CBLL1 in both the nucleus and cytoplasm, its subcellular localisation was next assessed. The effect of androgen treatment on the subcellular localisation of CBLL1 was also investigated. LNCaP:C4-2 and LNCaP:C4-$2_{enzR}$ PCa cell lines were treated for 72 hours with either vehicle (100% ethanol) or R1881 (1nM) before cells were harvested and the nuclear and cytoplasmic protein fractions isolated. HDAC1 and GAPDH were used as nuclear and cytoplasmic controls, respectively, and confirmed good separation

of the protein fractions (**Figure 3.7**). CBLL1 was expressed in both the nuclear and cytoplasmic compartments but enriched in the nucleus in both cell lines (**Figure 3.7**). No significant difference in subcellular localisation was seen in response to androgen, however both nuclear and cytoplasmic CBLL1 expression did appear to be increased following androgen treatment (**Figure 3.7**). E-cadherin was similarly expressed in both the nuclear and cytoplasmic compartments however, in contrast to CBLL1, its expression was markedly enriched in the cytoplasm (**Figure 3.7**). As with CBLL1, androgen did not induce a significant difference in E-cadherin subcellular localisation, however in LNCaP:C4-2 cells an increase in cytoplasmic E-cadherin expression was observed in response to androgen treatment (**Figure 3.7A**). Conversely, in LNCaP:C4-$2_{enzR}$ cells a decrease in cytoplasmic E-cadherin expression was seen following androgen treatment (**Figure 3.7B**). Androgen treatment had no significant effect on nuclear E-cadherin expression (**Figure 3.7**).

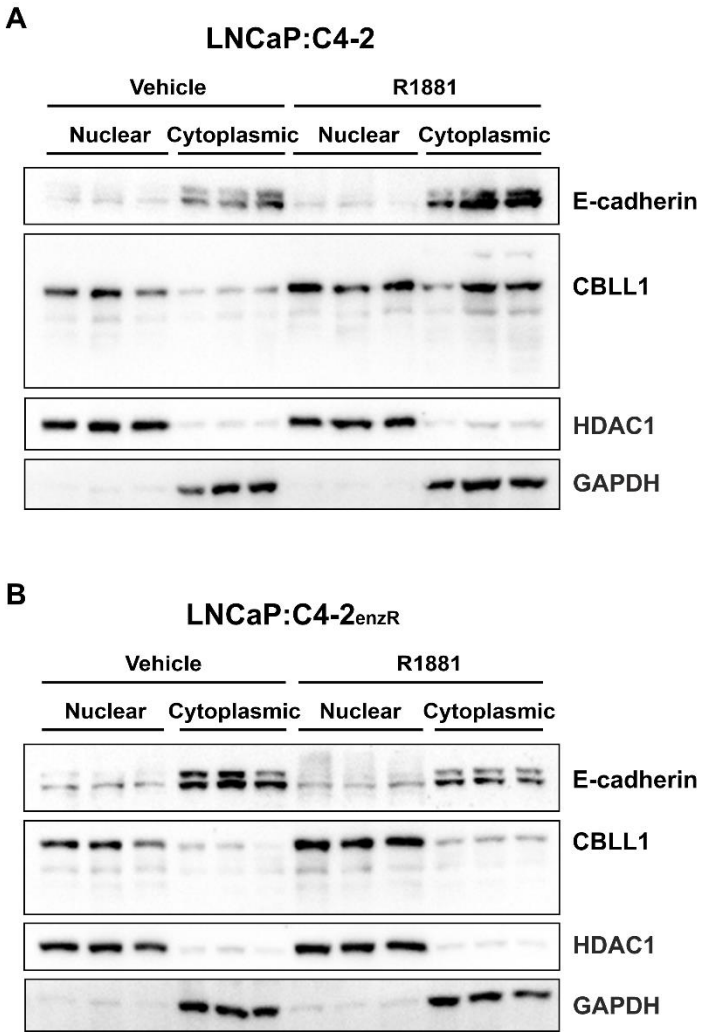


**Figure 3.7 CBLL1 protein localisation expression in prostate cancer cell lines in response to androgen treatment**

CBLL1 protein expression was analysed by western blot in LNCaP:C4-2 and LNCaP:C4-2$_{enzR}$ PCa cell lines following vehicle or R1881 (1nM) treatment for 72 hours and subsequent extraction of cytoplasmic and nuclear protein fractions. GAPDH and HDAC1 were used as cytoplasmic and nuclear loading controls, respectively. (**A**) CBLL1 and E-cadherin protein expression in LNCaP:C4-2 (n=3). (**B**) CBLL1 and E-cadherin protein expression in LNCaP:C4-2$_{enzR}$ (n=3). $_{enzR}$= Enzalutamide-resistant.

To elucidate further the potential androgen regulation of CBLL1 expression, analysis of publicly available data was carried out to determine androgen regulation of the *CBLL1* gene (**Figure 3.8**). The GSE154633 dataset (Huang et al., 2021) was viewed using the Integrative Genomics Viewer (Robinson et al., 2011). The androgen-regulated gene *KLK3* (also known as *PSA*) was used as a positive control, demonstrating androgen regulation of the proximal promoter region at the 5' end that extended across the majority of the entire gene (**Figure 3.8B**). Similarly, androgen regulation of the proximal promoter region in the 5' end in the *CBLL1* gene was also observed (**Figure 3.8A**).

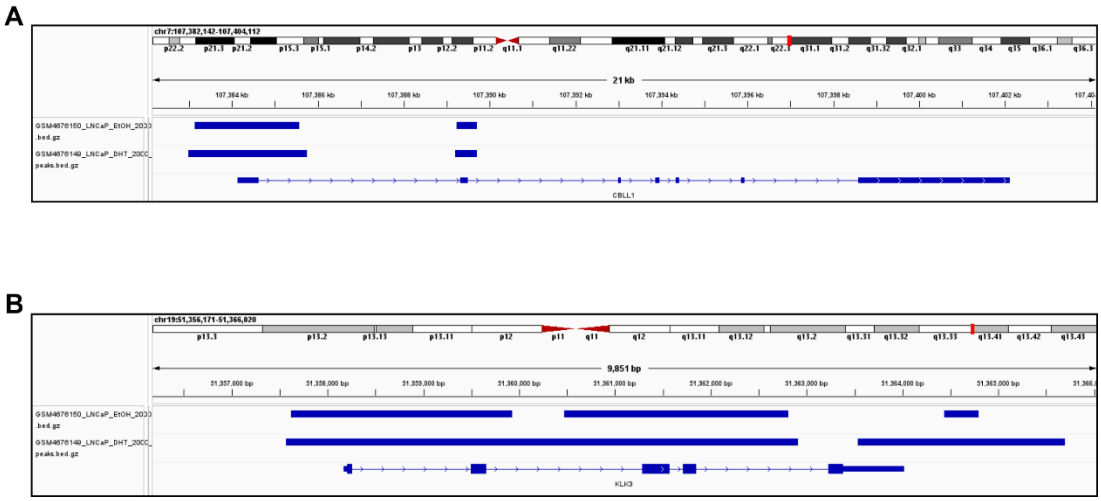


**Figure 3.8 STARR-Seq profiling of the *CBLL1* locus**

The Integrative Genomics Viewer (Robinson et al., 2011) was used to analyse STARR-Seq data (GEO accession GSE154633; Huang et al., 2021) from the NCBI GEO database (Barrett et al., 2013) detailing androgen regulation of the *CBLL1* locus. (**A**) AR binding site within the *CBLL1* gene. (**B**) AR binding site within the *KLK3* gene.

### 3.2.4 CBLL1 expression in prostate tissue specimens from Nottingham patient cohort

To investigate the expression of CBLL1 protein in PCa patients, immunohistochemistry (IHC) was carried out on a prostate tissue micro-array (TMA) comprising both non-malignant prostate (n=43) and tumour (n=99) specimens from patients in the Nottingham cohort (**Figure 3.10**). As described in chapter 2, CBLL1 staining in both the nucleus and cytoplasm of prostate glandular cells was assessed and assigned a H-score, with validation from a second scorer following an independent staining evaluation of 20% of the tissue cores. Concordance between independent scorers of >0.8 intraclass correlation was confirmed. The H-scores for both nuclear and cytoplasmic CBLL1 staining were then divided into three approximately equal groups of low, moderate and high CBLL1 expression. Examples of these three levels of staining intensities are shown in **Figure 3.9**.

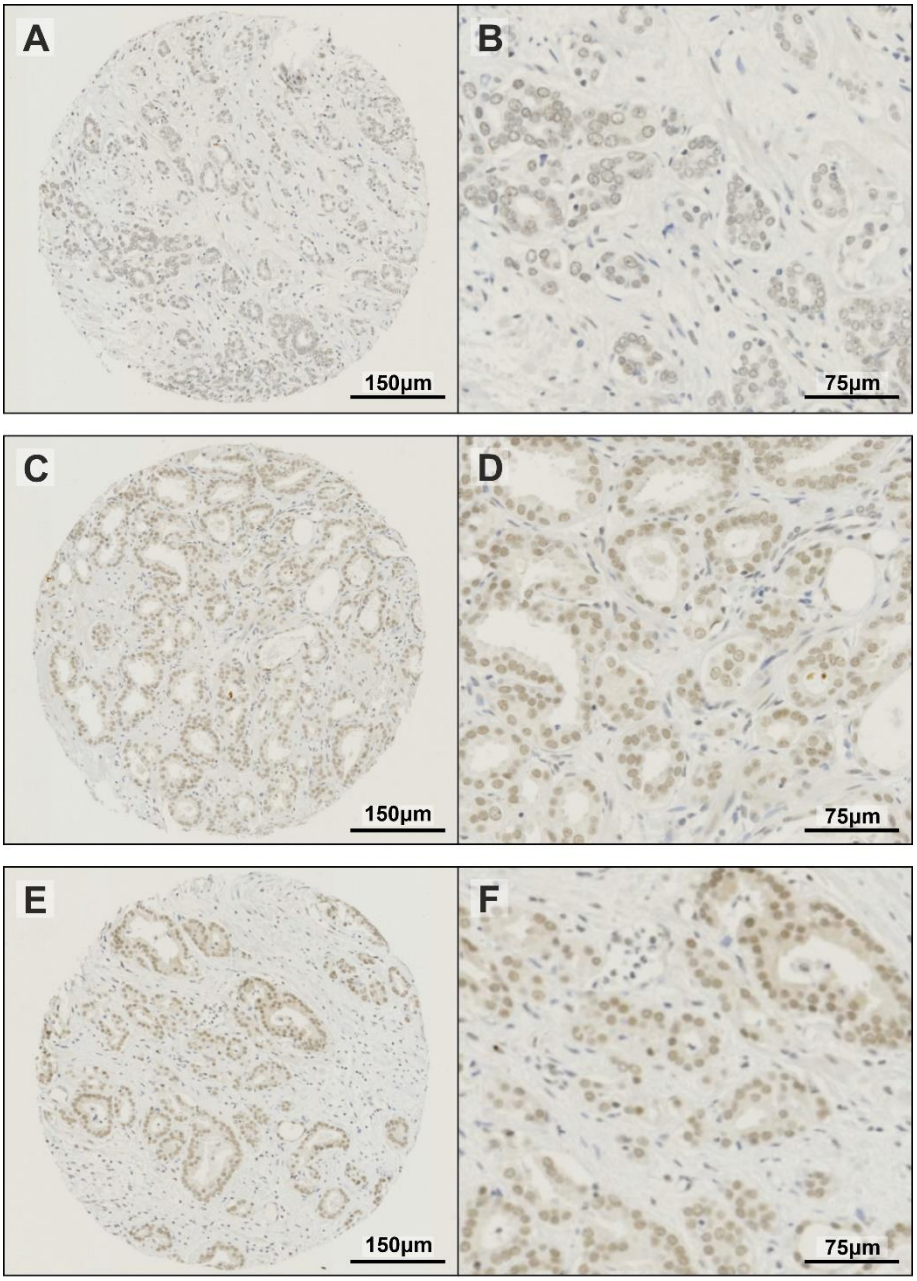


**Figure 3.9 Representative images of CBLL1 IHC staining of Nottingham cohort TMA of prostate cancer tissue**

IHC staining of prostate cancer patient tissue samples was carried out to determine the nuclear and cytoplasmic expression of CBLL1. (**A** and **B**) Representative images of low level CBLL1 expression. (**C** and **D**) Representative images of moderate level CBLL1 expression. (**E** and **F**) Representative images of high level CBLL1 expression.

Analysis of CBLL1 expression in non-malignant and tumour specimens identified that cytoplasmic expression was higher in PCa when compared with non-malignant prostatic tissue (p=0.009; **Figure 3.10B**). Nuclear CBLL1 expression showed a similar trend but did not reach statistical significance (p=0.219; **Figure 3.10A**).

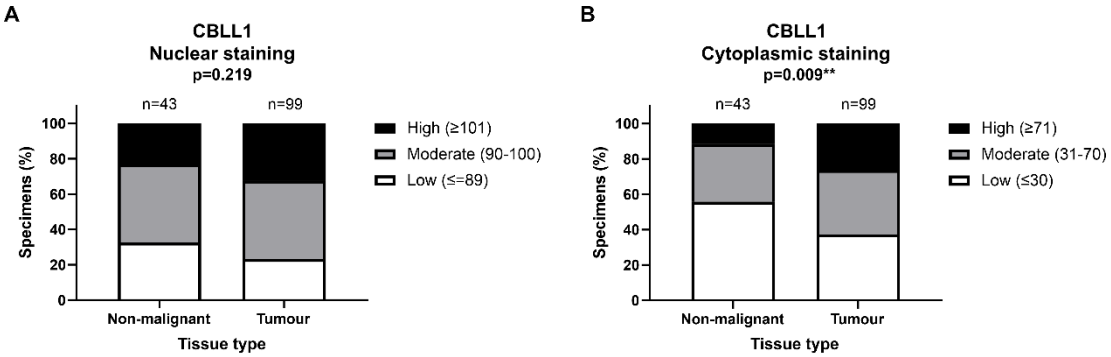


**Figure 3.10 CBLL1 expression in non-malignant prostate and tumour patient tissue samples in Nottingham cohort TMA**

IHC staining of 142 patient samples was assessed by H-score, divided into high, moderate, and low expression groups and correlated with prostate tissue malignancy. CBLL1 nuclear staining, low: ≤89, moderate: 90-100, high: ≥101; CBLL1 cytoplasmic staining, low: ≤30, moderate: 31-70, high: ≥71. (**A**) Correlation of CBLL1 nuclear staining and prostate malignancy (n=142). (**B**) Correlation of CBLL1 cytoplasmic staining and prostate malignancy (n=142). Analysed by $\chi^2$ test.

CBLL1 expression in tumour samples (n=99) was subsequently correlated with deidentified clinicopathological parameters (**Figure 3.11**, **Appendix 1** and **Appendix 2**). Nuclear CBLL1 expression was significantly higher in patients with a higher overall Gleason grade at diagnosis (p=0.031; **Figure 3.11A**). Interestingly, lower cytoplasmic expression was seen in PCa patients with concurrent high-grade PIN (p=0.037; **Figure 3.11C**). PCa recurrence occurred in 32 patients, and of those, 15 patients experienced recurrence within two years, and 17 after two years. It was found that both nuclear (p=0.047; **Figure 3.11B**) and cytoplasmic (p=0.040; **Figure 3.11D**) CBLL1 expression was significantly higher in patients with more rapid PCa recurrence (within two years) compared with those whose PCa recurred later (n=32).

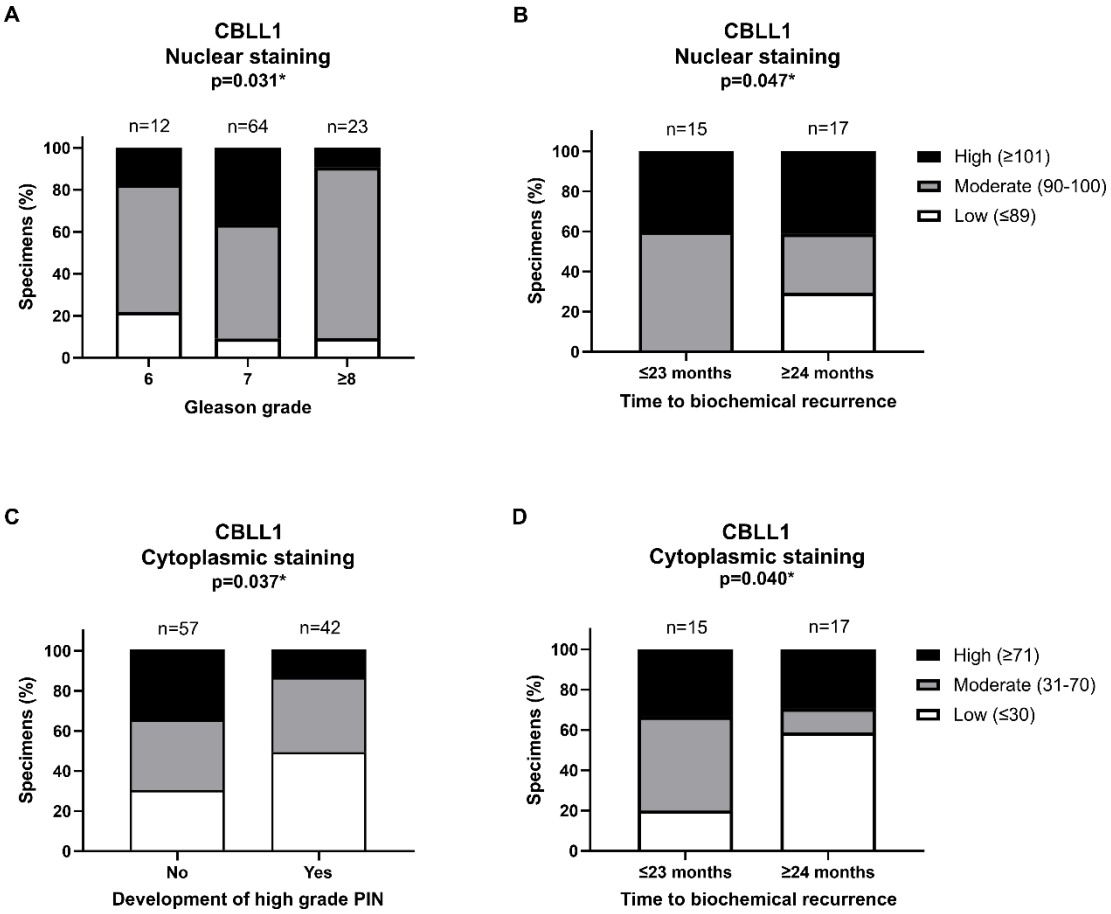


**Figure 3.11 Significant correlations of clinicopathological parameters with CBLL1 expression in prostate cancer patient tissue samples in Nottingham cohort TMA**

IHC analysis of patient tumour samples (n=99) were assessed by H-score, stratified into low (<89 nuclear CBLL1; ≤30 cytoplasmic CBLL1), moderate (90-100 nuclear CBLL1; 31-70 cytoplasmic CBLL1) and high (≥101 nuclear CBLL1; ≥71 cytoplasmic CBLL1) expression groups and correlated with Gleason grade, biochemical recurrence, and high-grade PIN. (**A**) Correlation of CBLL1 nuclear staining and overall Gleason grade (n=99). (**B**) Correlation of CBLL1 nuclear staining and time to biochemical recurrence (n=32). (**C**) Correlation of CBLL1 cytoplasmic staining and high-grade PIN (n=99). (**D**) Correlation of CBLL1 cytoplasmic staining and time to biochemical recurrence (n=32). Analysed by $\chi^2$ test.

The clinical significance of CBLL1 in PCa was further investigated by correlating nuclear and cytoplasmic expression with time to biochemical recurrence (BCR) (n=32). CBLL1 expression was dichotomised into equal high and low H-score groups and correlated with BCR-free survival using Kaplan Meier analysis (**Figure 3.12**). Whilst no significant difference in BCR-free survival was seen between the two nuclear expression groups (p>0.05; **Figure 3.12A**), low cytoplasmic CBLL1 expression was associated with longer BCR-free survival (p=0.005; **Figure 3.12B**).

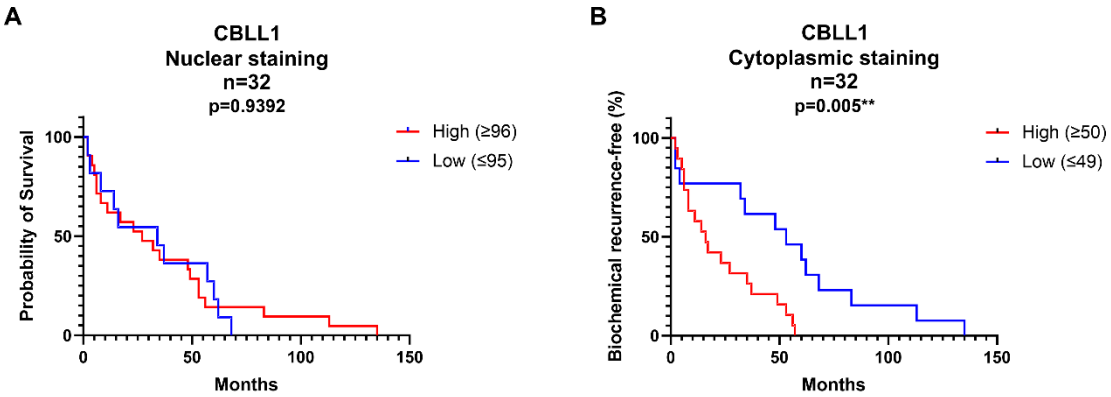


**Figure 3.12 CBLL1 expression correlated with biochemical recurrence-free survival in prostate cancer patients in Nottingham cohort TMA**

IHC staining of 32 patient samples was assessed by H-score, divided into high and low expression groups and correlated with biochemical recurrence-free survival. CBLL1 nuclear staining, low: ≤95, high: ≥96; CBLL1 cytoplasmic staining, low: ≤49, high: ≥50. (**A**) Correlation of CBLL1 nuclear staining and time to biochemical recurrence (n=32). (**B**) Correlation of CBLL1 cytoplasmic staining and time to biochemical recurrence (n=32). Correlated using Kaplan Meier estimate and analysed by log-rank test.

Due to its reported dual role both in the nucleus and cytoplasm, correlation of nuclear and cytoplasmic CBLL1 expression in both non-malignant and prostate tumour specimens was examined (n=142; **Figure 3.13**). No association was found between the level of nuclear and cytoplasmic CBLL1 expression in non-malignant prostatic tissue (n=43; **Figure 3.13A**). A weak positive trend was observed in PCa tumour samples (n=99; **Figure 3.13B**) and in all tissues combined (n=142; **Figure 3.13C**), however this was not statistically significant ($p>0.05$).

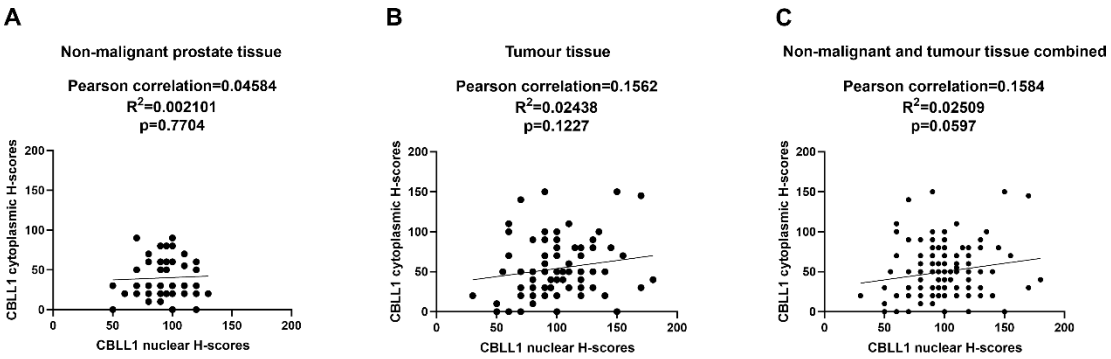


**Figure 3.13 Correlation of nuclear and cytoplasmic expression of CBLL1 in prostate cancer patient tissue samples in Nottingham cohort TMA**

CBLL1 staining H-scores in both the nuclear and cytoplasmic compartment of prostatic luminal cells were correlated to determine association of expression (n=142). (**A**) Correlation of CBLL1 nuclear and cytoplasmic expression in non-malignant prostate tissue (n=43). (**B**) Correlation of CBLL1 nuclear and cytoplasmic expression in tumour tissue (n=99). (**C**) Correlation of CBLL1 nuclear and cytoplasmic expression in non-malignant and tumour tissue combined (n=142). Linear regression and statistical analysis performed using Graphpad Prism, goodness of fit expressed as $R^2$, significance of slope difference from zero expressed as p-value.

Following the previous results that examined the effect of androgen on CBLL1 expression in PCa cell lines, the association between AR and CBLL1 expression in PCa patients was then analysed (**Figure 3.14**). A moderate positive correlation was observed between nuclear CBLL1 and AR expression in non-malignant ($p<0.0001$; **Figure 3.14A**), tumour ($p<0.0001$; **Figure 3.14B**), and both tissue types combined ($p<0.0001$; **Figure 3.14C**). A weak positive correlation was also found between cytoplasmic CBLL1 and AR expression in tumour tissue ($p=0.0014$; **Figure 3.14E**) , although no significant correlation was seen in non-malignant tissue ($p>0.05$; **Figure 3.14D**) or tumour and non-malignant tissue combined ($p>0.05$; **Figure 3.14F**).

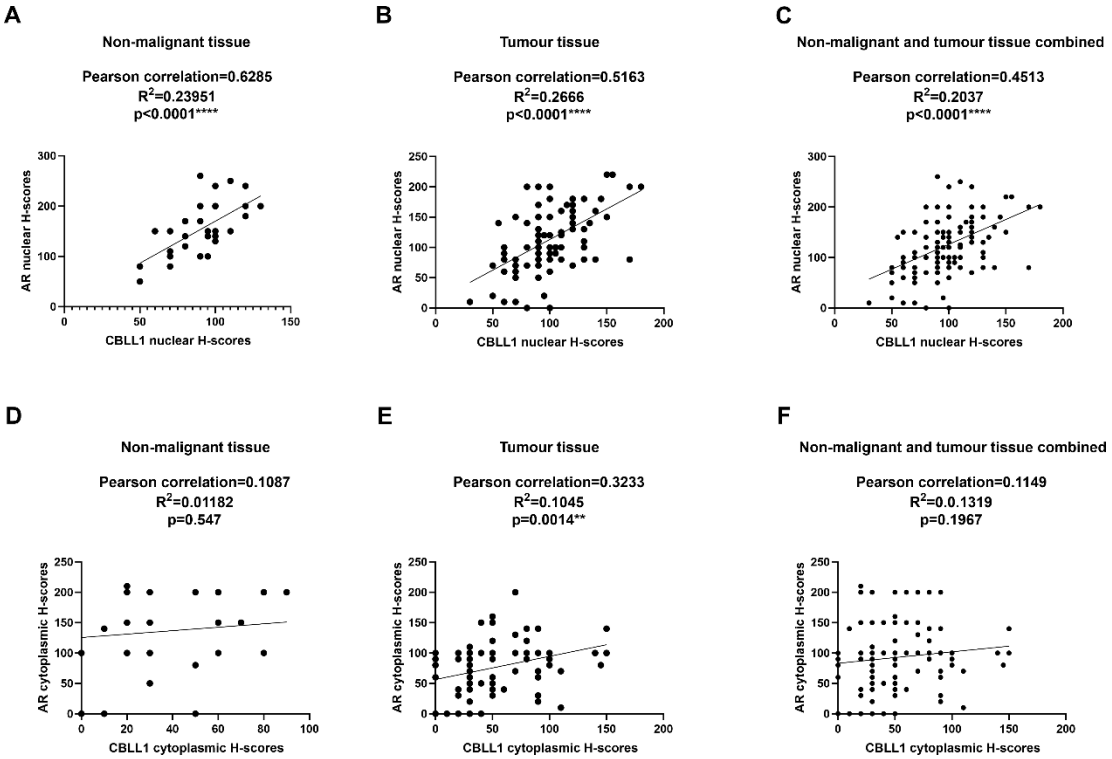


**Figure 3.14 Correlation of CBLL1 and AR expression in prostate cancer patient tissue samples in Nottingham cohort TMA**

CBLL1 and AR staining H-scores in both the nuclear and cytoplasmic compartment of prostatic luminal cells were correlated to determine association of expression (n=128). (**A**) Correlation of CBLL1 and AR nuclear expression in non-malignant prostate tissue (n=33). (**B**) Correlation of CBLL1 and AR nuclear expression in tumour tissue (n=95). (**C**) Correlation of CBLL1 and AR nuclear expression in non-malignant and tumour tissue combined (n=128). (**D**) Correlation of CBLL1 and AR cytoplasmic expression in non-malignant prostate tissue (n=33). (**E**) Correlation of CBLL1 and AR cytoplasmic expression in tumour tissue (n=95). (**F**) Correlation of CBLL1 and AR cytoplasmic expression in non-malignant and tumour tissue combined (n=128). Linear regression and statistical analysis performed using GraphPad Prism, goodness of fit expressed as $R^2$, significance of slope difference from zero expressed as p-value.

### 3.2.5 CBLL1 expression in prostate tissue specimens from Weill Cornell Medicine patient cohorts

To further investigate the expression of CBLL1 protein in PCa patients, immunohistochemistry (IHC) was carried out on two further patient cohorts from Weill Cornell Medicine (WCM), New York, USA. The WCM cohort 1 TMA comprised both non-malignant prostate (n=62) and tumour (n=160) patient samples taken from prostatectomy specimens punched in triplicate (**Figure 3.16**).

As described in chapter 2, CBLL1 staining in both the nucleus and cytoplasm of prostate glandular cells was assessed and given a H-score, with validation from a second scorer following an independent staining evaluation of 10% of the triplicates of patient specimens. Concordance between independent scorers of >0.8 intraclass correlation was confirmed. The H-scores for both nuclear and cytoplasmic CBLL1 staining were then divided into three approximately equal groups of low, moderate and high CBLL1 expression. Examples of these three levels of staining intensities in the WCM cohort 1 are shown in **Figure 3.15**.

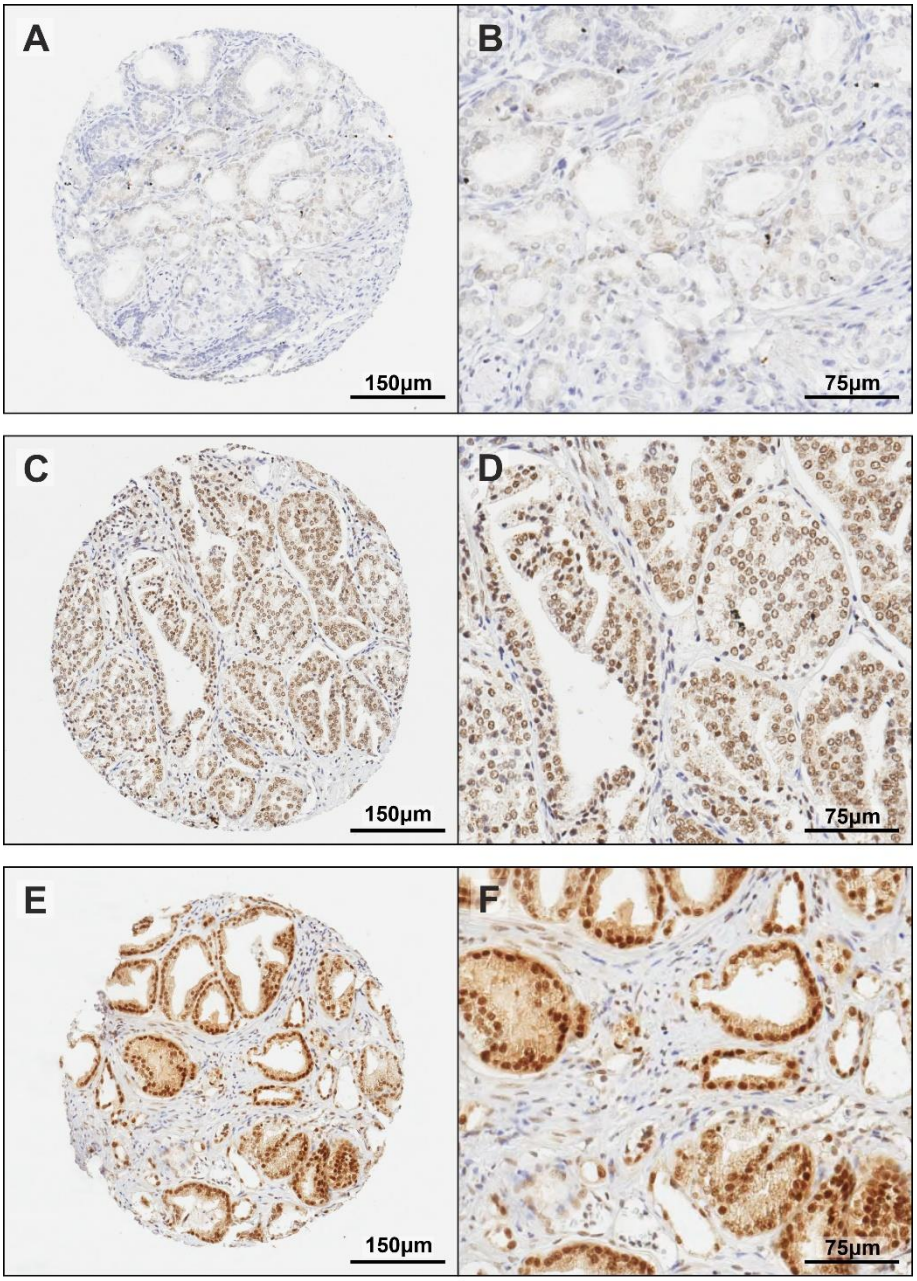


**Figure 3.15 Representative images of CBLL1 IHC staining of WCM cohort 1 TMA of prostate cancer tissue**

IHC staining of prostate cancer patient tissue samples was carried out to determine the nuclear and cytoplasmic expression of CBLL1. (**A** and **B**) Representative images of low level CBLL1 expression. (**C** and **D**) Representative images of moderate level CBLL1 expression. (**E** and **F**) Representative images of high level CBLL1 expression.

Analysis of CBLL1 staining in non-malignant and tumour specimens in the WCM cohort 1 identified that nuclear expression was significantly higher in non-malignant prostatic tissue compared with tumour (p=0.029; **Figure 3.16A**). Conversely, cytoplasmic expression of CBLL1 was found to be higher in tumour specimens compared with non-malignant tissue (p=0.033; **Figure 3.16B**).

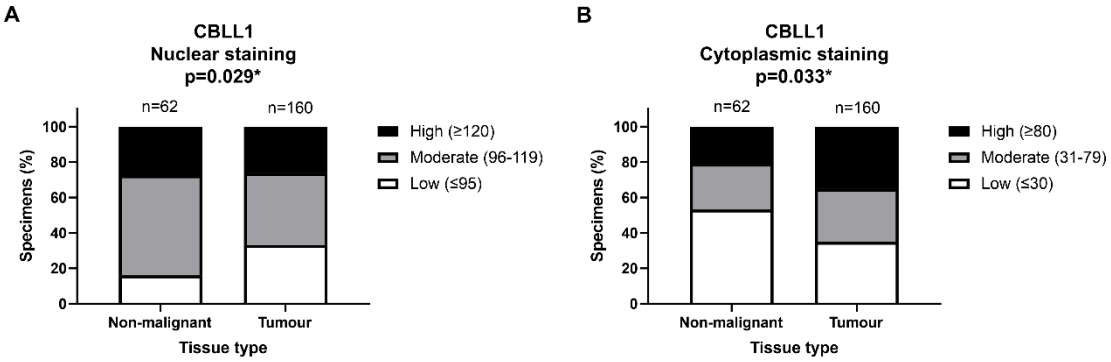


**Figure 3.16 CBLL1 expression in non-malignant prostate and tumour patient tissue samples in WCM cohort 1 TMA**

IHC staining of 222 patient samples was assessed by H-score, divided into high, moderate, and low expression groups and correlated with prostate tissue malignancy. CBLL1 nuclear staining, low: ≤95, moderate: 96-119, high: ≥120; CBLL1 cytoplasmic staining, low: ≤30, moderate: 31-79, high: ≥80. (**A**) Correlation of CBLL1 nuclear staining and prostate malignancy (n=222). (**B**) Correlation of CBLL1 cytoplasmic staining and prostate malignancy (n=222). Analysed by $\chi^2$ test.

CBLL1 expression in the WCM cohort 1 tumour samples was subsequently correlated with clinicopathological parameters from patients' medical records (n=91; **Figure 3.11**, **Appendix 3** and **Appendix 4**). No statistically significant association between either nuclear or cytoplasmic CBLL1 expression with overall Gleason grade at diagnosis was found ($p>0.05$), however a trend of higher nuclear expression (**Figure 3.17A**), but lower cytoplasmic expression (**Figure 3.17B**), was seen in cases with a higher Gleason grade. Similarly, no significant correlation was found between CBLL1 expression and TNM stage ($p>0.05$), however a trend of higher expression was observed in cases with a lower TNM stage (**Figure 3.17C**&**D**). Likewise, no significant association was found between CBLL1 expression and BCR ($p>0.05$), however a trend of lower expression was seen in cases with BCR (**Figure 3.17E**&**F**).

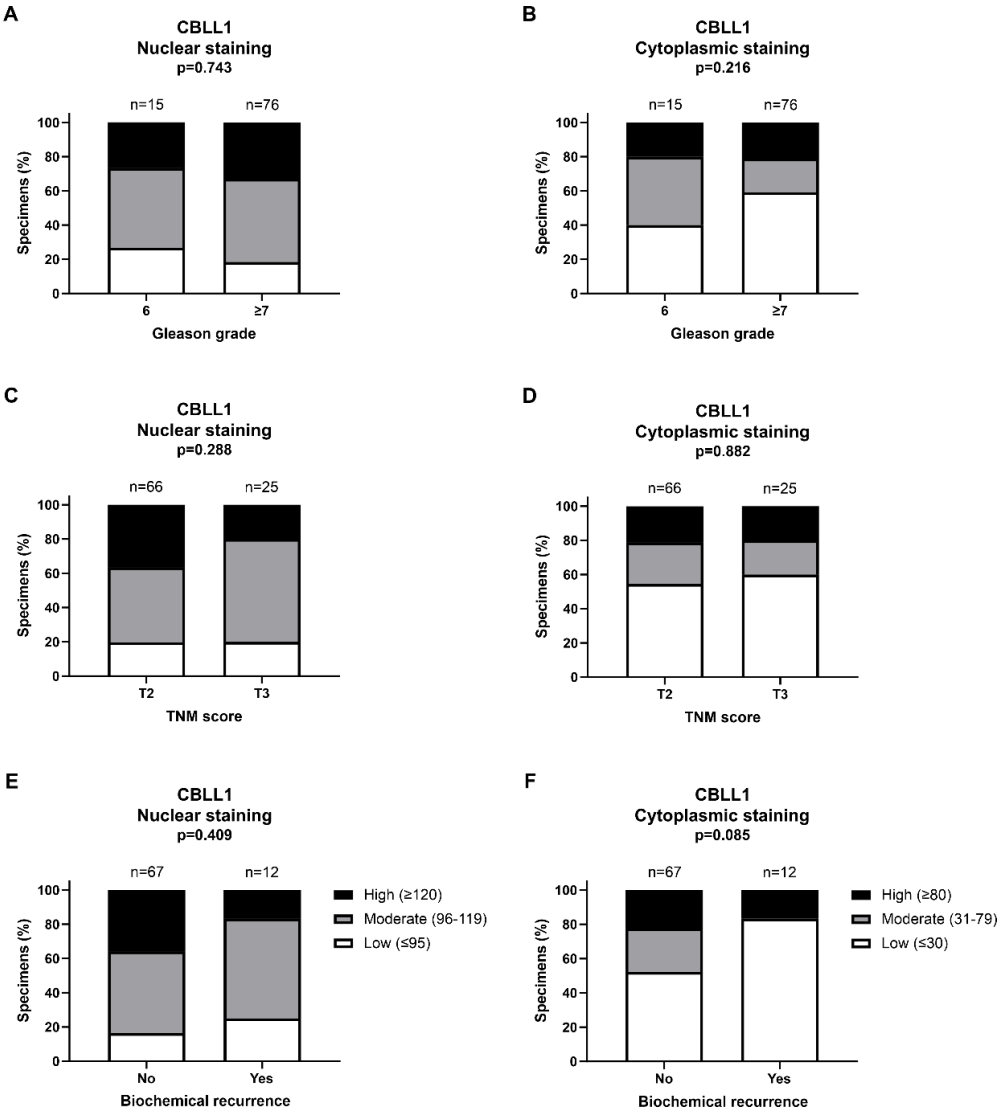


**Figure 3.17 Correlations of clinicopathological parameters with CBLL1 expression in prostate cancer patient specimens in WCM cohort 1 TMA**

IHC staining of 91 patient samples was assessed by H-score, divided into high, moderate, and low expression groups and correlated with Gleason grade, TNM score, and BCR. CBLL1 nuclear staining, low: ≤95, moderate: 96-119, high: ≥120; CBLL1 cytoplasmic staining, low: ≤30, moderate: 31-79, high: ≥80. (**A**) Correlation of CBLL1 nuclear staining and Gleason grade (n=91). (**B**) Correlation of CBLL1 cytoplasmic staining and Gleason grade (n=91). (**C**) Correlation of CBLL1 nuclear staining and TNM score (n=91). (**D**) Correlation of CBLL1 cytoplasmic staining and TNM score (n=91). (**E**) Correlation of CBLL1 nuclear staining and BCR (n=79). (**F**) Correlation of CBLL1 cytoplasmic staining and BCR (n=79). TNM = tumour, node, metastasis; BCR= biochemical recurrence. Analysed by $\chi^2$ test.

The WCM cohort 2 TMA comprised a further set of non-malignant prostate (n=29) and tumour (n=131) patient specimens taken at rapid autopsy and then punched in triplicate (**Figure 3.19**). In cohort 2 the tumour samples were stratified into primary adenocarcinoma (n=42) and advanced PCa (n=89) cases. The advanced PCa group comprised cases of locally advanced, metastatic, CRPC and NEPC (**Figure 3.19**). Examples of the three levels of staining intensities in the WCM cohort 2 are shown in **Figure 3.18**.

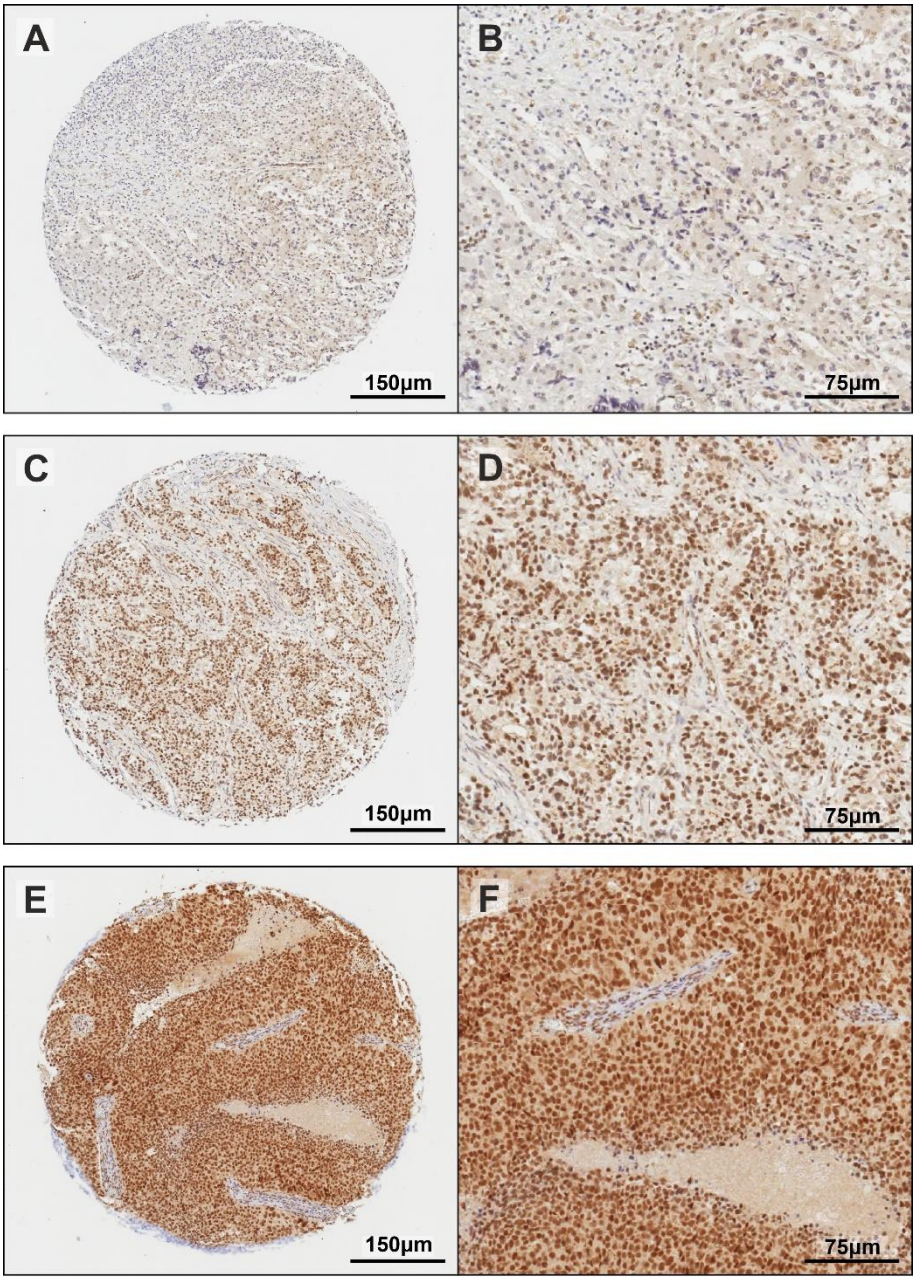


**Figure 3.18 Representative images of CBLL1 IHC staining of WCM cohort 2 TMA of prostate cancer tissue**

IHC staining of prostate cancer patient tissue samples was carried out to determine the expression of CBLL1. (**A** and **B**) Representative images of low level CBLL1 expression. (**C** and **D**) Representative images of moderate level CBLL1 expression. (**E** and **F**) Representative images of high level CBLL1 expression.

Analysis of CBLL1 staining in non-malignant and tumour specimens in the WCM cohort 2 revealed no significant correlation between either nuclear or cytoplasmic CBLL1 expression and malignancy ($p>0.05$), however a trend of higher expression in tumour tissue was seen (**Figure 3.19A**&**B**). Cytoplasmic expression of CBLL1 was found to be higher in cases of advanced PCa than in primary adenocarcinoma ($p<0.0001$; **Figure 3.19D**). Whilst statistical significance was not achieved, the opposite trend was observed in nuclear CBLL1 expression ($p>0.05$; **Figure 3.19C**).

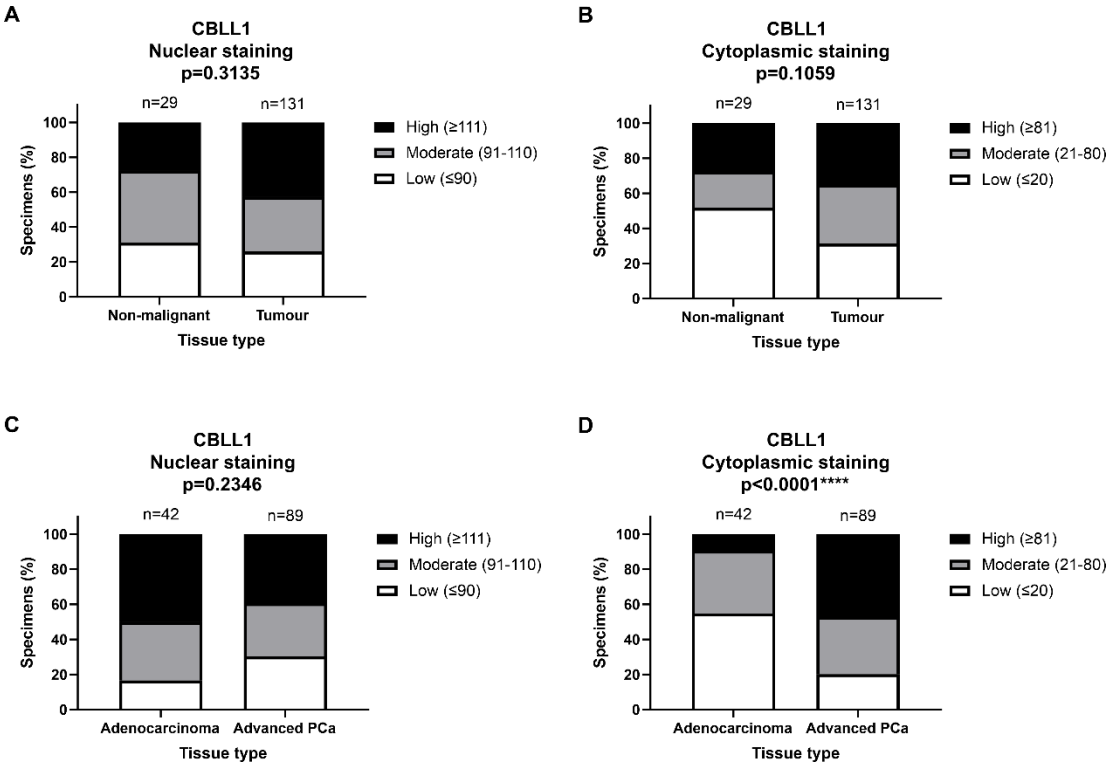


**Figure 3.19 CBLL1 expression in non-malignant prostate and tumour patient tissue samples in WCM cohort 2 TMA**

IHC staining of 162 patient samples was assessed by H-score, divided into high, moderate, and low expression groups and correlated with prostate tissue malignancy. CBLL1 nuclear staining, low: ≤90, moderate: 91-110, high: ≥111; CBLL1 cytoplasmic staining, low: ≤20, moderate: 21-80, high: ≥81. (**A**) Association of CBLL1 nuclear staining and prostate malignancy (n=162). (**B**) Association of CBLL1 cytoplasmic staining and prostate malignancy (n=162). (**C**) Association of CBLL1 nuclear staining and progression of PCa (n=131). (**D**) Association of CBLL1 cytoplasmic staining and progression of PCa (n=131). Advanced PCa comprises cases of locally advanced and metastatic PCa, CRPC and NEPC. Analysed by $\chi^2$ test. CRPC= Castrate-resistant PCa; NEPC= Neuroendocrine PCa.

As with the Nottingham cohort, correlation of nuclear and cytoplasmic CBLL1 expression in patient specimens was subsequently examined in both WCM cohorts combined (n=406; **Figure 3.20**). A moderate positive correlation was observed between nuclear and cytoplasmic CBLL1 expression in non-malignant (p<0.0001; **Figure 3.20A**), tumour (p<0.0001; **Figure 3.20B**), and non-malignant, high-grade PIN and tumour tissues combined (p<0.0001; **Figure 3.20C**).

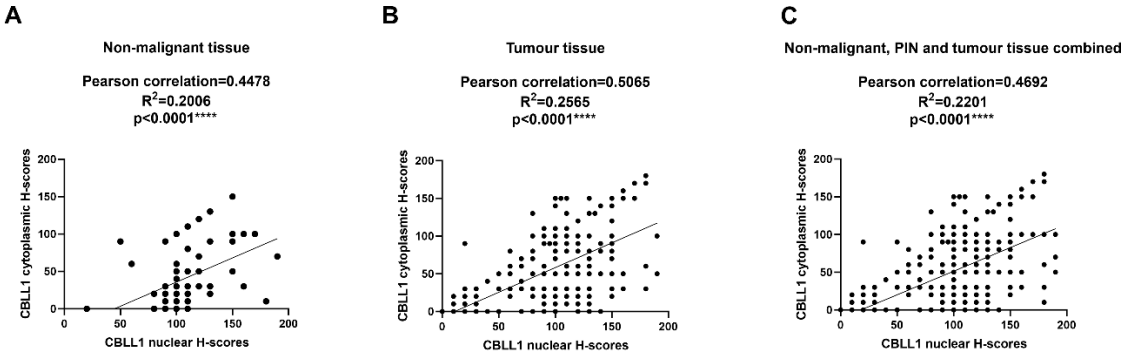


**Figure 3.20 Correlation of nuclear and cytoplasmic expression of CBLL1 in prostate cancer patient tissue samples in WCM cohorts 1 and 2 TMA**

CBLL1 staining H-scores in both the nuclear and cytoplasmic compartment of prostatic luminal cells were correlated to determine association of expression (n=406). (**A**) Association of CBLL1 nuclear and cytoplasmic expression in non-malignant prostate tissue (n=91). (**B**) Association of CBLL1 nuclear and cytoplasmic expression in tumour tissue (n=291). (**C**) Association of CBLL1 nuclear and cytoplasmic expression in non-malignant, PIN and tumour tissue combined (n=406). Linear regression and statistical analysis performed using Graphpad Prism, goodness of fit expressed as $R^2$, significance of slope difference from zero expressed as p-value.

A summary of the correlations of subcellular location of CBLL1 expression with tissue type and patient outcome in the different cohorts analysed is presented in **Table 3.1**. Cytoplasmic CBLL1 expression was found to be significantly higher in tumour compared with non-malignant prostate tissue in both the Nottingham ($p=0.009$) and WCM 1 ($p=0.033$) cohorts, with a similar trend seen in the WCM cohort 2 ($p>0.05$). Conversely, nuclear CBLL1 expression was significantly lower in tumour than non-malignant tissue in the WCM cohort 1 ($p=0.029$), although the opposite trend, which aligns with the cytoplasmic findings, was observed in both the Nottingham and WCM 2 cohorts ($p>0.05$). Moreover, cytoplasmic CBLL1 expression was found to be significantly higher in advanced PCa than in primary adenocarcinoma cases ($p<0.0001$), whilst the inverse trend was seen with nuclear expression ($p>0.05$). In the Nottingham cohort higher expression of nuclear and cytoplasmic CBLL1 was associated with a number of poorer patient outcomes ($p<0.05$), however no significant associations were seen in the WCM cohort 1 ($p>0.05$).

| | Nottingham TMA | | WCM Cohort 1 TMA | | WCM Cohort 2 TMA | |
|---|---|---|---|---|---|---|
| **Key findings** | **Nuclear CBLL1 expression** | **Cytoplasmic CBLL1 expression** | **Nuclear CBLL1 expression** | **Cytoplasmic CBLL1 expression** | **Nuclear CBLL1 expression** | **Cytoplasmic CBLL1 expression** |
| CBLL1 expression level associated with tumour vs non-malignant tissue | High p=0.219 | **High p=0.009**** | **Low p=0.029*** | **High p=0.033*** | High p=0.314 | High p=0.106 |
| CBLL1 expression level associated with advanced PCa | - | - | - | - | Low p=0.235 | **High p<0.0001****** |
| CBLL1 expression level associated with poorer patient outcomes | **High p=0.030*; 0.047*** | **High p=0.005**; 0.037*** | No association | No association | - | - |

**Table 3.1 CBLL1 IHC staining summary**

Summary of nuclear and cytoplasmic CBLL1 IHC H-scores and their observed association with prostatic malignancy, advanced PCa, and poorer patient outcomes and prognostic indicators across the Nottingham and both WCM cohorts 1 and 2. Statistical p-values determined by $\chi^2$-test and $p \leq 0.05$ highlighted in bold.

## 3.3 Discussion

A number of recent studies have implicated components of the $m^6A$ methyltransferase protein complex in many cancer types, including PCa (Bansal et al., 2014, Liu et al., 2018b, Paris et al., 2019, Vu et al., 2017, Wang et al., 2020b, Zhou et al., 2020). However, there is currently a lack of detailed clinical and mechanistic understanding of the expression of the distinct methyltransferase components in PCa (Cotter et al., 2021, Haigh et al., 2022) and the function and clinical relevance of CBLL1 in PCa remains poorly understood.

This chapter focussed on the role of CBLL1 in PCa patient specimens and cell lines, which has not previously been reported. One prior study focussed on E-cadherin expression did describe changes in CBLL1 expression in response to silibinin treatment in the PCa cell lines PC3, PC3MM2 and LNCaP:C4-2B (Deep et al., 2011). Another recent study reported on *CBLL1* mRNA expression only in a publicly available PCa patient database without independent protein validation in other cohorts (Su et al., 2021). This study therefore provides the first detailed analysis of CBLL1 expression in PCa cell lines and patients in order to elucidate its potential role in PCa development and progression.

Initially, bioinformatic analysis was carried out on published PCa datasets using the cBioPortal for Cancer Genomics (Cerami et al., 2012, Gao et al., 2013). *CBLL1* copy number was most frequently altered, and indeed amplified, in patients with metastatic PCa, compared with primary adenocarcinoma patients and, interestingly, not altered at all in patients with CRPC or NEPC (**Figure 3.1A**). Where mRNA expression of *CBLL1* was altered it was most frequently upregulated (**Figure 3.1B**). This may suggest an association

between *CBLL1* and more advanced PCa. Whilst little is currently known about the role of *CBLL1* in PCa, these findings may suggest an oncogenic function. This is supported by previous reports of increased *CBLL1* expression in other cancer types (Castosa et al., 2018, Figueroa et al., 2009b, Hui et al., 2019) and of *CBLL1* knockdown resulting in arrested cell cycle and reduced cellular proliferation (Horiuchi et al., 2013).

The majority of cases in both the primary adenocarcinoma and metastatic PCa cohorts are diploid for *CBLL1.* However, a trend of increased *CBLL1* expression was seen in those limited cases with copy number gain and amplification, with decreased expression seen in the few cases with copy number shallow and deep deletion (**Figure 3.2**). Taken together these findings suggested a role for aberrant *CBLL1* expression in PCa that warrants further investigation.

No significant difference in *CBLL1* expression was found between normal prostate and primary tumour tissue in the TCGA Firehose Legacy patient dataset (Goldman et al., 2020) (**Figure 3.3A**), nor between different outcomes following therapy (**Figure 3.3B**), or between cases with or without BCR (**Figure 3.3C**).

In order to further understand the role of CBLL1 in PCa, its expression was analysed at both the mRNA and protein level in PCa cell lines and compared with the non-malignant control cell line PNT1A. *CBLL1* was expressed in all cells examined, and moreover expressed at a significantly higher level in all PCa cell lines except PC3 when compared with non-malignant PNT1A cells (**Figure 3.4A**). Within the PCa cell lines, the highest *CBLL1* expression was

observed in the AR-expressing androgen-responsive cell lines, with ~30 to 45-fold higher *CBLL1* expression observed in the LNCaP, LNCaP:C4-$2_{LT}$, LNCaP:C4-$2_{enzR}$ and 22Rv1 cell lines (**Figure 3.4A**). CBLL1 protein expression was detected in all cell lines examined and was largely consistent with *CBLL1* mRNA (**Figure 3.4B**). These findings are consistent with prior studies which analysed CBLL1 expression both at the mRNA and protein level and found that this was higher in colon tumours than in non-malignant colon tissue, with CBLL1 expression progressively higher in tissue from carcinoma of advancing stage (Castosa et al., 2018). Similarly, other studies have reported higher expression of CBLL1 in lung cancer and hepatocellular carcinoma compared with non-malignant cells and tissue (Hui et al., 2019, Liu et al., 2018b, Liu et al., 2018c). Taken together, these results support a possible role for CBLL1 in PCa development and progression.

Given that the highest expression of *CBLL1* was observed in the androgen-responsive PCa cell lines, it was decided to establish whether *CBLL1* expression was androgen-regulated. As circulating androgens and their interactions with the AR are known to be essential both for normal prostate physiology as well as PCa development (Shen and Abate-Shen, 2010), a mechanistic link between *CBLL1* and androgen signalling would be a key finding in establishing its role in PCa. *CBLL1* mRNA expression was found to be significantly upregulated following androgen treatment in LNCaP (**Figure 3.5A**), LNCaP:C4-2 (**Figure 3.5B**) and LNCaP:C4-$2_{enzR}$ (**Figure 3.5D**), but interestingly was significantly downregulated in 22Rv1 cells (**Figure 3.5C**). One explanation for this could be that 22Rv1 cells express the alternatively-spliced AR variant ARv7, which lacks the ligand binding domain and is able to induce

a different transcriptional profile to the full-length AR (Hu et al., 2012, Jenster et al., 1991). In the one available publication that has mentioned *CBLL1* with respect to androgen regulation of gene expression, analysis of four microarray studies suggested that *CBLL1* may be androgen-regulated (Jin et al., 2013). STARR-Seq analysis supports androgen regulation of both the proximal promoter region at the 5' end and the second exon of the *CBLL1* gene (**Figure 3.8**), suggesting that *CBLL1* is indeed androgen-regulated.

When looking at the whole protein, androgen treatment did not induce detectable changes in CBLL1 expression in the androgen-responsive PCa cell lines, under the conditions employed (**Figure 3.6**). However, when the nuclear and cytoplasmic protein fractions were isolated and examined, CBLL1 expression in both subcellular compartments was obviously increased in response to androgen treatment (**Figure 3.7**).

The influence of androgen on subcellular localisation and expression of CBLL1 in PCa cell lines was investigated due to its reported dual role in both nuclear m6A methylation (Horiuchi et al., 2013, Ruzicka et al., 2017) and cytoplasmic regulation of E-cadherin (Fujita et al., 2002). CBLL1 was expressed in both the nuclear and cytoplasmic protein fractions but was particularly enriched in the nuclear fraction, and expression in both fractions increased following androgen treatment (**Figure 3.7**). One study found that CBLL1 protein was found mostly in the nucleus of mouse embryonic stem cells, but that the zinc finger protein ZC3H13 is required for the nuclear localisation of the CBLL1-WTAP-VIRMA protein complex, which in turn is important for m$^6$A RNA methylation (Wen et al., 2018). In the absence of ZC3H13, a significantly higher proportion of CBLL1 was found to be located in the cytoplasm (Wen et al., 2018). Another

study reported a predominantly nuclear localisation of CBLL1 in a number of kidney and breast cancer cell lines (Figueroa et al., 2009a).

The clinical relevance of CBLL1 protein expression in PCa patients was subsequently investigated by carrying out IHC staining and analysis of PCa TMA specimens from the Nottingham and two Weil Cornell Medicine patient cohorts. IHC analysis concurred with the previously discussed western blot findings (**Figure 3.7**) and the reported nuclear (Horiuchi et al., 2013, Ruzicka et al., 2017) and cytoplasmic (Fujita et al., 2002) roles of CBLL1, and expression of CBLL1 was detected and analysed in both the nuclear and cytoplasmic compartments of PCa cells. More intense CBLL1 expression was seen in the nucleus of both malignant and non-malignant prostate cells, compared to the cytoplasm (**Figure 3.9**, **Figure 3.15** and **Figure 3.18**). CBLL1 nuclear and cytoplasmic staining in the three patient cohorts was assessed using H-score, stratified and correlated with a number of clinicopathological parameters (**Appendices 1-4**).

The level of CBLL1 expression was compared between non-malignant and prostate tumour samples across all cohorts (**Figure 3.10**, **Figure 3.16**, **Figure 3.19** and **Table 3.1**). Significantly higher cytoplasmic expression of CBLL1 was observed in tumour samples compared with non-malignant prostate tissue in both the Nottingham and WCM 1 cohorts, with the same trend seen in the WCM 2 cohort. Cytoplasmic CBLL1 expression was also found to be significantly higher in advanced PCa specimens than in primary adenocarcinoma (**Figure 3.19D**). Nuclear CBLL1 expression was not as concordant across the different patient cohorts. Trends of higher nuclear expression in tumour compared with non-malignant tissue in both the Nottingham and WCM 2 cohorts were seen,

although these did not achieve statistical significance. Conversely, nuclear CBLL1 expression was significantly lower in the WCM 1 patient cohort in tumour vs non-malignant tissue (**Figure 3.16A**). A similar trend of lower nuclear CBLL1 expression in advanced PCa compared with primary adenocarcinoma was observed in the WCM cohort 2 (**Figure 3.19C**), although this did not reach statistical significance.

Correlations of CBLL1 expression and all available deidentified patient clinicopathological data were then completed to determine the potential clinical relevance and prognostic value of CBLL1 in PCa in the Nottingham and WCM 1 cohorts (**Figure 3.11**, **Figure 3.12**, **Figure 3.17**, **Table 3.1** and **Appendices 1-4**). No clinical data were available for the WCM cohort 2. In the Nottingham cohort, nuclear CBLL1 expression was significantly higher in patients with a higher overall Gleason grade at diagnosis (**Figure 3.11A**), a poor prognostic indicator (Gleason, 1966, Gleason and Mellinger, 1974, Gordetsky and Epstein, 2016), and in those patients whose PCa recurred within 2 years (**Figure 3.11B**). Cytoplasmic CBLL1 expression was also significantly higher in those patients with a more rapid biochemical recurrence (**Figure 3.12B**), although interestingly was higher in patients whose PCa recurred within 23 months (**Figure 3.11D**). Cytoplasmic CBLL1 expression was found to be lower in patients with high-grade PIN (**Figure 3.11C**), a PCa precursor lesion widely considered to be associated with poorer outcomes (Trabzonlu et al., 2019). No significant associations were seen between nuclear or cytoplasmic CBLL1 expression and any clinicopathological parameter examined in the WCM 1 cohort (**Figure 3.17**).

Taken together these findings suggest a pro-oncogenic role for CBLL1 in PCa and support previous studies that reported significantly higher CBLL1 protein expression in other cancer types compared with non-malignant tissues (Castosa et al., 2018, Figueroa et al., 2009b, Hui et al., 2019). Moreover, consistent with this study's findings of higher CBLL1 expression in more advanced PCa, increased CBLL1 expression has also been reported in colon carcinoma tissue with advancing stage (Castosa et al., 2018).

Given the two reported functions of CBLL1, nuclear and cytoplasmic expression of CBLL1 in all cohorts was correlated to determine any association between them (**Figure 3.13** and **Figure 3.20**). H-scores from the WCM cohorts were combined and significant positive correlations between nuclear and cytoplasmic CBLL1 expression were seen in non-malignant, high-grade PIN and tumour tissue (**Figure 3.20**). Whilst no significant correlation between nuclear and cytoplasmic expression was found in the Nottingham cohort, consistent with the results obtained in the WCM cohort, a weak positive trend was observed in all tissue types (**Figure 3.13**). This positive correlation may suggest that the potential oncogenic action of CBLL1 may function both through its role as part of the nuclear methyltransferase protein complex and its impact on E-cadherin degradation in the cytoplasm simultaneously.

Expression of AR and CBLL1 was correlated in the Nottingham patient cohort. A significant positive correlation was observed between nuclear CBLL1 and AR expression in both non-malignant and tumour tissue, and between cytoplasmic CBLL1 and AR expression in tumour tissue (**Figure 3.14**). This is supported by Chip-Seq analysis that found that AR binds in the proximal promoter region of *CBLL1*, is a direct AR target (**Figure 3.8**), and accords with

a previous study that reported that *CBLL1* may be regulated by androgen (Jin et al., 2013). Taken together these findings strongly suggest that *CBLL1* expression is androgen-regulated.

It is interesting that CBLL1 expression was positively correlated with cytoplasmic AR expression in patient samples in the Nottingham PCa cohort (**Figure 3.14**). Whilst not currently well understood, there is increasing evidence that the cytoplasmic function of AR is important, and may contribute to the development of AR variants and progression to a castrate-resistant state (Jenster et al., 1993, Ni et al., 2013, Zhan et al., 2017).

In summary, bioinformatic analysis of *CBLL1* revealed that copy number gain, gene amplification and increased mRNA expression are the most common genomic alterations affecting this locus in PCa. CBLL1 was expressed at the mRNA and protein level in both non-malignant and PCa cells, with the highest expression levels seen in AR-expressing PCa cell lines sensitive to androgen. *CBLL1* expression appears to be androgen-regulated, with androgen treatment significantly upregulating expression of *CBLL1* in LNCaP, LNCaP:C4-2 and LNCaP:C4-$2_{enzR}$ cells but downregulating it in 22Rv1 cells. This result in 22Rv1 cells may be due to the expression of AR variants which are known to modulate and alter AR-signalling, thereby altering the transcriptional profile from the full-length AR (Basil et al., 2022, Li et al., 2020c, Tietz and Dehm, 2020, Zadra et al., 2019). Furthermore, correlation of CBLL1 and AR in PCa tissue samples showed a positive association in the expression of these two proteins. Work in both PCa cell lines and patient PCa specimens demonstrated that CBLL1 protein is expressed both in the nucleus and cytoplasm as expected from its dual reported roles in both locations, but is enriched in the nucleus. IHC

analysis of three different cohorts of PCa patient tissue specimens demonstrated that overall, higher expression of CBLL1 in both the nucleus and cytoplasm was associated with malignancy and poorer patient outcomes. These results implicate a role for CBLL1 in the development and progression of PCa and further work is indicated to further elucidate its potential as prognostic indicator or therapeutic target.

# Chapter 4

## Functional role of CBLL1 in prostate cancer cell lines

# 4 Functional role of CBLL1 in prostate cancer cell lines

## 4.1 Introduction

PCa continues to be a global health problem, as the most commonly diagnosed cancer types in males in the western hemisphere, and second most commonly diagnosed cancer worldwide (Sung et al., 2021). Androgen signalling through the androgen receptor (AR) is the main driver of prostate adenocarcinoma initiation and progression, with suppression of this via androgen deprivation therapy (ADT) a cornerstone of treatment for advanced PCa (Heidenreich et al., 2014). However, in the majority of cases, despite an initial positive response to ADT, within approximately two years ADT often fails as the PCa progresses to an androgen-independent or castrate-resistant state (Gravis et al., 2013, Sweeney et al., 2015, van der Kwast et al., 1991). However, even within this so-called androgen-independent phase of PCa progression, it has been found that AR signalling persists through a number of mechanisms including mutation and/or amplification of the *AR* gene, expression of *AR* variants, altered androgen biosynthesis, and co-regulator modification (Chandrasekar et al., 2015, Jernberg et al., 2017).

Alternative splicing, whereby different transcripts and ultimately different proteins are encoded by the same gene (Ast, 2004), has been implicated in many cancer types, including prostate (He et al., 2009, Kahles et al., 2018, Paschalis et al., 2018). Steroid hormone receptors have been associated with significantly changing alternative splicing events in target genes through the recruitment of a number of coregulators (Auboeuf et al., 2004, Auboeuf et al., 2005). A number of pathogenic AR splice variants have been identified in

castrate-resistant PCa (CRPC) patients that enable persistent AR signalling despite a low-level androgen environment (Jernberg et al., 2017). Arguably the most clinically relevant in CRPC is ARv7, known to function independently of its androgen ligand due to the absence of the C-terminal ligand-binding domain and therefore contributes to resistance to a number of ADTs, including enzalutamide (Antonarakis et al., 2014, Cao et al., 2014, Dehm and Tindall, 2011).

A number of studies have reported a role for the RNA $m^6A$ modification and many of its individual 'writer', 'reader' and 'eraser' proteins in alternative splicing (Alarcón et al., 2015, Dominissini et al., 2012, Haigh et al., 2022, Haussmann et al., 2016, Horiuchi et al., 2013, Lence et al., 2016, Lothion-Roy et al., 2022, Ping et al., 2014, Su et al., 2022, Yang et al., 2018, Zhao et al., 2014). However, there has been limited examination of the role of CBLL1 specifically in alternative splicing or PCa.

Several genes have been reported as key drivers of enzalutamide resistance in PCa. These include *MET*, which encodes a tyrosine kinase receptor that has been linked to PCa progression through upregulation of both the ATM/ATR and PI3K/Akt signalling pathways (Lee and Smith, 2013, Qiao et al., 2016, Zhou et al., 2021c), and *VEGFR*, encoding the vascular endothelial growth factor receptor (Lee and Smith, 2013, Modena et al., 2016). Additionally, the proneuronal transcription factor encoded by *ASCL1* has also been implicated in enzalutamide resistance through stimulating progression to a neuroendocrine phenotype (Nouruzi et al., 2022).

In chapter 3 it was found that CBLL1-expression is androgen-regulated and that the highest CBLL1 expression was seen in AR-expressing PCa cell lines. Moreover, in the patient samples examined, it was found that both nuclear and cytoplasmic expression of CBLL1 were associated with malignancy and negative patient outcomes. These findings are supported by a number of studies in other cancer types of the gastrointestinal tract and lung, which reported that CBLL1 expression was associated with malignancy and cancer progression (Castosa et al., 2018, Figueroa et al., 2009b, Hui et al., 2019, Liu et al., 2018b, Liu et al., 2018c). However, the results presented in chapter 3, as well as those reported in the numerous studies mentioned above, are in contrast with the one previous PCa-specific study which analysed *CBLL1* mRNA, but not protein expression, in publicly available PCa patient datasets (Su et al., 2021). Su and colleagues (2021) found CBLL1 to be a crucial $m^6A$ regulator in PCa, reporting that lower *CBLL1* expression was associated with PCa development and progression.

Given the association between CBLL1 and PCa found in chapter 3, the functional role of CBLL1 in PCa gene regulation and androgen signalling was investigated here. Moreover, the role of CBLL1 was investigated in the development of castrate resistance, signified by resistance to the ADT enzalutamide. The effect of siRNA-mediated *CBLL1* depletion, both with and without androgen treatment, was therefore analysed in the AR-expressing PCa cell line LNCaP:C4-2 and compared with its enzalutamide-resistant counterpart LNCaP:C4-$2_{enzR}$. Knockdown of *CBLL1* was confirmed both at the protein and mRNA level, before its effect on AR expression and PCa cell phenotype was assessed. The impact of siRNA-mediated *CBLL1* depletion and

androgen treatment on gene expression and splicing was then analysed by RNA-Seq. Collectively, these results reveal the functional role of CBLL1 in PCa, progression to a castrate-resistant disease state, and androgen signalling.

## 4.2 Results

### 4.2.1 siRNA depletion of *CBLL1* in prostate cancer cell lines

To investigate the role of CBLL1 in the regulation of androgen signalling, siRNA-mediated functional depletion of *CBLL1* (si*CBLL1*) was initially carried out in the AR-expressing castrate-resistant PCa cell lines LNCaP:C4-2, both parental and enzalutamide-resistant (LNCap:C4-$2_{enzR}$), and 22Rv1, which also expresses AR variants. Cells were transfected twice during a six day experiment with either si*CBLL1* or scrambled control (si*Scr*) and were treated with either vehicle or R1881 (as described in chapter 2) prior to harvesting for analysis of protein and mRNA by western blot and qRT-PCR, respectively.

*CBLL1* knockdown was confirmed at the protein level in LNCaP:C4-2 parental cells, with a ~5-fold decrease ($p<0.01$) in expression observed between vehicle-treated cells, with a more modest decrease in CBLL1 expression observed between androgen-treated cells which did not reach statistical significance ($p>0.05$; **Figure 4.1A** and **Figure 4.1D**). Consistent with direct androgen upregulation of *CBLL1* expression, R1881 treatment partially opposed *siCBLL1*-mediated knockdown (**Figure 4.1A** and **Figure 4.1D**), although this did not reach statistical significance ($p>0.05$). Depletion of *CBLL1* resulted in no statistically significant changes in AR expression, although the androgen induction of AR expression did appear to be attenuated by *CBLL1* knockdown ($p>0.05$; **Figure 4.1A** and **Figure 4.1G**).

Significant *CBLL1* knockdown was similarly confirmed at the protein level in LNCaP:C4-$2_{enzR}$ cells, with a ~2-fold decrease ($p<0.05$) in expression observed between vehicle-treated cells, with, again, a more modest decrease in CBLL1 expression observed between androgen-treated cells which did not reach statistical significance ($p>0.05$; **Figure 4.1B** and **Figure 4.1E**). In contrast to the parental LNCaP:C42 cell line, R1881 treatment did not significantly oppose *siCBLL1*-mediated knockdown in LNCaP:$C42_{enzR}$ ($p>0.05$; **Figure 4.1B** and **Figure 4.1E**). Depletion of *CBLL1* resulted in no statistically significant changes in AR expression in LNCaP:C4-$2_{enzR}$ cells, although, unlike in the parental LNCaP:C4-2 cells, there was no apparent attenuation of androgen induction of AR expression by *CBLL1* knockdown, with AR expression higher in *CBLL1*-depleted LNCaP:C4-$2_{enzR}$ cells treated with R1881 than with vehicle ($p<0.05$; **Figure 4.1B** and **Figure 4.1H**).

Significant *CBLL1* knockdown could not be confirmed in vehicle-treated 22Rv1 cells ($p>0.05$) however, significant knockdown was observed in *CBLL1*-depleted 22Rv1 cells treated with R1881 ($p<0.05$; **Figure 4.1C** and **Figure 4.1F**). In contrast to the LNCaP:C4-2 parental cells, androgen did not oppose *siCBLL1*-mediated knockdown by R1881 treatment ($p>0.05$; **Figure 4.1C** and **Figure 4.1F**). No statistically significant changes in AR expression were observed in response to *CBLL1* depletion, including no attenuation of androgen-induced AR expression, rather the opposite effect was observed ($p>0.05$; **Figure 4.1C** and **Figure 4.1I**). It should be noted that the AR signal was too weak to allow visualisation of the AR variants present in 22Rv1, however their presence was subsequently verified on later western blots and through transcript quantification (data not shown).

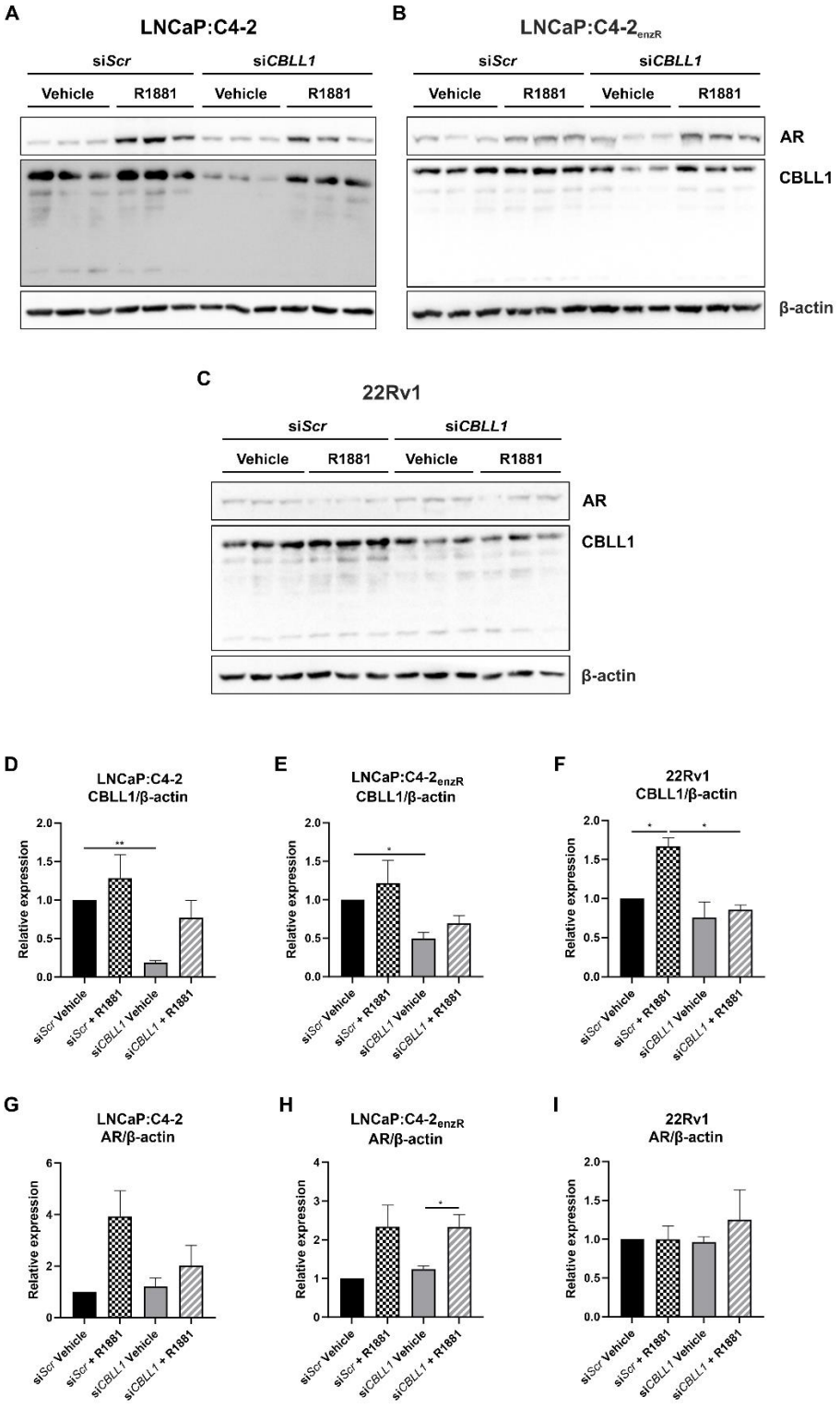


**Figure 4.1 Effect of siRNA-mediated CBLL1 knockdown and R1881 treatment on protein expression in LNCaP:C4-2, LNCaP:C4-2$_{enzR}$ and 22Rv1 cells**

CBLL1 and AR protein expression was analysed by western blot with β-actin loading control following siRNA-mediated knockdown of *CBLL1* and

subsequent treatment for 72 hours with vehicle or R1881. (**A**) AR and CBLL1 protein expression in LNCaP:C4-2 cells following *CBLL1* siRNA-mediated knockdown treated with vehicle or R1881 (n=3). (**B**) AR and CBLL1 protein expression in LNCaP:C4-$2_{enzR}$ cells following *CBLL1* siRNA-mediated knockdown treated with vehicle or R1881 (n=3). (**C**) AR and CBLL1 protein expression in 22Rv1 cells following *CBLL1* siRNA-mediated knockdown treated with vehicle or R1881 (n=3). (**D**) Quantification of CBLL1 protein expression following *CBLL1* siRNA-mediated knockdown treated with vehicle or R1881 in LNCaP:C4-2 cells (n=3). (**E**) Quantification of CBLL1 protein expression following *CBLL1* siRNA-mediated knockdown treated with vehicle or R1881 in LNCaP:C4-$2_{enzR}$ cells (n=3). (**F**) Quantification of CBLL1 protein expression following *CBLL1* siRNA-mediated knockdown treated with vehicle or R1881 in 22Rv1 cells (n=3). (**G**) Quantification of AR protein expression following *CBLL1* siRNA-mediated knockdown treated with vehicle or R1881 in LNCaP:C4-2 cells (n=3). (**H**) Quantification of AR protein expression following *CBLL1* siRNA-mediated knockdown treated with vehicle or R1881 in LNCaP:C4-$2_{enzR}$ cells (n=3). (**I**) Quantification of AR protein expression following *CBLL1* siRNA-mediated knockdown treated with vehicle or R1881 in 22Rv1 cells (n=3). * = $p \leq 0.05$, ** = $p \leq 0.01$, *** = $p \leq 0.001$, **** = $p \leq 0.0001$ by paired t-test.

*CBLL1* knockdown was subsequently examined at the mRNA level in LNCaP:C4-2 parental, LNCaP:C4-$2_{enzR}$ and 22Rv1 cells (**Figure 4.2**). In LNCaP:C4-2 cells a ~3-fold decrease in *CBLL1* expression was observed with *CBLL1* knockdown in both vehicle- and R1881-treated cells ($p<0.0001$; **Figure 4.2A**). Similar to the trend observed at the protein level, R1881 induced *CBLL1* expression and opposed *siCBLL1*-mediated knockdown (~1.5-fold; $p<0.0001$; **Figure 4.2A**).

In LNCaP:C4-$2_{enzR}$ cells a ~2-fold decrease in *CBLL1* expression was observed with *CBLL1* knockdown in vehicle-treated cells ($p<0.0001$; **Figure 4.2B**), with a ~3-fold decrease in expression observed between androgen-treated cells ($p<0.0001$; **Figure 4.2B**). Similar to the trend observed at the protein level, R1881 induced *CBLL1* expression in scrambled control cells, and did not significantly oppose *siCBLL1*-mediated knockdown ($p>0.05$; **Figure 4.2B**).

Whilst significant knockdown of *CBLL1* expression following si*CBLL1* treatment was observed in 22Rv1 cells in both vehicle- and R1881-treated conditions ($p<0.01$), this was only a ~0.2 fold-change (**Figure 4.2C**). Given the small magnitude of *CBLL1* knockdown achieved in 22Rv1 cells at both at the protein and mRNA level despite repeated attempts, the decision was made to prioritise analysis of the LNCaP:C4-2 parental and LNCaP:C4-$2_{enzR}$ cell lines where a more biologically, as well as statistically, significant *CBLL1* depletion had been demonstrated.

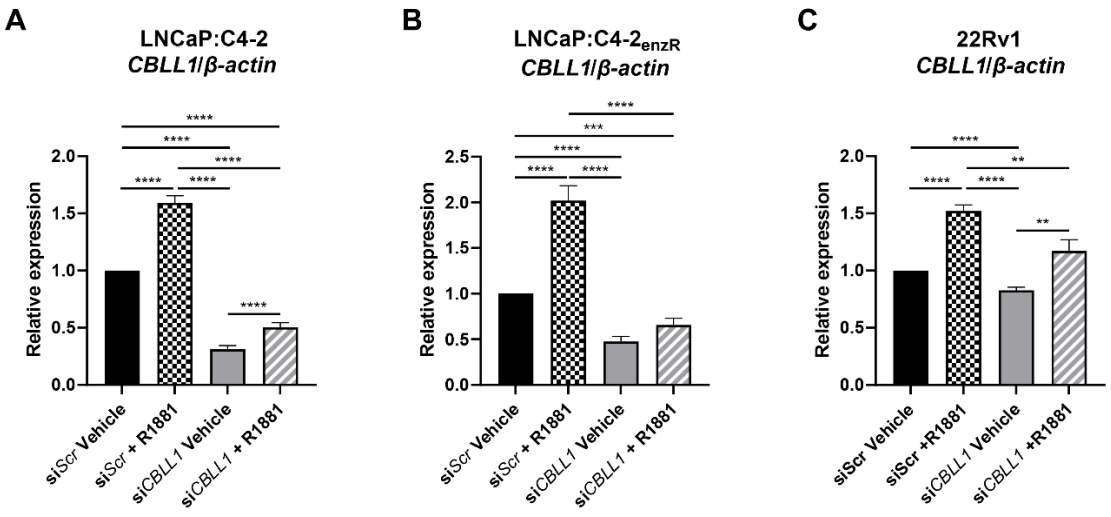


**Figure 4.2 Effect of siRNA-mediated *CBLL1* knockdown and R1881 treatment on *CBLL1* mRNA expression in LNCaP:C4-2, LNCaP:C4-2$_{enzR}$ and 22Rv1 cells**

*CBLL1* mRNA expression in LNCaP:C4-2, LNCaP:C4-2$_{enzR}$ and 22Rv1 cells was analysed by qRT-PCR relative to *β-actin* following siRNA-mediated knockdown of *CBLL1* and subsequent treatment for 72 hours with vehicle or R1881. (**A**) *CBLL1* mRNA expression following *CBLL1* siRNA-mediated knockdown treated with vehicle or R1881 in LNCaP:C4-2 cells (n=6). (**B**) *CBLL1* mRNA expression following *CBLL1* siRNA-mediated knockdown treated with vehicle or R1881 in LNCaP:C4-2$_{enzR}$ cells (n=6). (**C**) *CBLL1* mRNA expression following *CBLL1* siRNA-mediated knockdown treated with vehicle or R1881 in 22Rv1 cells (n=6). * = p ≤0.05, ** = p ≤0.01, *** = p ≤0.001, **** = p ≤0.0001 by paired t-test.

In order to further examine the role of CBLL1 on androgen-regulated gene expression, the impact of *CBLL1* knockdown on the *AR* and the androgen-regulated gene *KLK3*, which encodes the PSA protein used as a biomarker in the detection of PCa, was assessed. *AR* expression was significantly increased with *CBLL1* knockdown in vehicle-treated LNCaP:C4-2 cells (p<0.05; **Figure 4.3A**). Expression of *AR* was significantly decreased by R1881 treatment in

*CBLL1*-depleted cells ($p<0.01$; **Figure 4.3A**), however no significant change in *AR* expression was seen with R1881 treatment in scrambled control cells ($p>0.05$; **Figure 4.3A**). *KLK3* expression was markedly induced (over 100-fold) by R1881 treatment in both scrambled control and *CBLL1*-depleted LNCaP:C4-2 cells ($p<0.0001$; **Figure 4.3B**). A significant increase in *KLK3* expression was also seen with *CBLL1* knockdown in vehicle-treated cells ($p<0.05$). However, *CBLL1* depletion had no significant effect on *KLK3* expression between scrambled control and CBLL1-depleted R1881-treated cells ($p>0.05$; **Figure 4.3B**).

*AR* expression in LNCaP:C4-$2_{enzR}$ cells followed a similar trend to that observed in the parental cell line, with a significant decrease observed in response to R1881 treatment in *CBLL1*-depleted cells ($p<0.05$; **Figure 4.3C**). However, despite the same trend of higher *AR* expression in vehicle-treated *CBLL1*-depleted cells compared with the scrambled control being observed, this did not reach statistical significance ($p>0.05$; **Figure 4.3C**). Likewise, *KLK3* expression in LNCaP:C4-$2_{enzR}$ cells followed a similar trend to that observed in the parental cell line, with R1881 treatment in both scrambled control and *CBLL1*-depleted cells inducing *KLK3* expression, although this induction was lower than in the parental cell line. A ~55-fold and ~20-fold increase in *KLK3* expression was observed in scrambled control and *CBLL1*-depleted cells, respectively, following R1881 treatment ($p<0.0001$; **Figure 4.3B**&**D**). A modest, yet significant, increase in *KLK3* expression was also observed with *CBLL1* knockdown in vehicle-treated cells, with a significant decrease in expression seen in R1881-treated cells ($p<0.05$; **Figure 4.3D**).

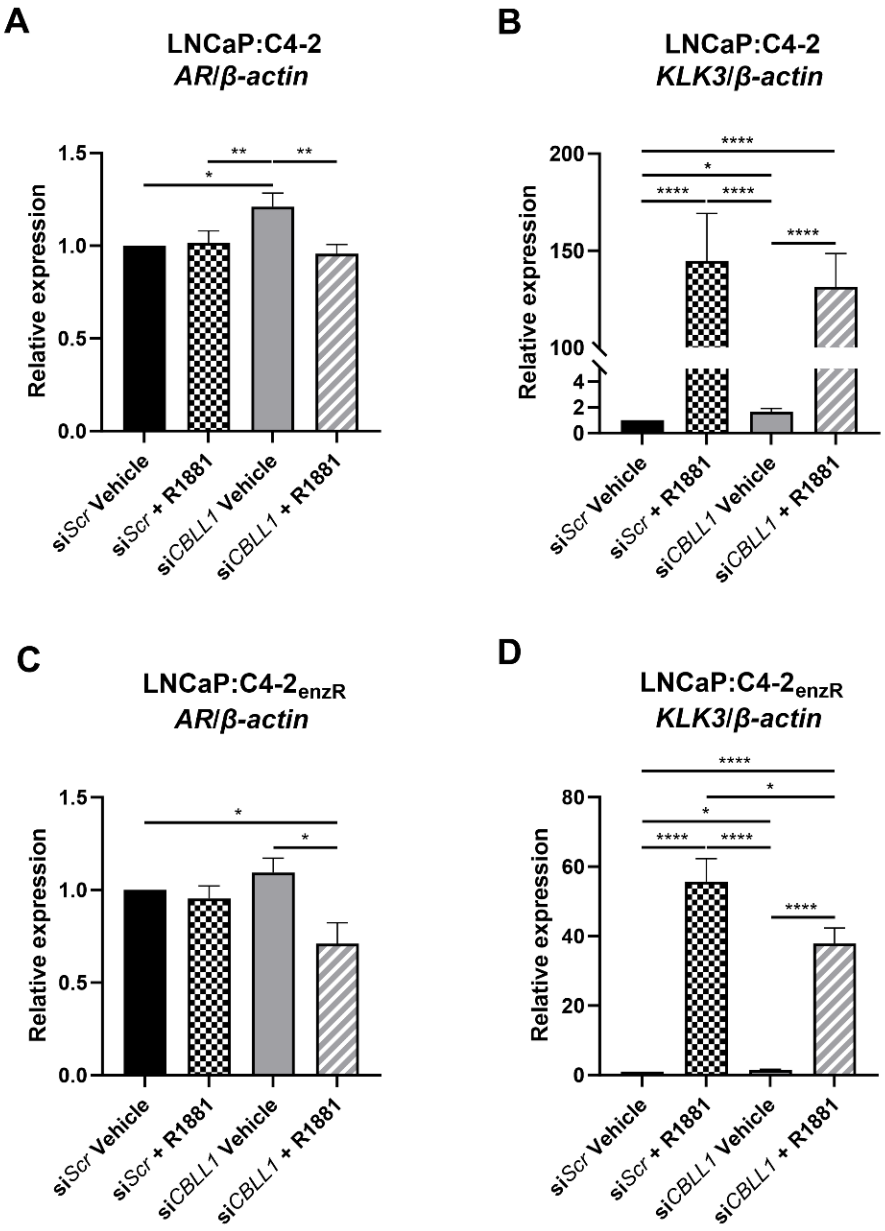


**Figure 4.3 Effect of siRNA-mediated *CBLL1* knockdown and R1881 treatment on mRNA expression in LNCaP:C4-2 and LNCaP:C4-2$_{enzR}$ cells**

*AR* and *KLK3* mRNA expression in LNCaP:C4-2 and LNCaP:C4-2$_{enzR}$ cells was analysed by qRT-PCR relative to *β-actin* following siRNA-mediated knockdown of *CBLL1* and subsequent treatment for 72 hours with vehicle or R1881. (**A**) *AR* mRNA expression following *CBLL1* siRNA-mediated knockdown treated with vehicle or R1881 in LNCaP:C4-2 cells (n=6). (**B**) *KLK3* mRNA expression following *CBLL1* siRNA-mediated knockdown treated with vehicle or R1881 LNCaP:C4-2 cells (n=6). (**C**) *AR* mRNA expression following *CBLL1* siRNA-mediated knockdown treated with vehicle or R1881 in

LNCaP:C4-$2_{enzR}$ cells (n=6). (**D**) *KLK3* mRNA expression following *CBLL1* siRNA-mediated knockdown treated with vehicle or R1881 in LNCaP:C4-$2_{enzR}$ cells (n=6). * = p ≤0.05, ** = p ≤0.01, *** = p ≤0.001, **** = p ≤0.0001 by paired t-test.

### 4.2.2 Phenotypic effect of siRNA depletion of *CBLL1* in prostate cancer cell lines

To further investigate the functional role of CBLL1 in PCa, the effect of *CBLL1* depletion and R1881 treatment in LNCaP:C4-2 and LNCaP:C4-$2_{enzR}$ cells on proliferation was assessed (**Figure 4.4**). No significant difference in cellular proliferation was observed between any of the conditions in either LNCaP:C4-2 (p>0.05; **Figure 4.4A**) or LNCaP:C4-$2_{enzR}$ cells (p>0.05; **Figure 4.4B**).

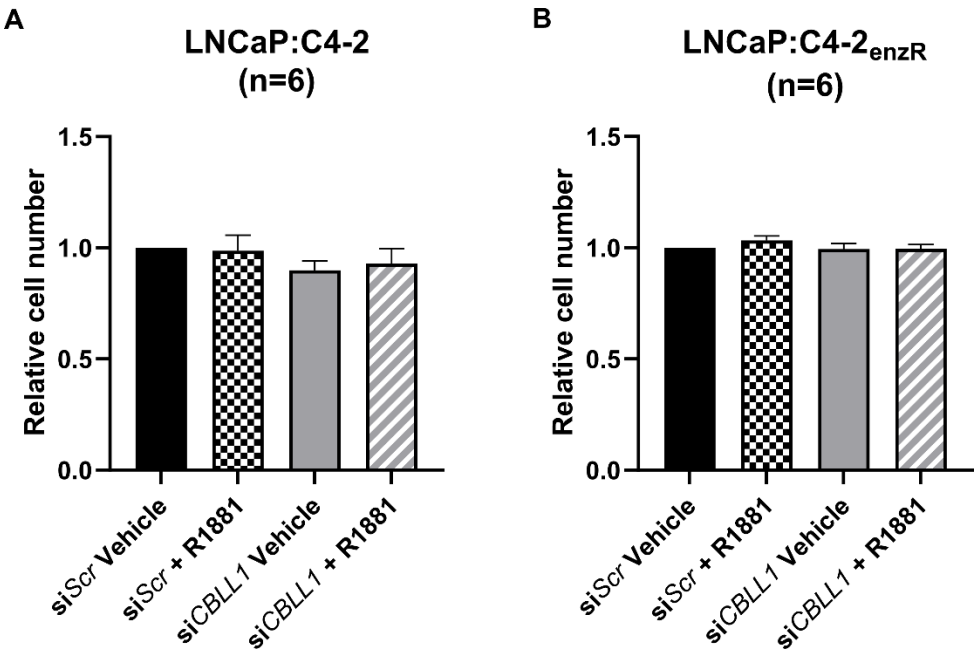


**Figure 4.4 Phenotypic effect of siRNA-mediated *CBLL1* knockdown and R1881 treatment in LNCaP:C4-2 and LNCaP:C4-2$_{enzR}$ cells**

Cellular proliferation of LNCaP:C4-2 and LNCaP:C4-2$_{enzR}$ cells was analysed by CyQUANT™ Direct Cell Proliferation Assay following siRNA-mediated knockdown of *CBLL1* and subsequent treatment for 72 hours with vehicle or R1881. (**A**) Cellular proliferation in LNCaP:C4-2 cells following *CBLL1* siRNA-mediated knockdown treated with vehicle or R1881 (n=6). (**B**) Cellular proliferation in LNCaP:C4-2$_{enzR}$ cells following *CBLL1* siRNA-mediated knockdown treated with vehicle or R1881 (n=6). * = p ≤0.05, ** = p ≤0.01, *** = p ≤0.001, **** = p ≤0.0001 by paired t-test.

### 4.2.3 Effect of siRNA depletion of *CBLL1* on differential gene expression in control and androgen-treated LNCaP:C4-2 and LNCaP:C4-2$_{enzR}$ cells

In order to further understand the function of CBLL1 in PCa, RNA-Seq was used to analyse the effects of siRNA-mediated functional depletion of *CBLL1* on the androgen-regulated transcriptome in LNCaP:C4-2 and LNCaP:C4-2$_{enzR}$ cells. Significantly differentially expressed genes (DEGs) were identified based

on a fold change (FC) of ≥1.5 or ≤-1.5 and a false discovery rate (FDR) of <0.05.

Initially the differentially expressed genes (DEGs) and their associated pathways were analysed between control conditions of LNCaP:C4-2 and LNCaP:C4-$2_{enzR}$ cells in order to establish the baseline differences between the parental cell line and its enzalutamide resistant counterpart. It should be noted there no significant difference in *CBLL1* expression was observed between vehicle-treated scrambled control LNCaP:C4-2 and LNCaP:C4-$2_{enzR}$ cells. This was also demonstrated at both the mRNA and protein level in **Figure 3.4**.

It was found that 1816 genes were differentially expressed between vehicle-treated scrambled control LNCaP:C4-2 cells compared with LNCaP:C4-$2_{enzR}$ cells, with expression of 969 genes higher in LNCaP:C4-$2_{enzR}$ compared with LNCaP:C4-2 (including the androgen-regulated genes *KLK3/PSA* and *TMPRSS2*, and the enzalutamide resistance-associated genes *MET* and *ASCL1*), and 849 genes downregulated in LNCaP:C4-$2_{enzR}$ (**Figure 4.5A**).

Following DEG analysis, pathway analysis was carried out using WebGestalt (Liao et al., 2019) to identify the significantly enriched KEGG pathways involved in resistance to enzalutamide. A total of 18 significantly enriched pathways associated with the DEGs were identified between the vehicle-treated scrambled control LNCaP:C4-2 and LNCaP:C4-$2_{enzR}$ cells (**Figure 4.5C**). Interestingly, several cancer-specific pathways were enriched, including central carbon metabolism in cancer (hsa05230), transcriptional misregulation in cancer (hsa05202) and pathways in cancer (hsa05200), as well as the PI3K-

Akt signalling (hsa04151) and MAPK signalling (hsa04010) pathways that are commonly altered in cancer.

Next, the effect of androgen on differential gene expression between the two cell lines was analysed. It was found that 172 genes were differentially expressed between R1881-treated scrambled control LNCaP:C4-2 and LNCaP:C4-$2_{enzR}$ cells, with expression of 63 genes lower in LNCaP:C4-2 compared with LNCaP:C4-$2_{enzR}$, including components of the PI3K pathway (*IGF1* and *FGFR3*), and 109 genes higher in LNCaP:C4-2, including *MR* and *PRKCA,* (**Figure 4.5B**).

Subsequent KEGG pathway analysis using WebGestalt (Liao et al., 2019) identified nine significantly enriched pathways associated with the DEGs between the R1881-treated scrambled control LNCaP:C4-2 and LNCaP:C4-$2_{enzR}$ cells (**Figure 4.5D**). Interestingly, 44.4% of the enriched pathways in R1881-treated scrambled control cells (**Figure 4.5D**) were common to those enriched in the vehicle-treated scrambled control cells (**Figure 4.5C**) and comprised the TGF-beta (hsa04350) and Ras (hsa04014) signalling pathways, as well as the pathways in cancer (hsa05200) and MAPK signalling (hsa04010) pathways mentioned above.

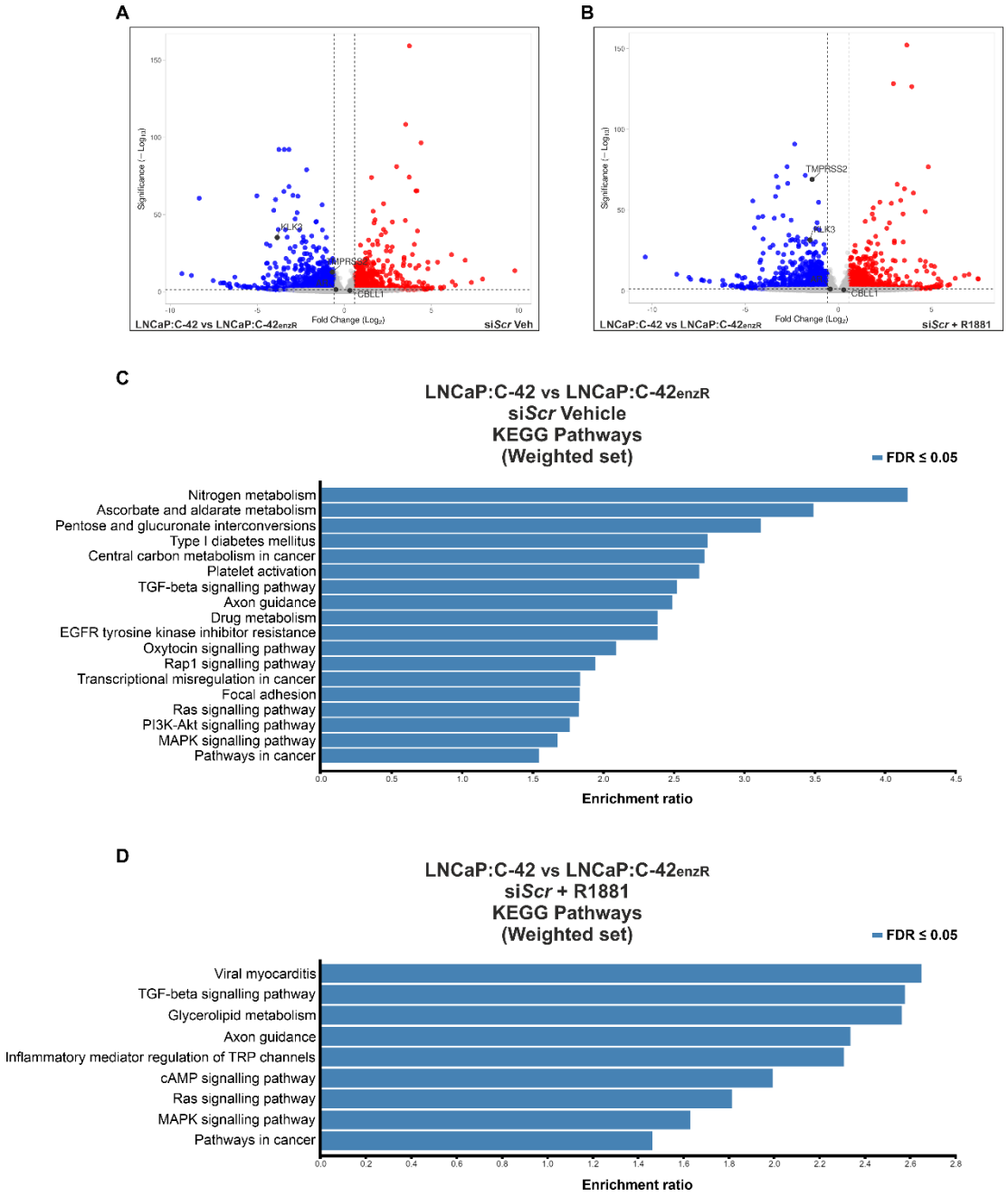


**Figure 4.5 Comparison of differential gene expression and associated over-represented KEGG pathways in scrambled control LNCaP:C4-2 and LNCaP:C4-2$_{enzR}$ cells in response to R1881**

Differential gene expression was analysed following RNA-Seq of LNCaP:C4-2 and LNCaP:C4-2$_{enzR}$ cells subjected to scrambled control siRNA transfection and subsequent treatment for 72 hours with vehicle or R1881 followed by pathway analysis using WebGestalt (Liao et al., 2019). (**A**) Differential gene expression compared between scrambled control vehicle-treated LNCaP:C4-2

and LNCaP:C4-$2_{enzR}$ cells (n=3). (**B**) Differential gene expression compared between scrambled control R1881-treated LNCaP:C4-2 and LNCaP:C4-$2_{enzR}$ cells (n=3). (**C**) Summary of significantly enriched KEGG pathways associated with DEGs in vehicle-treated scrambled control LNCaP:C4-2 and LNCaP:C4-$2_{enzR}$ cells (n=3). (**D**) Summary of significantly enriched KEGG pathways associated with DEGs in R1881-treated scrambled control LNCaP:C4-2 and LNCaP:C4-$2_{enzR}$ cells (n=3). Genes with significantly higher expression in the first condition listed on each volcano plot are highlighted in red, genes with significantly lower expression in the first condition are highlighted in blue. Genes without any significant differential expression between the two listed conditions are marked in grey. Significant gene expression= FC ± 1.5 and FDR <0.05. Veh= Vehicle.

The effect of CBLL1 on basal transcription was subsequently assessed through the analysis of *CBLL1* depletion on differential gene expression in both vehicle-treated LNCaP:C4-2 and LNCaP:C4-$2_{enzR}$ cells. It was found that 194 genes were differentially expressed between vehicle-treated scrambled control and *CBLL1*-depleted LNCaP:C4-2 cells, with 70 genes downregulated in vehicle-treated scrambled control compared with *CBLL1*-depleted cells, including *CA9*, *IGF1*, *GHR* and *ALDH1A1*. Upregulation of 124 genes was observed, including *MR* (**Figure 4.6A**).

In LNCaP:C4-$2_{enzR}$ cells 83 genes were differentially expressed between vehicle-treated scrambled control and *CBLL1*-depleted cells, with 46 genes downregulated in vehicle-treated scrambled control compared with *CBLL1*-depleted cells, and 37 genes upregulated (**Figure 4.6B**).

KEGG pathway analysis was then carried out using WebGestalt (Liao et al., 2019) to identify the significantly enriched pathways in which CBLL1

expression is involved. A total of 9 significantly enriched pathways associated with the DEGs were identified between the vehicle-treated scrambled control and CBLL1-depleted LNCaP:C4-2 cells (**Figure 4.6C** and **Appendix 8**). The majority of the pathways identified were associated with detoxification, including steroid hormone biosynthesis (hsa00140), drug metabolism (hsa00982), drug metabolism_1 (hsa00983), metabolism of xenobiotics by cytochrome P450 (hsa00980). However, interestingly, in vehicle-treated LNCaP:C4-$2_{enzR}$ cells, no significantly enriched pathways associated with DEGs were identified, with the CBLL1 regulation of the pathways listed above in the parental LNCaP:C4-2 cell line no longer present in the enzalutamide-resistant cell line (**Figure 4.6D**). This suggests that enzalutamide resistance enables LNCaP:C4-2 cells to function independently of CBLL1 regulation.

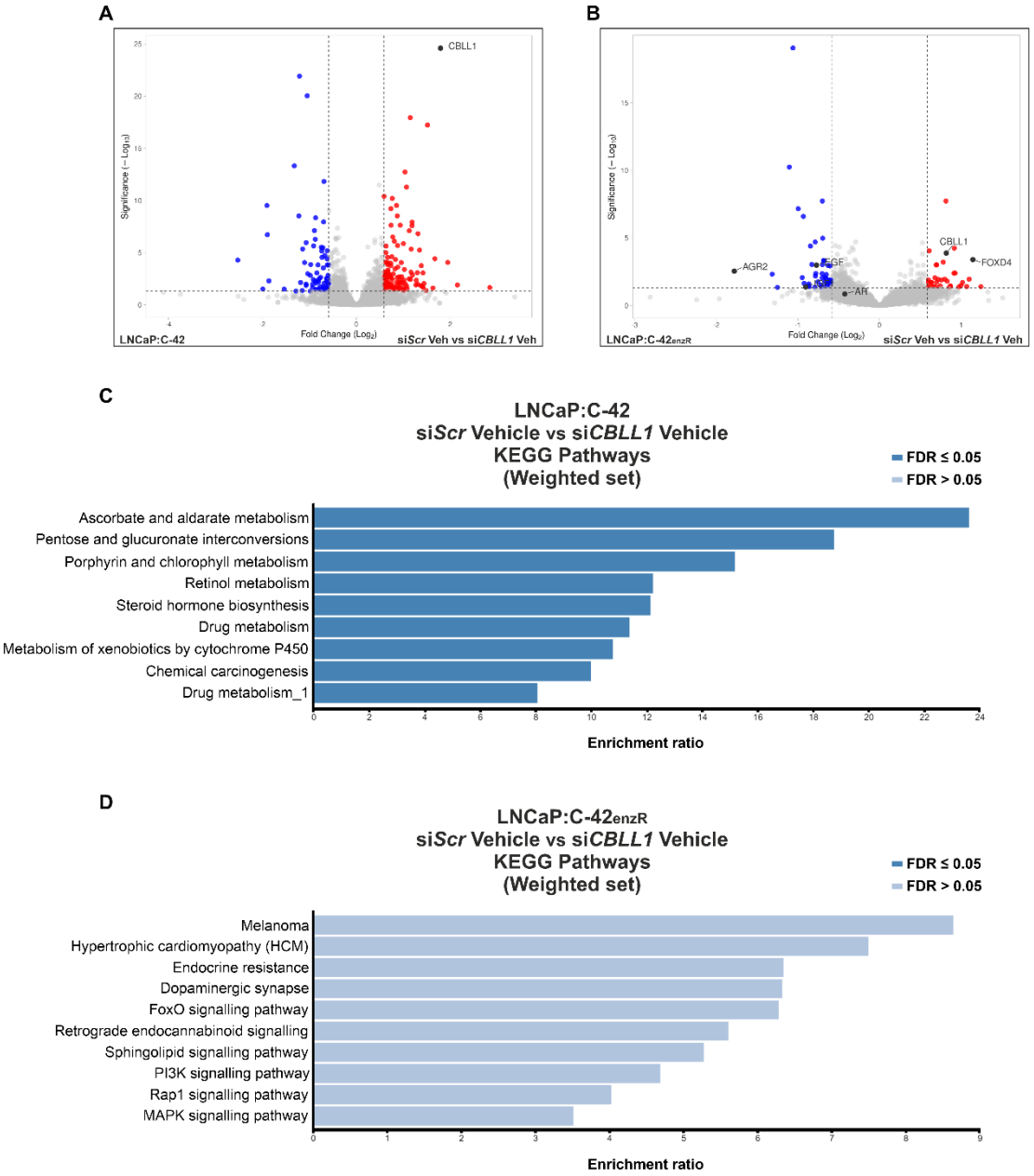


**Figure 4.6 Differential gene expression and associated over-represented KEGG pathways in vehicle-treated LNCaP:C4-2 and LNCaP:C4-2$_{enzR}$ cells in response to siRNA-mediated *CBLL1* knockdown**

Differential gene expression was analysed following RNA-Seq of LNCaP:C4-2 and LNCaP:C4-2$_{enzR}$ cells subjected to siRNA-mediated knockdown of *CBLL1* and subsequent treatment for 72 hours with vehicle followed by pathway analysis using WebGestalt (Liao et al., 2019). (**A**) Differential gene expression compared between vehicle-treated scrambled control and *CBLL1*-depleted LNCaP:C4-2 cells (n=3). (**B**) Differential gene expression compared between vehicle-treated scrambled control and *CBLL1*-depleted LNCaP:C4-2$_{enzR}$ cells

(n=3). (**C**) Summary of significantly enriched KEGG pathways associated with DEGs in vehicle-treated scrambled control and *CBLL1*-depleted LNCaP:C4-2 cells (n=3). (**D**) Summary of the top ten enriched KEGG pathways associated with DEGs in vehicle-treated scrambled control and *CBLL1*-depleted LNCaP:C4-$2_{enzR}$ cells (n=3). Genes with significantly higher expression in the first condition listed on each volcano plot are highlighted in red, genes with significantly lower expression in the first condition are highlighted in blue. Genes without any significant differential expression between the two listed conditions are marked in grey. Significant gene expression= FC ± 1.5 and FDR <0.05. Veh= Vehicle.

The effect of androgen on the CBLL1-regulated transcriptome was then analysed through examination of the effect of R1881 treatment on differential gene expression in both scrambled control LNCaP:C4-2 and LNCaP:C4-$2_{enzR}$ cells. A total of 1728 genes were differentially expressed between vehicle-treated and R1881-treated scrambled control LNCaP:C4-2 cells, with 910 genes downregulated in vehicle-treated compared with R1881-treated scrambled control cells (including the prototypical androgen-regulated genes *NKX3-1*, *KLK3/PSA* and *TMPRSS2*), and 818 genes upregulated (**Figure 4.7A**).

Subsequent KEGG pathway analysis using WebGestalt (Liao et al., 2019) identified 29 significantly enriched pathways with many directly associated with cancer, including basal cell carcinoma (hsa05217), central carbon metabolism in cancer (hsa05230), prostate cancer (hsa05215), breast cancer (hsa05224), gastric cancer (hsa05226), transcriptional misregulation in cancer (hsa05202), pathways in cancer (hsa05200) and proteoglycans in cancer (hsa05205), as

well as the PI3K-Akt signalling (hsa04151) pathways (**Figure 4.7C** and **Appendix 5**).

Focussing on the pathways in cancer KEGG pathway, *IGF1*, *VEGFA*, *MYC*, *NKX3-1* and *MTOR* were all upregulated by androgen treatment in scrambled control LNCaP:C4-2 cells, as were *GHR*, *IGF1R*, *MYC* and *MTOR* in the PI3K-Akt signalling pathway, and *NKX3-1*, *KLK3/PSA* and *TMPRSS2* in the prostate cancer pathways. In contrast, *PIK3R3* was downregulated in response to androgen in the PI3K-Akt signalling pathway.

In LNCaP:C4-$2_{enzR}$ cells 1895 genes were differentially expressed between vehicle-treated and R1881-treated scrambled control cells, with 966 genes downregulated in vehicle-treated compared with R1881-treated scrambled control cells (including the prototypical androgen-regulated genes *NKX3-1*, *KLK3/PSA* and *TMPRSS2*), and 929 genes upregulated (**Figure 4.7B**).

Fewer DEG-associated significantly enriched KEGG pathways (n=18) were identified in LNCaP:C4-$2_{enzR}$ (**Figure 4.7D** and **Appendix 11**), compared with the parental cell line (n=29) (**Figure 4.7C** and **Appendix 5**), although interestingly, again, 44.4% were common to those enriched in parental LNCaP:C4-2 cells. The majority of significantly enriched pathways were directly cancer-associated and included the basal cell carcinoma (hsa05217), prostate cancer (hsa05215), pancreatic cancer (05212), acute myeloid leukaemia (05221), non-small cell lung cancer (05223), melanoma (05218), breast cancer (hsa05224), gastric cancer (hsa05226), transcriptional misregulation in cancer (hsa05202), and pathways in cancer (hsa05200) pathways (**Figure 4.7D** and **Appendix 11**).

In the significantly enriched pathways in cancer KEGG pathway, as in the parental cell line, in enzalutamide-resistant scrambled control LNCaP:C4-2 cells *IGF1*, *VEGFA*, *NKX3-1* and *MTOR* were all upregulated by androgen treatment, however, in contrast, *MYC* was not differentially expressed. In addition, different DEGS appeared in the prostate cancer pathway, including *IGF1* and *MTOR*, both of whose expression was significantly induced by androgen. Taken together these results suggest that enzalutamide resistance reduces the effect of androgen in regulating the transcriptome in PCa.

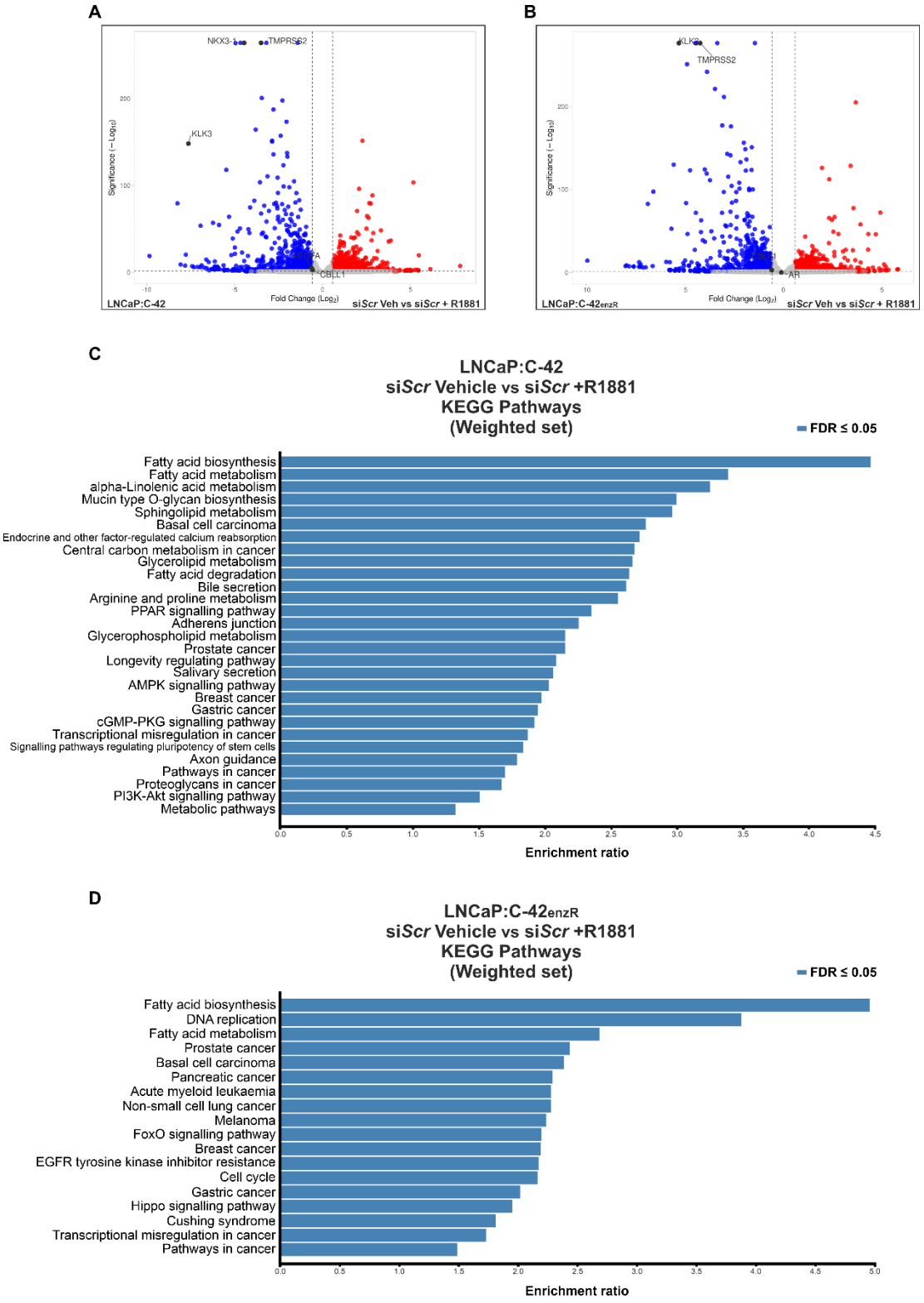


**Figure 4.7 Differential gene expression and associated over-represented KEGG pathways in scrambled control LNCaP:C4-2 and LNCaP:C4-2$_{enzR}$ cells in response to R1881 treatment**

Differential gene expression was analysed following RNA-Seq of LNCaP:C4-2 and LNCaP:C4-2$_{enzR}$ cells subjected to scrambled control siRNA transfection and subsequent treatment for 72 hours with vehicle or R1881 followed by pathway analysis using WebGestalt (Liao et al., 2019). (**A**) Differential gene expression compared between scrambled control LNCaP:C4-2 cells treated with vehicle or R1881 (n=3). (**B**) Differential gene expression compared between scrambled control LNCaP:C4-2$_{enzR}$ cells treated with vehicle or R1881 (n=3). (**C**) Summary of significantly enriched KEGG pathways associated with DEGs in scrambled control LNCaP:C4-2 cells treated with vehicle or R1881 (n=3). (**D**) Summary of significantly enriched KEGG pathways associated with DEGs in scrambled control LNCaP:C4-2 $_{enzR}$ cells treated vehicle or with R1881 (n=3). Genes with significantly higher expression in the first condition listed on each volcano plot are highlighted in red, genes with significantly lower expression in the first condition are highlighted in blue. Genes without any significant differential expression between the two listed conditions are marked in grey. Significant gene expression= FC ± 1.5 and FDR <0.05. Veh= Vehicle.

The effect of *CBLL1*-depletion on the androgen-regulated transcriptome was then analysed through examination of the effect of R1881 treatment on differential gene expression in both *CBLL1*-depleted LNCaP:C4-2 and LNCaP:C4-2$_{enzR}$ cells. A total of 1683 genes were differentially expressed between vehicle-treated and R1881-treated *CBLL1*-depleted LNCaP:C4-2 cells, with 785 genes downregulated in vehicle-treated compared with R1881-treated *CBLL1*-depleted cells (including the androgen-regulated genes *KLK3/PSA* and *TMPRSS2*), and 898 genes upregulated (**Figure 4.8A**).

KEGG pathway analysis using WebGestalt (Liao et al., 2019) identified 12 significantly enriched DEG-associated pathways, most notably the pathways in cancer (hsa05200) pathway (**Figure 4.8C** and **Appendix 9**).

In LNCaP:C4-$2_{enzR}$ cells 1897 genes were differentially expressed between vehicle-treated and R1881-treated *CBLL1*-depleted cells, with 959 genes downregulated in vehicle-treated compared with R1881-treated *CBLL1*-depleted cells (including the androgen-regulated genes *NKX3-1* and *TMPRSS2*), and 938 genes upregulated (**Figure 4.8B**).

As found in scrambled control cells (**Figure 4.7**), fewer DEG-associated significantly enriched KEGG pathways (n=8) were identified in LNCaP:C4-$2_{enzR}$ (**Figure 4.8D** and **Appendix 12**), compared with the parental cell line (n=12) (**Figure 4.8C** and **Appendix 9**), although interestingly, only the pathways in cancer KEGG pathway was significantly enriched in both the parental and enzalutamide-resistant LNCaP:C4-2 cells. Therefore, the remaining 11 significantly enriched pathways seen in *CBLL1*-depleted R1881-treated LNCaP:C4-2 cells (**Figure 4.8C** and **Appendix 9**) lose their androgen regulation in the process of enzalutamide resistance.

In contrast to LNCaP:C4-2, in androgen-treated *CBLL1*-depleted LNCaP:C4-$2_{enzR}$ cells, more significantly enriched pathways were directly linked to cancer, including the basal cell carcinoma (hsa05217), prostate cancer (hsa05215), breast cancer (hsa05224), gastric cancer (hsa05226), and pathways in cancer (hsa05200) pathways (**Figure 4.8D** and **Appendix 12**).

It is notable that despite pathways in cancer being significantly enriched in both *CBLL1*-depleted LNCaP:C4-2 cells and LNCaP:C4-$2_{enzR}$ cells, the genes altered within those pathways differ, demonstrating both that enzalutamide resistance is altering androgen-regulated transcription, and that the absence of CBLL1 alters a subset of androgen-regulated genes.

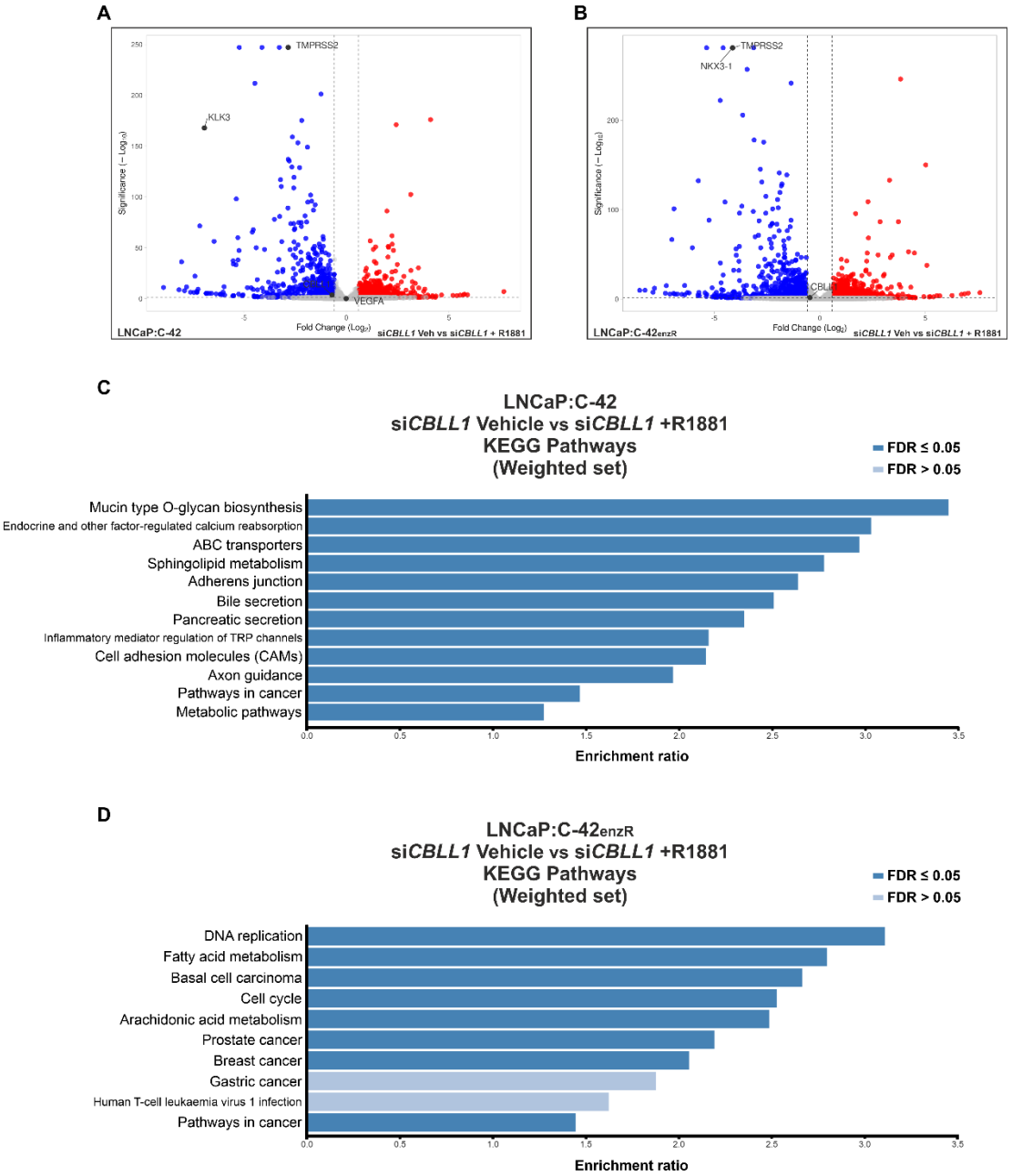


**Figure 4.8 Differential gene expression and associated over-represented KEGG pathways in *CBLL1*-depleted LNCaP:C4-2 and LNCaP:C4-2$_{enzR}$ cells in response to R1881 treatment**

Differential gene expression was analysed following RNA-Seq of LNCaP:C4-2 and LNCaP:C4-2$_{enzR}$ cells subjected to siRNA-mediated knockdown of *CBLL1* and subsequent treatment for 72 hours with vehicle or R1881 followed by pathway analysis using WebGestalt (Liao et al., 2019). (**A**) Differential gene expression compared between *CBLL1*-depleted LNCaP:C4-2 cells treated with vehicle or R1881 (n=3). (**B**) Differential gene expression compared between

*CBLL1*-depleted LNCaP:C4-2$_{enzR}$ cells treated with vehicle or R1881 (n=3). (**C**) Summary of significantly enriched KEGG pathways associated with DEGs in *CBLL1*-depleted LNCaP:C4-2 cells treated with vehicle or R1881 (n=3). (**D**) Summary of significantly enriched KEGG pathways associated with DEGs in *CBLL1*-depleted LNCaP:C4-2 $_{enzR}$ cells treated with vehicle or R1881 (n=3). Genes with significantly higher expression in the first condition listed on each volcano plot are highlighted in red, genes with significantly lower expression in the first condition are highlighted in blue. Genes without any significant differential expression between the two listed conditions are marked in grey. Significant gene expression= FC ± 1.5 and FDR <0.05. Veh= Vehicle.

Examination of the enriched KEGG pathways in both scrambled control (**Figure 4.7D** and **Appendix 11**) and *CBLL1*-depleted R1881-treated LNCaP:C4-2$_{enzR}$ cells (**Figure 4.8D** and **Appendix 12**) revealed different DEGs. A total of 75 DEGs were observed across all conditions, with just 15 (20.0%) DEGs common to both scrambled control and *CBLL1*-depleted LNCaP:C4-2$_{enzR}$ cells treated with vehicle or R1881 conditions, seven (9.3%) DEGs exclusive to scrambled control conditions, and 53 (70.7%) DEGs exclusive to *CBLL1*-depleted conditions.

Of the seven DEGs exclusive to scrambled control LNCaP:C4-2$_{enzR}$ cells treated with vehicle or R1881, the most notable is *TMPRSS2*, an androgen-regulated gene, whose androgen regulation is impaired by CBLL1 depletion. This supports a role for CBLL1 in androgen regulation of a subset of AR-regulated genes. Conversely, CBLL1 depletion enabled androgen regulation of *HIF1A* and *NCOA1*, which was not observed in scramble control cells. Thus, loss of CBLL1 relieves repression of, and induces other, androgen-regulated

genes. This suggests, therefore, that CBLL1 has a dual function of supporting the activation and repression of specific androgen-regulated genes.

For example, the pathways in cancer KEGG pathway is significantly enriched in both scrambled control (**Figure 4.7C** and **Appendix 5**), and *CBLL1*-depleted (**Figure 4.8C** and **Appendix 9**) LNCaP:C4-2 cells treated with vehicle or R1881, yet the specific DEGs in this pathway differ. Within this pathway are 91 DEGs in both scrambled control and *CBLL1*-depleted LNCaP:C4-2 cells treated with vehicle or androgen, with 51 (56.0%) DEGs common to both conditions (i.e. they are differentially expressed regardless of the presence of CBLL1), 26 (28.6%) DEGs exclusive to scrambled control conditions, and 14 (15.4%) DEGs exclusive to *CBLL1*-depleted conditions. Included within the 26 DEGs exclusive to scrambled control LNCaP:C4-2 cells treated with vehicle or R1881 are notable PCa-related genes including *VEGFA*, *PIK3R3*, *MYC* and *MTOR*. When *CBLL1* is depleted, androgen regulation of these genes is lost, suggesting that CBLL1 plays a role in maintaining androgen regulation of these key genes.

### 4.2.4 Effect of siRNA depletion of *CBLL1* on significantly enriched KEGG pathways associated with differential gene expression in basal and androgen-treated LNCaP:C4-2 and LNCaP:C4-2$_{enzR}$ cells

Further analysis was carried out in order to understand the overlapping and distinct androgen-regulated DEG-associated KEGG pathways between scrambled control and *CBLL1*-depleted LNCaP:C4-2 and LNCaP:C4-2$_{enzR}$ cells.

A comparison of significantly enriched DEG-associated KEGG pathways in scrambled control cells treated with vehicle or androgen between LNCaP:C4-

2 and LNCaP:C4-2$_{enzR}$ cells revealed 39 DEG-associated enriched pathways, of which only 8 (20.5%) were common to both the parental and enzalutamide-resistant cell lines, including the pathways in cancer and prostate cancer KEGG pathways (**Figure 4.9A**). This further supports the earlier findings that enzalutamide resistance has a profound effect on androgen-regulated gene expression. Of the enriched pathways, 21 (53.9%) were exclusive to scrambled control LNCaP:C4-2 cells treated with vehicle or R1881, including the PI3K-Akt signalling pathway, with ten (25.6%) pathways exclusively enriched in scrambled control LNCaP:C4-2$_{enzR}$ cells treated with vehicle or R1881. These included several cancer-specific pathways, including pancreatic cancer, non-small cell lung cancer, melanoma and acute myeloid leukaemia. This loss of androgen regulation of pathways in enzalutamide resistance, and the fact that the majority of the remaining significantly enriched pathways are directly linked to cancer, further demonstrates the contribution of enzalutamide resistance to PCa progression.

**Figure 4.9B** illustrates the overlapping and distinct enriched pathways between vehicle-treated LNCaP:C4-2 and LNCaP:C4-2$_{enzR}$ cells upon *CBLL1* knockdown. A total of nine DEG-associated pathways were significantly enriched in LNCaP:C4-2 cells exclusively, including key pathways associated with detoxification such as the steroid hormone biosynthesis, drug metabolism, drug metabolism_1, and metabolism of xenobiotics by cytochrome P450 pathways. Intriguingly, in vehicle-treated LNCaP:C4-2$_{enzR}$ cells no pathways are significantly enriched following *CBLL1*-depletion, highlighting the marked impact of enzalutamide resistance on CBLL1 regulation of gene expression,

with its presence rendering LNCaP:C4-2 cells independent of CBLL1's influence.

A comparison of significantly enriched DEG-associated KEGG pathways in *CBLL1*-depleted cells treated with vehicle or R1881 between LNCaP:C4-2 and LNCaP:C4-$2_{enzR}$ cells revealed 19 DEG-associated enriched pathways, of which just one (5.3%) was common to both the parental and enzalutamide-resistant cell lines, namely the pathways in cancer KEGG pathway (**Figure 4.9C**). As noted earlier, despite the same pathway being enriched in both cell lines, different genes within this pathway were differentially expressed, further emphasising that enzalutamide resistance has a profound effect on androgen-regulated gene expression, both in the presence and absence of CBLL1. There were 11 (57.9%) enriched pathways exclusive to *CBLL1*-depleted vehicle or R1881-treated LNCaP:C4-2 cells, none of which were directly associated with cancer. In *CBLL1*-depleted LNCaP:C4-$2_{enzR}$ cells treated with R1881, seven (36.8%) pathways were exclusively enriched, three of which were directly associated with cancer, including the breast cancer, prostate cancer and basal cell carcinoma KEGG pathways, as well as the cell cycle and DNA replication pathways implicated in cancer development and progression. The differences in significant enrichment of DEG-associated KEGG pathways between the presence and absence and *CBLL1* across both LNCaP:C4-2 and LNCaP:C4-$2_{enzR}$ highlights the key role of both CBLL1 expression and enzalutamide resistance in androgen-regulated gene expression in PCa and in progression of the disease.

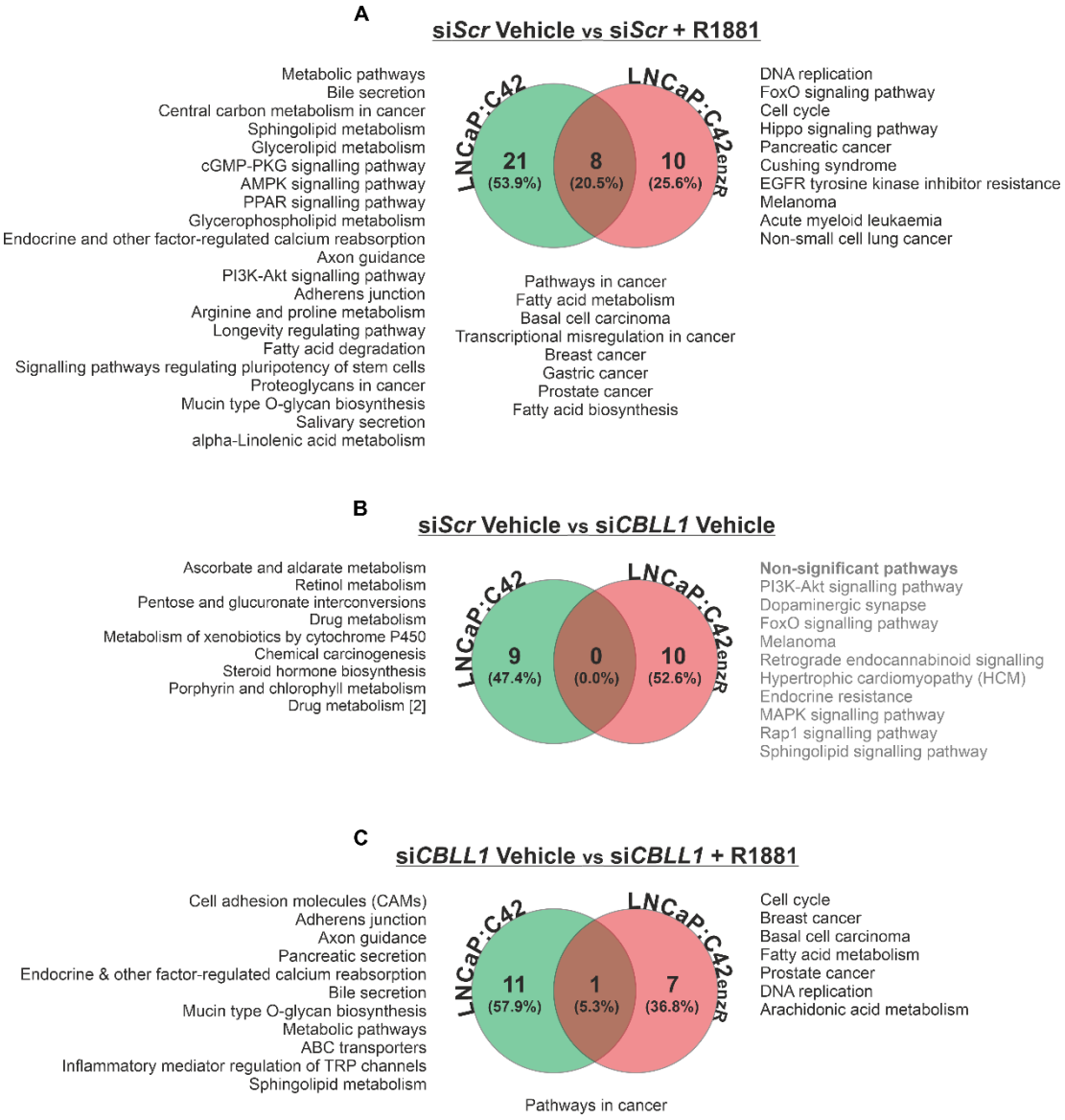


**Figure 4.9 Summary of over-represented pathways associated with differentially expressed genes in LNCaP:C4-2 and LNCaP:C4-2$_{enzR}$ cells in response to siRNA-mediated *CBLL1* knockdown and R1881 treatment**

Differential gene expression was analysed following RNA-Seq of LNCaP:C4-2 and LNCaP:C4-2$_{enzR}$ cells subjected to siRNA-mediated knockdown of *CBLL1* and subsequent treatment for 72 hours with vehicle or R1881, followed by pathway analysis using WebGestalt (Liao et al., 2019). (**A**) Summary of over-represented KEGG pathways across Scrambled control LNCaP:C4-2 and LNCaP:C4-2$_{enzR}$ cells treated with vehicle or R1881 (n=3). (**B**) Summary of over-represented pathways across vehicle-treated LNCaP:C4-2 and LNCaP:C4-2$_{enzR}$ cells in response to siRNA-mediated knockdown of *CBLL1*

(n=3). (**C**) Summary of over-represented pathways across *CBLL1*-depleted LNCaP:C4-2 and LNCaP:C4-$2_{enzR}$ cells treated with vehicle or R1881 (n=3). Over-represented pathways associated exclusively with LNCaP:C4-2 are listed to the left of each Venn diagram, with LNCaP:C4-$2_{enzR}$ to the right, and pathways associated with both cell lines are listed centrally. Pathways not significantly enriched are listed in grey. Significant gene expression= FC ± 1.5 and FDR <0.05. Veh= Vehicle.

### 4.2.5 Effect of siRNA depletion of *CBLL1* on alternative splicing in control and androgen-treated LNCaP:C4-2 and LNCaP:C4-$2_{enzR}$ cells

Given the key impact of *CBLL1* expression and enzalutamide resistance on differential gene expression, together with the previously reported association between $m^6A$ and alternative splicing, the effect of *CBLL1* knockdown on alternative splicing in both vehicle- and R1881-treated LNCaP:C4-2 and LNCaP:C4-$2_{enzR}$ cells was investigated.

The five classes of alternative splicing analysed were alternative 5' splice site (A5SS), mutually exclusive exon (MXE), retained intron (RI), skipped exon (SE), and alternative 3' splice site (A3SS). Differential splicing events were sorted by difference in percentage spliced in (dPSI ≥5%) and FDR (<0.05) to give the total number of significant splicing events (**Figure 4.10**). Both differentially spliced transcripts (DSTs) and differentially spliced genes (DSGs) were assessed and contextualised relative to the number and identity of DEGs detected, allowing the effect of elevated expression-associated alternative splicing as a confounding variable to be excluded.

A similar overall profile of the numbers and types of alternative splice events were seen in all conditions in both LNCaP:C4-2 and LNCaP:C4-$2_{enzR}$ cells

(**Figure 4.10**). However, a number of changes between the cell lines were observed, with the greatest number of DSTs and DSGs (n= 2810 and n=2200, respectively) in LNCaP:C4-2 cells found upon *CBLL1* knockdown in R1881-treated cells (**Figure 4.10E**), whereas in LNCaP:C4-$2_{enzR}$ cells the greatest number of DSGs and DSTs (n= 3476 and n=2561, respectively) were observed in scrambled control cells treated with vehicle or R1881 (**Figure 4.10B**). The differences between conditions were more evident in LNCaP:C4-$2_{enzR}$ cells, with a ~30% decrease in DST events observed between the condition with the highest total number of DSTs (n=3476; R1881 treatment in scrambled control cells; **Figure 4.10B**) and the lowest (n=2470; *CBLL1* knockdown in vehicle-treated cells; **Figure 4.10D**). In contrast, in LNCaP:C4-2 cells there was only a ~11% reduction in DSTs between the condition with the highest number (n=2810; *CBLL1* knockdown in R1881-treated cells; **Figure 4.10E**) and the lowest (n=2497; *CBLL1* knockdown in vehicle-treated cells; **Figure 4.10C**).

The most frequent alternative splicing event observed in all conditions in both cell lines was SE, particularly following R1881 treatment (**Figure 4.10A** and **Figure 4.10B**). In scrambled control LNCaP:C4-2 cells, R1881 induced SE in *NKX3-1*, whilst CBLL1 depletion induced SE in the *PTEN* and *XRCC3* transcripts in vehicle-treated LNCaP:C4-2 cells.

The second most frequently observed splicing event class in LNCaP:C4-2 cells was MXE in all conditions (**Figure 4.10A**, **Figure 4.10C** and **Figure 4.10E**). In R1881-treated LNCaP:C4-2 cells, *CBLL1* depletion induced MXE events in *NCOA1*, *FOXA1* and *PIK3CB*. In vehicle-treated LNCaP:C4-$2_{enzR}$ cells, *CBLL1* depletion induced MXE in *PIK3CB,* a key component of the PI3K pathway. In LNCaP:C4-$2_{enzR}$ cells the second most common event type was A5SS (**Figure**

**4.10B**, **Figure 4.10D** and **Figure 4.10F**). The number of alternative splicing events in LNCaP:C4-2$_{enzR}$ cells was ~10% higher than in the parental cell line, suggesting a role for enzalutamide resistance and CBLL1 in splicing orchestration. Although expression of putative AR variants was detected in androgen-treated LNCaP:C4-2$_{enzR}$ cells (**Figure 3.6**), Kallisto transcript level analysis did not detect significant differential expression of the ARv7 transcript (ENST00000504326) between LNCaP:C4-2 and LNCaP:C4-2$_{enzR}$ cell lines. This may indicate that translational regulation of AR-variant expression is associated with enzalutamide resistance.

KEGG pathway analysis of DSGs in LNCaP:C4-2 cells revealed a relatively small number of significantly enriched pathways when compared with the number enriched due to DEGs. In all conditions, only two pathways were enriched (**Appendix 14**). In scrambled control cells treated with vehicle or R1881, the only significantly enriched pathway (metabolic pathways: hsa01100) was associated with MXE events. The only other significantly enriched pathway (pyrimidine metabolism: hsa00240) was found in R1881-treated cells with CBLL1 depletion associated with SE events.

Similarly, KEGG pathway analysis of DSGs in LNCaP:C4-2$_{enzR}$ cells revealed a small number of significantly enriched pathways compared to those enriched due to DEGs, with just five pathways enriched (**Appendix 15**). In scrambled control cells treated with vehicle or R1881, four pathways were significantly enriched in association with DSGs with SE events. These comprised the Fanconi anaemia pathway (hsa03460), other types of O-glycan biosynthesis (hsa00514), ubiquitin-mediated proteolysis (hsa04120) and metabolic pathways (01100) KEGG pathways. The only other significantly enriched

pathway (lysine degradation (hsa00310) was found in vehicle-treated cells upon *CBLL1* depletion associated with DSGs with A3SS events.

It is notable that the number of DSGs in both LNCaP:C4-2 (n=5365) and LNCaP:C4-$2_{enzR}$ (n=5495) cells is far greater than the number of DEGs (n=2094 in LNCaP:C4-2, n=3809 in LNCaP:C4-$2_{enzR}$). However, the number of significantly enriched pathways associated with DSGs is much reduced, due to the large number of DSGs that are non-coding. In scrambled control LNCaP:C4-2 cells treated with vehicle or R1881, 1728 DEGs and 1785 DSGs were observed, however only 177 (5.3%) of these genes overlapped. Similarly, in vehicle-treated LNCaP:C4-2 cells with *CBLL1* knockdown only 0.9% of DEGs and DSGs were common, and in R1881-treated LNCaP:C4-2 cells with *CBLL1* knockdown only 0.8% of genes overlapped.

A similar trend was observed in LNCaP:C4-$2_{enzR}$ cells, where in scrambled control cells treated with vehicle or R1881 a total of 1895 DEGs and 2133 DSGs were observed, however only 247 (6.5%) of these genes overlapped. Likewise, in vehicle-treated cells with *CBLL1* knockdown only 5.3% of DEGs and DSGs were common, and in R1881-treated LNCaP:C4-$2_{enzR}$ cells with *CBLL1* knockdown only 0.1% of genes overlapped.

Taken together, these results demonstrate a role for CBLL1 in selective regulation of splicing in PCa.

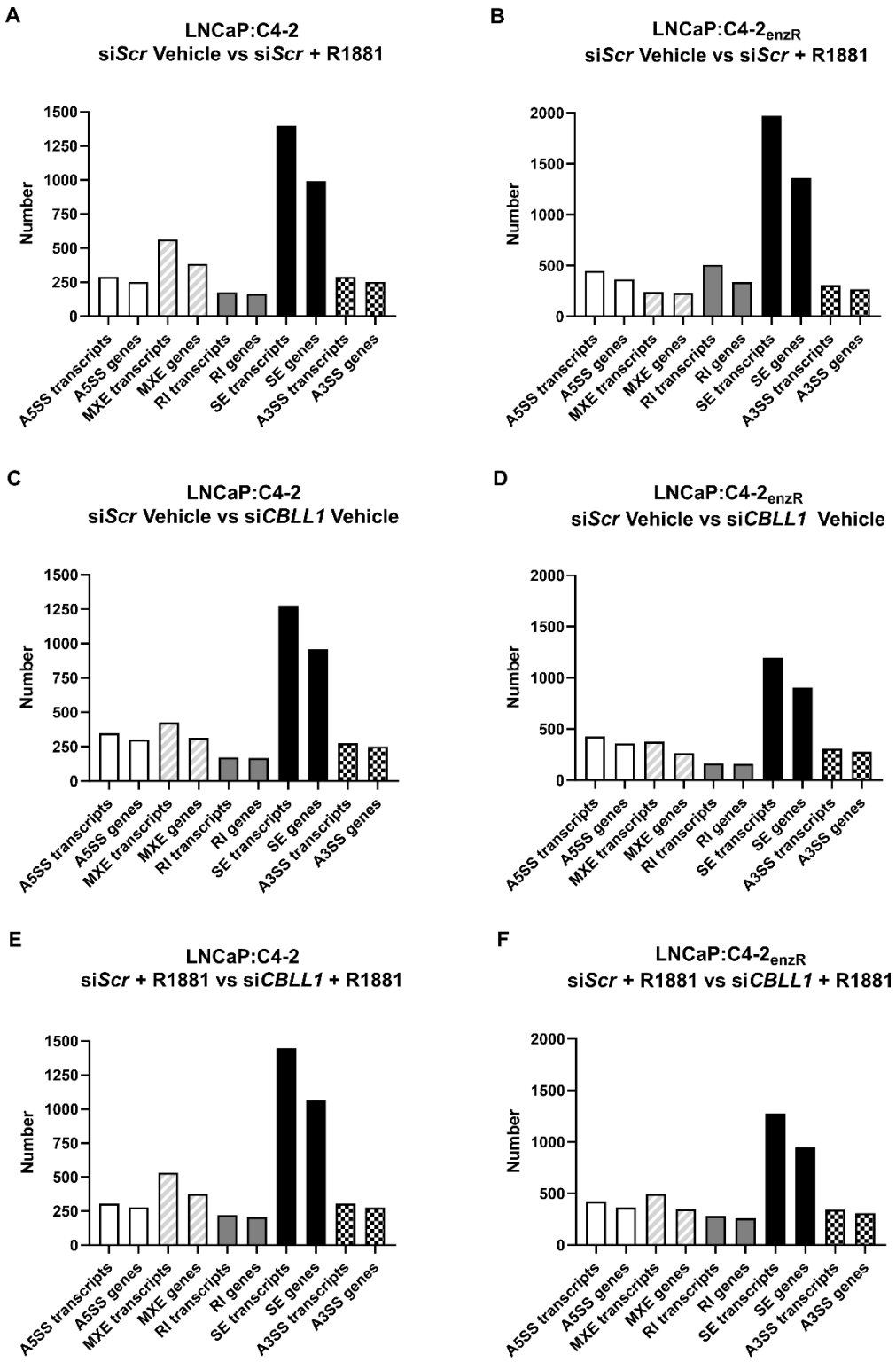


**Figure 4.10 Significant alternative splicing event types in LNCaP:C4-2 and LNCaP:C4-2$_{enzR}$ cells in response to siRNA-mediated CBLL1 knockdown and R1881 treatment**

Alternative splicing analysis using rMATS (Shen et al., 2014) was carried out following RNA-Seq of LNCaP:C4-2 and LNCaP:C4-2$_{enzR}$ cells subjected to

siRNA-mediated knockdown of *CBLL1* and subsequent treatment for 72 hours with vehicle or R1881. Differentially spliced transcript and differentially spliced gene numbers are shown for each alternative splicing event type. LNCaP:C4-2 and LNCaP:C4-$2_{enzR}$ cells treated with vehicle or R1881 (n=3). (**A**) Number of significant alternative splicing events compared between LNCaP:C4-2 scrambled control cells treated with vehicle or R1881 (n=3). (**B**) Number of significant alternative splicing events compared between LNCaP:C4-$2_{enzR}$ scrambled control cells treated with vehicle or R1881 (n=3). (**C**) Number of significant alternative splicing events compared between vehicle-treated scrambled control and *CBLL1*-depleted LNCaP:C4-2 cells (n=3). (**D**) Number of significant alternative splicing events compared between vehicle-treated scrambled control and *CBLL1*-depleted LNCaP:C4-$2_{enzR}$ cells (n=3). (**E**) Number of significant alternative splicing events compared between R1881-treated scrambled control and *CBLL1*-depleted LNCaP:C4-2 cells (n=3). (**F**) Number of significant alternative splicing events compared between R1881-treated scrambled control and *CBLL1*-depleted LNCaP:C4-$2_{enzR}$ cells (n=3). Significant alternative splice event= dPSI ≥5% and FDR <0.05. A5SS= alternative 5’ splice site (A5SS); MXE= mutually exclusive exon; RI= retained intron; SE= skipped exon; A3SS= alternative 3’ splice site.

## 4.3 Discussion

The findings presented in chapter 3 suggested a role for CBLL1 in PCa, with the highest CBLL1 expression seen in PCa cells, and in particular AR-expressing cells, compared with non-malignant prostate cells. These observations are consistent with prior studies that have reported CBLL1 expression to be positively associated with oncogenic features in a number of other cancer types (Castosa et al., 2018, Hui et al., 2019, Liu et al., 2018b, Liu et al., 2018c), although contrast with the one previous *CBLL1* study in PCa patients which found *CBLL1* mRNA expression to be negatively associated with PCa development and progression (Su et al., 2021).

With that in mind, siRNA-mediated depletion of *CBLL1* coupled with RNA-Seq was performed in the androgen-sensitive LNCaP:C4-2 cell line and its enzalutamide-resistant counterpart LNCaP:C4-$2_{enzR}$ to determine the function of *CBLL1* in the basal and androgen-regulated transcriptome.

Consistent with results presented in Chapter 3, androgen increased *CBLL1* expression in LNCaP:C4-2 and LNCaP:C4-$2_{enzR}$ cells at both the protein (**Figure 4.1A**&**B** and **Figure 4.1D**&**E**) and mRNA (**Figure 4.2A**&**B**) level. In LNCaP:C4-2 cells androgen treatment also appeared to oppose *CBLL1* depletion at both the protein (**Figure 4.1A**&**D**) and mRNA level (**Figure 4.2A**) although this was not observed in LNCaP:C4-$2_{enzR}$ cells (**Figure 4.1B**&**E** and **Figure 4.2B**).

The impact of *CBLL1* depletion on expression of AR and KLK3/PSA expression was next examined. At the protein and mRNA levels, AR expression appeared lower in LNCaP:C4-$2_{enzR}$ compared with LNCaP:C4-2 cells, and whilst expression of AR was androgen-regulated in both cell lines, it was more

pronounced in the enzalutamide-resistant cells (**Figure 4.1** and **Figure 4.3**). Additionally, examination of our RNA-Seq data revealed no significant change in *AR* expression between vehicle-treated scrambled control LNCaP:C4-2 compared with LNCaP:C4-2$_{enzR}$ cells. This is in contrast to a number of studies which have reported higher AR expression in CRPC compared with hormone-sensitive tumours, however it should be noted that amplification of the *AR* gene was only observed in ~20% of patients in these studies, and therefore additional mechanisms of castrate resistance were suggested to be of equal or greater importance (Edwards et al., 2003, Koivisto et al., 1997, Miyoshi et al., 2000).

The effect of *CBLL1* knockdown on expression of *KLK3*, a classical AR target gene (Olsen et al., 2016), was also analysed at the mRNA level. As expected, androgen treatment markedly induced *KLK3* expression in both scrambled control LNCaP:C4-2 and LNCaP:C4-2$_{enzR}$ cells (**Figure 4.3B**&**D**). Interestingly *CBLL1* knockdown also modestly, but significantly, induced *KLK3* expression in both cell lines in the absence of androgen (**Figure 4.3B**&**D**), and significantly attenuated androgen induction of *KLK3* expression in LNCaP:C4-2$_{enzR}$ cells (**Figure 4.3D**). These results indicate a role for *CBLL1* within androgen signalling and support amplified androgen signalling in castrate-resistant enzalutamide-resistant cells.

It was interesting to observe that, despite the effects of *CBLL1* depletion discussed above, *CBLL1* knockdown had no significant impact on cellular proliferation in either LNCaP:C4-2 and LNCaP:C4-2$_{enzR}$ cells (**Figure 4.4**). This lack of effect on cellular phenotype following *CBLL1* depletion contrasts with a number of reports of higher CBLL1 expression being associated with a pro-

oncogenic features in other cancer types (Liu et al., 2018b, Liu et al., 2018c, Castosa et al., 2018) and, indeed, with the one known study that reported an association of higher CBLL1 expression with reduced proliferation (Gong et al., 2010). Interestingly, our research group have recently reported conflicting findings with regard to the effect of knockdown of *METTL3* on PCa cell proliferation (encoding the catalytic subunit of the m6A methyltransferase complex), with shRNA-mediated knockdown of *METTL3* resulting in increased proliferation of LNCaP:C4-2 cells (Lothion-Roy et al., 2022), but short-term inhibition of METTL3 using the small molecule inhibitor STM4257 resulting in reduced proliferation of LNCaP:C4-2 cells (Haigh et al., 2022). No studies are known to have examined the effect of CBLL1 on cellular proliferation in PCa cells.

RNA-Seq analysis of vehicle- and androgen-treated scrambled control and *CBLL1*-depleted LNCaP:C4-2 and LNCaP:C4-$2_{enzR}$ cells allowed analysis of the role of CBLL1 in the regulation of basal and androgen-regulated gene expression in PCa. The baseline effect of enzalutamide resistance was initially examined through the analysis of DEGs and associated enriched pathways between vehicle-treated scrambled control LNCaP:C4-2 and LNCaP:C4-$2_{enzR}$ cells (**Figure 4.5**). Key genes upregulated in LNCaP:C4-$2_{enzR}$ compared with LNCaP:C4-2 cells included *KLK3/PSA*, *TMPRSS2*, *MET* and *ASCL1*).

Unsurprisingly, *KLK3* was upregulated in LNCaP:C4-$2_{enzR}$ compared with LNCaP:C4-2 cells. This is consistent with numerous previous studies that have observed increased expression of this AR-target gene in PCa, with expression continuing to increase as PCa progresses (Olsen et al., 2016, Wu et al., 2022).

*TMPRSS2* is another target gene of the AR that is known to fuse with *ERG*, an oncogenic member of the erythroblast transformation-specific (ETS) transcription factor family, in the majority of PCa patients (Tomlins et al., 2005, Yu et al., 2010). The *TMPRSS2-ERG* fusion is the most common gene fusion observed in human cancer and is believed to play a key role in PCa development and progression (Park et al., 2014, Tomlins et al., 2005, Tomlins et al., 2008). The results presented in this chapter are consistent with these previous studies, in that increased *TMPRSS2* expression is associated with the LNCaP:C4-$2_{enzR}$ cell line, a model for a more advanced form of PCa compared with parental LNCaP:C4-2 cells.

Expression of the *MET* oncogene was also upregulated in the LNCaP:C4-$2_{enzR}$ cell line compared with LNCaP:C4-2. *MET* has been reported to function as an important driver of enzalutamide resistance and is known to play a key role in PCa progression through upregulation the ATM/ATR and PI3K/Akt signalling pathways (Lee and Smith, 2013, Qiao et al., 2016, Zhou et al., 2021c).

Similarly, it was found that *ASCL1* expression was upregulated in LNCaP:C4-$2_{enzR}$ cells. This observation is also consistent with previous reports of the association of *ASCL1* with enzalutamide resistance through influencing transition to a neuroendocrine phenotype (Nouruzi et al., 2022). Therefore, the results presented in this chapter are validated by the findings reported in these earlier studies.

The effect of androgen on enzalutamide resistance was next examined in R1881-treated scrambled control LNCaP:C4-2 and LNCaP:C4-$2_{enzR}$ cells. Key genes upregulated by androgen in LNCaP:C4-$2_{enzR}$ compared with LNCaP:C4-

2 cells included *IGF1* and *FGFR3* (components of the PI3K-Akt pathway), with *MR* and *PRKCA* key downregulated genes.

Increased insulin-like growth factor-1 (*IGF1*) expression, stimulated by growth hormone (GH), has a systemic effect on promoting cellular proliferation and inhibiting apoptosis (Gubbi et al., 2018, Yakar et al., 2002). IGF1 has been associated with cancer, with elevated levels of IGF1 detected in the blood of patients correlated with increased risk of a number of types of cancer, including PCa (Giovannucci et al., 2000, Hankinson et al., 1998, Murphy et al., 2020, Shi et al., 2001).

*FGFR3* encodes one of the family of four fibroblast growth factor receptors, a transmembrane receptor tyrosine kinase that regulates signalling cascades involved in a myriad of physiological processes including cellular proliferation and survival, embryological development and angiogenesis (Haugsten et al., 2010, Perez-Garcia et al., 2018). Aberrant FGFR signalling has been implicated in carcinogenesis, disease progression and therapy resistance in a number of cancer types (Brooks et al., 2012, Dienstmann et al., 2014, Turner and Grose, 2010).

*MR* (encoding the mineralocorticoid receptor) has been reported to have an inhibitory effect on AR signalling and an overall tumour suppressor role in PCa (Kim et al., 2014, Shiota et al., 2019), and moreover to increase PCa cell sensitivity to enzalutamide (Shiota et al., 2018). Indeed, it has been found that androgen hormones can bind the MR and then function as potent MR antagonists in human kidney cells (Takeda et al., 2007). There is also complex physiological interplay between endogenous MR-agonists such as

aldosterone, cortisol and androgens, and these in turn are reflected in the complex interactions of ADTs and therapeutic corticosteroids in patients (Khalaf et al., 2019, Kim et al., 2014, Nagata et al., 2019, Shiota et al., 2018, Zhao et al., 2022).

*PRKCA* encodes protein kinase C alpha, a serine/threonine kinase that functions as an intracellular transductor (Lahn et al., 2004, Nishizuka, 1988). PRKCA has been reported to promote tumour cell growth in a range of cancer types, including PCa, by activating the MAPK pathway (Basu, 1993, Lahn et al., 2004, Pages et al., 2015).

A number of enriched cancer-related KEGG pathways were associated with the DEGs identified between vehicle-treated scrambled control LNCaP:C4-2 and LNCaP:C4-$2_{enzR}$ cells (**Figure 4.5C**). These included the pathways in cancer, PI3K-Akt signalling and MAPK signalling pathways. Key enriched cancer-related KEGG pathways associated with DEGs identified between R1881-treated scrambled control LNCaP:C4-2 and LNCaP:C4-$2_{enzR}$ cells included the pathways in cancer and MAPK signalling pathways (**Figure 4.5D**).

The phosphatidylinositol-3-kinase/protein kinase B (PI3K-Akt) pathway is commonly altered in cancer and has been associated with therapy resistance (Fresno Vara et al., 2004). Indeed, almost half of all metastatic CRPC tumours are reported to have altered expression of the PI3K pathway (Robinson et al., 2015). It has been demonstrated that PI3K-mediated phosphorylation is induced by androgen, through its direct interaction with the AR (Baron et al., 2004), and moreover, that the PI3K-Akt pathway can function to activate expression of AR mRNA and protein, therefore potentially contributing to the

progression to a castrate-resistant state (Yang et al., 2005). It is interesting, therefore, that the PI3K-Akt pathway was only enriched in vehicle-treated scrambled control LNCaP:C4-2 vs LNCaP:C4-$2_{enzR}$ cells, and not the same cells treated with R1881.

The mitogen-activated protein kinase (MAPK) signalling pathway has also been associated with cancer progression, most notably that the rate of increase and degree of MAPK activation can be positively correlated with PCa grade and stage (Gioeli et al., 1999, Weber and Gioeli, 2004). It has also been reported that constitutively active MAPK signalling sensitises the AR in PCa cells to low environmental levels of androgen, rendering them less reliant on androgen for their continued growth and AR-regulated gene expression (Bakin et al., 2003). Indeed, it has also been reported that downstream signalling pathways of both MAPK and PI3K are amplified in CRPC (Edwards et al., 2003).

Taken together these results confirm the molecular mechanism of enzalutamide resistance in the LNCaP:C4-$2_{enzR}$ cells used in this study, and the association of enzalutamide resistance with poorer prognostic factors in PCa.

The effect of *CBLL1* depletion on basal transcription through analysis of differential gene expression and their associated enriched pathways was then examined between vehicle-treated LNCaP:C4-2 and LNCaP:C4-$2_{enzR}$ cells (**Figure 4.6**). Key genes upregulated by *CBLL1* depletion in LNCaP:C4-2 cells included *CA9*, *IGF1* and *GHR*, with *MR* a key downregulated gene.

The carbonic anhydrase 9 (*CA9*) gene is a marker of tumour hypoxia, transcription of which is upregulated in the hypoxic and, inevitably, acidotic, tumour environment to aid in pH regulation, giving tumour cells a greater tolerance to acidosis (McDonald et al., 2019, Wilson and Hay, 2011). It is considered to be a negative prognostic biomarker in many cancer types, including prostate (Chiche et al., 2009, Lin et al., 2019, McDonald et al., 2019). It is intriguing that *CA9*, a gene whose transcriptional upregulation should usually only be triggered by hypoxic conditions was upregulated in LNCaP:C4-2 cells as a result of *CBLL1* depletion. This suggests that CBLL1 is mimicking the normoxic environment, and that loss of CBLL1 expression therefore mimics hypoxia. Interestingly, this effect was lost in LNCaP:C4-$2_{enzR}$ cells, where no differential expression in *CA9* was observed between scrambled control and *CBLL1*-depleted cells.

Similarly upregulated by *CBLL1* depletion in vehicle-treated LNCaP:C4-2 cells were insulin-like growth factor-1 (*IGF1*) and the growth hormone receptor (*GHR*). The growth hormone (GH)-IGF1 axis is integral to the regulation of cell growth, differentiation and death (Werner and Laron, 2020). Dysregulation of the GH/GHR axis has been associated with many cancer types, with upregulation of *GHR* expression and GH-induced activation of signalling pathways implicated in PCa progression (Basu et al., 2018, Gebre-Medhin et al., 2001, Weiss-Messer et al., 2004). The findings presented in this chapter demonstrate that both *IGF1* and *GHR* are CBLL1-regulated independent of androgen, and that loss of CBLL1 results in their upregulation. Again, as with *CA9*, this tumour suppressor effect of CBLL1 is lost in the enzalutamide

resistant cell line, suggesting that enzalutamide resistance allows gene expression within PCa cells to function independently of CBLL1 regulation.

In contrast, the gene encoding the mineralocorticoid receptor (*MR*), discussed earlier, was significantly downregulated by *CBLL1* depletion in vehicle-treated LNCaP:C4-2 cells.

Nine enriched cancer-related KEGG pathways were associated with the DEGs identified between vehicle-treated LNCaP:C4-2 cells upon *CBLL1* depletion (**Figure 4.6C**). These included many pathways involved in detoxification, including the steroid biosynthesis pathway. It is notable that the same conditions in LNCaP:C4-$2_{enzR}$ cells resulted in no significantly enriched KEGG pathways (**Figure 4.6D**), and therefore that the CBLL1 regulation of genes within these pathways is lost with enzalutamide resistance.

Next, androgen-regulated genes dependent on CBLL1 were assessed through analysis of differential gene expression and the associated enriched pathways elicited by androgen treatment in scrambled control LNCaP:C4-2 and LNCaP:C4-$2_{enzR}$ cells (**Figure 4.7**). Key genes upregulated by R1881 treatment in both scrambled control LNCaP:C4-2 and LNCaP:C4-$2_{enzR}$ cells included, unsurprisingly, the prototypical androgen-regulated genes *NKX3-1*, *KLK3* and *TMPRSS2*.

As discussed above, *KLK3* is a well-characterised androgen-regulated gene, and its expression is known to be upregulated by androgen exposure (Clegg et al., 2002). Likewise, *TMPRSS2* is a well-studied AR target gene, whose transcription is stimulated by androgen (Grönberg, 2003, Lin et al., 2009).

Expression of *NKX3.1*, the gene encoding the prostate-specific homeobox protein NKX3.1 is similarly induced by androgen (Prescott et al., 1998).

The findings presented in this study are consistent with the literature, with *NKX3-1*, *KLK3* and *TMPRSS2* previously shown to be androgen-regulated in PCa. However, in *CBLL1*-depleted conditions in LNCaP:C4-2 cells *NKX3-1* loses its androgen regulation, and in LNCaP:C4-$2_{enzR}$ cells *KLK3* is no longer regulated by androgen (**Figure 4.8)**. This suggests that in LNCaP:C4-2 cells androgen regulation of *NKX3-1* is CBLL1-dependent. CBLL1 is essential to maintain androgen regulation of *KLK3* once enzalutamide resistance has occurred. Taken together these results implicate a role for CBLL1 in the progression of PCa to a castrate-resistant state.

*TMPRSS2* is another AR-target gene that is known to form onco-fusion proteins with *ERG* and other members of the erythroblast transformation-specific (ETS) transcription factor family, in the majority of PCa patients (Tomlins et al., 2005, Yu et al., 2010). The *TMPRSS2-ERG* gene fusion has been associated with the PCa precursor high grade PIN and is believed to play a role in PCa development and progression (Park et al., 2014, Tomlins et al., 2008). The results presented in this chapter are consistent with these previous studies, in that increased *TMPRSS2* expression is associated with the LNCaP:C4-$2_{enzR}$ cell line, a model for a more advanced form of PCa compared with parental LNCaP:C4-2 cells.

Twenty-nine enriched KEGG pathways were associated with the DEGs identified between scrambled control LNCaP:C4-2 cells upon R1881 treatment (**Figure 4.7C**). These included many directly cancer-associated pathways,

including most notably the pathways in cancer, prostate cancer, and PI3-Akt signalling pathways. In contrast, ~40% fewer KEGG pathways were enriched in LNCaP:C4-$2_{enzR}$ cells (**Figure 4.7D**), the majority of which were cancer-related. This highlights the castrate-resistant phenotype of these PCa cells, in that they are no longer reliant on androgen-regulated pathways. In common with the parental cell line, these enriched pathways included the pathways in cancer and prostate cancer KEGG pathways, however regulation of the PI3K-Akt signalling pathway was lost with enzalutamide resistance. It is also remarkable that even within the 44.4% of enriched pathways common to both the parental and enzalutamide-resistant cell lines the DEGs within those pathways alter. For example, in scrambled control LNCaP:C4-2 cells, the enriched pathways in cancer KEGG pathway contained a number of DEGs upregulated with R1881 treatment, including *IGF1*, *VEGFA*, *MYC*, *NKX3-1*, and *MTOR*.

IGF1 is a peptide hormone with a marked mitogenic effect in PCa, and its expression is positively correlated with carcinogenesis, both in PCa and in a number of other cancer types (Giovannucci et al., 2000, Hankinson et al., 1998, Murphy et al., 2020, Shi et al., 2001). IGF1 expression is also known to be stimulated by androgen hormones (Hakuno and Takahashi, 2018, Vendola et al., 1999). IGF1 signalling has been demonstrated to stimulate PCa cell proliferation through the activation of local prostate MAPK and PI3K-Akt signalling (Hakuno and Takahashi, 2018, Matsushita et al., 2021).

*VEGFA*, formerly known simply as *VEGF*, encodes one of the vascular endothelial-derived growth factor family of cytokines that promotes normal angiogenesis both *in utero* and in adult wound healing, however in cancer, it is

a primary driver of tumour angiogenesis (Carmeliet, 2005, Claesson-Welsh and Welsh, 2013). Overexpression of VEGFA has been reported in PCa, with VEGFA positively correlated with distant metastasis and poorer prognosis (Duque et al., 1999, Green et al., 2007, Wegiel et al., 2005). Androgen is known to upregulate *VEGFA* expression, although the precise mechanism for this has not yet been fully elucidated (Eisermann and Fraizer, 2017, Kashyap et al., 2013).

MYC, a master transcription factor and oncoprotein, is widely reported to be a critical driver of PCa development and progression (Qiu et al., 2022). Overexpression or structural alteration of *MYC* is believed to be present in over 70% of human cancer types, including PCa (Dang, 2012, Meyer and Penn, 2008, Qiu et al., 2022). Indeed, such is the oncogenic potential of MYC, that its overexpression alone within normal mouse prostatic luminal cells is sufficient to initiate PCa (Ellwood-Yen et al., 2003).

*MTOR* encodes the mammalian target of rapamycin protein, which is a downstream effector the PI3K signalling pathway (Sutherland et al., 2014). mTOR is a master controller of cellular growth and metabolism (Hall, 2008, Wullschleger et al., 2006). mTOR signalling is commonly activated in cancer to induce metabolic reprogramming of tumour cells, which in turn impacts upon mTOR signalling (Mossmann et al., 2018). Furthermore, mTOR has been found to interact with the AR, with expression of mTOR known to be increased in the presence of androgen in PCa, and mTOR regulating AR expression (Mossmann et al., 2018, Shorning et al., 2020).

In scrambled control LNCaP:C4-2 cells the enriched prostate cancer pathway contained several DEGs upregulated with R1881 treatment including, unsurprisingly, the known androgen-regulated genes *NKX3-1*, KLK3, and *TMPRSS2*. Interestingly, *PIK3R3* (encoding the phosphoinositide-3-kinase (PI3K) regulatory subunit 3) which is overexpressed in a number of cancer types (Ibrahim et al., 2018, Zhang et al., 2007, Zhou et al., 2012) was downregulated in response to androgen.

Another enriched pathway associated with DEGs in scrambled control LNCaP:C4-2 cells was the PI3K-Akt pathway. Upregulated genes in response to R1881 treatment within this pathway included *GHR*, *IGF1R*, *MYC* and *MTOR*, all of which, together with their role in PCa, have been discussed above. Interestingly, no enrichment of the PI3K-Akt pathway was seen in the enzalutamide-resistant cell line, suggesting that androgen regulation of this pathway is lost in the progression to CRPC.

Consistent with the literature it was found the genes listed above were androgen-regulated in the LNCaP:C4-2 cells used in this study. However, in scrambled control LNCaP:C4-$2_{enzR}$ cells, whilst *IGF1*, *VEGFA*, *NKX3-1*, and *MTOR* remained differentially expressed in response to androgen within the pathways in cancer pathway, *MYC* was no longer regulated by androgen. Similarly, in the prostate cancer KEGG pathway, the prototypical androgen-regulated genes *NKX3-1*, *KLK3* and *TMPRSS2* that were differentially expressed in the parental cell line were no longer androgen-regulated in LNCaP:C4-$2_{enzR}$ cells. Moreover, androgen was no longer able to suppress the expression of the oncogene *PIK3R3* once enzalutamide resistance had occurred, likely a key contributor to the poor prognosis associated with CRPC.

The effect of *CBLL1* knockdown on the androgen-regulated transcriptome was subsequently examined through analysis of differential gene expression and the associated enriched pathways elicited by androgen treatment in CBLL1-depleted LNCaP:C4-2 and LNCaP:C4-$2_{enzR}$ cells (**Figure 4.8**). These results provide evidence that CBLL1 is implicated in the progression of PCa to a more advanced disease state.

Twelve enriched KEGG pathways were associated with the DEGs altered by androgen treatment in scrambled control versus *CBLL1*-depleted LNCaP:C4-2 cells (**Figure 4.8C**). Only eight pathways were enriched with R1881 treatment in *CBLL1*-depleted LNCaP:C4-$2_{enzR}$ cells (**Figure 4.8D**), with only one pathway in common with the parental cell line (pathways in cancer), and the other 11 pathways enriched in the parental cell line no longer androgen-regulated in enzalutamide-resistant cells. This limited 5% overlap of pathways between *CBLL1*-depleted parental and enzalutamide-resistant LNCaP:C42 cells contrasts with the 44.4% overlap of pathways seen between the two cell lines in scrambled control conditions (**Figure 4.7**), and supports an important role for CBLL1 in regulating the androgen-regulated transcriptome, both in enzalutamide-sensitive and -resistant PCa.

Within the one commonly enriched KEGG pathway, pathways in cancer, it was noted that in scrambled control parental cells, the differentially expressed oncogenes *VEGFA*, *MYC*, *PIK3R3* and *MTOR* were all androgen-regulated. However, in *CBLL1*-depleted cells this androgen regulation of *VEGFA* and *MYC* was lost, again supporting a role for CBLL1 in maintaining androgen regulation of these key PCa-associated genes. In scrambled control LNCaP:C4-$2_{enzR}$ cells, *VEGFA*, *PIK3R3* and *MTOR* were androgen-regulated,

however, in the transition to enzalutamide resistance, the regulation of *MYC* expression by androgen was lost. This was the same in *CBLL1*-depleted enzalutamide-resistant cells however, in these conditions, androgen regulation of *PIK3R3* expression was also lost, suggesting an essential role for CBLL1 in the androgen regulation of the *PIK3R3* oncogene.

In addition to the prototypical androgen-regulated genes referenced above, which, interestingly, were observed to have altered androgen regulation in the face of *CBLL1* knockdown and enzalutamide resistance, other key genes upregulated by R1881 treatment in *CBLL1*-depleted LNCaP:C4-2 cells included *HIF1A*, *NCOA1* and *MTOR*.

The hypoxia inducible factor-1 alpha (*HIF1A*) gene encodes one of the two subunits of HIF-1, a transcriptional activator that is a master regulator of oxygen homeostatic pathways (Semenza, 2001). Expression of HIF-1α is induced by a hypoxic cellular environment (Jiang et al., 1996), which in turn regulates a number of target genes that are fundamental in the response to hypoxia, including through altering cellular metabolism and angiogenesis (Semenza, 2000). In tumour cells, *HIF1A* expression can be aberrantly upregulated in response to the loss of function of the p53 tumour suppressor, which results in upregulation of downstream target genes such as *VEGFA* (Maxwell et al., 1999, Ravi et al., 2000). It has been reported that HIF-1α is overexpressed in advanced PCa, and that HIF-1α can promote prostate cancer stem cell survival through its interaction with the PI3K-Akt-mTOR pathway (Bai et al., 2010, Mimeault and Batra, 2013, Zhang et al., 2021). Moreover, it has been reported that HIF-1α is androgen-regulated and its expression is induced by androgen (Kimbro and Simons, 2006). These previous studies are

consistent with the results presented in this chapter, although it is interesting to observe that *HIF1A* was only androgen-regulated in the absence of *CBLL1*. Similarly, no differential expression of *HIF1A* was observed in LNCaP:C4-$2_{enzR}$ cells, suggesting that enzalutamide resistance results in loss of the androgen regulation of the *HIF1A* gene.

The *NCOA1* gene encodes the nuclear receptor coactivator 1, also known as Src1, which directly binds nuclear receptors, including the AR, and stimulates transcription in a hormone-dependent fashion (Lonard et al., 2007, Peng et al., 2022, Stashi et al., 2014, Walsh et al., 2012). As an AR coactivator, NCOA1 has a pro-oncogenic function in PCa, with higher NCOA1 expression in androgen-dependent tumours associated with metastasis (Agoulnik et al., 2005). It has also been implicated in castrate resistance, with higher levels of NCOA1 reported in CRPC compared with androgen-dependent tumours, leading to the suggestion that NCOA1 may be responsible for the reactivation of AR-mediated transcription despite the low-level androgen environment (Gregory et al., 2001, Mäki et al., 2006, Walsh et al., 2012).

These previous studies are consistent with the results presented in this chapter, that both *HIF1A* and *NCOA1* are androgen-regulated, however it is interesting to observe that they are only androgen-regulated in the absence of *CBLL1*, therefore suggesting an inhibitory function of CBLL1 on androgen upregulation of these genes. Similarly, no differential expression of *HIF1A* or *NCOA1* was observed in LNCaP:C4-$2_{enzR}$ cells, suggesting that enzalutamide resistance results in the loss of androgen regulation of these genes that is present in less advanced models of PCa.

Interestingly, *MTOR* is differentially expressed in response to androgen treatment in both scrambled control and *CBLL1*-depleted LNCaP:C4-2$_{enzR}$ cells treated with vehicle or R1881, however this is in contrast to the findings in LNCaP:C4-2 cells, where it is only androgen-regulated in the presence of CBLL1 (scrambled control condition). This interesting change of *MTOR* regulation in LNCaP:C4-2$_{enzR}$ cells may contribute to the emergence of enzalutamide resistance.

Overall, comparison of the significantly enriched DEG-associated KEGG pathways with androgen treatment between scrambled control and *CBLL1*-depleted LNCaP:C4-2 and LNCaP:C4-2$_{enzR}$ cells demonstrates not only the intrinsic difference in CBLL1-regulated basal transcription between the parental and enzalutamide-resistant cell lines, but also the difference in androgen-regulated transcription, with the presence of androgen unable to compensate for the lack of CBLL1 in *CBLL1*-depleted cells. This indicates a key role for CBLL1 in androgen-regulated gene expression in PCa as it progresses.

The contribution of CBLL1 to enzalutamide resistance in the progression of PCa was highlighted by comparing the DEG-associated significantly enriched KEGG pathways in scrambled control LNCaP:C4-2 and LNCaP:C4-2$_{enzR}$ cells /-+R1881 (**Figure 4.9A**). Only ~20% of pathways were common to both cell lines, and fewer pathways were enriched in the enzalutamide-resistant cells, yet a greater proportion of these were directly related to cancer than in the parental cell line. *CBLL1* depletion in LNCaP:C4-2 and LNCaP:C4-2$_{enzR}$ cells treated with vehicle or R1881 resulted in fewer than half the number of significantly enriched pathways (**Figure 4.9C**) compared with scrambled

control cells (**Figure 4.9A**). Only one KEGG pathway was common to *CBLL1*-depleted parental and enzalutamide-resistant cells (hsa05200 pathways in cancer). Of the significantly enriched pathways in *CBLL1*-depleted enzalutamide-resistant cells treated with vehicle or R1881, 87.5% were common to scrambled control enzalutamide-resistant cells treated with vehicle or R1881, the overwhelming majority of which were directly linked to cancer. However, in *CBLL1*-depleted parental cells treated with vehicle or R1881, only 66.7% were common to scrambled control parental cells treated with vehicle or R1881, with none, apart from pathways in cancer, directly associated with cancer. Key pathways that were no longer enriched in *CBLL1*-depleted parental cells treated with vehicle or R1881 included the PI3K-Akt signalling pathway, central carbon metabolism in cancer, proteoglycans in cancer, and the prostate cancer pathway. This suggests a key role for CBLL1 in maintaining the normal androgen regulation of a number of key cancer-related pathways in both androgen-dependent PCa and CRPC.

It is interesting that *CBLL1* knockdown of vehicle-treated LNCaP:C4-2 and LNCaP:C4-$2_{enzR}$ cells resulted in no significantly enriched pathways in enzalutamide-resistant cells compared with nine in parental LNCaP:C4-2 cells. This confirms the remarkable impact of enzalutamide resistance on the basal transcriptome, whereby the basal transcriptome of LNCaP:C4-$2_{enzR}$ is no longer influenced by CBLL1.

Following analysis of DEGs, alternative splicing in response to *CBLL1* depletion and androgen treatment was assessed in both LNCaP:C4-2 and LNCaP:C4-$2_{enzR}$ cells. Alternative splicing has been implicated in PCa, with pathogenic splice variants of the AR representing one of the key mechanisms

of the progression to castrate resistance (Jernberg et al., 2017). $m^6A$ is implicated in regulating context-dependent splicing *in vivo* (Haussmann et al., 2016, Lence et al., 2016), however the exact contribution of $m^6A$ to alternative splicing, exon selection and transcript stability has been debated (Darnell et al., 2018, Ke et al., 2015, Ke et al., 2017, Zhao et al., 2018). However, no studies have yet investigated the role of CBLL1 in alternative splicing in PCa. It is also known that steroid hormones affect expression of splicing (Auboeuf et al., 2004), therefore DSGs and their associated pathways were analysed in the context of *CBLL1* presence or depletion and R1881 treatment in LNCaP:C4-2 and LNCaP:C4-$2_{enzR}$ cells (**Figure 4.10**).

As expected in light of the DEGs already discussed, many differences in alternative splicing events were observed between the parental LNCaP:C4-2 cell line and the enzalutamide-resistant LNCaP:C4-$2_{enzR}$.

Firstly, it was remarkable how the number of DSGs was approximately double that of the number of DEGS in the parental LNCaP:C4-2 cell line, and ~50% higher than the number of DEGs in LNCaP:C4-$2_{enzR}$ cells, yet the number of significantly enriched pathways associated with DSGs was minimal in comparison. This is largely attributable to the large number of non-coding RNAs that were found to be alternatively spliced. Indeed, one important limitation to existing pathway analysis tools and databases is these are generally restricted to protein coding genes as current understanding of the function of non-coding RNAs lags behind the decades of research underpinning protein pathway databases. It was also remarkable how little overlap was seen between the ~2000 DEGs and DSGs across all of the

conditions in both LNCaP:C4-2 and LNCaP:C4-$2_{enzR}$ cells. This demonstrates a role for CBLL1 in selective regulation of splicing in PCa.

In the parental cell line, the greatest effect on differential splicing was seen with *CBLL1* knockdown in R1881-treated cells, suggesting a role for CBLL1 in splicing (**Figure 4.10** and **Appendix 14**). In LNCaP:C4-$2_{enzR}$ cells the greatest number of alternative splicing events was seen in response to androgen treatment in scrambled control cells (**Figure 4.10** and **Appendix 15**). This does, however, accord with the findings reported above with regard to differential gene expression, that the influence of CBLL1 is attenuated with castrate resistance in PCa cells.

Skipped exon was the most common splicing event type across all conditions and in both cell lines. In the parental LNCaP:C4-2 cell line notable DSGs with SE events were *NKX3-1* (in scrambled control cells treated with vehicle or R1881) and *PTEN* (in vehicle-treated cells upon *CBLL1* depletion), both well-characterised tumour suppressor genes in PCa.

*NKX3-1* is an androgen-regulated largely prostate-specific gene, with at least five reported splice variants (Korkmaz et al., 2000). Whilst the function and significance of these splice variants is not yet well understood, it has been reported that loss of function of *NKX3-1* is associated with PCa carcinogenesis (Abate-Shen et al., 2008).

*PTEN* encodes the phosphatase and tensin homolog and is a well-established tumour suppressor gene that is commonly inactivated in ~20% of localised and ~50% of advanced PCa cases (Trotman et al., 2003). Its function is to negatively regulate the PI3K-Akt signalling pathway, which in turn regulates

cell growth, proliferation and survival (Chalhoub and Baker, 2009). Therefore *PTEN* inactivation gives way to unregulated and constitutive activation of the PI3K-Akt signalling pathway and the uncontrolled cellular proliferation that results (Okumura et al., 2011). Whilst differential splicing of *PTEN* has been implicated in cancer, there are limited reports as to the clinical relevance of *PTEN* splice variants (Okumura et al., 2011).

Mutually exclusive exons was the second most common splicing event type in the parental LNCaP:C4-2 cell line. Notable DSGs with MXE events were *NCOA1*, *FOXA1* and *PIK3CB*, (in R1881-treated cells upon *CBLL1* depletion), all oncogenes in PCa.

As previously discussed, *NCOA1* is an AR coactivator with an oncogenic function in PCa (Agoulnik et al., 2005). It has been reported to be susceptible to alternative splicing (Sorek et al., 2004), with *NCOA1* splice variants implicated in the generation of a fusion protein that forms a genetic signature for a subset of soft tissue sarcomas (Wachtel et al., 2004).

*FOXA1* encodes the forkhead box A1 protein, a pioneer factor that functions to open chromatin to allow binding by transcription factors such as the AR (Teng et al., 2021). It directly interacts with the AR and is widely reported to drive prostate carcinogenesis and PCa progression (Barbieri et al., 2012, Gerhardt et al., 2012, Sahu et al., 2011). FOXA1 has been reported to be a primary orchestrator of dysregulation of alternative splicing in PCa (Del Giudice et al., 2022).

*PIK3CB* encodes the phosphatidylinositol-4,5-bisphosphate 3-kinase catalytic subunit beta protein, a catalytic subunit of a class IA PI3K that also comprises

a regulatory subunit such as PIK3R3, as discussed earlier (Zhang et al., 2020b). PI3K protein complexes play a pivotal role in the PI3K-Akt pathway and have also been reported to be a key driver of widespread alternative splicing (Ladewig et al., 2022). *PIK3CB* was also a notable DSG associated with MXE events in R1881-treated LNCaP:C4-$2_{enzR}$ cells upon *CBLL1* depletion.

It is notable that very few significantly enriched KEGG pathways were associated with the DSGs identified in either the parental or enzalutamide-resistant cell lines, particularly when compared with the number of enriched pathways associated with DEGs. In scrambled control LNCaP:C4-2 cells treated with vehicle or R1881 only one pathway (metabolic pathways) was significantly enriched associated with MXE events. The only other significantly enriched pathway (pyrimidine metabolism) was observed in R1881-treated LNCaP:C4-2 cells upon *CBLL1* depletion associated with a SE event.

DSG-associated significantly enriched pathways were observed slightly more frequently in LNCaP:C4-$2_{enzR}$ cells. Across all conditions, just five pathways were enriched (**Appendix 15**). In scrambled control LNCaP:C4-$2_{enzR}$ cells treated with vehicle or R1881, four pathways were significantly enriched in association with DSGs with SE events. These comprised the Fanconi anaemia pathway, other types of O-glycan biosynthesis, ubiquitin mediated proteolysis, and metabolic pathways KEGG pathways. One DSG-associated pathway (lysine degradation) was enriched in vehicle-treated LNCaP:C4-$2_{enzR}$ cells upon *CBLL1* knockdown associated with A3SS events.

The Fanconi anaemia pathway is associated with DNA damage repair, and its dysregulation is known to result in genomic instability and chemotherapy resistance in cancer (Liu et al., 2020).

Together with the metabolic pathways KEGG pathway, the other types of O-glycan biosynthesis pathway is also classified as a type of metabolism within the KEGG pathways. It is widely reported that cancer cells alter their metabolism in order to sustain their rapid proliferation (Chen et al., 2014, Feng et al., 2014, Wong et al., 2017, Yasumoto et al., 2016), with a key feature of this characterised as the 'Warburg effect' whereby cells switch from oxidative phosphorylation to aerobic glycolysis (Warburg, 1956).

Ubiquitin mediated proteolysis is fundamental in maintaining protein homeostasis by removing damaged or abnormal protein from cells, primarily via the lysosome or proteasome (Burger and Seth, 2004, Rock and Goldberg, 1999). Aberrations in this pathway are associated with a number of pathologies, particularly cancer (Adams, 2003, Glickman and Ciechanover, 2002). Given the reported function of CBLL1 as an E3 ubiquitin ligase (Aparicio et al., 2012, Fujita et al., 2002), it is somewhat unsurprising that *CBLL1* should be associated with this pathway, however it is interesting that this pathway was only enriched in scrambled control cells and was not induced by *CBLL1* knockdown. Taken together these results suggest a role for enzalutamide resistance in the regulation of cellular metabolism, DNA damage repair and ubiquitin-mediated proteolysis genes through alternative splicing in PCa.

To summarise, functional depletion of *CBLL1* was carried out to assess the effect of *CBLL1* on cellular phenotype, differential gene expression and

alternative splicing, and the associated enriched KEGG pathways. In conclusion, examination of differential gene expression and splicing revealed thousands of DEGs and DSGs regulated by androgen, *CBLL1* and enzalutamide resistance.

CBLL1 was demonstrated to have a key role in maintaining normal androgen-regulation of a number of pivotal oncogenes and tumour suppressor genes in parental LNCaP:C4-2 cells. The enzalutamide-resistant phenotype of the LNCaP:C4-$2_{enzR}$ cells was associated with upregulation of key genes associated with prostate cancer progression, including reduced androgen regulation of known AR-target genes. Similarly, CBLL1-regulated genes in the parental cell line were also observed to lose their regulation by CBLL1 in LNCaP:C4-$2_{enzR}$ cells, demonstrating the transcriptome-wide impact of enzalutamide resistance, whereby LNCaP:C4-$2_{enzR}$ cells become independent of the influence of CBLL1 on gene regulation.

With respect to alternative splicing, CBLL1 was found to play a role in selective regulation of splicing in both LNCaP:C4-2 and LNCaP:C4-$2_{enzR}$ cells.

These results have demonstrated a key role for CBLL1 in maintaining the normal androgen regulation of a number of key cancer-related genes and pathways in both androgen-sensitive PCa and CRPC. Furthermore, they provide more insight into the findings presented in chapter 3, and yet more evidence for a role for CBLL1 in the progression of PCa.

# Chapter 5

## Molecular and clinical significance of CBLL1 expression in breast cancer patient samples and cell lines

# 5 Expression of CBLL1 in breast cancer patient samples and cell lines

## 5.1 Introduction

E-cadherin is a transmembrane glycoprotein found on the plasma membrane of epithelial cells that functions as a key cell-to-cell adhesion mediator (Nollet et al., 1999, Riethmacher et al., 1995, Takeichi, 1991). E-cadherin expression is tightly regulated in differentiated cells, and its downregulation or indeed, loss of expression, is a key feature of cancer progression, and is associated with a more invasive phenotype in a large number of cancer cell types (Nollet et al., 1999, Jiang, 1996), most notably, in the context of this study, breast (Alsaleem et al., 2019, Berx et al., 1996, Berx and Van Roy, 2001). Downregulation of E-cadherin can occur via a variety of mechanisms, including via mutations and transcriptional and post-transcriptional modifications (Berx et al., 1995, Lamouille et al., 2014, Paredes et al., 2012). Additionally, it has been found that downregulation of cell surface E-cadherin expression can occur through its ubiquitination and subsequent degradation following binding by its specific ubiquitin E3 ligase CBLL1, also known as HAKAI (Aparicio et al., 2012, Fujita et al., 2002).

The second reported function of CBLL1 as an adaptor protein to the METTL3-methyltransferase protein complex responsible for $m^6A$ regulation is less well understood (Horiuchi et al., 2013, Ruzicka et al., 2017, Sun et al., 2019, Wen et al., 2018, Yue et al., 2018). Whilst METTL3 expression has been associated with BCa (Achour et al., 2023, Cai et al., 2018, Hu et al., 2022), relatively little is known about the role of CBLL1 in BCa. Indeed, whilst expression of CBLL1 is known to be increased in a number of cancer types (Castosa et al., 2018,

Figueroa et al., 2009b, Hui et al., 2019, Liu et al., 2018c), two BCa studies have reported results that accord with those published in other cancers (Liu et al., 2022b, Ma et al., 2023). One study found that knockdown of *CBLL1* resulted in reduced invasive potential of BCa cells (Liu et al., 2022b), whilst a second reported reduced CBLL1 and increased E-cadherin expression resulting in an anti-metastatic effect (Ma et al., 2023). However, in another BCa study, CBLL1 was reported to act as a co-repressor of the ERα, competitively binding it and thus interfering with recruitment of coactivators and inhibiting ER-positive BCa cell proliferation and migration (Gong et al., 2010). Another study reported somewhat conflicting findings of higher CBLL1 expression in normal breast tissue compared with BCa, yet found higher expression to be associated with better relapse-free and overall survival in BCa patients (Zheng et al., 2021). A final study reported no significant associations between CBLL1 expression and either prognostic factors or survival in a small cohort of BCa patient specimens (Makdissi et al., 2009).

Whilst the role of dysregulated $m^6A$ RNA methylation in cancer has been recently widely reported, little has been published regarding the specific impact of CBLL1 on this process, and indeed how dysregulation of CBLL1 may impact the development and progression of BCa. The E-cadherin-dependent contribution to BCa carcinogenesis has been relatively well characterised, though the potential contribution of CBLL1 remains unclear. The aim of this chapter is, therefore, to further elucidate the role of CBLL1 in BCa, both as a potential ubiquitin E3 ligase and its impact on E-cadherin, and as a “writer” of the $m^6A$ methyltransferase complex, and to determine if CBLL1 might represent a novel prognostic marker or therapeutic target in BCa.

To this end, CBLL1 and E-cadherin expression was analysed in a large well-characterised patient cohort as well as publicly available data sets. Expression of CBLL1 and E-cadherin was also investigated in BCa cell lines, and the effect of estrogen on *CBLL1* and *CDH1* mRNA and protein expression examined. These results provide novel insights into the regulation, expression and clinical significance of CBLL1 in BCa.

## 5.2 Results

### 5.2.1 CBLL1 expression and copy number alterations in breast cancer patients

The expression of *CBLL1* was analysed in publicly-available datasets of BCa patients using the cBioPortal for Cancer Genomics (Cerami et al., 2012, Gao et al., 2013). Two patient cohorts were examined: the TCGA Firehose Legacy breast invasive carcinoma study (n=1108) (Liu et al., 2018a) and the METABRIC breast cancer cohort (n=2509) (Curtis et al., 2012, Pereira et al., 2016) (retrieved 17 April 2023).

Comparative analysis of mutations and putative copy number alterations (CNA) from GISTIC was carried out to determine the frequency of genetic alterations affecting *CBLL1* and *CDH1* in BCa patients. Altered *CBLL1* expression was found to be rare, occurring in ~0.9% of BCa patients in both the TCGA and METABRIC cohorts (**Figure 5.1A**). Amplification was the most common single copy number alteration seen in the TCGA cohort, occurring in 0.27% of cases, and the only CNA seen in 0.88% of patients of the METABRIC cohort (**Figure 5.1A**).

Altered *CDH1* expression was more common, occurring in ~10-12% of BCa patients across both cohorts (**Figure 5.1B**). Multiple types of CNA were most

commonly seen in both cohorts, present in 10.25% of patients in the TCGA cohort and 4.82% of patients in the METABRIC cohort, followed by mutation in 1.1% and 4.78% of patients in the TCGA and METABRIC cohorts, respectively (**Figure 5.1B**). In contrast to the *CBLL1* findings, amplification of *CDH1* was only seen in 0.08% of patients from the METABRIC cohort, and not present at all in the TCGA cohort (**Figure 5.1B**).

To evaluate the clinical relevance of CBLL1 in BCa, mRNA expression of *CBLL1* and *CDH1* was assessed in the two patient cohorts (**Figure 5.1C** and **Figure 5.1D**). Altered expression of *CBLL1* mRNA in BCa patients was both elevated (13.72% in TCGA, 11% in METABRIC) and decreased (15.37% in TCGA, 11.96% in METABRIC) in both cohorts (**Figure 5.1C**). More discordant results were seen between the TCGA and METABRIC cohorts when looking at altered *CDH1* mRNA expression (**Figure 5.1D**). Increased *CDH1* (in 7.04% of cases) and decreased *CDH1* (in 20.86% of cases) expression was observed in the TCGA cohort, whereas *CDH1* was higher in 10.76% and lower in 6.06% of cases in the METABRIC cohort (**Figure 5.1D**).

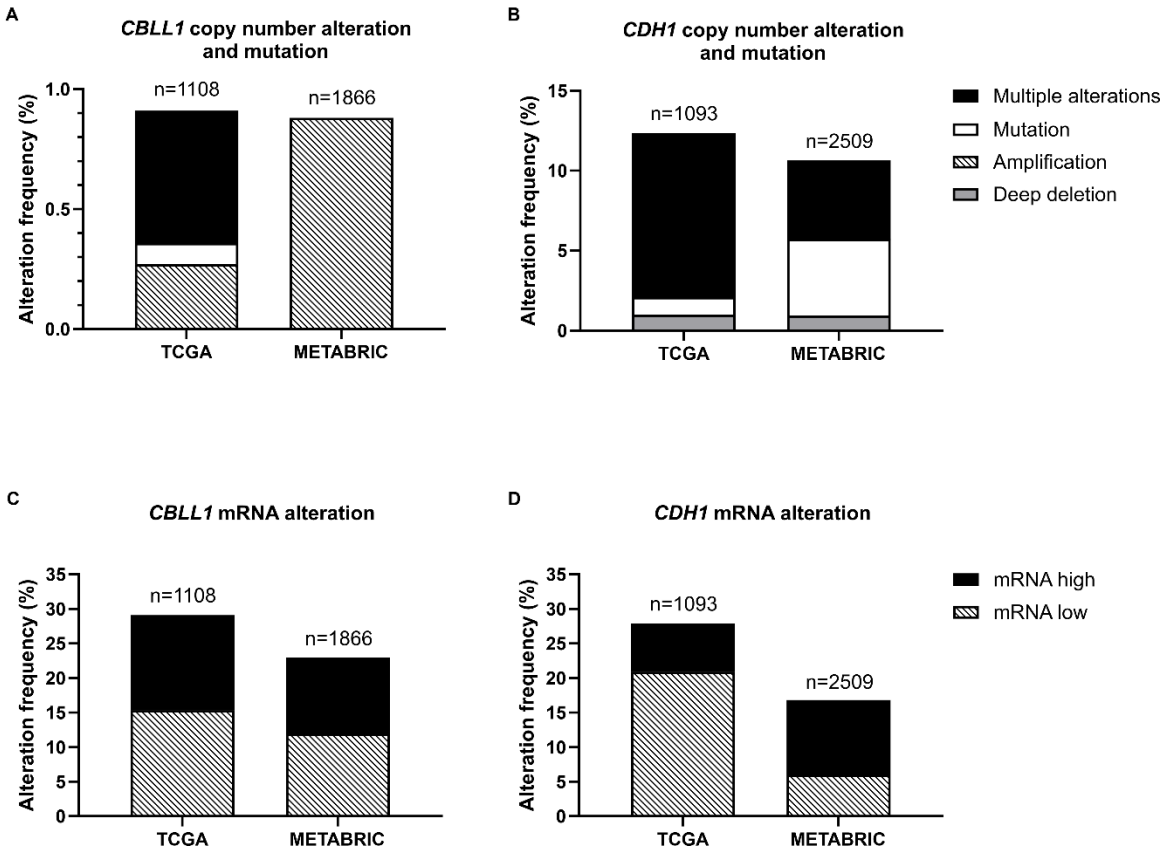


**Figure 5.1 *CBLL1* and *CDH1* alteration frequency in breast cancer**

The cBioPortal for Cancer Genomics (Cerami et al., 2012, Gao et al., 2013) was utilised to assess the incidence of *CBLL1* and *CDH1* amplification, deep deletion and mutation, together with mRNA expression in BCa patients from the TCGA Firehose Legacy breast invasive carcinoma study (Liu et al., 2018a) and the METABRIC breast cancer cohort (Curtis et al., 2012, Pereira et al., 2016). (**A**) Copy number alterations and mutations in *CBLL1* in BCa patients. (**B**) Copy number alterations and mutations in *CDH1* in BCa patients. (**C**) Alterations in mRNA expression of *CBLL1* in BCa patients. (**D**) Alterations in mRNA expression of *CDH1* in BCa patients (z score threshold ± 1).

The effect of copy number alterations (CNA) on *CBLL1* mRNA expression in the TCGA (Liu et al., 2018a) and METABRIC (Curtis et al., 2012, Pereira et al., 2016) breast invasive carcinoma patient cohorts was assessed (**Figure 5.2A** and **Figure 5.2B**). Whilst the majority of cases were diploid for the *CBLL1* locus, the most frequently observed CNA was amplification (**Figure 5.2A** and **Figure 5.2B**). *CDH1* expression was subsequently assessed in association with CNA in both patient cohorts (**Figure 5.2C** and **Figure 5.2D**). Again, the majority of cases were diploid, however the most frequently observed CNA was shallow deletion (**Figure 5.2C** and **Figure 5.2D**). A similar trend was observed between both *CBLL1* and *CDH1* expression and copy number across both cohorts, with higher mRNA expression in cases with copy number gain and amplification, and lower mRNA expression seen with shallow and deep deletion (**Figure 5.2**).

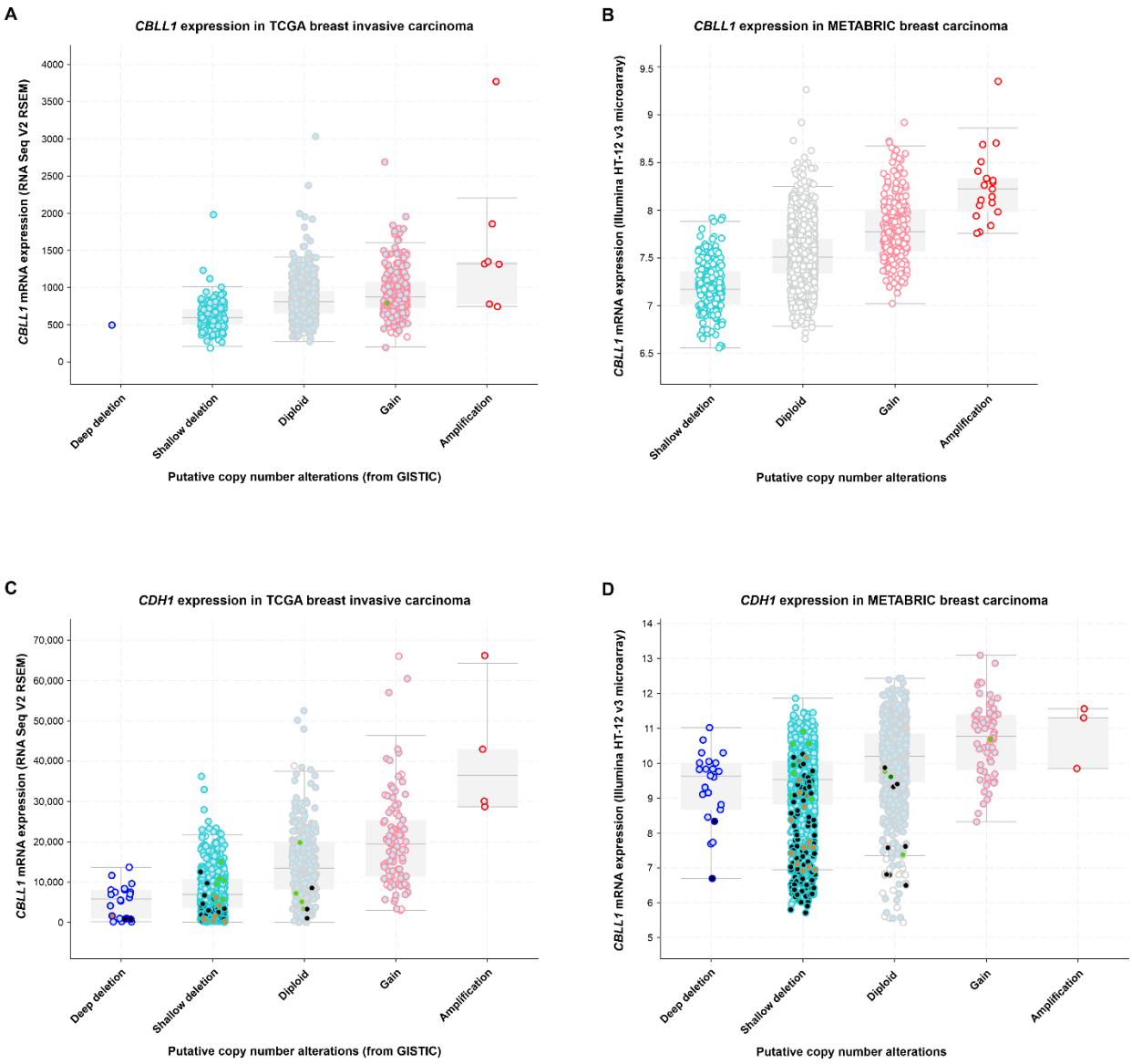


**Figure 5.2 *CBLL1* and *CDH1* copy number alterations in breast cancer**

The cBioPortal for Cancer Genomics (Cerami et al., 2012, Gao et al., 2013) was utilised to assess *CBLL1* putative copy number alterations in BCa patients and their association with mRNA expression in both the TCGA (Liu et al., 2018a) and METABRIC (Curtis et al., 2012, Pereira et al., 2016) cohorts. (**A**) *CBLL1* putative copy number alterations in BCa patients (n=1108) (Liu et al., 2018a). (**B**) *CBLL1* putative copy number alterations in BCa patients (n=2509) (Curtis et al., 2012, Pereira et al., 2016). (**C**) *CDH1* putative copy number alterations in BCa patients (n=1108) (Liu et al., 2018a). (**D**) *CDH1* putative copy number alterations in BCa patients (n=2509) (Curtis et al., 2012, Pereira et al., 2016).

The UCSC Xena browser (Goldman et al., 2020) was used to further investigate *CBLL1* and *CDH1* expression in the GDC TCGA Breast Cancer patient cohort (Liu et al., 2018a) in association with malignancy (retrieved 17 April 2023) (**Figure 5.3**). No significant difference was seen in *CBLL1* expression between normal breast (n=113), primary tumour (n=1097) and metastatic (n=7) tissue (p>0.05; **Figure 5.3A**). Conversely, *CDH1* expression was significantly associated with malignancy, with higher expression observed in primary tumour compared with normal breast tissue, and higher still in metastatic tissue (p<0.0001; **Figure 5.3B**).

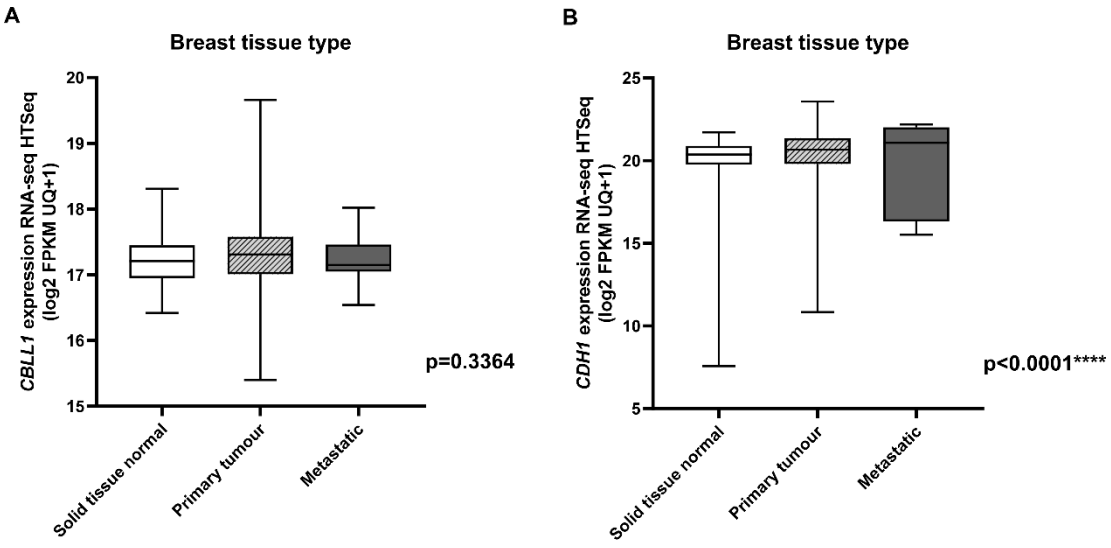


**Figure 5.3 *CBLL1* and *CDH1* mRNA expression and correlation with clinicopathological parameters**

The UCSC Xena browser (Goldman et al., 2020) was utilised to assess *CBLL1* and *CDH1* expression and its correlation with clinicopathological parameters in the GDC TCGA Breast Cancer patient cohort (Liu et al., 2018a). (**A**) *CBLL1* mRNA expression in primary tumour (n=1097) and metastatic (n=7) cases compared with normal breast tissue (n=113). (**B**) *CDH1* mRNA expression in primary tumour (n=1097) and metastatic (n=7) cases compared with normal breast tissue (n=113). Analysed by one-way Anova.

The Kaplan-Meier Plotter online tool (Győrffy, 2021) was then used to further investigate the prognostic value of *CBLL1* in BCa, and compared with *CDH1* (**Figure 5.4**). *CBLL1* expression was significantly higher in BCa patients with extended overall survival (OS) (p=0.0034; **Figure 5.4A**), and relapse-free survival (RFS) (p<0.0001; **Figure 5.4C**), but was not significantly associated with distant metastasis-free survival (DMFS) (p>0.05; **Figure 5.4E**). Interestingly, the inverse was observed for *CDH1* expression, where higher expression was associated with poorer RFS (p=0.0003; **Figure 5.4D**), with similar trends observed with both OS (**Figure 5.4B**) and DMFS (**Figure 5.4F**), however these did not achieve statistical significance (p>0.05). No significant association between *CBLL1* expression and survival (OS, RFS or DMFS) was observed when patients were stratified by hormone receptor positivity.

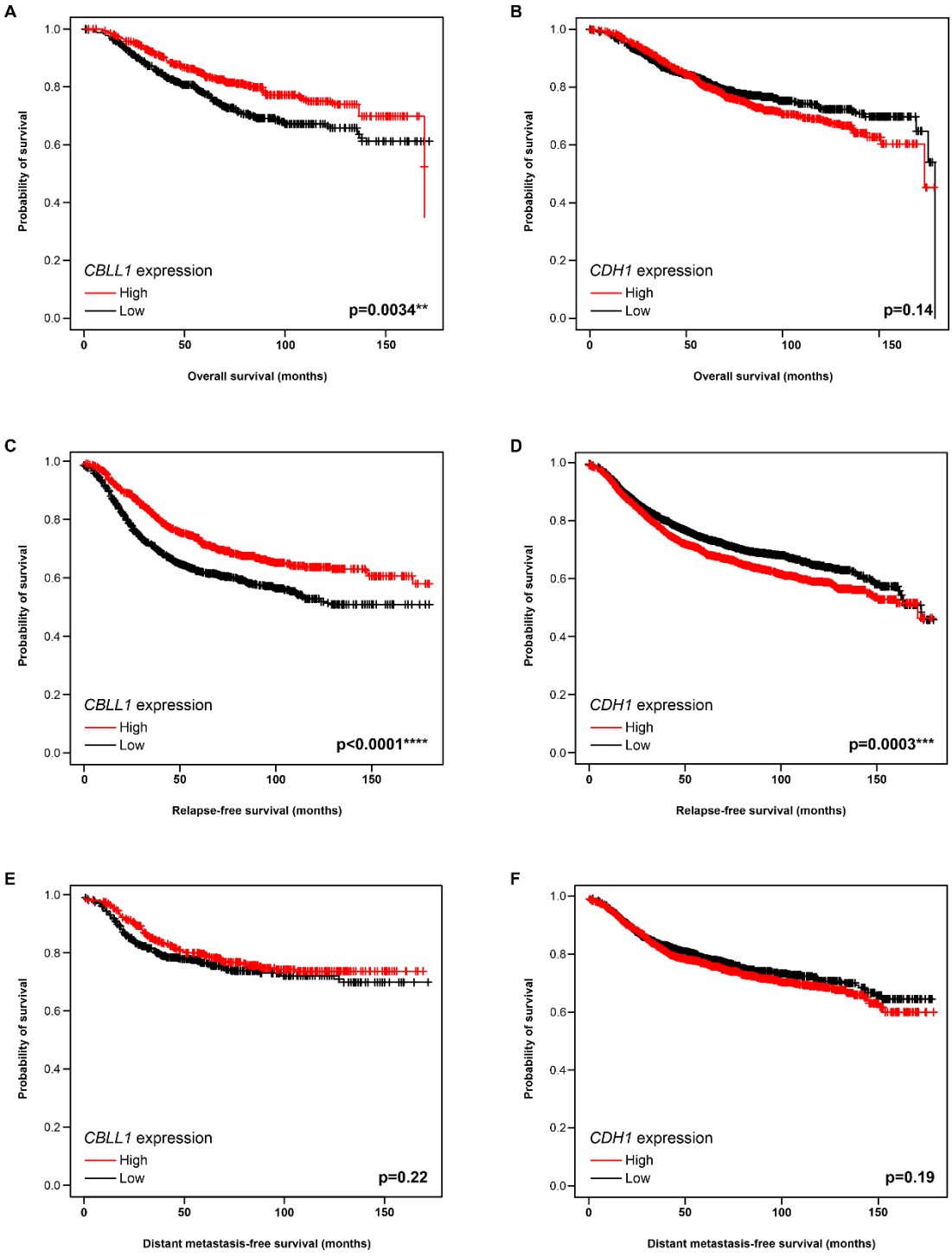


**Figure 5.4 *CBLL1* and *CDH1* expression and correlation with different survival types**

The Kaplan-Meier Plotter online tool (Győrffy, 2021) was utilised to assess *CBLL1* and *CDH1* mRNA expression and its correlation with patient survival. (**A**) *CBLL1* mRNA expression correlated with overall survival (n=943). (**B**) *CDH1* mRNA expression correlated with overall survival (n=1823). (**C**) *CBLL1*

mRNA expression correlated with relapse-free survival (n=2008). (**D**) *CDH1* mRNA expression correlated with relapse-free survival (n=4934). (**E**) *CBLL1* mRNA expression correlated with distant metastasis-free survival (n=958). (**F**) *CDH1* mRNA expression correlated with distant metastasis-free survival (n=2693).

The Genome to Outcome web server (Pongor et al., 2015) was additionally used to investigate the prognostic value of *CBLL1* and *CDH1* in BCa in a second larger patient dataset (The Cancer Genome Atlas et al., 2012) (**Figure 5.5**). *CBLL1* expression was significantly lower in BCa patients with increased OS (p<0.0001; **Figure 5.5A**). The inverse was seen with *CDH1* expression, where higher expression was associated with increased OS (p<0.0001; **Figure 5.5B**).

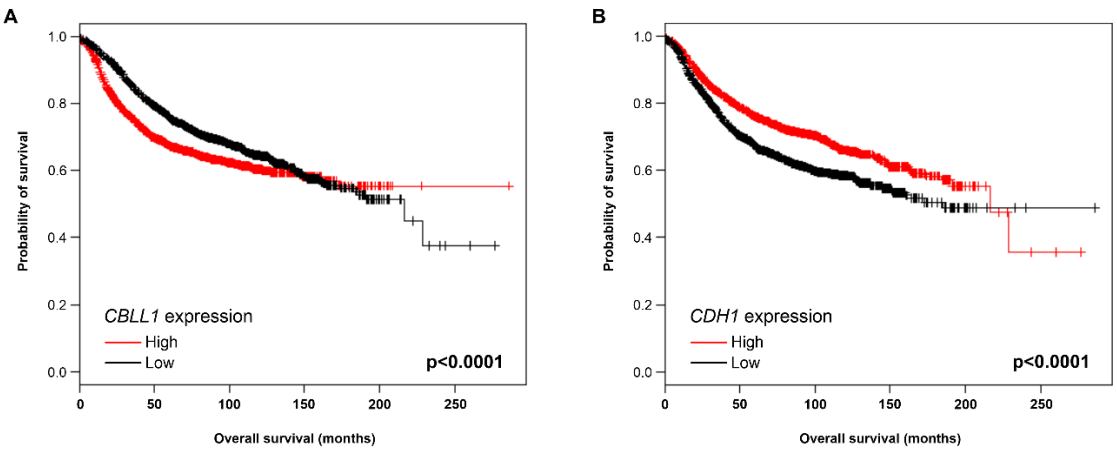


**Figure 5.5 *CBLL1* and *CDH1* expression and correlation with overall survival**

The Genome to Outcome web server (Pongor et al., 2015) was utilised to assess *CBLL1* and *CDH1* mRNA expression and its correlation with patient survival. (**A**) *CBLL1* mRNA expression correlated with overall survival (n=6,697). (**B**) *CDH1* mRNA expression correlated with overall survival (n=6,697).

### 5.2.2 CBLL1 expression in breast cancer cell lines

Basal expression of CBLL1 mRNA and protein was analysed in the BCa cell lines ERα-positive MCF7, T-47D, triple negative MDA-MB-453 and MDA-MB-231, and non-malignant HMEC and MCF10A breast cell lines (**Figure 5.6**). *CBLL1* mRNA was expressed in all cell lines and was significantly higher in all BCa cell lines except MDA-MB-453 compared with HMEC ($p<0.01$; **Figure 5.6A**). No significant difference was seen in *CBLL1* expression between the non-malignant immortalised cell line MCF10A and the normal HMEC control cell line ($p>0.05$; **Figure 5.6A**). *CBLL1* was expressed at the highest level in those cell lines expressing ERα and thus responsive to estrogen (**Figure 5.6A**). At the protein level, CBLL1 was expressed in all cell lines, with higher expression observed in all BCa cell lines compared with the normal HMEC control cell line (**Figure 5.6C**). Expression of ERα was also confirmed in the MCF7 and T-47D cell lines (**Figure 5.6C**).

*CDH1* mRNA was expressed in all cell lines except MDA-MB-231, with lowest expression detected in MDA-MB-453 (**Figure 5.6B**). *CDH1* expression was significantly higher in the ERα-expressing cell lines MCF7 and T-47D compared with HMEC ($p<0.01$; **Figure 5.6B**), yet significantly lower in MCF10A ($p<0.0001$; **Figure 5.6B**). At the protein level, E-cadherin expression was not detected in MDA-MB-231 or MDA-MB-453. Higher E-cadherin expression was observed in the ERα-expressing cell lines MCF7 and T-47D compared with normal HMEC and non-malignant MCF10A (**Figure 5.6C**).

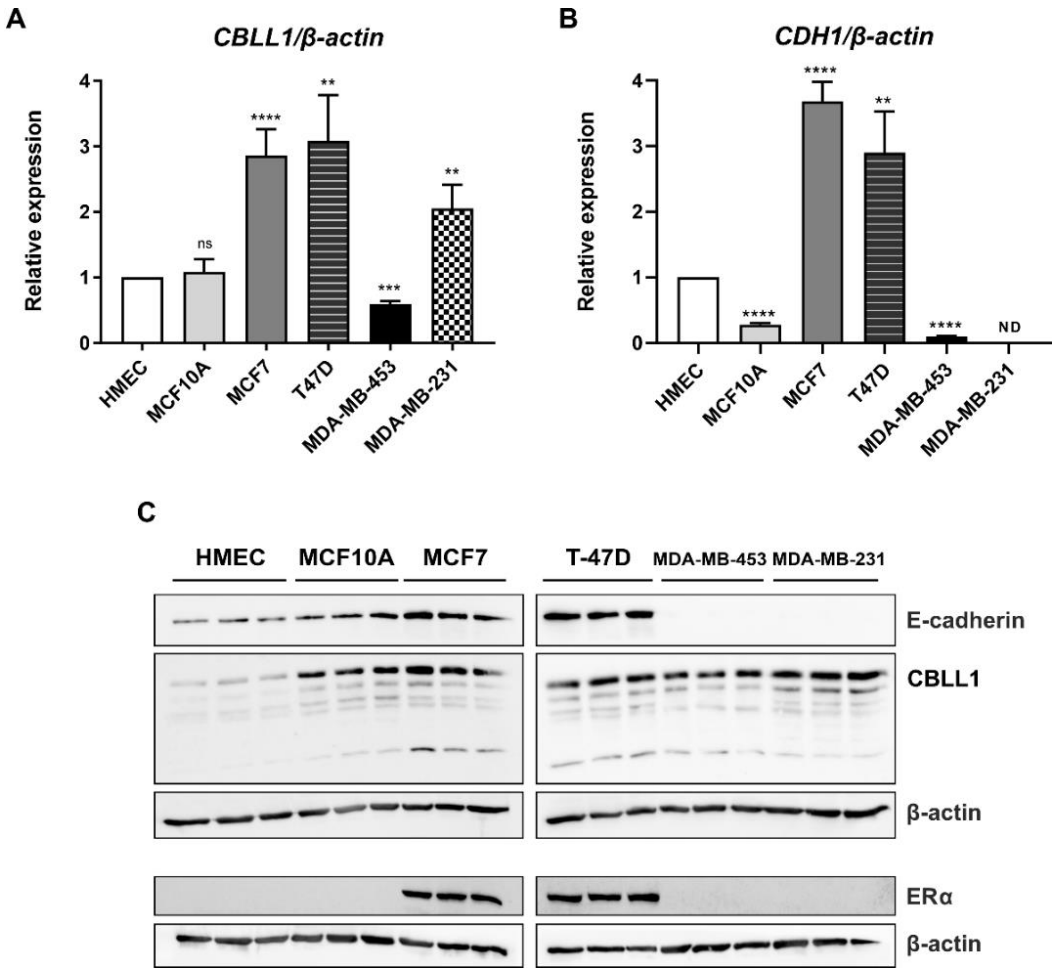


**Figure 5.6 CBLL1 and E-cadherin expression in non-malignant and breast cancer cell lines**

Expression of *CBLL1* and *CDH1* mRNA was analysed by qRT-PCR relative to *β-actin* and CBLL1 and E-cadherin protein expression was analysed by western blot with β-actin loading control. (**A**) *CBLL1* mRNA expression in non-malignant MCF10A and BCa cell lines MCF7, T-47D, MDA-MB-453 and MDA-MB-231 compared with the normal breast control cell line HMEC (n=6, except MDA-MB-453 when n=4). (**B**) *CDH1* mRNA expression in non-malignant MCF10A and BCa cell lines MCF7, T-47D, MDA-MB-453 and MDA-MB-231 compared with the normal breast control cell line HMEC (n=6, except MDA-MB-453 when n=4). (**C**) E-cadherin, CBLL1 and ERα protein expression in non-malignant MCF10A and BCa cell lines MCF7, T-47D, MDA-MB-453 and MDA-MB-231 compared with the normal breast control cell line HMEC (n=3). * = p≤0.05, ** = p≤0.01, *** = p≤0.001, **** = p<0.0001, ND= not detected, by unpaired t-test.

### 5.2.3 Estrogen regulation of CBLL1 expression in breast cancer cell lines

As *CBLL1* expression was highest in the ERα-expressing BCa cell lines, the effect of estrogen ($\beta E_2$) on *CBLL1* and *CDH1* mRNA expression was next examined (**Figure 5.7**). The estrogen-sensitive cell lines MCF7 and T-47D were treated for 72 hours with either vehicle (100% DMSO) or $\beta E_2$ (10nM). *CBLL1* expression was downregulated in MCF7 in response to estrogen treatment ($p=0.0001$; **Figure 5.7A**), but no significant change in expression was seen in the T-47D cell line ($p>0.05$; **Figure 5.7B**). Similar observations were made with respect to *CDH1* expression, with downregulation seen following estrogen treatment in MCF7 cells ($p<0.0001$; **Figure 5.7C**), but with no significant difference in the T-47D cell line ($p>0.05$; **Figure 5.7D**).

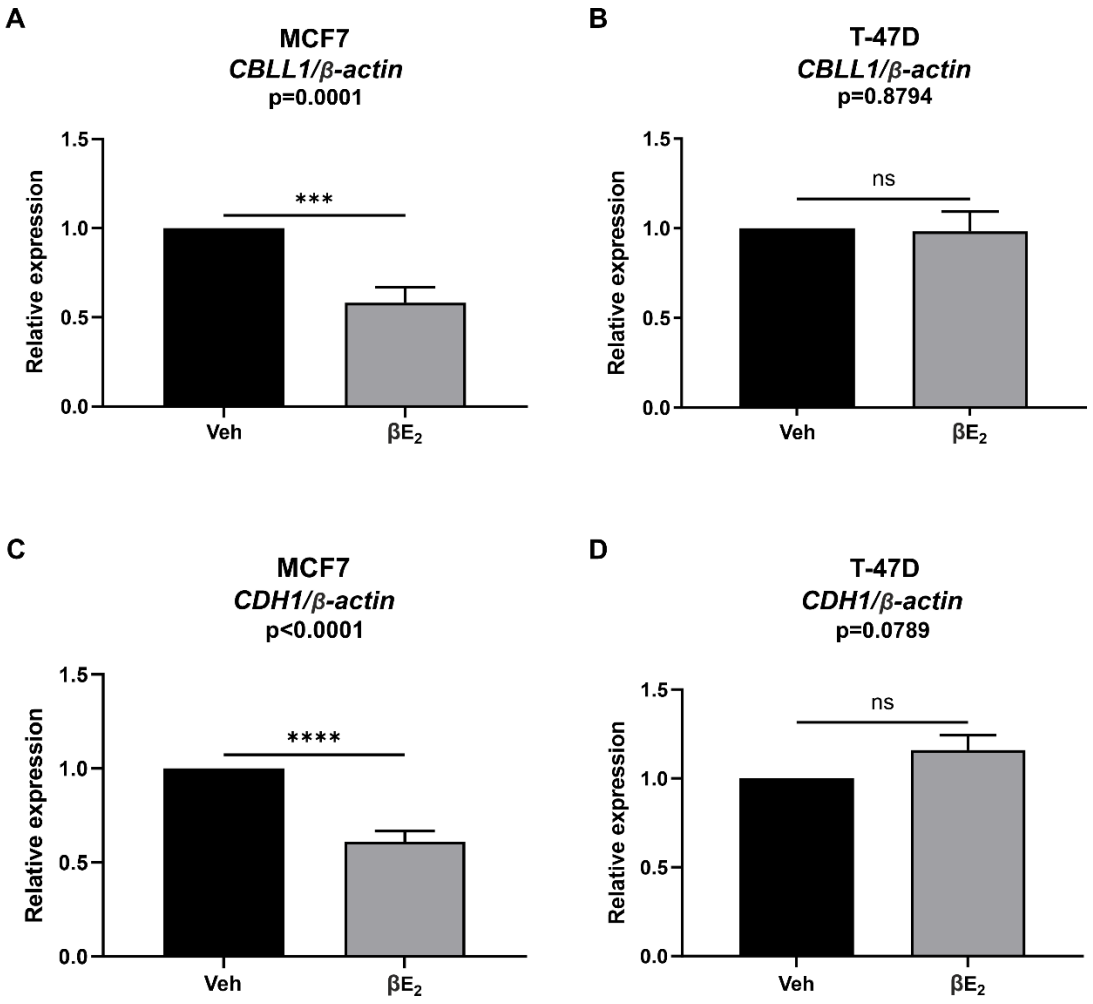


**Figure 5.7 *CBLL1* and *CDH1* expression in breast cancer cell lines in response to estradiol treatment**

*CBLL1* and *CDH1* mRNA expression was analysed by qRT-PCR relative to *β-actin* following vehicle (100% DMSO) or $\beta E_2$ (10nM) treatment for 72 hours in BCa cell lines. (**A**) *CBLL1* mRNA expression in MCF7 (n=6). (**B**) *CBLL1* mRNA expression in T-47D (n=5). (**C**) *CDH1* mRNA expression in MCF7 (n=6). (**D**) *CDH1* mRNA expression in T-47D (n=5). Veh=Vehicle. ns= not significant, * = p≤0.05, ** = p≤0.01, *** = p≤0.001, **** = p<0.0001 by paired t-test.

The expression of CBLL1 and E-cadherin protein in response to estrogen ($\beta E_2$) treatment was next investigated (**Figure 5.8**). The estrogen-sensitive cell lines MCF7 and T-47D were treated for 72 hours with either vehicle (100% DMSO) or $\beta E_2$ (10nM) before harvesting. A modest increase in CBLL1 expression was observed in both cell lines following estrogen treatment (**Figure 5.8A and Figure 5.8B**). Conversely, a modest decrease in E-cadherin expression was seen in both cell lines in response to estrogen treatment (**Figure 5.8A and Figure 5.8B**)

.

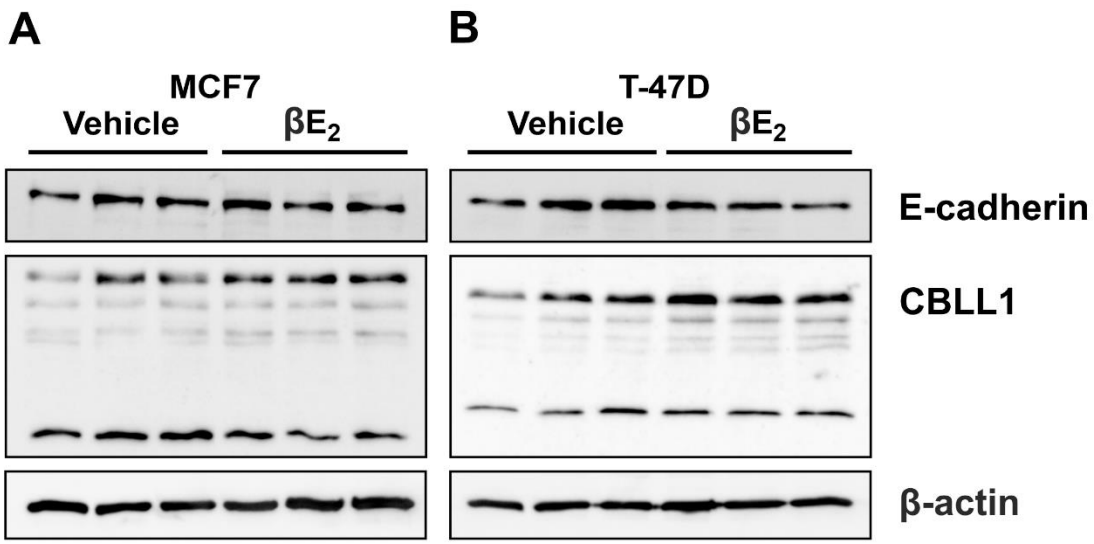


**Figure 5.8 CBLL1 expression in breast cancer cell lines in response to estradiol treatment**

CBLL1 and E-cadherin protein expression was analysed by western blot with β-actin loading control following vehicle (100% DMSO) or $\beta E_2$ (10nM) treatment for 72 hours in BCa cell lines. (**A**) CBLL1 and E-cadherin protein expression in MCF7 (n=3). (**B**) CBLL1 and E-cadherin protein expression in T-47D (n=3).

Given the dual reported roles of CBLL1 in both the nucleus and cytoplasm, its subcellular localisation was next assessed, alongside E-cadherin. The effect of estrogen treatment on cellular location was simultaneously investigated. MCF7 and T-47D BCa cell lines were treated for 72 hours with either vehicle (100% DMSO) or $\beta E_2$ (10nM) before cells were harvested and the nuclear and cytoplasmic protein fractions isolated. The HDAC1 nuclear loading control and GAPDH cytoplasmic loading control confirmed good separation of the protein fractions (**Figure 5.9**). CBLL1 was observed to be expressed in both the nuclear and cytoplasmic cellular compartments, but enriched in the nucleus in MCF7 (**Figure 5.9A**), however only trace expression of CBLL1 was seen in the cytoplasm of T-47D cells (**Figure 5.9B**). No significant difference in subcellular localisation was seen in response to estrogen, however both nuclear and cytoplasmic CBLL1 expression did appear to be increased following estrogen treatment (**Figure 5.9**). In contrast, E-cadherin was expressed in both the nuclear and cytoplasmic cellular compartments, but enriched in the cytoplasm in both cell lines (**Figure 5.9**and **Figure 5.9B**). No significant difference in E-cadherin expression or subcellular localisation was seen in response to estrogen treatment in either cell line however, interestingly, a second band became visible on the western blot following splitting of the E-cadherin protein fractions (**Figure 5.9**) that was not detectable when the whole cell lysate was analysed (**Figure 5.6** and **Figure 5.8**).

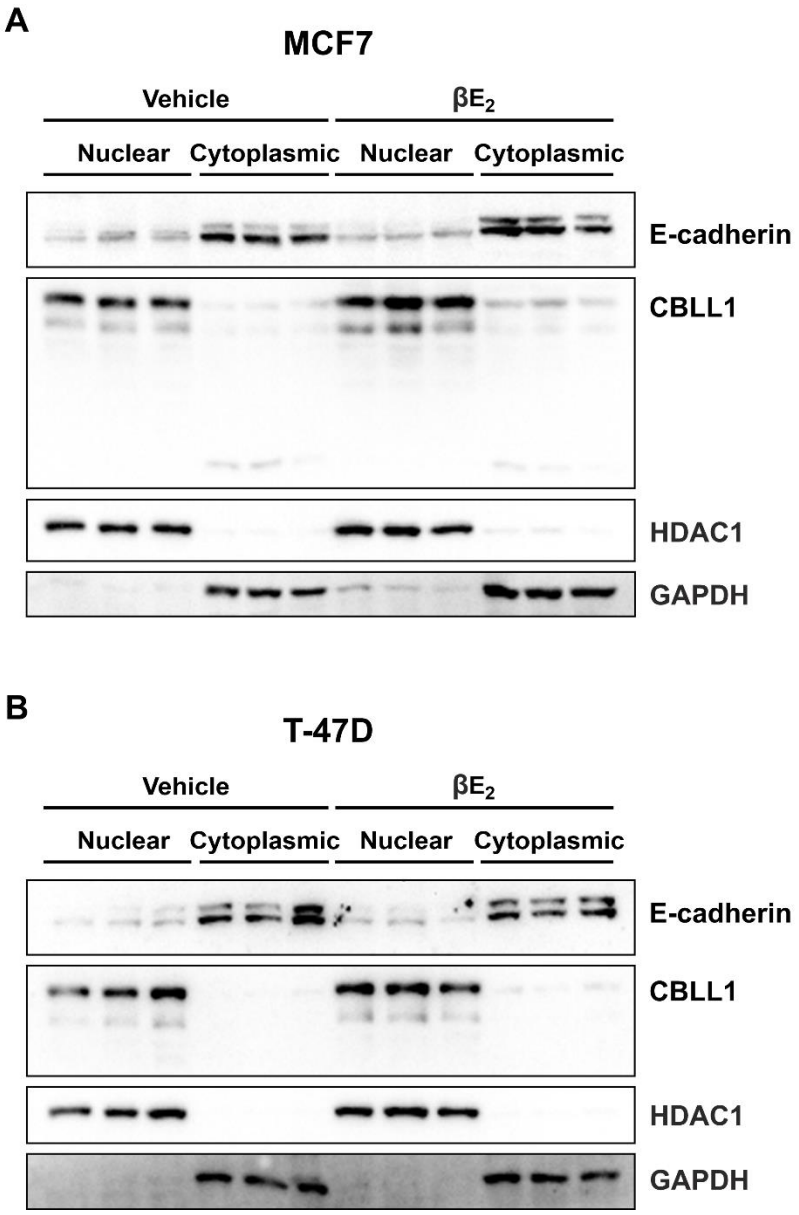


**Figure 5.9 CBLL1 and E-cadherin protein localisation expression in breast cancer cell lines in response to estradiol treatment**

CBLL1 and E-cadherin protein expression was analysed by western blot in MCF7 and T-47D cell lines following vehicle (100% DMSO) or $\beta E_2$ (10nM) treatment for 72 hours and subsequent extraction of cytoplasmic and nuclear protein fractions. GAPDH and HDAC1 were used as cytoplasmic and nuclear loading controls, respectively. (**A**) CBLL1 and E-cadherin protein expression in MCF7 (n=3). (**B**) CBLL1 and E-cadherin protein expression in T-47D (n=3).

To elucidate further the potential estrogen regulation of *CBLL1* expression, analysis of publicly available data was carried out to determine epigenetic regulation of the *CBLL1* gene (**Figure 5.10**). H3K4me3, a mark of transcriptionally active chromatin, had been assessed genome-wide by Chromatin Immunoprecipitation with massive parallel sequencing (ChIP-Seq) as previously described (Huang et al., 2021) and the data then downloaded from the NCBI Gene Expression Omnibus (GEO) database (Barrett et al., 2013), under accession number GSE40867 (Jansen et al., 2013, Nevedomskaya et al., 2014) and viewed using the Integrative Genomics Viewer (Robinson et al., 2011). The estrogen-regulated gene *TFF1* (also known as *PS2*) was used as a positive control, demonstrating H3K4me3 in the proximal promoter region at the 5' end that extended across almost the entirety of the gene (**Figure 5.10B**). Similarly, H3K4me3 was also found to bind in the proximal promoter region in the 5' end in the *CBLL1* gene (**Figure 5.10A**).

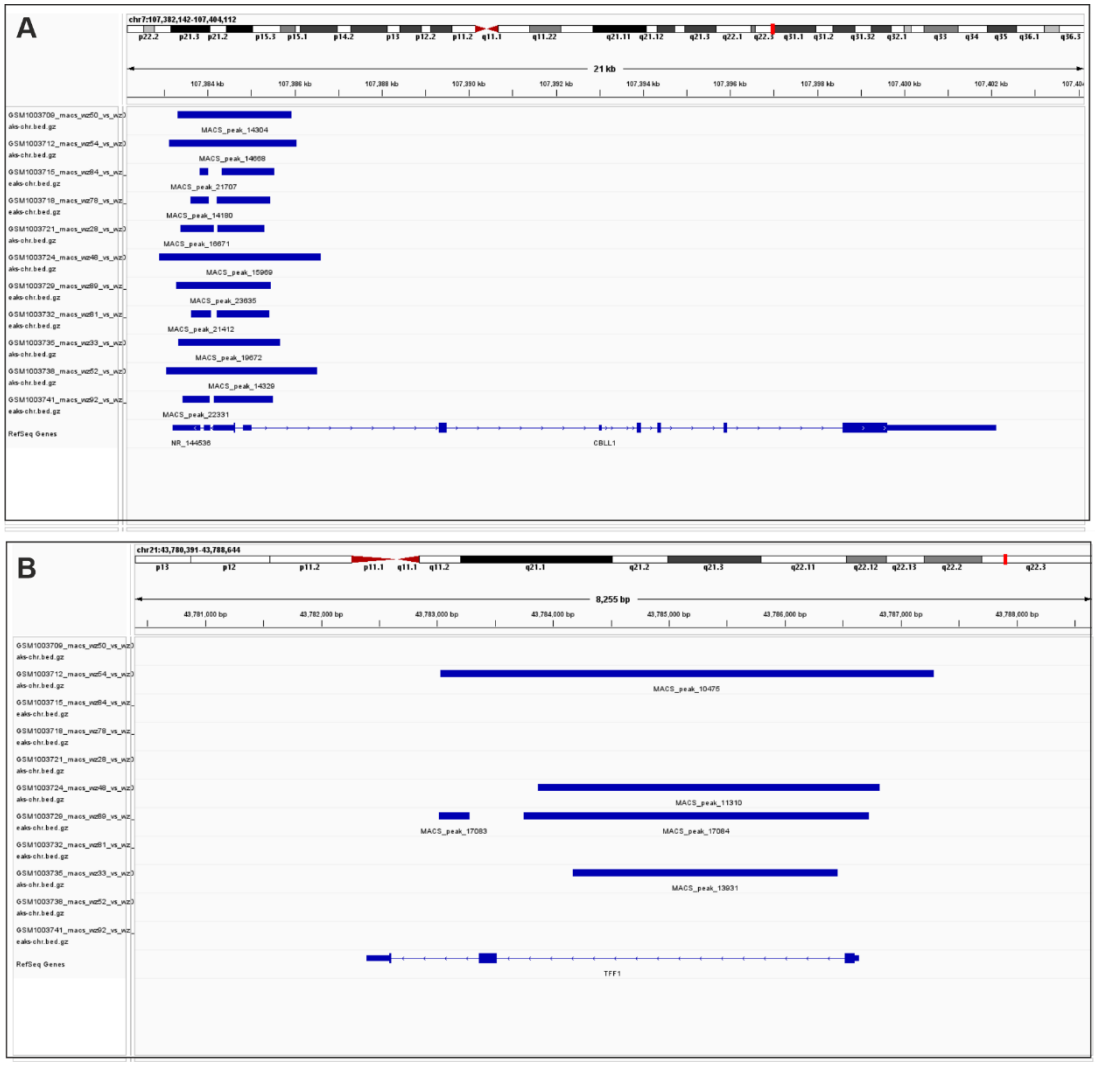


**Figure 5.10 Chromatin binding profile of H3K4me3, a mark of active chromatin, within the *CBLL1* gene**

The Integrative Genomics Viewer (Robinson et al., 2011) was used to analyse ChIP-Seq data (GEO accession GSM1003709; (Jansen et al., 2013, Nevedomskaya et al., 2014)) from the NCBI GEO database (Barrett et al., 2013) detailing the chromatin context with respect to H3K4me3 in the *CBLL1* gene. (**A**) H3K4me3 within the *CBLL1* gene. (**B**) H3K4me3 within the *TFF1* gene.

### 5.2.4 CBLL1 expression in breast tissue specimens from Nottingham patient cohorts

To investigate the expression and clinical relevance of CBLL1 protein in BCa patients, immunohistochemistry (IHC) was carried out on a large, well-characterised TMA comprising tumour specimens (n=1499) from patients in the Nottingham cohorts. As described in Chapter 2, CBLL1 staining in both the nucleus and cytoplasm of breast luminal cells was assessed and given a H-score, with validation from a second scorer following an independent staining evaluation of 10% of the tissue cores. Concordance between independent scorers of >0.8 intraclass correlation was confirmed. The H-scores for both nuclear and cytoplasmic CBLL1 staining were then dichotomised into two equal groups of low and high CBLL1 expression based on the median H-score. Examples of these two levels of staining intensities are shown in **Figure 5.11**. E-cadherin staining was also assessed, with examples of staining intensities presented in **Appendix 18**.

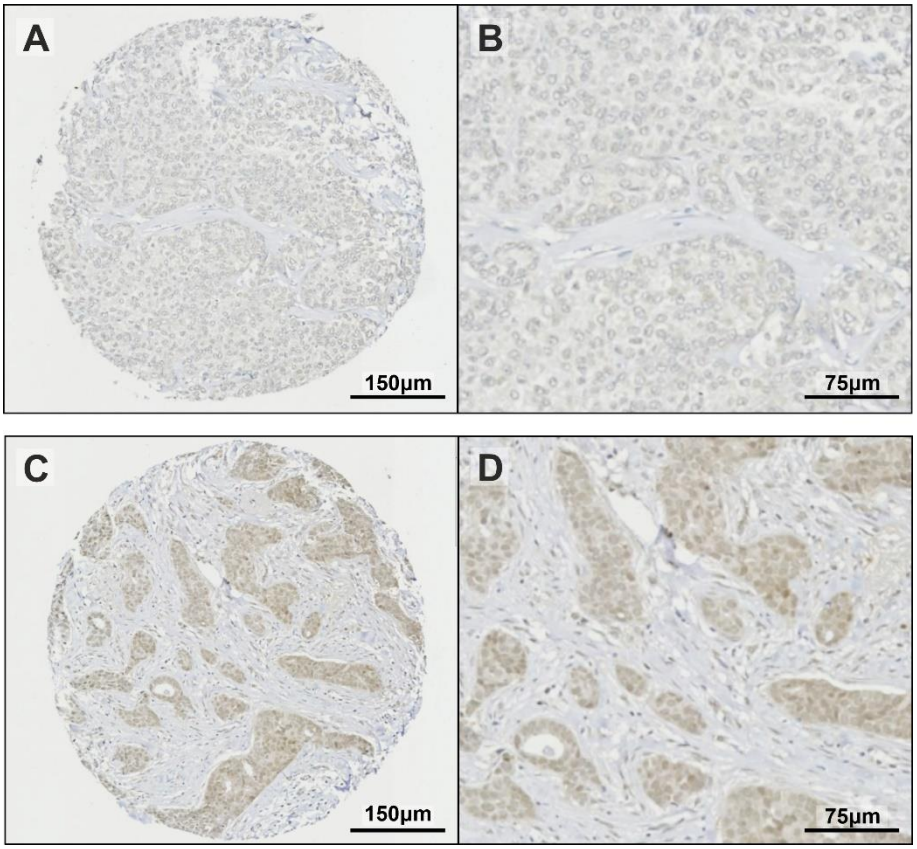


**Figure 5.11 Representative images of CBLL1 IHC staining of Nottingham cohort TMA of breast cancer tissue**

IHC staining of breast cancer patient tissue samples was carried out to determine the nuclear and cytoplasmic expression of CBLL1. (**A** and **B**) Representative images of low level CBLL1 expression. (**C** and **D**) Representative images of high level CBLL1 expression.

CBLL1 expression in tumour samples (n=1499) was subsequently correlated with deidentified clinicopathological parameters (**Figure 5.12**, **Appendix 16** and **Appendix 17**). Nuclear CBLL1 expression was significantly higher in patients with a lower grade at diagnosis (p<0.0001; **Figure 5.12A**), a better NPI prognostic group (p<0.0001; **Figure 5.12C**), ER positive status (p<0.0001; **Figure 5.12E**), and with non-TN status (p<0.0001; **Figure 5.12G**). Similarly, higher nuclear CBLL1 was significantly associated with a lower tubular differentiation, nuclear pleiomorphism and mitotic count score, a smaller tumour size, lower Ki67 index, PR positive and HER2 negative status, as well as histological tumour types and molecular classes with a more favourable prognosis (p<0.0001; **Appendix 17**).

Conversely, higher cytoplasmic CBLL1 expression was significantly associated with higher grade at diagnosis (p=0.014; **Figure 5.12B**), a poorer NPI prognostic group (p=0.005; **Figure 5.12D**), ER negative status (p=0.042; **Figure 5.12F**), and with TN status (p=0.032; **Figure 5.12H**). Additionally, cytoplasmic CBLL1 expression was significantly higher in patients with a higher nuclear pleiomorphism and mitotic count score, and a lower age and pre-menopausal status at diagnosis (p<0.05; **Appendix 17**). Interestingly, higher cytoplasmic CBLL1 expression was also associated with histological tumour types with a more favourable prognosis (p<0.0001; **Appendix 17**).

E-cadherin membrane expression was also assessed in patient tumour samples (n=2126) and correlated with clinicopathological parameters (**Appendix 19** and **Appendix 20**). Results were similar to those observed with nuclear CBLL1 expression, with higher E-cadherin expression significantly associated with lower grade at diagnosis (p<0.0001; **Appendix 20**), ER-

positive status ($p<0.0001$; **Appendix 20**), and with non-TN status ($p<0.0001$; **Appendix 20**). Likewise, higher E-cadherin expression was also significantly higher in patients with a lower tubular differentiation and mitotic count score, small tumour size, lower Ki67 index, and PR positive status, as well as significantly associated with histological tumour types and molecular classes with a more favourable prognosis ($p<0.0001$; **Appendix 20**). However, higher E-cadherin expression was also significantly associated with lymph node positive status and with vascular invasion ($p<0.05$; **Appendix 20**).

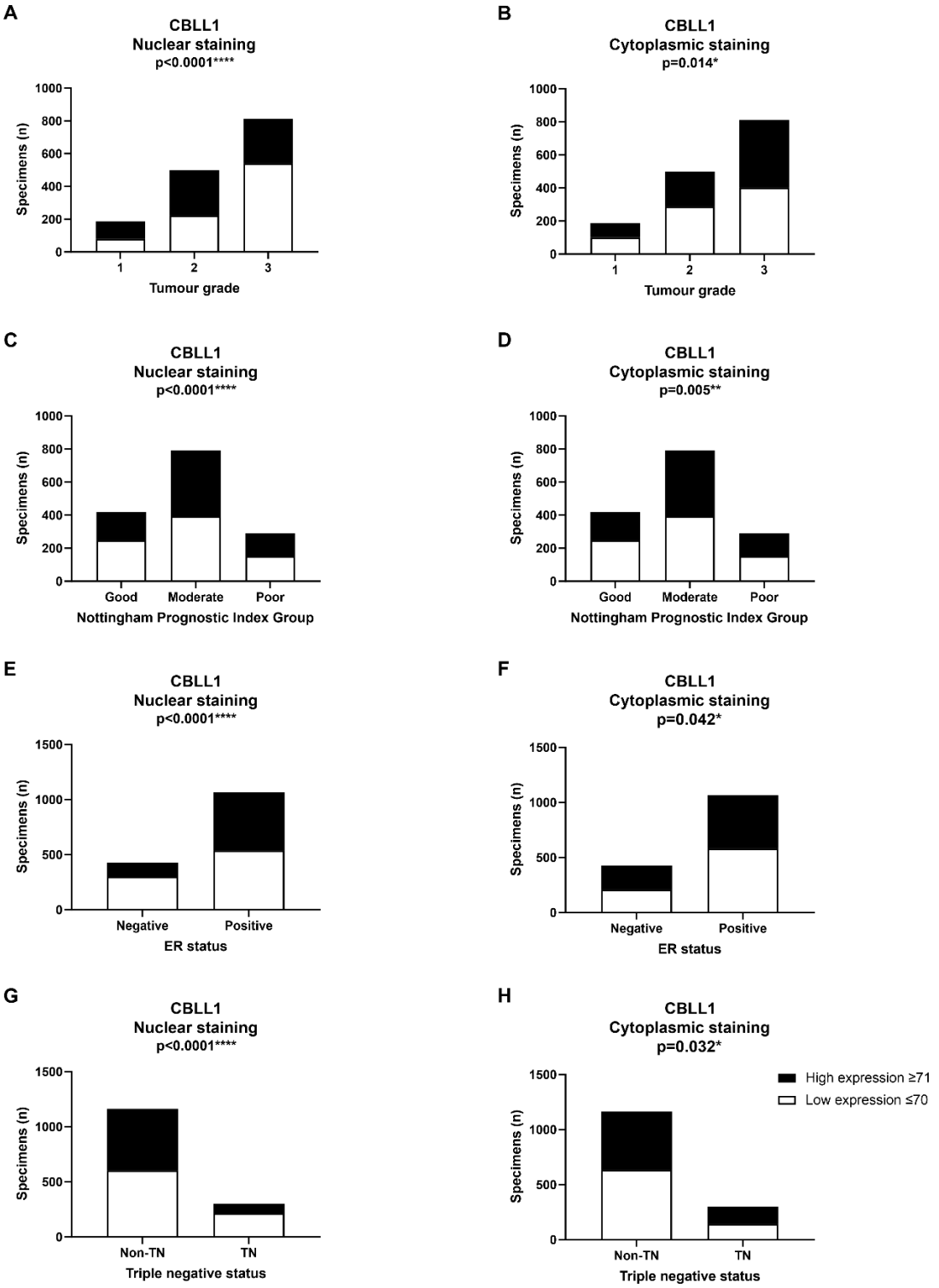


**Figure 5.12 Significant correlations of clinicopathological parameters with CBLL1 expression in breast cancer patient tissue samples**

IHC staining of 1499 patient tumour samples was assessed by H-score, divided into high and low expression groups and correlated with tumour grade, NPI group, ER status and TNBC status. CBLL1 nuclear and cytoplasmic staining,

low: ≤70, high: ≥71. (**A**) Correlation of CBLL1 nuclear staining and tumour grade (n=1499). (**B**) Correlation of CBLL1 cytoplasmic staining and tumour grade (n=1499). (**C**) Correlation of CBLL1 nuclear staining and NPI group (n=1499). (**D**) Correlation of CBLL1 cytoplasmic staining and NPI group (n=1499). (**E**) Correlation of CBLL1 nuclear staining and ER status (n=1493). (**F**) Correlation of CBLL1 cytoplasmic staining and ER status (n=1493). (**G**) Correlation of CBLL1 nuclear staining and TNBC status (n=1465). (**H**) Correlation of CBLL1 cytoplasmic staining and TNBC status (n=1465). Analysed by $\chi^2$ test.

The clinical significance of CBLL1 in BCa was further investigated by correlating nuclear and cytoplasmic expression with different survival parameters using Kaplan Meier analysis (**Figure 5.13**). Higher nuclear CBLL1 expression was significantly associated with both longer breast cancer specific survival (BCSS) and distant metastasis-free survival (DMFS) ($p<0.0001$; **Figure 5.13A** and **Figure 5.13B**). Conversely, no significant association was observed between cytoplasmic CBLL1 expression and BCSS or DMFS ($p>0.05$; **Figure 5.13C** and **Figure 5.13D**).

It was also found that higher membrane E-cadherin expression was significantly associated with both longer breast cancer specific survival (BCSS) ($p=0.001$; **Figure 5.13E**) and distant metastasis-free survival (DMFS) ($p=0.002$; **Figure 5.13F**).

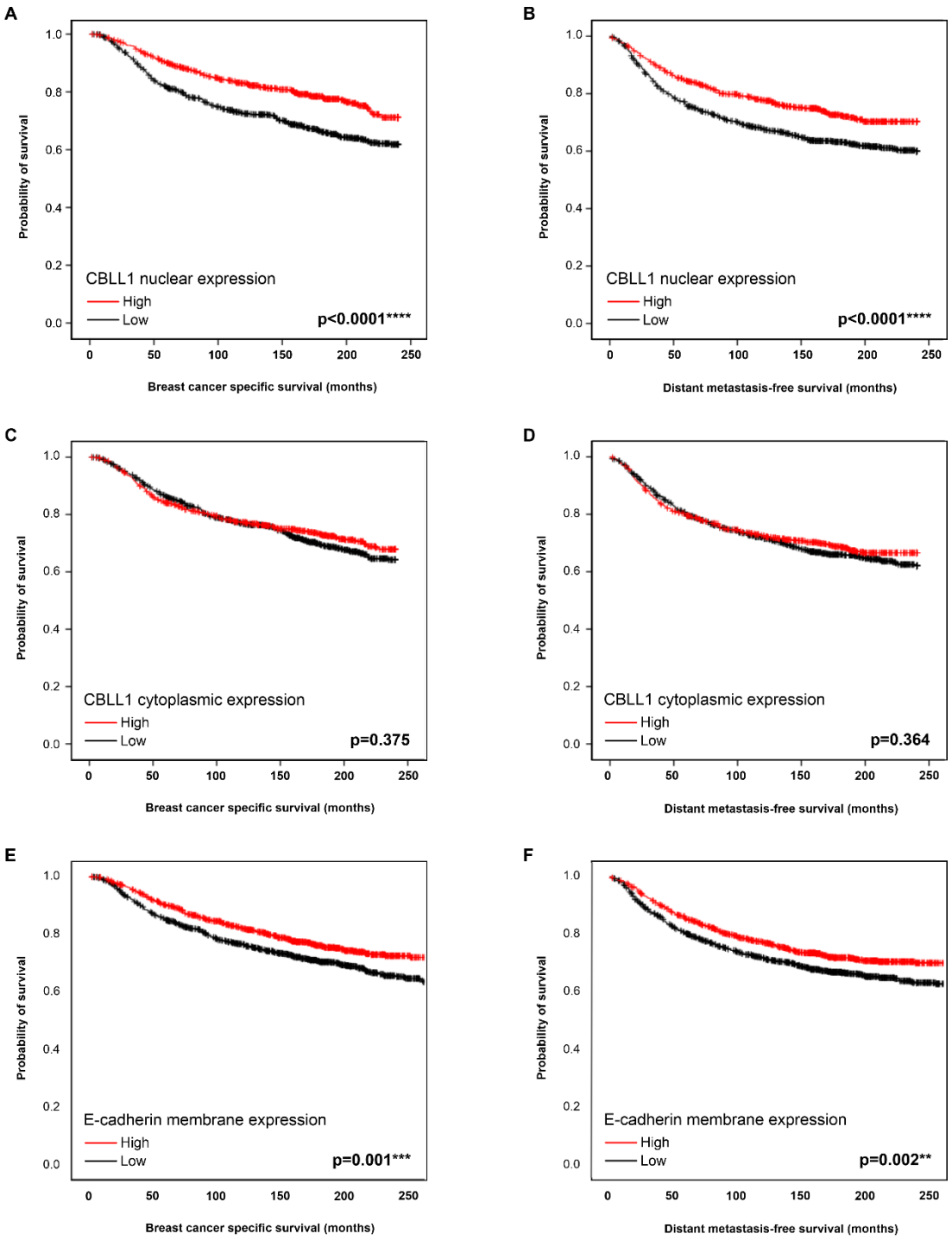


**Figure 5.13 CBLL1 expression correlated with survival in breast cancer patients**

IHC staining of 1499 patient samples was assessed by H-score, divided into high and low expression groups and correlated with BCSS and DMFS. CBLL1 nuclear and cytoplasmic staining, low: ≤70, high: ≥71. E-cadherin membrane staining, low: ≤130, high: ≥131. (**A**) Correlation of CBLL1 nuclear staining and

BCSS (n=1499). (**B**) Correlation of CBLL1 nuclear staining and DMFS (n=1499). (**C**) Correlation of CBLL1 cytoplasmic staining and BCSS (n=1499). (**D**) Correlation of CBLL1 cytoplasmic staining and DMFS (n=1499). (**E**) Correlation of E-cadherin membrane staining and BCSS (n=2126). (**F**) Correlation of E-cadherin membrane staining and DMFS (n=2126). Correlated using Kaplan Meier estimate and analysed by log-rank test.

Due to its reported dual role both in the nucleus and cytoplasm, correlation of nuclear and cytoplasmic CBLL1 expression in breast tumour specimens was subsequently independently examined (n=1499; **Figure 5.14**). A weak but statistically significant positive correlation was found between the level of nuclear and cytoplasmic CBLL1 expression (p=0.0125; **Figure 5.14**).

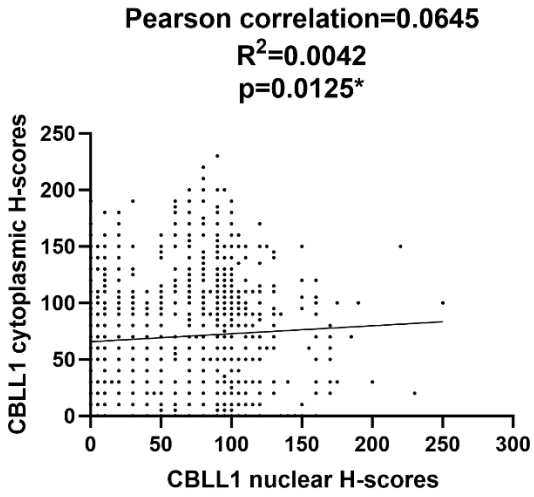


**Figure 5.14 Correlation of nuclear and cytoplasmic expression of CBLL1 in breast cancer patient tissue samples**

CBLL1 staining H-scores in both the nuclear and cytoplasmic compartments of breast luminal cells in BCa patient specimens were correlated to determine association of expression (n=1499). Linear regression and statistical analysis performed using Graphpad Prism, goodness of fit expressed as $R^2$, significance of slope difference from zero expressed as p-value.

To determine the prognostic significance of CBLL1, a multivariate Cox regression analysis was performed alongside other established prognostic indicators for BCSS and DMFS in BCa (**Figure 5.15**). It was found that nuclear CBLL1 expression in BCa is an independent positive prognostic factor in both BCSS ($p<0.0001$; **Figure 5.15A**) and DMFS ($p=0.001$; **Figure 5.15B**) alongside tumour size, grade and stage. Similarly, E-cadherin membrane expression was also determined to be an independent positive prognostic factor in BCSS ($p=0.002$; **Figure 5.15E**) and DMFS ($p=0.003$; **Figure 5.15F**). However, cytoplasmic CBLL1 expression was not an independent prognostic factor in either BCSS or DMFS when compared with tumour size, grade and stage ($p>0.05$; **Figure 5.15C** and **Figure 5.15D**).

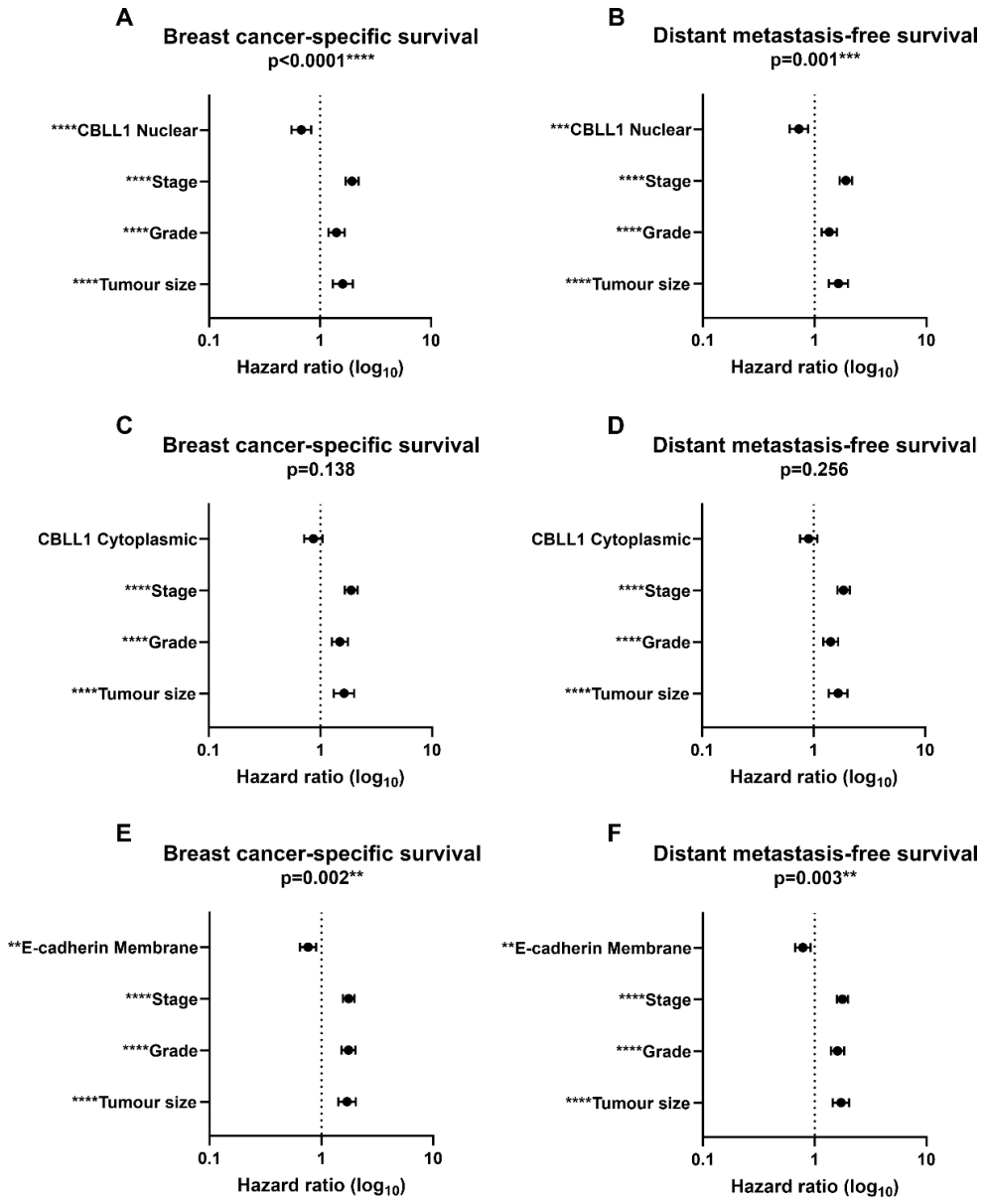


**Figure 5.15 Multivariate Cox regression analysis of CBLL1 and E-cadherin expression and survival in BCa patients**

Multivariate analysis was conducted to assess the prognostic value of both CBLL1 and E-cadherin expression, together with tumour stage, grade and size, with BCSS and DMFS. (**A**) Association of CBLL1 nuclear staining and BCSS (n=1496). (**B**) Association of CBLL1 nuclear staining and DMFS (n=1499). (**C**) Association of CBLL1 cytoplasmic staining and BCSS (n=1496). (**D**) Association of CBLL1 cytoplasmic staining and DMFS (n=1499). (**E**) Association of E-cadherin membrane staining and BCSS (n=2123). (**F**) Association of E-cadherin membrane staining and DMFS (n=2126).

Multivariate Cox regression analysis performed using SPSS, hazard ratio represented by black circle, 95% confidence interval represented by black line. * = p≤0.05, ** = p≤0.01, *** = p≤0.001, **** = p<0.0001 by Cox's proportional hazard model.

Given the similar prognostic significance of CBLL1 and E-cadherin expression, the association between the level of CBLL1 and E-cadherin expression in BCa patients was then analysed (**Figure 5.16**). A weak positive correlation was observed both between nuclear CBLL1 and membrane E-cadherin expression (p<0.0001; **Figure 5.16A**), and cytoplasmic CBLL1 and membrane E-cadherin expression in breast tumour specimens (p<0.0001; **Figure 5.16B**).

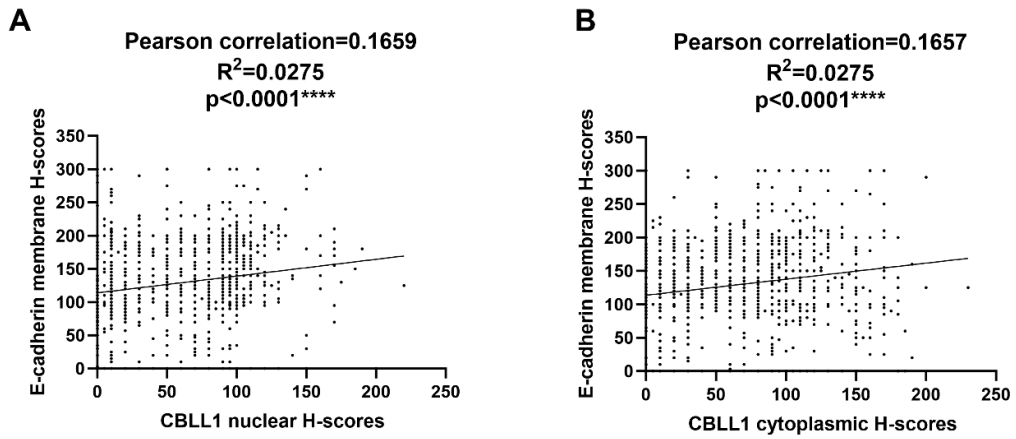


**Figure 5.16 of CBLL1 and E-cadherin expression in breast cancer patient tissue samples**

CBLL1 and E-cadherin staining H-scores in both the nuclear and cytoplasmic compartments of breast luminal cells were correlated to determine association of expression (n=1097). (**A**) Correlation of nuclear CBLL1 and membrane E-cadherin in BCa tissue (n=1097). (**B**) Correlation of cytoplasmic CBLL1 and membrane E-cadherin in BCa tissue (n=1097). Linear regression and statistical analysis performed using GraphPad Prism, goodness of fit expressed as $R^2$, significance of slope difference from zero expressed as p-value.

Expression of CBLL1 was subsequently correlated with expression of a number of other proteins implicated in BCa that had previously been analysed by IHC in the Nottingham BCa TMA. Nuclear CBLL1 was significantly positively correlated with both AR and ERα, and with the nuclear and cytoplasmic expression of the ER variant S118ER ($p<0.0001$; **Table 5.1**). Likewise, a significant positive correlation was observed between nuclear CBLL1 expression and expression of the p53 variant Ac_p53_K373, nuclear BRCA1, cytoplasmic BRCA2, FOXA1, ALKBH5 nuclear and cytoplasmic, and METTL3 nuclear expression ($p<0.05$; **Table 5.1**). A significant negative correlation was observed between nuclear CBLL1 expression and cytoplasmic expression of the p53 variant Ac_p53_K120, as well as N-cadherin, P-cadherin, and cytoplasmic FTO expression ($p<0.05$; **Table 5.1**). Cytoplasmic CBLL1 expression was significantly positively correlated with nuclear and cytoplasmic expression of the ER variant S118ER and BRCA1, as well as BRCA2 cytoplasmic, together with P-cadherin, TFF1, FTO nuclear and cytoplasmic, CCNB2 and ALKBH5 cytoplasmic expression ($p<0.05$; **Table 5.1**). A significant negative correlation was observed between cytoplasmic CBLL1 expression and nuclear and cytoplasmic expression of the p53 variant Ac_p53_K120 as well as N-cadherin expression ($p<0.05$; **Table 5.1**).

| Protein | | CBLL1 Nuclear | CBLL1 Cytoplasmic |
|---|---|---|---|
| **Ac_p53_K120 Nuclear** | Correlation coefficient | -0.127 | **-0.197** |
| | p value | p 0.073 | **p 0.005**** |
| | N | 201 | **201** |
| **Ac_p53_K120 Cytoplasmic** | Correlation coefficient | **-0.228** | **-0.233** |
| | p value | **p 0.001***** | **p 0.001***** |
| | N | **201** | **201** |
| **Ac_p53_K373** | Correlation coefficient | **0.151** | 0.123 |
| | p value | **p 0.025*** | p 0.066 |
| | N | **223** | 223 |
| **S118ER Nuclear** | Correlation coefficient | **0.413** | **0.267** |
| | p value | **p <0.0001****** | **p <0.0001****** |
| | N | **572** | **572** |
| **S118ER Cytoplasmic** | Correlation coefficient | **0.192** | **0.325** |
| | p value | **p <0.0001****** | **p <0.0001****** |
| | N | **572** | **572** |
| **AR** | Correlation coefficient | **0.309** | 0.052 |
| | p value | **p <0.0001****** | p 0.174 |
| | N | **687** | 687 |
| **BRCA1 Nuclear** | Correlation coefficient | **0.169** | **0.112** |
| | p value | **p <0.0001****** | **p 0.006**** |
| | N | **617** | **617** |
| **BRCA1 Cytoplasmic** | Correlation coefficient | -0.078 | **0.176** |
| | p value | p 0.053 | **p <0.0001****** |
| | N | 616 | **616** |
| **BRCA2 Nuclear** | Correlation coefficient | -0.073 | -0.030 |
| | p value | p 0.100 | p 0.508 |
| | N | 504 | 504 |
| **BRCA2 Cytoplasmic** | Correlation coefficient | **0.142** | **0.270** |
| | p value | **p 0.001***** | **p <0.0001****** |
| | N | **504** | **504** |
| **ER alpha** | Correlation coefficient | **0.192** | 0.000 |
| | p value | **p <0.0001****** | p 0.998 |
| | N | **745** | 745 |

| Protein | | CBLL1 Nuclear | CBLL1 Cytoplasmic |
|---|---|---|---|
| **FOXA1** | Correlation coefficient | **0.241** | 0.057 |
| | p value | **p <0.0001****** | p 0.200 |
| | N | **506** | 506 |
| **N-cadherin** | Correlation coefficient | **-0.120** | **-0.139** |
| | p value | **p 0.005**** | **p 0.001***** |
| | N | **545** | **545** |
| **P-cadherin** | Correlation coefficient | **-0.117** | **0.114** |
| | p value | **p 0.003**** | **p 0.004**** |
| | N | **624** | **624** |
| **TFF1** | Correlation coefficient | 0.029 | **0.168** |
| | p value | p 0.533 | **p <0.0001****** |
| | N | 458 | **458** |
| **FTO Nuclear** | Correlation coefficient | 0.064 | **0.095** |
| | p value | p 0.188 | **p 0.049*** |
| | N | 428 | **428** |
| **FTO Cytoplasmic** | Correlation coefficient | **-0.099** | **0.127** |
| | p value | **p 0.040*** | **p 0.009**** |
| | N | **428** | **428** |
| **CCNB2** | Correlation coefficient | -0.039 | **0.127** |
| | p value | p 0.330 | **p 0.002**** |
| | N | 617 | **617** |
| **ALKBH5 Nuclear** | Correlation coefficient | **0.237** | 0.077 |
| | p value | **p <0.0001****** | p 0.081 |
| | N | **513** | 513 |
| **ALKBH5 Cytoplasmic** | Correlation coefficient | **0.126** | **0.261** |
| | p value | **p 0.004**** | **p <0.0001****** |
| | N | **513** | **513** |
| **METTL3 Nuclear** | Correlation coefficient | **0.095** | 0.034 |
| | p value | **p 0.041*** | p 0.463 |
| | N | **460** | 460 |
| **METTL3 Cytoplasmic** | Correlation coefficient | -0.028 | -0.042 |
| | p value | p 0.542 | p 0.365 |
| | N | 460 | 460 |

**Table 5.1 Correlations of CBLL1 expression with other breast cancer-related proteins**

Correlations of both CBLL1 nuclear and cytoplasmic expression with expression of other proteins implicated in BCa assessed via IHC in the Nottingham BCa cohort. Statistical p-values determined by Spearman's correlation and p≤0.05 highlighted in bold.

## 5.3 Discussion

A small number of studies have examined the association of CBLL1 with BCa (Gong et al., 2010, Liu et al., 2022b, Ma et al., 2023, Makdissi et al., 2009, Zheng et al., 2021), however the function and clinical relevance of CBLL1 in BCa remains poorly understood.

This chapter focussed on the role of CBLL1 both in BCa cell lines and in a large, well-characterised independent BCa patient cohort, which has not previously been reported. This study therefore provides the first detailed analysis of CBLL1 expression in BCa cell lines and in ~1500 BCa patients in order to elucidate its potential role in E-cadherin expression and BCa development and progression.

Initially, bioinformatic analysis was carried out on published BCa datasets using the cBioPortal for Cancer Genomics (Cerami et al., 2012, Gao et al., 2013). Whilst altered *CBLL1* expression in BCa patients was found to be rare, where it was altered, *CBLL1* was most commonly amplified (**Figure 5.1A**). This may suggest an association between *CBLL1* and malignancy in BCa. This finding is consistent with recent studies that found that higher *CBLL1* expression in BCa cells was associated with a more aggressive phenotype (Liu et al., 2022b, Ma et al., 2023). Altered mRNA expression of *CBLL1* was more common (**Figure 5.1C**).

In contrast, alterations in *CDH1* expression were present in ~10-12 fold the number of BCa patients as *CBLL1* alterations. Multiple CNA types were most commonly observed, with amplification the rarest alteration seen (**Figure 5.1B**). In the TCGA cohort, altered *CDH1* mRNA expression was most commonly downregulated, although interestingly in the METABRIC cohort it

was most commonly upregulated (**Figure 5.1D**). Taken together these findings support the large number of other studies that have found that downregulation or total loss of E-cadherin is associated with malignancy and cancer progression (Christofori and Semb, 1999, Nollet et al., 1999, Siitonen et al., 1996).

The majority of cases were found to be diploid for both *CBLL1* and *CDH1* across both patient cohorts, with amplification the most common CNA in *CBLL1* expression (**Figure 5.2A** and **Figure 5.2B**), and shallow deletion in *CDH1* expression (**Figure 5.2C** and **Figure 5.2D**). Across both genes a trend of increased expression was seen in cases with copy number gain and amplification, with decreased expression seen in cases with copy number shallow and deep deletion (**Figure 5.2**). Taken together these findings suggest a role for aberrant *CBLL1* expression in BCa that warrants further investigation.

Further analysis into publicly available data sets revealed that whilst no significant difference in *CBLL1* expression was found between normal breast, primary tumour or metastatic tissue (**Figure 5.3A**), higher *CBLL1* expression was significantly associated with increased overall and relapse-free survival (**Figure 5.4A** and **Figure 5.4C**, respectively). These findings accord with a previous study which also found higher CBLL1 expression to be associated with better OS and RFS (Zheng et al., 2021). However, further analysis into an additional patient dataset found the inverse, that lower *CBLL1* expression was significantly associated with better OS (**Figure 5.5A**). This result is consistent with previous studies in other cancer types that found that lower *CBLL1* expression was associated with better overall survival in ovarian cancer (Tan et al., 2023), and more favourable prognostic factors in HCC (Gu et al., 2022).

*CDH1* expression was significantly higher in primary tumour, and higher still in metastatic patient specimens when compared with normal breast tissue (**Figure 5.3B**). Similarly, higher *CDH1* expression was significantly associated with poorer RFS (**Figure 5.4D**). These findings are somewhat surprising, given the wealth of literature that has reported higher E-cadherin expression to be a positive prognostic factor in many cancer types, including breast (Berx et al., 1996, Berx and Van Roy, 2001, Nollet et al., 1999, Rakha et al., 2005). However, it is increasingly understood that E-cadherin expression varies by tumour type and grade (Alsaleem et al., 2019, Jeschke et al., 2007, Rakha et al., 2010, Rakha et al., 2013), with some studies reporting higher E-cadherin expression to be significantly associated with negative prognostic factors in certain breast tumour types (Gillett et al., 2001, Kurozumi et al., 2018, Jeschke et al., 2007).

Further analysis using an additional patient dataset found a contrasting result, with higher *CDH1* expression significantly associated with better OS (**Figure 5.5B**). Other studies have found similar associations between disease-free survival and E-cadherin protein expression (Heimann et al., 2000, Siitonen et al., 1996). E-cadherin expression has been demonstrated to vary widely depending on the tumour histological subtype in BCa. For example, loss of E-cadherin expression is such a characteristic of invasive lobular carcinomas, it has been argued that this feature could be diagnostic (Korkola et al., 2003). However, the most common BCa subtype, invasive ductal carcinoma of no special type (IDC-NST) usually retains E-cadherin expression (Alsaleem et al., 2019, Cleton-Jansen, 2001, Rakha et al., 2013, Roylance et al., 2003, Siitonen et al., 1996), although reduced expression is more frequently seen in more

advanced and higher-grade NST tumours (Gillett et al., 2001, Oka et al., 1993). Indeed, some cohorts of mixed tumour subtypes have reported no correlation between E-cadherin expression and key prognostic factors or survival (Lipponen et al., 1994). There is overall consensus in the literature however that reduced or loss of E-cadherin expression is associated with aggressive and metastatic BCa regardless of subtype (Alsaleem et al., 2019, Jeschke et al., 2007, Mahler-Araujo et al., 2008, Siitonen et al., 1996). Further investigation into the histological subtype, grade and stage of the tumours studied in these cohorts is therefore warranted in order to further elucidate the significance of *CDH1* expression within them.

In order to further understand the expression of CBLL1 in BCa, its expression was analysed at both the mRNA and protein level in BCa cell lines. *CBLL1* was expressed in all cells examined, and moreover expressed at a significantly higher level in the ERα-expressing estrogen-responsive cell lines, with ~3 to 4-fold higher *CBLL1* expression observed in the MCF7 and T-47D cell lines compared with normal HMEC cells (**Figure 5.6A**). CBLL1 protein expression was detected in all cell lines, with higher expression seen in the malignant compared with the non-malignant cell lines (**Figure 5.6C**). These findings correspond with those of prior studies which reported higher *CBLL1* expression in tumour compared with non-malignant cells and tissue (Castosa et al., 2018, Hui et al., 2019, Liu et al., 2018b, Liu et al., 2018c), and with the results reported in PCa in Chapter 3. These results support a possible role for CBLL1 in BCa development and progression.

Consistent with the literature, E-cadherin protein was not expressed in the triple negative cell lines MDA-MB-231 and MDA-MB-453 (**Figure 5.6C**) as

previously described (Anzai et al., 2017, Lombaerts et al., 2006), with *CDH1* mRNA only just detectable in MDA-MB-453 (**Figure 5.6B**). Consistent with *CBLL1* expression, both the expression of mRNA and protein of E-cadherin was highest in the ERα- expressing cell lines MCF7 and T-47D (**Figure 5.6B** and **Figure 5.6C**). It is interesting that the expression patterns of CBLL1 and E-cadherin mirror one another and are not the inverse, as might be expected from the expression patterns found in the bioinformatic prognostic tools reported in **Figure 5.4** and **Figure 5.5,** and as described by other authors (Castosa et al., 2018, Figueroa et al., 2009b, Fujita et al., 2002).

The BioGRID tool (Oughtred et al., 2019) reports a direct interaction between the CBLL1 and ERα proteins, with another study reporting that CBLL1 can function as a co-repressor of the transcriptional activity of ERα (Gong et al., 2010). With this in mind, and given that the highest expression of *CBLL1* was observed in the estrogen-responsive BCa cell lines, the effect of estrogen on *CBLL1* expression was assessed. Estrogen is implicated in the development and progression of a number of cancer types, including breast, ovarian, colorectal and prostate (Ascenzi et al., 2006, Deroo and Korach, 2006). Therefore, it was important to establish any association in expression of *CBLL1* with estrogen in order to better understand its role in BCa.

Interestingly, estrogen treatment resulted in significantly lower expression of both *CBLL1* in MCF7 cells, as previously described (Gong et al., 2010), as well as *CDH1*, but had no effect in T-47D cells (**Figure 5.7**). Similarly, it has been demonstrated that estrogen can down-regulate *CDH1* transcription in ER-positive BCa cells (Oesterreich et al., 2003), and furthermore that the *CDH1* promoter is bound by ERα whether or not estrogen is present, and is repressed

in the presence of estrogen (Cardamone et al., 2009). These results appear to support these earlier findings, with the differences observed in the T-47D cell line potentially linked to the numerous bioenergetic differences between MCF7 and T-47D cells, including lower expression of ERα in T-47D cells (Radde et al., 2014).

Interestingly, in contrast to the mRNA findings, CBLL1 protein expression was modestly increased in response to estrogen treatment in both the MCF7 and T-47D cell lines, yet E-cadherin expression was modestly decreased in both cell lines (**Figure 5.8**). The effect of estrogen on protein expression in MCF7 and T-47D cells was further investigated by analysing protein subcellular localisation (**Figure 5.9**). CBLL1 expression was predominantly nuclear, with comparatively lower cytoplasmic expression in vehicle-treated MCF7 and T-47D cells, according with the reported nuclear (Horiuchi et al., 2013, Ruzicka et al., 2017) and cytoplasmic (Fujita et al., 2002) dual roles of CBLL1, and with previous studies that described a predominantly nuclear localisation of CBLL1 protein in mouse embryonic stem cells (Wen et al., 2018) and in a range of cancer cell types, including MCF7 (Figueroa et al., 2009a). Consistent with the findings in **Figure 5.8**, CBLL1 expression in both the nuclear and cytoplasmic fractions was increased following $\beta E_2$ treatment (**Figure 5.9**). In contrast, E-cadherin expression was enriched in the cytoplasm and modestly expressed in the nucleus in both cell lines, as previously described (Du et al., 2014, Ohishi et al., 2011), with no discernible change in expression seen in response to $\beta E_2$ treatment (**Figure 5.9**).

Evidence from recently reported ChIP-Seq data supports epigenetic regulation of *CBLL1* expression in at least a subset of patients and clinical contexts (Jansen et al., 2013, Nevedomskaya et al., 2014).

The clinical relevance of CBLL1 protein expression in BCa patients was subsequently investigated by carrying out IHC staining and analysis of BCa TMA specimens from two combined large well-characterised Nottingham patient cohorts. IHC staining of patient samples further confirmed the protein subcellular localisation observed in **Figure 5.9**, with CBLL1 staining most abundant in the nucleus and much weaker in the cytoplasm (**Figure 5.11**), and E-cadherin staining strongest at the cell membrane, followed by the cytoplasm, then the nucleus (**Appendix 18**).

Correlations of CBLL1 expression with deidentified patient clinicopathological data were then completed to determine the potential clinical relevance and prognostic value of CBLL1 in BCa (**Figure 5.12**, **Figure 5.13**, **Figure 5.15** and **Appendices 16** & **17**). Higher nuclear CBLL1 expression was significantly associated with a large number of positive prognostic factors, most particularly lower grade at diagnosis, better NPI prognostic group, ER and PR positive and non-TN status, as well as longer BCSS and DMFS (**Figure 5.12**, **Figure 5.13**, and **Appendix 17**). In contrast, higher cytoplasmic CBLL1 expression was significantly associated with a number of negative prognostic factors, most particularly higher grade at diagnosis, poorer NPI prognostic group, and both ER-negative and TN status (**Figure 5.12** and **Appendix 17**). Cytoplasmic CBLL1 expression was not significantly associated with survival (**Figure 5.13**). Interestingly, one study has reported that increased nuclear expression of CBLL1 in Madin-Darby canine kidney (MDCK) cells was associated with an

epithelial phenotype, with increasing cytoplasmic CBLL1 expression resulting in disrupted intercellular adhesions and a more fibroblastic phenotype (Figueroa et al., 2009a).

Only two studies are known to have been published examining CBLL1 expression in BCa patient samples, with one failing to find any significant associations with E-cadherin expression, malignancy or prognostic factors, however this was limited by the small sample size (n=30) (Makdissi et al., 2009). Another study reported conflicting findings, of lower CBLL1 expression in normal breast tissue compared with BCa yet found higher expression to be associated with better relapse-free and overall survival in BCa patients (n=134) (Zheng et al., 2021). This is consistent with the nuclear CBLL1 staining assessed in this chapter, that was found to also be similarly associated with survival (**Figure 5.13**).

The prognostic value of CBLL1 was further confirmed in the current study following its analysis alongside other established prognostic factors (**Figure 5.15**). Nuclear CBLL1 was found to be a significant positive prognostic factor, with higher CBLL1 an independent prognostic marker for improved survival (**Figure 5.15A** and **Figure 5.15B**), together with E-cadherin (**Figure 5.15E** and **Figure 5.15F**). Cytoplasmic CBLL1 expression, on the other hand, was not found to be an independent prognostic factor in BCa survival (**Figure 5.15E** and **Figure 5.15F**).

In **Table 5.1** CBLL1 nuclear and cytoplasmic expression was correlated with other proteins of interest with respect to BCa and $m^6A$. Nuclear CBLL1 was most commonly positively correlated with proteins associated with better

prognosis in BCa such as BRCA1, BRCA2, ERα and FOXA1 (Brohet et al., 2014, Kuchenbaecker et al., 2017, Sørlie et al., 2001, Thorat et al., 2008), whereas a significant negative correlation was seen only exclusively with markers associated with poorer prognosis such as N-cadherin and P-cadherin (Kotb et al., 2011, Qi et al., 2022).

Cytoplasmic CBLL1 expression was also exclusively negatively correlated with those markers associated with poor prognosis including the p53 tumour suppressor mutant Ac_p53_K120 and N-cadherin (Leszczynska et al., 2015). However positive correlations were more equivocally split between those markers associated with better prognosis such as BRCA1, BRCA2 and ALKBH5 (Brohet et al., 2014, Kuchenbaecker et al., 2017) and those associated with poorer prognosis such as P-cadherin (Qi et al., 2022).

A weak positive correlation was observed between the level of nuclear and cytoplasmic CBLL1 expression (**Figure 5.14**). A positive correlation was also observed in the PCa patient specimens reported in Chapter 3, however, interestingly, whilst as in BCa higher cytoplasmic expression of CBLL1 was associated with poorer prognostic factors, so too was higher nuclear CBLL1 expression in PCa. In contrast, in BCa it was found that higher nuclear CBLL1 expression was significantly correlated with better prognostic factors and with other proteins associated with better outcomes.

These nuclear findings are consistent with a previous study that suggested a tumour suppressor role for CBLL1 in BCa, reporting an association between higher CBLL1 expression and reduced proliferation and migration in BCa cells (Gong et al., 2010). However they do contrast with two other studies in BCa

cell lines where higher CBLL1 expression was associated with increased invasive and metastatic potential (Liu et al., 2022b, Ma et al., 2023), and with an oncogenic function purported in other cancer types (Castosa et al., 2018, Figueroa et al., 2009b, Hui et al., 2019).

E-cadherin membrane expression was also assessed via IHC in our large BCa patient cohort. Higher E-cadherin expression was significantly associated with a number of positive prognostic factors, most particularly lower grade at diagnosis and PR positive status, as well as longer BCSS and DMFS (**Figure 5.13**, and **Appendix 20**). These results accord with many studies that found higher E-cadherin expression to be associated with positive prognostic factors, (Heimann et al., 2000, Jeschke et al., 2007, Siitonen et al., 1996), including a meta-analysis of E-cadherin expression in over 7000 patients from 33 different individual studies (Li et al., 2017d). The fact that two of the negative prognostic factors investigated (lymph node status and vascular invasion) were significantly associated with higher E-cadherin expression (**Appendix 20**) is likely due to the fact that the majority of samples in our patient cohort were IDC-NST, where higher E-cadherin expression and association with poorer prognosis has been reported (Gillett et al., 2001, Oka et al., 1993).

Interestingly, a weak positive correlation was found between both nuclear and cytoplasmic CBLL1 expression and E-cadherin expression in the BCa patient cohort (**Figure 5.16**). This is consistent with the findings in **Figure 5.6**, however contrasts with the bioinformatic analysis presented in **Figure 5.4** and **Figure 5.5** and with reports from other authors, that CBLL1 and E-cadherin expression are negatively correlated (Castosa et al., 2018, Figueroa et al., 2009b, Fujita et al., 2002). This positive correlation, together with the low levels of CBLL1

cytoplasmic expression observed in BCa cells and tissues, suggests that the E-cadherin degradation function reported of CBLL1 may not play a key role in BCa.

Taken together the results presented in this chapter with regard to E-cadherin expression accord with those previously reported by others, that it is higher in ERα-positive tumours compared with normal tissue, and significantly lower or lost completely in TNBC as evidenced by the cell line findings reported in **Figure 5.6**. Likewise, it was observed that E-cadherin expression is downregulated by estrogen, and that E-cadherin is an independent positive prognostic marker in BCa patients.

To summarise, bioinformatic analysis of *CBLL1* found that gene amplification was the most common genomic alteration and that higher *CBLL1* expression was significantly associated with both increased and decreased survival in BCa depending on the patient cohort. CBLL1 was expressed at the mRNA and protein level in both non-malignant and BCa cells, with the highest expression levels seen in ERα-expressing BCa cell lines sensitive to estrogen. CBLL1 expression appears to be estrogen-regulated at the protein level, however results at the mRNA level were less obvious. Furthermore, correlation of CBLL1 and ERα in BCa tissue samples showed a positive association in the expression of these two proteins. Work in both BCa cell lines and patient BCa specimens demonstrated that CBLL1 protein is expressed both in the nucleus and cytoplasm as expected from its dual reported roles in both locations, but is markedly enriched in the nucleus. IHC analysis of a large cohort of BCa patient tissue specimens demonstrated that, overall, higher expression of nuclear CBLL1 was associated with better prognostic factors, better survival, and

moreover was demonstrated to be an independent positive prognostic indicator for patient survival. Cytoplasmic results were more equivocal, with higher cytoplasmic CBLL1 associated more frequently with negative prognostic factors, however it was not found to be an independent prognostic indicator and had no significant correlations with patient survival. These results implicate CBLL1 in BCa, however continued work is indicated to further elucidate its prognostic potential or utility as a therapeutic target.

# Chapter 6

## Functional role of CBLL1 in breast cancer cell lines

# 6 Functional role of CBLL1 in breast cancer cell lines

## 6.1 Introduction

BCa continues to be a global health problem, as the most commonly diagnosed cancer type in females and disease incidence continues to increase (Nolan et al., 2023, Sung et al., 2021). A number of non-genetic and genetic risk factors have been identified in BCa (Danaei et al., 2005, Hankinson et al., 2004).

A key non-genetic risk factor for BCa is increased exposure to estrogen (through early menarche, late menopause and consumption of exogenous hormones in oral contraceptives and post-menopausal therapies) (Henderson, 1989, Hsieh et al., 1990). One of the first genetic risk factors discovered was a hereditary mutation in the Breast Cancer 1 (*BRCA1*) gene that confers BCa susceptibility (Hall et al., 1990, Miki et al., 1994). Multi-gene expression assays have also been developed, whereby the level of mRNA expression of a defined set of genes can be correlated with robust prognostic indicators (Paik et al., 2004, Cardoso et al., 2016, van 't Veer et al., 2002).

Alternative splicing has been linked to a large number of cancer types, including breast (He et al., 2009, Kahles et al., 2018). Indeed, it has been found that alternative splicing in BCa can both influence the tumour phenotype and constitute a prognostic molecular signature in patients (Bjørklund et al., 2017, Wen et al., 2015). Estrogen treatment has been demonstrated to significantly change alternative splicing events in target genes in ERα-expressing cancer cells, including the BCa cell line T-47D but, interestingly, not in MCF7 cells (Auboeuf et al., 2002, Auboeuf et al., 2004).

Many studies have reported a role for the m$^6$A RNA modification in alternative splicing (Alarcón et al., 2015, Dominissini et al., 2012, Haigh et al., 2022, Haussmann et al., 2016, Horiuchi et al., 2013, Lence et al., 2016, Lothion-Roy et al., 2022, Ping et al., 2014, Su et al., 2022, Yang et al., 2018, Zhao et al., 2014), however, there has been limited examination of the role of CBLL1 in alternative splicing. One research group has reported that CBLL1 interacts with polypyrimidine tract-binding protein-associated splicing factor (PSF) in the nucleus of MCF7 BCa cells, and has a crucial role in the ability of PSF to bind RNA (Figueroa et al., 2009a, Figueroa et al., 2009b). PSF regulates a number of cellular process, including transcription, pre-mRNA splicing and retention of edited RNA in the nucleus (Patton et al., 1993, Shav-Tal and Zipori, 2002), and has been associated with tumourigenesis in both colon and prostate cancer (Takayama et al., 2017, Tsukahara et al., 2013). More recently, PSF has been implicated in BCa, with PSF expression associated with post-transcriptional regulation of *ESR1* and poorer prognosis in patients with ER-positive BCa (Mitobe et al., 2020).

In chapter 5 it was reported that CBLL1-expression is estrogen-regulated and that the highest CBLL1 expression was seen in ERα-expressing BCa cell lines. However, when examining patient data, it was found that nuclear expression of CBLL1 was an independent positive prognostic indicator, although cytoplasmic CBLL1 expression was associated with negative patient outcomes. Previous studies in BCa have found that higher CBLL1 expression was associated with increased BCa cell invasion and metastasis (Liu et al., 2022a, Ma et al., 2023), Interestingly, another study found that CBLL1

physically interacts with the ERα and inhibits ER-positive BCa cell proliferation and migration (Gong et al., 2010).

Given the association between CBLL1 and BCa, the functional role of CBLL1 in BCa gene regulation and estrogen signalling was investigated here. The effect of siRNA-mediated *CBLL1* depletion, with and without estrogen treatment, in the ERα-expressing cell lines MCF7 and T-47D was analysed. Knockdown of *CBLL1* was confirmed both at the protein and mRNA level, before its effect on ERα expression and BCa cell phenotype was assessed. The impact of siRNA-mediated *CBLL1* depletion and estrogen treatment on gene expression and splicing was then analysed by RNA-Seq. Collectively, these results further elucidate the functional role of CBLL1 in BCa and estrogen signalling.

## 6.2 Results

### 6.2.1 siRNA depletion of *CBLL1* in breast cancer cell lines

To investigate the role of CBLL1 in the regulation of E-cadherin expression and estrogen signalling, siRNA-mediated functional depletion of *CBLL1* (si*CBLL1*) was carried out in the ERα-expressing BCa cell lines MCF7 and T-47D. Cells received a double transfection of either si*CBLL1* or scrambled control (si*Scr*) and were treated with vehicle or $\beta E_2$ (as described in chapter 2) prior to harvesting for analysis of protein and mRNA by western blot and qRT-PCR, respectively.

*CBLL1* knockdown was confirmed at the protein level in MCF7 cells, with a ~4-fold decrease ($p<0.05$) in expression observed between vehicle-treated cells, and an even greater decrease (~15-fold; $p<0.05$) in CBLL1 expression seen in $\beta E_2$-treated cells (**Figure 6.1A** and **Figure 6.1C**). Consistent with direct estrogen upregulation of *CBLL1* expression, $\beta E_2$ treatment partially opposed *siCBLL1*-mediated knockdown (**Figure 6.1A** and **Figure 6.1C**), although this did not reach statistical significance ($p>0.05$).

No statistically significant difference was observed in E-cadherin expression in MCF7 cells following *CBLL1* knockdown ($p>0.05$; **Figure 6.1A** and **Figure 6.1E**). ERα was expressed across all conditions in MCF7 cells, with no obvious difference in expression observed following *CBLL1* knockdown (**Figure 6.1A**).

Significant *CBLL1* knockdown was likewise confirmed at the protein level in T-47D cells, with a ~4-fold decrease ($p<0.01$) in expression observed between vehicle-treated cells, and a similar decrease (~4-fold; $p<0.01$) in CBLL1 expression seen in $\beta E_2$-treated cells (**Figure 6.1B** and **Figure 6.1D**).

Interestingly, $\beta E_2$ treatment also significantly increased CBLL1 expression even with *CBLL1* knockdown (~2-fold; $p<0.05$; **Figure 6.1B** and **Figure 6.1D**).

E-cadherin expression was significantly reduced in $\beta E_2$-treated T-47D cells following *CBLL1* knockdown ($p<0.01$), and although expression was reduced with *CBLL1* depletion in vehicle-treated cells, this did not reach statistical significance ($p>0.05$; **Figure 6.1B** and **Figure 6.1F**). ERα was expressed in all conditions in T-47D cells, with no detectable difference in expression following *CBLL1* knockdown (**Figure 6.1B**).

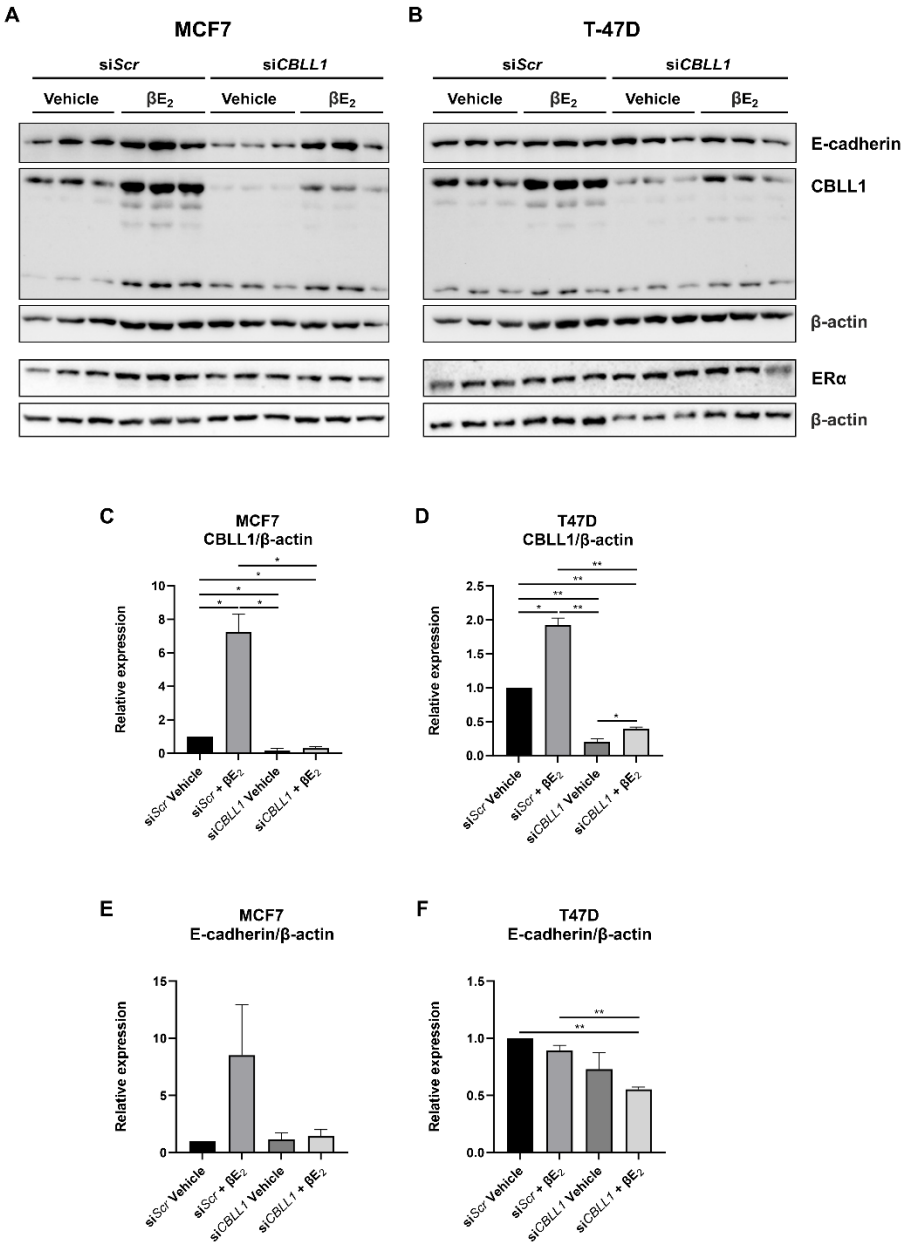


**Figure 6.1 Effect of siRNA-mediated *CBLL1* knockdown and $\beta E_2$ treatment on protein expression in MCF7 and T47D cells**

CBLL1, E-cadherin and ERα protein expression was analysed by western blot with β-actin loading control following siRNA-mediated knockdown of *CBLL1* and subsequent treatment for 72 hours with vehicle or $\beta E_2$. (**A**) E-cadherin, CBLL1 and ERα protein expression in MCF7 cells following *CBLL1* siRNA-mediated knockdown treated with vehicle or $\beta E_2$ (n=3). (**B**) E-cadherin, CBLL1 and ERα protein expression in T-47D cells following *CBLL1* siRNA-mediated knockdown treated with vehicle or $\beta E_2$ (n=3). (**C**) Quantification of CBLL1

protein expression following *CBLL1* siRNA-mediated knockdown treated with vehicle or $\beta E_2$ in MCF7 cells (n=3). (**D**) Quantification of CBLL1 protein expression following *CBLL1* siRNA-mediated knockdown treated with vehicle or $\beta E_2$ in T-47D cells (n=3). (**E**) Quantification of E-cadherin protein expression following *CBLL1* siRNA-mediated knockdown treated with vehicle or $\beta E_2$ in MCF7 cells (n=3). (**F**) Quantification of E-cadherin protein expression following *CBLL1* siRNA-mediated knockdown treated with vehicle or $\beta E_2$ in T-47D cells (n=3). * = p ≤0.05, ** = p ≤0.01, *** = p ≤0.001, **** = p ≤0.0001 by paired t-test.

*CBLL1* knockdown was subsequently confirmed at the mRNA level in both MCF7 and T-47D cells (**Figure 6.2** and **Figure 6.3**). In MCF7 cells a minimum ~5-fold decrease in *CBLL1* expression was observed across all *CBLL1* knockdown conditions ($p<0.05$), again with the greatest decrease in *CBLL1* expression (~10-fold; $P<0.0001$) seen between $\beta E_2$-treated cells (**Figure 6.2A**). Similar to the trend observed at the protein level, $\beta E_2$ induced *CBLL1* expression and opposed *siCBLL1*-mediated knockdown (~2-fold; $p<0.0001$; **Figure 6.2A**).

*CDH1* expression was modestly, yet significantly, reduced in vehicle-treated MCF7 cells following *CBLL1* knockdown ($p<0.001$), and although expression did also appear to be reduced with *CBLL1* depletion in $\beta E_2$-treated cells, this did not reach statistical significance ($p>0.05$; **Figure 6.2B**). *ESR1* expression was increased in vehicle-treated MCF7 cells following *CBLL1* knockdown (~1.5-fold; $p<0.0001$), with expression significantly higher in vehicle-treated compared with $\beta E_2$-treated *CBLL1* knockdown cells (~1.5-fold; $p<0.001$; **Figure 6.2C**). No significant difference in the expression of the ER-regulated gene *PS2* (also known as *TFF1*) was seen in response to *CBLL1* knockdown,

although a similar trend to the *ESR1* findings was observed (p>0.05; **Figure 6.2D**).

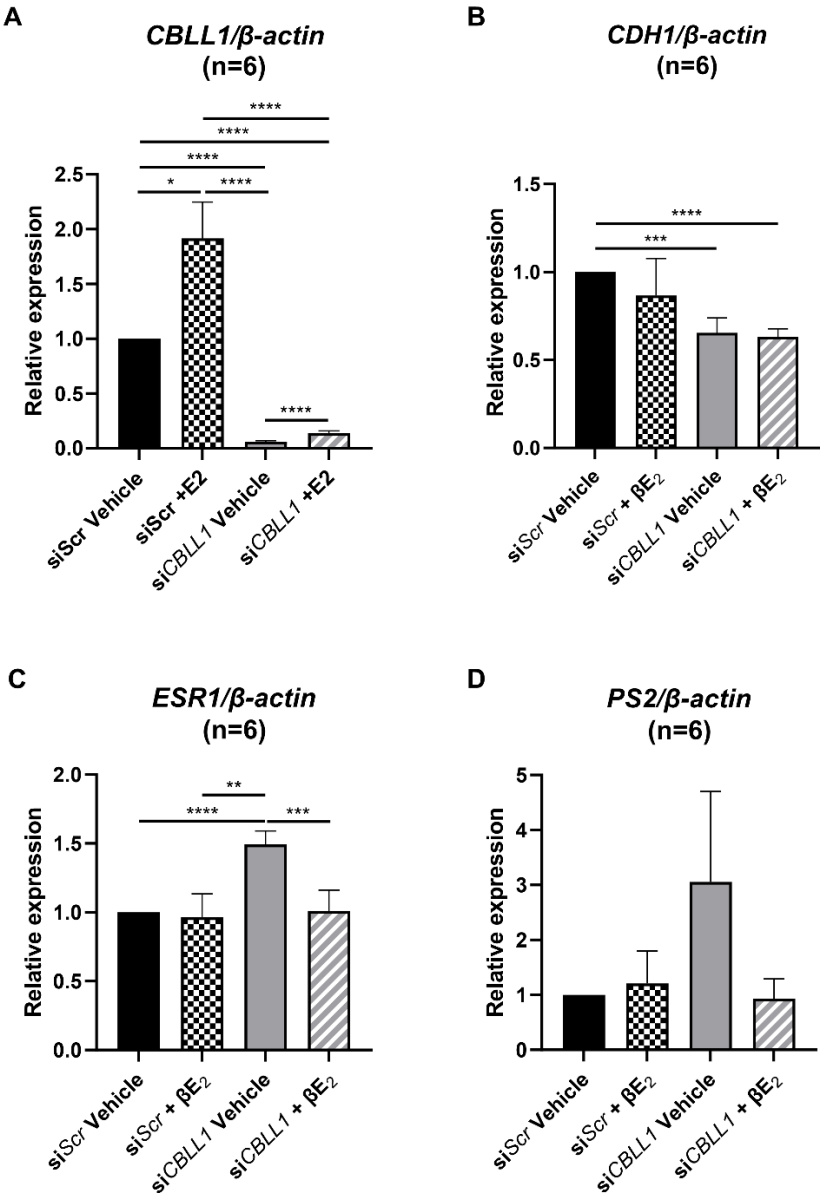


**Figure 6.2 Effect of siRNA-mediated *CBLL1* knockdown and $\beta E_2$ treatment on mRNA expression in MCF7 cells**

*CBLL1*, *CDH1, ESR1* and *PS2* mRNA expression in MCF7 cells was analysed by qRT-PCR relative to *β-actin* following siRNA-mediated knockdown of *CBLL1* and subsequent treatment for 72 hours with vehicle or $\beta E_2$. (**A**) *CBLL1* mRNA expression following *CBLL1* siRNA-mediated knockdown treated with

vehicle or $\beta E_2$ (n=6). (**B**) *CDH1* mRNA expression following *CBLL1* siRNA-mediated knockdown treated with vehicle or $\beta E_2$ (n=6). (**C**) *ESR1* mRNA expression following *CBLL1* siRNA-mediated knockdown treated with vehicle or $\beta E_2$ (n=6). (**D**) *PS2* mRNA expression following *CBLL1* siRNA-mediated knockdown treated with vehicle or $\beta E_2$ (n=6). * = $p \leq 0.05$, ** = $p \leq 0.01$, *** = $p \leq 0.001$, **** = $p \leq 0.0001$ by paired t-test.

In T-47D cells a minimum ~3-fold decrease in *CBLL1* expression was observed in all *CBLL1* knockdown conditions ($p<0.0001$), again with the greatest decrease in *CBLL1* expression (~4-fold; $p<0.0001$) seen between $\beta E_2$-treated cells (**Figure 6.3A**). Consistent with the findings observed at the protein level, $\beta E_2$ treatment also modestly, yet significantly, increased *CBLL1* expression and opposed *CBLL1* knockdown ($p<0.01$; **Figure 6.3A**).

No significant difference in *CDH1* expression was observed in T-47D cells following *CBLL1* knockdown ($p>0.05$; **Figure 6.3B**), however a similar trend was observed to that seen at the protein level (**Figure 6.1B**), and at the mRNA level in MCF7 cells (**Figure 6.2B**), whereby *CDH1* expression appeared to be modestly reduced following *CBLL1* depletion.

*ESR1* expression was significantly increased in vehicle-treated T-47D cells following *CBLL1* knockdown (~3-fold; $p<0.01$, **Figure 6.3C**). In contrast to MCF7 cells, *ESR1* expression was significantly higher in $\beta E_2$-treated compared with vehicle-treated across both scrambled control (~5-fold) and *CBLL1*-depleted (~1.5-fold) cells (both $p<0.01$; **Figure 6.3C**). In contrast to the findings in MCF7 cells, *PS2* expression was significantly lower in vehicle-treated T-47D cells following *CBLL1* knockdown (~2-fold; $p<0.0001$), yet induced following $\beta E_2$ treatment in scrambled control (~30-fold) and *CBLL1*-depleted (~25-fold)

cells (both $p<0.01$; **Figure 6.3D**). Moreover, this induction appeared to be attenuated with *CBLL1* knockdown, however this observation did not reach statistical significance ($p>0.05$; **Figure 6.3D**).

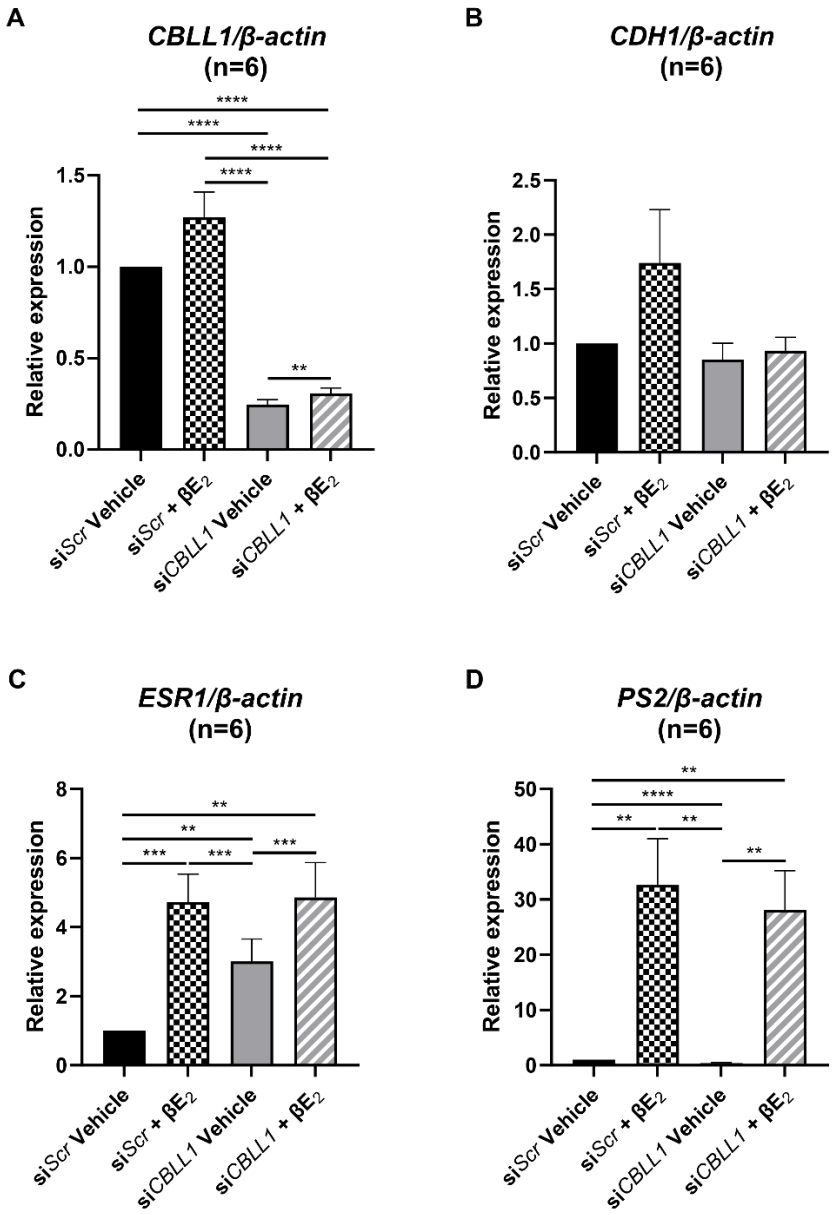


**Figure 6.3 Effect of siRNA-mediated *CBLL1* knockdown and $\beta E_2$ treatment on mRNA expression in T-47D cells**

*CBLL1*, *CDH1, ESR1* and *PS2* mRNA expression in T-47D cells was analysed by qRT-PCR relative to *β-actin* following siRNA-mediated knockdown of *CBLL1* and subsequent treatment for 72 hours with vehicle or $\beta E_2$. (**A**) *CBLL1* mRNA expression following *CBLL1* siRNA-mediated knockdown treated with vehicle or $\beta E_2$ (n=6). (**B**) *CDH1* mRNA expression following *CBLL1* siRNA-mediated knockdown treated with vehicle or $\beta E_2$ (n=6). (**C**) *ESR1* mRNA expression following *CBLL1* siRNA-mediated knockdown treated with vehicle or $\beta E_2$ (n=6). (**D**) *PS2* mRNA expression following *CBLL1* siRNA-mediated

knockdown treated with vehicle or $\beta E_2$ (n=6). * = p ≤0.05, ** = p ≤0.01, *** = p ≤0.001, **** = p ≤0.0001 by paired t-test.

### 6.2.2 Phenotypic effect of siRNA depletion of *CBLL1* in breast cancer cell lines

To further investigate the functional role of CBLL1 in BCa, the effect of *CBLL1* depletion -/+ $\beta E_2$ treatment in MCF7 and T-47D cells on proliferation was assessed (**Figure 6.4**). In MCF7 cells, proliferation was modestly, yet significantly, increased (~1.2-fold; $p<0.01$) in response to $\beta E_2$ treatment in scrambled control cells, however no change in proliferation was seen in *CBLL1*-depleted cells, with proliferation therefore significantly reduced (~1.2-fold) in $\beta E_2$-treated *CBLL1*-depleted cells, compared with $\beta E_2$-treated scrambled control cells ($p<0.05$; **Figure 6.4A**). No significant difference in cellular proliferation was observed in vehicle-treated MCF7 cells following *CBLL1* knockdown ($p>0.05$; **Figure 6.4A**).

No significant difference in cellular proliferation was observed between any of the conditions in T-47D cells ($p>0.05$; **Figure 6.4B**).

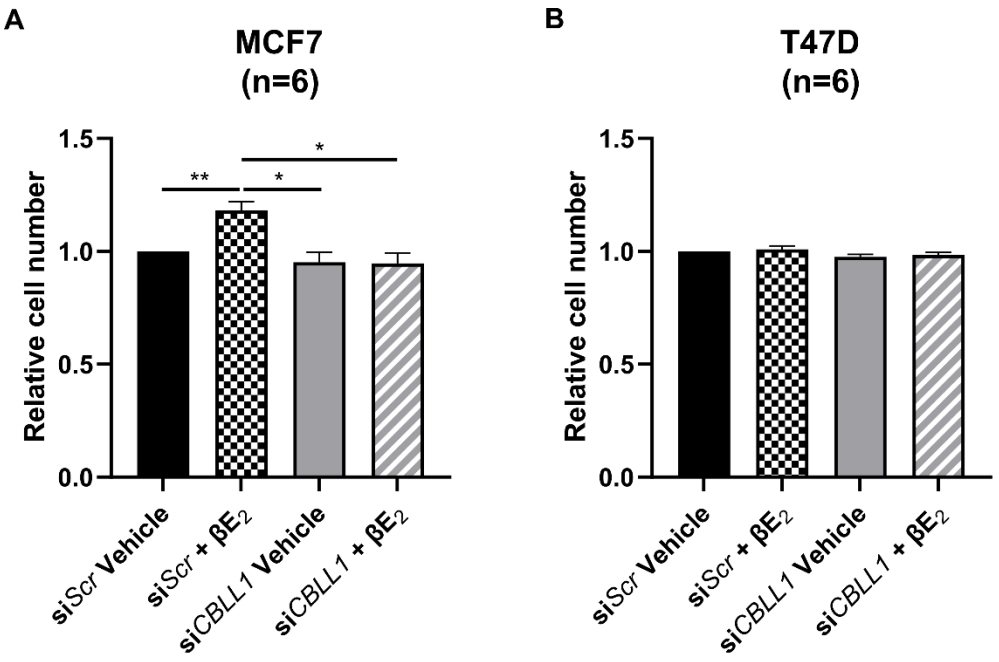


**Figure 6.4 Phenotypic effect of siRNA-mediated *CBLL1* knockdown and $\beta E_2$ treatment in MCF7 and T-47D cells**

Cellular proliferation of MCF7 and T-47D cells was analysed by CyQUANT™ Direct Cell Proliferation Assay following siRNA-mediated knockdown of *CBLL1* and subsequent treatment for 72 hours with vehicle or $\beta E_2$. (**A**) Cellular proliferation in MCF7 cells following *CBLL1* siRNA-mediated knockdown treated with vehicle or $\beta E_2$ (n=6). (**B**) Cellular proliferation in T-47D cells following *CBLL1* siRNA-mediated knockdown treated with vehicle or $\beta E_2$ (n=6). * = p ≤0.05, ** = p ≤0.01, *** = p ≤0.001, **** = p ≤0.0001 by paired t-test.

### 6.2.3 Effect of siRNA depletion of *CBLL1* on differential gene expression in basal and estrogen-treated MCF7 cells

In order to further understand the function of CBLL1 in BCa, RNA-Seq was used to analyse the effects of siRNA-mediated functional depletion of *CBLL1* on the estrogen-regulated transcriptome in MCF7 cells. Significantly differentially expressed genes (DEGs) were identified based on a fold change (FC) of ≥1.5 or ≤-1.5 and a false discovery rate (FDR) of <0.05.

In scrambled control MCF7 cells 8665 genes were found to be estrogen-regulated, with 3583 genes (including the estrogen-regulated gene *TFF1/PS2* and, interestingly, *METTL3*) induced by $\beta E_2$ treatment, and 5082 genes downregulated by $\beta E_2$ (**Figure 6.5A** and **Figure 6.6A**). Where *CBLL1* was depleted, 5532 estrogen-regulated genes were identified, with 2290 genes (including *TFF1/PS2* as well as *H19*, *METTL3* and *PGR*) induced by $\beta E_2$ treatment and 3242 genes downregulated by $\beta E_2$ in the absence of *CBLL1* (**Figure 6.5D** and **Figure 6.6A**).

Functional depletion of *CBLL1* in vehicle-treated (basal) cells resulted in the significant differential expression of 486 genes, of which 278 were induced by *CBLL1* (including *H19*, *PPL* and *TFEB*) and 208 were downregulated by *CBLL1* (including *INHA*) (**Figure 6.5B**). In the presence of $\beta E_2$, depletion of *CBLL1* resulted in 420 genes being differentially expressed, with 153 induced by $\beta E_2$, and 267 genes (including *PPL* and *TFEB*) downregulated by $\beta E_2$ in the absence of *CBLL1* (**Figure 6.5C**).

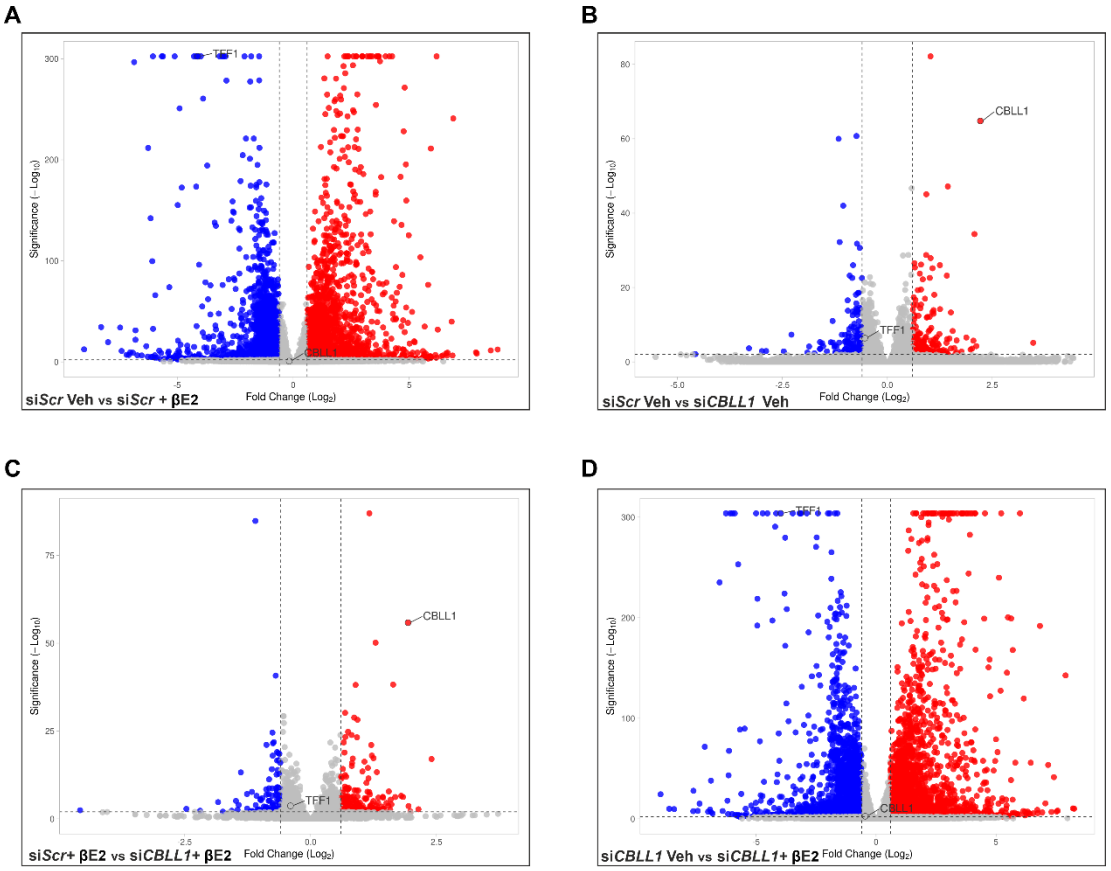


**Figure 6.5 Differential gene expression in MCF7 cells in response to siRNA-mediated *CBLL1* knockdown and $\beta E_2$ treatment**

Differential gene expression was analysed following RNA-Seq of MCF7 cells subjected to siRNA-mediated knockdown of *CBLL1* and subsequent treatment for 72 hours with vehicle or $\beta E_2$. (**A**) Differential gene expression compared between scrambled control cells treated with vehicle or $\beta E_2$ (n=3). (**B**) Differential gene expression compared between vehicle-treated scrambled control and *CBLL1*-depleted cells (n=3). (**C**) Differential gene expression compared between $\beta E_2$-treated scrambled control and *CBLL1*-depleted cells (n=3). (**D**) Differential gene expression compared between *CBLL1*-depleted cells treated with vehicle or $\beta E_2$ (n=3). Genes with significantly higher expression in the first condition listed on each plot are highlighted in red, genes with significantly lower expression in the first condition are highlighted in blue. Genes without any significant differential expression between the two listed conditions are marked in grey. Significant gene expression= FC ± 1.5 and FDR <0.05. Veh= Vehicle.

Of the 9640 DEGs identified in all four experiment conditions in MCF7 cells, 42.6% were found to be CBLL1-dependent estrogen-regulated, with 10.1% only estrogen-regulated in the absence of CBLL1 (**Figure 6.6A**). The remaining 47.3% of DEGs were found to be estrogen-regulated independent of CBLL1 expression (**Figure 6.6A**).

Following DEG analysis, pathway analysis was carried out using WebGestalt to identify significantly enriched KEGG pathways (Liao et al., 2019). KEGG pathway analysis revealed 41 significantly enriched pathways associated with the DEGs identified following $\beta E_2$ treatment in scrambled control MCF7 cells (**Figure 6.6B** and **Appendix 21**) and 42 significantly enriched pathways following $\beta E_2$ treatment in *CBLL1*-depleted MCF7 cells (**Figure 6.6B** and **Appendix 22**). Interestingly, 43.1% of these pathways were common to both the vehicle- or $\beta E_2$-treated scrambled control and *CBLL1*-depleted cells, and included many associated with cell cycle, DNA replication and repair, and cancer (**Appendix 21**, **Appendix 22** and **Appendix 23**). Interestingly, several cancer-specific pathways were also enriched, including basal cell carcinoma (hsa05217) in vehicle- or $\beta E_2$-treated scrambled control cells (**Appendix 21**), and colorectal cancer (hsa05210), hepatocellular carcinoma (hsa05225), small cell lung cancer (hsa05222) and gastric cancer (hsa05226) in vehicle- or $\beta E_2$-treated *CBLL1*-depleted MCF7 cells (**Appendix 22**).

No significantly enriched pathways were associated with DEGs either in vehicle-treated scrambled control and *CBLL1*-depleted MCF7 cells, or in $\beta E_2$-treated scrambled control and *CBLL1*-depleted MCF7 cells (**Appendix 22**), suggesting that *CBLL1* is required for estrogen signalling in cell cycle and DNA repair mechanisms.

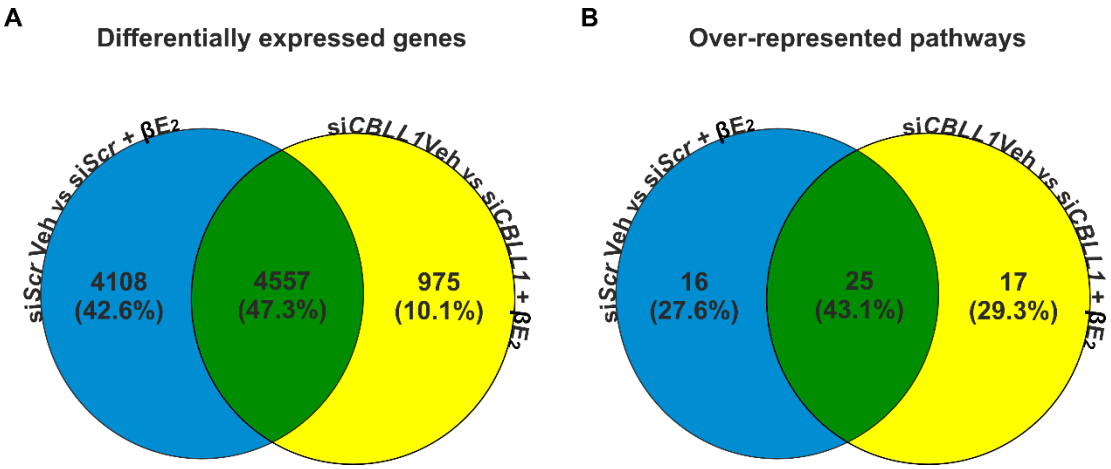


**Figure 6.6 Summary of differentially expressed genes and over-represented KEGG pathways in MCF7 cells in response to siRNA-mediated *CBLL1* knockdown and $\beta E_2$ treatment**

Differential gene expression was analysed following RNA-Seq of MCF7 cells subjected to siRNA-mediated knockdown of *CBLL1* and subsequent treatment for 72 hours with vehicle or $\beta E_2$, followed by pathway analysis using WebGestalt (Liao et al., 2019). (**A**) Summary of DEGs across scrambled control and *CBLL1*-depleted cells treated with vehicle or $\beta E_2$ (n=3). (**B**) Summary of over-represented KEGG pathways across scrambled control and *CBLL1*-depleted cells treated with vehicle or $\beta E_2$ (n=3). Significant gene expression= FC ± 1.5 and FDR <0.05. Veh= Vehicle.

Further analysis revealed the ten most significantly enriched KEGG pathways associated with the identified DEGs in MCF7 cells (**Figure 6.7**). These included pathways associated with cell cycle and cancer, but interestingly, also associated with E-cadherin expression such as the cell adhesion molecules pathway (hsa04514; **Figure 6.7A**) and the lysosome pathway (hsa04142; **Figure 6.7B**). The Fanconi anaemia pathway (hsa03460), associated with DNA damage repair, was the most significantly enriched pathway in *CBLL1*-depleted cells treated with vehicle or $\beta E_2$ (**Figure 6.7B**), and was also enriched in scrambled control cells treated with vehicle or $\beta E_2$ (**Appendix 21**). It is striking that the pathways in cancer (hsa05200) and cell cycle (hsa04110) pathways were significantly enriched in both scrambled control and *CBLL1*-depleted MCF7 cells when treated with vehicle or $\beta E_2$, again suggesting that *CBLL1* may have a role in estrogen signalling in the cell cycle, DNA repair, and carcinogenesis.

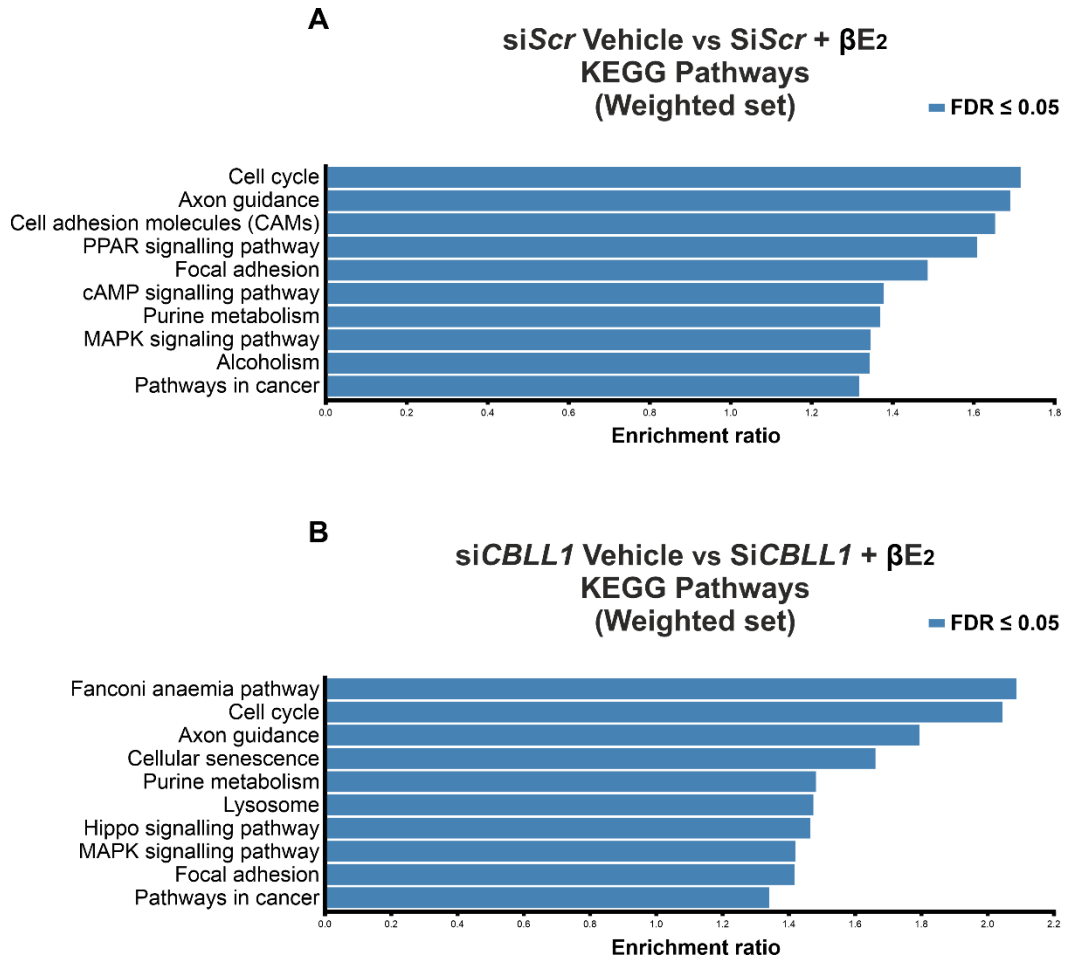


**Figure 6.7 Ten most significantly enriched KEGG pathways in MCF7 cells in response to siRNA-mediated *CBLL1* knockdown and $\beta E_2$ treatment**

Pathway analysis using WebGestalt (Liao et al., 2019) was carried out following differential gene expression analysis of RNA-Seq of MCF7 cells subjected to siRNA-mediated knockdown of *CBLL1* and subsequent treatment for 72 hours with vehicle or $\beta E_2$. (**A**) Weighted set of significantly enriched KEGG pathways associated with DEGs in scrambled control cells treated with vehicle or $\beta E_2$ (n=3). (**B**) Weighted set of significantly enriched KEGG pathways associated with DEGs in *CBLL1*-depleted cells treated with vehicle or $\beta E_2$ (n=3).

The DEGs common to both the vehicle- or $\beta E_2$-treated scrambled control and *CBLL1*-depleted MCF7 cells involved in the pathways in cancer KEGG pathway (hsa05200) are illustrated in **Figure 6.8**.

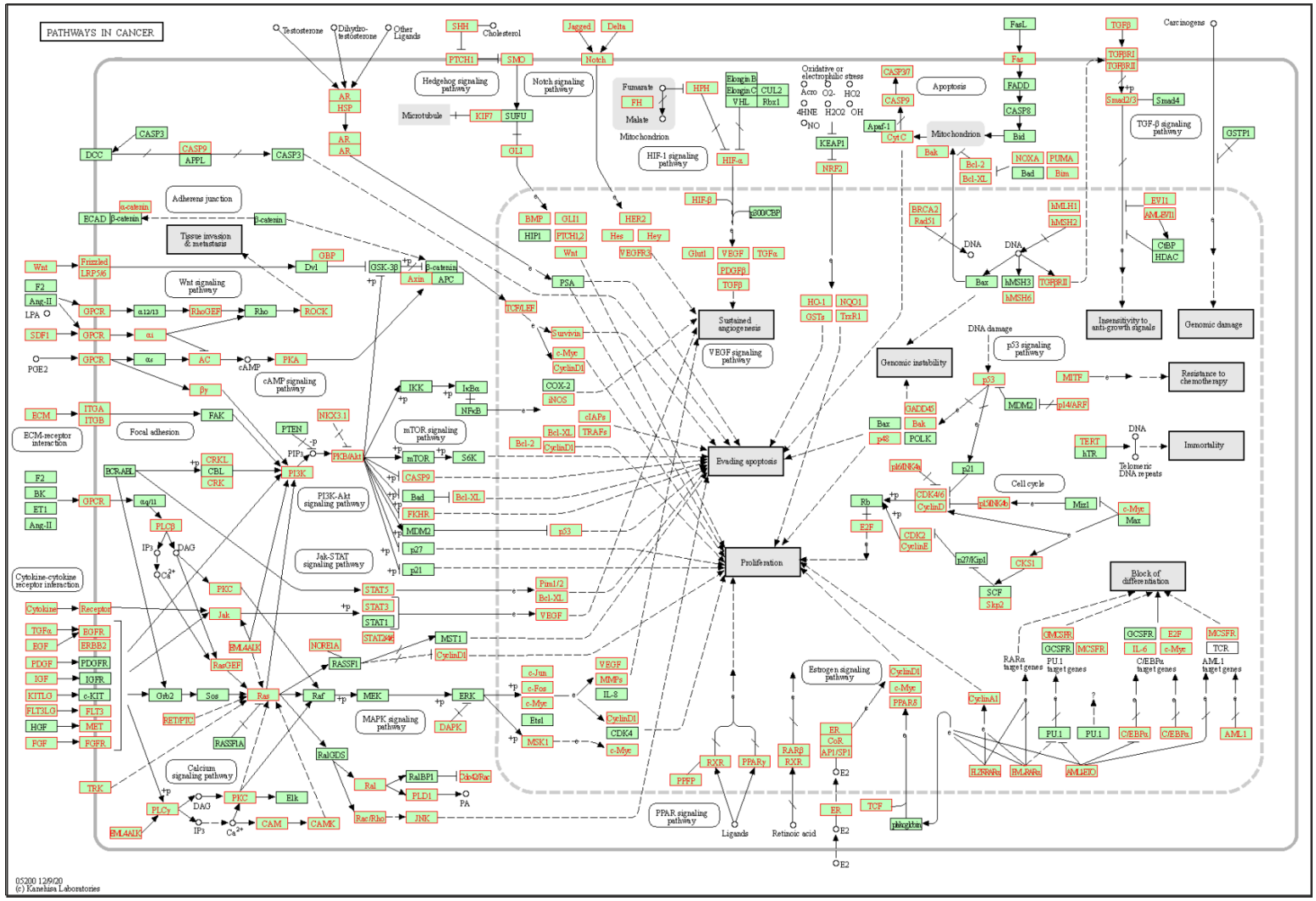


**Figure 6.8 Pathways in cancer KEGG pathway with commonly differentially expressed genes in scrambled control and *CBLL1*-depleted MCF7 and T47D cells in response to estrogen.**

Pathways in cancer KEGG pathway with significantly differentially expressed genes in response to $\beta E_2$ treatment in both scrambled control and *CBLL1*-depleted MCF7 and T47D cells highlighted in red.

### 6.2.4 Effect of siRNA depletion of *CBLL1* on differential gene expression in basal and estrogen-treated T-47D cells

To gain further understanding of the impact of siRNA-mediated functional depletion of *CBLL1* on the estrogen-regulated transcriptome, RNA-Seq analysis was also carried out in T-47D cells. Significant DEGs were identified based on a fold change (FC) of ≥1.5 or ≤-1.5 and a false discovery rate (FDR) of <0.05.

In scrambled control T-47D cells 3888 genes were found to be estrogen-regulated, with 1963 genes (including the estrogen-regulated gene *TFF1/PS2*) induced by $\beta E_2$ treatment, and 1925 genes downregulated by $\beta E_2$ (**Figure 6.9A** and **Figure 6.10A**). Where *CBLL1* was depleted, 4033 estrogen-regulated genes were identified, with 1898 genes (including *TFF1/PS2*) induced by $\beta E_2$ treatment and 2135 genes downregulated by $\beta E_2$ in the absence of *CBLL1* (**Figure 6.9D** and **Figure 6.10A**).

Functional depletion of *CBLL1* in vehicle-treated cells resulted in the significant differential expression of 819 genes, of which 253 were induced by *CBLL1* and 566 were downregulated by *CBLL1* (including *AMH*, *EIF4A1*, *INHA* and *MYC*) (**Figure 6.9B**). In the presence of $\beta E_2$, depletion of *CBLL1* resulted in just 167 genes being differentially expressed, with 97 induced by $\beta E_2$ and 70 downregulated by $\beta E_2$ in the absence of *CBLL1* (**Figure 6.9C**).

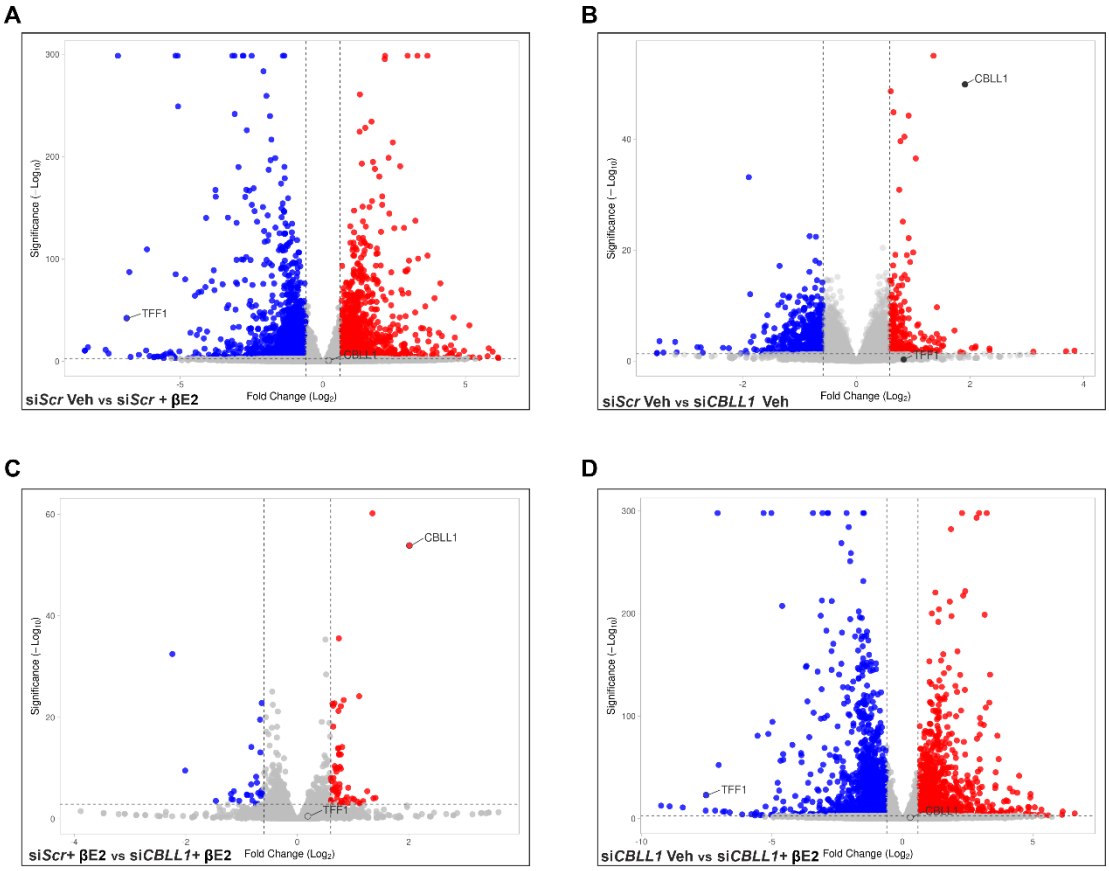


**Figure 6.9 Differential gene expression in T-47D cells in response to siRNA-mediated *CBLL1* knockdown and $\beta E_2$ treatment**

Differential gene expression was analysed following RNA-Seq of T-47D cells subjected to siRNA-mediated knockdown of *CBLL1* and subsequent treatment for 72 hours with vehicle or $\beta E_2$. (**A**) Differential gene expression compared between scrambled control cells treated with vehicle or $\beta E_2$ (n=3). (**B**) Differential gene expression compared between vehicle-treated scrambled control and *CBLL1*-depleted cells (n=3). (**C**) Differential gene expression compared between $\beta E_2$-treated scrambled control and *CBLL1*-depleted cells (n=3). (**D**) Differential gene expression compared between *CBLL1*-depleted cells treated with vehicle or $\beta E_2$ (n=3). Genes with significantly higher expression in the first condition listed on each plot are highlighted in red, genes with significantly lower expression in the first condition are highlighted in blue. Genes without any significant differential expression between the two listed conditions are marked in grey. Significant gene expression= FC ± 1.5 and FDR <0.05. Veh= Vehicle.

Of the 5052 DEGs identified across all four experiment conditions in T-47D cells, 20.2% were found to be *CBLL1*-dependent and estrogen-regulated, with 23.0% only estrogen-regulated in the absence of *CBLL1* (**Figure 6.10A**). The remaining 56.8% of DEGs were found to be estrogen-regulated independent of *CBLL1* expression (**Figure 6.10A**). This is in comparison with MCF7 cells, where 42.6% of estrogen-regulated DEGs were dependent on *CBLL1* expression, 10.1% were dependent on *CBLL1* depletion, and 47.3% were estrogen-regulated regardless of *CBLL1* expression (**Figure 6.6A**).

Following DEG analysis, pathway analysis was carried out using WebGestalt to identify significantly enriched KEGG pathways (Liao et al., 2019). KEGG pathway analysis revealed 12 significantly enriched pathways associated with the DEGs identified following $\beta E_2$ treatment in scrambled control T-47D cells (**Figure 6.10B** and **Appendix 24**) and 14 significantly enriched pathways following $\beta E_2$ treatment in *CBLL1*-depleted T-47D cells (**Figure 6.10B** and **Appendix 25**). Interestingly, 62.5% of these pathways were common to both the vehicle- or $\beta E_2$-treated scrambled control and *CBLL1*-depleted cells, and, consistent with the findings in MCF7 cells, included pathways associated with cell cycle, DNA replication and repair, and cancer (**Appendix 24**, **Appendix 25** and **Appendix 26**). A number of cancer-specific pathways were also enriched, but only in -/+ $\beta E_2$-treated *CBLL1*-depleted T-47D cells. These included human T-cell leukaemia virus-1 infection (hsa05166), proteoglycans in cancer (hsa05205) and small cell lung cancer (hsa05222) (**Appendix 25**).

No significantly enriched pathways were associated with DEGs either in vehicle-treated scrambled control and *CBLL1*-depleted T-47D cells, or in $\beta E_2$-treated scrambled control and *CBLL1*-depleted T-47D cells (**Appendix 25**),

supporting the findings observed in MCF7 cells that suggest *CBLL1* is required for estrogen signalling in cell cycle and DNA repair mechanisms.

.

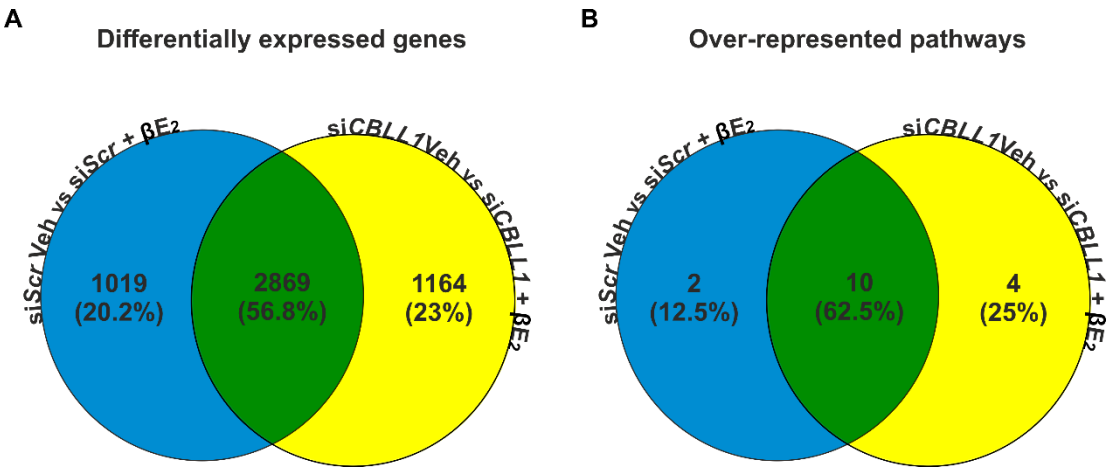


**Figure 6.10 Summary of differentially expressed genes and over-represented pathways in T-47D cells in response to siRNA-mediated *CBLL1* knockdown and $\beta E_2$ treatment**

Differential gene expression was analysed following RNA-Seq of T-47D cells subjected to siRNA-mediated knockdown of *CBLL1* and subsequent treatment for 72 hours with vehicle or $\beta E_2$, followed by pathway analysis using WebGestalt (Liao et al., 2019). (**A**) Summary of DEGs across scrambled control and *CBLL1*-depleted cells treated with vehicle or $\beta E_2$ (n=3). (**B**) Summary of over-represented pathways across scrambled control and *CBLL1*-depleted cells treated with vehicle or $\beta E_2$ (n=3). Significant gene expression= FC ± 1.5 and FDR <0.05. Veh= Vehicle.

Further analysis revealed the ten most significantly enriched KEGG pathways associated with the identified DEGs in T-47D cells (

**Figure 6.11**). As with MCF7, these included pathways involved in cell cycle and cancer, however, strikingly, 80% of the most enriched pathways were common to both scrambled control and *CBLL1*-depleted T47D cells treated with vehicle or $\beta E_2$. These included the cell cycle (hsa04110), DNA replication (hsa03030), p53 signalling (hsa04115) and pathways in cancer (hsa05200) KEGG pathways (

**Figure 6.11A** and

**Figure 6.11B**), further supporting the role of *CBLL1* in cell cycle and carcinogenesis.

It should be noted that despite the high degree of commonality in terms of the enriched pathways associated with DEGs in both MCF7 and T-47D cells, the DEGs within those pathways do differ between cell lines. For example, the pathways in cancer KEGG pathway is enriched in both MCF7 and T-47D, however it is only in T-47D cells that *CBLL1* is demonstrated to regulate *ESR1* expression in this pathway.

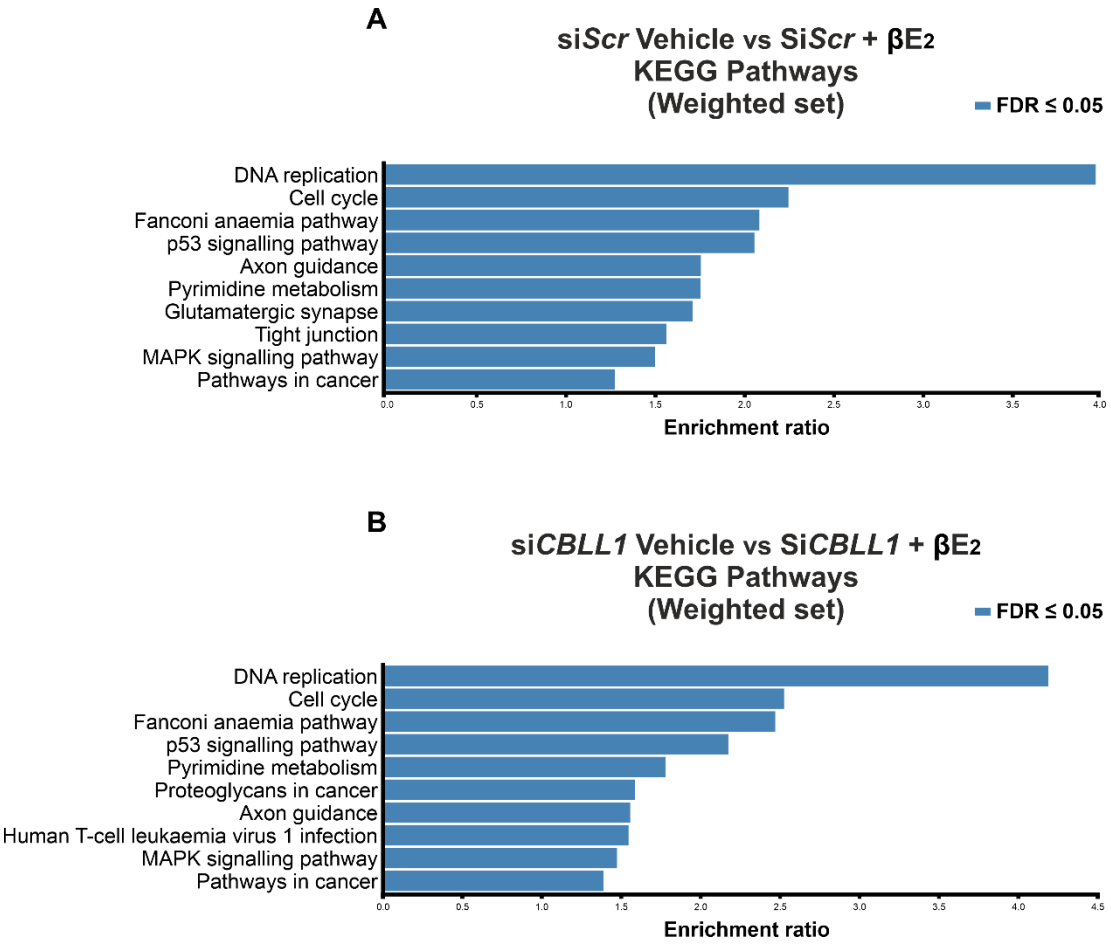


**Figure 6.11 Ten most significantly enriched KEGG pathways in T-47D cells in response to siRNA-mediated *CBLL1* knockdown and $\beta E_2$ treatment**

Pathway analysis using WebGestalt (Liao et al., 2019) was carried out following differential gene expression analysis of RNA-Seq of T-47D cells subjected to siRNA-mediated knockdown of *CBLL1* and subsequent treatment for 72 hours with vehicle or $\beta E_2$. (**A**) Weighted set of significantly enriched KEGG pathways associated with DEGs in scrambled control cells treated with vehicle or $\beta E_2$ (n=3). (**B**) Weighted set of significantly enriched KEGG pathways associated with DEGs in *CBLL1*-depleted cells treated with vehicle or $\beta E_2$ (n=3).

Comparisons between DEGs in the MCF7 and T-47D cell lines showed that of the 6974 total number of genes that were differentially expressed, 755 of these were common to both cell lines and across all conditions (**Appendix 27**). In scrambled control cells, 3583 DEGs were upregulated by estrogen treatment in MCF7, and 3888 in T-47D cells, of which 27.6% DEGs were common to both cell lines and thus *CBLL1*-dependent and estrogen-regulated. Downregulation occurred in response to estrogen in 5082 DEGs in scrambled control MCF7 cells and in 1925 DEGs in T-47D cells, of which 25.2% were common to both cell lines (**Appendix 27**). In *CBLL1*-depleted cells, 2290 DEGs were upregulated by estrogen treatment in MCF7, and 1898 in T-47D cells, of which 43.1% DEGs were common to both cell lines. Downregulation occurred in response to estrogen in 3242 DEGs in *CBLL1*-depleted MCF7 cells and in 2135 DEGs in T-47D cells, of which just 4.0% were common to both cell lines (**Appendix 27**). These DEGs were therefore estrogen-regulated only in the absence of *CBLL1* expression.

Of the 41 significantly enriched pathways associated with DEGs in scrambled control MCF7 cells -/+ $\beta E_2$, 7 (17.1%) were common to T-47D cells (**Appendix 21** and **Appendix 24**). Notably these included a number of key pathways linked to carcinogenesis, including cell cycle (hsa04110), DNA replication (hsa03030), Fanconi anaemia pathway (associated with DNA damage repair; hsa03460), and pathways in cancer (hsa05200). Similarly, of the 42 significantly enriched pathways associated with DEGs in *CBLL1*-depleted MCF7 cells treated with vehicle or $\beta E_2$, nine (21.4%) were common to T-47D cells (**Appendix 22** and **Appendix 25**). Again, these included the same key

carcinogenesis pathways as listed above, as well as the p53 signalling (hsa04115).

The significant number of genes dependent on *CBLL1* for estrogen regulation, together with their association with cancer-related pathways, suggest an essential role for CBLL1 in BCa cells.

### 6.2.5 Effect of siRNA depletion of *CBLL1* on alternative splicing in basal and estrogen-treated MCF7 and T-47D cells

Given the previously reported association between $m^6A$ and alternative splicing, the effect of *CBLL1* knockdown on alternative splicing in both vehicle- and $\beta E_2$-treated MCF7 and T-47D cells was investigated.

The five classes of alternative splicing analysed comprised A5SS, MXE, RI, SE, and A3SS. Differential splicing events were sorted by difference in percentage spliced in (dPSI ≥5%) and FDR (<0.05) to give the total number of significant splicing events (**Figure 6.12**). Both differentially spliced transcripts (DSTs) and differentially spliced genes (DSGs) were assessed.

In MCF7 cells the greatest number of total alternative splice events were seen between states of vehicle and estrogen treatment in both scrambled control cells (n=4185 DSTs, n=2948 DSGs; **Figure 6.12A**) and *CBLL1*-depleted cells (n=5486 DSTs, n=3658 DSGs; **Figure 6.12D**). Conversely, only ~half the number of significant alternative splice events were observed following *CBLL1* knockdown in both vehicle-treated (n=2423 DSTs, n=1916 DSGs; **Figure 6.12B**) and $\beta E_2$-treated (n=2667 DSTs, n=2040 DSGs; **Figure 6.12C**) MCF7 cells. The most frequent alternative splicing event observed across all conditions was SE, particularly in response to $\beta E_2$ treatment (**Figure 6.12A** and **Figure 6.12D**). The second most frequently observed event type was MXE

across all conditions (**Figure 6.12**). The significantly reduced number of alternative splicing events in response to *CBLL1* depletion suggests a key role for CBLL1 in splicing orchestration.

KEGG pathway analysis of DSGs in MCF7 cells revealed a relatively small number of significantly enriched pathways when compared with the number enriched due to DEGs. Across all conditions, 16 pathways were enriched (**Appendix 28**). In scrambled control cells -/+ $\beta E_2$ significantly enriched pathways were only found in association with DSGs with SE events. Of the seven enriched pathways identified, most notable were the central carbon metabolism in cancer (hsa05230) and adherens junction (hsa04520) pathways (**Appendix 28**). Eight significantly enriched pathways in *CBLL1*-depleted cells -/+ $\beta E_2$ were identified, including the ubiquitin-mediated proteolysis (hsa04120) and RNA transport (hsa03013) pathways (**Appendix 28**). Taken together these results support the previously reported findings of *CBLL1* being linked with E-cadherin expression.

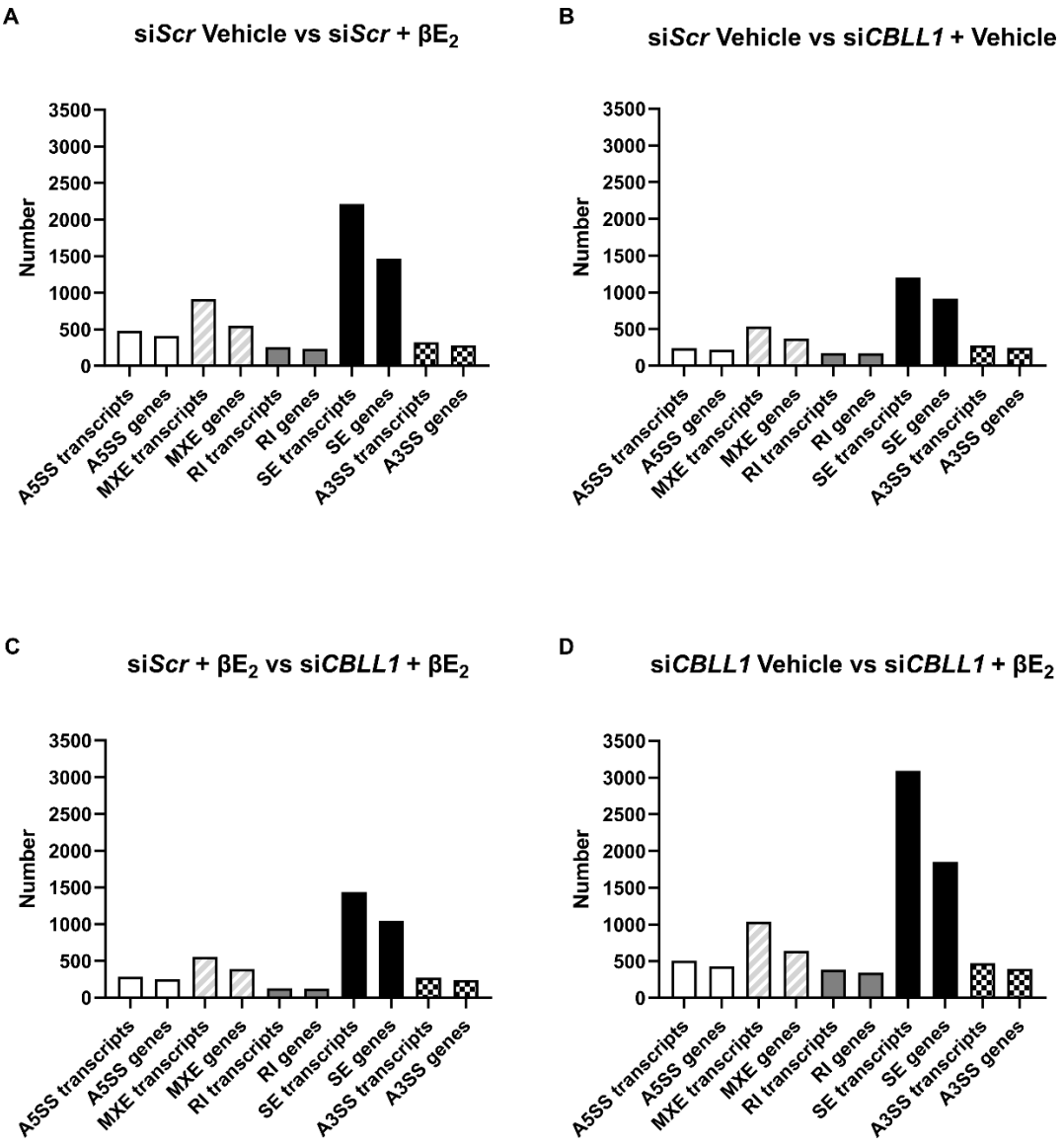


**Figure 6.12 Significant alternative splicing event types in MCF7 cells in response to siRNA-mediated *CBLL1* knockdown and $\beta E_2$ treatment**

Alternative splicing analysis using rMATS (Shen et al., 2014) was carried out following RNA-Seq of MCF7 cells subjected to siRNA-mediated knockdown of *CBLL1* and subsequent treatment for 72 hours with vehicle or $\beta E_2$. Differentially spliced transcript and differentially spliced gene numbers are shown for each alternative splicing event type. (**A**) Number of significant alternative splicing events compared between scrambled control cells treated with vehicle or $\beta E_2$ (n=3). (**B**) Number of significant alternative splicing events compared between vehicle-treated scrambled control and *CBLL1*-depleted cells (n=3). (**C**) Number of significant alternative splicing events compared between $\beta E_2$-treated scrambled control and *CBLL1*-depleted cells (n=3). (**D**) Number of significant

alternative splicing events compared between *CBLL1*-depleted cells treated with vehicle or $\beta E_2$ (n=3). Significant alternative splice event= dPSI ≥5% and FDR <0.05. A5SS= alternative 5' splice site (A5SS); MXE= mutually exclusive exon; RI= retained intron; SE= skipped exon; A3SS= alternative 3' splice site.

Estrogen and CBLL1-regulated alternative splicing events were less common in T-47D, but followed a similar trend as observed in MCF7 cells, with the greatest number of total alternative splicing events similarly seen between states of vehicle and estrogen treatment in both scrambled control cells (n=2622 DSTs, n=1961 DSGs; **Figure 6.13A**) and *CBLL1*-depleted cells (n=2937 DSTs, n=2186 DSGs; **Figure 6.13D**). Fewer alternative splicing events were observed in response to *CBLL1* knockdown in both vehicle-treated (n=2012 DSTs, n=1588 DSGs; **Figure 6.13B**) and $\beta E_2$-treated (n=1753 DSTs, n=1336 DSGs; **Figure 6.13C**) T-47D cells.

As in MCF7 cells, SE was also the most frequent alternative splicing event in all conditions in T-47D cells, particularly in response to $\beta E_2$ treatment (**Figure 6.13A** and **Figure 6.13D**), with MXE similarly the second most frequently observed event type across all conditions (**Figure 6.13**). In both MCF7 and T47D cells the overall profile of alternative splicing event types across all conditions and both cell lines was similar (**Figure 6.12** and **Figure 6.13**).

Unlike in MCF7 cells, KEGG pathway analysis of DSGs in T-47D cells revealed a similar number of significantly enriched pathways when compared with the number enriched due to DEGs. A total of 20 pathways were significantly enriched, all within *CBLL1*-depleted cells -/+ $\beta E_2$, 19 of which were associated with MXE events (**Appendix 29**). Notable significantly enriched cancer-related

pathways include the renal cell carcinoma (hsa05211), pancreatic cancer (hsa05212), colorectal cancer (hsa05210), proteoglycans in cancer (hsa05205), and the VEGF signalling pathway (hsa04370) (**Appendix 29**). Taken together these results may implicate an estrogen-regulated role for *CBLL1* in cancer and carcinogenesis.

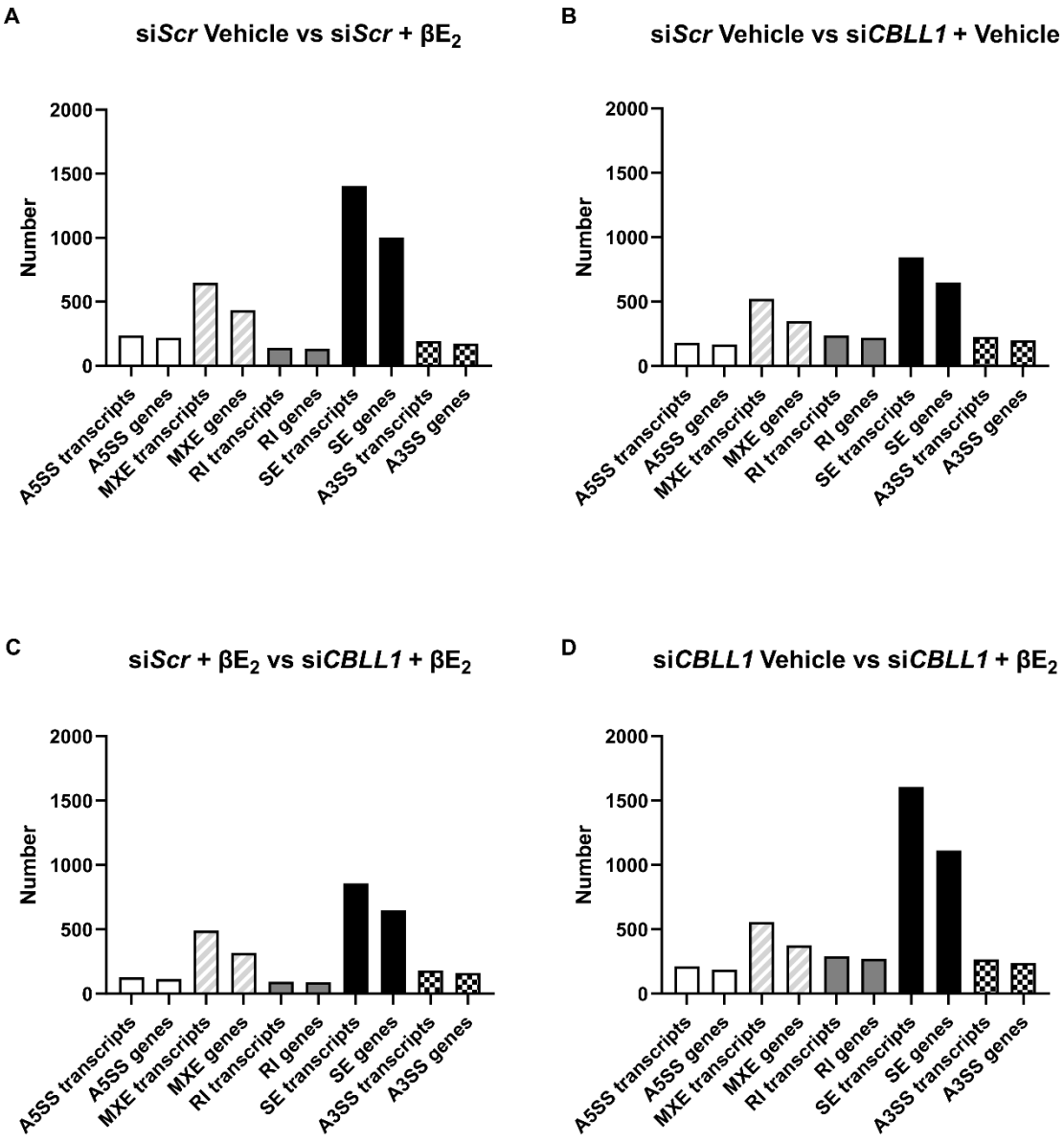


**Figure 6.13 Significant alternative splicing event types in T-47D cells in response to siRNA-mediated *CBLL1* knockdown and $\beta E_2$ treatment**

Alternative splicing analysis using rMATS (Shen et al., 2014) was carried out following RNA-Seq of T-47D cells subjected to siRNA-mediated knockdown of *CBLL1* and subsequent treatment for 72 hours with vehicle or $\beta E_2$. Differentially spliced transcript and differentially spliced gene numbers are shown for each alternative splicing event type. (**A**) Number of significant alternative splicing events compared between scrambled control cells treated with vehicle or $\beta E_2$ (n=3). (**B**) Number of significant alternative splicing events compared between vehicle-treated scrambled control and *CBLL1*-depleted cells (n=3). (**C**) Number of significant alternative splicing events compared between $\beta E_2$-treated

scrambled control and *CBLL1*-depleted cells (n=3). (**D**) Number of significant alternative splicing events compared between *CBLL1*-depleted cells treated with vehicle or $\beta E_2$ (n=3). Significant alternative splice event= dPSI ≥5% and FDR <0.05. A5SS= alternative 5' splice site (A5SS); MXE= mutually exclusive exon; RI= retained intron; SE= skipped exon; A3SS= alternative 3' splice site.

## 6.3 Discussion

The findings presented in chapter 5 suggested a role for CBLL1 in BCa, with the highest level of expression seen in BCa cells, and in particular ERα-expressing cells, compared with non-malignant mammary cells. These observations are consistent with other studies that have reported CBLL1 to be positively associated with oncogenic features in BCa (Liu et al., 2022b, Ma et al., 2023) and a number of other cancer types (Castosa et al., 2018, Hui et al., 2019, Liu et al., 2018b, Liu et al., 2018c).

With that in mind, siRNA-mediated depletion of *CBLL1* coupled with RNA-Seq was performed in the estrogen-sensitive MCF7 and T-47D cell lines to determine the function of *CBLL1* in the basal and estrogen-regulated transcriptome.

Consistent with results presented in Chapter 5, estrogen increased *CBLL1* expression and opposed *CBLL1* knockdown (**Figure 6.1A-D**, **Figure 6.2A** and **Figure 6.3A**). Estrogen treatment of basal MCF7 and T-47D cells similarly resulted in a moderate increase in CBLL1 protein expression (**Figure 5.8A**&**B**). *CBLL1* mRNA expression was, in contrast, reduced in basal MCF7 and unchanged in basal T-47D cells in response to estrogen treatment (**Figure 5.7A**&**B**). The only other study known to have studied *CBLL1* expression in MCF7 cells also found it to be reduced in response to estrogen treatment, however the T-47D cell line was not examined (Gong et al., 2010). It should be noted, however, that Gong and colleagues used a concentration of 100nM $\beta E_2$ over just 24 hours (Gong et al., 2010), whereas the current study used 10nM $\beta E_2$ over a 72 hour treatment period. Different $\beta E_2$ concentrations are known to elicit distinct biological effects *in vivo* (Strom et al., 2009). Indeed,

physiological $\beta E_2$ concentrations are reported to have a large range and fluctuate throughout the menstrual cycle and between pre- and post-menopausal women, (Celojevic et al., 2011). However 10nM, as employed here, is a widely used concentration to represent moderate physiological $\beta E_2$ levels (Ma et al., 2013, Pacheco-Velázquez et al., 2022).

The impact of *CBLL1* depletion on expression of E-cadherin, ERa and *PS2* was also examined. In MCF7 cells, expression of the E-cadherin-encoding gene *CDH1* was significantly reduced following *CBLL1* knockdown, but only in vehicle-treated cells (**Figure 6.2B**), with E-cadherin protein expression also appearing to be decreased (**Figure 6.1A**), however this did not reach statistical significance on quantification (**Figure 6.1E**). In T-47D cells, *CBLL1* knockdown resulted in no significant change in *CDH1* expression (**Figure 6.2B**), with a modest, yet significant, reduction in E-cadherin protein expression seen in estrogen-treated cells (**Figure 6.1B**&**D**). In contrast with other studies, which have reported that *CDH1* is downregulated by estrogen (Cardamone et al., 2009), in particular in ER-positive BCa cells (Oesterreich et al., 2003), no significant change in E-cadherin expression at either the mRNA or protein level was observed following estrogen treatment in MCF7 or T-47D cells .

No significant changes were detected in ERα protein expression following *CBLL1* knockdown in either MCF7 or T-47D cells (**Figure 6.1A**), although at the mRNA level, expression of *ESR1* (the ERα-encoding gene) was highest in vehicle-treated *CBLL1*-depleted MCF7 cells, which supports a role for CBLL1 in fine-tuning ERα expression (**Figure 6.2C**). In *PS2* (also known as *TFF1*), another estrogen-regulated gene, the same trend was observed, although this did not reach statistical significance (**Figure 6.2D**). In contrast, in T-47D, the

highest levels of *ESR1* expression were seen in both the estrogen-treated scrambled control and *CBLL1*-depleted cells, with expression also significantly higher in vehicle-treated *CBLL1*-depleted T-47D cells compared with scrambled control (**Figure 6.2C**). *PS2* expression was also significantly highest in the estrogen-treated cells, however the lowest level of expression was seen in *CBLL1*-depleted T-47D cells (**Figure 6.2D**). These findings may suggest that CBLL1 functions to inhibit *ESR1* expression in BCa, resulting in higher expression of *ESR1,* and therefore of *PS2*, when *CBLL1* is depleted. This hypothesis is consistent with another study that suggested that CBLL1 acts as a co-repressor of ERα (Gong et al., 2010).

Gong and colleagues reported that *CBLL1* overexpression in MCF7 cells reduced *PS2* expression (Gong et al., 2010). In this chapter it was found that knockdown of *CBLL1* had no significant effect on *PS2* expression in either vehicle- or estrogen- treated MCF7 cells (**Figure 6.2D**) but, interestingly, in contrast to previously reported findings (Gong et al., 2010), appeared to modestly reduce *PS2* expression in T-47D cells, significantly in vehicle-treated cells (**Figure 6.2D**). MCF7 and T-47D harbour many differences in cellular mechanisms which may explain the different findings between these cell lines, including that of reduced ERα expression in T47D (Radde et al., 2014). With that being said, it is interesting that in the current study, *ESR1* expression increased 5-fold in T-47D cells in response to estrogen, and only a maximum of 1.5-fold in MCF7 cells (**Figure 6.2C** and **Figure 6.3C**). This may reflect distinct mechanisms of ERα regulation in these two cells and the data presented here suggests a potential role for CBLL1 in this pathway.

Examination of the phenotypic effect of *CBLL1* depletion revealed, somewhat surprisingly, that no significant difference in proliferation was seen in T-47D cells (**Figure 6.4B**). In MCF7 cells, whilst no difference in cellular proliferation was observed with *CBLL1* knockdown in vehicle-treated cells, a modest, yet significant reduction in proliferation was seen in estrogen-treated cells (**Figure 6.4A**). This reduced proliferation seen with *CBLL1* knockdown in MCF7 is consistent with reports of higher CBLL1 expression being associated with pro-oncogenic phenotypes in BCa cells, including MCF7 (Liu et al., 2022b, Ma et al., 2023), and in a number of other cancer types (Liu et al., 2018b, Liu et al., 2018c, Castosa et al., 2018). It is in contrast, however, to another study that found increased CBLL1 expression in MCF7 cells was associated with reduced migration and an anti-proliferative role (Gong et al., 2010). No studies are known to have examined the effect of CBLL1 on cellular proliferation in T-47D cells.

RNA-Seq analysis of vehicle- and estrogen-treated MCF7 and T-47D scrambled control and *CBLL1*-depleted cells allowed analysis of the role of CBLL1 in the regulation of basal and estrogen-regulated gene expression in BCa. A total of 9640 DEGs was identified in MCF7 cells between conditions. Interestingly, 4108 *CBLL1*-dependent estrogen-regulated DEGs were found, including *PPL*, *TFEB* and *PTBP1*, which are highlighted here.

*PPL* was found to be downregulated following estrogen treatment and suppressed further with *CBLL1* knockdown. The *PPL* gene encodes the periplakin protein, a component of desmosomes in keratinocytes (DiColandrea et al., 2000), with a key role in cellular cytoskeleton homeostasis (Boczonadi and Määttä, 2012, Groot et al., 2004, Kazerounian and Aho, 2003).

Downregulated periplakin expression has been associated with carcinogenesis in a number of cancer types (Li et al., 2017c, Matsumoto et al., 2014, Otsubo et al., 2015), and has been implicated in brain metastasis in TNBC (Choi et al., 2013). As higher *CBLL1* expression was linked to higher *PPL* expression, this interaction may be one of the mechanisms that helps to explain why higher nuclear expression of CBLL1 was found to be an independent positive prognostic factor in our large cohort of BCa patients as described in chapter 5.

*TFEB* demonstrated the same expression pattern as *PPL,* downregulated with estrogen treatment and further suppressed with *CBLL1* knockdown. The *TFEB* gene encodes the transcription factor EB, a master regulator of several essential cellular processes, including autophagy, cellular energy metabolism, lysosome regulation, and immune response (Napolitano et al., 2018, Settembre et al., 2011, Settembre et al., 2012, Zhang et al., 2022b). Given its critical role in autophagy-lysosomal biogenesis, altered *TFEB* expression has been associated with a wide range of diseases as a result of accumulation of undegraded substances (Tan et al., 2022). These include neurodegenerative diseases such as Alzheimer's and Parkinson's (Dehay et al., 2010, Polito et al., 2014), lysosomal storage disorders (Song et al., 2013, Spampanato et al., 2013), as well as many types of cancer (Giatromanolaki et al., 2015, Klein et al., 2016, Liang et al., 2018, Sakamoto et al., 2018). In early stage BCa, high TFEB expression has been associated with a poorer prognosis in patients (Giatromanolaki et al., 2017), although another study found that increased TFEB expression reduced breast tumour development through modulation of tumour-associated macrophages, and concluded that TFEB activation represented a promising therapeutic target (Li et al., 2020b). Higher *CBLL1*

expression was linked to higher *TFEB* expression in MCF7 cells, a model of early-stage BCa. It would be interesting in future work to analyse the relationship between *CBLL1* and *TFEB* expression in cell lines representative of later stage and more aggressive tumours and therefore see whether our data support the findings of Giatromanolaki and colleagues or Li and colleagues.

*PTBP1* was found to be induced by estrogen treatment in a *CBLL1*-dependent manner. The *PTBP1* gene encodes the polypyrimidine tract binding protein 1 associated with the polypyrimidine tract-binding protein (PTB)-associated splicing factor (also known as PSF). As discussed earlier in this chapter CBLL1 has been demonstrated to interact with PSF in the nucleus, potentially impacting upon PSF's crucial role in binding RNA and its regulation of transcription and pre-mRNA splicing (Figueroa et al., 2009a, Figueroa et al., 2009b, Patton et al., 1993, Shav-Tal and Zipori, 2002). PTB is a member of the heterogeneous nuclear ribonucleoprotein (hnRNP) family that influences pre-mRNA alternative splicing, as well as mRNA metabolism and transport (Dai et al., 2022, Lin and Patton, 1995, Patton et al., 1991). Upregulated PTB expression has been reported in a number of cancer types (Barbagallo et al., 2018, Jiang et al., 2017, Takahashi et al., 2015, Xie et al., 2019, Zhang et al., 2020c). In BCa, PTB has been associated with carcinogenesis and contributing to the Warburg effect, with *PTBP1* depletion suggested as a target for therapy (He et al., 2014, Wang et al., 2018). As higher *PTBP1* expression was seen following estrogen treatment only when *CBLL1* expression was maintained (in scrambled control cells), this interaction could be linked to the observations of

higher CBLL1 expression in estrogen-sensitive BCa cell lines compared with non-malignant cells (as described in chapter 5).

A total of 975 DEGS were found to be estrogen-regulated but repressed by *CBLL1*. Of note is *PGR* which encodes the progesterone receptor (PR) which in turn mediates the physiological effects of progesterone, and is a master regulator of developmental processes in female reproductive tissues, also controlling the menstrual cycle and pregnancy (Grimm et al., 2016, Obr and Edwards, 2012). Progesterone signalling is vital for mammary gland development, both during puberty and pregnancy, and for epithelial proliferation in adulthood (Graham and Clarke, 1997, Grimm et al., 2016, Lydon et al., 1995). An increase in progesterone signalling and subsequent proliferation of PR positive breast cells is associated with increased risk of developing BCa (Khan et al., 1994, Lawson et al., 2002, Shoker et al., 1999). Indeed, it has been shown that *BRCA1* deletion in mice leads to PR overexpression in the mammary gland and hyperproliferation in response to progesterone, and moreover that the development of tumours in such cases is dependent on PR (Ma et al., 2006, Poole et al., 2006). However, whilst an initial increase in proliferation is seen in BCa cells in response to progesterone, its long-term effect is to inhibit proliferation (Groshong et al., 1997, Skildum et al., 2005). That being said, although the proliferative effects of progesterone are well documented, together with its attendant risk for BCa development, once BCa has developed the presence of PR is an independent positive prognostic factor, associated with a less invasive tumour phenotype and improved survival (Bardou et al., 2003, Grimm et al., 2016). In chapter 5 it was reported that higher nuclear CBLL1 expression was associated with PR positive status in

BCa patients. The fact that the absence of *CBLL1* results in differential expression of *PGR* suggests a role for CBLL1 in carcinogenesis and disease progression in BCa.

A further 4557 genes were differentially expressed under the influence of estrogen but independently of *CBLL1*. These included *METTL3*, *HI9*, *BRCA1*, *BRCA2*, *INHA* and *TFF1*. *METTL3* encodes the catalytic subunit of the $m^6A$ methyltransferase complex and its expression has been found to be upregulated in BCa (Hu et al., 2022, Wang et al., 2020a). Whilst estrogen regulation of *METTL3* expression doesn't appear to have been reported in the literature, our research group has recently determined that *METTL3* expression is estrogen-regulated in BCa cells (AH thesis), consistent with the results presented here.

*H19* encodes a long non-coding RNA that functions as a tumour suppressor in many cancer types (Hao et al., 1993, Yoshimizu et al., 2008). Inactivation of *H19* has been reported in Wilms' tumour samples (Moulton et al., 1994, Steenman et al., 1994). Interestingly, *WTAP* (another component of the $m^6A$ methyltransferase complex) was originally discovered in partnership with the Wilms' tumour suppressor gene (*WT1*) (Little et al., 2000), where it was found to regulate cell proliferation and quiescence (Penalva et al., 2000, Small et al., 2007). However, interestingly, *H19* has been reported to show no tumour suppressor effect in some tumour types, potentially acting as an oncogene in some cancers (Ariel et al., 1995, Lustig-Yariv et al., 1997).

*BRCA1* and *BRCA2* encode tumour suppressor proteins, and their mutation is significantly associated with increased susceptibility to BCa, as well as many other cancer types (Brohet et al., 2014, Miki et al., 1994, Wooster et al., 1995,

Yoshida and Miki, 2004). Consistent with the results presented in this chapter, *BRCA1* is widely reported to be estrogen-regulated, with *BRCA1* promoter activity directly stimulated by estradiol (Hilakivi-Clarke, 2000, Seery et al., 1999, Werner, 2022). Likewise, this chapter's results accord with the literature, that *BRCA2* too is induced by estrogen (Suba, 2014, Suba, 2015). However, whilst no direct relationship was observed at the level of gene expression, it is interesting that IHC analysis in chapter 5 revealed a significant positive correlation between BRCA1 and BRCA2 protein expression with both nuclear and cytoplasmic CBLL1 (**Table 5.1**).

*INHA* encodes a member of the transforming growth factor-beta (TGF-beta) protein superfamily, a preproprotein which generates multiple products, including the alpha subunit of the inhibin α and β protein complexes (Ball et al., 2004). Inhibins have a diverse range of regulatory functions, including inhibition of secretion of a number of hormones, including those from the hypothalamus, pituitary gland, and gonads (Rivier et al., 1985, Seachrist and Keri, 2019). Inhibin α subunit expression has been demonstrated to decrease in BCa compared with normal breast tissue or DCIS, becoming undetectable as BCa progresses (Di Loreto et al., 1999, Mylonas et al., 2005). Our finding that *INHA* appears to be repressed by estrogen accords with other studies, who found *INHA* expression was negatively regulated by estrogen (Billiar et al., 2003, Drummond and Fuller, 2012).

*TFF1* (also known as *PS2*) encoding trefoil factor 1 is a secretory protein expressed in the gastric mucosa (Rio et al., 1988), however it is also expressed in a number of tumours (Welter et al., 1994). Its alias, BCEI (breast cancer estrogen-inducible protein), is appropriately descriptive, given how its

expression has been associated with BCa (Welter et al., 1994, Xue et al., 2022). In accordance with the findings presented in this chapter, *TFF1* is known to be induced by estrogen (Jakowlew et al., 1984, Masiakowski et al., 1982).

WebGestalt analysis of significantly enriched KEGG pathways (Liao et al., 2019) in MCF7 identified 41 pathways associated with estrogen-regulated, *CBLL1*-induced DEGs, and 42 associated with estrogen-regulated, *CBLL1*-repressed DEGs (**Figure 6.6B**, **Appendix 21**, **Appendix 22** and **Appendix 23**). A large number of enriched KEGG pathways related to DEGs were found to be related to several key groups, notably DNA replication and repair (DNA replication, p53 signalling, mismatch repair, homologous recombination, Fanconi anaemia pathway), nucleotide metabolism (purine metabolism, pyrimidine metabolism), cellular adhesion (cell adhesion molecules, focal adhesion, gap junction), cell cycle and fate (cell cycle, cellular senescence), as well as cancer-specific (pathways in cancer, basal cell carcinoma, small cell lung cancer, gastric cancer, hepatocellular carcinoma, colorectal cancer, proteoglycans in cancer). Almost half (43.1%) of all enriched pathways were common to both scrambled control and *CBLL1*-depleted MCF7 cells treated with vehicle or $\beta E_2$. Interestingly, all the cell fate pathways were enriched both in the presence and absence of *CBLL1* knockdown, suggesting a *CBLL1*-independent estrogen regulation of cell cycle and senescence in BCa.

Whilst the majority of DNA replication and repair pathways were enriched across both scrambled control and *CBLL1*-depleted cells, the p53 signalling pathway was enriched by estrogen only when *CBLL1* was knocked down. The p53 protein is encoded by the *TP53* gene, a well-characterised tumour suppressor gene that mediates cell cycle arrest, senescence, apoptosis and

DNA damage response (Toledo and Wahl, 2006), with loss of expression associated with significantly increased cancer risk (Vousden and Lane, 2007). Enrichment of the p53 signalling pathway associated with DEGs reported in this chapter is consistent with other findings in our research group, which found *METTL3* functional depletion in PCa cells also influenced p53 signalling (DH thesis), and with another study which reported DEGs and DSGs within the p53 signalling pathway in response to *METTL3* knockdown (Dominissini et al., 2012). The fact that p53 signalling is only altered when *CBLL1* is depleted implicates a role for CBLL1 in maintaining normal p53 signalling. This potential effect of CBLL1 on p53 signalling may be a contributing factor to the findings reported in chapter 5, where nuclear CBLL1 expression was found to be an independent positive prognostic indicator.

Additionally, the TGF-beta signalling pathway was enriched by estrogen only when *CBLL1* was depleted. The TGF-beta pathway has a prominent role in regulating cell growth and differentiation and has been widely reported to be essential for tumour progression (Pickup et al., 2013). The role of TGF-beta is complex in cancer as in the early stages of tumourigenesis it functions as a tumour suppressor by inhibiting cell growth, however in later stages it promotes cancer progression through initiating EMT, increased invasion, and metastasis, particularly to the bones in BCa (Fournier et al., 2015, Pickup et al., 2013, Yin et al., 1999).

Exclusively in *CBLL1* knockdown cells, significant enrichment of four cancer-specific pathways was also seen: colorectal cancer (CRC), hepatocellular carcinoma (HCC), small cell lung cancer (SCLC) and gastric cancer (GC). Common mechanisms of action have been reported in carcinogenesis between

BCa and CRC (Cai et al., 2020), BCa and HCC (Jia et al., 2021), BCa and SCLC (Wang et al., 2022b) and BCa and GC (Hansford et al., 2015). Likewise, the platinum drug resistance pathway was enriched in with estrogen treatment only in *CBLL1*-depleted cells. Platinum-based drugs are a part of common chemotherapy protocols in BCa, particularly TNBC, and the development of resistance to these compounds inevitably leads to poorer patient outcomes (Lin et al., 2022, Yu et al., 2020).

Taken together, these findings support a role for CBLL1 in BCa and, as with p53, demonstrate that these carcinogenic pathways are usually repressed by the presence of CBLL1, again suggesting a possible protective effect of CBLL1 in BCa.

Two significantly enriched pathways were observed exclusively in scrambled control cells treated with vehicle or $\beta E_2$. It is interesting that the cell adhesion molecules pathway, which contains the cadherin proteins, was enriched, despite *CDH1* not being significantly differentially expressed. This suggests that *CBLL1* has effects on cellular adhesion outside of its reported role in E-cadherin degradation.

The second messenger 3'-5'-cyclic adenosine monophosphate (cAMP) plays a key role in a wide range of vital cellular process including energy metabolism, steroidogenesis and immune function, where it is reported to have an overall anti-inflammatory action (Gerlo et al., 2011, McKnight, 1991, Serezani et al., 2008, Tasken and Ruppelt, 2006). Upregulated intracellular cAMP expression has been reported to inhibit cellular proliferation via apoptosis induction or cell cycle arrest in a wide variety of cancer types including BCa (Cho-Chung et al., 1981, Kim et al., 2001, Santore et al., 2002). However, there are some

conflicting studies in the literature, that have found cAMP expression in cancer to be associated with poorer outcomes. For example, cAMP expression has been observed to promote NEPC development in PCa (Bang et al., 1994, Burchardt et al., 1999), a feature of PCa progression (Abrahamsson et al., 1989). Moreover, in one study it was found that cAMP is an independent negative prognostic factor in early stage BCa (Miller et al., 1990). The findings reported in the current study concur with other reports that cAMP signalling is modulated by the $m^6A$ mRNA modification in solid tumours (Huang et al., 2020). As the cAMP signalling pathway was only enriched by estrogen in the presence of *CBLL1,* this suggests a role for *CBLL1* for maintaining normal cAMP signalling in BCa.

As no significantly enriched pathways were associated with DEGs following *CBLL1* knockdown in either vehicle- or estrogen-treated MCF7 cells (**Appendix 22**), this suggests that *CBLL1* plays a role in estrogen signalling in cell cycle, DNA repair and carcinogenesis mechanisms.

RNA-Seq analysis of *CBLL1* knockdown in T-47D cells identified a total of 5052 DEGs between all conditions. Interestingly, 1019 *CBLL1*-dependent estrogen-regulated DEGs were found, including *AMH* and *PTBP1*.

*AMH* encodes anti-Mullerian hormone, a ligand of the TGF-beta protein superfamily (Pepinsky et al., 1988, Peregrin-Alvarez et al., 2021). Once bound to TGF-beta receptors, AMH activates a number of transcription factors that regulate gene expression (Howard et al., 2022). AMH plays a key role in regulating a number of reproductive functions, including embryonic sex organ development and follicular development in adult females (Cate et al., 1986). It has been reported that AMH can inhibit tumour growth in Mullerian duct-related

tissues, including the ovary and endometrium (Cate et al., 1986, Donahoe et al., 1981, Fuller et al., 1985). AMH has more recently been demonstrated to inhibit *BRCA1* expression in the ovarian cortex of mice, although the authors suggested a beneficial effect of AMH by suppressing expression of *BRCA1* in women with mutation(s) in this gene (Peregrin-Alvarez et al., 2021). In the current study it was found that *AMH* expression was induced by estrogen in the presence of *CBLL1*, but was also induced by *CBLL1* knockdown, however, interestingly, once *CBLL1* was depleted, estrogen could no longer stimulate expression. These data may suggest a potential role for *CBLL1* in estrogen-regulated *AMH* expression and thus, ultimately, on *BRCA1* expression. This may be one explanation for the significant correlation between CBLL1 and BRCA1 protein expression in the BCa patient samples reported in chapter 5.

The identical finding in T-47D and in MCF7, that expression of the purported oncogene *PTBP1* (Barbagallo et al., 2018, Takahashi et al., 2015, Xie et al., 2019) is induced by estrogen treatment and is *CBLL1*-dependent, further supports the hypothesis that this association could be linked to the observations of higher CBLL1 expression in estrogen-sensitive BCa cell lines compared with non-malignant breast cells (as described in chapter 5).

*CBLL1* was found to induce expression of 566 genes independent of estrogen in T-47D cells. In particular, expression of *EIF4A1* and *MYC* were downregulated with *CBLL1* depletion. *EIF4A1* encodes eukaryotic translation initiation factor 4A, a RNA helicase forming part of the EIF4F complex involved in mRNA ribosomal binding and regulating translation initiation (Gingras et al., 1999). EIF4A1 has been demonstrated to support an oncogenic translation program in a number of different cancer types (Chan et al., 2019, Wolfe et al.,

2014, Wang et al., 2022a). In BCa it has been demonstrated to be an independent negative prognostic indicator in patients with ER negative tumours (Modelska et al., 2015) and has been implicated in chemotherapy resistance in TNBC (Sridharan et al., 2019). Interestingly, *EIF4A1* has been reported to interact with *MYC* (Howard et al., 2020), a proto-oncogene encoding a nuclear phosphoprotein that regulates transcription and plays a vital role in the cell cycle, apoptosis and cellular transformation (Beaulieu et al., 2020). Indeed, the key carcinogenic functions of the EIF4F complex are reported to be mediated through a number of EIF4F-dependent oncogenic mRNAs, including *MYC* (Graff et al., 2007, Howard et al., 2020). The EIF4F complex and MYC operate in a positive feedback loop with one another, with MYC expression regulated by EIF4F, and MYC in turn transcriptionally regulating components of the EIF4F complex (Lin et al., 2008, Polunovsky et al., 1996, Ruggero et al., 2004), including EIF4A1 (Howard et al., 2020). Moreover, therapeutic inhibition of MYC is known to result in decreased EIF4A1 expression (Howard et al., 2020).

Overexpression or structural alteration of *MYC* is believed to be present in over 70% of human cancer types (Dang, 2012, Meyer and Penn, 2008), with increasingly aggressive tumour phenotypes generally seen with increasing expression (Dang, 2012, Schaub et al., 2018). *MYC* amplification is seen in ~30% of all breast tumours (Schaub et al., 2018, Vita and Henriksson, 2006), although this increases up to 44% in cases of TNBC (AlSultan et al., 2021). Inhibition of *MYC* results in decreased cell growth and increased apoptosis in BCa cells, and inhibited tumour growth and increased survival in mouse BCa models (AlSultan et al., 2021, Castell et al., 2022).

The fact that *CBLL1* induces expression of *EIF4A1* and *MYC* in T-47D cells may explain the oncogenic findings presented in chapter 5, whereby *CBLL1* expression was found to be significantly associated with poorer outcomes in some BCa patient cohorts and significantly higher in BCa cells compared with non-malignant breast cells. Likewise, in our own large BCa patient cohort, high cytoplasmic expression of CBLL1 protein was associated with poorer prognostic factors. However, in contrast, nuclear CBLL1 expression was found to be an independent positive prognostic factor, suggesting more complex mechanisms of action for CBLL1 in breast carcinogenesis.

Interestingly, and consistent with MCF7, the largest proportion of DEGs in T-47D were those that were differentially expressed under the influence of estrogen but independently of *CBLL1* (n=2869). As in MCF7, this group included, most notably, the tumour suppressor genes essential for DNA repair, *BRCA1* and *BRCA2* (Brohet et al., 2014, Miki et al., 1994, Venkitaraman, 2002, Wooster et al., 1995).

Unlike in MCF7, *METTL3* was not significantly differentially expressed in T-47D cells. Of further note is that none of the other components of the $m^6A$ methyltransferase complex (including *METTL14, WTAP* and *VIRMA*), nor the $m^6A$ demethylases *FTO* and *ALKBH5*, or indeed, the E-cadherin encoding gene *CDH1*, were significantly differentially expressed in any condition in either MCF7 or T-47D cells. Nolan and colleagues recently reported a number of key genes most often mutated in BCa: *PIK3CA*, *GATA3*, *MAP3K1* and, interestingly, *CDH1* (Nolan et al., 2023). Analysis of our RNA-Seq data found that none of these genes were differentially expressed in any condition in either MCF7 or T-47D cells.

WebGestalt analysis of significantly enriched KEGG pathways (Liao et al., 2019) in T-47D identified 12 pathways associated with estrogen-regulated, CBLL1-induced DEGs, and 14 associated with estrogen-regulated, CBLL1-repressed DEGs (**Figure 6.10B**, **Appendix 24**, **Appendix 25** and **Appendix 26**). As in MCF7, the majority of the enriched KEGG pathways related to DEGs in T-47D cells could be grouped, most notably as pathways of DNA replication and repair (DNA replication, p53 signalling, mismatch repair, homologous recombination, Fanconi anaemia pathway, base excision repair), nucleotide metabolism (pyrimidine metabolism), cell cycle (cell cycle), as well as cancer-specific (pathways in cancer, small cell lung cancer, proteoglycans in cancer). An even greater proportion (62.5%) of enriched pathways were common to both scrambled control and *CBLL1*-depleted T-47D cells treated with vehicle or $\beta E_2$ than in MCF7 cells. Interestingly, all the cell cycle and pyrimidine metabolism pathways were enriched both in the presence and absence of *CBLL1* knockdown, suggesting estrogen regulation of cell cycle and nucleotide metabolism in BCa is *CBLL1*-independent.

A large proportion of the enriched pathways associated with DEGs were common in both MCF7 and T-47D cells, however some distinct DEGs within those pathways were found between cell lines. For example, in the enriched pathways in cancer KEGG pathway in both MCF7 and T-47D cell lines, only in T-47D cells was it seen that *CBLL1* regulates *ESR1* expression. Whilst the BioGRID online tool has provided evidence that CBLL1 physically interacts with ERα (Oughtred et al., 2019), however this is now the first evidence that CBLL1 transcriptionally regulates *ESR1*.

As in MCF7, in T-47D cells the majority of DNA replication and repair pathways were enriched across both scrambled control and *CBLL1*-depleted cells, with just the mismatch repair pathway enriched by estrogen exclusively when *CBLL1* was knocked down. The mismatch repair pathway is a key component of the DNA damage repair system (Scarbrough et al., 2016), responsible for correcting single base pair mismatches and misaligned short nucleotide reads that can cause frameshift mutations (Jiang et al., 2020, Martin et al., 2009). Defects in expression of genes within the mismatch repair pathway are associated with the development of a number of cancer types (Hampel et al., 2005, Kandoth et al., 2013, Ruemmele et al., 2009), and germline sequencing of a number of key mismatch repair pathway genes is often carried out to detect impaired mismatch repair in patients (Le et al., 2017). Whilst altered mismatch repair does intuitively increase cancer risk, interestingly, it has also been demonstrated to increase the susceptibility of tumour cells to certain chemotherapeutic drugs, preventing them from repairing the DNA damage inflicted during treatment (Martin et al., 2009).

The other pathways enriched by estrogen in *CBLL1*-depleted T-47D cells treated with vehicle or $\beta E_2$ are both cancer-specific. The small cell lung cancer pathway was significantly enriched in this group of cells as it was in MCF7. Similarly, the proteoglycans in cancer pathway was also enriched in this cell group (it was enriched in both scrambled control and *CBLL1*-depleted MCF7 cells). Proteoglycans are macromolecules in the tumour microenvironment that regulate critical signalling pathways, and have been reported to contribute to tumour progression by influencing cellular proliferation, angiogenesis and metastasis in many cancer types (Mellai et al., 2020, Piperigkou et al., 2022,

Wade et al., 2013) including BCa (Insua-Rodríguez and Oskarsson, 2016, Karousou et al., 2014). Many studies have reported that higher expression of a number of proteoglycans in BCa is associated with poorer outcomes (Auvinen et al., 2014, Kischel et al., 2010, Leivonen et al., 2004, Okuda et al., 2012), although some of the small leucine-rich proteoglycans, namely decorin and lumican, have been reported to function as tumour suppressors (Neill et al., 2012, Troup et al., 2003). The proteoglycans pathway also includes genes encoding the PI3K:AKT network (*AKT3, ERBB, EGFR, Fas, Frizzled receptors, Wnts, TGFb1, TGFb2* and *MYC*). Focussing here on *MYC* expression, estrogen was observed to induce *MYC* expression in scrambled control MCF-7 (~2-fold) and T-47D (~3-fold) cells, and this is modestly reduced in *CBLL1*-depleted MCF- (~1.5-fold) and T-47D (2.6-fold) cells. This is consistent with a fine-tuning role for CBLL in estrogen signalling.

The fact that these three cancer-related pathways are only altered when *CBLL1* is depleted again supports a potential tumour suppressor role for CBLL1. Taken together, and with the effect on p53 discussed in MCF7, these factors may help to explain the findings reported in chapter 5, where nuclear CBLL1 expression was found to be an independent positive prognostic indicator.

As in MCF7 cells, only two significantly enriched pathways were observed exclusively in scrambled control T-47D cells treated with vehicle or $\beta E_2$. Whilst the cell adhesion molecules, focal adhesion, and gap junction pathways were enriched in MCF7 cells, in T-47D it was the tight junctions pathway that was significantly enriched in scrambled control cells. Tight junctions sit alongside, and are interdependent upon, adherens junctions (mediated by the cadherin

proteins among others) at sites of cell-to-cell contact, and mediate the passage between cells of small molecules and ions (Campbell et al., 2017). Loss of tight junctions is a feature of EMT, a hallmark of metastasis, markers of which are, in turn, associated with poorer patient outcomes in a wide range of tumour types (Jin et al., 2010, Olmeda et al., 2007, Wang et al., 2013), including BCa (Moody et al., 2005). Dysregulation of tight junctions has been observed in a number of types of cancer, including BCa, and their targeting for cancer detection and therapy has been suggested (Agarwal et al., 2005, Brennan et al., 2010).

Also enriched in the scrambled control T-47D cells -/+ $\beta E_2$ was the glutamatergic synapse pathway. Dysregulated glutamate-mediated signalling has been implicated in a number of cancer types, with higher glutamate and glutamate receptor expression associated with carcinogenesis (Li and Hanahan, 2013, Takano et al., 2001, Zeng et al., 2019). In BCa higher expression of several glutamate receptors has been associated with breast to brain metastasis (Zeng et al., 2019).

As the tight junctions and glutamatergic synapse pathways, which have both been associated with cancer, are only enriched by estrogen in the presence of *CBLL1*, this suggests that normal gene expression in these pathways is reliant on *CBLL1* depletion. These mechanisms may contribute to the oncogenic characteristics displayed by CBLL1 in BCa cell lines and when expressed in the cytoplasm of BCa cells in patient specimens.

Following analysis of DEGs, alternative splicing in response to *CBLL1* depletion and estrogen treatment was assessed in both MCF7 and T-47D cells. Alternative splicing has been implicated in BCa and constitutes a prognostic

molecular signature in patients (Bjørklund et al., 2017, He et al., 2009, Kahles et al., 2018, Wen et al., 2015). Indeed, dysregulation of alternative splicing has been identified in BCa and has been associated with poorer TNBC patient outcomes (Forootan et al., 2016, Yang et al., 2022). There is evidence to support a role for $m^6A$ in regulating context-dependent splicing *in vivo* (Haussmann et al., 2016, Lence et al., 2016), however no studies have yet investigated the role of CBLL1 in alternative splicing outside of its association with PSF (Figueroa et al., 2009a, Figueroa et al., 2009b). It is known that steroid hormones affect expression of splicing (Auboeuf et al., 2004), therefore DSGs and their associated pathways were analysed in the context of *CBLL1* presence or depletion treated with vehicle or $\beta E_2$.

In MCF7, almost twice as many alternative splicing events were observed in scrambled control cells treated with vehicle or $\beta E_2$ compared with *CBLL1*-depleted, suggesting a role for CBLL1 in splicing (**Figure 6.12** and **Appendix 28**). Skipped exon was the most common splicing event type across all conditions and the only type associated with significantly enriched pathways in scrambled control cells -/+ $\beta E_2$. Seven enriched pathways were associated with DSGs in scrambled control cells -/+ $\beta E_2$, most notably the adherens junction and central carbon metabolism in cancer pathways. E-cadherin plays an integral role in adherens junctions (Hartsock and Nelson, 2008), however, despite this pathway being enriched, the *CDH1* gene was not significantly differentially spliced, again supporting the findings reported above that CBLL1 impacts upon cellular adhesion independent of its interaction with E-cadherin.

The key component of the central carbon metabolism in cancer pathway is the Warburg effect, whereby cancer cells develop their own distinct metabolism in

order to sustain their rapid proliferation, characterised by a switch from oxidative phosphorylation to aerobic glycolysis (Warburg, 1956, Wong et al., 2017). Similarly, cancer stem cells (CSCs), also known as tumour-initiating cells, have been demonstrated to have a different metabolic phenotype to bulk cancer cells in a number of tumour types, including breast (Chen et al., 2014, Feng et al., 2014, Magee et al., 2012, Yasumoto et al., 2016, Zhou et al., 2011b). This altered metabolic phenotype has been shown to be remarkably similar to normal stem cells, suggesting the importance of this pathway in promoting stemness (Folmes et al., 2011). That *CBLL1* is essential in mediating estrogen regulation of this pathway suggests a role for *CBLL1* in altered cellular metabolism in BCa.

Eight enriched pathways were associated with DSGs in *CBLL1*-depleted cells treated with vehicle or $\beta E_2$, i.e. only regulated by estrogen in the absence of CBLL1. These included the ubiquitin mediated proteolysis, homologous recombination and metabolic pathways.

Ubiquitin-mediated proteolysis is a highly conserved system in eukaryotes that is fundamental in maintaining protein homeostasis by removing damaged or abnormal protein from cells, primarily via the lysosome or proteasome (Burger and Seth, 2004, Rock and Goldberg, 1999). Protein degradation is a vital part of a wide range of normal physiological processes (Goldberg et al., 1995), and any aberrations in this pathway are associated with a number of pathologies, particularly cancer (Adams, 2003, Glickman and Ciechanover, 2002). Given the reported function of CBLL1 as an E3 ubiquitin ligase (Aparicio et al., 2012, Fujita et al., 2002), it is somewhat unsurprising that *CBLL1* should be

associated with this pathway, and provides further evidence to support this reported role.

As with the mismatch repair pathway discussed earlier, the homologous recombination repair (HRR) pathway is another of the main components of the DNA damage repair system (Scarbrough et al., 2016), responsible for maintaining genome stability through double strand break repair (Lieber, 2010). Key genes within the HRR pathway include *BRCA1* and *BRCA2*, and alterations in expression of these genes are associated with the development of cancer, particularly breast (Rennert et al., 2007, Walsh et al., 2011). In *CBLL1*-depleted MCF7 cells, estrogen induced differential splicing of *BRCA1*, suggesting a role for *CBLL1* in maintaining canonical splicing in BCa cells. Significant enrichment of this pathway with *CBLL1* knockdown supports an earlier study that reported a role for the $m^6A$ catalytic subunit METTL3 in DNA repair, introducing modifications at double strand break sites that enabled recruitment of DNA repair factors (Xiang et al., 2017).

As described above, cancer cells can exploit metabolic processes to promote tumour growth, both encompassed in and independent of the Warburg effect (Eidelman et al., 2017, Wong et al., 2017). Our research group has also reported that knockdown of other $m^6A$ regulators in PCa cells, namely *METTL3*, *FTO* and *ALKBH5* resulted in DSGs that significantly alter metabolic pathways (Haigh et al., 2022, Lothion-Roy et al., 2022). Taken together, these results suggest that a function of *CBLL1* may be to aid in the regulation of metabolic reprogramming of BCa cells.

In T-47D, alternative splicing events were less frequent than in MCF7 and the overall number of splicing events was higher in estrogen-treated cells (both

scrambled control and *CBLL1* depleted) than in vehicle-treated (**Figure 6.13** and **Appendix 29**). As in MCF7, SE was the most common splicing event type across all conditions, however only MXE and RI events resulted in any significantly enriched pathways (**Appendix 29**). A total of 20 enriched pathways were associated with DSGs and all were in *CBLL1*-depleted cells treated with vehicle or $\beta E_2$. A number of cancer-associated pathways were enriched, including the proteoglycans in cancer pathway, cAMP signalling pathway, Rap1 signalling pathway, VEGF signalling pathway, and the ErbB signalling pathway, as well as three pathways directly related to other cancer types, namely renal cell carcinoma, pancreatic cancer and colorectal cancer.

The proteoglycans in cancer pathway was enriched in T-47D *CBLL1*-depleted cells -/+ $\beta E_2$ , as it was with MCF7 DEGs, where, as discussed previously, it has been found that the majority of proteoglycans contribute to tumorigenesis by driving cellular proliferation and metastasis in many types of cancer (Karousou et al., 2014, Mellai et al., 2020, Piperigkou et al., 2022, Wade et al., 2013) and result in poorer outcomes in BCa (Auvinen et al., 2014, Kischel et al., 2010, Leivonen et al., 2004, Okuda et al., 2012).

As in MCF7 DEGs, significant enrichment of the cAMP signalling pathway associated with DSGs in *CBLL1*-depleted T-47D cells was observed. As discussed above, cAMP can have paradoxical roles in cancer, with many reports of a tumour suppressor function, including in BCa (Cho-Chung et al., 1981, Kim et al., 2001, Santore et al., 2002). However others have found cAMP expression in cancer to be associated with poorer outcomes (Bang et al., 1994, Burchardt et al., 1999), even reporting it to be an independent negative prognostic factor in early stage BCa (Miller et al., 1990). In contrast to the

findings reported in MCF7, the cAMP signalling pathway was only enriched by estrogen in the absence of *CBLL1,* suggesting a more complex and cell type-dependent role for *CBLL1* for maintaining normal cAMP signalling in BCa.

The Rap1 (Ras-associated protein-1) signalling pathway can be activated by cAMP signalling (Lyle et al., 2008), and was also significantly enriched in *CBLL1*-depleted T-47D cells. Rap1 has been reported to play key regulatory roles in stimulating tumour cell invasion and metastasis in many cancer types, including BCa (Bailey et al., 2009, Huang et al., 2012, McSherry et al., 2011, Takahashi et al., 2013). However, in some cancer types, Rap1 has been found to have a tumour suppressor function, instead working to inhibit invasion and metastasis (Lyle et al., 2008, Vallés et al., 2004). These different responses reflect the huge number of downstream signalling pathways to Rap1 (Zhang et al., 2017). One such downstream pathway is the activation of VEGF (vascular endothelial-derived growth factor), whereby Rap1 has been found to promote angiogenesis in hypoxic conditions (Menon et al., 2012).

The VEGF signalling pathway was another enriched pathway in *CBLL1*-depleted T-47D cells. Under normal conditions, VEGF promotes angiogenesis both *in utero* and in adult wound healing, however in cancer, it is the key regulator of angiogenesis (Carmeliet, 2005). mRNA expression of *VEGF* is increased in the majority of tumour types (including breast) and is correlated with tumour invasion, metastasis, recurrence and prognosis (Kerbel, 2008, Sohn et al., 2018).

The ErbB signalling pathway comprises the human epidermal growth factor (EGFR) family of four receptor tyrosine kinases (RTK) which regulate a diverse range of cellular responses, including cellular proliferation, differentiation and

survival (Roskoski, 2014). Members of the ErbB RTK family represent some of the most commonly altered proteins in cancer, with aberrant expression of their encoding genes associated with many cancer types, including BCa (Kumagai et al., 2021, Roskoski, 2014, Yarden and Pines, 2012). A notable RTK from the ErbB family in the context of BCa is ErbB-2, otherwise known as HER2 (human epidermal growth factor receptor 2) (Kumagai et al., 2021). Overexpression of HER2 is seen in 15-30% of invasive breast tumours (Burstein, 2005), and is associated with higher risk of recurrence and shorter disease-free survival than normal HER2 expression (Press et al., 1993, Seshadri et al., 1993). HER2 has become a therapeutic target in BCa recent years, with HER2 inhibition via monoclonal antibodies such as trastuzumab (Herceptin®) and pertuzumab dual therapy, or tyrosine kinase inhibitors such as tucatinib, now the standard of care in HER2 over-expressing breast tumours (Murthy et al., 2020, Pernas and Tolaney, 2022, Piccart et al., 2021).

The enrichment of all these cancer-related pathways only in the absence of *CBLL1* suggests a role for *CBLL1* in preventing carcinogenesis and again provides insight into the finding of nuclear CBLL1 being an independent positive prognostic factor in BCa patients (presented in chapter 5).

To summarise, functional depletion of *CBLL1* was carried out in ERα-expressing BCa cell lines to assess the effect of *CBLL1* on cellular phenotype, differential gene expression and alternative splicing, and the associated enriched KEGG pathways.

Interestingly, knockdown of *CBLL1* had little impact on E-cadherin expression, either at the mRNA or protein level, or on cellular proliferation in either cell type,

although a modest decrease in proliferation was seen in *CBLL1*-depleted MCF7 cells treated with estrogen compared with scrambled controls.

In conclusion, examination of differential gene expression and splicing revealed thousands of DEGs and DSGs regulated by estrogen and *CBLL1,* including many that are cancer-related and associated with DNA repair and cancer-specific KEGG pathways. It was notable how many genes in both MCF7 and T-47D cells were dependent on *CBLL1* expression for their estrogen regulation. Whilst many of the pathways identified were associated with pro-oncogenic processes, some were associated with tumour suppression. These diverse and complex mechanisms provide more insight into the processes behind some of the conflicting results presented in chapter 5, particularly in the analysis of our BCa patient cohort and publicly available patient datasets, and provide more evidence for a role for CBLL1 in the development and progression of BCa.

# Chapter 7

Conclusions and future work

# 7 Conclusions and future work

PCa and BCa continue to be huge global clinical challenges, being among the most commonly diagnosed and deadly cancer types in men and women, respectively (Sung et al., 2021). Whilst the hormones largely responsible for driving these cancer types form the main focus of targeted therapy (ATAC, 2002, Cornford et al., 2017, Francis et al., 2014, Hussain et al., 2018, Semenas et al., 2012), when resistance to these therapies develops, or the hormone receptor targets are not present in the first place, very few effective treatment options remain (Denkert et al., 2017, Gillessen et al., 2020). It is, therefore, essential to find new specific therapeutic targets in PCa and BCa in order to offer these patients improved outcomes.

In recent years, technological advances have enabled study of the epitranscriptome which has deepened understanding of the proteins involved in the dynamic regulation of the $m^6A$ RNA modification (Dominissini et al., 2012, Meyer et al., 2012). Given the important role $m^6A$ plays in fundamental biological processes it is unsurprising that regulators of $m^6A$ are now implicated in numerous cancer types (Bansal et al., 2014, Barbieri et al., 2017, Cai et al., 2018, Chen et al., 2018, Guan et al., 2022, Jia et al., 2011, Knuckles et al., 2018, Kong et al., 2020, Li et al., 2020a, Wang et al., 2020c, Zhang et al., 2016a). In particular, the methyltransferase protein complex responsible for 'writing' $m^6A$ has garnered a lot of interest as a possible drug target, particularly the catalytic subunit METTL3 (Bedi et al., 2020, Du et al., 2022, Fiorentino et al., 2023, Li and Gregory, 2021, Yankova et al., 2021). Indeed, small molecule inhibitors of METTL3 are currently in clinical trials, and have thus far shown preclinical potential to treat haematological cancers (Yankova et al., 2021) and

solid tumours (Haigh et al., 2022, Sun et al., 2023, Wang et al., 2023, Zhang et al., 2022c). One of the adaptor proteins to the $m^6A$ methyltransferase complex, CBLL1, has been implicated in several cancer types, mostly through its interaction with E-cadherin (Castosa et al., 2018, Figueroa et al., 2009b, Hui et al., 2019, Liu et al., 2018b, Liu et al., 2018c), but its role in $m^6A$ RNA modification in PCa and BCa remains poorly understood. It has been suggested that CBLL1 expression may also be hormone-regulated (Gong et al., 2010, Jin et al., 2013), therefore indicating further investigation into the function and role of CBLL1 in the two most important hormone-driven cancers, PCa and BCa.

The majority of studies that have examined CBLL1 in cancer have reported a pro-oncogenic role (Castosa et al., 2018, Figueroa et al., 2009b, Hui et al., 2019, Liu et al., 2018b, Liu et al., 2018c, Rodriguez-Rigueiro et al., 2011). In BCa cells, several studies have also reported a positive association between CBLL1 expression and oncogenic features, including increased invasive potential and metastasis (Liu et al., 2022b, Ma et al., 2023). One study of BCa patient specimens reported conflicting findings, of lower CBLL1 expression in normal breast tissue compared with BCa yet observed better relapse-free and overall survival in samples with higher expression of CBLL1 (Zheng et al., 2021). Another study reported that CBLL1 inhibited proliferation and migration in BCa cells, and that estrogen treatment inhibited CBLL1 expression (Gong et al., 2010). One of the only studies available in PCa reported a tumour suppressor role for CBLL1, with lower expression associated with PCa development and progression (Su et al., 2021).

This study examined the expression of CBLL1 in PCa cell lines and patient specimens. Given the dual roles reported for CBLL1, both in the nucleus as part of the $m^6A$ methyltransferase complex and in the cytoplasm as a ubiquitin E3 ligase of E-cadherin, here it was found that CBLL1 was primarily expressed in the nucleus. The highest CBLL1 expression was observed in AR-expressing PCa cells compared with non-malignant controls at both the mRNA and protein level and was indeed found to be androgen-regulated. Moreover, bioinformatic analysis of publicly available patient datasets revealed that elevated *CBLL1* expression was associated with PCa. Multiple PCa patient cohorts from two separate institutions were analysed using IHC and found that overall, higher expression of CBLL1 in both the nucleus and cytoplasm were associated with malignancy and poorer patient outcomes. Taken together, these positive associations between CBLL1 expression and PCa cells and tumour samples suggest a pro-oncogenic role for CBLL1 in PCa.

This was explored further through functional depletion of *CBLL1* using siRNA, in order to assess the effect on cellular phenotype, differential gene expression and alternative splicing, and the associated enriched KEGG pathways. The role of CBLL1 in ADT resistance was simultaneously examined, and this analysis revealed thousands of DEGs and DSGs regulated by androgen, *CBLL1* and enzalutamide resistance. CBLL1 was implicated in the regulation of androgen signalling in PCa. No effect on cell phenotype was observed, although additional future studies are required to confirm this result. CBLL1 was demonstrated to have a key role in maintaining normal androgen regulation of a number of pivotal oncogenes and tumour suppressor genes and their related pathways in PCa cells. It was also found that enzalutamide

resistance causes PCa cells to become independent of the influence of CBLL1 on gene regulation. Moreover, CBLL1 was demonstrated to play a role in selective regulation of splicing in PCa, in both androgen-sensitive and enzalutamide-resistant cells. These results support a pro-oncogenic role for CBLL1 in PCa, and moreover a role in ADT resistance and disease progression.

Future exploration of the function of CBLL1 in PCa would be aided by examining the effect of *CBLL1* depletion in alternative cell lines. It was found that the normal androgen regulation of the *TMPRSS2* gene is impaired by *CBLL1* depletion. The *TMPRSS2-ERG* fusion is a key driver of PCa, and since this is lacking in the LNCaP:C42 cell line exclusively used in this study, it would be beneficial to assess the effect of *CBLL1* depletion in the VCaP cell line which harbours this fusion. Our collaboration with WCM also gives us access to their PCa patient-derived organoids. Examination of the effect of *CBLL1* depletion within a three-dimensional structure that more closely replicates the complex microenvironment of tumours in the body would be of incredible utility in order to assess whether CBLL1 may be of value as a therapeutic target for a new wave of $m^6A$ small molecule inhibitors in PCa. Additionally, with the likely technological advances in the years to come, it would be helpful to revisit the splicing analysis carried out in this study following *CBLL1* knockdown. The currently available tools do not have the capability to analyse the functional significance of all the non-coding RNAs that were found to be alternatively spliced as a result of *CBLL1* knockdown in the PCa cells analysed in this study. Therefore, elucidation of the role and function of these non-coding RNAs may be a key piece of the puzzle we are currently missing.

This study also examined the expression of CBLL1 in BCa cell lines and patient specimens. As in PCa, CBLL1 was also found to be expressed most abundantly in the nucleus of BCa cells. Also, similar to PCa, the highest levels of CBLL1 expression were observed in hormone receptor-positive (ERα) BCa cells compared with non-malignant and triple negative cell lines. Additionally, as in PCa, it was found that CBLL1 expression in BCa was regulated by the key hormone implicated in the disease, estrogen. However, bioinformatic analysis of publicly available patient datasets revealed a less clear picture, that whilst the most common alteration associated with BCa was amplification of the *CBLL1* gene, the effect of *CBLL1* expression on BCa patient survival varied depending on the cohort. IHC analysis of two large well-characterised BCa patient cohorts found that, in contrast to PCa, higher nuclear expression of CBLL1 was associated with more favourable clinicopathological parameters and was demonstrated to be an independent positive prognostic indicator for patient survival. Correlations of cytoplasmic CBLL1 expression with clinicopathological parameters were more equivocal, with higher cytoplasmic CBLL1 associated more frequently with negative prognostic factors, however it was not found to be significantly associated with patient survival. Interestingly, a positive correlation was observed between E-cadherin and CBLL1 expression in both BCa cell lines and patient samples. Taken together these results implicate a more complex role for CBLL1 in BCa, with the higher expression associated with malignancy in BCa cell lines not replicated in BCa patient specimens.

It should be noted, however, that whilst an incredibly valuable resource, the BCa TMAs comprised only early stage BCa samples and no matched non-

malignant breast tissue specimens. It would be helpful in future to assess and compare CBLL1 expression in normal/non-malignant breast tissue and also in DCIS and TNBC TMAs which have recently become available to our research group. It would be interesting to assess how CBLL1 expression changes across the spectrum of disease and analyse if nuclear CBLL1 still does have a tumour suppressor effect.

This potential tumour suppressor role of CBLL1 in BCa was explored further through siRNA-mediated *CBLL1* depletion, again to assess the effect on cellular phenotype, differential gene expression and alternative splicing, and the associated enriched KEGG pathways. Unlike in PCa cells, *CBLL1* depletion resulted in a modest, yet significant, decrease in proliferation in MCF7 cells. Examination of differential gene expression and splicing revealed thousands of DEGs and DSGs regulated by estrogen and *CBLL1,* including many that were cancer-related and associated with DNA repair and cancer-specific KEGG pathways. As in PCa, CBLL1 was implicated in the regulation of hormone (estrogen) signalling in BCa, with CBLL1 shown to again have a role in maintaining normal estrogen regulation of a number of oncogenes and tumour suppressor genes and their related pathways in BCa cells. Taken together, the findings in BCa cells and in patient samples indicate a diverse and complex role for CBLL1 in BCa.

As discussed earlier, IHC examination of different tissue types across the spectrum of different BCa subtypes would be useful, as would examination of the effect of *CBLL1* depletion in different molecular subtype cell line models of disease. Plans for future work include *CBLL1* knockdown experiments in the MDA-MB-231 triple negative cell line in order to compare the effects to the

current results in ERα-positive cells. As it has been suggested that CBLL1 is responsible for stabilising the METTL3-METTL14 complex, there are also plans to carry out combination experiments looking at the effect of *CBLL1*, together with *METTL3* and *METTL14*, knockdown in multiple BCa cell lines in collaboration with other members of our lab group. As discussed with PCa, it would additionally be valuable to replicate these *CBLL1* depletion experiments in organoid models in order to assess the impact of the tumour micro-environment on the function of CBLL1.

In conclusion, this study has reported for the first time an extensive assessment of the role of CBLL1 in PCa and BCa cell lines and patient samples. Additionally, to date only the post-translational effects of CBLL1 on E-cadherin have been reported, and this study presents for the first time the transcriptional and translational impact of CBLL1 on E-cadherin expression. This study has reported a role for CBLL1 in both gene expression, alternative splicing and hormone regulation in both PCa and BCa. A primarily pro-oncogenic role for CBLL1 in PCa has been revealed, together with a role in ADT resistance and associated disease progression. In BCa, there was some discordance between the results seen in BCa cell lines, which suggested a pro-oncogenic role for CBLL1, and in patient samples, which found CBLL1 to be an independent positive prognostic factor for survival. This may be a function of the broad variety of intrinsic and molecular subtypes seen in BCa and further work is now indicated to examine the role of CBLL1 across the spectrum of different BCa subtypes.

The early success of $m^6A$ small molecule inhibitors offers hope that a new avenue of targeted cancer therapies may be opening up. The results presented

in thesis support continued investigation of CBLL1 as a specific drug target, particularly in advanced hormone-independent cancers, which currently hold a bleak outlook for patients.

# References


AALDRIKS, A. A., GILTAY, E. J., LE CESSIE, S., VAN DER GEEST, L. G., PORTIELJE, J. E., TANIS, B. C., NORTIER, J. W. & MAARTENSE, E. 2013. Prognostic value of geriatric assessment in older patients with advanced breast cancer receiving chemotherapy. *Breast,* 22**,** 753-60.

ABATE-SHEN, C., SHEN, M. M. & GELMANN, E. 2008. Integrating differentiation and cancer: the Nkx3.1 homeobox gene in prostate organogenesis and carcinogenesis. *Differentiation,* 76**,** 717-27.

ABEDIN, M. & KING, N. 2008. The premetazoan ancestry of cadherins. *Science,* 319**,** 946-8.

ABIDA, W., CYRTA, J., HELLER, G., PRANDI, D., ARMENIA, J., COLEMAN, I., CIESLIK, M., BENELLI, M., ROBINSON, D., VAN ALLEN, E. M., SBONER, A., FEDRIZZI, T., MOSQUERA, J. M., ROBINSON, B. D., DE SARKAR, N., KUNJU, L. P., TOMLINS, S., WU, Y. M., NAVA RODRIGUES, D., LODA, M., GOPALAN, A., REUTER, V. E., PRITCHARD, C. C., MATEO, J., BIANCHINI, D., MIRANDA, S., CARREIRA, S., RESCIGNO, P., FILIPENKO, J., VINSON, J., MONTGOMERY, R. B., BELTRAN, H., HEATH, E. I., SCHER, H. I., KANTOFF, P. W., TAPLIN, M. E., SCHULTZ, N., DEBONO, J. S., DEMICHELIS, F., NELSON, P. S., RUBIN, M. A., CHINNAIYAN, A. M. & SAWYERS, C. L. 2019. Genomic correlates of clinical outcome in advanced prostate cancer. *Proc Natl Acad Sci U S A,* 116**,** 11428-11436.

ABRAHAMSSON, P. A., FALKMER, S., FÄLT, K. & GRIMELIUS, L. 1989. The course of neuroendocrine differentiation in prostatic carcinomas. An immunohistochemical study testing chromogranin A as an "endocrine marker". *Pathol Res Pract,* 185**,** 373-80.

ACHOUR, C., BHATTARAI, D. P., GROZA, P., ROMÁN Á, C. & AGUILO, F. 2023. METTL3 regulates breast cancer-associated alternative splicing switches. *Oncogene,* 42**,** 911-925.

ACS 2015. National Cancer Database, 2013 Data Submission. *American College of Surgeons, Commission on Cancer.* Chicago, IL: American College of Surgeons.

ADAMS, J. 2003. The proteasome: structure, function, and role in the cell. *Cancer treatment reviews,* 29**,** 3-9.

ADES, E. W., CANDAL, F. J., SWERLICK, R. A., GEORGE, V. G., SUMMERS, S., BOSSE, D. C. & LAWLEY, T. J. 1992. HMEC-1: Establishment of an Immortalized Human Microvascular Endothelial Cell Line. *Journal of Investigative Dermatology,* 99**,** 683-690.

AFSHAR, M., EVISON, F., JAMES, N. D. & PATEL, P. 2015. Shifting paradigms in the estimation of survival for castration-resistant prostate cancer: A tertiary academic center experience. *Urologic Oncology: Seminars and Original Investigations,* 33**,** 338.e1-338.e7.

AGARWAL, R., D'SOUZA, T. & MORIN, P. J. 2005. Claudin-3 and claudin-4 expression in ovarian epithelial cells enhances invasion and is associated with increased matrix metalloproteinase-2 activity. *Cancer research,* 65**,** 7378-7385.

AGOULNIK, I. U., VAID, A., BINGMAN, W. E., 3RD, ERDEME, H., FROLOV, A., SMITH, C. L., AYALA, G., ITTMANN, M. M. & WEIGEL, N. L. 2005. Role of SRC-1 in the promotion of prostate cancer cell growth and tumor progression. *Cancer Res,* 65**,** 7959-67.

AIK, W., DEMETRIADES, M., HAMDAN, M. K., BAGG, E. A., YEOH, K. K., LEJEUNE, C., ZHANG, Z., MCDONOUGH, M. A. & SCHOFIELD, C. J. 2013. Structural basis for inhibition of the fat mass and obesity associated protein (FTO). *J Med Chem,* 56**,** 3680-8.

AL-HAJJ, M., WICHA, M. S., BENITO-HERNANDEZ, A., MORRISON, S. J. & CLARKE, M. F. 2003. Prospective identification of tumorigenic breast cancer cells. *Proc Natl Acad Sci U S A,* 100**,** 3983-8.

ALARCÓN, C. R., GOODARZI, H., LEE, H., LIU, X., TAVAZOIE, S. & TAVAZOIE, S. F. 2015. HNRNPA2B1 Is a Mediator of m(6)A-Dependent Nuclear RNA Processing Events. *Cell,* 162**,** 1299-308.

ALBERTSEN, P. C., HANLEY, J. A., GLEASON, D. F. & BARRY, M. J. 1998. Competing Risk Analysis of Men Aged 55 to 74 Years at Diagnosis Managed Conservatively for Clinically Localized Prostate Cancer. *JAMA,* 280**,** 975-980.

ALLAN, G. F., TSAI, S. Y., O'MALLEY, B. W. & TSAI, M. J. 1991. Steroid hormone receptors and in vitro transcription. *Bioessays,* 13**,** 73-8.

ALSALEEM, M., TOSS, M. S., JOSEPH, C., ALESKANDARANY, M., KUROZUMI, S., ALSHANKYTY, I., OGDEN, A., RIDA, P. C. G., ELLIS, I. O., ANEJA, R., GREEN, A. R., MONGAN, N. P. & RAKHA, E. A. 2019. The molecular mechanisms underlying reduced E-cadherin expression in invasive ductal carcinoma of the breast: high throughput analysis of large cohorts. *Mod Pathol,* 32**,** 967-976.

ALSULTAN, D., KAVANAGH, E., O'GRADY, S., EUSTACE, A. J., CASTELL, A., LARSSON, L. G., CROWN, J., MADDEN, S. F. & DUFFY, M. J. 2021. The novel low molecular weight MYC antagonist MYCMI-6 inhibits proliferation and induces apoptosis in breast cancer cells. *Invest New Drugs,* 39**,** 587-594.

AMOS, H. & KORN, M. 1958. 5-Methyl cytosine in the RNA of Escherichia coli. *Biochimica et biophysica acta,* 29**,** 444-445.

ANDRIOLE, G. L., CRAWFORD, E. D., GRUBB, R. L., BUYS, S. S., CHIA, D., CHURCH, T. R., FOUAD, M. N., GELMANN, E. P., KVALE, P. A., REDING, D. J., WEISSFELD, J. L., YOKOCHI, L. A., O'BRIEN, B., CLAPP, J. D., RATHMELL, J. M., RILEY, T. L., HAYES, R. B., KRAMER, B. S., IZMIRLIAN, G., MILLER, A. B., PINSKY, P. F., PROROK, P. C., GOHAGAN, J. K. & BERG, C. D. 2009. Mortality Results from a Randomized Prostate-Cancer Screening Trial. *New England Journal of Medicine,* 360**,** 1310-1319.

ANTONARAKIS, E. S., LU, C., LUBER, B., WANG, H., CHEN, Y., ZHU, Y., SILBERSTEIN, J. L., TAYLOR, M. N., MAUGHAN, B. L. & DENMEADE, S. R. 2017. Clinical significance of androgen receptor splice variant-7 mRNA detection in circulating tumor cells of men with metastatic castration-resistant prostate cancer treated with first-and second-line abiraterone and enzalutamide. *Journal of Clinical Oncology,* 35**,** 2149.

ANTONARAKIS, E. S., LU, C., WANG, H., LUBER, B., NAKAZAWA, M., ROESER, J. C., CHEN, Y., MOHAMMAD, T. A., CHEN, Y., FEDOR, H. L., LOTAN, T. L., ZHENG, Q., DE MARZO, A. M., ISAACS, J. T., ISAACS, W. B., NADAL, R., PALLER, C. J., DENMEADE, S. R.,

CARDUCCI, M. A., EISENBERGER, M. A. & LUO, J. 2014. AR-V7 and resistance to enzalutamide and abiraterone in prostate cancer. *N Engl J Med,* 371**,** 1028-38.

ANTONIOU, A. C., CUNNINGHAM, A. P., PETO, J., EVANS, D. G., LALLOO, F., NAROD, S. A., RISCH, H. A., EYFJORD, J. E., HOPPER, J. L., SOUTHEY, M. C., OLSSON, H., JOHANNSSON, O., BORG, A., PASINI, B., RADICE, P., MANOUKIAN, S., ECCLES, D. M., TANG, N., OLAH, E., ANTON-CULVER, H., WARNER, E., LUBINSKI, J., GRONWALD, J., GORSKI, B., TRYGGVADOTTIR, L., SYRJAKOSKI, K., KALLIONIEMI, O. P., EEROLA, H., NEVANLINNA, H., PHAROAH, P. D. & EASTON, D. F. 2008. The BOADICEA model of genetic susceptibility to breast and ovarian cancers: updates and extensions. *Br J Cancer,* 98**,** 1457-66.

ANZAI, E., HIRATA, K., SHIBAZAKI, M., YAMADA, C., MORII, M., HONDA, T., YAMAGUCHI, N. & YAMAGUCHI, N. 2017. FOXA1 Induces E-Cadherin Expression at the Protein Level via Suppression of Slug in Epithelial Breast Cancer Cells. *Biological and Pharmaceutical Bulletin,* 40**,** 1483-1489.

APARICIO, L. A., VALLADARES, M., BLANCO, M., ALONSO, G. & FIGUEROA, A. 2012. Biological influence of Hakai in cancer: a 10-year review. *Cancer Metastasis Rev,* 31**,** 375-86.

ARIEL, I., LUSTIG, O., SCHNEIDER, T., PIZOV, G., SAPPIR, M., DE-GROOT, N. & HOCHBERG, A. 1995. The imprinted H19 gene as a tumor marker in bladder carcinoma. *Urology,* 45**,** 335-8.

ARMSTRONG, A. J., HALABI, S., LUO, J., NANUS, D. M., GIANNAKAKOU, P., SZMULEWITZ, R. Z., DANILA, D. C., HEALY, P., ANAND, M., ROTHWELL, C. J., RASMUSSEN, J., THORNBURG, B., BERRY, W. R., WILDER, R. S., LU, C., CHEN, Y., SILBERSTEIN, J. L., KEMENY, G., GALLETTI, G., SOMARELLI, J. A., GUPTA, S., GREGORY, S. G., SCHER, H. I., DITTAMORE, R., TAGAWA, S. T., ANTONARAKIS, E. S. & GEORGE, D. J. 2019. Prospective Multicenter Validation of Androgen Receptor Splice Variant 7 and Hormone Therapy Resistance in High-Risk Castration-Resistant Prostate Cancer: The PROPHECY Study. *J Clin Oncol,* 37**,** 1120-1129.

ASCENZI, P., BOCEDI, A. & MARINO, M. 2006. Structure–function relationship of estrogen receptor α and β: Impact on human health. *Molecular Aspects of Medicine,* 27**,** 299-402.

AST, G. 2004. How did alternative splicing evolve? *Nat Rev Genet,* 5**,** 773-82.

ATAC 2002. The ATAC (Arimidex, Tamoxifen Alone or in Combination) Trialists' Group: Anastrozole alone or in combination with tamoxifen versus tamoxifen alone for adjuvant treatment of postmenopausal women with early breast cancer: first results of the ATAC randomised trial. *The Lancet,* 359**,** 2131-2139.

ATTAR, R. M., TAKIMOTO, C. H. & GOTTARDIS, M. M. 2009. Castration-Resistant Prostate Cancer: Locking Up the Molecular Escape Routes. *Clinical Cancer Research,* 15**,** 3251-3255.

AUBOEUF, D., DOWHAN, D. H., DUTERTRE, M., MARTIN, N., BERGET, S. M. & O'MALLEY, B. W. 2005. A subset of nuclear receptor coregulators act as coupling proteins during synthesis and maturation of RNA transcripts. *Mol Cell Biol,* 25**,** 5307-16.

AUBOEUF, D., DOWHAN, D. H., KANG, Y. K., LARKIN, K., LEE, J. W., BERGET, S. M. & O'MALLEY, B. W. 2004. Differential recruitment of nuclear receptor coactivators may determine alternative RNA splice site choice in target genes. *Proc Natl Acad Sci U S A,* 101**,** 2270-4.

AUBOEUF, D., HÖNIG, A., BERGET, S. M. & O'MALLEY, B. W. 2002. Coordinate regulation of transcription and splicing by steroid receptor coregulators. *Science,* 298**,** 416-9.

AUVINEN, P., RILLA, K., TUMELIUS, R., TAMMI, M., SIRONEN, R., SOINI, Y., KOSMA, V.-M., MANNERMAA, A., VIIKARI, J. & TAMMI, R. 2014. Hyaluronan synthases (HAS1–3) in stromal and malignant cells correlate with breast cancer grade and predict patient survival. *Breast cancer research and treatment,* 143**,** 277-286.

BAI, G., LIU, Y., ZHANG, H., SU, D., TAO, D., YANG, Y., MA, Y. & ZHANG, S. 2010. Promoter demethylation mediates the expression of ZNF645, a novel cancer/testis gene. *BMB Rep,* 43**,** 400-6.

BAILEY, C. L., KELLY, P. & CASEY, P. J. 2009. Activation of Rap1 promotes prostate cancer metastasis. *Cancer Res,* 69**,** 4962-8.

BAJRAMI, I., MARLOW, R., VAN DE VEN, M., BROUGH, R., PEMBERTON, H. N., FRANKUM, J., SONG, F., RAFIQ, R., KONDE, A., KRASTEV, D. B., MENON, M., CAMPBELL, J., GULATI, A., KUMAR, R., PETTITT, S. J., GURDEN, M. D., CARDENOSA, M. L., CHONG, I., GAZINSKA, P., WALLBERG, F., SAWYER, E. J., MARTIN, L.-A., DOWSETT, M., LINARDOPOULOS, S., NATRAJAN, R., RYAN, C. J., DERKSEN, P. W. B., JONKERS, J., TUTT, A. N. J., ASHWORTH, A. & LORD, C. J. 2018. E-Cadherin/ROS1 Inhibitor Synthetic Lethality in Breast Cancer. *Cancer Discovery,* 8**,** 498-515.

BAKIN, R. E., GIOELI, D., SIKES, R. A., BISSONETTE, E. A. & WEBER, M. J. 2003. Constitutive activation of the Ras/mitogen-activated protein kinase signaling pathway promotes androgen hypersensitivity in LNCaP prostate cancer cells. *Cancer Res,* 63**,** 1981-9.

BALL, E. M. A., MELLOR, S. L. & RISBRIDGER, G. P. 2004. Cancer progression: is inhibin α from Venus or Mars? *Cytokine & Growth Factor Reviews,* 15**,** 291-296.

BANG, Y. J., PIRNIA, F., FANG, W. G., KANG, W. K., SARTOR, O., WHITESELL, L., HA, M. J., TSOKOS, M., SHEAHAN, M. D., NGUYEN, P., NIKLINSKI, W. T., MYERS, C. E. & TREPEL, J. B. 1994. Terminal neuroendocrine differentiation of human prostate carcinoma cells in response to increased intracellular cyclic AMP. *Proc Natl Acad Sci U S A,* 91**,** 5330-4.

BANSAL, H., YIHUA, Q., IYER, S. P., GANAPATHY, S., PROIA, D., PENALVA, L. O., UREN, P. J., SURESH, U., CAREW, J. S., KARNAD, A. B., WEITMAN, S., TOMLINSON, G. E., RAO, M. K., KORNBLAU, S. M. & BANSAL, S. 2014. WTAP is a novel oncogenic protein in acute myeloid leukemia. *Leukemia,* 28**,** 1171.

BARANWAL, S. & ALAHARI, S. K. 2009. Molecular mechanisms controlling E-cadherin expression in breast cancer. *Biochem Biophys Res Commun,* 384**,** 6-11.

BARBAGALLO, D., CAPONNETTO, A., CIRNIGLIARO, M., BREX, D., BARBAGALLO, C., D'ANGELI, F., MORRONE, A., CALTABIANO, R., BARBAGALLO, G. M., RAGUSA, M., DI PIETRO, C., HANSEN, T. B. & PURRELLO, M. 2018. CircSMARCA5 Inhibits Migration of Glioblastoma

Multiforme Cells by Regulating a Molecular Axis Involving Splicing Factors SRSF1/SRSF3/PTB. *International Journal of Molecular Sciences* [Online], 19.

BARBER, A. G., CASTILLO-MARTIN, M., BONAL, D. M., JIA, A. J., RYBICKI, B. A., CHRISTIANO, A. M. & CORDON-CARDO, C. 2015. PI3K/AKT pathway regulates E-cadherin and Desmoglein 2 in aggressive prostate cancer. *Cancer Medicine,* 4**,** 1258-1271.

BARBER, L., GERKE, T., MARKT, S. C., PEISCH, S. F., WILSON, K. M., AHEARN, T., GIOVANNUCCI, E., PARMIGIANI, G. & MUCCI, L. A. 2018. Family History of Breast or Prostate Cancer and Prostate Cancer Risk. *Clin Cancer Res,* 24**,** 5910-5917.

BARBIERI, C. E., BACA, S. C., LAWRENCE, M. S., DEMICHELIS, F., BLATTNER, M., THEURILLAT, J. P., WHITE, T. A., STOJANOV, P., VAN ALLEN, E., STRANSKY, N., NICKERSON, E., CHAE, S. S., BOYSEN, G., AUCLAIR, D., ONOFRIO, R. C., PARK, K., KITABAYASHI, N., MACDONALD, T. Y., SHEIKH, K., VUONG, T., GUIDUCCI, C., CIBULSKIS, K., SIVACHENKO, A., CARTER, S. L., SAKSENA, G., VOET, D., HUSSAIN, W. M., RAMOS, A. H., WINCKLER, W., REDMAN, M. C., ARDLIE, K., TEWARI, A. K., MOSQUERA, J. M., RUPP, N., WILD, P. J., MOCH, H., MORRISSEY, C., NELSON, P. S., KANTOFF, P. W., GABRIEL, S. B., GOLUB, T. R., MEYERSON, M., LANDER, E. S., GETZ, G., RUBIN, M. A. & GARRAWAY, L. A. 2012. Exome sequencing identifies recurrent SPOP, FOXA1 and MED12 mutations in prostate cancer. *Nat Genet,* 44**,** 685-9.

BARBIERI, I., TZELEPIS, K., PANDOLFINI, L., SHI, J., MILLÁN-ZAMBRANO, G., ROBSON, S. C., ASPRIS, D., MIGLIORI, V., BANNISTER, A. J., HAN, N., DE BRAEKELEER, E., PONSTINGL, H., HENDRICK, A., VAKOC, C. R., VASSILIOU, G. S. & KOUZARIDES, T. 2017. Promoter-bound METTL3 maintains myeloid leukaemia by m6A-dependent translation control. *Nature,* 552**,** 126.

BARDOU, V.-J., ARPINO, G., ELLEDGE, R. M., OSBORNE, C. K. & CLARK, G. M. 2003. Progesterone receptor status significantly improves outcome prediction over estrogen receptor status alone for adjuvant endocrine therapy in two large breast cancer databases. *Journal of clinical oncology,* 21**,** 1973-1979.

BARON, S., MANIN, M., BEAUDOIN, C., LEOTOING, L., COMMUNAL, Y., VEYSSIERE, G. & MOREL, L. 2004. Androgen receptor mediates non-genomic activation of phosphatidylinositol 3-OH kinase in androgen-sensitive epithelial cells. *J Biol Chem,* 279**,** 14579-86.

BARRETT, T., WILHITE, S. E., LEDOUX, P., EVANGELISTA, C., KIM, I. F., TOMASHEVSKY, M., MARSHALL, K. A., PHILLIPPY, K. H., SHERMAN, P. M., HOLKO, M., YEFANOV, A., LEE, H., ZHANG, N., ROBERTSON, C. L., SEROVA, N., DAVIS, S. & SOBOLEVA, A. 2013. NCBI GEO: archive for functional genomics data sets—update. *Nucleic Acids Research,* 41**,** D991-D995.

BASIL, P., ROBERTSON, M. J., BINGMAN, W. E., 3RD, DASH, A. K., KRAUSE, W. C., SHAFI, A. A., PIYARATHNA, B., COARFA, C. & WEIGEL, N. L. 2022. Cistrome and transcriptome analysis identifies unique androgen receptor (AR) and AR-V7 splice variant chromatin binding and transcriptional activities. *Sci Rep,* 12**,** 5351.

BASU, A. 1993. The potential of protein kinase C as a target for anticancer treatment. *Pharmacol Ther,* 59**,** 257-80.

BASU, R., QIAN, Y. & KOPCHICK, J. J. 2018. MECHANISMS IN ENDOCRINOLOGY: Lessons from growth hormone receptor gene-disrupted mice: are there benefits of endocrine defects? *European Journal of Endocrinology,* 178**,** R155-R181.

BEATO, M. 1989. Gene regulation by steroid hormones. *Cell,* 56**,** 335-44.

BEAULIEU, M.-E., CASTILLO, F. & SOUCEK, L. 2020. Structural and Biophysical Insights into the Function of the Intrinsically Disordered Myc Oncoprotein. *Cells* [Online], 9.

BECKER, K.-F., ATKINSON, M. J., REICH, U., BECKER, I., NEKARDA, H., SIEWERT, J. R. & HÖFLER, H. 1994. E-Cadherin Gene Mutations Provide Clues to Diffuse Type Gastric Carcinomas. *Cancer Research,* 54**,** 3845-3852.

BEDI, R. K., HUANG, D., EBERLE, S. A., WIEDMER, L., ŚLEDŹ, P. & CAFLISCH, A. 2020. Small-Molecule Inhibitors of METTL3, the Major Human Epitranscriptomic Writer. *ChemMedChem,* 15**,** 744-748.

BEER, T. M., ARMSTRONG, A. J., RATHKOPF, D. E., LORIOT, Y., STERNBERG, C. N., HIGANO, C. S., IVERSEN, P., BHATTACHARYA, S., CARLES, J., CHOWDHURY, S., DAVIS, I. D., DE BONO, J. S., EVANS, C. P., FIZAZI, K., JOSHUA, A. M., KIM, C. S., KIMURA, G., MAINWARING, P., MANSBACH, H., MILLER, K., NOONBERG, S. B., PERABO, F., PHUNG, D., SAAD, F., SCHER, H. I., TAPLIN, M. E., VENNER, P. M. & TOMBAL, B. 2014. Enzalutamide in metastatic prostate cancer before chemotherapy. *N Engl J Med,* 371**,** 424-33.

BELTRAN, H., PRANDI, D., MOSQUERA, J. M., BENELLI, M., PUCA, L., CYRTA, J., MAROTZ, C., GIANNOPOULOU, E., CHAKRAVARTHI, B. V., VARAMBALLY, S., TOMLINS, S. A., NANUS, D. M., TAGAWA, S. T., VAN ALLEN, E. M., ELEMENTO, O., SBONER, A., GARRAWAY, L. A., RUBIN, M. A. & DEMICHELIS, F. 2016. Divergent clonal evolution of castration-resistant neuroendocrine prostate cancer. *Nat Med,* 22**,** 298-305.

BELTRAN, H., RICKMAN, D. S., PARK, K., CHAE, S. S., SBONER, A., MACDONALD, T. Y., WANG, Y., SHEIKH, K. L., TERRY, S., TAGAWA, S. T., DHIR, R., NELSON, J. B., DE LA TAILLE, A., ALLORY, Y., GERSTEIN, M. B., PERNER, S., PIENTA, K. J., CHINNAIYAN, A. M., WANG, Y., COLLINS, C. C., GLEAVE, M. E., DEMICHELIS, F., NANUS, D. M. & RUBIN, M. A. 2011. Molecular characterization of neuroendocrine prostate cancer and identification of new drug targets. *Cancer Discov,* 1**,** 487-95.

BELTRAN, H., TOMLINS, S., APARICIO, A., ARORA, V., RICKMAN, D., AYALA, G., HUANG, J., TRUE, L., GLEAVE, M. E., SOULE, H., LOGOTHETIS, C. & RUBIN, M. A. 2014. Aggressive variants of castration-resistant prostate cancer. *Clin Cancer Res,* 20**,** 2846-50.

BENNETT, N. C., GARDINER, R. A., HOOPER, J. D., JOHNSON, D. W. & GOBE, G. C. 2010. Molecular cell biology of androgen receptor signalling. *Int J Biochem Cell Biol,* 42**,** 813-27.

BERGET, S. M., MOORE, C. & SHARP, P. A. 1977. Spliced segments at the 5' terminus of adenovirus 2 late mRNA. *Proc Natl Acad Sci U S A,* 74**,** 3171-5.

BERX, G., CLETON-JANSEN, A. M., STRUMANE, K., DE LEEUW, W. J., NOLLET, F., VAN ROY, F. & CORNELISSE, C. 1996. E-cadherin is inactivated in a majority of invasive human lobular breast cancers by truncation mutations throughout its extracellular domain. *Oncogene,* 13**,** 1919-1925.

BERX, G., STAES, K., VAN HENGEL, J., MOLEMANS, F., BUSSEMAKERS, M. J., VAN BOKHOVEN, A. & VAN ROY, F. 1995. Cloning and characterization of the human invasion suppressor gene E-cadherin (CDH1). *Genomics,* 2*6***,** 281-9.

BERX, G. & VAN ROY, F. 2001. The E-cadherin/catenin complex: an important gatekeeper in breast cancer tumorigenesis and malignant progression. *Breast Cancer Res,* 3**,** 289-93.

BEVAN, C. & PARKER, M. 1999. The role of coactivators in steroid hormone action. *Exp Cell Res,* 253**,** 349-56.

BEVERS, T. B., HELVIE, M., BONACCIO, E., CALHOUN, K. E., DALY, M. B., FARRAR, W. B., GARBER, J. E., GRAY, R., GREENBERG, C. C., GREENUP, R., HANSEN, N. M., HARRIS, R. E., HEERDT, A. S., HELSTEN, T., HODGKISS, L., HOYT, T. L., HUFF, J. G., JACOBS, L., LEHMAN, C. D., MONSEES, B., NIELL, B. L., PARKER, C. C., PEARLMAN, M., PHILPOTTS, L., SHEPARDSON, L. B., SMITH, M. L., STEIN, M., TUMYAN, L., WILLIAMS, C., BERGMAN, M. A. & KUMAR, R. 2018. Breast Cancer Screening and Diagnosis, Version 3.2018, NCCN Clinical Practice Guidelines in Oncology. *J Natl Compr Canc Netw,* 16**,** 1362-1389.

BIGNELL, G. R., WARREN, W., SEAL, S., TAKAHASHI, M., RAPLEY, E., BARFOOT, R., GREEN, H., BROWN, C., BIGGS, P. J., LAKHANI, S. R., JONES, C., HANSEN, J., BLAIR, E., HOFMANN, B., SIEBERT, R., TURNER, G., EVANS, D. G., SCHRANDER-STUMPEL, C., BEEMER, F. A., VAN DEN OUWELAND, A., HALLEY, D., DELPECH, B., CLEVELAND, M. G., LEIGH, I., LEISTI, J., RASMUSSEN, S., WALLACE, M. R., FENSKE, C., BANERJEE, P., OISO, N., CHAGGAR, R., MERRETT, S., LEONARD, N., HUBER, M., HOHL, D., CHAPMAN, P., BURN, J., SWIFT, S., SMITH, A., ASHWORTH, A. & STRATTON, M. R. 2000. Identification of the familial cylindromatosis tumour-suppressor gene. *Nature Genetics,* 2*5***,** 160-165.

BILLIAR, R. B., ZACHOS, N. C., BURCH, M. G., ALBRECHT, E. D. & PEPE, G. J. 2003. Up-Regulation of α-Inhibin Expression in the Fetal Ovary of Estrogen-Suppressed Baboons Is Associated with Impaired Fetal Ovarian Folliculogenesis1. *Biology of Reproduction,* 68**,** 1989-1996.

BJØRKLUND, S. S., PANDA, A., KUMAR, S., SEILER, M., ROBINSON, D., GHEEYA, J., YAO, M., ALNÆS, G. I. G., TOPPMEYER, D., RIIS, M., NAUME, B., BØRRESEN-DALE, A.-L., KRISTENSEN, V. N., GANESAN, S. & BHANOT, G. 2017. Widespread alternative exon usage in clinically distinct subtypes of Invasive Ductal Carcinoma. *Scientific Reports,* 7**,** 5568.

BLAMEY, R. W., ELLIS, I. O., PINDER, S. E., LEE, A. H. S., MACMILLAN, R. D., MORGAN, D. A. L., ROBERTSON, J. F. R., MITCHELL, M. J., BALL, G. R., HAYBITTLE, J. L. & ELSTON, C. W. 2007. Survival of invasive breast cancer according to the Nottingham Prognostic Index in cases diagnosed in 1990–1999. *European Journal of Cancer,* 43**,** 1548-1555.

BOCCALETTO, P., MACHNICKA, M. A., PURTA, E., PIĄTKOWSKI, P., BAGIŃSKI, B., WIRECKI, T. K., DE CRÉCY-LAGARD, V., ROSS, R., LIMBACH, P. A., KOTTER, A., HELM, M. & BUJNICKI, J. M. 2017. MODOMICS: a database of RNA modification pathways. 2017 update. *Nucleic Acids Research,* 46**,** D303-D307.

BOCQUEL, M. T., KUMAR, V., STRICKER, C., CHAMBON, P. & GRONEMEYER, H. 1989. The contribution of the N- and C-terminal regions of steroid receptors to activation of transcription is both receptor and cell-specific. *Nucleic Acids Res,* 17**,** 2581-95.

BOCZONADI, V. & MÄÄTTÄ, A. 2012. Annexin A9 is a periplakin interacting partner in membrane-targeted cytoskeletal linker protein complexes. *FEBS Lett,* 586**,** 3090-6.

BOHL, C. E., MILLER, D. D., CHEN, J., BELL, C. E. & DALTON, J. T. 2005. Structural basis for accommodation of nonsteroidal ligands in the androgen receptor. *J Biol Chem,* 280**,** 37747-54.

BOKAR, J. A. 2005. The biosynthesis and functional roles of methylated nucleosides in eukaryotic mRNA. *In:* GROSJEAN, H. (ed.) *Fine-Tuning of RNA Functions by Modification and Editing.* Berlin, Heidelberg: Springer Berlin Heidelberg.

BOSTWICK, D. G. & BRAWER, M. K. 1987. Prostatic intra-epithelial neoplasia and early invasion in prostate cancer. *Cancer,* 59**,** 788-94.

BOSTWICK, D. G., LIU, L., BRAWER, M. K. & QIAN, J. 2004. High-grade prostatic intraepithelial neoplasia. *Rev Urol,* 6**,** 171-9.

BOUKOVALA, M., SPETSIERIS, N. & EFSTATHIOU, E. 2019. Systemic Treatment of Prostate Cancer in Elderly Patients: Current Role and Safety Considerations of Androgen-Targeting Strategies. *Drugs & Aging,* 36**,** 701-717.

BRACKE, M. E., CHARLIER, C., BRUYNEEL, E. A., LABIT, C., MAREEL, M. M. & CASTRONOVO, V. 1994. Tamoxifen Restores the E-Cadherin Function in Human Breast Cancer MCF-7/6 Cells and Suppresses Their Invasive Phenotype. *Cancer Research,* 54**,** 4607-4609.

BRASCH, J., HARRISON, O. J., AHLSEN, G., CARNALLY, S. M., HENDERSON, R. M., HONIG, B. & SHAPIRO, L. 2011. Structure and Binding Mechanism of Vascular Endothelial Cadherin: A Divergent Classical Cadherin. *Journal of Molecular Biology,* 408**,** 57-73.

BRATT, O., DREVIN, L., AKRE, O., GARMO, H. & STATTIN, P. 2016. Family History and Probability of Prostate Cancer, Differentiated by Risk Category: A Nationwide Population-Based Study. *JNCI: Journal of the National Cancer Institute,* 108.

BRAY, F., FERLAY, J., SOERJOMATARAM, I., SIEGEL, R. L., TORRE, L. A. & JEMAL, A. 2018. Global cancer statistics 2018: GLOBOCAN estimates of incidence and mortality worldwide for 36 cancers in 185 countries. *CA Cancer J Clin,* 68**,** 394-424.

BRENNAN, K., OFFIAH, G., MCSHERRY, E. A. & HOPKINS, A. M. 2010. Tight junctions: a barrier to the initiation and progression of breast cancer? *J Biomed Biotechnol,* 2010**,** 460607.

BROHET, R. M., VELTHUIZEN, M. E., HOGERVORST, F. B., MEIJERS-HEIJBOER, H. E., SEYNAEVE, C., COLLEE, M. J., VERHOEF, S., AUSEMS, M. G., HOOGERBRUGGE, N., VAN ASPEREN, C. J., GOMEZ GARCIA, E., MENKO, F., OOSTERWIJK, J. C., DEVILEE, P., VAN'T VEER, L. J., VAN LEEUWEN, F. E., EASTON, D. F., ROOKUS,

M. A. & ANTONIOU, A. C. 2014. Breast and ovarian cancer risks in a large series of clinically ascertained families with a high proportion of BRCA1 and BRCA2 Dutch founder mutations. *J Med Genet,* 51**,** 98-107.
BROOKS, A. N., KILGOUR, E. & SMITH, P. D. 2012. Molecular pathways: fibroblast growth factor signaling: a new therapeutic opportunity in cancer. *Clin Cancer Res,* 18**,** 1855-62.
BURCHARDT, T., BURCHARDT, M., CHEN, M. W., CAO, Y., DE LA TAILLE, A., SHABSIGH, A., HAYEK, O., DORAI, T. & BUTTYAN, R. 1999. Transdifferentiation of prostate cancer cells to a neuroendocrine cell phenotype in vitro and in vivo. *J Urol,* 162**,** 1800-5.
BURGER, A. M. & SETH, A. K. 2004. The ubiquitin-mediated protein degradation pathway in cancer: therapeutic implications. *Eur J Cancer,* 40**,** 2217-29.
BURSTEIN, H. J. 2005. The distinctive nature of HER2-positive breast cancers. *N Engl J Med,* 353**,** 1652-4.
BUSSEMAKERS, M. J. G., VAN BOKHOVEN, A., TOMITA, K., JANSEN, C. F. J. & SCHALKEN, J. A. 2000. Complex cadherin expression in human prostate cancer cells. *International Journal of Cancer,* 85**,** 446-450.
CAI, C., LONG, J., HUANG, Q., HAN, Y., PENG, Y., GUO, C., LIU, S., CHEN, Y., SHEN, E., LONG, K., WANG, X., YU, J., SHEN, H. & ZENG, S. 2021. M6A "Writer" Gene METTL14: A Favorable Prognostic Biomarker and Correlated With Immune Infiltrates in Rectal Cancer. *Front Oncol,* 11**,** 615296.
CAI, J., YANG, F., ZHAN, H., SITU, J., LI, W., MAO, Y. & LUO, Y. 2019. RNA m(6)A Methyltransferase METTL3 Promotes The Growth Of Prostate Cancer By Regulating Hedgehog Pathway. *Onco Targets Ther,* 12**,** 9143-9152.
CAI, X., WANG, X., CAO, C., GAO, Y., ZHANG, S., YANG, Z., LIU, Y., ZHANG, X., ZHANG, W. & YE, L. 2018. HBXIP-elevated methyltransferase METTL3 promotes the progression of breast cancer via inhibiting tumor suppressor let-7g. *Cancer Lett,* 415**,** 11-19.
CAI, Y., YOUSEF, A., GRANDIS, J. R. & JOHNSON, D. E. 2020. NSAID therapy for PIK3CA-Altered colorectal, breast, and head and neck cancer. *Adv Biol Regul,* 75**,** 100653.
CAILLEAU, R., OLIVÉ, M. & CRUCIGER, Q. V. 1978. Long-term human breast carcinoma cell lines of metastatic origin: preliminary characterization. *In Vitro,* 14**,** 911-5.
CAILLEAU, R., YOUNG, R., OLIVÉ, M. & REEVES, W. J., JR. 1974. Breast tumor cell lines from pleural effusions. *J Natl Cancer Inst,* 53**,** 661-74.
CALDON, C. E. 2014. Estrogen signaling and the DNA damage response in hormone dependent breast cancers. *Front Oncol,* 4**,** 106.
CALZA, S., HALL, P., AUER, G., BJÖHLE, J., KLAAR, S., KRONENWETT, U., LIU, E. T., MILLER, L., PLONER, A., SMEDS, J., BERGH, J. & PAWITAN, Y. 2006. Intrinsic molecular signature of breast cancer in a population-based cohort of 412 patients. *Breast Cancer Research,* 8**,** R34.
CAMPBELL, H. K., MAIERS, J. L. & DEMALI, K. A. 2017. Interplay between tight junctions & adherens junctions. *Exp Cell Res,* 358**,** 39-44.
CAO, B., QI, Y., ZHANG, G., XU, D., ZHAN, Y., ALVAREZ, X., GUO, Z., FU, X., PLYMATE, S. R., SARTOR, O., ZHANG, H. & DONG, Y. 2014. Androgen receptor splice variants activating the full-length receptor in

mediating resistance to androgen-directed therapy. *Oncotarget,* 5**,** 1646-56.

CAO, Y. & MA, J. 2011. Body mass index, prostate cancer-specific mortality, and biochemical recurrence: a systematic review and meta-analysis. *Cancer Prev Res (Phila),* 4**,** 486-501.

CARDAMONE, M. D., BARDELLA, C., GUTIERREZ, A., DI CROCE, L., ROSENFELD, M. G., DI RENZO, M. F. & DE BORTOLI, M. 2009. ERalpha as ligand-independent activator of CDH-1 regulates determination and maintenance of epithelial morphology in breast cancer cells. *Proc Natl Acad Sci U S A,* 106**,** 7420-5.

CARDOSO, F., VAN'T VEER, L. J., BOGAERTS, J., SLAETS, L., VIALE, G., DELALOGE, S., PIERGA, J.-Y., BRAIN, E., CAUSERET, S., DELORENZI, M., GLAS, A. M., GOLFINOPOULOS, V., GOULIOTI, T., KNOX, S., MATOS, E., MEULEMANS, B., NEIJENHUIS, P. A., NITZ, U., PASSALACQUA, R., RAVDIN, P., RUBIO, I. T., SAGHATCHIAN, M., SMILDE, T. J., SOTIRIOU, C., STORK, L., STRAEHLE, C., THOMAS, G., THOMPSON, A. M., VAN DER HOEVEN, J. M., VUYLSTEKE, P., BERNARDS, R., TRYFONIDIS, K., RUTGERS, E. & PICCART, M. 2016. 70-Gene Signature as an Aid to Treatment Decisions in Early-Stage Breast Cancer. *New England Journal of Medicine,* 375**,** 717-729.

CARMELIET, P. 2005. VEGF as a key mediator of angiogenesis in cancer. *Oncology,* 69 Suppl 3**,** 4-10.

CASTELL, A., YAN, Q., FAWKNER, K., BAZZAR, W., ZHANG, F., WICKSTRÖM, M., ALZRIGAT, M., FRANCO, M., KRONA, C., CAMERON, D. P., DYBERG, C., OLSEN, T. K., VERSCHUT, V., SCHMIDT, L., LIM, S. Y., MAHMOUD, L., HYDBRING, P., LEHMANN, S., BARANELLO, L., NELANDER, S., JOHNSEN, J. I. & LARSSON, L. G. 2022. MYCMI-7: A Small MYC-Binding Compound that Inhibits MYC: MAX Interaction and Tumor Growth in a MYC-Dependent Manner. *Cancer Res Commun,* 2**,** 182-201.

CASTOSA, R., MARTINEZ-IGLESIAS, O., ROCA-LEMA, D., CASAS-PAIS, A., DIAZ-DIAZ, A., IGLESIAS, P., SANTAMARINA, I., GRANA, B., CALVO, L., VALLADARES-AYERBES, M., CONCHA, A. & FIGUEROA, A. 2018. Hakai overexpression effectively induces tumour progression and metastasis in vivo. *Sci Rep,* 8**,** 3466.

CATE, R. L., MATTALIANO, R. J., HESSION, C., TIZARD, R., FARBER, N. M., CHEUNG, A., NINFA, E. G., FREY, A. Z., GASH, D. J., CHOW, E. P., FISHER, R. A., BERTONIS, J. M., TORRES, G., WALLNER, B. P., RAMACHANDRAN, K. L., RAGIN, R. C., MANGANARO, T. F., MACLAUGHLIN, D. T. & DONAHOE, P. K. 1986. Isolation of the bovine and human genes for müllerian inhibiting substance and expression of the human gene in animal cells. *Cell,* 45**,** 685-698.

CELOJEVIC, D., PETERSEN, A., KARLSSON, J. O., BEHNDIG, A. & ZETTERBERG, M. 2011. Effects of 17β-estradiol on proliferation, cell viability and intracellular redox status in native human lens epithelial cells. *Mol Vis,* 17**,** 1987-96.

CERAMI, E., GAO, J., DOGRUSOZ, U., GROSS, B. E., SUMER, S. O., AKSOY, B. A., JACOBSEN, A., BYRNE, C. J., HEUER, M. L., LARSSON, E., ANTIPIN, Y., REVA, B., GOLDBERG, A. P., SANDER, C. & SCHULTZ, N. 2012. The cBio cancer genomics portal: an open

platform for exploring multidimensional cancer genomics data. *Cancer Discov,* 2**,** 401-4.

CGHFBC 2002. Collaborative Group on Hormonal Factors in Breast Cancer-Breast cancer and breastfeeding: collaborative reanalysis of individual data from 47 epidemiological studies in 30 countries, including 50 302 women with breast cancer and 96 973 women without the disease. *The Lancet,* 360**,** 187-195.

CHALHOUB, N. & BAKER, S. J. 2009. PTEN and the PI3-kinase pathway in cancer. *Annu Rev Pathol,* 4**,** 127-50.

CHAN, K., ROBERT, F., OERTLIN, C., KAPELLER-LIBERMANN, D., AVIZONIS, D., GUTIERREZ, J., HANDLY-SANTANA, A., DOUBROVIN, M., PARK, J., SCHOEPFER, C., DA SILVA, B., YAO, M., GORTON, F., SHI, J., THOMAS, C. J., BROWN, L. E., PORCO, J. A., JR., POLLAK, M., LARSSON, O., PELLETIER, J. & CHIO, I. I. C. 2019. eIF4A supports an oncogenic translation program in pancreatic ductal adenocarcinoma. *Nat Commun,* 10**,** 5151.

CHANDRASEKAR, T., YANG, J. C., GAO, A. C. & EVANS, C. P. 2015. Mechanisms of resistance in castration-resistant prostate cancer (CRPC). *Transl Androl Urol,* 4**,** 365-80.

CHEN, C. D., WELSBIE, D. S., TRAN, C., BAEK, S. H., CHEN, R., VESSELLA, R., ROSENFELD, M. G. & SAWYERS, C. L. 2004. Molecular determinants of resistance to antiandrogen therapy. *Nat Med,* 10**,** 33-9.

CHEN, K.-Y., LIU, X., BU, P., LIN, C.-S., RAKHILIN, N., LOCASALE, J. W. & SHEN, X. A metabolic signature of colon cancer initiating cells. 2014 36th annual international conference of the IEEE Engineering in Medicine and Biology Society, 2014. IEEE, 4759-4762.

CHEN, L. & WANG, X. 2018. Relationship between the genetic expression of WTAP and bladder cancer and patient prognosis. *Oncol Lett,* 16**,** 6966-6970.

CHEN, M., WEI, L., LAW, C. T., TSANG, F. H., SHEN, J., CHENG, C. L., TSANG, L. H., HO, D. W., CHIU, D. K., LEE, J. M., WONG, C. C., NG, I. O. & WONG, C. M. 2018. RNA N6-methyladenosine methyltransferase-like 3 promotes liver cancer progression through YTHDF2-dependent posttranscriptional silencing of SOCS2. *Hepatology,* 67**,** 2254-2270.

CHEN, R. C., RUMBLE, B., LOBLAW, A., FINELLI, A., EHDAIE, B., COOPERBERG, M. R., MORGAN, S. C., TYLDESLEY, S., HALUSCHAK, J. J. & TAN, W. 2016. Active surveillance for the management of localized prostate cancer (Cancer Care Ontario Guideline): American Society of Clinical Oncology clinical practice guideline endorsement. *Journal of Clinical Oncology,* 34.

CHICHE, J., ILC, K., LAFERRIERE, J., TROTTIER, E., DAYAN, F., MAZURE, N. M., BRAHIMI-HORN, M. C. & POUYSSÉGUR, J. 2009. Hypoxia-inducible carbonic anhydrase IX and XII promote tumor cell growth by counteracting acidosis through the regulation of the intracellular pH. *Cancer research,* 69**,** 358-368.

CHO-CHUNG, Y. S., CLAIR, T., BODWIN, J. S. & BERGHOFFER, B. 1981. Growth arrest and morphological change of human breast cancer cells by dibutyryl cyclic AMP and L-arginine. *Science,* 214**,** 77-9.

CHOI, Y. K., WOO, S. M., CHO, S. G., MOON, H. E., YUN, Y. J., KIM, J. W., NOH, D. Y., JANG, B. H., SHIN, Y. C., KIM, J. H., SHIN, H. D., PAEK,

S. H. & KO, S. G. 2013. Brain-metastatic triple-negative breast cancer cells regain growth ability by altering gene expression patterns. *Cancer Genomics Proteomics,* 10**,** 265-75.
CHRISTGEN, M., BALLMAIER, M., BRUCHHARDT, H., VON WASIELEWSKI, R., KREIPE, H. & LEHMANN, U. 2007. Identification of a distinct side population of cancer cells in the Cal-51 human breast carcinoma cell line. *Molecular and Cellular Biochemistry,* 306**,** 201-212.
CHRISTOFORI, G. & SEMB, H. 1999. The role of the cell-adhesion molecule E-cadherin as a tumour-suppressor gene. *Trends Biochem Sci,* 24**,** 73-6.
CLAESSENS, F., DENAYER, S., VAN TILBORGH, N., KERKHOFS, S., HELSEN, C. & HAELENS, A. 2008. Diverse roles of androgen receptor (AR) domains in AR-mediated signaling. *Nucl Recept Signal,* 6**,** e008.
CLAESSON-WELSH, L. & WELSH, M. 2013. VEGFA and tumour angiogenesis. *J Intern Med,* 273**,** 114-27.
CLAUS, E. B., RISCH, N. & THOMPSON, W. D. 1993. The calculation of breast cancer risk for women with a first degree family history of ovarian cancer. *Breast Cancer Res Treat,* 28**,** 115-20.
CLEARY, M. P. & GROSSMANN, M. E. 2009. Obesity and Breast Cancer: The Estrogen Connection. *Endocrinology,* 150**,** 2537-2542.
CLEGG, N., EROGLU, B., FERGUSON, C., ARNOLD, H., MOORMAN, A. & NELSON, P. S. 2002. Digital expression profiles of the prostate androgen-response program. *The Journal of Steroid Biochemistry and Molecular Biology,* 80**,** 13-23.
CLETON-JANSEN, A.-M. 2001. E-cadherin and loss of heterozygosity at chromosome 16 in breast carcinogenesis: different genetic pathways in ductal and lobular breast cancer? *Breast Cancer Research,* 4**,** 5.
COOPER, J. A., KANEKO, T. & LI, S. S. 2015. Cell regulation by phosphotyrosine-targeted ubiquitin ligases. *Mol Cell Biol,* 35**,** 1886-97.
CORNFORD, P., BELLMUNT, J., BOLLA, M., BRIERS, E., DE SANTIS, M., GROSS, T., HENRY, A. M., JONIAU, S., LAM, T. B., MASON, M. D., VAN DER POEL, H. G., VAN DER KWAST, T. H., ROUVIÈRE, O., WIEGEL, T. & MOTTET, N. 2017. EAU-ESTRO-SIOG Guidelines on Prostate Cancer. Part II: Treatment of Relapsing, Metastatic, and Castration-Resistant Prostate Cancer. *European Urology,* 71**,** 630-642.
COTTER, K. A., GALLON, J., UEBERSAX, N., RUBIN, P., MEYER, K. D., PISCUOGLIO, S., JAFFREY, S. R. & RUBIN, M. A. 2021. Mapping of m(6)A and Its Regulatory Targets in Prostate Cancer Reveals a METTL3-Low Induction of Therapy Resistance. *Mol Cancer Res,* 19**,** 1398-1411.
CRUK. 2017. *Lifetime risk of cancer* [Online]. Cancer Research UK. Available: https://www.cancerresearchuk.org/health-professional/cancer-statistics/risk/lifetime-risk#heading-One [Accessed 9 June 2023].
CURTIS, C., SHAH, S. P., CHIN, S. F., TURASHVILI, G., RUEDA, O. M., DUNNING, M. J., SPEED, D., LYNCH, A. G., SAMARAJIWA, S., YUAN, Y., GRÄF, S., HA, G., HAFFARI, G., BASHASHATI, A., RUSSELL, R., MCKINNEY, S., LANGERØD, A., GREEN, A., PROVENZANO, E., WISHART, G., PINDER, S., WATSON, P., MARKOWETZ, F., MURPHY, L., ELLIS, I., PURUSHOTHAM, A., BØRRESEN-DALE, A. L., BRENTON, J. D., TAVARÉ, S., CALDAS, C. & APARICIO, S. 2012.

The genomic and transcriptomic architecture of 2,000 breast tumours reveals novel subgroups. *Nature,* 486**,** 346-52.
CUSSENOT, O., BERTHON, P., BERGER, R., MOWSZOWICZ, I., FAILLE, A., HOJMAN, F., TEILLAC, P., LE DUC, A. & CALVO, F. 1991. Immortalization of human adult normal prostatic epithelial cells by liposomes containing large T-SV40 gene. *J Urol,* 146**,** 881-6.
CUTRESS, M. L., WHITAKER, H. C., MILLS, I. G., STEWART, M. & NEAL, D. E. 2008. Structural basis for the nuclear import of the human androgen receptor. *J Cell Sci,* 121**,** 957-68.
DAGENAIS, G. R., LEONG, D. P., RANGARAJAN, S., LANAS, F., LOPEZ-JARAMILLO, P., GUPTA, R., DIAZ, R., AVEZUM, A., OLIVEIRA, G. B. F., WIELGOSZ, A., PARAMBATH, S. R., MONY, P., ALHABIB, K. F., TEMIZHAN, A., ISMAIL, N., CHIFAMBA, J., YEATES, K., KHATIB, R., RAHMAN, O., ZATONSKA, K., KAZMI, K., WEI, L., ZHU, J., ROSENGREN, A., VIJAYAKUMAR, K., KAUR, M., MOHAN, V., YUSUFALI, A., KELISHADI, R., TEO, K. K., JOSEPH, P. & YUSUF, S. 2020. Variations in common diseases, hospital admissions, and deaths in middle-aged adults in 21 countries from five continents (PURE): a prospective cohort study. *The Lancet,* 395**,** 785-794.
DAI, D., WANG, H., ZHU, L., JIN, H. & WANG, X. 2018. N6-methyladenosine links RNA metabolism to cancer progression. *Cell Death Dis,* 9**,** 124.
DAI, S., WANG, C., ZHANG, C., FENG, L., ZHANG, W., ZHOU, X., HE, Y., XIA, X., CHEN, B. & SONG, W. 2022. PTB: Not just a polypyrimidine tract-binding protein. *Journal of Cellular Physiology,* 237**,** 2357-2373.
DAI, X., LI, T., BAI, Z., YANG, Y., LIU, X., ZHAN, J. & SHI, B. 2015. Breast cancer intrinsic subtype classification, clinical use and future trends. *Am J Cancer Res,* 5**,** 2929-43.
DANAEI, G., VANDER HOORN, S., LOPEZ, A. D., MURRAY, C. J. L. & EZZATI, M. 2005. Causes of cancer in the world: comparative risk assessment of nine behavioural and environmental risk factors. *The Lancet,* 366**,** 1784-1793.
DANG, CHI V. 2012. MYC on the Path to Cancer. *Cell,* 149**,** 22-35.
DARNELL, R. B., KE, S. & DARNELL, J. E., JR. 2018. Pre-mRNA processing includes N(6) methylation of adenosine residues that are retained in mRNA exons and the fallacy of "RNA epigenetics". *RNA,* 24**,** 262-267.
DAVIDSON, D., BOSTWICK, D. G., QIAN, J., WOLLAN, P. C., OESTERLING, J. E., RUDDERS, R. A., SIROKY, M. & STILMANT, M. 1995. Prostatic intraepithelial neoplasia is a risk factor for adenocarcinoma: predictive accuracy in needle biopsies. *J Urol,* 154**,** 1295-9.
DAVIS, M. A., IRETON, R. C. & REYNOLDS, A. B. 2003. A core function for p120-catenin in cadherin turnover. *The Journal of Cell Biology,* 163**,** 525-534.
DE BROT, S., NTEKIM, A., CARDENAS, R., JAMES, V., ALLEGRUCCI, C., HEERY, D. M., BATES, D. O., ØDUM, N., PERSSON, J. L. & MONGAN, N. P. 2015. Regulation of vascular endothelial growth factor in prostate cancer. *Endocr Relat Cancer,* 22**,** R107-23.
DE GREVE, J., SERMIJN, E., DE BRAKELEER, S., REN, Z. & TEUGELS, E. 2008. Hereditary breast cancer: from bench to bedside. *Curr Opin Oncol,* 20**,** 605-13.
DE ROOIJ, M., HAMOEN, E. H. J., WITJES, J. A., BARENTSZ, J. O. & ROVERS, M. M. 2016. Accuracy of Magnetic Resonance Imaging for

Local Staging of Prostate Cancer: A Diagnostic Meta-analysis. *European Urology,* 70**,** 233-245.
DEEP, G., GANGAR, S. C., AGARWAL, C. & AGARWAL, R. 2011. Role of E-cadherin in antimigratory and antiinvasive efficacy of silibinin in prostate cancer cells. *Cancer Prev Res (Phila),* 4**,** 1222-32.
DEHAY, B., BOVÉ, J., RODRÍGUEZ-MUELA, N., PERIER, C., RECASENS, A., BOYA, P. & VILA, M. 2010. Pathogenic lysosomal depletion in Parkinson's disease. *J Neurosci,* 30**,** 12535-44.
DEHM, S. M. & TINDALL, D. J. 2011. Alternatively spliced androgen receptor variants. *Endocr Relat Cancer,* 18**,** R183-96.
DEL GIUDICE, M., FOSTER, J. G., PEIRONE, S., RISSONE, A., CAIZZI, L., GAUDINO, F., PARLATO, C., ANSELMI, F., ARKELL, R., GUARRERA, S., OLIVIERO, S., BASSO, G., RAJAN, P. & CEREDA, M. 2022. FOXA1 regulates alternative splicing in prostate cancer. *Cell Rep,* 40**,** 111404.
DENG, R., CHENG, Y., YE, S., ZHANG, J., HUANG, R., LI, P., LIU, H., DENG, Q., WU, X., LAN, P. & DENG, Y. 2019. m(6)A methyltransferase METTL3 suppresses colorectal cancer proliferation and migration through p38/ERK pathways. *Onco Targets Ther,* 12**,** 4391-4402.
DENKERT, C., LIEDTKE, C., TUTT, A. & VON MINCKWITZ, G. 2017. Molecular alterations in triple-negative breast cancer—the road to new treatment strategies. *The Lancet,* 389**,** 2430-2442.
DEROO, B. J. & KORACH, K. S. 2006. Estrogen receptors and human disease. *The Journal of Clinical Investigation,* 116**,** 561-570.
DESANTIS, C., SIEGEL, R., BANDI, P. & JEMAL, A. 2011. Breast cancer statistics, 2011. *CA Cancer J Clin,* 61**,** 409-18.
DESROSIERS, R., FRIDERICI, K. & ROTTMAN, F. 1974. Identification of Methylated Nucleosides in Messenger RNA from Novikoff Hepatoma Cells. *Proceedings of the National Academy of Sciences,* 71**,** 3971-3975.
DHAR, S., KUMAR, A., GOMEZ, C. R., AKHTAR, I., HANCOCK, J. C., LAGE, J. M., POUND, C. R. & LEVENSON, A. S. 2017. MTA1-activated Epi-microRNA-22 regulates E-cadherin and prostate cancer invasiveness. *FEBS Letters,* 591**,** 924-933.
DHIMAN, V. K., BOLT, M. J. & WHITE, K. P. 2018. Nuclear receptors in cancer - uncovering new and evolving roles through genomic analysis. *Nat Rev Genet,* 19**,** 160-174.
DI LORETO, C., REIS, F. M., CATALDI, P., ZUIANI, C., LUISI, S., BELTRAMI, C. A. & PETRAGLIA, F. 1999. Human mammary gland and breast carcinoma contain immunoreactive inhibin/activin subunits: evidence for a secretion into cystic fluid. *Eur J Endocrinol,* 141**,** 190-4.
DIAZ-DIAZ, A., CASAS-PAIS, A., CALAMIA, V., CASTOSA, R., MARTINEZ-IGLESIAS, O., ROCA-LEMA, D., SANTAMARINA, I., VALLADARES-AYERBES, M., CALVO, L., CHANTADA, V. & FIGUEROA, A. 2017. Proteomic Analysis of the E3 Ubiquitin-Ligase Hakai Highlights a Role in Plasticity of the Cytoskeleton Dynamics and in the Proteasome System. *J Proteome Res,* 16**,** 2773-2788.
DICOLANDREA, T., KARASHIMA, T., MÄÄTTÄ, A. & WATT, F. M. 2000. Subcellular distribution of envoplakin and periplakin: insights into their role as precursors of the epidermal cornified envelope. *J Cell Biol,* 151**,** 573-86.

DIENSTMANN, R., RODON, J., PRAT, A., PEREZ-GARCIA, J., ADAMO, B., FELIP, E., CORTES, J., IAFRATE, A. J., NUCIFORO, P. & TABERNERO, J. 2014. Genomic aberrations in the FGFR pathway: opportunities for targeted therapies in solid tumors. *Ann Oncol,* 25**,** 552-563.

DOBIN, A., DAVIS, C. A., SCHLESINGER, F., DRENKOW, J., ZALESKI, C., JHA, S., BATUT, P., CHAISSON, M. & GINGERAS, T. R. 2013. STAR: ultrafast universal RNA-seq aligner. *Bioinformatics,* 29**,** 15-21.

DOMINISSINI, D., MOSHITCH-MOSHKOVITZ, S., SCHWARTZ, S., SALMON-DIVON, M., UNGAR, L., OSENBERG, S., CESARKAS, K., JACOB-HIRSCH, J., AMARIGLIO, N., KUPIEC, M., SOREK, R. & RECHAVI, G. 2012. Topology of the human and mouse m6A RNA methylomes revealed by m6A-seq. *Nature,* 485**,** 201.

DONAHOE, P. K., FULLER, A. F., JR., SCULLY, R. E., GUY, S. R. & BUDZIK, G. P. 1981. Mullerian inhibiting substance inhibits growth of a human ovarian cancer in nude mice. *Ann Surg,* 194**,** 472-80.

DRUMMOND, A. E. & FULLER, P. J. 2012. Activin and inhibin, estrogens and NFκB, play roles in ovarian tumourigenesis is there crosstalk? *Molecular and Cellular Endocrinology,* 359**,** 85-91.

DU, H., ZHAO, Y., HE, J., ZHANG, Y., XI, H., LIU, M., MA, J. & WU, L. 2016. YTHDF2 destabilizes m6A-containing RNA through direct recruitment of the CCR4–NOT deadenylase complex. *Nature Communications,* 7**,** 12626.

DU, W., LIU, X., FAN, G., ZHAO, X., SUN, Y., WANG, T., ZHAO, R., WANG, G., ZHAO, C., ZHU, Y., YE, F., JIN, X., ZHANG, F., ZHONG, Z. & LI, X. 2014. From cell membrane to the nucleus: an emerging role of E-cadherin in gene transcriptional regulation. *J Cell Mol Med,* 18**,** 1712-9.

DU, Y., YUAN, Y., XU, L., ZHAO, F., WANG, W., XU, Y. & TIAN, X. 2022. Discovery of METTL3 Small Molecule Inhibitors by Virtual Screening of Natural Products. *Front Pharmacol,* 13**,** 878135.

DUQUE, J. L., LOUGHLIN, K. R., ADAM, R. M., KANTOFF, P. W., ZURAKOWSKI, D. & FREEMAN, M. R. 1999. Plasma levels of vascular endothelial growth factor are increased in patients with metastatic prostate cancer. *Urology,* 54**,** 523-7.

EDWARDS, J., KRISHNA, N. S., GRIGOR, K. M. & BARTLETT, J. M. 2003. Androgen receptor gene amplification and protein expression in hormone refractory prostate cancer. *Br J Cancer,* 89**,** 552-6.

EIDELMAN, E., TWUM-AMPOFO, J., ANSARI, J. & SIDDIQUI, M. M. 2017. The Metabolic Phenotype of Prostate Cancer. *Front Oncol,* 7**,** 131.

EISERMANN, K. & FRAIZER, G. 2017. The Androgen Receptor and VEGF: Mechanisms of Androgen-Regulated Angiogenesis in Prostate Cancer. *Cancers (Basel),* 9.

ELLIS, I. O., GALEA, M., BROUGHTON, N., LOCKER, A., BLAMEY, R. W. & ELSTON, C. W. 1992. Pathological prognostic factors in breast cancer. II. Histological type. Relationship with survival in a large study with long-term follow-up. *Histopathology,* 20**,** 479-489.

ELLWOOD-YEN, K., GRAEBER, T. G., WONGVIPAT, J., IRUELA-ARISPE, M. L., ZHANG, J., MATUSIK, R., THOMAS, G. V. & SAWYERS, C. L. 2003. Myc-driven murine prostate cancer shares molecular features with human prostate tumors. *Cancer Cell,* 4**,** 223-38.

ELSTON, C. W. & ELLIS, I. O. 1991. Pathological prognostic factors in breast cancer. I. The value of histological grade in breast cancer: experience from a large study with long-term follow-up. *Histopathology,* 19**,** 403-10.
ELSTON, C. W. & ELLIS, I. O. 2002. Pathological prognostic factors in breast cancer. I. The value of histological grade in breast cancer: experience from a large study with long-term follow-up. C. W. Elston & I. O. Ellis. Histopathology 1991; 19; 403–410. *Histopathology,* 41**,** 151-151.
ELSTRODT, F., HOLLESTELLE, A., NAGEL, J. H., GORIN, M., WASIELEWSKI, M., VAN DEN OUWELAND, A., MERAJVER, S. D., ETHIER, S. P. & SCHUTTE, M. 2006. BRCA1 mutation analysis of 41 human breast cancer cell lines reveals three new deleterious mutants. *Cancer Res,* 66**,** 41-5.
EPSTEIN, J. I. 2000. Gleason score 2-4 adenocarcinoma of the prostate on needle biopsy: a diagnosis that should not be made. *Am J Surg Pathol,* 24**,** 477-8.
EPSTEIN, J. I., ALLSBROOK, W. C., JR., AMIN, M. B. & EGEVAD, L. L. 2005. The 2005 International Society of Urological Pathology (ISUP) Consensus Conference on Gleason Grading of Prostatic Carcinoma. *Am J Surg Pathol,* 29**,** 1228-42.
EPSTEIN, J. I., EGEVAD, L., AMIN, M. B., DELAHUNT, B., SRIGLEY, J. R. & HUMPHREY, P. A. 2016. The 2014 International Society of Urological Pathology (ISUP) Consensus Conference on Gleason Grading of Prostatic Carcinoma: Definition of Grading Patterns and Proposal for a New Grading System. *Am J Surg Pathol,* 40**,** 244-52.
EROLES, P., BOSCH, A., ALEJANDRO PÉREZ-FIDALGO, J. & LLUCH, A. 2012. Molecular biology in breast cancer: Intrinsic subtypes and signaling pathways. *Cancer Treatment Reviews,* 38**,** 698-707.
EVANS, A. J. 2018. Treatment effects in prostate cancer. *Mod Pathol,* 31**,** S110-121.
FAN, H. N., CHEN, Z. Y., CHEN, X. Y., CHEN, M., YI, Y. C., ZHU, J. S. & ZHANG, J. 2022. METTL14-mediated m(6)A modification of circORC5 suppresses gastric cancer progression by regulating miR-30c-2-3p/AKT1S1 axis. *Mol Cancer,* 21**,** 51.
FENG, W., GENTLES, A., NAIR, R. V., HUANG, M., LIN, Y., LEE, C. Y., CAI, S., SCHEEREN, F. A., KUO, A. H. & DIEHN, M. 2014. Targeting unique metabolic properties of breast tumor initiating cells. *Stem cells,* 32**,** 1734-1745.
FENG, Y., SPEZIA, M., HUANG, S., YUAN, C., ZENG, Z., ZHANG, L., JI, X., LIU, W., HUANG, B., LUO, W., LIU, B., LEI, Y., DU, S., VUPPALAPATI, A., LUU, H. H., HAYDON, R. C., HE, T. C. & REN, G. 2018. Breast cancer development and progression: Risk factors, cancer stem cells, signaling pathways, genomics, and molecular pathogenesis. *Genes Dis,* 5**,** 77-106.
FERLAY, J., COLOMBET, M., SOERJOMATARAM, I., MATHERS, C., PARKIN, D. M., PIÑEROS, M., ZNAOR, A. & BRAY, F. 2019. Estimating the global cancer incidence and mortality in 2018: GLOBOCAN sources and methods. *International Journal of Cancer,* 144**,** 1941-1953.
FERLAY, J., SOERJOMATARAM, I., DIKSHIT, R., ESER, S., MATHERS, C., REBELO, M., PARKIN, D. M., FORMAN, D. & BRAY, F. 2015. Cancer incidence and mortality worldwide: sources, methods and major patterns in GLOBOCAN 2012. *Int J Cancer,* 136**,** E359-86.

FIGUEROA, A., FUJITA, Y. & GOROSPE, M. 2009a. Hacking RNA: Hakai promotes tumorigenesis by enhancing the RNA-binding function of PSF. *Cell Cycle,* 8**,** 3648-51.

FIGUEROA, A., KOTANI, H., TODA, Y., MAZAN-MAMCZARZ, K., MUELLER, E. C., OTTO, A., DISCH, L., NORMAN, M., RAMDASI, R. M., KESHTGAR, M., GOROSPE, M. & FUJITA, Y. 2009b. Novel roles of hakai in cell proliferation and oncogenesis. *Mol Biol Cell,* 20**,** 3533-42.

FIORENTINO, F., MENNA, M., ROTILI, D., VALENTE, S. & MAI, A. 2023. METTL3 from Target Validation to the First Small-Molecule Inhibitors: A Medicinal Chemistry Journey. *J Med Chem,* 66**,** 1654-1677.

FIZAZI, K., TRAN, N., FEIN, L., MATSUBARA, N., RODRIGUEZ-ANTOLIN, A., ALEKSEEV, B. Y., ÖZGÜROĞLU, M., YE, D., FEYERABEND, S., PROTHEROE, A., DE PORRE, P., KHEOH, T., PARK, Y. C., TODD, M. B. & CHI, K. N. 2017. Abiraterone plus Prednisone in Metastatic, Castration-Sensitive Prostate Cancer. *N Engl J Med,* 377**,** 352-360.

FLUG, M. & KÖPF-MAIER, P. 1995. The basement membrane and its involvement in carcinoma cell invasion. *Acta Anat (Basel),* 152**,** 69-84.

FOLMES, C. D., NELSON, T. J., MARTINEZ-FERNANDEZ, A., ARRELL, D. K., LINDOR, J. Z., DZEJA, P. P., IKEDA, Y., PEREZ-TERZIC, C. & TERZIC, A. 2011. Somatic oxidative bioenergetics transitions into pluripotency-dependent glycolysis to facilitate nuclear reprogramming. *Cell metabolism,* 14**,** 264-271.

FOROOTAN, S. S., BUTLER, J. M., GARDENER, D., JONES, D., BAIRD, A. E., DODSON, A., DARBY, A., KENNY, J., HALL, N., COSSINS, A. R., FOSTER, C. S. & GOSDEN, C. M. 2016. Transcriptome sequencing of human breast cancer reveals aberrant intronic transcription in amplicons and dysregulation of alternative splicing with major therapeutic implications. *Int J Oncol,* 48**,** 130-44.

FORWARD, D. P., CHEUNG, K. L., JACKSON, L. & ROBERTSON, J. F. R. 2004. Clinical and endocrine data for goserelin plus anastrozole as second-line endocrine therapy for premenopausal advanced breast cancer. *British Journal of Cancer,* 90**,** 590-594.

FOURNIER, P. G., JUÁREZ, P., JIANG, G., CLINES, G. A., NIEWOLNA, M., KIM, H. S., WALTON, H. W., PENG, X. H., LIU, Y., MOHAMMAD, K. S., WELLS, C. D., CHIRGWIN, J. M. & GUISE, T. A. 2015. The TGF-β Signaling Regulator PMEPA1 Suppresses Prostate Cancer Metastases to Bone. *Cancer Cell,* 27**,** 809-21.

FRANCIS, P. A., REGAN, M. M., FLEMING, G. F., LÁNG, I., CIRUELOS, E., BELLET, M., BONNEFOI, H. R., CLIMENT, M. A., DA PRADA, G. A., BURSTEIN, H. J., MARTINO, S., DAVIDSON, N. E., GEYER, C. E., WALLEY, B. A., COLEMAN, R., KERBRAT, P., BUCHHOLZ, S., INGLE, J. N., WINER, E. P., RABAGLIO-PORETTI, M., MAIBACH, R., RUEPP, B., GIOBBIE-HURDER, A., PRICE, K. N., COLLEONI, M., VIALE, G., COATES, A. S., GOLDHIRSCH, A. & GELBER, R. D. 2014. Adjuvant Ovarian Suppression in Premenopausal Breast Cancer. *New England Journal of Medicine,* 372**,** 436-446.

FRANKS, L. M. 1954. Latent carcinoma of the prostate. *The Journal of Pathology and Bacteriology,* 68**,** 603-616.

FRAY, R. G. & SIMPSON, G. G. 2015. The Arabidopsis epitranscriptome. *Curr Opin Plant Biol,* 27**,** 17-21.

FRESNO VARA, J. A., CASADO, E., DE CASTRO, J., CEJAS, P., BELDA-INIESTA, C. & GONZÁLEZ-BARÓN, M. 2004. PI3K/Akt signalling pathway and cancer. *Cancer Treat Rev,* 30**,** 193-204.

FUJITA, Y., KRAUSE, G., SCHEFFNER, M., ZECHNER, D., LEDDY, H. E., BEHRENS, J., SOMMER, T. & BIRCHMEIER, W. 2002. Hakai, a c-Cbl-like protein, ubiquitinates and induces endocytosis of the E-cadherin complex. *Nat Cell Biol,* 4**,** 222-31.

FULLER, A. F., JR., KRANE, I. M., BUDZIK, G. P. & DONAHOE, P. K. 1985. Mullerian inhibiting substance reduction of colony growth of human gynecologic cancers in a stem cell assay. *Gynecol Oncol,* 22**,** 135-48.

FUSTIN, J.-M., DOI, M., YAMAGUCHI, Y., HIDA, H., NISHIMURA, S., YOSHIDA, M., ISAGAWA, T., MORIOKA, MASAKI S., KAKEYA, H., MANABE, I. & OKAMURA, H. 2013. RNA-Methylation-Dependent RNA Processing Controls the Speed of the Circadian Clock. *Cell,* 155**,** 793-806.

GAIL, M. H., BRINTON, L. A., BYAR, D. P., CORLE, D. K., GREEN, S. B., SCHAIRER, C. & MULVIHILL, J. J. 1989. Projecting Individualized Probabilities of Developing Breast Cancer for White Females Who Are Being Examined Annually. *JNCI: Journal of the National Cancer Institute,* 81**,** 1879-1886.

GALEA, M. H., BLAMEY, R. W., ELSTON, C. E. & ELLIS, I. O. 1992. The Nottingham Prognostic Index in primary breast cancer. *Breast Cancer Res Treat,* 22**,** 207-19.

GANN, P. H. 2002. Risk factors for prostate cancer. *Reviews in urology,* 4 Suppl 5**,** S3-S10.

GANN, P. H., MA, J., GIOVANNUCCI, E., WILLETT, W., SACKS, F. M., HENNEKENS, C. H. & STAMPFER, M. J. 1999. Lower prostate cancer risk in men with elevated plasma lycopene levels: results of a prospective analysis. *Cancer Res,* 59**,** 1225-30.

GAO, J., AKSOY, B. A., DOGRUSOZ, U., DRESDNER, G., GROSS, B., SUMER, S. O., SUN, Y., JACOBSEN, A., SINHA, R., LARSSON, E., CERAMI, E., SANDER, C. & SCHULTZ, N. 2013. Integrative analysis of complex cancer genomics and clinical profiles using the cBioPortal. *Sci Signal,* 6**,** pl1.

GEBRE-MEDHIN, M., KINDBLOM, L.-G., WENNBO, H., TÖRNELL, J. & MEIS-KINDBLOM, J. M. 2001. Growth hormone receptor is expressed in human breast cancer. *The American journal of pathology,* 158**,** 1217-1222.

GERHARDT, J., MONTANI, M., WILD, P., BEER, M., HUBER, F., HERMANNS, T., MÜNTENER, M. & KRISTIANSEN, G. 2012. FOXA1 promotes tumor progression in prostate cancer and represents a novel hallmark of castration-resistant prostate cancer. *Am J Pathol,* 180**,** 848-61.

GERLO, S., KOOIJMAN, R., BECK, I. M., KOLMUS, K., SPOOREN, A. & HAEGEMAN, G. 2011. Cyclic AMP: a selective modulator of NF-κB action. *Cell Mol Life Sci,* 68**,** 3823-41.

GERMAIN, P., STAELS, B., DACQUET, C., SPEDDING, M. & LAUDET, V. 2006. Overview of nomenclature of nuclear receptors. *Pharmacol Rev,* 58**,** 685-704.

GEULA, S., MOSHITCH-MOSHKOVITZ, S., DOMINISSINI, D., MANSOUR, A. A., KOL, N., SALMON-DIVON, M., HERSHKOVITZ, V., PEER, E.,

MOR, N., MANOR, Y. S., BEN-HAIM, M. S., EYAL, E., YUNGER, S., PINTO, Y., JAITIN, D. A., VIUKOV, S., RAIS, Y., KRUPALNIK, V., CHOMSKY, E., ZERBIB, M., MAZA, I., RECHAVI, Y., MASSARWA, R., HANNA, S., AMIT, I., LEVANON, E. Y., AMARIGLIO, N., STERN-GINOSSAR, N., NOVERSHTERN, N., RECHAVI, G. & HANNA, J. H. 2015. Stem cells. m6A mRNA methylation facilitates resolution of naive pluripotency toward differentiation. *Science,* 347**,** 1002-6.

GIATROMANOLAKI, A., KALAMIDA, D., SIVRIDIS, E., KARAGOUNIS, I. V., GATTER, K. C., HARRIS, A. L. & KOUKOURAKIS, M. I. 2015. Increased expression of transcription factor EB (TFEB) is associated with autophagy, migratory phenotype and poor prognosis in non-small cell lung cancer. *Lung Cancer,* 90**,** 98-105.

GIATROMANOLAKI, A., SIVRIDIS, E., KALAMIDA, D. & KOUKOURAKIS, M. I. 2017. Transcription Factor EB Expression in Early Breast Cancer Relates to Lysosomal/Autophagosomal Markers and Prognosis. *Clinical Breast Cancer,* 17**,** e119-e125.

GILLESSEN, S., ATTARD, G., BEER, T. M., BELTRAN, H., BJARTELL, A., BOSSI, A., BRIGANTI, A., BRISTOW, R. G., CHI, K. N., CLARKE, N., DAVIS, I. D., DE BONO, J., DRAKE, C. G., DURAN, I., EELES, R., EFSTATHIOU, E., EVANS, C. P., FANTI, S., FENG, F. Y., FIZAZI, K., FRYDENBERG, M., GLEAVE, M., HALABI, S., HEIDENREICH, A., HEINRICH, D., HIGANO, C. T. S., HOFMAN, M. S., HUSSAIN, M., JAMES, N., KANESVARAN, R., KANTOFF, P., KHAULI, R. B., LEIBOWITZ, R., LOGOTHETIS, C., MALUF, F., MILLMAN, R., MORGANS, A. K., MORRIS, M. J., MOTTET, N., MRABTI, H., MURPHY, D. G., MURTHY, V., OH, W. K., OST, P., O'SULLIVAN, J. M., PADHANI, A. R., PARKER, C., POON, D. M. C., PRITCHARD, C. C., REITER, R. E., ROACH, M., RUBIN, M., RYAN, C. J., SAAD, F., SADE, J. P., SARTOR, O., SCHER, H. I., SHORE, N., SMALL, E., SMITH, M., SOULE, H., STERNBERG, C. N., STEUBER, T., SUZUKI, H., SWEENEY, C., SYDES, M. R., TAPLIN, M. E., TOMBAL, B., TÜRKERI, L., VAN OORT, I., ZAPATERO, A. & OMLIN, A. 2020. Management of Patients with Advanced Prostate Cancer: Report of the Advanced Prostate Cancer Consensus Conference 2019. *Eur Urol,* 77**,** 508-547.

GILLETT, C. E., MILES, D. W., RYDER, K., SKILTON, D., LIEBMAN, R. D., SPRINGALL, R. J., BARNES, D. M. & HANBY, A. M. 2001. Retention of the expression of E-cadherin and catenins is associated with shorter survival in grade III ductal carcinoma of the breast. *J Pathol,* 193**,** 433-41.

GINGRAS, A. C., RAUGHT, B. & SONENBERG, N. 1999. eIF4 initiation factors: effectors of mRNA recruitment to ribosomes and regulators of translation. *Annu Rev Biochem,* 68**,** 913-63.

GIOELI, D., MANDELL, J. W., PETRONI, G. R., FRIERSON, H. F., JR. & WEBER, M. J. 1999. Activation of mitogen-activated protein kinase associated with prostate cancer progression. *Cancer Res,* 59**,** 279-84.

GIOVANNUCCI, E., LIU, Y., PLATZ, E. A., STAMPFER, M. J. & WILLETT, W. C. 2007. Risk factors for prostate cancer incidence and progression in the health professionals follow-up study. *International Journal of Cancer,* 121**,** 1571-1578.

GIOVANNUCCI, E., POLLAK, M. N., PLATZ, E. A., WILLETT, W. C., STAMPFER, M. J., MAJEED, N., COLDITZ, G. A., SPEIZER, F. E. & HANKINSON, S. E. 2000. A prospective study of plasma insulin-like growth factor-1 and binding protein-3 and risk of colorectal neoplasia in women. *Cancer Epidemiology Biomarkers & Prevention,* 9**,** 345-349.

GJYREZI, A., GALLETTI, G., ZHANG, J., WORROLL, D., SIGOUROS, M., KIM, S., COOLEY, V., BALLMAN, K. V., OCEAN, A. J., SHAH, M. A., SCANDURA, J. M., SBONER, A., NANUS, D. M., BELTRAN, H., TAGAWA, S. & GIANNAKAKOU, P. 2021. Androgen receptor variant shows heterogeneous expression in prostate cancer according to differentiation stage. *Commun Biol,* 4**,** 785.

GLEASON, D. 1966. Classification of prostatic carcinomas. *Cancer chemotherapy reports. Part 1,* 50.

GLEASON, D. F. & MELLINGER, G. T. 1974. Prediction of prognosis for prostatic adenocarcinoma by combined histological grading and clinical staging. *J Urol,* 111**,** 58-64.

GLICKMAN, M. H. & CIECHANOVER, A. 2002. The ubiquitin-proteasome proteolytic pathway: destruction for the sake of construction. *Physiological reviews*.

GOLDBERG, A. L., STEIN, R. & ADAMS, J. 1995. New insights into proteasome function: from archaebacteria to drug development. *Chemistry & biology,* 2**,** 503-508.

GOLDHIRSCH, A., WOOD, W. C., COATES, A. S., GELBER, R. D., THURLIMANN, B. & SENN, H. J. 2011. Strategies for subtypes--dealing with the diversity of breast cancer: highlights of the St. Gallen International Expert Consensus on the Primary Therapy of Early Breast Cancer 2011. *Ann Oncol,* 22**,** 1736-47.

GOLDMAN, M. J., CRAFT, B., HASTIE, M., REPEČKA, K., MCDADE, F., KAMATH, A., BANERJEE, A., LUO, Y., ROGERS, D., BROOKS, A. N., ZHU, J. & HAUSSLER, D. 2020. Visualizing and interpreting cancer genomics data via the Xena platform. *Nature Biotechnology,* 38**,** 675-678.

GONG, E. Y., PARK, E. & LEE, K. 2010. Hakai acts as a coregulator of estrogen receptor alpha in breast cancer cells. *Cancer Sci,* 101**,** 2019-25.

GORDETSKY, J. & EPSTEIN, J. 2016. Grading of prostatic adenocarcinoma: current state and prognostic implications. *Diagnostic pathology,* 11**,** 25-25.

GOTTLIEB, B., BEITEL, L. K., NADARAJAH, A., PALIOURAS, M. & TRIFIRO, M. 2012. The androgen receptor gene mutations database: 2012 update. *Hum Mutat,* 33**,** 887-94.

GOULDING, H., PINDER, S., CANNON, P., PEARSON, D., NICHOLSON, R., SNEAD, D., BELL, J., ELSTON, C. W., ROBERTSON, J. F., BLAMEY, R. W. & ET AL. 1995. A new immunohistochemical antibody for the assessment of estrogen receptor status on routine formalin-fixed tissue samples. *Hum Pathol,* 26**,** 291-4.

GRAFF, J. R., KONICEK, B. W., VINCENT, T. M., LYNCH, R. L., MONTEITH, D., WEIR, S. N., SCHWIER, P., CAPEN, A., GOODE, R. L., DOWLESS, M. S., CHEN, Y., ZHANG, H., SISSONS, S., COX, K., MCNULTY, A. M., PARSONS, S. H., WANG, T., SAMS, L., GEEGANAGE, S., DOUGLASS, L. E., NEUBAUER, B. L., DEAN, N. M., BLANCHARD, K.,

SHOU, J., STANCATO, L. F., CARTER, J. H. & MARCUSSON, E. G. 2007. Therapeutic suppression of translation initiation factor eIF4E expression reduces tumor growth without toxicity. *J Clin Invest,* 117**,** 2638-48.

GRAHAM, J. D. & CLARKE, C. L. 1997. Physiological Action of Progesterone in Target Tissues*. *Endocrine Reviews,* 18**,** 502-519.

GRASSO, C. S., WU, Y. M., ROBINSON, D. R., CAO, X., DHANASEKARAN, S. M., KHAN, A. P., QUIST, M. J., JING, X., LONIGRO, R. J., BRENNER, J. C., ASANGANI, I. A., ATEEQ, B., CHUN, S. Y., SIDDIQUI, J., SAM, L., ANSTETT, M., MEHRA, R., PRENSNER, J. R., PALANISAMY, N., RYSLIK, G. A., VANDIN, F., RAPHAEL, B. J., KUNJU, L. P., RHODES, D. R., PIENTA, K. J., CHINNAIYAN, A. M. & TOMLINS, S. A. 2012. The mutational landscape of lethal castration-resistant prostate cancer. *Nature,* 487**,** 239-43.

GRAVIS, G., FIZAZI, K., JOLY, F., OUDARD, S., PRIOU, F., ESTERNI, B., LATORZEFF, I., DELVA, R., KRAKOWSKI, I., LAGUERRE, B., ROLLAND, F., THÉODORE, C., DEPLANQUE, G., FERRERO, J. M., POUESSEL, D., MOUREY, L., BEUZEBOC, P., ZANETTA, S., HABIBIAN, M., BERDAH, J. F., DAUBA, J., BACIUCHKA, M., PLATINI, C., LINASSIER, C., LABOUREY, J. L., MACHIELS, J. P., EL KOURI, C., RAVAUD, A., SUC, E., EYMARD, J. C., HASBINI, A., BOUSQUET, G. & SOULIE, M. 2013. Androgen-deprivation therapy alone or with docetaxel in non-castrate metastatic prostate cancer (GETUG-AFU 15): a randomised, open-label, phase 3 trial. *The Lancet Oncology,* 14**,** 149-158.

GREEN, M. M., HILEY, C. T., SHANKS, J. H., BOTTOMLEY, I. C., WEST, C. M., COWAN, R. A. & STRATFORD, I. J. 2007. Expression of vascular endothelial growth factor (VEGF) in locally invasive prostate cancer is prognostic for radiotherapy outcome. *Int J Radiat Oncol Biol Phys,* 67**,** 84-90.

GREGORY, C. W., HE, B., JOHNSON, R. T., FORD, O. H., MOHLER, J. L., FRENCH, F. S. & WILSON, E. M. 2001. A mechanism for androgen receptor-mediated prostate cancer recurrence after androgen deprivation therapy. *Cancer Res,* 61**,** 4315-9.

GRIMM, S. L., HARTIG, S. M. & EDWARDS, D. P. 2016. Progesterone Receptor Signaling Mechanisms. *Journal of Molecular Biology,* 428**,** 3831-3849.

GRITSINA, G., GAO, W. Q. & YU, J. 2019. Transcriptional repression by androgen receptor: roles in castration-resistant prostate cancer. *Asian J Androl,* 21**,** 215-223.

GRÖNBERG, H. 2003. Prostate cancer epidemiology. *Lancet,* 361**,** 859-64.

GRONER, A. C., BROWN, M. & THEURILLAT, J.-P. 2016. Targeting transcriptional co-activators in advanced prostate cancer. *Cell cycle (Georgetown, Tex.),* 15**,** 3333-3334.

GROOT, K. R., SEVILLA, L. M., NISHI, K., DICOLANDREA, T. & WATT, F. M. 2004. Kazrin, a novel periplakin-interacting protein associated with desmosomes and the keratinocyte plasma membrane. *J Cell Biol,* 166**,** 653-9.

GROSHONG, S. D., OWEN, G. I., GRIMISON, B., SCHAUER, I. E., TODD, M. C., LANGAN, T. A., SCLAFANI, R. A., LANGE, C. A. & HORWITZ, K. B. 1997. Biphasic regulation of breast cancer cell growth by

progesterone: role of the cyclin-dependent kinase inhibitors, p21 and p27Kip1. *Molecular endocrinology,* 11**,** 1593-1607.
GU, Z., DU, Y., ZHAO, X. & WANG, C. 2022. Diagnostic, Therapeutic, and Prognostic Value of the m(6)A Writer Complex in Hepatocellular Carcinoma. *Front Cell Dev Biol,* 10**,** 822011.
GUAN, Q., LIN, H., MIAO, L., GUO, H., CHEN, Y., ZHUO, Z. & HE, J. 2022. Functions, mechanisms, and therapeutic implications of METTL14 in human cancer. *J Hematol Oncol,* 15**,** 13.
GUBBI, S., QUIPILDOR, G. F., BARZILAI, N., HUFFMAN, D. M. & MILMAN, S. 2018. 40 YEARS of IGF1: IGF1: the Jekyll and Hyde of the aging brain. *J Mol Endocrinol,* 61**,** T171-t185.
GUILFORD, P., HOPKINS, J., HARRAWAY, J., MCLEOD, M., MCLEOD, N., HARAWIRA, P., TAITE, H., SCOULAR, R., MILLER, A. & REEVE, A. E. 1998. E-cadherin germline mutations in familial gastric cancer. *Nature,* 392**,** 402-405.
GUO, Z., YANG, X., SUN, F., JIANG, R., LINN, D. E., CHEN, H., CHEN, H., KONG, X., MELAMED, J., TEPPER, C. G., KUNG, H. J., BRODIE, A. M., EDWARDS, J. & QIU, Y. 2009. A novel androgen receptor splice variant is up-regulated during prostate cancer progression and promotes androgen depletion-resistant growth. *Cancer Res,* 69**,** 2305-13.
GYŐRFFY, B. 2021. Survival analysis across the entire transcriptome identifies biomarkers with the highest prognostic power in breast cancer. *Computational and Structural Biotechnology Journal,* 19**,** 4101-4109.
HAHN, W. C., COUNTER, C. M., LUNDBERG, A. S., BEIJERSBERGEN, R. L., BROOKS, M. W. & WEINBERG, R. A. 1999. Creation of human tumour cells with defined genetic elements. *Nature,* 400**,** 464-8.
HAIGH, D. B., WOODCOCK, C. L., LOTHION-ROY, J., HARRIS, A. E., METZLER, V. M., PERSSON, J. L., ROBINSON, B. D., KHANI, F., ALSALEEM, M., NTEKIM, A., MADHUSUDAN, S., DAVIS, M. B., LAURSEN, K. B., GUDAS, L. J., RUTLAND, C. S., TOSS, M. S., ARCHER, N., BODI, Z., RAKHA, E. A., FRAY, R. G., JEYAPALAN, J. N. & MONGAN, N. P. 2022. The METTL3 RNA Methyltransferase Regulates Transcriptional Networks in Prostate Cancer. *Cancers,* 14**,** 5148.
HAKUNO, F. & TAKAHASHI, S. I. 2018. IGF1 receptor signaling pathways. *J Mol Endocrinol,* 61**,** T69-t86.
HALL, J., LEE, M., NEWMAN, B., MORROW, J., ANDERSON, L., HUEY, B. & KING, M. 1990. Linkage of early-onset familial breast cancer to chromosome 17q21. *Science,* 250**,** 1684-1689.
HALL, M. N. 2008. mTOR-what does it do? *Transplant Proc,* 40**,** S5-8.
HAMAJIMA, N., HIROSE, K., TAJIMA, K., ROHAN, T., CALLE, E. E., HEATH, C. W., JR., COATES, R. J., LIFF, J. M., TALAMINI, R., CHANTARAKUL, N., KOETSAWANG, S., RACHAWAT, D., MORABIA, A., SCHUMAN, L., STEWART, W., SZKLO, M., BAIN, C., SCHOFIELD, F., SISKIND, V., BAND, P., COLDMAN, A. J., GALLAGHER, R. P., HISLOP, T. G., YANG, P., KOLONEL, L. M., NOMURA, A. M. Y., HU, J., JOHNSON, K. C., MAO, Y., DE SANJOSÉ, S., LEE, N., MARCHBANKS, P., ORY, H. W., PETERSON, H. B., WILSON, H. G., WINGO, P. A., EBELING, K., KUNDE, D., NISHAN, P., HOPPER, J. L., COLDITZ, G., GAJALANSKI, V., MARTIN, N., PARDTHAISONG, T.,

SILPISORNKOSOL, S., THEETRANONT, C., BOOSIRI, B., CHUTIVONGSE, S., JIMAKORN, P., VIRUTAMASEN, P., WONGSRICHANALAI, C., EWERTZ, M., ADAMI, H. O., BERGKVIST, L., MAGNUSSON, C., PERSSON, I., CHANG-CLAUDE, J., PAUL, C., SKEGG, D. C. G., SPEARS, G. F. S., BOYLE, P., EVSTIFEEVA, T., DALING, J. R., HUTCHINSON, W. B., MALONE, K., NOONAN, E. A., STANFORD, J. L., THOMAS, D. B., WEISS, N. S., WHITE, E., ANDRIEU, N., BRÊMOND, A., CLAVEL, F., GAIRARD, B., LANSAC, J., PIANA, L., RENAUD, R., IZQUIERDO, A., VILADIU, P., CUEVAS, H. R., ONTIVEROS, P., PALET, A., SALAZAR, S. B., ARISTIZABEL, N., CUADROS, A., TRYGGVADOTTIR, L., TULINIUS, H., BACHELOT, A., LÊ, M. G., PETO, J., FRANCESCHI, S., LUBIN, F., MODAN, B., RON, E., WAX, Y., FRIEDMAN, G. D., HIATT, R. A., LEVI, F., BISHOP, T., KOSMELJ, K., et al. 2002. Alcohol, tobacco and breast cancer--collaborative reanalysis of individual data from 53 epidemiological studies, including 58,515 women with breast cancer and 95,067 women without the disease. *British journal of cancer,* 87**,** 1234-1245.

HAMPEL, H., FRANKEL, W. L., MARTIN, E., ARNOLD, M., KHANDUJA, K., KUEBLER, P., NAKAGAWA, H., SOTAMAA, K., PRIOR, T. W., WESTMAN, J., PANESCU, J., FIX, D., LOCKMAN, J., COMERAS, I. & DE LA CHAPELLE, A. 2005. Screening for the Lynch syndrome (hereditary nonpolyposis colorectal cancer). *N Engl J Med,* 352**,** 1851-60.

HANAHAN, D. & WEINBERG, R. A. 2000. The Hallmarks of Cancer. *Cell,* 100**,** 57-70.

HANAHAN, D. & WEINBERG, ROBERT A. 2011. Hallmarks of Cancer: The Next Generation. *Cell,* 144**,** 646-674.

HANKINSON, S. E., COLDITZ, G. A. & WILLETT, W. C. 2004. Towards an integrated model for breast cancer etiology: The lifelong interplay of genes, lifestyle, and hormones. *Breast Cancer Research,* 6**,** 213.

HANKINSON, S. E., WILLETT, W. C., COLDITZ, G. A., HUNTER, D. J., MICHAUD, D. S., DEROO, B., ROSNER, B., SPEIZER, F. E. & POLLAK, M. 1998. Circulating concentrations of insulin-like growth factor I and risk of breast cancer. *The Lancet,* 351**,** 1393-1396.

HANSEN, A. R., MASSARD, C., OTT, P. A., HAAS, N. B., LOPEZ, J. S., EJADI, S., WALLMARK, J. M., KEAM, B., DELORD, J. P., AGGARWAL, R., GOULD, M., YANG, P., KEEFE, S. M. & PIHA-PAUL, S. A. 2018. Pembrolizumab for advanced prostate adenocarcinoma: findings of the KEYNOTE-028 study. *Ann Oncol,* 29**,** 1807-1813.

HANSFORD, S., KAURAH, P., LI-CHANG, H., WOO, M., SENZ, J., PINHEIRO, H., SCHRADER, K. A., SCHAEFFER, D. F., SHUMANSKY, K., ZOGOPOULOS, G., SANTOS, T. A., CLARO, I., CARVALHO, J., NIELSEN, C., PADILLA, S., LUM, A., TALHOUK, A., BAKER-LANGE, K., RICHARDSON, S., LEWIS, I., LINDOR, N. M., PENNELL, E., MACMILLAN, A., FERNANDEZ, B., KELLER, G., LYNCH, H., SHAH, S. P., GUILFORD, P., GALLINGER, S., CORSO, G., ROVIELLO, F., CALDAS, C., OLIVEIRA, C., PHAROAH, P. D. & HUNTSMAN, D. G. 2015. Hereditary Diffuse Gastric Cancer Syndrome: CDH1 Mutations and Beyond. *JAMA Oncol,* 1**,** 23-32.

HAO, Y., CRENSHAW, T., MOULTON, T., NEWCOMB, E. & TYCKO, B. 1993. Tumour-suppressor activity of H19 RNA. *Nature,* 365**,** 764-767.

HARA, T., MIYAZAKI, J.-I., ARAKI, H., YAMAOKA, M., KANZAKI, N., KUSAKA, M. & MIYAMOTO, M. 2003. Novel Mutations of Androgen Receptor. *A Possible Mechanism of Bicalutamide Withdrawal Syndrome,* 63**,** 149-153.

HARTMAN, T. J., SISTI, J. S., HANKINSON, S. E., XU, X., ELIASSEN, A. H. & ZIEGLER, R. 2016. Alcohol Consumption and Urinary Estrogens and Estrogen Metabolites in Premenopausal Women. *Hormones and Cancer,* 7**,** 65-74.

HARTSOCK, A. & NELSON, W. J. 2008. Adherens and tight junctions: structure, function and connections to the actin cytoskeleton. *Biochim Biophys Acta,* 1778**,** 660-9.

HASSIOTOU, F. & GEDDES, D. 2013. Anatomy of the human mammary gland: Current status of knowledge. *Clin Anat,* 26**,** 29-48.

HAUGSTEN, E. M., WIEDLOCHA, A., OLSNES, S. & WESCHE, J. 2010. Roles of fibroblast growth factor receptors in carcinogenesis. *Mol Cancer Res,* 8**,** 1439-52.

HAUSSMANN, I. U., BODI, Z., SANCHEZ-MORAN, E., MONGAN, N. P., ARCHER, N., FRAY, R. G. & SOLLER, M. 2016. m(6)A potentiates Sxl alternative pre-mRNA splicing for robust Drosophila sex determination. *Nature,* 540**,** 301-304.

HAYBITTLE, J. L., BLAMEY, R. W., ELSTON, C. W., JOHNSON, J., DOYLE, P. J., CAMPBELL, F. C., NICHOLSON, R. I. & GRIFFITHS, K. 1982. A prognostic index in primary breast cancer. *Br J Cancer,* 45**,** 361-6.

HE, C., ZHOU, F., ZUO, Z., CHENG, H. & ZHOU, R. 2009. A global view of cancer-specific transcript variants by subtractive transcriptome-wide analysis. *PLoS One,* 4**,** e4732.

HE, X., ARSLAN, A. D., HO, T. T., YUAN, C., STAMPFER, M. R. & BECK, W. T. 2014. Involvement of polypyrimidine tract-binding protein (PTBP1) in maintaining breast cancer cell growth and malignant properties. *Oncogenesis,* 3**,** e84.

HEIDENREICH, A., ABRAHAMSSON, P.-A., ARTIBANI, W., CATTO, J., MONTORSI, F., VAN POPPEL, H., WIRTH, M. & MOTTET, N. 2013. Early Detection of Prostate Cancer: European Association of Urology Recommendation. *European Urology,* 64**,** 347-354.

HEIDENREICH, A., BASTIAN, P. J., BELLMUNT, J., BOLLA, M., JONIAU, S., VAN DER KWAST, T., MASON, M., MATVEEV, V., WIEGEL, T., ZATTONI, F. & MOTTET, N. 2014. EAU Guidelines on Prostate Cancer. Part 1: Screening, Diagnosis, and Local Treatment with Curative Intent—Update 2013. *European Urology,* 65**,** 124-137.

HEIMANN, R., LAN, F., MCBRIDE, R. & HELLMAN, S. 2000. Separating favorable from unfavorable prognostic markers in breast cancer: the role of E-cadherin. *Cancer Res,* 60**,** 298-304.

HEINLEIN, C. A. & CHANG, C. 2004. Androgen receptor in prostate cancer. *Endocr Rev,* 25**,** 276-308.

HEMMINKI, K. 2012. Familial risk and familial survival in prostate cancer. *World Journal of Urology,* 30**,** 143-148.

HENDERSON, B. E. 1989. Endogenous and exogenous endocrine factors. *Hematol Oncol Clin North Am,* 3**,** 577-98.

HENDERSON, B. E. & FEIGELSON, H. S. 2000. Hormonal carcinogenesis. *Carcinogenesis,* 21**,** 427-433.

HENDERSON, B. E., ROSS, R. & BERNSTEIN, L. 1988. Estrogens as a Cause of Human Cancer: The Richard and Hinda Rosenthal Foundation Award Lecture. *Cancer Research,* 48**,** 246-253.

HILAKIVI-CLARKE, L. 2000. Estrogens, BRCA1, and breast cancer. *Cancer Res,* 60**,** 4993-5001.

HJELMBORG, J. B., SCHEIKE, T., HOLST, K., SKYTTHE, A., PENNEY, K. L., GRAFF, R. E., PUKKALA, E., CHRISTENSEN, K., ADAMI, H.-O., HOLM, N. V., NUTTALL, E., HANSEN, S., HARTMAN, M., CZENE, K., HARRIS, J. R., KAPRIO, J. & MUCCI, L. A. 2014. The heritability of prostate cancer in the Nordic Twin Study of Cancer. *Cancer epidemiology, biomarkers & prevention : a publication of the American Association for Cancer Research, cosponsored by the American Society of Preventive Oncology,* 2**3,** 2303-2310.

HOERNES, T. P. & ERLACHER, M. D. 2017. Translating the epitranscriptome. *Wiley Interdisciplinary Reviews: RNA,* 8**,** e1375.

HORIUCHI, K., KAWAMURA, T., IWANARI, H., OHASHI, R., NAITO, M., KODAMA, T. & HAMAKUBO, T. 2013. Identification of Wilms' tumor 1-associating protein complex and its role in alternative splicing and the cell cycle. *J Biol Chem,* 288**,** 33292-302.

HOROSZEWICZ, J. S., LEONG, S. S., KAWINSKI, E., KARR, J. P., ROSENTHAL, H., CHU, T. M., MIRAND, E. A. & MURPHY, G. P. 1983. LNCaP model of human prostatic carcinoma. *Cancer Res,* 43**,** 1809-18.

HOWARD, C. M., ESTRADA, M., TERRERO, D., TIWARI, A. K. & RAMAN, D. 2020. Identification of Cardiac Glycosides as Novel Inhibitors of eIF4A1-Mediated Translation in Triple-Negative Breast Cancer Cells. *Cancers (Basel),* 12.

HOWARD, J. A., HART, K. N. & THOMPSON, T. B. 2022. Molecular Mechanisms of AMH Signaling. *Front Endocrinol (Lausanne),* 13**,** 927824.

HSIEH, C. C., TRICHOPOULOS, D., KATSOUYANNI, K. & YUASA, S. 1990. Age at menarche, age at menopause, height and obesity as risk factors for breast cancer: associations and interactions in an international case-control study. *Int J Cancer,* 46**,** 796-800.

HU, R., DUNN, T. A., WEI, S., ISHARWAL, S., VELTRI, R. W., HUMPHREYS, E., HAN, M., PARTIN, A. W., VESSELLA, R. L., ISAACS, W. B., BOVA, G. S. & LUO, J. 2009. Ligand-independent androgen receptor variants derived from splicing of cryptic exons signify hormone-refractory prostate cancer. *Cancer Res,* 69**,** 16-22.

HU, R., LU, C., MOSTAGHEL, E. A., YEGNASUBRAMANIAN, S., GUREL, M., TANNAHILL, C., EDWARDS, J., ISAACS, W. B., NELSON, P. S., BLUEMN, E., PLYMATE, S. R. & LUO, J. 2012. Distinct transcriptional programs mediated by the ligand-dependent full-length androgen receptor and its splice variants in castration-resistant prostate cancer. *Cancer research,* 72**,** 3457-3462.

HU, S., SONG, Y., ZHOU, Y., JIAO, Y. & LI, G. 2022. METTL3 Accelerates Breast Cancer Progression via Regulating EZH2 m(6)A Modification. *J Healthc Eng,* 2022**,** 5794422.

HUANG, C. F., LINGADAHALLI, S., MOROVA, T., OZTURAN, D., HU, E., YU, I. P. L., LINDER, S., HOOGSTRAAT, M., STELLOO, S., SAR, F., VAN DER POEL, H., ALTINTAS, U. B., SAFFARZADEH, M., LE BIHAN, S., MCCONEGHY, B., GOKBAYRAK, B., FENG, F. Y., GLEAVE, M. E.,

BERGMAN, A. M., COLLINS, C., HACH, F., ZWART, W., EMBERLY, E. & LACK, N. A. 2021. Functional mapping of androgen receptor enhancer activity. *Genome Biol,* 22**,** 149.

HUANG, H., WANG, Y., KANDPAL, M., ZHAO, G., CARDENAS, H., JI, Y., CHAPARALA, A., TANNER, E. J., CHEN, J., DAVULURI, R. V. & MATEI, D. 2020. FTO-Dependent N (6)-Methyladenosine Modifications Inhibit Ovarian Cancer Stem Cell Self-Renewal by Blocking cAMP Signaling. *Cancer Res,* 80**,** 3200-3214.

HUANG, H., WENG, H., SUN, W., QIN, X., SHI, H., WU, H., ZHAO, B. S., MESQUITA, A., LIU, C., YUAN, C. L., HU, Y.-C., HÜTTELMAIER, S., SKIBBE, J. R., SU, R., DENG, X., DONG, L., SUN, M., LI, C., NACHTERGAELE, S., WANG, Y., HU, C., FERCHEN, K., GREIS, K. D., JIANG, X., WEI, M., QU, L., GUAN, J.-L., HE, C., YANG, J. & CHEN, J. 2018. Recognition of RNA N6-methyladenosine by IGF2BP proteins enhances mRNA stability and translation. *Nature Cell Biology,* 20**,** 285-295.

HUANG, M., ANAND, S., MURPHY, E. A., DESGROSELLIER, J. S., STUPACK, D. G., SHATTIL, S. J., SCHLAEPFER, D. D. & CHERESH, D. A. 2012. EGFR-dependent pancreatic carcinoma cell metastasis through Rap1 activation. *Oncogene,* 31**,** 2783-93.

HUANG, Y., YAN, J., LI, Q., LI, J., GONG, S., ZHOU, H., GAN, J., JIANG, H., JIA, G. F., LUO, C. & YANG, C. G. 2015. Meclofenamic acid selectively inhibits FTO demethylation of m6A over ALKBH5. *Nucleic Acids Res,* 43**,** 373-84.

HUGGINS, C. & HODGES, C. V. 1941. Studies on prostatic cancer: I. The effect of castration, of estrogen and of androgen injection on serum phosphatases in metastatic carcinoma of the prostate. 1941. *Cancer Res,* 1.

HUGGINS, C. & NEAL, W. 1942. COAGULATION AND LIQUEFACTION OF SEMEN : PROTEOLYTIC ENZYMES AND CITRATE IN PROSTATIC FLUID. *J Exp Med,* 76**,** 527-41.

HUI, L., ZHANG, S., WUDU, M., REN, H., XU, Y., ZHANG, Q. & QIU, X. 2019. CBLL1 is highly expressed in non-small cell lung cancer and promotes cell proliferation and invasion. *Thorac Cancer,* 10**,** 1479-1488.

HUMPHREY, P. A. 2012. Histological variants of prostatic carcinoma and their significance. *Histopathology,* 60**,** 59-74.

HUSSAIN, M., FIZAZI, K., SAAD, F., RATHENBORG, P., SHORE, N., FERREIRA, U., IVASHCHENKO, P., DEMIRHAN, E., MODELSKA, K., PHUNG, D., KRIVOSHIK, A. & STERNBERG, C. N. 2018. Enzalutamide in Men with Nonmetastatic, Castration-Resistant Prostate Cancer. *The New England journal of medicine,* 378**,** 2465-2474.

IBRAHIM, S., LI, G., HU, F., HOU, Z., CHEN, Q., LI, G., LUO, X., HU, J. & FENG, Y. 2018. PIK3R3 promotes chemotherapeutic sensitivity of colorectal cancer through PIK3R3/NF-kB/TP pathway. *Cancer Biol Ther,* 19**,** 222-229.

ILIC, D., DJULBEGOVIC, M., JUNG, J. H., HWANG, E. C., ZHOU, Q., CLEVES, A., AGORITSAS, T. & DAHM, P. 2018. Prostate cancer screening with prostate-specific antigen (PSA) test: a systematic review and meta-analysis. *Bmj,* 362**,** k3519.

ILIC, D., O'CONNOR, D., GREEN, S. & WILT, T. 2007. Screening for prostate cancer: A Cochrane systematic review. *Cancer Causes & Control,* 18**,** 279-285.

IMPERATO-MCGINLEY, J., GUERRERO, L., GAUTIER, T. & PETERSON, R. E. 1974. Steroid 5alpha-reductase deficiency in man: an inherited form of male pseudohermaphroditism. *Science,* 186**,** 1213-5.

INSUA-RODRÍGUEZ, J. & OSKARSSON, T. 2016. The extracellular matrix in breast cancer. *Adv Drug Deliv Rev,* 97**,** 41-55.

ISAKOFF, S. J., MAYER, E. L., HE, L., TRAINA, T. A., CAREY, L. A., KRAG, K. J., RUGO, H. S., LIU, M. C., STEARNS, V., COME, S. E., TIMMS, K. M., HARTMAN, A.-R., BORGER, D. R., FINKELSTEIN, D. M., GARBER, J. E., RYAN, P. D., WINER, E. P., GOSS, P. E. & ELLISEN, L. W. 2015. TBCRC009: A Multicenter Phase II Clinical Trial of Platinum Monotherapy With Biomarker Assessment in Metastatic Triple-Negative Breast Cancer. *Journal of clinical oncology : official journal of the American Society of Clinical Oncology,* 33**,** 1902-1909.

ITTMANN, M. 2018. Anatomy and Histology of the Human and Murine Prostate. *Cold Spring Harb Perspect Med,* 8.

JAKOWLEW, S. B., BREATHNACH, R., JELTSCH, J. M., MASIAKOWSKI, P. & CHAMBON, P. 1984. Sequence of the pS2 mRNA induced by estrogen in the human breast cancer cell line MCF-7. *Nucleic Acids Res,* 12**,** 2861-78.

JANDA, E., NEVOLO, M., LEHMANN, K., DOWNWARD, J., BEUG, H. & GRIECO, M. 2006. Raf plus TGFbeta-dependent EMT is initiated by endocytosis and lysosomal degradation of E-cadherin. *Oncogene,* 25**,** 7117-30.

JANSEN, M. P., KNIJNENBURG, T., REIJM, E. A., SIMON, I., KERKHOVEN, R., DROOG, M., VELDS, A., VAN LAERE, S., DIRIX, L., ALEXI, X., FOEKENS, J. A., WESSELS, L., LINN, S. C., BERNS, E. M. & ZWART, W. 2013. Hallmarks of aromatase inhibitor drug resistance revealed by epigenetic profiling in breast cancer. *Cancer Res,* 73**,** 6632-41.

JENSTER, G., TRAPMAN, J. & BRINKMANN, A. O. 1993. Nuclear import of the human androgen receptor. *Biochem J,* 293 ( Pt 3)**,** 761-8.

JENSTER, G., VAN DER KORPUT, H. A. G. M., VAN VROONHOVEN, C., VAN DER KWAST, T. H., TRAPMAN, J. & BRINKMANN, A. O. 1991. Domains of the Human Androgen Receptor Involved in Steroid Binding, Transcriptional Activation, and Subcellular Localization. *Molecular Endocrinology,* 5**,** 1396-1404.

JERNBERG, E., BERGH, A. & WIKSTRÖM, P. 2017. Clinical relevance of androgen receptor alterations in prostate cancer. *Endocr Connect,* 6**,** R146-r161.

JESCHKE, U., MYLONAS, I., KUHN, C., SHABANI, N., KUNERT-KEIL, C., SCHINDLBECK, C., GERBER, B. & FRIESE, K. 2007. Expression of E-cadherin in human ductal breast cancer carcinoma in situ, invasive carcinomas, their lymph node metastases, their distant metastases, carcinomas with recurrence and in recurrence. *Anticancer Res,* 27**,** 1969-74.

JESELSOHN, R., BUCHWALTER, G., DE ANGELIS, C., BROWN, M. & SCHIFF, R. 2015. ESR1 mutations—a mechanism for acquired endocrine resistance in breast cancer. *Nature Reviews Clinical Oncology,* 12**,** 573.

JESINGER, R. A. 2014. Breast Anatomy for the Interventionalist. *Techniques in Vascular and Interventional Radiology,* 17**,** 3-9.
JI, G., HUANG, C., HE, S., GONG, Y., SONG, G., LI, X. & ZHOU, L. 2020. Comprehensive analysis of m6A regulators prognostic value in prostate cancer. *Aging (Albany NY),* 12**,** 14863-14884.
JIA, G., FU, Y., ZHAO, X., DAI, Q., ZHENG, G., YANG, Y., YI, C., LINDAHL, T., PAN, T., YANG, Y. G. & HE, C. 2011. N6-methyladenosine in nuclear RNA is a major substrate of the obesity-associated FTO. *Nat Chem Biol,* 7**,** 885-7.
JIA, H., WANG, Z., ZHANG, J. & FENG, F. 2021. γ-Secretase inhibitors for breast cancer and hepatocellular carcinoma: From mechanism to treatment. *Life Sci,* 268**,** 119007.
JIANG, B.-H., SEMENZA, G. L., BAUER, C. & MARTI, H. H. 1996. Hypoxia-inducible factor 1 levels vary exponentially over a physiologically relevant range of O2 tension. *American Journal of Physiology-Cell Physiology,* 271**,** C1172-C1180.
JIANG, J., CHEN, X., LIU, H., SHAO, J., XIE, R., GU, P. & DUAN, C. 2017. Polypyrimidine Tract-Binding Protein 1 promotes proliferation, migration and invasion in clear-cell renal cell carcinoma by regulating alternative splicing of PKM. *Am J Cancer Res,* 7**,** 245-259.
JIANG, M., JIA, K., WANG, L., LI, W., CHEN, B., LIU, Y., WANG, H., ZHAO, S., HE, Y. & ZHOU, C. 2020. Alterations of DNA damage repair in cancer: from mechanisms to applications. *Ann Transl Med,* 8**,** 1685.
JIANG, W. G. 1996. E-cadherin and its associated protein catenins, cancer invasion and metastasis. *BJS (British Journal of Surgery),* 83**,** 437-446.
JIN, H., YU, Y., ZHANG, T., ZHOU, X., ZHOU, J., JIA, L., WU, Y., ZHOU, B. P. & FENG, Y. 2010. Snail is critical for tumor growth and metastasis of ovarian carcinoma. *International journal of cancer,* 126**,** 2102-2111.
JIN, H. J., KIM, J. & YU, J. 2013. Androgen receptor genomic regulation. *Transl Androl Urol,* 2**,** 157-177.
JONES, M. E., SCHOEMAKER, M. J., WRIGHT, L. B., ASHWORTH, A. & SWERDLOW, A. J. 2017. Smoking and risk of breast cancer in the Generations Study cohort. *Breast Cancer Res,* 19**,** 118.
KAHLES, A., LEHMANN, K. V., TOUSSAINT, N. C., HÜSER, M., STARK, S. G., SACHSENBERG, T., STEGLE, O., KOHLBACHER, O., SANDER, C. & RÄTSCH, G. 2018. Comprehensive Analysis of Alternative Splicing Across Tumors from 8,705 Patients. *Cancer Cell,* 34**,** 211-224.e6.
KAIDO, M., WADA, H., SHINDO, M. & HAYASHI, S. 2009. Essential requirement for RING finger E3 ubiquitin ligase Hakai in early embryonic development of Drosophila. *Genes Cells,* 14**,** 1067-77.
KAIGHN, M. E., NARAYAN, K. S., OHNUKI, Y., LECHNER, J. F. & JONES, L. W. 1979. Establishment and characterization of a human prostatic carcinoma cell line (PC-3). *Invest Urol,* 17**,** 16-23.
KALLURI, R. & WEINBERG, R. A. 2009. The basics of epithelial-mesenchymal transition. *The Journal of Clinical Investigation,* 119**,** 1420-1428.
KANDOTH, C., SCHULTZ, N., CHERNIACK, A. D., AKBANI, R., LIU, Y., SHEN, H., ROBERTSON, A. G., PASHTAN, I., SHEN, R., BENZ, C. C., YAU, C., LAIRD, P. W., DING, L., ZHANG, W., MILLS, G. B., KUCHERLAPATI, R., MARDIS, E. R. & LEVINE, D. A. 2013. Integrated genomic characterization of endometrial carcinoma. *Nature,* 497**,** 67-73.

KANTOFF, P. W., HIGANO, C. S., SHORE, N. D., BERGER, E. R., SMALL, E. J., PENSON, D. F., REDFERN, C. H., FERRARI, A. C., DREICER, R., SIMS, R. B., XU, Y., FROHLICH, M. W. & SCHELLHAMMER, P. F. 2010. Sipuleucel-T immunotherapy for castration-resistant prostate cancer. *N Engl J Med,* 363**,** 411-22.

KANTOR, E. D., HANEUSE, S., VALDIMARSDOTTIR, U. A., WILLIAMS, D. R., SIGNORELLO, L. B. & RIDER, J. R. 2019. Socioenvironmental adversity and risk of prostate cancer in non-Hispanic black and white men. *Cancer Causes Control,* 30**,** 997-1007.

KAROUSOU, E., D'ANGELO, M. L., KOUVIDI, K., VIGETTI, D., VIOLA, M., NIKITOVIC, D., DE LUCA, G. & PASSI, A. 2014. Collagen VI and hyaluronan: the common role in breast cancer. *BioMed research international,* 2014.

KASHYAP, V., AHMAD, S., NILSSON, E. M., HELCZYNSKI, L., KENNA, S., PERSSON, J. L., GUDAS, L. J. & MONGAN, N. P. 2013. The lysine specific demethylase-1 (LSD1/KDM1A) regulates VEGF-A expression in prostate cancer. *Mol Oncol,* 7**,** 555-66.

KAZEROUNIAN, S. & AHO, S. 2003. Characterization of periphilin, a widespread, highly insoluble nuclear protein and potential constituent of the keratinocyte cornified envelope. *J Biol Chem,* 278**,** 36707-17.

KE, S., ALEMU, E. A., MERTENS, C., GANTMAN, E. C., FAK, J. J., MELE, A., HARIPAL, B., ZUCKER-SCHARFF, I., MOORE, M. J., PARK, C. Y., VAGBO, C. B., KUSSNIERCZYK, A., KLUNGLAND, A., DARNELL, J. E., JR. & DARNELL, R. B. 2015. A majority of m6A residues are in the last exons, allowing the potential for 3' UTR regulation. *Genes Dev,* 29**,** 2037-53.

KE, S., PANDYA-JONES, A., SAITO, Y., FAK, J. J., VAGBO, C. B., GEULA, S., HANNA, J. H., BLACK, D. L., DARNELL, J. E., JR. & DARNELL, R. B. 2017. m(6)A mRNA modifications are deposited in nascent pre-mRNA and are not required for splicing but do specify cytoplasmic turnover. *Genes Dev,* 31**,** 990-1006.

KELSEY, J. L., GAMMON, M. D. & JOHN, E. M. 1993. Reproductive factors and breast cancer. *Epidemiol Rev,* 15**,** 36-47.

KENFIELD, S. A., STAMPFER, M. J., CHAN, J. M. & GIOVANNUCCI, E. 2011. Smoking and Prostate Cancer Survival and Recurrence. *JAMA,* 305**,** 2548-2555.

KERBEL, R. S. 2008. Tumor angiogenesis. *N Engl J Med,* 358**,** 2039-49.

KEYDAR, I., CHEN, L., KARBY, S., WEISS, F. R., DELAREA, J., RADU, M., CHAITCIK, S. & BRENNER, H. J. 1979. Establishment and characterization of a cell line of human breast carcinoma origin. *Eur J Cancer,* 15**,** 659-70.

KHALAF, D. J., ANNALA, M., TAAVITSAINEN, S., FINCH, D. L., OJA, C., VERGIDIS, J., ZULFIQAR, M., SUNDERLAND, K., AZAD, A. A., KOLLMANNSBERGER, C. K., EIGL, B. J., NOONAN, K., WADHWA, D., ATTWELL, A., KEITH, B., ELLARD, S. L., LE, L., GLEAVE, M. E., WYATT, A. W. & CHI, K. N. 2019. Optimal sequencing of enzalutamide and abiraterone acetate plus prednisone in metastatic castration-resistant prostate cancer: a multicentre, randomised, open-label, phase 2, crossover trial. *Lancet Oncol,* 20**,** 1730-1739.

KHAN, S. A., ROGERS, M. A., OBANDO, J. A. & TAMSEN, A. 1994. Estrogen receptor expression of benign breast epithelium and its association with breast cancer. *Cancer research,* 54**,** 993-997.

KIM, S., AU, C. C., JAMALRUDDIN, M. A. B., ABOU-GHALI, N. E., MUKHTAR, E., PORTELLA, L., BERGER, A., WORROLL, D., VATSA, P., RICKMAN, D. S., NANUS, D. M. & GIANNAKAKOU, P. 2022. AR-V7 exhibits non-canonical mechanisms of nuclear import and chromatin engagement in castrate-resistant prostate cancer. *Elife,* 11.

KIM, S. N., AHN, Y. H., KIM, S. G., PARK, S. D., CHO-CHUNG, Y. S. & HONG, S. H. 2001. 8-Cl-cAMP induces cell cycle-specific apoptosis in human cancer cells. *Int J Cancer,* 93**,** 33-41.

KIM, W., JONES, J. O., DIAMOND, M., HAQQ, C., MOLINA, A., SMALL, E. J. & RYAN, C. J. 2014. Inhibition of the androgen receptor by mineralocorticoids at levels physiologically achieved in serum in patients treated with abiraterone acetate. *Prostate Cancer Prostatic Dis,* 17**,** 292-9.

KIMBRO, K. S. & SIMONS, J. W. 2006. Hypoxia-inducible factor-1 in human breast and prostate cancer. *Endocr Relat Cancer,* 13**,** 739-49.

KISCHEL, P., WALTREGNY, D., DUMONT, B., TURTOI, A., GREFFE, Y., KIRSCH, S., DE PAUW, E. & CASTRONOVO, V. 2010. Versican overexpression in human breast cancer lesions: known and new isoforms for stromal tumor targeting. *International journal of cancer,* 126**,** 640-650.

KISHINO, T., LALANDE, M. & WAGSTAFF, J. 1997. UBE3A/E6-AP mutations cause Angelman syndrome. *Nature Genetics,* 15**,** 70-73.

KLEIN, K., WERNER, K., TESKE, C., SCHENK, M., GIESE, T., WEITZ, J. & WELSCH, T. 2016. Role of TFEB-driven autophagy regulation in pancreatic cancer treatment. *Int J Oncol,* 49**,** 164-172.

KNOWLES, M. & SELBY, P. 2005. *Introduction to the Cellular and Molecular Biology of Cancer,* Oxford, Oxford University Press.

KNUCKLES, P., LENCE, T., HAUSSMANN, I. U., JACOB, D., KREIM, N., CARL, S. H., MASIELLO, I., HARES, T., VILLASEÑOR, R., HESS, D., ANDRADE-NAVARRO, M. A., BIGGIOGERA, M., HELM, M., SOLLER, M., BÜHLER, M. & ROIGNANT, J.-Y. 2018. Zc3h13/Flacc is required for adenosine methylation by bridging the mRNA-binding factor Rbm15/Spenito to the m6A machinery component Wtap/Fl(2)d. *Genes & development,* 32**,** 415-429.

KNUDSEN, K. E. & PENNING, T. M. 2010. Partners in crime: deregulation of AR activity and androgen synthesis in prostate cancer. *Trends in Endocrinology & Metabolism,* 21**,** 315-324.

KOBOLDT, D. C., FULTON, R. S., MCLELLAN, M. D., SCHMIDT, H., KALICKI-VEIZER, J., MCMICHAEL, J. F., FULTON, L. L., DOOLING, D. J., DING, L., MARDIS, E. R., WILSON, R. K., ALLY, A., BALASUNDARAM, M., BUTTERFIELD, Y. S. N., CARLSEN, R., CARTER, C., CHU, A., CHUAH, E., CHUN, H.-J. E., COOPE, R. J. N., DHALLA, N., GUIN, R., HIRST, C., HIRST, M., HOLT, R. A., LEE, D., LI, H. I., MAYO, M., MOORE, R. A., MUNGALL, A. J., PLEASANCE, E., GORDON ROBERTSON, A., SCHEIN, J. E., SHAFIEI, A., SIPAHIMALANI, P., SLOBODAN, J. R., STOLL, D., TAM, A., THIESSEN, N., VARHOL, R. J., WYE, N., ZENG, T., ZHAO, Y., BIROL, I., JONES, S. J. M., MARRA, M. A., CHERNIACK, A. D., SAKSENA, G., ONOFRIO, R. C., PHO, N.

H., CARTER, S. L., SCHUMACHER, S. E., TABAK, B., HERNANDEZ, B., GENTRY, J., NGUYEN, H., CRENSHAW, A., ARDLIE, K., BEROUKHIM, R., WINCKLER, W., GETZ, G., GABRIEL, S. B., MEYERSON, M., CHIN, L., PARK, P. J., KUCHERLAPATI, R., HOADLEY, K. A., TODD AUMAN, J., FAN, C., TURMAN, Y. J., SHI, Y., LI, L., TOPAL, M. D., HE, X., CHAO, H.-H., PRAT, A., SILVA, G. O., IGLESIA, M. D., ZHAO, W., USARY, J., BERG, J. S., ADAMS, M., BOOKER, J., WU, J., GULABANI, A., BODENHEIMER, T., HOYLE, A. P., SIMONS, J. V., SOLOWAY, M. G., MOSE, L. E., JEFFERYS, S. R., BALU, S., PARKER, J. S., NEIL HAYES, D., PEROU, C. M., MALIK, S., MAHURKAR, S., SHEN, H., WEISENBERGER, D. J., TRICHE JR, T., et al. 2012. Comprehensive molecular portraits of human breast tumours. *Nature,* 490**,** 61-70.

KOEPP, D. M. 2014. Cell Cycle Regulation by Protein Degradation. *In:* NOGUCHI, E. & GADALETA, M. C. (eds.) *Cell Cycle Control: Mechanisms and Protocols.* New York, NY: Springer New York.

KOIVISTO, P., KONONEN, J., PALMBERG, C., TAMMELA, T., HYYTINEN, E., ISOLA, J., TRAPMAN, J., CLEUTJENS, K., NOORDZIJ, A., VISAKORPI, T. & KALLIONIEMI, O. P. 1997. Androgen receptor gene amplification: a possible molecular mechanism for androgen deprivation therapy failure in prostate cancer. *Cancer Res,* 57**,** 314-9.

KONG, F., LIU, X., ZHOU, Y., HOU, X., HE, J., LI, Q., MIAO, X. & YANG, L. 2020. Downregulation of METTL14 increases apoptosis and autophagy induced by cisplatin in pancreatic cancer cells. *Int J Biochem Cell Biol,* 122**,** 105731.

KOOISTRA, B., WAUTERS, C., STROBBE, L. & WOBBES, T. 2010. Preoperative cytological and histological diagnosis of breast lesions: A critical review. *Eur J Surg Oncol,* 36**,** 934-40.

KORKMAZ, K. S., KORKMAZ, C. G., RAGNHILDSTVEIT, E., KIZILDAG, S., PRETLOW, T. G. & SAATCIOGLU, F. 2000. Full-length cDNA sequence and genomic organization of human NKX3A - alternative forms and regulation by both androgens and estrogens. *Gene,* 260**,** 25-36.

KORKOLA, J. E., DEVRIES, S., FRIDLYAND, J., HWANG, E. S., ESTEP, A. L. H., CHEN, Y.-Y., CHEW, K. L., DAIRKEE, S. H., JENSEN, R. M. & WALDMAN, F. M. 2003. Differentiation of Lobular versus Ductal Breast Carcinomas by Expression Microarray Analysis1. *Cancer Research,* 63**,** 7167-7175.

KORPAL, M., KORN, J. M., GAO, X., RAKIEC, D. P., RUDDY, D. A., DOSHI, S., YUAN, J., KOVATS, S. G., KIM, S., COOKE, V. G., MONAHAN, J. E., STEGMEIER, F., ROBERTS, T. M., SELLERS, W. R., ZHOU, W. & ZHU, P. 2013. An F876L mutation in androgen receptor confers genetic and phenotypic resistance to MDV3100 (enzalutamide). *Cancer Discov,* 3**,** 1030-43.

KOTB, A. M., HIERHOLZER, A. & KEMLER, R. 2011. Replacement of E-cadherin by N-cadherin in the mammary gland leads to fibrocystic changes and tumor formation. *Breast Cancer Res,* 13**,** R104.

KRAUSCH, M., RAFFEL, A., ANLAUF, M., SCHOTT, M., WILLENBERG, H., LEHWALD, N., HAFNER, D., CUPISTI, K., EISENBERGER, C. F. & KNOEFEL, W. T. 2011. Loss of PTEN expression in neuroendocrine pancreatic tumors. *Horm Metab Res,* 43**,** 865-71.

KUCHENBAECKER, K. B., HOPPER, J. L., BARNES, D. R., PHILLIPS, K.-A., MOOIJ, T. M., ROOS-BLOM, M.-J., JERVIS, S., VAN LEEUWEN, F. E., MILNE, R. L., ANDRIEU, N., GOLDGAR, D. E., TERRY, M. B., ROOKUS, M. A., EASTON, D. F., ANTONIOU, A. C., BRCA1, A. T. & CONSORTIUM, B. C. 2017. Risks of Breast, Ovarian, and Contralateral Breast Cancer for BRCA1 and BRCA2 Mutation CarriersRisks of Breast, Ovarian, and Contralateral Breast Cancer Among BRCA Mutation CarriersRisks of Breast, Ovarian, and Contralateral Breast Cancer Among BRCA Mutation Carriers. *JAMA,* 317**,** 2402-2416.

KUMAGAI, S., KOYAMA, S. & NISHIKAWA, H. 2021. Antitumour immunity regulated by aberrant ERBB family signalling. *Nat Rev Cancer,* 21**,** 181-197.

KUROZUMI, S., JOSEPH, C., SONBUL, S., ALESKANDARANY, M. A., PIGERA, M., ALSALEEM, M., ALSAEED, S., KARIRI, Y., NOLAN, C. C., DIEZ-RODRIGUEZ, M., JOHNSTON, S., MONGAN, N. P., FUJII, T., SHIRABE, K., MARTIN, S. G., ELLIS, I. O., GREEN, A. R. & RAKHA, E. A. 2018. Clinicopathological and prognostic significance of Ras association and pleckstrin homology domains 1 (RAPH1) in breast cancer. *Breast Cancer Research and Treatment,* 172**,** 61-68.

KWON, O.-J., ZHANG, L., ITTMANN, M. M. & XIN, L. 2014. Prostatic inflammation enhances basal-to-luminal differentiation and accelerates initiation of prostate cancer with a basal cell origin. *Proceedings of the National Academy of Sciences,* 111**,** E592-E600.

LADEWIG, E., MICHELINI, F., JHAVERI, K., CASTEL, P., CARMONA, J., FAIRCHILD, L., ZUNIGA, A. G., ARRUABARRENA-ARISTORENA, A., COCCO, E., BLAWSKI, R., KITTANE, S., ZHANG, Y., SALLAKU, M., BALDINO, L., HRISTIDIS, V., CHANDARLAPATY, S., ABDEL-WAHAB, O., LESLIE, C., SCALTRITI, M. & TOSKA, E. 2022. The Oncogenic PI3K-Induced Transcriptomic Landscape Reveals Key Functions in Splicing and Gene Expression Regulation. *Cancer Res,* 82**,** 2269-2280.

LAHN, M., SUNDELL, K., GLEAVE, M., LADAN, F., SU, C., LI, S., MA, D., PATERSON, B. M. & BUMOL, T. F. 2004. Protein kinase C-α in prostate cancer. *BJU International,* 93**,** 1076-1081.

LAKHANI, S. R., ELLIS, I. O., SCHNITT, S. J., TAN, P. H. & VAN DE VIJVER, M. J. 2012. *WHO Classification of Tumours of the Breast,* Lyon, IARC.

LAMBERTINI, M., SANTORO, L., DEL MASTRO, L., NGUYEN, B., LIVRAGHI, L., UGOLINI, D., PECCATORI, F. A. & AZIM, H. A. 2016. Reproductive behaviors and risk of developing breast cancer according to tumor subtype: A systematic review and meta-analysis of epidemiological studies. *Cancer Treatment Reviews,* 49**,** 65-76.

LAMOUILLE, S., XU, J. & DERYNCK, R. 2014. Molecular mechanisms of epithelial–mesenchymal transition. *Nature Reviews Molecular Cell Biology,* 15**,** 178.

LANGDON, W. Y., HARTLEY, J. W., KLINKEN, S. P., RUSCETTI, S. K. & MORSE, H. C. 1989a. v-cbl, an oncogene from a dual-recombinant murine retrovirus that induces early B-lineage lymphomas. *Proceedings of the National Academy of Sciences,* 86**,** 1168-1172.

LANGDON, W. Y., HYLAND, C. D., GRUMONT, R. J. & MORSE, H. C. 1989b. The c-cbl proto-oncogene is preferentially expressed in thymus and testis tissue and encodes a nuclear protein. *Journal of Virology,* 63**,** 5420-5424.

LARUE, L., OHSUGI, M., HIRCHENHAIN, J. & KEMLER, R. 1994. E-cadherin null mutant embryos fail to form a trophectoderm epithelium. *Proc Natl Acad Sci U S A,* 91**,** 8263-7.

LAWSON, J. S., FIELD, A. S., TRAN, D. D., KILLEEN, J., MASKARENIC, G., ISHIKURA, H. & TRICHOPOULOS, D. 2002. Breast cancer incidence and estrogen receptor α in normal mammary tissue—An epidemiologic study among Japanese women in Japan and Hawaii. *International journal of cancer,* 97**,** 685-687.

LE, D. T., DURHAM, J. N., SMITH, K. N., WANG, H., BARTLETT, B. R., AULAKH, L. K., LU, S., KEMBERLING, H., WILT, C., LUBER, B. S., WONG, F., AZAD, N. S., RUCKI, A. A., LAHERU, D., DONEHOWER, R., ZAHEER, A., FISHER, G. A., CROCENZI, T. S., LEE, J. J., GRETEN, T. F., DUFFY, A. G., CIOMBOR, K. K., EYRING, A. D., LAM, B. H., JOE, A., KANG, S. P., HOLDHOFF, M., DANILOVA, L., COPE, L., MEYER, C., ZHOU, S., GOLDBERG, R. M., ARMSTRONG, D. K., BEVER, K. M., FADER, A. N., TAUBE, J., HOUSSEAU, F., SPETZLER, D., XIAO, N., PARDOLL, D. M., PAPADOPOULOS, N., KINZLER, K. W., ESHLEMAN, J. R., VOGELSTEIN, B., ANDERS, R. A. & DIAZ, L. A., JR. 2017. Mismatch repair deficiency predicts response of solid tumors to PD-1 blockade. *Science,* 357**,** 409-413.

LEE, R. J. & SMITH, M. R. 2013. Targeting MET and vascular endothelial growth factor receptor signaling in castration-resistant prostate cancer. *Cancer J,* 19**,** 90-8.

LEE, S., ROY, F., GALMARINI, C. M., ACCARDI, R., MICHELON, J., VILLER, A., CROS, E., DUMONTET, C. & SYLLA, B. S. 2004. Frameshift mutation in the Dok1 gene in chronic lymphocytic leukemia. *Oncogene,* 23**,** 2287-97.

LEIVONEN, M., LUNDIN, J., NORDLING, S., VON BOGUSLAWSKI, K. & HAGLUND, C. 2004. Prognostic value of syndecan-1 expression in breast cancer. *Oncology,* 67**,** 11-18.

LEK, N., TADOKORO-CUCCARO, R., WHITCHURCH, J. B., MAZUMDER, B., MILES, H., PRENTICE, P., BUNCH, T., ZIELIŃSKA, K., METZLER, V., MONGAN, N. P., HEERY, D. M. & HUGHES, I. A. 2018. Predicting puberty in partial androgen insensitivity syndrome: Use of clinical and functional androgen receptor indices. *EBioMedicine,* 36**,** 401-409.

LENCE, T., AKHTAR, J., BAYER, M., SCHMID, K., SPINDLER, L., HO, C. H., KREIM, N., ANDRADE-NAVARRO, M. A., POECK, B., HELM, M. & ROIGNANT, J.-Y. 2016. m6A modulates neuronal functions and sex determination in Drosophila. *Nature,* 540**,** 242.

LESZCZYNSKA, K. B., FOSKOLOU, I. P., ABRAHAM, A. G., ANBALAGAN, S., TELLIER, C., HAIDER, S., SPAN, P. N., O'NEILL, E. E., BUFFA, F. M. & HAMMOND, E. M. 2015. Hypoxia-induced p53 modulates both apoptosis and radiosensitivity via AKT. *J Clin Invest,* 125**,** 2385-98.

LI, A., CHEN, Y.-S., PING, X.-L., YANG, X., XIAO, W., YANG, Y., SUN, H.-Y., ZHU, Q., BAIDYA, P., WANG, X., BHATTARAI, D. P., ZHAO, Y.-L., SUN, B.-F. & YANG, Y.-G. 2017a. Cytoplasmic m6A reader YTHDF3 promotes mRNA translation. *Cell Research,* 27**,** 444.

LI, B., JIANG, J., ASSARAF, Y. G., XIAO, H., CHEN, Z. S. & HUANG, C. 2020a. Surmounting cancer drug resistance: New insights from the perspective of N(6)-methyladenosine RNA modification. *Drug Resist Updat,* 53**,** 100720.

LI, J. & GREGORY, R. I. 2021. Mining for METTL3 inhibitors to suppress cancer. *Nat Struct Mol Biol,* 28**,** 460-462.
LI, L. & HANAHAN, D. 2013. Hijacking the neuronal NMDAR signaling circuit to promote tumor growth and invasion. *Cell,* 153**,** 86-100.
LI, X., TANG, J., HUANG, W., WANG, F., LI, P., QIN, C., QIN, Z., ZOU, Q., WEI, J., HUA, L., YANG, H. & WANG, Z. 2017b. The M6A methyltransferase METTL3: acting as a tumor suppressor in renal cell carcinoma. *Oncotarget,* 8**,** 96103-96116.
LI, X., ZHANG, G., WANG, Y., ELGEHAMA, A., SUN, Y., LI, L., GU, Y., GUO, W. & XU, Q. 2017c. Loss of periplakin expression is associated with the tumorigenesis of colorectal carcinoma. *Biomed Pharmacother,* 87**,** 366-374.
LI, Y., CHAN, S. C., BRAND, L. J., HWANG, T. H., SILVERSTEIN, K. A. & DEHM, S. M. 2013. Androgen receptor splice variants mediate enzalutamide resistance in castration-resistant prostate cancer cell lines. *Cancer Res,* 73**,** 483-9.
LI, Y., HODGE, J., LIU, Q., WANG, J., WANG, Y., EVANS, T. D., ALTOMARE, D., YAO, Y., MURPHY, E. A., RAZANI, B. & FAN, D. 2020b. TFEB is a master regulator of tumor-associated macrophages in breast cancer. *J Immunother Cancer,* 8.
LI, Y., YANG, R., HENZLER, C. M., HO, Y., PASSOW, C., AUCH, B., CARREIRA, S., NAVA RODRIGUES, D., BERTAN, C., HWANG, T. H., QUIGLEY, D. A., DANG, H. X., MORRISSEY, C., FRASER, M., PLYMATE, S. R., MAHER, C. A., FENG, F. Y., DE BONO, J. S. & DEHM, S. M. 2020c. Diverse AR Gene Rearrangements Mediate Resistance to Androgen Receptor Inhibitors in Metastatic Prostate Cancer. *Clin Cancer Res,* 26**,** 1965-1976.
LI, Z., YIN, S., ZHANG, L., LIU, W. & CHEN, B. 2017d. Prognostic value of reduced E-cadherin expression in breast cancer: a meta-analysis. *Oncotarget,* 8**,** 16445-16455.
LIANG, J., JIA, X., WANG, K. & ZHAO, N. 2018. High expression of TFEB is associated with aggressive clinical features in colorectal cancer. *Onco Targets Ther,* 11**,** 8089-8098.
LIAO, Y., SMYTH, G. K. & SHI, W. 2014. featureCounts: an efficient general purpose program for assigning sequence reads to genomic features. *Bioinformatics,* 30**,** 923-30.
LIAO, Y., WANG, J., JAEHNIG, E. J., SHI, Z. & ZHANG, B. 2019. WebGestalt 2019: gene set analysis toolkit with revamped UIs and APIs. *Nucleic Acids Res,* 47**,** W199-W205.
LIEBER, M. R. 2010. The mechanism of double-strand DNA break repair by the nonhomologous DNA end-joining pathway. *Annual review of biochemistry,* 79**,** 181-211.
LIN, C., CUI, J., PENG, Z., QIAN, K., WU, R., CHENG, Y. & YIN, W. 2022. Efficacy of platinum-based and non-platinum-based drugs on triple-negative breast cancer: meta-analysis. *Eur J Med Res,* 27**,** 201.
LIN, C., YANG, L., TANASA, B., HUTT, K., JU, B. G., OHGI, K., ZHANG, J., ROSE, D. W., FU, X. D., GLASS, C. K. & ROSENFELD, M. G. 2009. Nuclear receptor-induced chromosomal proximity and DNA breaks underlie specific translocations in cancer. *Cell,* 139**,** 1069-83.
LIN, C. H. & PATTON, J. G. 1995. Regulation of alternative 3' splice site selection by constitutive splicing factors. *Rna,* 1**,** 234-45.

LIN, C. J., CENCIC, R., MILLS, J. R., ROBERT, F. & PELLETIER, J. 2008. c-Myc and eIF4F are components of a feedforward loop that links transcription and translation. *Cancer Res,* 68**,** 5326-34.

LIN, C. Y., WANG, S. S., YANG, C. K., LI, J. R., CHEN, C. S., HUNG, S. C., CHIU, K. Y., CHENG, C. L., OU, Y. C. & YANG, S. F. 2019. Genetic polymorphism and carbonic anhydrase 9 expression can predict nodal metastatic prostate cancer risk in patients with prostate-specific antigen levels ≤10 ng/ml at initial biopsy. *Urol Oncol,* 37**,** 814.e9-814.e16.

LIN, S., CHOE, J., DU, P., TRIBOULET, R. & GREGORY, R. I. 2016. The m(6)A Methyltransferase METTL3 Promotes Translation in Human Cancer Cells. *Mol Cell,* 62**,** 335-345.

LIN, Z., HSU, P. J., XING, X., FANG, J., LU, Z., ZOU, Q., ZHANG, K.-J., ZHANG, X., ZHOU, Y., ZHANG, T., ZHANG, Y., SONG, W., JIA, G., YANG, X., HE, C. & TONG, M.-H. 2017. Mettl3-/Mettl14-mediated mRNA N6-methyladenosine modulates murine spermatogenesis. *Cell Research,* 27**,** 1216.

LINJA, M. J., SAVINAINEN, K. J., SARAMÄKI, O. R., TAMMELA, T. L. J., VESSELLA, R. L. & VISAKORPI, T. 2001. Amplification and Overexpression of Androgen Receptor Gene in Hormone-Refractory Prostate Cancer. *Cancer Research,* 61**,** 3550-3555.

LIPPONEN, P., SAARELAINEN, E., JI, H., AALTOMAA, S. & SYRJÄNEN, K. 1994. Expression of E-cadherin (E-CD) as related to other prognostic factors and survival in breast cancer. *The Journal of Pathology,* 174**,** 101-109.

LITTLE, N. A., HASTIE, N. D. & DAVIES, R. C. 2000. Identification of WTAP, a novel Wilms' tumour 1-associating protein. *Human Molecular Genetics,* 9**,** 2231-2239.

LITTON, J. K., RUGO, H. S., ETTL, J., HURVITZ, S. A., GONÇALVES, A., LEE, K.-H., FEHRENBACHER, L., YERUSHALMI, R., MINA, L. A., MARTIN, M., ROCHÉ, H., IM, Y.-H., QUEK, R. G. W., MARKOVA, D., TUDOR, I. C., HANNAH, A. L., EIERMANN, W. & BLUM, J. L. 2018. Talazoparib in Patients with Advanced Breast Cancer and a Germline BRCA Mutation. *New England Journal of Medicine,* 379**,** 753-763.

LIU, J., LICHTENBERG, T., HOADLEY, K. A., POISSON, L. M., LAZAR, A. J., CHERNIACK, A. D., KOVATICH, A. J., BENZ, C. C., LEVINE, D. A., LEE, A. V., OMBERG, L., WOLF, D. M., SHRIVER, C. D., THORSSON, V. & HU, H. 2018a. An Integrated TCGA Pan-Cancer Clinical Data Resource to Drive High-Quality Survival Outcome Analytics. *Cell,* 173**,** 400-416.e11.

LIU, J., YUE, Y., HAN, D., WANG, X., FU, Y., ZHANG, L., JIA, G., YU, M., LU, Z., DENG, X., DAI, Q., CHEN, W. & HE, C. 2014. A METTL3-METTL14 complex mediates mammalian nuclear RNA N6-adenosine methylation. *Nat Chem Biol,* 10**,** 93-5.

LIU, M., JIANG, K., LIN, G., LIU, P., YAN, Y., YE, T., YAO, G., BARR, M. P., LIANG, D., WANG, Y., GONG, P., MENG, S. & PIAO, H. 2018b. Ajuba inhibits hepatocellular carcinoma cell growth via targeting of beta-catenin and YAP signaling and is regulated by E3 ligase Hakai through neddylation. *J Exp Clin Cancer Res,* 37**,** 165.

LIU, N., ZHOU, K. I., PARISIEN, M., DAI, Q., DIATCHENKO, L. & PAN, T. 2017. N6-methyladenosine alters RNA structure to regulate binding of a low-complexity protein. *Nucleic Acids Research,* 45**,** 6051-6063.

LIU, Q., LI, Z., HE, L., LI, K., HU, C., CHEN, J., ZHOU, F., WANG, J., LI, Y. & XIAO, H. 2022a. Molecular Characterization and Clinical Relevance of N(6)-Methyladenosine Regulators in Metastatic Prostate Cancer. *Front Oncol,* 12**,** 914692.

LIU, W., PALOVCAK, A., LI, F., ZAFAR, A., YUAN, F. & ZHANG, Y. 2020. Fanconi anemia pathway as a prospective target for cancer intervention. *Cell Biosci,* 10**,** 39.

LIU, Z., FAN, M., XUAN, X., XIA, C., HUANG, G. & MA, L. 2022b. Celastrol inhibits the migration and invasion and enhances the anti-cancer effects of docetaxel in human triple-negative breast cancer cells. *Medical Oncology,* 39**,** 189.

LIU, Z., WU, Y., TAO, Z. & MA, L. 2018c. E3 ubiquitin ligase Hakai regulates cell growth and invasion, and increases the chemosensitivity to cisplatin in nonsmallcell lung cancer cells. *Int J Mol Med,* 42**,** 1145-1151.

LLOYD, T., HOUNSOME, L., MEHAY, A., MEE, S., VERNE, J. & COOPER, A. 2015. Lifetime risk of being diagnosed with, or dying from, prostate cancer by major ethnic group in England 2008–2010. *BMC Medicine,* 13**,** 171.

LOBERG, R. D., BRADLEY, D. A., TOMLINS, S. A., CHINNAIYAN, A. M. & PIENTA, K. J. 2007. The lethal phenotype of cancer: the molecular basis of death due to malignancy. *CA Cancer J Clin,* 57**,** 225-41.

LOBERG, R. D., LOGOTHETIS, C. J., KELLER, E. T. & PIENTA, K. J. 2005. Pathogenesis and Treatment of Prostate Cancer Bone Metastases: Targeting the Lethal Phenotype. *Journal of Clinical Oncology,* 23**,** 8232-8241.

LODA, M., CUKOR, B., TAM, S. W., LAVIN, P., FIORENTINC, M., DRAETTA, G. F., JESSUP, J. M. & PAGANO, M. 1997. Increased proteasome-dependent degradation of the cyclin-dependent kinase inhibitor p27 in aggressive colorectal carcinomas. *Nature Medicine,* 3**,** 231-234.

LOMBAERTS, M., VAN WEZEL, T., PHILIPPO, K., DIERSSEN, J. W. F., ZIMMERMAN, R. M. E., OOSTING, J., VAN EIJK, R., EILERS, P. H., VAN DE WATER, B., CORNELISSE, C. J. & CLETON-JANSEN, A. M. 2006. E-cadherin transcriptional downregulation by promoter methylation but not mutation is related to epithelial-to-mesenchymal transition in breast cancer cell lines. *British Journal of Cancer,* 94**,** 661-671.

LONARD, D. M., LANZ, R. B. & O'MALLEY, B. W. 2007. Nuclear receptor coregulators and human disease. *Endocrine reviews,* 28**,** 575-587.

LONGO, D. L. 2010. New Therapies for Castration-Resistant Prostate Cancer. *New England Journal of Medicine,* 363**,** 479-481.

LORD, C. J. & ASHWORTH, A. 2017. PARP inhibitors: Synthetic lethality in the clinic. *Science,* 355**,** 1152-1158.

LOTHION-ROY, J., HAIGH, D. B., HARRIS, A. E., METZLER, V. M., ALSALEEM, M., TOSS, M. S., KARIRI, Y., NTEKIM, A., ROBINSON, B. D., KHANI, F., GUDAS, L. J., ALLEGRUCCI, C., JAMES, V. H., MADHUSUDAN, S., MATHER, M., EMES, R. D., ARCHER, N., FRAY, R. G., RAKHA, E., JEYAPALAN, J. N., RUTLAND, C. S., MONGAN, N. P. & WOODCOCK, C. L. 2022. Clinical and molecular significance of the RNA m(6)A methyltransferase complex in prostate cancer. *Front Genet,* 13**,** 1096071.

LOVE, M. I., HUBER, W. & ANDERS, S. 2014. Moderated estimation of fold change and dispersion for RNA-seq data with DESeq2. *Genome Biol,* 15**,** 550.

LUSTIG-YARIV, O., SCHULZE, E., KOMITOWSKI, D., ERDMANN, V., SCHNEIDER, T., DE GROOT, N. & HOCHBERG, A. 1997. The expression of the imprinted genes H19 and IGF-2 in choriocarcinoma cell lines. Is H19 a tumor suppressor gene? *Oncogene,* 15**,** 169-177.

LYDON, J. P., DEMAYO, F. J., FUNK, C. R., MANI, S. K., HUGHES, A. R., MONTGOMERY, C. A., JR., SHYAMALA, G., CONNEELY, O. M. & O'MALLEY, B. W. 1995. Mice lacking progesterone receptor exhibit pleiotropic reproductive abnormalities. *Genes Dev,* 9**,** 2266-78.

LYLE, K. S., RAAIJMAKERS, J. H., BRUINSMA, W., BOS, J. L. & DE ROOIJ, J. 2008. cAMP-induced Epac-Rap activation inhibits epithelial cell migration by modulating focal adhesion and leading edge dynamics. *Cell Signal,* 20**,** 1104-16.

MA, L., XUAN, X.-J., CHEN, X.-M., FAN, M.-H., LIU, J., HUANG, G.-Z. & LIU, Z. 2023. Ethoxysanguinarine Induces Apoptosis, Inhibits Metastasis and Sensitizes cells to Docetaxel in Breast Cancer Cells through Inhibition of Hakai. *Chemistry & Biodiversity,* 20**,** e202200284.

MA, Y.-L., QIN, P., LI, Y., SHEN, L., WANG, S.-Q., DONG, H.-L., HOU, W.-G. & XIONG, L.-Z. 2013. The effects of different doses of estradiol (E2) on cerebral ischemia in an in vitro model of oxygen and glucose deprivation and reperfusion and in a rat model of middle carotid artery occlusion. *BMC Neuroscience,* 14**,** 118.

MA, Y., KATIYAR, P., JONES, L. P., FAN, S., ZHANG, Y., FURTH, P. A. & ROSEN, E. M. 2006. The breast cancer susceptibility gene BRCA1 regulates progesterone receptor signaling in mammary epithelial cells. *Molecular endocrinology,* 20**,** 14-34.

MA, Z., GAO, Y., LIU, W., ZHENG, L., JIN, B., DUAN, B., XIE, H., GUO, P., ZENG, J., WANG, K., XU, S., WANG, X., HE, D. & LI, L. 2020. CD82 Suppresses ADAM17-Dependent E-Cadherin Cleavage and Cell Migration in Prostate Cancer. *Dis Markers,* 2020**,** 8899924.

MAAS, P., BARRDAHL, M., JOSHI, A. D., AUER, P. L., GAUDET, M. M., MILNE, R. L., SCHUMACHER, F. R., ANDERSON, W. F., CHECK, D., CHATTOPADHYAY, S., BAGLIETTO, L., BERG, C. D., CHANOCK, S. J., COX, D. G., FIGUEROA, J. D., GAIL, M. H., GRAUBARD, B. I., HAIMAN, C. A., HANKINSON, S. E., HOOVER, R. N., ISAACS, C., KOLONEL, L. N., LE MARCHAND, L., LEE, I.-M., LINDSTRÖM, S., OVERVAD, K., ROMIEU, I., SANCHEZ, M.-J., SOUTHEY, M. C., STRAM, D. O., TUMINO, R., VANDERWEELE, T. J., WILLETT, W. C., ZHANG, S., BURING, J. E., CANZIAN, F., GAPSTUR, S. M., HENDERSON, B. E., HUNTER, D. J., GILES, G. G., PRENTICE, R. L., ZIEGLER, R. G., KRAFT, P., GARCIA-CLOSAS, M. & CHATTERJEE, N. 2016. Breast Cancer Risk From Modifiable and Nonmodifiable Risk Factors Among White Women in the United StatesModifiable and Nonmodifiable Risk Factors and Breast Cancer RiskModifiable and Nonmodifiable Risk Factors and Breast Cancer Risk. *JAMA Oncology,* 2**,** 1295-1302.

MACACU, A., AUTIER, P., BONIOL, M. & BOYLE, P. 2015. Active and passive smoking and risk of breast cancer: a meta-analysis. *Breast Cancer Research and Treatment,* 154**,** 213-224.

MAGADI, W., EXARCHAKOU, A., RACHET, B., COLEMAN, M. P., JENKINS, J., BANNISTER, N., MURPHY, R. & ROWLANDS, S. 2016. *Cancer survival in England: Patients diagnosed between 2010 and 2014 and followed up to 2015* [Online]. Office for National Statistics. Available: https://www.ons.gov.uk/peoplepopulationandcommunity/healthandsocialcare/conditionsanddiseases/bulletins/cancersurvivalinenglandadultsdiagnosed/2010and2014andfollowedupto2015#5-year-survival [Accessed 8 August 2019].

MAGEE, J. A., PISKOUNOVA, E. & MORRISON, S. J. 2012. Cancer stem cells: impact, heterogeneity, and uncertainty. *Cancer cell,* 21**,** 283-296.

MAHLER-ARAUJO, B., SAVAGE, K., PARRY, S. & REIS-FILHO, J. S. 2008. Reduction of E-cadherin expression is associated with non-lobular breast carcinomas of basal-like and triple negative phenotype. *Journal of Clinical Pathology,* 61**,** 615.

MAKDISSI, F. B., MACHADO, L. V., OLIVEIRA, A. G., BENVENUTI, T. T., KATAYAMA, M. L., BRENTANI, M. M., OSORIO, C. A., MOURAO NETTO, M., LYRA, E. C., CARVALHO, F., GOES, J. C. & FOLGUEIRA, M. A. 2009. Expression of E-cadherin, Snail and Hakai in epithelial cells isolated from the primary tumor and from peritumoral tissue of invasive ductal breast carcinomas. *Braz J Med Biol Res,* 42**,** 1128-37.

MÄKI, H. E., WALTERING, K. K., WALLÉN, M. J., MARTIKAINEN, P. M., TAMMELA, T. L., VAN WEERDEN, W. M., VESSELLA, R. L. & VISAKORPI, T. 2006. Screening of genetic and expression alterations of SRC1 gene in prostate cancer. *Prostate,* 66**,** 1391-8.

MALIK, S. S., BATOOL, R., MASOOD, N. & YASMIN, A. 2018. Risk factors for prostate cancer: A multifactorial case-control study. *Curr Probl Cancer,* 42**,** 337-343.

MANGELSDORF, D. J., THUMMEL, C., BEATO, M., HERRLICH, P., SCHÜTZ, G., UMESONO, K., BLUMBERG, B., KASTNER, P., MARK, M., CHAMBON, P. & EVANS, R. M. 1995. The nuclear receptor superfamily: the second decade. *Cell,* 83**,** 835-9.

MARCIAS, G., ERDMANN, E., LAPOUGE, G., SIEBERT, C., BARTHÉLÉMY, P., DUCLOS, B., BERGERAT, J.-P., CÉRALINE, J. & KURTZ, J.-E. 2010. Identification of novel truncated androgen receptor (AR) mutants including unreported pre-mRNA splicing variants in the 22Rv1 hormone-refractory prostate cancer (PCa) cell line. *Human Mutation,* 31**,** 74-80.

MARMOT, M. G., ALTMAN, D. G., CAMERON, D. A., DEWAR, J. A., THOMPSON, S. G. & WILCOX, M. 2013. The benefits and harms of breast cancer screening: an independent review. *Br J Cancer,* 108**,** 2205-40.

MARTIN, M. 2011. Cutadapt removes adapter sequences from high-throughput sequencing reads. *2011,* 17**,** 3.

MARTIN, S. A., MCCARTHY, A., BARBER, L. J., BURGESS, D. J., PARRY, S., LORD, C. J. & ASHWORTH, A. 2009. Methotrexate induces oxidative DNA damage and is selectively lethal to tumour cells with defects in the DNA mismatch repair gene MSH2. *EMBO Mol Med,* 1**,** 323-37.

MARTINEZ-IGLESIAS, O., CASAS-PAIS, A., CASTOSA, R., DÍAZ-DÍAZ, A., ROCA-LEMA, D., CONCHA, Á., CORTÉS, Á., GAGO, F. & FIGUEROA, A. 2020. Hakin-1, a New Specific Small-Molecule Inhibitor for the E3

Ubiquitin-Ligase Hakai, Inhibits Carcinoma Growth and Progression. *Cancers (Basel),* 12.

MASHIMA, R., HISHIDA, Y., TEZUKA, T. & YAMANASHI, Y. 2009. The roles of Dok family adapters in immunoreceptor signaling. *Immunol Rev,* 232**,** 273-85.

MASIAKOWSKI, P., BREATHNACH, R., BLOCH, J., GANNON, F., KRUST, A. & CHAMBON, P. 1982. Cloning of cDNA sequences of hormone-regulated genes from the MCF-7 human breast cancer cell line. *Nucleic Acids Res,* 10**,** 7895-903.

MATSUMOTO, K., IKEDA, M., SATO, Y., KURUMA, H., KAMATA, Y., NISHIMORI, T., TOMONAGA, T., NOMURA, F., EGAWA, S. & IWAMURA, M. 2014. Loss of periplakin expression is associated with pathological stage and cancer-specific survival in patients with urothelial carcinoma of the urinary bladder. *Biomed Res,* 35**,** 201-6.

MATSUSHITA, M., FUJITA, K., HAYASHI, T., KAYAMA, H., MOTOOKA, D., HASE, H., JINGUSHI, K., YAMAMICHI, G., YUMIBA, S., TOMIYAMA, E., KOH, Y., HAYASHI, Y., NAKANO, K., WANG, C., ISHIZUYA, Y., KATO, T., HATANO, K., KAWASHIMA, A., UJIKE, T., UEMURA, M., IMAMURA, R., RODRIGUEZ PENA, M. D. C., GORDETSKY, J. B., NETTO, G. J., TSUJIKAWA, K., NAKAMURA, S., TAKEDA, K. & NONOMURA, N. 2021. Gut Microbiota-Derived Short-Chain Fatty Acids Promote Prostate Cancer Growth via IGF1 Signaling. *Cancer Res,* 81**,** 4014-4026.

MAXWELL, P. H., WIESENER, M. S., CHANG, G.-W., CLIFFORD, S. C., VAUX, E. C., COCKMAN, M. E., WYKOFF, C. C., PUGH, C. W., MAHER, E. R. & RATCLIFFE, P. J. 1999. The tumour suppressor protein VHL targets hypoxia-inducible factors for oxygen-dependent proteolysis. *Nature,* 399**,** 271-275.

MCDONALD, P. C., CHAFE, S. C., BROWN, W. S., SABERI, S., SWAYAMPAKULA, M., VENKATESWARAN, G., NEMIROVSKY, O., GILLESPIE, J. A., KARASINSKA, J. M., KALLOGER, S. E., SUPURAN, C. T., SCHAEFFER, D. F., BASHASHATI, A., SHAH, S. P., TOPHAM, J. T., YAPP, D. T., LI, J., RENOUF, D. J., STANGER, B. Z. & DEDHAR, S. 2019. Regulation of pH by Carbonic Anhydrase 9 Mediates Survival of Pancreatic Cancer Cells With Activated KRAS in Response to Hypoxia. *Gastroenterology,* 157**,** 823-837.

MCGUIRE, A., BROWN, J. A. L., MALONE, C., MCLAUGHLIN, R. & KERIN, M. J. 2015. Effects of Age on the Detection and Management of Breast Cancer. *Cancers,* 7**,** 908-929.

MCKNIGHT, G. S. 1991. Cyclic AMP second messenger systems. *Curr Opin Cell Biol,* 3**,** 213-7.

MCNEAL, J. E. 1988. Normal histology of the prostate. *Am J Surg Pathol,* 12**,** 619-33.

MCSHERRY, E. A., BRENNAN, K., HUDSON, L., HILL, A. D. & HOPKINS, A. M. 2011. Breast cancer cell migration is regulated through junctional adhesion molecule-A-mediated activation of Rap1 GTPase. *Breast Cancer Res,* 13**,** R31.

MELLAI, M., CASALONE, C., CORONA, C., CROCIARA, P., FAVOLE, A., CASSONI, P., SCHIFFER, D. & BOLDORINI, R. 2020. Chondroitin Sulphate Proteoglycans in the Tumour Microenvironment. *Adv Exp Med Biol,* 1272**,** 73-92.

MENON, J., DOEBELE, R. C., GOMES, S., BEVILACQUA, E., REINDL, K. M. & ROSNER, M. R. 2012. A novel interplay between Rap1 and PKA regulates induction of angiogenesis in prostate cancer. *PLoS One,* 7**,** e49893.

MEYER, K. D., SALETORE, Y., ZUMBO, P., ELEMENTO, O., MASON, C. E. & JAFFREY, S. R. 2012. Comprehensive analysis of mRNA methylation reveals enrichment in 3' UTRs and near stop codons. *Cell,* 149**,** 1635-46.

MEYER, N. & PENN, L. Z. 2008. Reflecting on 25 years with MYC. *Nat Rev Cancer,* 8**,** 976-90.

MIKI, Y., SWENSEN, J., SHATTUCK-EIDENS, D., FUTREAL, P. A., HARSHMAN, K., TAVTIGIAN, S., LIU, Q., COCHRAN, C., BENNETT, L. M., DING, W., BELL, R., ROSENTHAL, J., HUSSEY, C., TRAN, T., MCCLURE, M., FRYE, C., HATTIER, T., PHELPS, R., HAUGEN-STRANO, A., KATCHER, H., YAKUMO, K., GHOLAMI, Z., SHAFFER, D., STONE, S., BAYER, S., WRAY, C., BOGDEN, R., DAYANANTH, P., WARD, J., TONIN, P., NAROD, S., BRISTOW, P. K., NORRIS, F. H., HELVERING, L., MORRISON, P., ROSTECK, P., LAI, M., BARRETT, J. C., LEWIS, C., NEUHAUSEN, S., CANNON-ALBRIGHT, L., GOLDGAR, D., WISEMAN, R., KAMB, A. & SKOLNICK, M. H. 1994. A Strong Candidate for the Breast and Ovarian Cancer Susceptibility Gene BRCA1. *Science,* 266**,** 66-71.

MILLER, K. D., SIEGEL, R. L., LIN, C. C., MARIOTTO, A. B., KRAMER, J. L., ROWLAND, J. H., STEIN, K. D., ALTERI, R. & JEMAL, A. 2016. Cancer treatment and survivorship statistics, 2016. *CA: A Cancer Journal for Clinicians,* 66**,** 271-289.

MILLER, M. D., MARTY, M. A., BROADWIN, R., JOHNSON, K. C., SALMON, A. G., WINDER, B. & STEINMAUS, C. 2007. The association between exposure to environmental tobacco smoke and breast cancer: A review by the California Environmental Protection Agency. *Preventive Medicine,* 44**,** 93-106.

MILLER, W. R., ELTON, R. A., DIXON, J. M., CHETTY, U. & WATSON, D. M. 1990. Cyclic AMP binding proteins and prognosis in breast cancer. *Br J Cancer,* 61**,** 263-6.

MIMEAULT, M. & BATRA, S. K. 2013. Hypoxia-inducing factors as master regulators of stemness properties and altered metabolism of cancer- and metastasis-initiating cells. *J Cell Mol Med,* 17**,** 30-54.

MINCKWITZ, G. V., SCHNEEWEISS, A., SALAT, C., REZAI, M., ZAHM, D. M., KLARE, P., BLOHMER, J. U., TESCH, H., KHANDAN, F., JUD, S., JACKISCH, C., MEHTA, K., LOIBL, S., UNTCH, M. & GROUP, G. B. 2013. A randomized phase II trial investigating the addition of carboplatin to neoadjuvant therapy for triple-negative and HER2-positive early breast cancer (GeparSixto). *Journal of Clinical Oncology,* 31**,** 1004-1004.

MITOBE, Y., IINO, K., TAKAYAMA, K. I., IKEDA, K., SUZUKI, T., AOGI, K., KAWABATA, H., SUZUKI, Y., HORIE-INOUE, K. & INOUE, S. 2020. PSF Promotes ER-Positive Breast Cancer Progression via Posttranscriptional Regulation of ESR1 and SCFD2. *Cancer Res,* 80**,** 2230-2242.

MIYAKE, S., LUPHER, M. L., DRUKER, B. & BAND, H. 1998. The tyrosine kinase regulator Cbl enhances the ubiquitination and degradation of the

platelet-derived growth factor receptor α. *Proceedings of the National Academy of Sciences,* 95**,** 7927-7932.
MIYOSHI, Y., UEMURA, H., FUJINAMI, K., MIKATA, K., HARADA, M., KITAMURA, H., KOIZUMI, Y. & KUBOTA, Y. 2000. Fluorescence in situ hybridization evaluation of c-myc and androgen receptor gene amplification and chromosomal anomalies in prostate cancer in Japanese patients. *Prostate,* 43**,** 225-32.
MODELSKA, A., TURRO, E., RUSSELL, R., BEATON, J., SBARRATO, T., SPRIGGS, K., MILLER, J., GRÄF, S., PROVENZANO, E., BLOWS, F., PHAROAH, P., CALDAS, C. & LE QUESNE, J. 2015. The malignant phenotype in breast cancer is driven by eIF4A1-mediated changes in the translational landscape. *Cell Death Dis,* 6**,** e1603.
MODENA, A., MASSARI, F., CICCARESE, C., BRUNELLI, M., SANTONI, M., MONTIRONI, R., MARTIGNONI, G. & TORTORA, G. 2016. Targeting Met and VEGFR Axis in Metastatic Castration-Resistant Prostate Cancer: 'Game Over'? *Target Oncol,* 11**,** 431-46.
MOHAMMED, H., RUSSELL, I. A., STARK, R., RUEDA, O. M., HICKEY, T. E., TARULLI, G. A., SERANDOUR, A. A., BIRRELL, S. N., BRUNA, A., SAADI, A., MENON, S., HADFIELD, J., PUGH, M., RAJ, G. V., BROWN, G. D., D'SANTOS, C., ROBINSON, J. L. L., SILVA, G., LAUNCHBURY, R., PEROU, C. M., STINGL, J., CALDAS, C., TILLEY, W. D. & CARROLL, J. S. 2015. Progesterone receptor modulates ERα action in breast cancer. *Nature,* 523**,** 313.
MONGAN, N. P., TADOKORO-CUCCARO, R., BUNCH, T. & HUGHES, I. A. 2015. Androgen insensitivity syndrome. *Best Pract Res Clin Endocrinol Metab,* 29**,** 569-80.
MOODY, S. E., PEREZ, D., PAN, T.-C., SARKISIAN, C. J., PORTOCARRERO, C. P., STERNER, C. J., NOTORFRANCESCO, K. L., CARDIFF, R. D. & CHODOSH, L. A. 2005. The transcriptional repressor Snail promotes mammary tumor recurrence. *Cancer cell,* 8**,** 197-209.
MOORADIAN, A. D., MORLEY, J. E. & KORENMAN, S. G. 1987. Biological actions of androgens. *Endocr Rev,* 8**,** 1-28.
MORAS, D. & GRONEMEYER, H. 1998. The nuclear receptor ligand-binding domain: structure and function. *Curr Opin Cell Biol,* 10**,** 384-91.
MORRIS, P. G., HUDIS, C. A., GIRI, D., MORROW, M., FALCONE, D. J., ZHOU, X. K., DU, B., BROGI, E., CRAWFORD, C. B., KOPELOVICH, L., SUBBARAMAIAH, K. & DANNENBERG, A. J. 2011. Inflammation and increased aromatase expression occur in the breast tissue of obese women with breast cancer. *Cancer Prev Res (Phila),* 4**,** 1021-9.
MOSSMANN, D., PARK, S. & HALL, M. N. 2018. mTOR signalling and cellular metabolism are mutual determinants in cancer. *Nat Rev Cancer,* 18**,** 744-757.
MOTRICH, R. D., SALAZAR, F. C., BRESER, M. L., MACKERN-OBERTI, J. P., GODOY, G. J., OLIVERA, C., PAIRA, D. A. & RIVERO, V. E. 2018. Implications of prostate inflammation on male fertility. *Andrologia,* 50**,** e13093.
MOTTET, N., BELLMUNT, J., BOLLA, M., BRIERS, E., CUMBERBATCH, M. G., DE SANTIS, M., FOSSATI, N., GROSS, T., HENRY, A. M., JONIAU, S., LAM, T. B., MASON, M. D., MATVEEV, V. B., MOLDOVAN, P. C., VAN DEN BERGH, R. C. N., VAN DEN BROECK, T., VAN DER POEL,

H. G., VAN DER KWAST, T. H., ROUVIÈRE, O., SCHOOTS, I. G., WIEGEL, T. & CORNFORD, P. 2017. EAU-ESTRO-SIOG Guidelines on Prostate Cancer. Part 1: Screening, Diagnosis, and Local Treatment with Curative Intent. *European Urology,* 71**,** 618-629.

MOULTON, T., CRENSHAW, T., HAO, Y., MOOSIKASUWAN, J., LIN, N., DEMBITZER, F., HENSLE, T., WEISS, L., MCMORROW, L., LOEW, T., KRAUS, W., GERALD, W. & TYCKO, B. 1994. Epigenetic lesions at the H19 locus in Wilms' tumour patients. *Nature Genetics,* 7**,** 440-447.

MUCCI, L. A., HJELMBORG, J. B., HARRIS, J. R., CZENE, K., HAVELICK, D. J., SCHEIKE, T., GRAFF, R. E., HOLST, K., MÖLLER, S., UNGER, R. H., MCINTOSH, C., NUTTALL, E., BRANDT, I., PENNEY, K. L., HARTMAN, M., KRAFT, P., PARMIGIANI, G., CHRISTENSEN, K., KOSKENVUO, M., HOLM, N. V., HEIKKILÄ, K., PUKKALA, E., SKYTTHE, A., ADAMI, H. O. & KAPRIO, J. 2016. Familial Risk and Heritability of Cancer Among Twins in Nordic Countries. *Jama,* 315**,** 68-76.

MUCCI, N. R., AKDAS, G., MANELY, S. & RUBIN, M. A. 2000. Neuroendocrine expression in metastaticprostate cancer: Evaluation of high throughput tissue microarrays to detect heterogeneous protein expression. *Human pathology,* 31**,** 406-414.

MUELLER, S. O. & KORACH, K. S. 2001. Estrogen receptors and endocrine diseases: lessons from estrogen receptor knockout mice. *Curr Opin Pharmacol,* 1**,** 613-9.

MUKHERJEE, M., CHOW, S. Y., YUSOFF, P., SEETHARAMAN, J., NG, C., SINNIAH, S., KOH, X. W., ASGAR, N. F., LI, D., YIM, D., JACKSON, R. A., YEW, J., QIAN, J., IYU, A., LIM, Y. P., ZHOU, X., SZE, S. K., GUY, G. R. & SIVARAMAN, J. 2012. Structure of a novel phosphotyrosine-binding domain in Hakai that targets E-cadherin. *EMBO J,* 31**,** 1308-19.

MUKHERJEE, M., JING-SONG, F., RAMACHANDRAN, S., GUY, G. R. & SIVARAMAN, J. 2014. Dimeric switch of Hakai-truncated monomers during substrate recognition: insights from solution studies and NMR structure. *J Biol Chem,* 289**,** 25611-23.

MURPHY, N., KNUPPEL, A., PAPADIMITRIOU, N., MARTIN, R. M., TSILIDIS, K., SMITH-BYRNE, K., FENSOM, G., PEREZ-CORNAGO, A., TRAVIS, R. C. & KEY, T. J. 2020. Insulin-like growth factor-1, insulin-like growth factor-binding protein-3, and breast cancer risk: observational and Mendelian randomization analyses with~ 430 000 women. *Annals of Oncology,* 31**,** 641-649.

MURTHY, R. K., LOI, S., OKINES, A., PAPLOMATA, E., HAMILTON, E., HURVITZ, S. A., LIN, N. U., BORGES, V., ABRAMSON, V., ANDERS, C., BEDARD, P. L., OLIVEIRA, M., JAKOBSEN, E., BACHELOT, T., SHACHAR, S. S., MÜLLER, V., BRAGA, S., DUHOUX, F. P., GREIL, R., CAMERON, D., CAREY, L. A., CURIGLIANO, G., GELMON, K., HORTOBAGYI, G., KROP, I., LOIBL, S., PEGRAM, M., SLAMON, D., PALANCA-WESSELS, M. C., WALKER, L., FENG, W. & WINER, E. P. 2020. Tucatinib, Trastuzumab, and Capecitabine for HER2-Positive Metastatic Breast Cancer. *N Engl J Med,* 382**,** 597-609.

MYLONAS, I., JESCHKE, U., SHABANI, N., KUHN, C., FRIESE, K. & GERBER, B. 2005. Inhibin/activin subunits (inhibin-alpha, -betaA and -betaB) are differentially expressed in human breast cancer and their metastasis. *Oncol Rep,* 13**,** 81-8.

NAGATA, Y., GOTO, T. & MIYAMOTO, H. 2019. The role of mineralocorticoid receptor signaling in genitourinary cancers. *Nuclear Receptor Research,* 6**,** 1-7.
NAPOLITANO, G., ESPOSITO, A., CHOI, H., MATARESE, M., BENEDETTI, V., DI MALTA, C., MONFREGOLA, J., MEDINA, D. L., LIPPINCOTT-SCHWARTZ, J. & BALLABIO, A. 2018. mTOR-dependent phosphorylation controls TFEB nuclear export. *Nat Commun,* 9**,** 3312.
NATIONAL CENTER FOR CHRONIC DISEASE, P., HEALTH PROMOTION OFFICE ON, S. & HEALTH 2014. Reports of the Surgeon General. *The Health Consequences of Smoking-50 Years of Progress: A Report of the Surgeon General.* Atlanta (GA): Centers for Disease Control and Prevention (US).
NATT, E., MAGENIS, R. E., ZIMMER, J., MANSOURI, A. & SCHERER, G. 1989. Regional assignment of the human loci for uvomorulin (UVO) and chymotrypsinogen B (CTRB) with the help of two overlapping deletions on the long arm of chromosome 16. *Cytogenet Cell Genet,* 50**,** 145-8.
NEILL, T., SCHAEFER, L. & IOZZO, R. V. 2012. Decorin: a guardian from the matrix. *The American journal of pathology,* 181**,** 380-387.
NETTEY, O. S., WALKER, A. J., KEETER, M. K., SINGAL, A., NUGOORU, A., MARTIN, I. K., RUDEN, M., GOGANA, P., DIXON, M. A., OSUMA, T., HOLLOWELL, C. M. P., SHARIFI, R., SEKOSAN, M., YANG, X., CATALONA, W. J., KAJDACSY-BALLA, A., MACIAS, V., KITTLES, R. A. & MURPHY, A. B. 2018. Self-reported Black race predicts significant prostate cancer independent of clinical setting and clinical and socioeconomic risk factors. *Urol Oncol,* 36**,** 501 e1-501 e8.
NEUHOUSER, M. L., ARAGAKI, A. K., PRENTICE, R. L., MANSON, J. E., CHLEBOWSKI, R., CARTY, C. L., OCHS-BALCOM, H. M., THOMSON, C. A., CAAN, B. J., TINKER, L. F., URRUTIA, R. P., KNUDTSON, J. & ANDERSON, G. L. 2015. Overweight, Obesity, and Postmenopausal Invasive Breast Cancer Risk: A Secondary Analysis of the Women's Health Initiative Randomized Clinical TrialsObesity and Postmenopausal Invasive Breast Cancer RiskObesity and Postmenopausal Invasive Breast Cancer Risk. *JAMA Oncology,* 1**,** 611-621.
NEVEDOMSKAYA, E., WESSELS, L. & ZWART, W. 2014. Genome-wide epigenetic profiling of breast cancer tumors treated with aromatase inhibitors. *Genom Data,* 2**,** 195-8.
NI, L., LLEWELLYN, R., KESLER, C. T., KELLEY, J. B., SPENCER, A., SNOW, C. J., SHANK, L. & PASCHAL, B. M. 2013. Androgen induces a switch from cytoplasmic retention to nuclear import of the androgen receptor. *Mol Cell Biol,* 33**,** 4766-78.
NICE. 2016. *Quality statement 1: Timely diagnosis* [Online]. National Institute for Health and Care Excellence. Available: https://www.nice.org.uk/guidance/qs12/chapter/Quality-statement-1-Timely-diagnosis [Accessed 7 August 2019].
NICE. 2020. *Breast screening* [Online]. National Institute for Health and Care Excellence. Available: https://cks.nice.org.uk/topics/breast-screening/background-information/the-nhs-breast-screening-programme/ [Accessed 11 September 2020].
NISHIZUKA, Y. 1988. The molecular heterogeneity of protein kinase C and its implications for cellular regulation. *Nature,* 334**,** 661-5.

NOH, S. J., BAEK, H. A., PARK, H. S., JANG, K. Y., MOON, W. S., KANG, M. J., LEE, D. G., KIM, M. H., LEE, J. H. & CHUNG, M. J. 2013. Expression of SIRT1 and cortactin is associated with progression of non-small cell lung cancer. *Pathol Res Pract,* 209**,** 365-70.

NOLAN, E., LINDEMAN, G. J. & VISVADER, J. E. 2023. Deciphering breast cancer: from biology to the clinic. *Cell,* 186**,** 1708-1728.

NOLLET, F., BERX, G. & VAN ROY, F. 1999. The Role of the E-Cadherin/Catenin Adhesion Complex in the Development and Progression of Cancer. *Molecular Cell Biology Research Communications,* 2**,** 77-85.

NOURUZI, S., GANGULI, D., TABRIZIAN, N., KOBELEV, M., SIVAK, O., NAMEKAWA, T., THAPER, D., BACA, S. C., FREEDMAN, M. L., AGUDA, A., DAVIES, A. & ZOUBEIDI, A. 2022. ASCL1 activates neuronal stem cell-like lineage programming through remodeling of the chromatin landscape in prostate cancer. *Nat Commun,* 13**,** 2282.

OBR, A. E. & EDWARDS, D. P. 2012. The biology of progesterone receptor in the normal mammary gland and in breast cancer. *Molecular and Cellular Endocrinology,* 357**,** 4-17.

OESTERREICH, S., DENG, W., JIANG, S., CUI, X., IVANOVA, M., SCHIFF, R., KANG, K., HADSELL, D. L., BEHRENS, J. & LEE, A. V. 2003. Estrogen-mediated down-regulation of E-cadherin in breast cancer cells. *Cancer Res,* 63**,** 5203-8.

OHISHI, Y., ODA, Y., KURIHARA, S., KAKU, T., KOBAYASHI, H., WAKE, N. & TSUNEYOSHI, M. 2011. Nuclear localization of E-cadherin but not beta-catenin in human ovarian granulosa cell tumours and normal ovarian follicles and ovarian stroma. *Histopathology,* 58**,** 423-32.

OKA, H., SHIOZAKI, H., KOBAYASHI, K., INOUE, M., TAHARA, H., KOBAYASHI, T., TAKATSUKA, Y., MATSUYOSHI, N., HIRANO, S., TAKEICHI, M. & ET AL. 1993. Expression of E-cadherin cell adhesion molecules in human breast cancer tissues and its relationship to metastasis. *Cancer Res,* 53**,** 1696-701.

OKUDA, H., KOBAYASHI, A., XIA, B., WATABE, M., PAI, S. K., HIROTA, S., XING, F., LIU, W., PANDEY, P. R. & FUKUDA, K. 2012. Hyaluronan Synthase HAS2 Promotes Tumor Progression in Bone by Stimulating the Interaction of Breast Cancer Stem–Like Cells with Macrophages and Stromal CellsHAS2 Promotes Tumor Progression in Bone. *Cancer research,* 72**,** 537-547.

OKUMURA, N., YOSHIDA, H., KITAGISHI, Y., NISHIMURA, Y. & MATSUDA, S. 2011. Alternative splicings on p53, BRCA1 and PTEN genes involved in breast cancer. *Biochemical and Biophysical Research Communications,* 413**,** 395-399.

OLEFSKY, J. M. 2001. Nuclear receptor minireview series. *J Biol Chem,* 276**,** 36863-4.

OLMEDA, D., MORENO-BUENO, G., FLORES, J. M., FABRA, A., PORTILLO, F. & CANO, A. 2007. SNAI1 is required for tumor growth and lymph node metastasis of human breast carcinoma MDA-MB-231 cells. *Cancer research,* 67**,** 11721-11731.

OLSEN, J. R., AZEEM, W., HELLEM, M. R., MARVYIN, K., HUA, Y., QU, Y., LI, L., LIN, B., KE, X., ØYAN, A. M. & KALLAND, K. 2016. Context dependent regulatory patterns of the androgen receptor and androgen receptor target genes. *BMC Cancer,* 16**,** 377.

ONITILO, A. A., ENGEL, J. M., GREENLEE, R. T. & MUKESH, B. N. 2009. Breast cancer subtypes based on ER/PR and Her2 expression: comparison of clinicopathologic features and survival. *Clin Med Res,* 7**,** 4-13.

ORIHUELA, E. & GREEN, J. M. 2008. Ductal prostate cancer: contemporary management and outcomes. *Urol Oncol,* 26**,** 368-71.

OTSUBO, T., HAGIWARA, T., TAMURA-NAKANO, M., SEZAKI, T., MIYAKE, O., HINOHARA, C., SHIMIZU, T., YAMADA, K., DOHI, T. & KAWAMURA, Y. I. 2015. Aberrant DNA hypermethylation reduces the expression of the desmosome-related molecule periplakin in esophageal squamous cell carcinoma. *Cancer Med,* 4**,** 415-25.

OUGHTRED, R., STARK, C., BREITKREUTZ, B. J., RUST, J., BOUCHER, L., CHANG, C., KOLAS, N., O'DONNELL, L., LEUNG, G., MCADAM, R., ZHANG, F., DOLMA, S., WILLEMS, A., COULOMBE-HUNTINGTON, J., CHATR-ARYAMONTRI, A., DOLINSKI, K. & TYERS, M. 2019. The BioGRID interaction database: 2019 update. *Nucleic Acids Res,* 47**,** D529-d541.

PACHECO-VELÁZQUEZ, S. C., ORTEGA-MEJÍA, I. I., VARGAS-NAVARRO, J. L., PADILLA-FLORES, J. A., ROBLEDO-CADENA, D. X., TAPIA-MARTÍNEZ, G., PEÑALOSA-CASTRO, I., AGUILAR-PONCE, J. L., GRANADOS-RIVAS, J. C., MORENO-SÁNCHEZ, R. & RODRÍGUEZ-ENRÍQUEZ, S. 2022. 17-β Estradiol up-regulates energy metabolic pathways, cellular proliferation and tumor invasiveness in ER+ breast cancer spheroids. *Frontiers in Oncology,* 12.

PAGES, M., LACROIX, L., TAUZIEDE-ESPARIAT, A., CASTEL, D., DAUDIGEOS-DUBUS, E., RIDOLA, V., GILLES, S., FINA, F., ANDREIUOLO, F., POLIVKA, M., LECHAPT-ZALCMAN, E., PUGET, S., BODDAERT, N., LIU, X. Q., BRIDGE, J. A., GRILL, J., CHRETIEN, F. & VARLET, P. 2015. Papillary glioneuronal tumors: histological and molecular characteristics and diagnostic value of SLC44A1-PRKCA fusion. *Acta Neuropathol Commun,* 3**,** 85.

PAIK, S., SHAK, S., TANG, G., KIM, C., BAKER, J., CRONIN, M., BAEHNER, F. L., WALKER, M. G., WATSON, D., PARK, T., HILLER, W., FISHER, E. R., WICKERHAM, D. L., BRYANT, J. & WOLMARK, N. 2004. A Multigene Assay to Predict Recurrence of Tamoxifen-Treated, Node-Negative Breast Cancer. *New England Journal of Medicine,* 351**,** 2817-2826.

PAN, T. 2013. N6-methyl-adenosine modification in messenger and long non-coding RNA. *Trends in Biochemical Sciences,* 38**,** 204-209.

PANTELIDOU, C., SONZOGNI, O., DE OLIVERIA TAVEIRA, M., MEHTA, A. K., KOTHARI, A., WANG, D., VISAL, T., LI, M. K., PINTO, J., CASTRILLON, J. A., CHENEY, E. M., BOUWMAN, P., JONKERS, J., ROTTENBERG, S., GUERRIERO, J. L., WULF, G. M. & SHAPIRO, G. I. 2019. PARP Inhibitor Efficacy Depends on CD8(+) T-cell Recruitment via Intratumoral STING Pathway Activation in BRCA-Deficient Models of Triple-Negative Breast Cancer. *Cancer Discov,* 9**,** 722-737.

PAREDES, J., FIGUEIREDO, J., ALBERGARIA, A., OLIVEIRA, P., CARVALHO, J., RIBEIRO, A. S., CALDEIRA, J., COSTA, A. M., SIMÕES-CORREIA, J., OLIVEIRA, M. J., PINHEIRO, H., PINHO, S. S., MATEUS, R., REIS, C. A., LEITE, M., FERNANDES, M. S., SCHMITT, F., CARNEIRO, F., FIGUEIREDO, C., OLIVEIRA, C. & SERUCA, R.

2012. Epithelial E- and P-cadherins: Role and clinical significance in cancer. *Biochimica et Biophysica Acta - Reviews on Cancer,* 1826**,** 297-311.

PARIS, J., MORGAN, M., CAMPOS, J., SPENCER, G. J., SHMAKOVA, A., IVANOVA, I., MAPPERLEY, C., LAWSON, H., WOTHERSPOON, D. A., SEPULVEDA, C., VUKOVIC, M., ALLEN, L., SARAPUU, A., TAVOSANIS, A., GUITART, A. V., VILLACRECES, A., MUCH, C., CHOE, J., AZAR, A., VAN DE LAGEMAAT, L. N., VERNIMMEN, D., NEHME, A., MAZURIER, F., SOMERVAILLE, T. C. P., GREGORY, R. I., O'CARROLL, D. & KRANC, K. R. 2019. Targeting the RNA m(6)A Reader YTHDF2 Selectively Compromises Cancer Stem Cells in Acute Myeloid Leukemia. *Cell Stem Cell,* 25**,** 137-148.e6.

PARK, K., DALTON, J. T., NARAYANAN, R., BARBIERI, C. E., HANCOCK, M. L., BOSTWICK, D. G., STEINER, M. S. & RUBIN, M. A. 2014. TMPRSS2:ERG gene fusion predicts subsequent detection of prostate cancer in patients with high-grade prostatic intraepithelial neoplasia. *J Clin Oncol,* 32**,** 206-11.

PASCHALIS, A., SHARP, A., WELTI, J. C., NEEB, A., RAJ, G. V., LUO, J., PLYMATE, S. R. & DE BONO, J. S. 2018. Alternative splicing in prostate cancer. *Nat Rev Clin Oncol,* 15**,** 663-675.

PATERNI, I., GRANCHI, C., KATZENELLENBOGEN, J. A. & MINUTOLO, F. 2014. Estrogen receptors alpha (ERα) and beta (ERβ): subtype-selective ligands and clinical potential. *Steroids,* 90**,** 13-29.

PATIL, D. P., CHEN, C.-K., PICKERING, B. F., CHOW, A., JACKSON, C., GUTTMAN, M. & JAFFREY, S. R. 2016. m6A RNA methylation promotes XIST-mediated transcriptional repression. *Nature,* 537**,** 369.

PATTON, J. G., MAYER, S. A., TEMPST, P. & NADAL-GINARD, B. 1991. Characterization and molecular cloning of polypyrimidine tract-binding protein: a component of a complex necessary for pre-mRNA splicing. *Genes Dev,* 5**,** 1237-51.

PATTON, J. G., PORRO, E. B., GALCERAN, J., TEMPST, P. & NADAL-GINARD, B. 1993. Cloning and characterization of PSF, a novel pre-mRNA splicing factor. *Genes Dev,* 7**,** 393-406.

PAYNE, A. H. & HALES, D. B. 2004. Overview of steroidogenic enzymes in the pathway from cholesterol to active steroid hormones. *Endocr Rev,* 25**,** 947-70.

PECE, S. & GUTKIND, J. S. 2002. E-cadherin and Hakai: signalling, remodeling or destruction? *Nat Cell Biol,* 4**,** E72-4.

PEINADO, H., PORTILLO, F. & CANO, A. 2004. Transcriptional regulation of cadherins during development and carcinogenesis. *Int J Dev Biol,* 48**,** 365-75.

PEISCH, S. F., VAN BLARIGAN, E. L., CHAN, J. M., STAMPFER, M. J. & KENFIELD, S. A. 2017. Prostate cancer progression and mortality: a review of diet and lifestyle factors. *World Journal of Urology,* 35**,** 867-874.

PENALVA, L. O. F., RUIZ, M. F., ORTEGA, A., GRANADINO, B., VICENTE, L., SEGARRA, C., VALCÁRCEL, J. & SÁNCHEZ, L. 2000. The Drosophila fl(2)d Gene, Required for Female-Specific Splicing of Sxl and tra Pre-mRNAs, Encodes a Novel Nuclear Protein With a HQ-Rich Domain. *Genetics,* 155**,** 129-139.

PENG, H., CHEN, B., WEI, W., GUO, S., HAN, H., YANG, C., MA, J., WANG, L., PENG, S., KUANG, M. & LIN, S. 2022. N(6)-methyladenosine (m(6)A) in 18S rRNA promotes fatty acid metabolism and oncogenic transformation. *Nat Metab,* 4**,** 1041-1054.

PENG, S., XIAO, W., JU, D., SUN, B., HOU, N., LIU, Q., WANG, Y., ZHAO, H., GAO, C., ZHANG, S., CAO, R., LI, P., HUANG, H., MA, Y., WANG, Y., LAI, W., MA, Z., ZHANG, W., HUANG, S., WANG, H., ZHANG, Z., ZHAO, L., CAI, T., ZHAO, Y. L., WANG, F., NIE, Y., ZHI, G., YANG, Y. G., ZHANG, E. E. & HUANG, N. 2019. Identification of entacapone as a chemical inhibitor of FTO mediating metabolic regulation through FOXO1. *Sci Transl Med,* 11.

PEPINSKY, R. B., SINCLAIR, L. K., CHOW, E. P., MATTALIANO, R. J., MANGANARO, T. F., DONAHOE, P. K. & CATE, R. L. 1988. Proteolytic processing of mullerian inhibiting substance produces a transforming growth factor-beta-like fragment. *J Biol Chem,* 263**,** 18961-4.

PEREGRIN-ALVAREZ, I., FLETCHER, N. M., SAED, G. M., ROMAN, R. A. & DETTI, L. 2021. Anti-Müllerian Hormone (AMH) regulates BRCA1 and BRCA2 gene expression after ovarian cortex transplantation. *Gynecol Endocrinol,* 37**,** 349-352.

PEREIRA, B., CHIN, S. F., RUEDA, O. M., VOLLAN, H. K., PROVENZANO, E., BARDWELL, H. A., PUGH, M., JONES, L., RUSSELL, R., SAMMUT, S. J., TSUI, D. W., LIU, B., DAWSON, S. J., ABRAHAM, J., NORTHEN, H., PEDEN, J. F., MUKHERJEE, A., TURASHVILI, G., GREEN, A. R., MCKINNEY, S., OLOUMI, A., SHAH, S., ROSENFELD, N., MURPHY, L., BENTLEY, D. R., ELLIS, I. O., PURUSHOTHAM, A., PINDER, S. E., BØRRESEN-DALE, A. L., EARL, H. M., PHAROAH, P. D., ROSS, M. T., APARICIO, S. & CALDAS, C. 2016. The somatic mutation profiles of 2,433 breast cancers refines their genomic and transcriptomic landscapes. *Nat Commun,* 7**,** 11479.

PEREZ-GARCIA, J., MUÑOZ-COUSELO, E., SOBERINO, J., RACCA, F. & CORTES, J. 2018. Targeting FGFR pathway in breast cancer. *Breast,* 37**,** 126-133.

PERNAS, S. & TOLANEY, S. M. 2022. Clinical trial data and emerging strategies: HER2-positive breast cancer. *Breast Cancer Research and Treatment,* 193**,** 281-291.

PEROU, C. M. 2011. Molecular stratification of triple-negative breast cancers. *Oncologist,* 16 Suppl 1**,** 61-70.

PEROU, C. M., SORLIE, T., EISEN, M. B., VAN DE RIJN, M., JEFFREY, S. S., REES, C. A., POLLACK, J. R., ROSS, D. T., JOHNSEN, H., AKSLEN, L. A., FLUGE, O., PERGAMENSCHIKOV, A., WILLIAMS, C., ZHU, S. X., LONNING, P. E., BORRESEN-DALE, A. L., BROWN, P. O. & BOTSTEIN, D. 2000. Molecular portraits of human breast tumours. *Nature,* 406**,** 747-52.

PFAFFL, M. W. 2001. A new mathematical model for relative quantification in real-time RT-PCR. *Nucleic Acids Res,* 29**,** e45.

PICCART, M., PROCTER, M., FUMAGALLI, D., DE AZAMBUJA, E., CLARK, E., EWER, M. S., RESTUCCIA, E., JERUSALEM, G., DENT, S., REABY, L., BONNEFOI, H., KROP, I., LIU, T.-W., PIEŃKOWSKI, T., TOI, M., WILCKEN, N., ANDERSSON, M., IM, Y.-H., TSENG, L. M., LUECK, H.-J., COLLEONI, M., MONTURUS, E., SICOE, M., GUILLAUME, S., BINES, J., GELBER, R. D., VIALE, G. & THOMSSEN,

C. 2021. Adjuvant Pertuzumab and Trastuzumab in Early HER2-Positive Breast Cancer in the APHINITY Trial: 6 Years' Follow-Up. *Journal of Clinical Oncology,* 39**,** 1448-1457.

PICKART, C. M. 2001. Mechanisms Underlying Ubiquitination. *Annual Review of Biochemistry,* 70**,** 503-533.

PICKUP, M., NOVITSKIY, S. & MOSES, H. L. 2013. The roles of TGFβ in the tumour microenvironment. *Nat Rev Cancer,* 13**,** 788-99.

PIERORAZIO, P. M., WALSH, P. C., PARTIN, A. W. & EPSTEIN, J. I. 2013. Prognostic Gleason grade grouping: data based on the modified Gleason scoring system. *BJU Int,* 111**,** 753-60.

PING, X. L., SUN, B. F., WANG, L., XIAO, W., YANG, X., WANG, W. J., ADHIKARI, S., SHI, Y., LV, Y., CHEN, Y. S., ZHAO, X., LI, A., YANG, Y., DAHAL, U., LOU, X. M., LIU, X., HUANG, J., YUAN, W. P., ZHU, X. F., CHENG, T., ZHAO, Y. L., WANG, X., RENDTLEW DANIELSEN, J. M., LIU, F. & YANG, Y. G. 2014. Mammalian WTAP is a regulatory subunit of the RNA N6-methyladenosine methyltransferase. *Cell Res,* 24**,** 177-89.

PIPERIGKOU, Z., TZAFERI, K., MAKROKANIS, G., CHELI, K. & KARAMANOS, N. K. 2022. The microRNA-cell surface proteoglycan axis in cancer progression. *Am J Physiol Cell Physiol,* 322**,** C825-c832.

POKUTTA, S. & WEIS, W. I. 2007. Structure and Mechanism of Cadherins and Catenins in Cell-Cell Contacts. *Annual Review of Cell and Developmental Biology,* 23**,** 237-261.

POLITO, V. A., LI, H., MARTINI-STOICA, H., WANG, B., YANG, L., XU, Y., SWARTZLANDER, D. B., PALMIERI, M., DI RONZA, A., LEE, V. M., SARDIELLO, M., BALLABIO, A. & ZHENG, H. 2014. Selective clearance of aberrant tau proteins and rescue of neurotoxicity by transcription factor EB. *EMBO Mol Med,* 6**,** 1142-60.

POLUNOVSKY, V. A., ROSENWALD, I. B., TAN, A. T., WHITE, J., CHIANG, L., SONENBERG, N. & BITTERMAN, P. B. 1996. Translational control of programmed cell death: eukaryotic translation initiation factor 4E blocks apoptosis in growth-factor-restricted fibroblasts with physiologically expressed or deregulated Myc. *Mol Cell Biol,* 16**,** 6573-81.

PONGOR, L., KORMOS, M., HATZIS, C., PUSZTAI, L., SZABÓ, A. & GYŐRFFY, B. 2015. A genome-wide approach to link genotype to clinical outcome by utilizing next generation sequencing and gene chip data of 6,697 breast cancer patients. *Genome Med,* 7**,** 104.

POOLE, A. J., LI, Y., KIM, Y., LIN, S.-C. J., LEE, W.-H. & LEE, E. Y.-H. 2006. Prevention of Brca1-mediated mammary tumorigenesis in mice by a progesterone antagonist. *Science,* 314**,** 1467-1470.

PREKOVIC, S., VAN DEN BROECK, T., MORIS, L., SMEETS, E., CLAESSENS, F., JONIAU, S., HELSEN, C. & ATTARD, G. 2018. Treatment-induced changes in the androgen receptor axis: Liquid biopsies as diagnostic/prognostic tools for prostate cancer. *Molecular and Cellular Endocrinology,* 462**,** 56-63.

PRESCOTT, J. L., BLOK, L. & TINDALL, D. J. 1998. Isolation and androgen regulation of the human homeobox cDNA, NKX3.1. *Prostate,* 35**,** 71-80.

PRESS, M. F., PIKE, M. C., CHAZIN, V. R., HUNG, G., UDOVE, J. A., MARKOWICZ, M., DANYLUK, J., GODOLPHIN, W., SLIWKOWSKI, M., AKITA, R. & ET AL. 1993. Her-2/neu expression in node-negative breast

cancer: direct tissue quantitation by computerized image analysis and association of overexpression with increased risk of recurrent disease. *Cancer Res,* 53**,** 4960-70.

QI, R., LIN, J., CHEN, S., JIANG, J., ZHANG, X., YAO, B., ZHENG, H., JIN, Z., YUAN, Y., HOU, W., HUA, B. & GUO, Q. 2022. Breast cancer prognosis and P-cadherin expression: systematic review and study-level meta-analysis. *BMJ Support Palliat Care,* 12**,** e893-e905.

QIAO, Y., FENG, F. Y., WANG, Y., CAO, X., HAN, S., WILDER-ROMANS, K., NAVONE, N. M., LOGOTHETIS, C., TAICHMAN, R. S., KELLER, E. T., PALAPATTU, G. S., ALVA, A. S., SMITH, D. C., TOMLINS, S. A., CHINNAIYAN, A. M. & MORGAN, T. M. 2016. Mechanistic Support for Combined MET and AR Blockade in Castration-Resistant Prostate Cancer. *Neoplasia,* 18**,** 1-9.

QIU, X., BOUFAIED, N., HALLAL, T., FEIT, A., DE POLO, A., LUOMA, A. M., ALAHMADI, W., LAROCQUE, J., ZADRA, G., XIE, Y., GU, S., TANG, Q., ZHANG, Y., SYAMALA, S., SEO, J. H., BELL, C., O'CONNOR, E., LIU, Y., SCHAEFFER, E. M., JEFFREY KARNES, R., WEINMANN, S., DAVICIONI, E., MORRISSEY, C., CEJAS, P., ELLIS, L., LODA, M., WUCHERPFENNIG, K. W., POMERANTZ, M. M., SPRATT, D. E., COREY, E., FREEDMAN, M. L., SHIRLEY LIU, X., BROWN, M., LONG, H. W. & LABBÉ, D. P. 2022. MYC drives aggressive prostate cancer by disrupting transcriptional pause release at androgen receptor targets. *Nat Commun,* 13**,** 2559.

RADDE, BRANDIE N., IVANOVA, MARGARITA M., MAI, HUY X., SALABEI, JOSHUA K., HILL, BRADFORD G. & KLINGE, CAROLYN M. 2014. Bioenergetic differences between MCF-7 and T47D breast cancer cells and their regulation by oestradiol and tamoxifen. *Biochemical Journal,* 465**,** 49-61.

RAKHA, E. A., ABD EL REHIM, D., PINDER, S. E., LEWIS, S. A. & ELLIS, I. O. 2005. E-cadherin expression in invasive non-lobular carcinoma of the breast and its prognostic significance. *Histopathology,* 46**,** 685-693.

RAKHA, E. A., EL-SAYED, M. E., LEE, A. H., ELSTON, C. W., GRAINGE, M. J., HODI, Z., BLAMEY, R. W. & ELLIS, I. O. 2008. Prognostic significance of Nottingham histologic grade in invasive breast carcinoma. *J Clin Oncol,* 26**,** 3153-8.

RAKHA, E. A., PATEL, A., POWE, D. G., BENHASOUNA, A., GREEN, A. R., LAMBROS, M. B., REIS-FILHO, J. S. & ELLIS, I. O. 2010. Clinical and biological significance of E-cadherin protein expression in invasive lobular carcinoma of the breast. *Am J Surg Pathol,* 34**,** 1472-9.

RAKHA, E. A., TEOH, T. K., LEE, A. H., NOLAN, C. C., ELLIS, I. O. & GREEN, A. R. 2013. Further evidence that E-cadherin is not a tumour suppressor gene in invasive ductal carcinoma of the breast: an immunohistochemical study. *Histopathology,* 62**,** 695-701.

RAVI, R., MOOKERJEE, B., BHUJWALLA, Z. M., SUTTER, C. H., ARTEMOV, D., ZENG, Q., DILLEHAY, L. E., MADAN, A., SEMENZA, G. L. & BEDI, A. 2000. Regulation of tumor angiogenesis by p53-induced degradation of hypoxia-inducible factor 1α. *Genes & development,* 14**,** 34-44.

RENNERT, G., BISLAND-NAGGAN, S., BARNETT-GRINESS, O., BAR-JOSEPH, N., ZHANG, S., RENNERT, H. S. & NAROD, S. A. 2007. Clinical outcomes of breast cancer in carriers of BRCA1 and BRCA2 mutations. *New England Journal of Medicine,* 357**,** 115-123.

RIETHMACHER, D., BRINKMANN, V. & BIRCHMEIER, C. 1995. A targeted mutation in the mouse E-cadherin gene results in defective preimplantation development. *Proc Natl Acad Sci U S A,* 92**,** 855-9.

RIO, M. C., BELLOCQ, J. P., DANIEL, J. Y., TOMASETTO, C., LATHE, R., CHENARD, M. P., BATZENSCHLAGER, A. & CHAMBON, P. 1988. Breast cancer-associated pS2 protein: synthesis and secretion by normal stomach mucosa. *Science,* 241**,** 705-8.

RISINGER, J. I., BERCHUCK, A., KOHLER, M. F. & BOYD, J. 1994. Mutations of the E–cadherin gene in human gynecologic cancers. *Nature Genetics,* 7**,** 98-102.

RIVIER, J., SPIESS, J., MCCLINTOCK, R., VAUGHAN, J. & VALE, W. 1985. Purification and partial characterization of inhibin from porcine follicular fluid. *Biochem Biophys Res Commun,* 133**,** 120-7.

ROBINSON, D., VAN ALLEN, E. M., WU, Y.-M., SCHULTZ, N., LONIGRO, R. J., MOSQUERA, J.-M., MONTGOMERY, B., TAPLIN, M.-E., PRITCHARD, C. C. & ATTARD, G. 2015. Integrative clinical genomics of advanced prostate cancer. *Cell,* 161**,** 1215-1228.

ROBINSON, J. T., THORVALDSDÓTTIR, H., WINCKLER, W., GUTTMAN, M., LANDER, E. S., GETZ, G. & MESIROV, J. P. 2011. Integrative genomics viewer. *Nat Biotechnol,* 29**,** 24-6.

ROBSON, M., IM, S. A., SENKUS, E., XU, B., DOMCHEK, S. M., MASUDA, N., DELALOGE, S., LI, W., TUNG, N., ARMSTRONG, A., WU, W., GOESSL, C., RUNSWICK, S. & CONTE, P. 2017. Olaparib for Metastatic Breast Cancer in Patients with a Germline BRCA Mutation. *N Engl J Med,* 377**,** 523-533.

ROCK, K. L. & GOLDBERG, A. L. 1999. DEGRADATION OF CELL PROTEINS AND THE GENERATION OF MHC CLASS I-PRESENTED PEPTIDES. *Annual Review of Immunology,* 17**,** 739-779.

RODRIGUEZ-RIGUEIRO, T., VALLADARES-AYERBES, M., HAZ-CONDE, M., APARICIO, L. A. & FIGUEROA, A. 2011. Hakai reduces cell-substratum adhesion and increases epithelial cell invasion. *BMC Cancer,* 11**,** 474.

ROSKOSKI, R., JR. 2014. The ErbB/HER family of protein-tyrosine kinases and cancer. *Pharmacol Res,* 79**,** 34-74.

ROTTMAN, F., SHATKIN, A. J. & PERRY, R. P. 1974. Sequences containing methylated nucleotides at the 5′ termini of messenger RNAs: Possible implications for processing. *Cell,* 3**,** 197-199.

ROYLANCE, R., DROUFAKOU, S., GORMAN, P., GILLETT, C., HART, I. R., HANBY, A. & TOMLINSON, I. 2003. The role of E-cadherin in low-grade ductal breast tumourigenesis. *The Journal of Pathology,* 200**,** 53-58.

RUBIN, M. A., MUCCI, N. R., FIGURSKI, J., FECKO, A., PIENTA, K. J. & DAY, M. L. 2001. E-cadherin expression in prostate cancer: A broad survey using high-density tissue microarray technology. *Human Pathology,* 32**,** 690-697.

RUEMMELE, P., DIETMAIER, W., TERRACCIANO, L., TORNILLO, L., BATAILLE, F., KAISER, A., WUENSCH, P. H., HEINMOELLER, E., HOMAYOUNFAR, K., LUETTGES, J., KLOEPPEL, G., SESSA, F., EDMONSTON, T. B., SCHNEIDER-STOCK, R., KLINKHAMMER-SCHALKE, M., PAUER, A., SCHICK, S., HOFSTAEDTER, F., BAUMHOER, D. & HARTMANN, A. 2009. Histopathologic features and

microsatellite instability of cancers of the papilla of vater and their precursor lesions. *Am J Surg Pathol,* 33**,** 691-704.

RUGGERO, D., MONTANARO, L., MA, L., XU, W., LONDEI, P., CORDON-CARDO, C. & PANDOLFI, P. P. 2004. The translation factor eIF-4E promotes tumor formation and cooperates with c-Myc in lymphomagenesis. *Nat Med,* 10**,** 484-6.

RUZICKA, K., ZHANG, M., CAMPILHO, A., BODI, Z., KASHIF, M., SALEH, M., EECKHOUT, D., EL-SHOWK, S., LI, H., ZHONG, S., DE JAEGER, G., MONGAN, N. P., HEJATKO, J., HELARIUTTA, Y. & FRAY, R. G. 2017. Identification of factors required for m(6) A mRNA methylation in Arabidopsis reveals a role for the conserved E3 ubiquitin ligase HAKAI. *New Phytol,* 215**,** 157-172.

SACHS, N., DE LIGT, J., KOPPER, O., GOGOLA, E., BOUNOVA, G., WEEBER, F., BALGOBIND, A. V., WIND, K., GRACANIN, A., BEGTHEL, H., KORVING, J., VAN BOXTEL, R., DUARTE, A. A., LELIEVELD, D., VAN HOECK, A., ERNST, R. F., BLOKZIJL, F., NIJMAN, I. J., HOOGSTRAAT, M., VAN DE VEN, M., EGAN, D. A., ZINZALLA, V., MOLL, J., BOJ, S. F., VOEST, E. E., WESSELS, L., VAN DIEST, P. J., ROTTENBERG, S., VRIES, R. G. J., CUPPEN, E. & CLEVERS, H. 2018. A Living Biobank of Breast Cancer Organoids Captures Disease Heterogeneity. *Cell,* 172**,** 373-386.e10.

SAHU, B., LAAKSO, M., OVASKA, K., MIRTTI, T., LUNDIN, J., RANNIKKO, A., SANKILA, A., TURUNEN, J. P., LUNDIN, M., KONSTI, J., VESTERINEN, T., NORDLING, S., KALLIONIEMI, O., HAUTANIEMI, S. & JÄNNE, O. A. 2011. Dual role of FoxA1 in androgen receptor binding to chromatin, androgen signalling and prostate cancer. *Embo j,* 30**,** 3962-76.

SAKAMOTO, H., YAMASHITA, K., OKAMOTO, K., KADOWAKI, T., SAKAI, E., UMEDA, M. & TSUKUBA, T. 2018. Transcription factor EB influences invasion and migration in oral squamous cell carcinomas. *Oral Diseases,* 24**,** 741-748.

SALINAS, C. A., TSODIKOV, A., ISHAK-HOWARD, M. & COONEY, K. A. 2014. Prostate cancer in young men: an important clinical entity. *Nature reviews. Urology,* 11**,** 317-323.

SANSONE, P., SAVINI, C., KURELAC, I., CHANG, Q., AMATO, L. B., STRILLACCI, A., STEPANOVA, A., IOMMARINI, L., MASTROLEO, C., DALY, L., GALKIN, A., THAKUR, B. K., SOPLOP, N., URYU, K., HOSHINO, A., NORTON, L., BONAFÉ, M., CRICCA, M., GASPARRE, G., LYDEN, D. & BROMBERG, J. 2017. Packaging and transfer of mitochondrial DNA via exosomes regulate escape from dormancy in hormonal therapy-resistant breast cancer. *Proceedings of the National Academy of Sciences,* 114**,** E9066-E9075.

SANTORE, T. A., CHEN, Y., SMIT, M. J. & IYENGAR, R. 2002. Adenovirus-directed expression of Q227L-G alpha(s) inhibits growth of established tumors of later-stage human breast cancer cells in athymic mice. *Proc Natl Acad Sci U S A,* 99**,** 1671-6.

SCARBROUGH, P. M., WEBER, R. P., IVERSEN, E. S., BRHANE, Y., AMOS, C. I., KRAFT, P., HUNG, R. J., SELLERS, T. A., WITTE, J. S., PHAROAH, P., HENDERSON, B. E., GRUBER, S. B., HUNTER, D. J., GARBER, J. E., JOSHI, A. D., MCDONNELL, K., EASTON, D. F., EELES, R., KOTE-JARAI, Z., MUIR, K., DOHERTY, J. A. &

SCHILDKRAUT, J. M. 2016. A Cross-Cancer Genetic Association Analysis of the DNA Repair and DNA Damage Signaling Pathways for Lung, Ovary, Prostate, Breast, and Colorectal Cancer. *Cancer Epidemiol Biomarkers Prev,* 25**,** 193-200.

SCARDINO, P. T., WEAVER, R. & HUDSON, M. L. A. 1992. Early detection of prostate cancer. *Human Pathology,* 23**,** 211-222.

SCHAEFER, M., KAPOOR, U. & JANTSCH, M. F. 2017. Understanding RNA modifications: the promises and technological bottlenecks of the ‘epitranscriptome&#x2019. *Open Biology,* 7**,** 170077.

SCHAUB, F. X., DHANKANI, V., BERGER, A. C., TRIVEDI, M., RICHARDSON, A. B., SHAW, R., ZHAO, W., ZHANG, X., VENTURA, A., LIU, Y., AYER, D. E., HURLIN, P. J., CHERNIACK, A. D., EISENMAN, R. N., BERNARD, B., GRANDORI, C., CAESAR-JOHNSON, S. J., DEMCHOK, J. A., FELAU, I., KASAPI, M., FERGUSON, M. L., HUTTER, C. M., SOFIA, H. J., TARNUZZER, R., WANG, Z., YANG, L., ZENKLUSEN, J. C., ZHANG, J., CHUDAMANI, S., LIU, J., LOLLA, L., NARESH, R., PIHL, T., SUN, Q., WAN, Y., WU, Y., CHO, J., DEFREITAS, T., FRAZER, S., GEHLENBORG, N., GETZ, G., HEIMAN, D. I., KIM, J., LAWRENCE, M. S., LIN, P., MEIER, S., NOBLE, M. S., SAKSENA, G., VOET, D., ZHANG, H., BERNARD, B., CHAMBWE, N., DHANKANI, V., KNIJNENBURG, T., KRAMER, R., LEINONEN, K., LIU, Y., MILLER, M., REYNOLDS, S., SHMULEVICH, I., THORSSON, V., ZHANG, W., AKBANI, R., BROOM, B. M., HEGDE, A. M., JU, Z., KANCHI, R. S., KORKUT, A., LI, J., LIANG, H., LING, S., LIU, W., LU, Y., MILLS, G. B., NG, K.-S., RAO, A., RYAN, M., WANG, J., WEINSTEIN, J. N., ZHANG, J., ABESHOUSE, A., ARMENIA, J., CHAKRAVARTY, D., CHATILA, W. K., DE BRUIJN, I., GAO, J., GROSS, B. E., HEINS, Z. J., KUNDRA, R., LA, K., LADANYI, M., LUNA, A., NISSAN, M. G., OCHOA, A., PHILLIPS, S. M., REZNIK, E., SANCHEZ-VEGA, F., SANDER, C., SCHULTZ, N., SHERIDAN, R., et al. 2018. Pan-cancer Alterations of the MYC Oncogene and Its Proximal Network across the Cancer Genome Atlas. *Cell Systems,* 6**,** 282-300.e2.

SCHEFFNER, M., WERNESS, B. A., HUIBREGTSE, J. M., LEVINE, A. J. & HOWLEY, P. M. 1990. The E6 oncoprotein encoded by human papillomavirus types 16 and 18 promotes the degradation of p53. *Cell,* 63**,** 1129-1136.

SCHER, H. I., FIZAZI, K., SAAD, F., TAPLIN, M. E., STERNBERG, C. N., MILLER, K., DE WIT, R., MULDERS, P., CHI, K. N., SHORE, N. D., ARMSTRONG, A. J., FLAIG, T. W., FLÉCHON, A., MAINWARING, P., FLEMING, M., HAINSWORTH, J. D., HIRMAND, M., SELBY, B., SEELY, L. & DE BONO, J. S. 2012. Increased survival with enzalutamide in prostate cancer after chemotherapy. *N Engl J Med,* 367**,** 1187-97.

SCHER, H. I., LU, D., SCHREIBER, N. A., LOUW, J., GRAF, R. P., VARGAS, H. A., JOHNSON, A., JENDRISAK, A., BAMBURY, R., DANILA, D., MCLAUGHLIN, B., WAHL, J., GREENE, S. B., HELLER, G., MARRINUCCI, D., FLEISHER, M. & DITTAMORE, R. 2016. Association of AR-V7 on Circulating Tumor Cells as a Treatment-Specific Biomarker With Outcomes and Survival in Castration-Resistant Prostate Cancer. *JAMA Oncol,* 2**,** 1441-1449.

SCHÖCK, F. & PERRIMON, N. 2002. Molecular Mechanisms of Epithelial Morphogenesis. *Annual Review of Cell and Developmental Biology,* 18**,** 463-493.

SCHWARTZ, S., MUMBACH, MAXWELL R., JOVANOVIC, M., WANG, T., MACIAG, K., BUSHKIN, G. G., MERTINS, P., TER-OVANESYAN, D., HABIB, N., CACCHIARELLI, D., SANJANA, NEVILLE E., FREINKMAN, E., PACOLD, MICHAEL E., SATIJA, R., MIKKELSEN, TARJEI S., HACOHEN, N., ZHANG, F., CARR, STEVEN A., LANDER, ERIC S. & REGEV, A. 2014. Perturbation of m6A Writers Reveals Two Distinct Classes of mRNA Methylation at Internal and 5′ Sites. *Cell Reports,* 8**,** 284-296.

SEACHRIST, D. D. & KERI, R. A. 2019. The Activin Social Network: Activin, Inhibin, and Follistatin in Breast Development and Cancer. *Endocrinology,* 160**,** 1097-1110.

SEERY, L. T., KNOWLDEN, J. M., GEE, J. M. W., ROBERTSON, J. F. R., KENNY, F. S., ELLIS, I. O. & NICHOLSON, R. I. 1999. BRCA1 expression levels predict distant metastasis of sporadic breast cancers. *International Journal of Cancer,* 84**,** 258-262.

SELBERG, S., BLOKHINA, D., AATONEN, M., KOIVISTO, P., SILTANEN, A., MERVAALA, E., KANKURI, E. & KARELSON, M. 2019. Discovery of Small Molecules that Activate RNA Methylation through Cooperative Binding to the METTL3-14-WTAP Complex Active Site. *Cell Reports,* 26**,** 3762-3771.e5.

SEMENAS, J., ALLEGRUCCI, C., A. BOORJIAN, S., P. MONGAN, N. & LIAO PERSSON, J. 2012. Overcoming Drug Resistance and Treating Advanced Prostate Cancer. *Current Drug Targets,* 13**,** 1308-1323.

SEMENZA, G. L. 2000. HIF-1 and human disease: one highly involved factor. *Genes & development,* 14**,** 1983-1991.

SEMENZA, G. L. 2001. HIF-1 and mechanisms of hypoxia sensing. *Current Opinion in Cell Biology,* 13**,** 167-171.

SEREZANI, C. H., BALLINGER, M. N., ARONOFF, D. M. & PETERS-GOLDEN, M. 2008. Cyclic AMP: master regulator of innate immune cell function. *Am J Respir Cell Mol Biol,* 39**,** 127-32.

SESHADRI, R., FIRGAIRA, F. A., HORSFALL, D. J., MCCAUL, K., SETLUR, V. & KITCHEN, P. 1993. Clinical significance of HER-2/neu oncogene amplification in primary breast cancer. The South Australian Breast Cancer Study Group. *J Clin Oncol,* 11**,** 1936-42.

SETTEMBRE, C., DI MALTA, C., POLITO, V. A., GARCIA ARENCIBIA, M., VETRINI, F., ERDIN, S., ERDIN, S. U., HUYNH, T., MEDINA, D., COLELLA, P., SARDIELLO, M., RUBINSZTEIN, D. C. & BALLABIO, A. 2011. TFEB links autophagy to lysosomal biogenesis. *Science,* 332**,** 1429-33.

SETTEMBRE, C., ZONCU, R., MEDINA, D. L., VETRINI, F., ERDIN, S., ERDIN, S., HUYNH, T., FERRON, M., KARSENTY, G., VELLARD, M. C., FACCHINETTI, V., SABATINI, D. M. & BALLABIO, A. 2012. A lysosome-to-nucleus signalling mechanism senses and regulates the lysosome via mTOR and TFEB. *Embo j,* 31**,** 1095-108.

SGROI, D. C. 2010. Preinvasive breast cancer. *Annu Rev Pathol,* 5**,** 193-221.

SHAH, R. B., MEHRA, R., CHINNAIYAN, A. M., SHEN, R., GHOSH, D., ZHOU, M., MACVICAR, G. R., VARAMBALLY, S., HARWOOD, J., BISMAR, T. A., KIM, R., RUBIN, M. A. & PIENTA, K. J. 2004. Androgen-independent

prostate cancer is a heterogeneous group of diseases: lessons from a rapid autopsy program. *Cancer research,* 64**,** 9209-9216.

SHARP, A., COLEMAN, I., YUAN, W., SPRENGER, C., DOLLING, D., RODRIGUES, D. N., RUSSO, J. W., FIGUEIREDO, I., BERTAN, C., SEED, G., RIISNAES, R., UO, T., NEEB, A., WELTI, J., MORRISSEY, C., CARREIRA, S., LUO, J., NELSON, P. S., BALK, S. P., TRUE, L. D., DE BONO, J. S. & PLYMATE, S. R. 2019. Androgen receptor splice variant-7 expression emerges with castration resistance in prostate cancer. *J Clin Invest,* 129**,** 192-208.

SHAV-TAL, Y. & ZIPORI, D. 2002. PSF and p54(nrb)/NonO--multi-functional nuclear proteins. *FEBS Lett,* 531**,** 109-14.

SHEN, M. M. & ABATE-SHEN, C. 2010. Molecular genetics of prostate cancer: new prospects for old challenges. *Genes Dev,* 24**,** 1967-2000.

SHEN, S., PARK, J. W., LU, Z. X., LIN, L., HENRY, M. D., WU, Y. N., ZHOU, Q. & XING, Y. 2014. rMATS: robust and flexible detection of differential alternative splicing from replicate RNA-Seq data. *Proc Natl Acad Sci U S A,* 111**,** E5593-601.

SHI, R., BERKEL, H. & YU, H. 2001. Insulin-like growth factor-I and prostate cancer: a meta-analysis. *British journal of cancer,* 85**,** 991-996.

SHIMURA, H., HATTORI, N., KUBO, S.-I., MIZUNO, Y., ASAKAWA, S., MINOSHIMA, S., SHIMIZU, N., IWAI, K., CHIBA, T., TANAKA, K. & SUZUKI, T. 2000. Familial Parkinson disease gene product, parkin, is a ubiquitin-protein ligase. *Nature Genetics,* 25**,** 302-305.

SHIOTA, M., FUJIMOTO, N., HIGASHIJIMA, K., IMADA, K., KASHIWAGI, E., TAKEUCHI, A., INOKUCHI, J., TATSUGAMI, K., KAJIOKA, S., UCHIUMI, T. & ETO, M. 2018. Mineralocorticoid receptor signaling affects therapeutic effect of enzalutamide. *Prostate*.

SHIOTA, M., FUJIMOTO, N., KASHIWAGI, E. & ETO, M. 2019. The Role of Nuclear Receptors in Prostate Cancer. *Cells,* 8.

SHOKER, B. S., JARVIS, C., CLARKE, R. B., ANDERSON, E., HEWLETT, J., DAVIES, M. P., SIBSON, D. R. & SLOANE, J. P. 1999. Estrogen receptor-positive proliferating cells in the normal and precancerous breast. *The American journal of pathology,* 155**,** 1811-1815.

SHORNING, B. Y., DASS, M. S., SMALLEY, M. J. & PEARSON, H. B. 2020. The PI3K-AKT-mTOR Pathway and Prostate Cancer: At the Crossroads of AR, MAPK, and WNT Signaling. *Int J Mol Sci,* 21.

SIITONEN, S. M., KONONEN, J. T., HELIN, H. J., RANTALA, I. S., HOLLI, K. A. & ISOLA, J. J. 1996. Reduced E-Cadherin Expression is Associated With Invasiveness and Unfavorable Prognosis in Breast Cancer. *American Journal of Clinical Pathology,* 105**,** 394-402.

SIOUDA, M., YUE, J., SHUKLA, R., GUILLERMIER, S., HERCEG, Z., CREVEAUX, M., ACCARDI, R., TOMMASINO, M. & SYLLA, B. S. 2012. Transcriptional regulation of the human tumor suppressor DOK1 by E2F1. *Mol Cell Biol,* 32**,** 4877-90.

SKILDUM, A., FAIVRE, E. & LANGE, C. A. 2005. Progesterone receptors induce cell cycle progression via activation of mitogen-activated protein kinases. *Molecular endocrinology,* 19**,** 327-339.

SLAMON, D. J., LEYLAND-JONES, B., SHAK, S., FUCHS, H., PATON, V., BAJAMONDE, A., FLEMING, T., EIERMANN, W., WOLTER, J., PEGRAM, M., BASELGA, J. & NORTON, L. 2001. Use of Chemotherapy plus a Monoclonal Antibody against HER2 for Metastatic

Breast Cancer That Overexpresses HER2. *New England Journal of Medicine,* 344**,** 783-792.
SMALL, T. W., PENALVA, L. O. & PICKERING, J. G. 2007. Vascular Biology and the Sex of Flies: Regulation of Vascular Smooth Muscle Cell Proliferation by Wilms' Tumor 1–Associating Protein. *Trends in Cardiovascular Medicine,* 17**,** 230-234.
SMITTENAAR, C. R., PETERSEN, K. A., STEWART, K. & MOITT, N. 2016. Cancer incidence and mortality projections in the UK until 2035. *Br J Cancer,* 115**,** 1147-1155.
SOHN, E. J., JUNG, D. B., LEE, H., HAN, I., LEE, J., LEE, H. & KIM, S. H. 2018. CNOT2 promotes proliferation and angiogenesis via VEGF signaling in MDA-MB-231 breast cancer cells. *Cancer Lett,* 412**,** 88-98.
SONG, W., WANG, F., SAVINI, M., AKE, A., DI RONZA, A., SARDIELLO, M. & SEGATORI, L. 2013. TFEB regulates lysosomal proteostasis. *Hum Mol Genet,* 22**,** 1994-2009.
SORCI, M., IANNIELLO, Z., CRUCIANI, S., LARIVERA, S., GINISTRELLI, L. C., CAPUANO, E., MARCHIONI, M., FAZI, F. & FATICA, A. 2018. METTL3 regulates WTAP protein homeostasis. *Cell Death & Disease,* 9**,** 796.
SOREK, R., SHEMESH, R., COHEN, Y., BASECHESS, O., AST, G. & SHAMIR, R. 2004. A non-EST-based method for exon-skipping prediction. *Genome research,* 14**,** 1617-1623.
SØRENSEN, M. B., STOLTENBERG, M., DANSCHER, G. & ERNST, E. 1999. Chelation of intracellular zinc ions affects human sperm cell motility. *Mol Hum Reprod,* 5**,** 338-41.
SØRLIE, T., PEROU, C. M., TIBSHIRANI, R., AAS, T., GEISLER, S., JOHNSEN, H., HASTIE, T., EISEN, M. B., VAN DE RIJN, M., JEFFREY, S. S., THORSEN, T., QUIST, H., MATESE, J. C., BROWN, P. O., BOTSTEIN, D., LØNNING, P. E. & BØRRESEN-DALE, A.-L. 2001. Gene expression patterns of breast carcinomas distinguish tumor subclasses with clinical implications. *Proceedings of the National Academy of Sciences,* 98**,** 10869-10874.
SOULE, H. D., MALONEY, T. M., WOLMAN, S. R., PETERSON, W. D., JR., BRENZ, R., MCGRATH, C. M., RUSSO, J., PAULEY, R. J., JONES, R. F. & BROOKS, S. C. 1990. Isolation and characterization of a spontaneously immortalized human breast epithelial cell line, MCF-10. *Cancer Res,* 50**,** 6075-86.
SOULE, H. D., VAZGUEZ, J., LONG, A., ALBERT, S. & BRENNAN, M. 1973. A human cell line from a pleural effusion derived from a breast carcinoma. *J Natl Cancer Inst,* 51**,** 1409-16.
SPAMPANATO, C., FEENEY, E., LI, L., CARDONE, M., LIM, J. A., ANNUNZIATA, F., ZARE, H., POLISHCHUK, R., PUERTOLLANO, R., PARENTI, G., BALLABIO, A. & RABEN, N. 2013. Transcription factor EB (TFEB) is a new therapeutic target for Pompe disease. *EMBO Mol Med,* 5**,** 691-706.
SRAMKOSKI, R. M., PRETLOW, T. G., 2ND, GIACONIA, J. M., PRETLOW, T. P., SCHWARTZ, S., SY, M. S., MARENGO, S. R., RHIM, J. S., ZHANG, D. & JACOBBERGER, J. W. 1999. A new human prostate carcinoma cell line, 22Rv1. *In Vitro Cell Dev Biol Anim,* 35**,** 403-9.
SRIDHARAN, S., ROBESON, M., BASTIHALLI-TUKARAMRAO, D., HOWARD, C. M., SUBRAMANIYAN, B., TILLEY, A. M. C., TIWARI, A.

K. & RAMAN, D. 2019. Targeting of the Eukaryotic Translation Initiation Factor 4A Against Breast Cancer Stemness. *Front Oncol,* 9**,** 1311.

STAMEY, T. A., FREIHA, F. S., MCNEAL, J. E., REDWINE, E. A., WHITTEMORE, A. S. & SCHMID, H.-P. 1993. Localized prostate cancer. Relationship of tumor volume to clinical significance for treatment of prostate cancer. *Cancer,* 71**,** 933-938.

STAMEY, T. A. & KABALIN, J. N. 1989. Prostate specific antigen in the diagnosis and treatment of adenocarcinoma of the prostate. I. Untreated patients. *The Journal of urology,* 141**,** 1070-1075.

STAMEY, T. A., YANG, N., HAY, A. R., MCNEAL, J. E., FREIHA, F. S. & REDWINE, E. 1987. Prostate-Specific Antigen as a Serum Marker for Adenocarcinoma of the Prostate. *New England Journal of Medicine,* 317**,** 909-916.

STASHI, E., YORK, B. & O'MALLEY, B. W. 2014. Steroid receptor coactivators: servants and masters for control of systems metabolism. *Trends in Endocrinology & Metabolism,* 25**,** 337-347.

STEENMAN, M. J., RAINIER, S., DOBRY, C. J., GRUNDY, P., HORON, I. L. & FEINBERG, A. P. 1994. Loss of imprinting of IGF2 is linked to reduced expression and abnormal methylation of H19 in Wilms' tumour. *Nature genetics,* 7**,** 433-439.

STONE, K. R., MICKEY, D. D., WUNDERLI, H., MICKEY, G. H. & PAULSON, D. F. 1978. Isolation of a human prostate carcinoma cell line (DU 145). *Int J Cancer,* 21**,** 274-81.

STROM, J. O., THEODORSSON, A. & THEODORSSON, E. 2009. Dose-Related Neuroprotective versus Neurodamaging Effects of Estrogens in Rat Cerebral Ischemia: A Systematic Analysis. *Journal of Cerebral Blood Flow & Metabolism,* 29**,** 1359-1372.

SU, H., WANG, Y. & LI, H. 2021. RNA m6A Methylation Regulators Multi-Omics Analysis in Prostate Cancer. *Front Genet,* 12**,** 768041.

SU, R., DONG, L., LI, Y., GAO, M., HAN, L., WUNDERLICH, M., DENG, X., LI, H., HUANG, Y., GAO, L., LI, C., ZHAO, Z., ROBINSON, S., TAN, B., QING, Y., QIN, X., PRINCE, E., XIE, J., QIN, H., LI, W., SHEN, C., SUN, J., KULKARNI, P., WENG, H., HUANG, H., CHEN, Z., ZHANG, B., WU, X., OLSEN, M. J., MÜSCHEN, M., MARCUCCI, G., SALGIA, R., LI, L., FATHI, A. T., LI, Z., MULLOY, J. C., WEI, M., HORNE, D. & CHEN, J. 2020. Targeting FTO Suppresses Cancer Stem Cell Maintenance and Immune Evasion. *Cancer Cell,* 38**,** 79-96.e11.

SU, S., LI, S., DENG, T., GAO, M., YIN, Y., WU, B., PENG, C., LIU, J., MA, J. & ZHANG, K. 2022. Cryo-EM structures of human m(6)A writer complexes. *Cell Res,* 32**,** 982-994.

SUBA, Z. 2014. Triple-negative breast cancer risk in women is defined by the defect of estrogen signaling: preventive and therapeutic implications. *Onco Targets Ther,* 7**,** 147-64.

SUBA, Z. 2015. DNA stabilization by the upregulation of estrogen signaling in BRCA gene mutation carriers. *Drug Des Devel Ther,* 9**,** 2663-75.

SUN, S., SPRENGER, C. C., VESSELLA, R. L., HAUGK, K., SORIANO, K., MOSTAGHEL, E. A., PAGE, S. T., COLEMAN, I. M., NGUYEN, H. M., SUN, H., NELSON, P. S. & PLYMATE, S. R. 2010. Castration resistance in human prostate cancer is conferred by a frequently occurring androgen receptor splice variant. *J Clin Invest,* 120**,** 2715-30.

SUN, T., WU, R. & MING, L. 2019. The role of m6A RNA methylation in cancer. *Biomedicine & Pharmacotherapy,* 112**,** 108613.

SUN, Y., SHEN, W., HU, S., LYU, Q., WANG, Q., WEI, T., ZHU, W. & ZHANG, J. 2023. METTL3 promotes chemoresistance in small cell lung cancer by inducing mitophagy. *J Exp Clin Cancer Res,* 42**,** 65.

SUNG, H., FERLAY, J., SIEGEL, R. L., LAVERSANNE, M., SOERJOMATARAM, I., JEMAL, A. & BRAY, F. 2021. Global Cancer Statistics 2020: GLOBOCAN Estimates of Incidence and Mortality Worldwide for 36 Cancers in 185 Countries. *CA: A Cancer Journal for Clinicians,* 71**,** 209-249.

SUTHERLAND, S. I., PE BENITO, R., HENSHALL, S. M., HORVATH, L. G. & KENCH, J. G. 2014. Expression of phosphorylated-mTOR during the development of prostate cancer. *Prostate,* 74**,** 1231-9.

SWAMINATHAN, G. & CARTWRIGHT, C. A. 2012. Rack1 promotes epithelial cell-cell adhesion by regulating E-cadherin endocytosis. *Oncogene,* 31**,** 376-89.

SWEENEY, C., BERNARD, P. S., FACTOR, R. E., KWAN, M. L., HABEL, L. A., QUESENBERRY, C. P., JR., SHAKESPEAR, K., WELTZIEN, E. K., STIJLEMAN, I. J., DAVIS, C. A., EBBERT, M. T., CASTILLO, A., KUSHI, L. H. & CAAN, B. J. 2014. Intrinsic subtypes from PAM50 gene expression assay in a population-based breast cancer cohort: differences by age, race, and tumor characteristics. *Cancer Epidemiol Biomarkers Prev,* 23**,** 714-24.

SWEENEY, C. J., CHEN, Y.-H., CARDUCCI, M., LIU, G., JARRARD, D. F., EISENBERGER, M., WONG, Y.-N., HAHN, N., KOHLI, M., COONEY, M. M., DREICER, R., VOGELZANG, N. J., PICUS, J., SHEVRIN, D., HUSSAIN, M., GARCIA, J. A. & DIPAOLA, R. S. 2015. Chemohormonal Therapy in Metastatic Hormone-Sensitive Prostate Cancer. *New England Journal of Medicine,* 373**,** 737-746.

TAKAHASHI, H., NISHIMURA, J., KAGAWA, Y., KANO, Y., TAKAHASHI, Y., WU, X., HIRAKI, M., HAMABE, A., KONNO, M., HARAGUCHI, N., TAKEMASA, I., MIZUSHIMA, T., ISHII, M., MIMORI, K., ISHII, H., DOKI, Y., MORI, M. & YAMAMOTO, H. 2015. Significance of Polypyrimidine Tract–Binding Protein 1 Expression in Colorectal Cancer. *Molecular Cancer Therapeutics,* 14**,** 1705-1716.

TAKAHASHI, M., DILLON, T. J., LIU, C., KARIYA, Y., WANG, Z. & STORK, P. J. 2013. Protein kinase A-dependent phosphorylation of Rap1 regulates its membrane localization and cell migration. *J Biol Chem,* 288**,** 27712-23.

TAKANO, T., LIN, J. H.-C., ARCUINO, G., GAO, Q., YANG, J. & NEDERGAARD, M. 2001. Glutamate release promotes growth of malignant gliomas. *Nature medicine,* 7**,** 1010-1015.

TAKAYAMA, K. I., SUZUKI, T., FUJIMURA, T., YAMADA, Y., TAKAHASHI, S., HOMMA, Y., SUZUKI, Y. & INOUE, S. 2017. Dysregulation of spliceosome gene expression in advanced prostate cancer by RNA-binding protein PSF. *Proc Natl Acad Sci U S A,* 114**,** 10461-10466.

TAKEDA, A. N., PINON, G. M., BENS, M., FAGART, J., RAFESTIN-OBLIN, M. E. & VANDEWALLE, A. 2007. The synthetic androgen methyltrienolone (r1881) acts as a potent antagonist of the mineralocorticoid receptor. *Mol Pharmacol,* 71**,** 473-82.

TAKEICHI, M. 1991. Cadherin cell adhesion receptors as a morphogenetic regulator. *Science,* 251**,** 1451-5.

TAKEICHI, M., HATTA, K., NOSE, A. & NAGAFUCHI, A. 1988. Identification of a gene family of cadherin cell adhesion molecules. *Cell Differentiation and Development,* 25**,** 91-94.

TAN, A., PRASAD, R., LEE, C. & JHO, E. H. 2022. Past, present, and future perspectives of transcription factor EB (TFEB): mechanisms of regulation and association with disease. *Cell Death Differ,* 29**,** 1433-1449.

TAN, W., LIU, S., DENG, Z., DAI, F., YUAN, M., HU, W., LI, B. & CHENG, Y. 2023. Gene signature of m6A-related targets to predict prognosis and immunotherapy response in ovarian cancer. *Journal of Cancer Research and Clinical Oncology,* 149**,** 593-608.

TAPLIN, M. E., BUBLEY, G. J., SHUSTER, T. D., FRANTZ, M. E., SPOONER, A. E., OGATA, G. K., KEER, H. N. & BALK, S. P. 1995. Mutation of the androgen-receptor gene in metastatic androgen-independent prostate cancer. *N Engl J Med,* 332**,** 1393-8.

TASKEN, K. & RUPPELT, A. 2006. Negative regulation of T-cell receptor activation by the cAMP-PKA-Csk signalling pathway in T-cell lipid rafts. *Front Biosci,* 11**,** 2929-39.

TAVASSOLI, F. A. 2003. Pathology and Genetics of Tumours of the Breast and Female Genital Organs. *World Hhealth Organization Classification of Tumours*.

TENG, M., ZHOU, S., CAI, C., LUPIEN, M. & HE, H. H. 2021. Pioneer of prostate cancer: past, present and the future of FOXA1. *Protein Cell,* 12**,** 29-38.

TEO, M. Y., RATHKOPF, D. E. & KANTOFF, P. 2019. Treatment of Advanced Prostate Cancer. *Annu Rev Med,* 70**,** 479-499.

THADANI-MULERO, M., PORTELLA, L., SUN, S., SUNG, M., MATOV, A., VESSELLA, R. L., COREY, E., NANUS, D. M., PLYMATE, S. R. & GIANNAKAKOU, P. 2014. Androgen receptor splice variants determine taxane sensitivity in prostate cancer. *Cancer Res,* 74**,** 2270-2282.

THALMANN, G. N., ANEZINIS, P. E., CHANG, S. M., ZHAU, H. E., KIM, E. E., HOPWOOD, V. L., PATHAK, S., VON ESCHENBACH, A. C. & CHUNG, L. W. 1994. Androgen-independent cancer progression and bone metastasis in the LNCaP model of human prostate cancer. *Cancer Res,* 54**,** 2577-81.

THE CANCER GENOME ATLAS, N., KOBOLDT, D. C., FULTON, R. S., MCLELLAN, M. D., SCHMIDT, H., KALICKI-VEIZER, J., MCMICHAEL, J. F., FULTON, L. L., DOOLING, D. J., DING, L., MARDIS, E. R., WILSON, R. K., ALLY, A., BALASUNDARAM, M., BUTTERFIELD, Y. S. N., CARLSEN, R., CARTER, C., CHU, A., CHUAH, E., CHUN, H.-J. E., COOPE, R. J. N., DHALLA, N., GUIN, R., HIRST, C., HIRST, M., HOLT, R. A., LEE, D., LI, H. I., MAYO, M., MOORE, R. A., MUNGALL, A. J., PLEASANCE, E., GORDON ROBERTSON, A., SCHEIN, J. E., SHAFIEI, A., SIPAHIMALANI, P., SLOBODAN, J. R., STOLL, D., TAM, A., THIESSEN, N., VARHOL, R. J., WYE, N., ZENG, T., ZHAO, Y., BIROL, I., JONES, S. J. M., MARRA, M. A., CHERNIACK, A. D., SAKSENA, G., ONOFRIO, R. C., PHO, N. H., CARTER, S. L., SCHUMACHER, S. E., TABAK, B., HERNANDEZ, B., GENTRY, J., NGUYEN, H., CRENSHAW, A., ARDLIE, K., BEROUKHIM, R.,

WINCKLER, W., GETZ, G., GABRIEL, S. B., MEYERSON, M., CHIN, L., PARK, P. J., KUCHERLAPATI, R., HOADLEY, K. A., TODD AUMAN, J., FAN, C., TURMAN, Y. J., SHI, Y., LI, L., TOPAL, M. D., HE, X., CHAO, H.-H., PRAT, A., SILVA, G. O., IGLESIA, M. D., ZHAO, W., USARY, J., BERG, J. S., ADAMS, M., BOOKER, J., WU, J., GULABANI, A., BODENHEIMER, T., HOYLE, A. P., SIMONS, J. V., SOLOWAY, M. G., MOSE, L. E., JEFFERYS, S. R., BALU, S., PARKER, J. S., NEIL HAYES, D., PEROU, C. M., MALIK, S., MAHURKAR, S., SHEN, H., WEISENBERGER, D. J., et al. 2012. Comprehensive molecular portraits of human breast tumours. *Nature,* 490**,** 61.

THIERY, J. P., ACLOQUE, H., HUANG, R. Y. J. & NIETO, M. A. 2009. Epithelial-Mesenchymal Transitions in Development and Disease. *Cell,* 139**,** 871-890.

THORAT, M. A., MARCHIO, C., MORIMIYA, A., SAVAGE, K., NAKSHATRI, H., REIS-FILHO, J. S. & BADVE, S. 2008. Forkhead box A1 expression in breast cancer is associated with luminal subtype and good prognosis. *J Clin Pathol,* 61**,** 327-32.

TIETZ, K. T. & DEHM, S. M. 2020. Androgen receptor variants: RNA-based mechanisms and therapeutic targets. *Hum Mol Genet,* 29**,** R19-r26.

TOLEDO, F. & WAHL, G. M. 2006. Regulating the p53 pathway: in vitro hypotheses, in vivo veritas. *Nat Rev Cancer,* 6**,** 909-23.

TOMBAL, B. 2019. Androgen receptor-targeted agents in the management of advanced prostate cancer. *Lancet Oncol,* 20**,** 1628-1630.

TOMITA, K., VAN BOKHOVEN, A., VAN LEENDERS, G. J. L. H., RUIJTER, E. T. G., JANSEN, C. F. J., BUSSEMAKERS, M. J. G. & SCHALKEN, J. A. 2000. Cadherin Switching in Human Prostate Cancer Progression. *Cancer Research,* 60**,** 3650-3654.

TOMLINS, S. A., LAXMAN, B., VARAMBALLY, S., CAO, X., YU, J., HELGESON, B. E., CAO, Q., PRENSNER, J. R., RUBIN, M. A., SHAH, R. B., MEHRA, R. & CHINNAIYAN, A. M. 2008. Role of the TMPRSS2-ERG gene fusion in prostate cancer. *Neoplasia,* 10**,** 177-88.

TOMLINS, S. A., RHODES, D. R., PERNER, S., DHANASEKARAN, S. M., MEHRA, R., SUN, X.-W., VARAMBALLY, S., CAO, X., TCHINDA, J., KUEFER, R., LEE, C., MONTIE, J. E., SHAH, R. B., PIENTA, K. J., RUBIN, M. A. & CHINNAIYAN, A. M. 2005. Recurrent Fusion of TMPRSS2 and ETS Transcription Factor Genes in Prostate Cancer. *Science,* 310**,** 644-648.

TRABZONLU, L., KULAC, I., ZHENG, Q., HICKS, J. L., HAFFNER, M. C., NELSON, W. G., SFANOS, K. S., ERTUNC, O., LOTAN, T. L., HEAPHY, C. M., MEEKER, A. K., YEGNASUBRAMANIAN, S. & DE MARZO, A. M. 2019. Molecular Pathology of High-Grade Prostatic Intraepithelial Neoplasia: Challenges and Opportunities. *Cold Spring Harb Perspect Med,* 9.

TROTMAN, L. C., NIKI, M., DOTAN, Z. A., KOUTCHER, J. A., DI CRISTOFANO, A., XIAO, A., KHOO, A. S., ROY-BURMAN, P., GREENBERG, N. M., VAN DYKE, T., CORDON-CARDO, C. & PANDOLFI, P. P. 2003. Pten dose dictates cancer progression in the prostate. *PLoS Biol,* 1**,** E59.

TROUP, S., NJUE, C., KLIEWER, E. V., PARISIEN, M., ROSKELLEY, C., CHAKRAVARTI, S., ROUGHLEY, P. J., MURPHY, L. C. & WATSON, P. H. 2003. Reduced expression of the small leucine-rich proteoglycans,

lumican, and decorin is associated with poor outcome in node-negative invasive breast cancer. *Clinical cancer research,* 9**,** 207-214.
TSUKAHARA, T., HANIU, H. & MATSUDA, Y. 2013. PTB-associated splicing factor (PSF) is a PPARγ-binding protein and growth regulator of colon cancer cells. *PLoS One,* 8**,** e58749.
TURNER, N. & GROSE, R. 2010. Fibroblast growth factor signalling: from development to cancer. *Nat Rev Cancer,* 10**,** 116-29.
TYCZYNSKI, J., TARKOWSKI, W., PARKIN, D. M. & ZATONSKI, W. 1994. Cancer mortality among Polish migrants to Australia. *Eur J Cancer,* 30a**,** 478-84.
UEDA, Y., OOSHIO, I., FUSAMAE, Y., KITAE, K., KAWAGUCHI, M., JINGUSHI, K., HASE, H., HARADA, K., HIRATA, K. & TSUJIKAWA, K. 2017. AlkB homolog 3-mediated tRNA demethylation promotes protein synthesis in cancer cells. *Scientific Reports,* 7**,** 42271.
UHLEN, M. F., L.; HALLSTROM, B. M.; LINDSKOG, C.; OKSVOLD, P.; MARDINOGLU, A.; SIVERTSSON, A.; KAMPF, C. ; SJOSTEDT, E.; ASPLUND, A.; OLSSON, I.; EDLUND, K.; LUNDBERG, E.; NAVANI, S.; SZIGYARTO, C. A.; ODEBERG, J.; DJUREINOVIC, D.; TAKANEN, J. O.; HOBER, S.; ALM, T.; EDQVIST, P. H.; BERLING, H.; TEGEL, H.; MULDER, J.; ROCKBERG, J.; NILSSON, P.; SCHWENK, J. M.; HAMSTEN, M.; VON FEILITZEN, K.; FORSBERG, M.; PERSSON, L.; JOHANSSON, F.; ZWAHLEN, M.; VON HEIJNE, G.; NIELSEN, J.; PONTEN, F. 2015. Proteomics. Tissue-based map of the human proteome. *Science,* 347**,** 1260419.
UMBAS, R., ISAACS, W. B., BRINGUIER, P. P., SCHAAFSMA, H. E., KARTHAUS, H. F. M., OOSTERHOF, G. O. N., DEBRUYNE, F. M. J. & SCHALKEN, J. A. 1994. Decreased E-Cadherin Expression Is Associated with Poor Prognosis in Patients with Prostate Cancer. *Cancer Research,* 54**,** 3929-3933.
UMBAS, R., SCHALKEN, J. A., AALDERS, T. W., CARTER, B. S., KARTHAUS, H. F. M., SCHAAFSMA, H. K., DEBRUYNE, F. M. J. & ISAACS, W. B. 1992. Expression of the Cellular Adhesion Molecule E-Cadherin Is Reduced or Absent in High-Grade Prostate Cancer. *Cancer Research,* 52**,** 5104-5109.
VALLÉS, A. M., BEUVIN, M. & BOYER, B. 2004. Activation of Rac1 by paxillin-Crk-DOCK180 signaling complex is antagonized by Rap1 in migrating NBT-II cells. *J Biol Chem,* 279**,** 44490-6.
VAN 'T VEER, L. J., DAI, H., VAN DE VIJVER, M. J., HE, Y. D., HART, A. A. M., MAO, M., PETERSE, H. L., VAN DER KOOY, K., MARTON, M. J., WITTEVEEN, A. T., SCHREIBER, G. J., KERKHOVEN, R. M., ROBERTS, C., LINSLEY, P. S., BERNARDS, R. & FRIEND, S. H. 2002. Gene expression profiling predicts clinical outcome of breast cancer. *Nature,* 415**,** 530-536.
VAN DER KWAST, T. H., SCHALKEN, J., RUIZEVELD DE WINTER, J. A., VAN VROONHOVEN, C. C., MULDER, E., BOERSMA, W. & TRAPMAN, J. 1991. Androgen receptors in endocrine-therapy-resistant human prostate cancer. *Int J Cancer,* 48**,** 189-93.
VELDSCHOLTE, J., RIS-STALPERS, C., KUIPER, G. G., JENSTER, G., BERREVOETS, C., CLAASSEN, E., VAN ROOIJ, H. C., TRAPMAN, J., BRINKMANN, A. O. & MULDER, E. 1990. A mutation in the ligand binding domain of the androgen receptor of human LNCaP cells affects

steroid binding characteristics and response to anti-androgens. *Biochem Biophys Res Commun,* 173**,** 534-40.

VENDOLA, K., ZHOU, J., WANG, J. & BONDY, C. A. 1999. Androgens promote insulin-like growth factor-I and insulin-like growth factor-I receptor gene expression in the primate ovary. *Hum Reprod,* 14**,** 2328-32.

VENKITARAMAN, A. R. 2002. Cancer susceptibility and the functions of BRCA1 and BRCA2. *Cell,* 108**,** 171-82.

VERZE, P., CAI, T. & LORENZETTI, S. 2016. The role of the prostate in male fertility, health and disease. *Nat Rev Urol,* 13**,** 379-86.

VICTORA, C. G., BAHL, R., BARROS, A. J. D., FRANÇA, G. V. A., HORTON, S., KRASEVEC, J., MURCH, S., SANKAR, M. J., WALKER, N. & ROLLINS, N. C. 2016. Breastfeeding in the 21st century: epidemiology, mechanisms, and lifelong effect. *The Lancet,* 387**,** 475-490.

VISAKORPI, T., HYYTINEN, E., KOIVISTO, P., TANNER, M., KEINÄNEN, R., PALMBERG, C., PALOTIE, A., TAMMELA, T., ISOLA, J. & KALLIONIEMI, O.-P. 1995. In vivo amplification of the androgen receptor gene and progression of human prostate cancer. *Nature Genetics,* 9**,** 401-406.

VITA, M. & HENRIKSSON, M. 2006. The Myc oncoprotein as a therapeutic target for human cancer. *Seminars in Cancer Biology,* 16**,** 318-330.

VLEMINCKX, K., VAKAET, L., MAREEL, M., FIERS, W. & VAN ROY, F. 1991. Genetic manipulation of E-cadherin expression by epithelial tumor cells reveals an invasion suppressor role. *Cell,* 66**,** 107-119.

VOSS, G., HAFLIDADÓTTIR, B. S., JÄREMO, H., PERSSON, M., CATELA IVKOVIC, T., WIKSTRÖM, P. & CEDER, Y. 2020. Regulation of cell-cell adhesion in prostate cancer cells by microRNA-96 through upregulation of E-Cadherin and EpCAM. *Carcinogenesis,* 41**,** 865-874.

VOUSDEN, K. H. & LANE, D. P. 2007. p53 in health and disease. *Nat Rev Mol Cell Biol,* 8**,** 275-83.

VU, L. P., PICKERING, B. F., CHENG, Y., ZACCARA, S., NGUYEN, D., MINUESA, G., CHOU, T., CHOW, A., SALETORE, Y., MACKAY, M., SCHULMAN, J., FAMULARE, C., PATEL, M., KLIMEK, V. M., GARRETT-BAKELMAN, F. E., MELNICK, A., CARROLL, M., MASON, C. E., JAFFREY, S. R. & KHARAS, M. G. 2017. The N(6)-methyladenosine (m(6)A)-forming enzyme METTL3 controls myeloid differentiation of normal hematopoietic and leukemia cells. *Nat Med,* 23**,** 1369-1376.

WACHTEL, M., DETTLING, M., KOSCIELNIAK, E., STEGMAIER, S., TREUNER, J. R., SIMON-KLINGENSTEIN, K., BÜHLMANN, P., NIGGLI, F. K. & SCHÄFER, B. W. 2004. Gene Expression Signatures Identify Rhabdomyosarcoma Subtypes and Detect a Novel t(2;2)(q35;p23) Translocation Fusing PAX3 to NCOA1. *Cancer Research,* 64**,** 5539-5545.

WADE, A., ROBINSON, A. E., ENGLER, J. R., PETRITSCH, C., JAMES, C. D. & PHILLIPS, J. J. 2013. Proteoglycans and their roles in brain cancer. *Febs j,* 280**,** 2399-417.

WALSH, C. A., QIN, L., TIEN, J. C.-Y., YOUNG, L. S. & XU, J. 2012. The function of steroid receptor coactivator-1 in normal tissues and cancer. *International journal of biological sciences,* 8**,** 470.

WALSH, T., CASADEI, S., LEE, M. K., PENNIL, C. C., NORD, A. S., THORNTON, A. M., ROEB, W., AGNEW, K. J., STRAY, S. M. & WICKRAMANAYAKE, A. 2011. Mutations in 12 genes for inherited ovarian, fallopian tube, and peritoneal carcinoma identified by massively parallel sequencing. *Proceedings of the National Academy of Sciences,* 108**,** 18032-18037.

WANG, B., XIAO, Y., DING, B. B., ZHANG, N., YUAN, X., GUI, L., QIAN, K. X., DUAN, S., CHEN, Z., RAO, Y. & GENG, J. G. 2003. Induction of tumor angiogenesis by Slit-Robo signaling and inhibition of cancer growth by blocking Robo activity. *Cancer Cell,* 4**,** 19-29.

WANG, C., LEAVENWORTH, J., ZHANG, C., LIU, Z., YUAN, K. Y., WANG, Y., ZHANG, G., WANG, S., CUI, X., ZHANG, Y., BAE, S., ZHOU, J., WANG, L. & LIU, R. 2022a. Epigenetic regulation of EIF4A1 through DNA methylation and an oncogenic role of eIF4A1 through BRD2 signaling in prostate cancer. *Oncogene,* 41**,** 2778-2785.

WANG, H., XU, B. & SHI, J. 2020a. N6-methyladenosine METTL3 promotes the breast cancer progression via targeting Bcl-2. *Gene,* 722**,** 144076.

WANG, L., YANG, Q., ZHOU, Q., FANG, F., LEI, K., LIU, Z., ZHENG, G., ZHU, L., HUO, J., LI, X., PENG, S., KUANG, M., LIN, S., HUANG, M. & XU, L. 2023. METTL3-m(6)A-EGFR-axis drives lenvatinib resistance in hepatocellular carcinoma. *Cancer Lett,* 559**,** 216122.

WANG, M., LIU, J., ZHAO, Y., HE, R., XU, X., GUO, X., LI, X., XU, S., MIAO, J., GUO, J., ZHANG, H., GONG, J., ZHU, F., TIAN, R., SHI, C., PENG, F., FENG, Y., YU, S., XIE, Y., JIANG, J., LI, M., WEI, W., HE, C. & QIN, R. 2020b. Upregulation of METTL14 mediates the elevation of PERP mRNA N(6) adenosine methylation promoting the growth and metastasis of pancreatic cancer. *Mol Cancer,* 19**,** 130.

WANG, T., KONG, S., TAO, M. & JU, S. 2020c. The potential role of RNA N6-methyladenosine in Cancer progression. *Mol Cancer,* 19**,** 88.

WANG, X., LI, Y., FAN, Y., YU, X., MAO, X. & JIN, F. 2018. PTBP1 promotes the growth of breast cancer cells through the PTEN/Akt pathway and autophagy. *J Cell Physiol,* 233**,** 8930-8939.

WANG, X., ZENG, X., LI, D., ZHU, C., GUO, X., FENG, L. & YU, Z. 2022b. PARP inhibitors in small cell lung cancer: The underlying mechanisms and clinical implications. *Biomed Pharmacother,* 153**,** 113458.

WANG, Y., CHEN, J., GAO, W. Q. & YANG, R. 2022c. METTL14 promotes prostate tumorigenesis by inhibiting THBS1 via an m6A-YTHDF2-dependent mechanism. *Cell Death Discov,* 8**,** 143.

WANG, Y., LI, Y., TOTH, J. I., PETROSKI, M. D., ZHANG, Z. & ZHAO, J. C. 2014. N6-methyladenosine modification destabilizes developmental regulators in embryonic stem cells. *Nature Cell Biology,* 16**,** 191.

WANG, Y., SHI, J., CHAI, K., YING, X. & ZHOU, B. P. 2013. The Role of Snail in EMT and Tumorigenesis. *Curr Cancer Drug Targets,* 13**,** 963-972.

WARBURG, O. 1956. On the origin of cancer cells. *Science,* 123**,** 309-314.

WARD, A., BALWIERZ, A., ZHANG, J. D., KÜBLBECK, M., PAWITAN, Y., HIELSCHER, T., WIEMANN, S. & SAHIN, Ö. 2012. Re-expression of microRNA-375 reverses both tamoxifen resistance and accompanying EMT-like properties in breast cancer. *Oncogene,* 32**,** 1173.

WÄRNMARK, A., TREUTER, E., WRIGHT, A. P. & GUSTAFSSON, J. A. 2003. Activation functions 1 and 2 of nuclear receptors: molecular strategies for transcriptional activation. *Mol Endocrinol,* 17**,** 1901-9.

WATERMAN, H., LEVKOWITZ, G., ALROY, I. & YARDEN, Y. 1999. The RING Finger of c-Cbl Mediates Desensitization of the Epidermal Growth Factor Receptor. *Journal of Biological Chemistry,* 274**,** 22151-22154.

WEBER, M. J. & GIOELI, D. 2004. Ras signaling in prostate cancer progression. *J Cell Biochem,* 91**,** 13-25.

WEGIEL, B., BJARTELL, A., EKBERG, J., GADALEANU, V., BRUNHOFF, C. & PERSSON, J. L. 2005. A role for cyclin A1 in mediating the autocrine expression of vascular endothelial growth factor in prostate cancer. *Oncogene,* 24**,** 6385-93.

WEI, C.-M., GERSHOWITZ, A. & MOSS, B. 1975. Methylated nucleotides block 5′ terminus of HeLa cell messenger RNA. *Cell,* 4**,** 379-386.

WEI, X., HUO, Y., PI, J., GAO, Y., RAO, S., HE, M., WEI, Q., SONG, P., CHEN, Y., LU, D., SONG, W., LIANG, J., XU, L., WANG, H., HONG, G., GUO, Y., SI, Y., XU, J., WANG, X., MA, Y., YU, S., ZOU, D., JIN, J., WANG, F. & YU, J. 2022. METTL3 preferentially enhances non-m6A translation of epigenetic factors and promotes tumourigenesis. *Nature Cell Biology,* 24**,** 1278-1290.

WEIGELT, B., BAEHNER, F. L. & REIS-FILHO, J. S. 2010a. The contribution of gene expression profiling to breast cancer classification, prognostication and prediction: a retrospective of the last decade. *J Pathol,* 220**,** 263-80.

WEIGELT, B., GEYER, F. C. & REIS-FILHO, J. S. 2010b. Histological types of breast cancer: How special are they? *Molecular Oncology,* 4**,** 192-208.

WEISS-MESSER, E., MEROM, O., ADI, A., KARRY, R., BIDOSEE, M., BER, R., KAPLOUN, A., STEIN, A. & BARKEY, R. J. 2004. Growth hormone (GH) receptors in prostate cancer: gene expression in human tissues and cell lines and characterization, GH signaling and androgen receptor regulation in LNCaP cells. *Molecular and cellular endocrinology,* 220**,** 109-123.

WELTER, C., THEISINGER, B., RIO, M. C., SEITZ, G., SCHÜDER, G. & BLIN, N. 1994. Expression pattern of breast-cancer-associated protein pS2/BCEI in colorectal tumors. *International Journal of Cancer,* 56**,** 52-55.

WEN, J., LV, R., MA, H., SHEN, H., HE, C., WANG, J., JIAO, F., LIU, H., YANG, P., TAN, L., LAN, F., SHI, Y. G., HE, C., SHI, Y. & DIAO, J. 2018. Zc3h13 Regulates Nuclear RNA m(6)A Methylation and Mouse Embryonic Stem Cell Self-Renewal. *Mol Cell,* 69**,** 1028-1038 e6.

WEN, J., TOOMER, K. H., CHEN, Z. & CAI, X. 2015. Genome-wide analysis of alternative transcripts in human breast cancer. *Breast Cancer Res Treat,* 151**,** 295-307.

WENG, H., HUANG, H., WU, H., QIN, X., ZHAO, B. S., DONG, L., SHI, H., SKIBBE, J., SHEN, C., HU, C., SHENG, Y., WANG, Y., WUNDERLICH, M., ZHANG, B., DORE, L. C., SU, R., DENG, X., FERCHEN, K., LI, C., SUN, M., LU, Z., JIANG, X., MARCUCCI, G., MULLOY, J. C., YANG, J., QIAN, Z., WEI, M., HE, C. & CHEN, J. 2018. METTL14 Inhibits Hematopoietic Stem/Progenitor Differentiation and Promotes Leukemogenesis via mRNA m(6)A Modification. *Cell Stem Cell,* 22**,** 191-205.e9.

WERNER, H. 2022. BRCA1: An Endocrine and Metabolic Regulator. *Front Endocrinol (Lausanne),* 13**,** 844575.

WERNER, H. & LARON, Z. 2020. Role of the GH-IGF1 system in progression of cancer. *Mol Cell Endocrinol,* 518**,** 111003.

WILLIAMS, C. & LIN, C. Y. 2013. Oestrogen receptors in breast cancer: basic mechanisms and clinical implications. *Ecancermedicalscience,* 7**,** 370.

WILSON, W. R. & HAY, M. P. 2011. Targeting hypoxia in cancer therapy. *Nature Reviews Cancer,* 11**,** 393-410.

WOLFE, A. L., SINGH, K., ZHONG, Y., DREWE, P., RAJASEKHAR, V. K., SANGHVI, V. R., MAVRAKIS, K. J., JIANG, M., RODERICK, J. E., VAN DER MEULEN, J., SCHATZ, J. H., RODRIGO, C. M., ZHAO, C., RONDOU, P., DE STANCHINA, E., TERUYA-FELDSTEIN, J., KELLIHER, M. A., SPELEMAN, F., PORCO, J. A., JR., PELLETIER, J., RÄTSCH, G. & WENDEL, H. G. 2014. RNA G-quadruplexes cause eIF4A-dependent oncogene translation in cancer. *Nature,* 513**,** 65-70.

WONG, T. L., CHE, N. & MA, S. 2017. Reprogramming of central carbon metabolism in cancer stem cells. *Biochim Biophys Acta Mol Basis Dis,* 1863**,** 1728-1738.

WOOSTER, R., BIGNELL, G., LANCASTER, J., SWIFT, S., SEAL, S., MANGION, J., COLLINS, N., GREGORY, S., GUMBS, C., MICKLEM, G., BARFOOT, R., HAMOUDI, R., PATEL, S., RICES, C., BIGGS, P., HASHIM, Y., SMITH, A., CONNOR, F., ARASON, A., GUDMUNDSSON, J., FICENEC, D., KELSELL, D., FORD, D., TONIN, P., TIMOTHY BISHOP, D., SPURR, N. K., PONDER, B. A. J., EELES, R., PETO, J., DEVILEE, P., CORNELISSE, C., LYNCH, H., NAROD, S., LENOIR, G., EGILSSON, V., BJORK BARKADOTTIR, R., EASTON, D. F., BENTLEY, D. R., FUTREAL, P. A., ASHWORTH, A. & STRATTON, M. R. 1995. Identification of the breast cancer susceptibility gene BRCA2. *Nature,* 378**,** 789-792.

WU, J., GUO, S., WANG, L. & LIAO, Z. 2022. Correlation analysis between CD133, Klk3 and grhl2 expression and tumor characteristics in prostate cancer. *Cell Mol Biol (Noisy-le-grand),* 67**,** 68-73.

WU, L., WU, D., NING, J., LIU, W. & ZHANG, D. 2019. Changes of N6-methyladenosine modulators promote breast cancer progression. *BMC Cancer,* 19**,** 326.

WU, Q., XIE, X., HUANG, Y., MENG, S., LI, Y., WANG, H. & HU, Y. 2021. N6-methyladenosine RNA methylation regulators contribute to the progression of prostate cancer. *J Cancer,* 12**,** 682-692.

WULLSCHLEGER, S., LOEWITH, R. & HALL, M. N. 2006. TOR signaling in growth and metabolism. *Cell,* 124**,** 471-484.

XIANG, Y., LAURENT, B., HSU, C.-H., NACHTERGAELE, S., LU, Z., SHENG, W., XU, C., CHEN, H., OUYANG, J., WANG, S., LING, D., HSU, P.-H., ZOU, L., JAMBHEKAR, A., HE, C. & SHI, Y. 2017. RNA m6A methylation regulates the ultraviolet-induced DNA damage response. *Nature,* 543**,** 573.

XIE, R., CHEN, X., CHEN, Z., HUANG, M., DONG, W., GU, P., ZHANG, J., ZHOU, Q., DONG, W., HAN, J., WANG, X., LI, H., HUANG, J. & LIN, T. 2019. Polypyrimidine tract binding protein 1 promotes lymphatic metastasis and proliferation of bladder cancer via alternative splicing of MEIS2 and PKM. *Cancer Lett,* 449**,** 31-44.

XU, J., LAMOUILLE, S. & DERYNCK, R. 2009. TGF-beta-induced epithelial to mesenchymal transition. *Cell Res,* 19**,** 156-72.

XUE, F., MENG, Y. & JIANG, J. 2022. Diagnostic Value of Dynamic Enhanced Magnetic Resonance Imaging Combined with Serum CA15-3, CYFRA21-1, and TFF1 for Breast Cancer. *J Healthc Eng,* 2022**,** 7984591.

YAKAR, S., ROSEN, C. J., BEAMER, W. G., ACKERT-BICKNELL, C. L., WU, Y., LIU, J. L., OOI, G. T., SETSER, J., FRYSTYK, J., BOISCLAIR, Y. R. & LEROITH, D. 2002. Circulating levels of IGF-1 directly regulate bone growth and density. *J Clin Invest,* 110**,** 771-81.

YANG, L., XIE, S., JAMALUDDIN, M. S., ALTUWAIJRI, S., NI, J., KIM, E., CHEN, Y. T., HU, Y. C., WANG, L., CHUANG, K. H., WU, C. T. & CHANG, C. 2005. Induction of androgen receptor expression by phosphatidylinositol 3-kinase/Akt downstream substrate, FOXO3a, and their roles in apoptosis of LNCaP prostate cancer cells. *J Biol Chem,* 280**,** 33558-65.

YANG, X., ZHANG, S., HE, C., XUE, P., ZHANG, L., HE, Z., ZANG, L., FENG, B., SUN, J. & ZHENG, M. 2020. METTL14 suppresses proliferation and metastasis of colorectal cancer by down-regulating oncogenic long non-coding RNA XIST. *Mol Cancer,* 19**,** 46.

YANG, Y., HSU, P. J., CHEN, Y. S. & YANG, Y. G. 2018. Dynamic transcriptomic m(6)A decoration: writers, erasers, readers and functions in RNA metabolism. *Cell Res,* 28**,** 616-624.

YANG, Y. S., JIN, X., LI, Q., CHEN, Y. Y., CHEN, F., ZHANG, H., SU, Y., XIAO, Y., DI, G. H., JIANG, Y. Z., HUANG, S. & SHAO, Z. M. 2022. Superenhancer drives a tumor-specific splicing variant of MARCO to promote triple-negative breast cancer progression. *Proc Natl Acad Sci U S A,* 119**,** e2207201119.

YANKOVA, E., BLACKABY, W., ALBERTELLA, M., RAK, J., DE BRAEKELEER, E., TSAGKOGEORGA, G., PILKA, E. S., ASPRIS, D., LEGGATE, D., HENDRICK, A. G., WEBSTER, N. A., ANDREWS, B., FOSBEARY, R., GUEST, P., IRIGOYEN, N., ELEFTHERIOU, M., GOZDECKA, M., DIAS, J. M. L., BANNISTER, A. J., VICK, B., JEREMIAS, I., VASSILIOU, G. S., RAUSCH, O., TZELEPIS, K. & KOUZARIDES, T. 2021. Small-molecule inhibition of METTL3 as a strategy against myeloid leukaemia. *Nature,* 593**,** 597-601.

YARDEN, Y. & PINES, G. 2012. The ERBB network: at last, cancer therapy meets systems biology. *Nat Rev Cancer,* 12**,** 553-63.

YASUMOTO, Y., MIYAZAKI, H., VAIDYAN, L. K., KAGAWA, Y., EBRAHIMI, M., YAMAMOTO, Y., OGATA, M., KATSUYAMA, Y., SADAHIRO, H. & SUZUKI, M. 2016. Inhibition of fatty acid synthase decreases expression of stemness markers in glioma stem cells. *PloS one,* 11**,** e0147717.

YI, D., WANG, R., SHI, X., XU, L., YILIHAMU, Y. & SANG, J. 2020. METTL14 promotes the migration and invasion of breast cancer cells by modulating N6-methyladenosine and hsa-miR-146a-5p expression. *Oncol Rep,* 43**,** 1375-1386.

YIN, J. J., SELANDER, K., CHIRGWIN, J. M., DALLAS, M., GRUBBS, B. G., WIESER, R., MASSAGUÉ, J., MUNDY, G. R. & GUISE, T. A. 1999. TGF-beta signaling blockade inhibits PTHrP secretion by breast cancer cells and bone metastases development. *J Clin Invest,* 103**,** 197-206.

YOSHIDA, K., KAWANO, N., YOSHIIKE, M., YOSHIDA, M., IWAMOTO, T. & MORISAWA, M. 2008. Physiological roles of semenogelin I and zinc in

sperm motility and semen coagulation on ejaculation in humans. *Mol Hum Reprod,* 14**,** 151-6.

YOSHIDA, K. & MIKI, Y. 2004. Role of BRCA1 and BRCA2 as regulators of DNA repair, transcription, and cell cycle in response to DNA damage. *Cancer Science,* 95**,** 866-871.

YOSHIMIZU, T., MIROGLIO, A., RIPOCHE, M. A., GABORY, A., VERNUCCI, M., RICCIO, A., COLNOT, S., GODARD, C., TERRIS, B., JAMMES, H. & DANDOLO, L. 2008. The H19 locus acts in vivo as a tumor suppressor. *Proc Natl Acad Sci U S A,* 105**,** 12417-22.

YU, J., YU, J., MANI, R. S., CAO, Q., BRENNER, C. J., CAO, X., WANG, X., WU, L., LI, J., HU, M., GONG, Y., CHENG, H., LAXMAN, B., VELLAICHAMY, A., SHANKAR, S., LI, Y., DHANASEKARAN, S. M., MOREY, R., BARRETTE, T., LONIGRO, R. J., TOMLINS, S. A., VARAMBALLY, S., QIN, Z. S. & CHINNAIYAN, A. M. 2010. An integrated network of androgen receptor, polycomb, and TMPRSS2-ERG gene fusions in prostate cancer progression. *Cancer Cell,* 17**,** 443-54.

YU, K. D., YE, F. G., HE, M., FAN, L., MA, D., MO, M., WU, J., LIU, G. Y., DI, G. H., ZENG, X. H., HE, P. Q., WU, K. J., HOU, Y. F., WANG, J., WANG, C., ZHUANG, Z. G., SONG, C. G., LIN, X. Y., TOSS, A., RICCI, F., SHEN, Z. Z. & SHAO, Z. M. 2020. Effect of Adjuvant Paclitaxel and Carboplatin on Survival in Women With Triple-Negative Breast Cancer: A Phase 3 Randomized Clinical Trial. *JAMA Oncol,* 6**,** 1390-1396.

YUAN, Y., DU, Y., WANG, L. & LIU, X. 2020. The M6A methyltransferase METTL3 promotes the development and progression of prostate carcinoma via mediating MYC methylation. *J Cancer,* 11**,** 3588-3595.

YUE, Y., LIU, J., CUI, X., CAO, J., LUO, G., ZHANG, Z., CHENG, T., GAO, M., SHU, X., MA, H., WANG, F., WANG, X., SHEN, B., WANG, Y., FENG, X., HE, C. & LIU, J. 2018. VIRMA mediates preferential m6A mRNA methylation in 3′UTR and near stop codon and associates with alternative polyadenylation. *Cell Discovery,* 4**,** 10.

YUNIS, J. J. & BRUNNING, R. D. 1986. Prognostic significance of chromosomal abnormalities in acute leukaemias and myelodysplastic syndromes. *Clinics in haematology,* 15**,** 597-620.

ZADRA, G., RIBEIRO, C. F., CHETTA, P., HO, Y., CACCIATORE, S., GAO, X., SYAMALA, S., BANGO, C., PHOTOPOULOS, C., HUANG, Y., TYEKUCHEVA, S., BASTOS, D. C., TCHAICHA, J., LAWNEY, B., UO, T., D'ANELLO, L., CSIBI, A., KALEKAR, R., LARIMER, B., ELLIS, L., BUTLER, L. M., MORRISSEY, C., MCGOVERN, K., PALOMBELLA, V. J., KUTOK, J. L., MAHMOOD, U., BOSARI, S., ADAMS, J., PELUSO, S., DEHM, S. M., PLYMATE, S. R. & LODA, M. 2019. Inhibition of de novo lipogenesis targets androgen receptor signaling in castration-resistant prostate cancer. *Proc Natl Acad Sci U S A,* 116**,** 631-640.

ZENG, Q., MICHAEL, I. P., ZHANG, P., SAGHAFINIA, S., KNOTT, G., JIAO, W., MCCABE, B. D., GALVÁN, J. A., ROBINSON, H. P. C., ZLOBEC, I., CIRIELLO, G. & HANAHAN, D. 2019. Synaptic proximity enables NMDAR signalling to promote brain metastasis. *Nature,* 573**,** 526-531.

ZHAN, Y., ZHANG, G., WANG, X., QI, Y., BAI, S., LI, D., MA, T., SARTOR, O., FLEMINGTON, E. K., ZHANG, H., LEE, P. & DONG, Y. 2017. Interplay between Cytoplasmic and Nuclear Androgen Receptor Splice Variants Mediates Castration Resistance. *Mol Cancer Res,* 15**,** 59-68.

ZHANG, C., ZHI, W. I., LU, H., SAMANTA, D., CHEN, I., GABRIELSON, E. & SEMENZA, G. L. 2016a. Hypoxia-inducible factors regulate pluripotency factor expression by ZNF217- and ALKBH5-mediated modulation of RNA methylation in breast cancer cells. *Oncotarget,* 7**,** 64527-64542.

ZHANG, D., HU, Q., LIU, X., JI, Y., CHAO, H. P., LIU, Y., TRACZ, A., KIRK, J., BUONAMICI, S., ZHU, P., WANG, J., LIU, S. & TANG, D. G. 2020a. Intron retention is a hallmark and spliceosome represents a therapeutic vulnerability in aggressive prostate cancer. *Nat Commun,* 11**,** 2089.

ZHANG, D., ZHAO, S., LI, X., KIRK, J. S. & TANG, D. G. 2018. Prostate Luminal Progenitor Cells in Development and Cancer. *Trends Cancer,* 4**,** 769-783.

ZHANG, J., TSOI, H., LI, X., WANG, H., GAO, J., WANG, K., GO, M. Y., NG, S. C., CHAN, F. K., SUNG, J. J. & YU, J. 2016b. Carbonic anhydrase IV inhibits colon cancer development by inhibiting the Wnt signalling pathway through targeting the WTAP-WT1-TBL1 axis. *Gut,* 65**,** 1482-93.

ZHANG, L., HUANG, J., YANG, N., GRESHOCK, J., LIANG, S., HASEGAWA, K., GIANNAKAKIS, A., POULOS, N., O'BRIEN-JENKINS, A., KATSAROS, D., BUTZOW, R., WEBER, B. L. & COUKOS, G. 2007. Integrative genomic analysis of phosphatidylinositol 3'-kinase family identifies PIK3R3 as a potential therapeutic target in epithelial ovarian cancer. *Clin Cancer Res,* 13**,** 5314-21.

ZHANG, L., LI, Y., WANG, Q., CHEN, Z., LI, X., WU, Z., HU, C., LIAO, D., ZHANG, W. & CHEN, Z.-S. 2020b. The PI3K subunits, P110α and P110β are potential targets for overcoming P-gp and BCRP-mediated MDR in cancer. *Molecular Cancer,* 19**,** 10.

ZHANG, M., BODI, Z., MACKINNON, K., ZHONG, S., ARCHER, N., MONGAN, N. P., SIMPSON, G. G. & FRAY, R. G. 2022a. Two zinc finger proteins with functions in m(6)A writing interact with HAKAI. *Nat Commun,* 13**,** 1127.

ZHANG, Q., HAN, Z., ZHU, Y., CHEN, J. & LI, W. 2021. Role of hypoxia inducible factor-1 in cancer stem cells. *Molecular Medicine Reports,* 23**,** 1-1.

ZHANG, S., WAN, H. & ZHANG, X. 2020c. LncRNA LHFPL3-AS1 contributes to tumorigenesis of melanoma stem cells via the miR-181a-5p/BCL2 pathway. *Cell Death Dis,* 11**,** 950.

ZHANG, Y. L., WANG, R. C., CHENG, K., RING, B. Z. & SU, L. 2017. Roles of Rap1 signaling in tumor cell migration and invasion. *Cancer Biol Med,* 14**,** 90-99.

ZHANG, Z., CHEN, C., YANG, F., ZENG, Y. X., SUN, P., LIU, P. & LI, X. 2022b. Itaconate is a lysosomal inducer that promotes antibacterial innate immunity. *Mol Cell,* 82**,** 2844-2857.e10.

ZHANG, Z. W., TENG, X., ZHAO, F., MA, C., ZHANG, J., XIAO, L. F., WANG, Y., CHANG, M., TIAN, Y., LI, C., ZHANG, Z., SONG, S., TONG, W. M., LIU, P. & NIU, Y. 2022c. METTL3 regulates m(6)A methylation of PTCH1 and GLI2 in Sonic hedgehog signaling to promote tumor progression in SHH-medulloblastoma. *Cell Rep,* 41**,** 111530.

ZHAO, B. S., NACHTERGAELE, S., ROUNDTREE, I. A. & HE, C. 2018. Our views of dynamic N(6)-methyladenosine RNA methylation. *RNA,* 24**,** 268-272.

ZHAO, B. S., ROUNDTREE, I. A. & HE, C. 2016. Post-transcriptional gene regulation by mRNA modifications. *Nature Reviews Molecular Cell Biology,* 18**,** 31.

ZHAO, J. L., FIZAZI, K., SAAD, F., CHI, K. N., TAPLIN, M.-E., STERNBERG, C. N., ARMSTRONG, A. J., DE BONO, J. S., DUGGAN, W. T. & SCHER, H. I. 2022. The Effect of Corticosteroids on Prostate Cancer Outcome Following Treatment with Enzalutamide: A Multivariate Analysis of the Phase III AFFIRM Trial. *Clinical Cancer Research,* 28**,** 860-869.

ZHAO, X., YANG, Y., SUN, B. F., SHI, Y., YANG, X., XIAO, W., HAO, Y. J., PING, X. L., CHEN, Y. S., WANG, W. J., JIN, K. X., WANG, X., HUANG, C. M., FU, Y., GE, X. M., SONG, S. H., JEONG, H. S., YANAGISAWA, H., NIU, Y., JIA, G. F., WU, W., TONG, W. M., OKAMOTO, A., HE, C., RENDTLEW DANIELSEN, J. M., WANG, X. J. & YANG, Y. G. 2014. FTO-dependent demethylation of N6-methyladenosine regulates mRNA splicing and is required for adipogenesis. *Cell Res,* 24**,** 1403-19.

ZHENG, F., DU, F., QIAN, H., ZHAO, J., WANG, X., YUE, J., HU, N., SI, Y., XU, B. & YUAN, P. 2021. Expression and clinical prognostic value of m6A RNA methylation modification in breast cancer. *Biomark Res,* 9**,** 28.

ZHENG, G., DAHL, JOHN A., NIU, Y., FEDORCSAK, P., HUANG, C.-M., LI, CHARLES J., VÅGBØ, CATHRINE B., SHI, Y., WANG, W.-L., SONG, S.-H., LU, Z., BOSMANS, RALPH P. G., DAI, Q., HAO, Y.-J., YANG, X., ZHAO, W.-M., TONG, W.-M., WANG, X.-J., BOGDAN, F., FURU, K., FU, Y., JIA, G., ZHAO, X., LIU, J., KROKAN, HANS E., KLUNGLAND, A., YANG, Y.-G. & HE, C. 2013. ALKBH5 Is a Mammalian RNA Demethylase that Impacts RNA Metabolism and Mouse Fertility. *Molecular Cell,* 49**,** 18-29.

ZHOU, H., YIN, K., ZHANG, Y., TIAN, J. & WANG, S. 2021a. The RNA m6A writer METTL14 in cancers: Roles, structures, and applications. *Biochimica et Biophysica Acta (BBA) - Reviews on Cancer,* 1876**,** 188609.

ZHOU, J., CHEN, G. B., TANG, Y. C., SINHA, R. A., WU, Y., YAP, C. S., WANG, G., HU, J., XIA, X., TAN, P., GOH, L. K. & YEN, P. M. 2012. Genetic and bioinformatic analyses of the expression and function of PI3K regulatory subunit PIK3R3 in an Asian patient gastric cancer library. *BMC Med Genomics,* 5**,** 34.

ZHOU, L. L., XU, H., HUANG, Y. & YANG, C. G. 2021b. Targeting the RNA demethylase FTO for cancer therapy. *RSC Chem Biol,* 2**,** 1352-1369.

ZHOU, S., DAI, Z., WANG, L., GAO, X., YANG, L., WANG, Z., WANG, Q. & LIU, Z. 2021c. MET inhibition enhances PARP inhibitor efficacy in castration-resistant prostate cancer by suppressing the ATM/ATR and PI3K/AKT pathways. *J Cell Mol Med,* 25**,** 11157-11169.

ZHOU, W. J., GENG, Z. H., CHI, S., ZHANG, W., NIU, X. F., LAN, S. J., MA, L., YANG, X., WANG, L. J., DING, Y. Q. & GENG, J. G. 2011a. Slit-Robo signaling induces malignant transformation through Hakai-mediated E-cadherin degradation during colorectal epithelial cell carcinogenesis. *Cell Res,* 21**,** 609-26.

ZHOU, Y., BOLTON, E. C. & JONES, J. O. 2015. Androgens and androgen receptor signaling in prostate tumorigenesis. *J Mol Endocrinol,* 54**,** R15-29.

ZHOU, Y., ZHOU, Y., SHINGU, T., FENG, L., CHEN, Z., OGASAWARA, M., KEATING, M. J., KONDO, S. & HUANG, P. 2011b. Metabolic alterations in highly tumorigenic glioblastoma cells: preference for hypoxia and high dependency on glycolysis. *Journal of Biological Chemistry,* 286**,** 32843-32853.

ZHOU, Z., LV, J., YU, H., HAN, J., YANG, X., FENG, D., WU, Q., YUAN, B., LU, Q. & YANG, H. 2020. Mechanism of RNA modification N6-methyladenosine in human cancer. *Molecular Cancer,* 19**,** 104.

ZIEGLER, R. G., HOOVER, R. N., PIKE, M. C., HILDESHEIM, A., NOMURA, A. M., WEST, D. W., WU-WILLIAMS, A. H., KOLONEL, L. N., HORN-ROSS, P. L., ROSENTHAL, J. F. & HYER, M. B. 1993. Migration patterns and breast cancer risk in Asian-American women. *J Natl Cancer Inst,* 85**,** 1819-27.

# Appendices

# Appendix 1 Nottingham PCa TMA patient database

## Table ii Patient demographics and clinicopathological parameters examined in Nottingham PCa TMA.

The Nottingham PCa TMA comprised tissue cores from 104 patients acquired following prostatectomy. The number of patients in each parameter group is given. PIN = prostate intraepithelial neoplasia; PSA = prostate specific antigen; TNM = tumour, node, metastasis.

| Clinicopathological parameter | Number of patients |
|---|---|
| **Age at diagnosis** | |
| <60 years | 44 |
| ≥60 years | 60 |
| **Ethnicity** | |
| White | 94 |
| Black Caribbean/Mixed | 2 |
| Other | 2 |
| Not available | 6 |
| **Perineural invasion** | |
| No | 32 |
| Yes | 72 |
| **High grade PIN** | |
| No | 32 |
| Yes | 72 |
| **Positive surgical margins** | |
| No | 55 |
| Yes | 47 |
| Not available | 2 |
| **Extraprostatic extension** | |
| No | 66 |
| Yes | 36 |
| Not available | 2 |
| **Preoperative PSA level (ng/ml)** | |
| <10 | 55 |
| ≥10 | 46 |
| Not available | 3 |
| **Biochemical recurrence** | |
| No | 59 |
| Yes | 33 |
| Never tumour-free | 1 |
| **Time to biochemical recurrence (months)** | |
| ≤23 | 15 |
| ≥24 | 18 |
| **Gleason score** | |
| 6 | 12 |
| 7 | 68 |
| ≥8 | 23 |
| Not available | 1 |
| **TNM score** | |
| T1 & T2 | 66 |
| T3 | 33 |
| Not available | 5 |

# Appendix 2 Nottingham PCa TMA patient database and clinical correlations

### Table iii Correlation of CBLL1 staining with clinicopathological parameters in Nottingham cohort.

CBLL1 nuclear and cytoplasmic staining was correlated with relevant clinicopathological patient parameters. PIN = prostate intraepithelial neoplasia; PSA = prostate specific antigen; TNM = tumour, node, metastasis. Statistical p-values determined by $\chi 2$-test and $p \leq 0.05$ highlighted in bold.

| Clinico-pathological criteria | Nuclear CBLL1 protein expression (%) | | | $\chi^2$ (p value) | Cytoplasmic CBLL1 protein expression (%) | | | $\chi^2$ (p value) |
|---|---|---|---|---|---|---|---|---|
| | Low (≤89) | Moderate (90-100) | High (≥101) | | Low (≤30) | Moderate (31-70) | High (≥71) | |
| **Malignancy** | | | | | | | | |
| Non-malignant | 32.6 | 44.2 | 23.3 | 0.304 (0.219) | 55.8 | 32.6 | 11.6 | **9.51 (0.009)**** |
| Malignant | 23.2 | 44.4 | 32.3 | | 37.4 | 36.4 | 26.3 | |
| **Age at diagnosis** | | | | | | | | |
| <60 years | 24.4 | 41.5 | 34.1 | 0.252 (0.881) | 43.9 | 34.1 | 22.0 | 1.142 (0.565) |
| ≥60 years | 22.4 | 46.6 | 31.0 | | 33.9 | 37.3 | 28.8 | |
| **Perineural invasion** | | | | | | | | |
| No | 22.6 | 48.4 | 29.0 | 0.317 (0.853) | 43.8 | 34.4 | 21.9 | 0.752 (0.687) |
| Yes | 23.5 | 42.6 | 33.8 | | 35.3 | 36.8 | 27.9 | |
| **High grade PIN** | | | | | | | | |
| No | 23.2 | 44.6 | 32.1 | 0.002 (0.999) | 48.8 | 37.2 | 14.0 | **6.573 (0.037)*** |
| Yes | 23.3 | 44.2 | 32.6 | | 29.8 | 35.1 | 35.1 | |
| **Positive surgical margins** | | | | | | | | |
| No | 30.7 | 40.4 | 28.9 | 3.124 (0.21) | 44.2 | 30.8 | 25.0 | 2.087 (0.352) |
| Yes | 15.6 | 51.1 | 33.3 | | 30.4 | 41.3 | 28.3 | |
| **Extraprostatic extension** | | | | | | | | |
| No | 27.9 | 41.0 | 31.1 | 1.647 (0.439) | 41.9 | 35.5 | 22.6 | 2.307 (0.316) |
| Yes | 16.7 | 50.0 | 33.3 | | 27.8 | 38.9 | 33.3 | |
| **Pre-operative PSA level** | | | | | | | | |
| <10 ng/ml | 28.8 | 40.4 | 30.8 | 1.506 (0.471) | 40.4 | 36.5 | 23.1 | 0.832 (0.66) |
| ≥10 ng/ml | 18.2 | 47.7 | 34.1 | | 37.8 | 31.1 | 31.1 | |
| **Biochemical recurrence** | | | | | | | | |
| No | 29.1 | 41.8 | 29.1 | 2.721 (0.606) | 39.3 | 39.3 | 21.4 | 2.48 (0.648) |
| Yes | 17.1 | 45.7 | 37.1 | | 40.6 | 28.1 | 31.3 | |
| Never tumour free | 11.1 | 55.6 | 33.3 | | 25.0 | 41.7 | 33.3 | |
| **Biochemical recurrence within 2 years** | | | | | | | | |
| <2 years | 0.0 | 60.0 | 40.0 | **6.119 (0.047)*** | 20.0 | 46.7 | 33.3 | **6.447 (0.04)*** |
| ≥2 years | 29.4 | 29.4 | 41.2 | | 58.8 | 11.8 | 29.4 | |
| **Gleason score** | | | | | | | | |
| 6 | 41.6 | 33.3 | 25.0 | **10.646 (0.031)*** | 58.3 | 25.0 | 16.7 | 2.913 (0.572) |
| 7 | 21.9 | 37.5 | 40.6 | | 36.9 | 35.4 | 27.7 | |
| ≥8 | 17.4 | 69.6 | 13.0 | | 30.4 | 43.5 | 26.1 | |
| **TNM score** | | | | | | | | |
| T1 & 2 | 27.9 | 41.0 | 31.1 | 1.933 (0.38) | 43.5 | 35.5 | 21.0 | 1.614 (0.446) |
| T3 | 15.2 | 48.5 | 36.4 | | 10.0 | 14.0 | 9.0 | |

# Appendix 3 Weill Cornell Medicine PCa TMA patient database

### Table iv Patient demographics and clinicopathological parameters examined in WCM cohort 1 PCa TMA.

The WCM cohort 1 PCa TMA comprised tissue cores from 171 patients acquired following prostatectomy. The number of patients in each parameter group is given. TNM = tumour, node, metastasis.

| Clinicopathological parameter | Number of patients |
|---|---|
| **Age at diagnosis** | |
| <60 years | 73 |
| ≥60 years | 98 |
| **Ethnicity** | |
| White | 69 |
| African-American | 102 |
| **Gleason score** | |
| 6 | 29 |
| ≥7 | 142 |
| **TNM score** | |
| T2 | 129 |
| T3 | 42 |
| **Biochemical recurrence** | |
| No | 123 |
| Yes | 24 |
| Not available | 24 |

# Appendix 4 Weill Cornell Medicine PCa TMA patient database and clinical correlations

### Table v Correlation of CBLL1 staining with clinicopathological parameters in WCM cohort 1.

CBLL1 nuclear and cytoplasmic staining was correlated with relevant clinicopathological patient parameters. TNM = tumour, node, metastasis. Statistical p-values determined by χ2-test and p ≤ 0.05 highlighted in bold.

| Clinico-pathological criteria | Nuclear CBLL1 protein expression (%) | | | $\chi^2$ (p value) | Cytoplasmic CBLL1 protein expression (%) | | | $\chi^2$ (p value) |
|---|---|---|---|---|---|---|---|---|
| | Low (≤95) | Moderate (96-119) | High (≥120) | | Low (≤30) | Moderate (31-79) | High (≥80) | |
| <60 years | 13.9 | 47.2 | 38.9 | 1.982 (0.371) | 55.6 | 27.8 | 16.7 | 1.079 (0.583) |
| ≥60 years | 23.6 | 49.1 | 27.3 | | 56.4 | 20.0 | 23.6 | |
| White | 16.7 | 40.0 | 43.3 | 2.711 (0.258) | 56.7 | 13.3 | 30.0 | 3.627 (0.163) |
| African-American | 21.3 | 52.5 | 26.2 | | 55.7 | 27.9 | 16.4 | |
| 6 | 26.7 | 46.7 | 26.7 | 0.594 (0.743) | 40.0 | 40.0 | 20.0 | 3.061 (0.216) |
| ≥ 7 | 18.4 | 48.7 | 32.9 | | 59.2 | 19.7 | 21.1 | |
| T2 | 19.7 | 43.9 | 36.4 | 2.492 (0.288) | 54.5 | 24.2 | 21.2 | 0.250 (0.882) |
| T3 | 20.0 | 60.0 | 20.0 | | 60.0 | 20.0 | 20.0 | |
| No | 16.4 | 47.8 | 35.8 | 1.788 (0.409) | 52.2 | 25.4 | 22.4 | 4.927 (0.085) |
| Yes | 25.0 | 58.3 | 16.7 | | 83.3 | 0.0 | 11.8 | |
| Non-malignant | 16.1 | 56.5 | 27.4 | **- (0.029)*** | 53.2 | 25.8 | 21.0 | **- (0.033)*** |
| Malignant | 33.1 | 40.6 | 26.3 | | 35.0 | 30.0 | 35.0 | |

# Appendix 5 Analysis of KEGG pathways related to differentially expressed genes upon R1881 treatment in LNCaP:C4-2 scrambled control cells

**Table vi Analysis of significantly enriched KEGG pathways associated with differentially expressed genes (DEGs) upon R1881 treatment in LNCaP:C4-2 scrambled control cells (si*Scr* Vehicle vs si*Scr* R1881) (FDR<0.05).**

| All DEGs | Description | Size | Expect | Ratio | FDR |
|---|---|---|---|---|---|
| hsa05200 | Pathways in cancer | 526 | 45.283 | 1.7004 | 0.000489 |
| hsa01212 | Fatty acid metabolism | 48 | 4.1323 | 3.388 | 0.005337 |
| hsa01100 | Metabolic pathways | 1305 | 112.35 | 1.3263 | 0.007755 |
| hsa05217 | Basal cell carcinoma | 63 | 5.4236 | 2.7657 | 0.017392 |
| hsa04976 | Bile secretion | 71 | 6.1123 | 2.6177 | 0.017392 |
| hsa05230 | Central carbon metabolism in cancer | 65 | 5.5958 | 2.6806 | 0.017392 |
| hsa00600 | Sphingolipid metabolism | 47 | 4.0462 | 2.9658 | 0.019683 |
| hsa00561 | Glycerolipid metabolism | 61 | 5.2514 | 2.6659 | 0.019683 |
| hsa05202 | Transcriptional misregulation in cancer | 186 | 16.013 | 1.8735 | 0.019683 |
| hsa04022 | cGMP-PKG signalling pathway | 163 | 14.033 | 1.9241 | 0.020814 |
| hsa05224 | Breast cancer | 147 | 12.655 | 1.9755 | 0.020814 |
| hsa05226 | Gastric cancer | 149 | 12.827 | 1.949 | 0.023395 |
| hsa04152 | AMPK signalling pathway | 120 | 10.331 | 2.0328 | 0.028283 |
| hsa03320 | PPAR signalling pathway | 74 | 6.3706 | 2.3546 | 0.028283 |
| hsa00564 | Glycerophospholipid metabolism | 97 | 8.3506 | 2.1555 | 0.028283 |
| hsa05215 | Prostate cancer | 97 | 8.3506 | 2.1555 | 0.028283 |
| hsa04961 | Endocrine and other factor-regulated calcium reabsorption | 47 | 4.0462 | 2.7186 | 0.033611 |
| hsa04360 | Axon guidance | 175 | 15.066 | 1.7922 | 0.036039 |
| hsa04151 | PI3K-Akt signalling pathway | 354 | 30.476 | 1.5094 | 0.045796 |
| hsa04520 | Adherens junction | 72 | 6.1984 | 2.2586 | 0.045796 |
| hsa00330 | Arginine and proline metabolism | 50 | 4.3045 | 2.5555 | 0.045796 |
| hsa00061 | Fatty acid biosynthesis | 13 | 1.1192 | 4.4676 | 0.045796 |
| hsa04211 | Longevity regulating pathway | 89 | 7.6619 | 2.0882 | 0.045796 |
| hsa00071 | Fatty acid degradation | 44 | 3.7879 | 2.64 | 0.045796 |
| hsa04550 | Signalling pathways regulating pluripotency of stem cells | 139 | 11.966 | 1.8385 | 0.045796 |
| hsa05205 | Proteoglycans in cancer | 201 | 17.304 | 1.6759 | 0.045796 |
| hsa00512 | Mucin type O-glycan biosynthesis | 31 | 2.6688 | 2.9976 | 0.045796 |
| hsa04970 | Salivary secretion | 90 | 7.748 | 2.065 | 0.045796 |
| hsa00592 | alpha-Linolenic acid metabolism | 25 | 2.1522 | 3.2524 | 0.046686 |

# Appendix 6 Analysis of KEGG pathways related to differentially expressed genes upon R1881 treatment in LNCaP:C4-2 *CBLL1* knockdown cells

**Table vii Analysis of significantly enriched KEGG pathways associated with differentially expressed genes (DEGs) upon R1881 treatment in LNCaP:C4-2 *CBLL1* knockdown cells (si*CBLL1* Vehicle vs si*CBLL1* R1881) (FDR<0.05).**

| All DEGs | Description | Size | Expect | Ratio | FDR |
|---|---|---|---|---|---|
| hsa04514 | Cell adhesion molecules (CAMs) | 144 | 12.127 | 2.144 | 0.02515 |
| hsa04520 | Adherens junction | 72 | 6.0635 | 2.6388 | 0.02515 |
| hsa04360 | Axon guidance | 175 | 14.738 | 1.9678 | 0.02515 |
| hsa04972 | Pancreatic secretion | 96 | 8.0846 | 2.3501 | 0.02515 |
| hsa04961 | Endocrine and other factor-regulated calcium reabsorption | 47 | 3.9581 | 3.0318 | 0.02515 |
| hsa04976 | Bile secretion | 71 | 5.9792 | 2.5087 | 0.028614 |
| hsa00512 | Mucin type O-glycan biosynthesis | 31 | 2.6107 | 3.4474 | 0.028614 |
| hsa01100 | Metabolic pathways | 1305 | 109.9 | 1.2739 | 0.028614 |
| hsa02010 | ABC transporters | 44 | 3.7054 | 2.9686 | 0.028614 |
| hsa05200 | Pathways in cancer | 526 | 44.297 | 1.4674 | 0.028614 |
| hsa04750 | Inflammatory mediator regulation of TRP channels | 99 | 8.3373 | 2.159 | 0.039826 |
| hsa00600 | Sphingolipid metabolism | 47 | 3.9581 | 2.7791 | 0.039826 |

# Appendix 7 Summary of KEGG pathways related to differentially expressed genes in LNCaP:C4-2 cells grouped by R1881 treatment and *CBLL1* knockdown

**Table viii Summary of KEGG pathways associated with differentially expressed genes in LNCaP:C4-2 cells grouped by R1881 treatment and *CBLL1* knockdown (FDR<0.05).**

| **KEGG pathways unique to si*Scr* Vehicle vs si*Scr* R1881** | **KEGG pathways common to si*Scr* Vehicle vs si*Scr* R1881 & si*CBLL1* Vehicle vs si*CBLL1* R1881** | **KEGG pathways unique to si*CBLL1* Vehicle vs si*CBLL1* R1881** |
|---|---|---|
| Fatty acid metabolism<br>Basal cell carcinoma<br>Central carbon metabolism in cancer<br>Glycerolipid metabolism<br>Transcriptional misregulation in cancer<br>cGMP-PKG signalling pathway<br>Breast cancer<br>Gastric cancer<br>AMPK signalling pathway<br>PPAR signalling pathway<br>Glycerophospholipid metabolism<br>Prostate cancer<br>Axon guidance<br>PI3K-Akt signalling pathway<br>Arginine and proline metabolism<br>Fatty acid biosynthesis<br>Longevity regulating pathway<br>Fatty acid degradation<br>Signalling pathways regulating pluripotency of stem cells<br>Proteoglycans in cancer<br>Salivary secretion<br>alpha-Linolenic acid metabolism | Pathways in cancer<br>Metabolic pathways<br>Adherens junction<br>Endocrine and other factor-regulated calcium reabsorption<br>Bile secretion<br>Mucin type O-glycan biosynthesis<br>Sphingolipid metabolism | Cell adhesion molecules (CAMS)<br>Axon guidance<br>Pancreatic secretion<br>ABC transporters<br>Inflammatory mediator regulation of TRP channels |

# Appendix 8 Analysis of KEGG pathways related to differentially expressed genes upon *CBLL1* knockdown in vehicle-treated LNCaP:C4-2 cells

**Table ix Analysis of significantly enriched KEGG pathways associated with differentially expressed genes (DEGs) upon *CBLL1* knockdown in vehicle-treated LNCaP:C4-2 cells (si*Scr* Vehicle vs si*CBLL1* Vehicle) (FDR<0.05).**

| All DEGs | Description | Size | Expect | Ratio | FDR |
|---|---|---|---|---|---|
| hsa00053 | Ascorbate and aldarate metabolism | 27 | 0.29643 | 23.615 | 3.63E-06 |
| hsa00830 | Retinol metabolism | 67 | 0.73557 | 12.235 | 5.92E-06 |
| hsa00040 | Pentose and glucuronate interconversions | 34 | 0.37328 | 18.753 | 5.92E-06 |
| hsa00982 | Drug metabolism | 72 | 0.79047 | 11.386 | 5.92E-06 |
| hsa00980 | Metabolism of xenobiotics by cytochrome P450 | 76 | 0.83438 | 10.786 | 7.65E-06 |
| hsa05204 | Chemical carcinogenesis | 82 | 0.90025 | 9.9972 | 1.13E-05 |
| hsa00140 | Steroid hormone biosynthesis | 60 | 0.65872 | 12.145 | 1.13E-05 |
| hsa00860 | Porphyrin and chlorophyll metabolism | 42 | 0.46111 | 15.181 | 1.21E-05 |
| hsa00983 | Drug metabolism | 79 | 0.86732 | 8.0709 | 0.000832 |

# Appendix 9 Analysis of KEGG pathways related to differentially expressed genes upon *CBLL1* knockdown in R1881-treated LNCaP:C4-2 cells

**Table x Analysis of significantly enriched KEGG pathways associated with differentially expressed genes (DEGs) upon *CBLL1* knockdown in vehicle-treated LNCaP:C4-2 cells (si*Scr* R1881 vs si*CBLL1* R1881) (FDR<0.05).**

| All DEGs | Description | Size | Expect | Ratio | FDR |
|---|---|---|---|---|---|
| hsa04960 | Aldosterone-regulated sodium reabsorption | 37 | 0.35172 | 14.216 | 0.007621 |
| hsa04151 | PI3K-Akt signalling pathway | 354 | 3.3651 | 3.566 | 0.012233 |
| hsa00053 | Ascorbate and aldarate metabolism | 27 | 0.25666 | 15.585 | 0.012233 |
| hsa00040 | Pentose and glucuronate interconversions | 34 | 0.3232 | 12.376 | 0.023058 |
| hsa00982 | Drug metabolism | 72 | 0.68443 | 7.3054 | 0.034637 |
| hsa00860 | Porphyrin and chlorophyll metabolism | 42 | 0.39925 | 10.019 | 0.034637 |
| hsa00980 | Metabolism of xenobiotics by cytochrome P450 | 76 | 0.72245 | 6.9209 | 0.034637 |
| hsa05204 | Chemical carcinogenesis | 82 | 0.77949 | 6.4145 | 0.042834 |

# Appendix 10 Summary of KEGG pathways related to differentially expressed genes in LNCaP:C4-2 cells grouped by R1881 treatment and *CBLL1* knockdown (2)

**Table xi Summary of KEGG pathways associated with differentially expressed genes in LNCaP:C4-2 cells grouped by R1881 treatment and *CBLL1* knockdown (FDR<0.05).**

| **KEGG pathways unique to si*Scr* Vehicle vs si*CBLL1* Vehicle** | **KEGG pathways common to si*Scr* Vehicle vs si*CBLL1* Vehicle & si*Scr* R1881 vs si*CBLL1* R1881** | **KEGG pathways unique to si*Scr* R1881 vs si*CBLL1* R1881** |
|---|---|---|
| Retinol metabolism<br>Steroid hormone biosynthesis<br>Drug metabolism [2] | Ascorbate and aldarate metabolism<br>Pentose and glucuronate interconversions<br>Drug metabolism<br>Chemical carcinogenesis<br>Metabolism of xenobiotics by cytochrome P450<br>Porphyrin and chlorophyll metabolism | Aldosterone-regulated sodium reabsorption<br>PI3K-Akt signalling pathway |

# Appendix 11 Analysis of KEGG pathways related to differentially expressed genes upon R1881 treatment in LNCaP:C4-2$_{enzR}$ scrambled control cells

**Table xii Analysis of significantly enriched KEGG pathways associated with differentially expressed genes (DEGs) upon R1881 treatment in LNCaP:C4-2$_{enzR}$ scrambled control cells (si*Scr* Vehicle vs si*Scr* R1881) (FDR<0.05).**

| All DEGs | Description | Size | Expect | Ratio | FDR |
|---|---|---|---|---|---|
| hsa03030 | DNA replication | 36 | 3.3498 | 3.8808 | 0.003526 |
| hsa05224 | Breast cancer | 147 | 13.679 | 2.1932 | 0.004409 |
| hsa05215 | Prostate cancer | 97 | 9.026 | 2.4374 | 0.0053 |
| hsa04068 | FoxO signalling pathway | 132 | 12.283 | 2.1982 | 0.0053 |
| hsa04110 | Cell cycle | 124 | 11.538 | 2.1667 | 0.009997 |
| hsa05226 | Gastric cancer | 149 | 13.865 | 2.0195 | 0.011764 |
| hsa05200 | Pathways in cancer | 526 | 48.945 | 1.4915 | 0.011764 |
| hsa04390 | Hippo signalling pathway | 154 | 14.33 | 1.954 | 0.016063 |
| hsa00061 | Fatty acid biosynthesis | 13 | 1.2097 | 4.96 | 0.022491 |
| hsa01212 | Fatty acid metabolism | 48 | 4.4665 | 2.6867 | 0.036372 |
| hsa05212 | Pancreatic cancer | 75 | 6.9788 | 2.2926 | 0.036372 |
| hsa05217 | Basal cell carcinoma | 63 | 5.8622 | 2.3882 | 0.043886 |
| hsa05202 | Transcriptional misregulation in cancer | 186 | 17.308 | 1.7333 | 0.045133 |
| hsa04934 | Cushing syndrome | 154 | 14.33 | 1.8144 | 0.045133 |
| hsa01521 | EGFR tyrosine kinase inhibitor resistance | 79 | 7.3511 | 2.1766 | 0.045138 |
| hsa05218 | Melanoma | 72 | 6.6997 | 2.2389 | 0.045138 |
| hsa05221 | Acute myeloid leukaemia | 66 | 6.1414 | 2.2796 | 0.046647 |
| hsa05223 | Non-small cell lung cancer | 66 | 6.1414 | 2.2796 | 0.046647 |

# Appendix 12 Analysis of KEGG pathways related to differentially expressed genes upon R1881 treatment in LNCaP:C4-2$_{enzR}$ *CBLL1* knockdown cells

**Table xiii Analysis of significantly enriched KEGG pathways associated with differentially expressed genes (DEGs) upon R1881 treatment in LNCaP:C4-2$_{enzR}$ *CBLL1* knockdown cells (si*CBLL1* Vehicle vs si*CBLL1* R1881) (FDR<0.05).**

| All DEGs | Description | Size | Expect | Ratio | FDR |
|---|---|---|---|---|---|
| hsa04110 | Cell cycle | 124 | 11.074 | 2.5286 | 0.001007 |
| hsa05224 | Breast cancer | 147 | 13.127 | 2.0568 | 0.035366 |
| hsa05217 | Basal cell carcinoma | 63 | 5.6261 | 2.6662 | 0.035975 |
| hsa01212 | Fatty acid metabolism | 48 | 4.2865 | 2.7995 | 0.044195 |
| hsa05215 | Prostate cancer | 97 | 8.6623 | 2.1934 | 0.044195 |
| hsa03030 | DNA replication | 36 | 3.2149 | 3.1105 | 0.044195 |
| hsa05200 | Pathways in cancer | 526 | 46.973 | 1.4476 | 0.044195 |
| hsa00590 | Arachidonic acid metabolism | 63 | 5.6261 | 2.4884 | 0.044195 |

# Appendix 13 Summary of KEGG pathways related to differentially expressed genes in LNCaP:C4-2$_{enzR}$ cells grouped by R1881 treatment and *CBLL1* knockdown

**Table xiv Summary of KEGG pathways associated with differentially expressed genes in LNCaP:C4-2$_{enzR}$ cells grouped by R1881 treatment and *CBLL1* knockdown (FDR<0.05).**

| **KEGG pathways unique to si*Scr* Vehicle vs si*Scr* R1881** | **KEGG pathways common to si*Scr* Vehicle vs si*Scr* R1881 & si*CBLL1* Vehicle vs si*CBLL1* R1881** | **KEGG pathways unique to si*CBLL1* Vehicle vs si*CBLL1* R1881** |
|---|---|---|
| Transcriptional misregulation in cancer<br>FoxO signalling pathway<br>Gastric cancer<br>Hippo signalling pathway<br>Fatty acid biosynthesis<br>Pancreatic cancer<br>Cushing syndrome<br>EGFR tyrosine kinase inhibitor resistance<br>Melanoma<br>Acute myeloid leukaemia<br>Non-small cell lung cancer | Breast cancer<br>Prostate cancer<br>Cell cycle<br>Basal cell carcinoma<br>Fatty acid metabolism<br>DNA replication<br>Pathways in cancer | Arachidonic acid metabolism |

**N.B. No significantly over-represented pathways were identified in either LNCaP:C4-2$_{enzR}$ si*Scr* Vehicle vs si*CBLL1* Vehicle or LNCaP:C4-2$_{enzR}$ si*Scr* R1881 vs si*CBLL1* R1881.**

# Appendix 14 Analysis of KEGG pathways related to differentially spliced genes in LNCap:C4-2 cells

**Table xv Analysis of KEGG pathways associated with differentially spliced genes in LNCaP:C4-2 cells (dPSI ≥5%, FDR<0.05). Pathways listed in grey are not statistically significant.**

| si*Scr* Vehicle vs si*Scr* R1881 cells – A5SS events | | | | | |
|---|---|---|---|---|---|
| **All DSGs** | **Description** | **Size** | **Expect** | **Ratio** | **FDR** |
| hsa03420 | Nucleotide excision repair | 47 | 0.66073 | 7.5674 | 0.07158 |
| hsa00240 | Pyrimidine metabolism | 101 | 1.4199 | 4.93 | 0.07158 |
| hsa04120 | Ubiquitin mediated proteolysis | 137 | 1.926 | 4.1538 | 0.07158 |
| hsa05218 | Melanoma | 72 | 1.0122 | 4.9398 | 0.27229 |
| hsa04141 | Protein processing in endoplasmic reticulum | 165 | 2.3196 | 3.0178 | 0.45486 |
| hsa03410 | Base excision repair | 33 | 0.46392 | 6.4667 | 0.45486 |
| hsa05215 | Prostate cancer | 97 | 1.3636 | 3.6667 | 0.45486 |
| hsa05230 | Central carbon metabolism in cancer | 65 | 0.91378 | 4.3774 | 0.45486 |
| hsa04960 | Aldosterone-regulated sodium reabsorption | 37 | 0.52015 | 5.7676 | 0.45486 |
| hsa05214 | Glioma | 71 | 0.99813 | 4.0075 | 0.45486 |
| si*Scr* Vehicle vs si*Scr* R1881 cells – SE events | | | | | |
| **All DSGs** | **Description** | **Size** | **Expect** | **Ratio** | **FDR** |
| hsa03440 | Homologous recombination | 41 | 1.6358 | 4.2792 | 0.34483 |
| hsa01524 | Platinum drug resistance | 73 | 2.9126 | 3.0901 | 0.38361 |
| hsa00564 | Glycerophospholipid metabolism | 97 | 3.8701 | 2.5839 | 0.39696 |
| hsa04146 | Peroxisome | 83 | 3.3116 | 2.7178 | 0.39696 |
| hsa01523 | Antifolate resistance | 31 | 1.2368 | 4.0425 | 0.39696 |
| hsa04115 | p53 signalling pathway | 72 | 2.8727 | 2.7849 | 0.39696 |
| hsa04142 | Lysosome | 123 | 4.9075 | 2.2415 | 0.39696 |
| hsa00280 | Valine, leucine and isoleucine degradation | 48 | 1.9151 | 3.133 | 0.39696 |
| hsa05222 | Small cell lung cancer | 93 | 3.7105 | 2.4255 | 0.39696 |
| hsa03430 | Mismatch repair | 23 | 0.91766 | 4.3589 | 0.39696 |
| si*Scr* Vehicle vs si*Scr* R1881 cells – MXE events | | | | | |
| **All DSGs** | **Description** | **Size** | **Expect** | **Ratio** | **FDR** |
| hsa01100 | Metabolic pathways | 1305 | 22.364 | 1.7886 | **0.029406** |
| hsa03430 | Mismatch repair | 23 | 0.39416 | 10.148 | 0.093115 |
| hsa00983 | Drug metabolism | 79 | 1.3539 | 4.4318 | 0.24711 |
| hsa00240 | Pyrimidine metabolism | 101 | 1.7309 | 3.4664 | 0.62308 |
| hsa01200 | Carbon metabolism | 116 | 1.988 | 3.0182 | 0.94919 |
| hsa03450 | Non-homologous end-joining | 13 | 0.22279 | 8.9772 | 1 |
| hsa01230 | Biosynthesis of amino acids | 75 | 1.2853 | 3.1121 | 1 |
| hsa00600 | Sphingolipid metabolism | 47 | 0.80546 | 3.7246 | 1 |
| hsa03460 | Fanconi anaemia pathway | 54 | 0.92543 | 3.2418 | 1 |
| hsa00592 | alpha-Linolenic acid metabolism | 25 | 0.42844 | 4.6681 | 1 |

| si*Scr* Vehicle vs si*Scr* R1881 cells – RI events | | | | | |
|---|---|---|---|---|---|
| **All DSGs** | **Description** | **Size** | **Expect** | **Ratio** | **FDR** |
| hsa01100 | Metabolic pathways | 1305 | 12.056 | 1.7419 | 1 |
| hsa00603 | Glycosphingolipid biosynthesis | 15 | 0.13857 | 14.433 | 1 |
| hsa05213 | Endometrial cancer | 58 | 0.53581 | 5.599 | 1 |
| hsa00563 | Glycosylphosphatidylinositol (GPI)-anchor biosynthesis | 25 | 0.23095 | 8.6597 | 1 |
| hsa04520 | Adherens junction | 72 | 0.66515 | 4.5103 | 1 |
| hsa03010 | Ribosome | 153 | 1.4134 | 2.83 | 1 |
| hsa04122 | Sulphur relay system | 8 | 0.073905 | 13.531 | 1 |
| hsa04330 | Notch signalling pathway | 48 | 0.44343 | 4.5103 | 1 |
| hsa03008 | Ribosome biogenesis in eukaryotes | 105 | 0.97001 | 3.0928 | 1 |
| hsa00510 | N-Glycan biosynthesis | 49 | 0.45267 | 4.4182 | 1 |
| si*Scr* Vehicle vs si*Scr* R1881 cells – A3SS events | | | | | |
| **All DSGs** | **Description** | **Size** | **Expect** | **Ratio** | **FDR** |
| hsa05131 | Shigellosis | 65 | 0.82675 | 4.8382 | 0.98775 |
| hsa03030 | DNA replication | 36 | 0.45789 | 6.5518 | 0.98775 |
| hsa04662 | B cell receptor signalling pathway | 71 | 0.90307 | 4.4294 | 0.98775 |
| hsa00562 | Inositol phosphate metabolism | 74 | 0.94122 | 4.2498 | 0.98775 |
| hsa01230 | Biosynthesis of amino acids | 75 | 0.95394 | 4.1931 | 0.98775 |
| hsa04140 | Autophagy | 128 | 1.6281 | 3.0711 | 1 |
| hsa05222 | Small cell lung cancer | 93 | 1.1829 | 3.3816 | 1 |
| hsa03430 | Mismatch repair | 23 | 0.29254 | 6.8366 | 1 |
| hsa00564 | Glycerophospholipid metabolism | 97 | 1.2338 | 3.2421 | 1 |
| hsa04070 | Phosphatidylinositol signalling system | 99 | 1.2592 | 3.1766 | 1 |

| si*Scr* Vehicle vs si*CBLL1* Vehicle cells – A5SS events | | | | | |
|---|---|---|---|---|---|
| **All DSGs** | **Description** | **Size** | **Expect** | **Ratio** | **FDR** |
| hsa03022 | Basal transcription factors | 45 | 0.63864 | 7.8291 | 0.13405 |
| hsa05214 | Glioma | 71 | 1.0076 | 4.9621 | 0.35192 |
| hsa03430 | Mismatch repair | 23 | 0.32642 | 9.1907 | 0.35192 |
| hsa03420 | Nucleotide excision repair | 47 | 0.66702 | 5.9968 | 0.35192 |
| hsa04722 | Neurotrophin signalling pathway | 119 | 1.6888 | 3.5527 | 0.40137 |
| hsa00020 | Citrate cycle (TCA cycle) | 30 | 0.42576 | 7.0462 | 0.40137 |
| hsa00630 | Glyoxylate and dicarboxylate metabolism | 30 | 0.42576 | 7.0462 | 0.40137 |
| hsa04910 | Insulin signalling pathway | 137 | 1.9443 | 3.0859 | 0.41306 |
| hsa05152 | Tuberculosis | 179 | 2.5404 | 2.7555 | 0.41306 |
| hsa03030 | DNA replication | 36 | 0.51091 | 5.8719 | 0.41306 |

| si*Scr* Vehicle vs si*CBLL1* Vehicle cells – SE events | | | | | |
|---|---|---|---|---|---|
| **All DSGs** | **Description** | **Size** | **Expect** | **Ratio** | **FDR** |
| hsa03410 | Base excision repair | 33 | 1.215 | 4.9382 | 0.32761 |
| hsa04150 | mTOR signalling pathway | 151 | 5.5596 | 2.3383 | 0.32761 |
| hsa00240 | Pyrimidine metabolism | 101 | 3.7187 | 2.6891 | 0.32761 |
| hsa04120 | Ubiquitin mediated proteolysis | 137 | 5.0442 | 2.379 | 0.32761 |
| hsa01100 | Metabolic pathways | 1305 | 48.049 | 1.3528 | 0.32761 |
| hsa01212 | Fatty acid metabolism | 48 | 1.7673 | 3.395 | 0.3923 |
| hsa00970 | Aminoacyl-tRNA biosynthesis | 66 | 2.43 | 2.8806 | 0.3923 |
| hsa00061 | Fatty acid biosynthesis | 13 | 0.47865 | 6.2677 | 0.3923 |
| hsa03450 | Non-homologous end-joining | 13 | 0.47865 | 6.2677 | 0.3923 |
| hsa04110 | Cell cycle | 124 | 4.5655 | 2.1903 | 0.49454 |
| si*Scr* Vehicle vs si*CBLL1* Vehicle cells – MXE events | | | | | |
| **All DSGs** | **Description** | **Size** | **Expect** | **Ratio** | **FDR** |
| hsa00510 | N-Glycan biosynthesis | 49 | 0.73477 | 6.8048 | 0.25712 |
| hsa01100 | Metabolic pathways | 1305 | 19.569 | 1.533 | 1 |
| hsa00051 | Fructose and mannose metabolism | 33 | 0.49485 | 6.0625 | 1 |
| hsa04120 | Ubiquitin mediated proteolysis | 137 | 2.0544 | 2.9206 | 1 |
| hsa03420 | Nucleotide excision repair | 47 | 0.70478 | 4.2566 | 1 |
| hsa03430 | Mismatch repair | 23 | 0.34489 | 5.7989 | 1 |
| hsa00230 | Purine metabolism | 174 | 2.6092 | 2.2996 | 1 |
| hsa04977 | Vitamin digestion and absorption | 24 | 0.35989 | 5.5573 | 1 |
| hsa00020 | Citrate cycle (TCA cycle) | 30 | 0.44986 | 4.4458 | 1 |
| hsa01523 | Antifolate resistance | 31 | 0.46485 | 4.3024 | 1 |
| si*Scr* Vehicle vs si*CBLL1* Vehicle cells – RI events | | | | | |
| **All DSGs** | **Description** | **Size** | **Expect** | **Ratio** | **FDR** |
| hsa04215 | Apoptosis | 33 | 0.30044 | 9.9853 | 1 |
| hsa04530 | Tight junction | 170 | 1.5477 | 3.2305 | 1 |
| hsa04623 | Cytosolic DNA-sensing pathway | 63 | 0.57357 | 5.2304 | 1 |
| hsa05120 | Epithelial cell signalling in Helicobacter pylori infection | 68 | 0.61909 | 4.8458 | 1 |
| hsa04920 | Adipocytokine signalling pathway | 69 | 0.6282 | 4.7756 | 1 |
| hsa04142 | Lysosome | 123 | 1.1198 | 3.572 | 1 |
| hsa01523 | Antifolate resistance | 31 | 0.28223 | 7.0863 | 1 |
| hsa03020 | RNA polymerase | 31 | 0.28223 | 7.0863 | 1 |
| hsa04210 | Apoptosis | 136 | 1.2382 | 3.2305 | 1 |
| hsa05161 | Hepatitis B | 144 | 1.311 | 3.0511 | 1 |

| si*Scr* Vehicle vs si*CBLL1* Vehicle cells – A3SS events | | | | | |
|---|---|---|---|---|---|
| **All DSGs** | **Description** | **Size** | **Expect** | **Ratio** | **FDR** |
| hsa00515 | Mannose type O-glycan biosynthesis | 23 | 0.2987 | 10.043 | 0.57857 |
| hsa03018 | RNA degradation | 79 | 1.026 | 4.8734 | 0.57857 |
| hsa04714 | Thermogenesis | 229 | 2.974 | 2.69 | 0.90504 |
| hsa04150 | mTOR signalling pathway | 151 | 1.961 | 3.0596 | 0.90504 |
| hsa01100 | Metabolic pathways | 1305 | 16.948 | 1.5341 | 0.90504 |
| hsa04142 | Lysosome | 123 | 1.5974 | 3.1301 | 1 |
| hsa03460 | Fanconi anaemia pathway | 54 | 0.7013 | 4.2778 | 1 |
| hsa00564 | Glycerophospholipid metabolism | 97 | 1.2597 | 3.1753 | 1 |
| hsa01522 | Endocrine resistance | 98 | 1.2727 | 3.1429 | 1 |
| hsa03008 | Ribosome biogenesis in eukaryotes | 105 | 1.3636 | 2.9333 | 1 |

| si*Scr* R1881 vs si*CBLL1* R1881 cells – A5SS events | | | | | |
|---|---|---|---|---|---|
| **All DSGs** | **Description** | **Size** | **Expect** | **Ratio** | **FDR** |
| hsa00514 | Other types of O-glycan biosynthesis | 22 | 0.28866 | 13.857 | 0.055946 |
| hsa00900 | Terpenoid backbone biosynthesis | 22 | 0.28866 | 10.393 | 0.46303 |
| hsa01100 | Metabolic pathways | 1305 | 17.123 | 1.5768 | 0.91668 |
| hsa04218 | Cellular senescence | 160 | 2.0993 | 2.858 | 1 |
| hsa03022 | Basal transcription factors | 45 | 0.59044 | 5.081 | 1 |
| hsa03040 | Spliceosome | 134 | 1.7582 | 2.8438 | 1 |
| hsa03015 | mRNA surveillance pathway | 91 | 1.194 | 3.3501 | 1 |
| hsa05231 | Choline metabolism in cancer | 99 | 1.299 | 3.0794 | 1 |
| hsa00310 | Lysine degradation | 59 | 0.77413 | 3.8753 | 1 |
| hsa00020 | Citrate cycle (TCA cycle) | 30 | 0.39363 | 5.081 | 1 |

| si*Scr* R1881 vs si*CBLL1* R1881 cells – SE events | | | | | |
|---|---|---|---|---|---|
| **All DSGs** | **Description** | **Size** | **Expect** | **Ratio** | **FDR** |
| hsa00240 | Pyrimidine metabolism | 101 | 4.3272 | 3.6975 | **0.001697** |
| hsa00230 | Purine metabolism | 174 | 7.4548 | 2.4145 | 0.073385 |
| hsa03420 | Nucleotide excision repair | 47 | 2.0137 | 3.9729 | 0.083083 |
| hsa04623 | Cytosolic DNA-sensing pathway | 63 | 2.6992 | 3.3344 | 0.10231 |
| hsa03460 | Fanconi anaemia pathway | 54 | 2.3136 | 3.4579 | 0.10231 |
| hsa03410 | Base excision repair | 33 | 1.4138 | 4.2438 | 0.10231 |
| hsa00515 | Mannose type O-glycan biosynthesis | 23 | 0.98541 | 5.074 | 0.10231 |
| hsa03430 | Mismatch repair | 23 | 0.98541 | 5.074 | 0.10231 |
| hsa04115 | p53 signalling pathway | 72 | 3.0848 | 2.9176 | 0.12511 |
| hsa03030 | DNA replication | 36 | 1.5424 | 3.8901 | 0.12735 |

| si*Scr* R1881 vs si*CBLL1* R1881 cells – MXE events | | | | | |
|---|---|---|---|---|---|
| **All DSGs** | **Description** | **Size** | **Expect** | **Ratio** | **FDR** |
| hsa04932 | Non-alcoholic fatty liver disease (NAFLD) | 149 | 2.334 | 3.856 | 0.14245 |
| hsa00520 | Amino sugar and nucleotide sugar metabolism | 48 | 0.75191 | 6.6498 | 0.14245 |
| hsa04141 | Protein processing in endoplasmic reticulum | 165 | 2.5847 | 3.0952 | 0.27746 |
| hsa04068 | FoxO signalling pathway | 132 | 2.0677 | 3.3853 | 0.27746 |
| hsa04917 | Prolactin signalling pathway | 70 | 1.0965 | 4.5598 | 0.27746 |
| hsa03430 | Mismatch repair | 23 | 0.36029 | 8.3266 | 0.27746 |
| hsa05100 | Bacterial invasion of epithelial cells | 74 | 1.1592 | 4.3134 | 0.27746 |
| hsa04668 | TNF signalling pathway | 110 | 1.7231 | 3.4821 | 0.30525 |
| hsa04722 | Neurotrophin signalling pathway | 119 | 1.8641 | 3.2187 | 0.36733 |
| hsa04152 | AMPK signalling pathway | 120 | 1.8798 | 3.1919 | 0.36733 |
| si*Scr* R1881 vs si*CBLL1* R1881 cells – RI events | | | | | |
| **All DSGs** | **Description** | **Size** | **Expect** | **Ratio** | **FDR** |
| hsa01212 | Fatty acid metabolism | 48 | 0.44986 | 6.6688 | 1 |
| hsa03010 | Ribosome | 153 | 1.4339 | 3.4869 | 1 |
| hsa04136 | Autophagy | 32 | 0.29991 | 6.6688 | 1 |
| hsa03040 | Spliceosome | 134 | 1.2559 | 3.1851 | 1 |
| hsa00260 | Glycine, serine and threonine metabolism | 40 | 0.37488 | 5.335 | 1 |
| hsa05219 | Bladder cancer | 41 | 0.38425 | 5.2049 | 1 |
| hsa00270 | Cysteine and methionine metabolism | 47 | 0.44049 | 4.5404 | 1 |
| hsa04330 | Notch signalling pathway | 48 | 0.44986 | 4.4458 | 1 |
| hsa05110 | Vibrio cholerae infection | 50 | 0.4686 | 4.268 | 1 |
| hsa00920 | Sulphur metabolism | 9 | 0.084349 | 11.856 | 1 |

| si*Scr* R1881 vs si*CBLL1* R1881 cells – A3SS events | | | | | |
|---|---|---|---|---|---|
| **All DSGs** | **Description** | **Size** | **Expect** | **Ratio** | **FDR** |
| hsa03030 | DNA replication | 36 | 0.53019 | 9.4306 | 0.054517 |
| hsa03420 | Nucleotide excision repair | 47 | 0.69219 | 7.2234 | 0.09753 |
| hsa04520 | Adherens junction | 72 | 1.0604 | 4.7153 | 0.36533 |
| hsa03430 | Mismatch repair | 23 | 0.33873 | 8.8565 | 0.36533 |
| hsa00310 | Lysine degradation | 59 | 0.86892 | 4.6034 | 0.67461 |
| hsa03410 | Base excision repair | 33 | 0.48601 | 6.1727 | 0.67461 |
| hsa05131 | Shigellosis | 65 | 0.95729 | 4.1785 | 0.71219 |
| hsa05100 | Bacterial invasion of epithelial cells | 74 | 1.0898 | 3.6703 | 0.95825 |
| hsa01212 | Fatty acid metabolism | 48 | 0.70692 | 4.2438 | 1 |
| hsa00510 | N-Glycan biosynthesis | 49 | 0.72165 | 4.1571 | 1 |

| si*Scr* R1881 vs si*CBLL1* R1881 cells – A5SS events | | | | | |
|---|---|---|---|---|---|
| **All DSGs** | **Description** | **Size** | **Expect** | **Ratio** | **FDR** |
| hsa00514 | Other types of O-glycan biosynthesis | 22 | 0.28866 | 13.857 | 0.055946 |
| hsa00900 | Terpenoid backbone biosynthesis | 22 | 0.28866 | 10.393 | 0.46303 |
| hsa01100 | Metabolic pathways | 1305 | 17.123 | 1.5768 | 0.91668 |
| hsa04218 | Cellular senescence | 160 | 2.0993 | 2.858 | 1 |
| hsa03022 | Basal transcription factors | 45 | 0.59044 | 5.081 | 1 |
| hsa03040 | Spliceosome | 134 | 1.7582 | 2.8438 | 1 |
| hsa03015 | mRNA surveillance pathway | 91 | 1.194 | 3.3501 | 1 |
| hsa05231 | Choline metabolism in cancer | 99 | 1.299 | 3.0794 | 1 |
| hsa00310 | Lysine degradation | 59 | 0.77413 | 3.8753 | 1 |
| hsa00020 | Citrate cycle (TCA cycle) | 30 | 0.39363 | 5.081 | 1 |
| si*Scr* R1881 vs si*CBLL1* R1881 cells – SE events | | | | | |
| **All DSGs** | **Description** | **Size** | **Expect** | **Ratio** | **FDR** |
| hsa00240 | Pyrimidine metabolism | 101 | 4.3272 | 3.6975 | **0.001697** |
| hsa00230 | Purine metabolism | 174 | 7.4548 | 2.4145 | 0.073385 |
| hsa03420 | Nucleotide excision repair | 47 | 2.0137 | 3.9729 | 0.083083 |
| hsa04623 | Cytosolic DNA-sensing pathway | 63 | 2.6992 | 3.3344 | 0.10231 |
| hsa03460 | Fanconi anemia pathway | 54 | 2.3136 | 3.4579 | 0.10231 |
| hsa03410 | Base excision repair | 33 | 1.4138 | 4.2438 | 0.10231 |
| hsa00515 | Mannose type O-glycan biosynthesis | 23 | 0.98541 | 5.074 | 0.10231 |
| hsa03430 | Mismatch repair | 23 | 0.98541 | 5.074 | 0.10231 |
| hsa04115 | p53 signaling pathway | 72 | 3.0848 | 2.9176 | 0.12511 |
| hsa03030 | DNA replication | 36 | 1.5424 | 3.8901 | 0.12735 |
| si*Scr* R1881 vs si*CBLL1* R1881 cells – MXE events | | | | | |
| **All DSGs** | **Description** | **Size** | **Expect** | **Ratio** | **FDR** |
| hsa04932 | Non-alcoholic fatty liver disease (NAFLD) | 149 | 2.334 | 3.856 | 0.14245 |
| hsa00520 | Amino sugar and nucleotide sugar metabolism | 48 | 0.75191 | 6.6498 | 0.14245 |
| hsa04141 | Protein processing in endoplasmic reticulum | 165 | 2.5847 | 3.0952 | 0.27746 |
| hsa04068 | FoxO signalling pathway | 132 | 2.0677 | 3.3853 | 0.27746 |
| hsa04917 | Prolactin signalling pathway | 70 | 1.0965 | 4.5598 | 0.27746 |
| hsa03430 | Mismatch repair | 23 | 0.36029 | 8.3266 | 0.27746 |
| hsa05100 | Bacterial invasion of epithelial cells | 74 | 1.1592 | 4.3134 | 0.27746 |
| hsa04668 | TNF signalling pathway | 110 | 1.7231 | 3.4821 | 0.30525 |
| hsa04722 | Neurotrophin signalling pathway | 119 | 1.8641 | 3.2187 | 0.36733 |
| hsa04152 | AMPK signalling pathway | 120 | 1.8798 | 3.1919 | 0.36733 |

| si*Scr* R1881 vs si*CBLL1* R1881 cells – RI events | | | | | |
|---|---|---|---|---|---|
| **All DSGs** | **Description** | **Size** | **Expect** | **Ratio** | **FDR** |
| hsa01212 | Fatty acid metabolism | 48 | 0.44986 | 6.6688 | 1 |
| hsa03010 | Ribosome | 153 | 1.4339 | 3.4869 | 1 |
| hsa04136 | Autophagy | 32 | 0.29991 | 6.6688 | 1 |
| hsa03040 | Spliceosome | 134 | 1.2559 | 3.1851 | 1 |
| hsa00260 | Glycine, serine and threonine metabolism | 40 | 0.37488 | 5.335 | 1 |
| hsa05219 | Bladder cancer | 41 | 0.38425 | 5.2049 | 1 |
| hsa00270 | Cysteine and methionine metabolism | 47 | 0.44049 | 4.5404 | 1 |
| hsa04330 | Notch signalling pathway | 48 | 0.44986 | 4.4458 | 1 |
| hsa05110 | Vibrio cholerae infection | 50 | 0.4686 | 4.268 | 1 |
| hsa00920 | Sulphur metabolism | 9 | 0.084349 | 11.856 | 1 |

| si*Scr* R1881 vs si*CBLL1* R1881 cells – A3SS events | | | | | |
|---|---|---|---|---|---|
| **All DSGs** | **Description** | **Size** | **Expect** | **Ratio** | **FDR** |
| hsa03030 | DNA replication | 36 | 0.53019 | 9.4306 | 0.054517 |
| hsa03420 | Nucleotide excision repair | 47 | 0.69219 | 7.2234 | 0.09753 |
| hsa04520 | Adherens junction | 72 | 1.0604 | 4.7153 | 0.36533 |
| hsa03430 | Mismatch repair | 23 | 0.33873 | 8.8565 | 0.36533 |
| hsa00310 | Lysine degradation | 59 | 0.86892 | 4.6034 | 0.67461 |
| hsa03410 | Base excision repair | 33 | 0.48601 | 6.1727 | 0.67461 |
| hsa05131 | Shigellosis | 65 | 0.95729 | 4.1785 | 0.71219 |
| hsa05100 | Bacterial invasion of epithelial cells | 74 | 1.0898 | 3.6703 | 0.95825 |
| hsa01212 | Fatty acid metabolism | 48 | 0.70692 | 4.2438 | 1 |
| hsa00510 | N-Glycan biosynthesis | 49 | 0.72165 | 4.1571 | 1 |

# Appendix 15 Analysis of KEGG pathways related to differentially spliced genes in LNCap:C4-2$_{enzR}$ cells

**Table xvi Analysis of KEGG pathways associated with differentially spliced genes in LNCaP:C4-2$_{enzR}$ cells (dPSI ≥5%, FDR<0.05). All pathways marked in grey are not statistically significant.**

| si*Scr* Vehicle vs si*Scr* R1881 cells – A5SS events | | | | | |
|---|---|---|---|---|---|
| **All DSGs** | **Description** | **Size** | **Expect** | **Ratio** | **FDR** |
| hsa03440 | Homologous recombination | 41 | 0.60383 | 8.2805 | 0.10221 |
| hsa00630 | Glyoxylate and dicarboxylate metabolism | 30 | 0.44183 | 9.0533 | 0.14946 |
| hsa03430 | Mismatch repair | 23 | 0.33873 | 8.8565 | 0.4871 |
| hsa00310 | Lysine degradation | 59 | 0.86892 | 4.6034 | 0.85523 |
| hsa04120 | Ubiquitin mediated proteolysis | 137 | 2.0177 | 2.9737 | 0.85523 |
| hsa03030 | DNA replication | 36 | 0.53019 | 5.6583 | 0.85523 |
| hsa03420 | Nucleotide excision repair | 47 | 0.69219 | 4.334 | 1 |
| hsa00670 | One carbon pool by folate | 20 | 0.29455 | 6.79 | 1 |
| hsa03460 | Fanconi anaemia pathway | 54 | 0.79529 | 3.7722 | 1 |
| hsa00190 | Oxidative phosphorylation | 133 | 1.9588 | 2.5526 | 1 |
| **si*Scr* Vehicle vs si*Scr* R1881 cells – SE events** | | | | | |
| **All DSGs** | **Description** | **Size** | **Expect** | **Ratio** | **FDR** |
| hsa03460 | Fanconi anaemia pathway | 54 | 3.0076 | 3.9899 | 0.010123 |
| hsa00514 | Other types of O-glycan biosynthesis | 22 | 1.2253 | 5.7127 | 0.021272 |
| hsa04120 | Ubiquitin mediated proteolysis | 137 | 7.6305 | 2.49 | 0.021272 |
| hsa01100 | Metabolic pathways | 1305 | 72.684 | 1.3621 | 0.038063 |
| hsa00515 | Mannose type O-glycan biosynthesis | 23 | 1.281 | 4.6837 | 0.084947 |
| hsa04140 | Autophagy | 128 | 7.1292 | 2.104 | 0.26533 |
| hsa04931 | Insulin resistance | 107 | 5.9596 | 2.1814 | 0.27293 |
| hsa04152 | AMPK signalling pathway | 120 | 6.6836 | 2.0947 | 0.27293 |
| hsa00240 | Pyrimidine metabolism | 101 | 5.6254 | 2.1332 | 0.32941 |
| hsa04141 | Protein processing in endoplasmic reticulum | 165 | 9.19 | 1.8498 | 0.32941 |
| **si*Scr* Vehicle vs si*Scr* R1881 cells – MXE events** | | | | | |
| **All DSGs** | **Description** | **Size** | **Expect** | **Ratio** | **FDR** |
| hsa01100 | Metabolic pathways | 1305 | 21.491 | 1.7682 | 0.057081 |
| hsa03420 | Nucleotide excision repair | 47 | 0.774 | 6.46 | 0.16201 |
| hsa00260 | Glycine, serine and threonine metabolism | 40 | 0.65872 | 6.0724 | 0.36164 |
| hsa00270 | Cysteine and methionine metabolism | 47 | 0.774 | 5.168 | 0.36164 |
| hsa04120 | Ubiquitin mediated proteolysis | 137 | 2.2561 | 3.1027 | 0.36164 |
| hsa01230 | Biosynthesis of amino acids | 75 | 1.2351 | 4.0482 | 0.36164 |
| hsa00592 | alpha-Linolenic acid metabolism | 25 | 0.4117 | 7.2868 | 0.36164 |
| hsa01523 | Antifolate resistance | 31 | 0.51051 | 5.8765 | 0.51564 |
| hsa05016 | Huntington disease | 193 | 3.1783 | 2.517 | 0.51564 |
| hsa05010 | Alzheimer disease | 171 | 2.816 | 2.4858 | 0.70041 |

| si*Scr* Vehicle vs si*Scr* R1881 cells – RI events | | | | | |
|---|---|---|---|---|---|
| **All DSGs** | **Description** | **Size** | **Expect** | **Ratio** | **FDR** |
| hsa04142 | Lysosome | 123 | 1.3998 | 5.0008 | 0.15522 |
| hsa00514 | Other types of O-glycan biosynthesis | 22 | 0.25037 | 11.982 | 0.30823 |
| hsa01100 | Metabolic pathways | 1305 | 14.851 | 1.6833 | 0.46999 |
| hsa00240 | Pyrimidine metabolism | 101 | 1.1494 | 4.35 | 0.46999 |
| hsa03010 | Ribosome | 153 | 1.7412 | 2.8716 | 1 |
| hsa00592 | alpha-Linolenic acid metabolism | 25 | 0.28451 | 7.0296 | 1 |
| hsa05131 | Shigellosis | 65 | 0.73972 | 4.0556 | 1 |
| hsa05120 | Epithelial cell signalling in Helicobacter pylori infection | 68 | 0.77387 | 3.8766 | 1 |
| hsa00230 | Purine metabolism | 174 | 1.9802 | 2.525 | 1 |
| hsa04360 | Axon guidance | 175 | 1.9916 | 2.5106 | 1 |
| si*Scr* Vehicle vs si*Scr* R1881 cells – A3SS events | | | | | |
| **All DSGs** | **Description** | **Size** | **Expect** | **Ratio** | **FDR** |
| hsa04621 | NOD-like receptor signalling pathway | 168 | 2.2043 | 3.1756 | 0.8613 |
| hsa04120 | Ubiquitin mediated proteolysis | 137 | 1.7976 | 3.3379 | 0.8613 |
| hsa04933 | AGE-RAGE signalling pathway in diabetic complications | 99 | 1.299 | 3.8492 | 0.8613 |
| hsa05120 | Epithelial cell signalling in Helicobacter pylori infection | 68 | 0.89222 | 4.4832 | 0.8613 |
| hsa05165 | Human papillomavirus infection | 339 | 4.448 | 2.2482 | 0.8613 |
| hsa03018 | RNA degradation | 79 | 1.0366 | 3.859 | 0.89843 |
| hsa04110 | Cell cycle | 124 | 1.627 | 3.0732 | 0.89843 |
| hsa04961 | Endocrine and other factor-regulated calcium reabsorption | 47 | 0.61668 | 4.8647 | 0.89843 |
| hsa05164 | Influenza A | 171 | 2.2437 | 2.6742 | 0.89843 |
| hsa04068 | FoxO signalling pathway | 132 | 1.732 | 2.8869 | 0.92404 |

| si*Scr* Vehicle vs si*CBLL1* Vehicle cells – A5SS events | | | | | |
|---|---|---|---|---|---|
| **All DSGs** | **Description** | **Size** | **Expect** | **Ratio** | **FDR** |
| hsa03010 | Ribosome | 153 | 2.7859 | 3.5895 | 0.14884 |
| hsa00514 | Other types of O-glycan biosynthesis | 22 | 0.40059 | 7.489 | 0.998 |
| hsa04966 | Collecting duct acid secretion | 27 | 0.49163 | 6.1021 | 0.998 |
| hsa05418 | Fluid shear stress and atherosclerosis | 139 | 2.531 | 2.7657 | 0.998 |
| hsa00430 | Taurine and hypotaurine metabolism | 11 | 0.20029 | 9.9853 | 0.998 |
| hsa04370 | VEGF signalling pathway | 59 | 1.0743 | 3.7233 | 0.998 |
| hsa00564 | Glycerophospholipid metabolism | 97 | 1.7662 | 2.8309 | 0.998 |
| hsa05225 | Hepatocellular carcinoma | 168 | 3.059 | 2.2883 | 0.998 |
| hsa00190 | Oxidative phosphorylation | 133 | 2.4217 | 2.4776 | 0.998 |
| hsa00860 | Porphyrin and chlorophyll metabolism | 42 | 0.76476 | 3.9228 | 0.998 |

| si*Scr* Vehicle vs si*CBLL1* Vehicle cells – SE events | | | | | |
|---|---|---|---|---|---|
| **All DSGs** | **Description** | **Size** | **Expect** | **Ratio** | **FDR** |
| hsa01100 | Metabolic pathways | 1305 | 44.904 | 1.4698 | 0.16333 |
| hsa04621 | NOD-like receptor signalling pathway | 168 | 5.7807 | 2.2489 | 0.65672 |
| hsa00563 | Glycosylphosphatidylinositol (GPI)-anchor biosynthesis | 25 | 0.86022 | 4.65 | 0.65672 |
| hsa05212 | Pancreatic cancer | 75 | 2.5807 | 2.7125 | 0.65672 |
| hsa05160 | Hepatitis C | 131 | 4.5076 | 2.2185 | 0.65672 |
| hsa00310 | Lysine degradation | 59 | 2.0301 | 2.9555 | 0.65672 |
| hsa05162 | Measles | 132 | 4.542 | 2.2017 | 0.65672 |
| hsa04120 | Ubiquitin mediated proteolysis | 137 | 4.714 | 2.1213 | 0.65672 |
| hsa04623 | Cytosolic DNA-sensing pathway | 63 | 2.1678 | 2.7678 | 0.65672 |
| hsa03020 | RNA polymerase | 31 | 1.0667 | 3.75 | 0.65672 |
| si*Scr* Vehicle vs si*CBLL1* Vehicle cells – MXE events | | | | | |
| **All DSGs** | **Description** | **Size** | **Expect** | **Ratio** | **FDR** |
| hsa04962 | Vasopressin-regulated water reabsorption | 44 | 0.54786 | 7.3011 | 0.43807 |
| hsa04150 | mTOR signalling pathway | 151 | 1.8802 | 3.7231 | 0.43807 |
| hsa04142 | Lysosome | 123 | 1.5315 | 3.2647 | 0.91717 |
| hsa00120 | Primary bile acid biosynthesis | 17 | 0.21167 | 9.4485 | 0.91717 |
| hsa00531 | Glycosaminoglycan degradation | 19 | 0.23658 | 8.4539 | 0.91717 |
| hsa04714 | Thermogenesis | 229 | 2.8514 | 2.4549 | 0.91717 |
| hsa04923 | Regulation of lipolysis in adipocytes | 54 | 0.67238 | 4.4618 | 0.91717 |
| hsa00900 | Terpenoid backbone biosynthesis | 22 | 0.27393 | 7.3011 | 0.91717 |
| hsa01522 | Endocrine resistance | 98 | 1.2202 | 3.278 | 0.91717 |
| hsa00592 | alpha-Linolenic acid metabolism | 25 | 0.31129 | 6.4249 | 0.91717 |
| si*Scr* Vehicle vs si*CBLL1* Vehicle cells – RI events | | | | | |
| **All DSGs** | **Description** | **Size** | **Expect** | **Ratio** | **FDR** |
| hsa03440 | Homologous recombination | 41 | 0.33485 | 8.9592 | 1 |
| hsa04012 | ErbB signalling pathway | 85 | 0.6942 | 4.3215 | 1 |
| hsa04145 | Phagosome | 152 | 1.2414 | 3.2222 | 1 |
| hsa04066 | HIF-1 signalling pathway | 100 | 0.81671 | 3.6733 | 1 |
| hsa04660 | T cell receptor signalling pathway | 101 | 0.82488 | 3.6369 | 1 |
| hsa03013 | RNA transport | 171 | 1.3966 | 2.8642 | 1 |
| hsa04922 | Glucagon signalling pathway | 103 | 0.84121 | 3.5663 | 1 |
| hsa04625 | C-type lectin receptor signalling pathway | 104 | 0.84938 | 3.532 | 1 |
| hsa05166 | Human T-cell leukaemia virus 1 infection | 255 | 2.0826 | 2.4008 | 1 |
| hsa05165 | Human papillomavirus infection | 339 | 2.7686 | 2.1671 | 1 |

| si*Scr* Vehicle vs si*CBLL1* Vehicle cells – A3SS events | | | | | |
|---|---|---|---|---|---|
| **All DSGs** | **Description** | **Size** | **Expect** | **Ratio** | **FDR** |
| hsa04714 | Thermogenesis | 229 | 2.9434 | 3.3975 | 0.15035 |
| hsa00310 | Lysine degradation | 59 | 0.75833 | 6.5934 | 0.15035 |
| hsa04010 | MAPK signalling pathway | 295 | 3.7917 | 2.3736 | 0.96147 |
| hsa05225 | Hepatocellular carcinoma | 168 | 2.1593 | 2.7786 | 0.96147 |
| hsa01212 | Fatty acid metabolism | 48 | 0.61695 | 4.8626 | 0.96147 |
| hsa05210 | Colorectal cancer | 86 | 1.1054 | 3.6187 | 0.96147 |
| hsa05130 | Pathogenic Escherichia coli infection | 55 | 0.70692 | 4.2438 | 0.96147 |
| hsa04925 | Aldosterone synthesis and secretion | 96 | 1.2339 | 3.2418 | 0.96147 |
| hsa04261 | Adrenergic signalling in cardiomyocytes | 144 | 1.8509 | 2.7015 | 0.96147 |
| hsa05213 | Endometrial cancer | 58 | 0.74548 | 4.0242 | 0.96147 |
| si*Scr* R1881 vs si*CBLL1* R1881 cells – A5SS events | | | | | |
| **All DSGs** | **Description** | **Size** | **Expect** | **Ratio** | **FDR** |
| hsa04120 | Ubiquitin mediated proteolysis | 137 | 2.4946 | 3.6078 | 0.18799 |
| hsa04914 | Progesterone-mediated oocyte maturation | 99 | 1.8027 | 3.8832 | 0.18799 |
| hsa04218 | Cellular senescence | 160 | 2.9134 | 3.0892 | 0.18799 |
| hsa05160 | Hepatitis C | 131 | 2.3853 | 3.3538 | 0.18799 |
| hsa00051 | Fructose and mannose metabolism | 33 | 0.60088 | 6.6569 | 0.18799 |
| hsa04370 | VEGF signalling pathway | 59 | 1.0743 | 4.6542 | 0.23217 |
| hsa05222 | Small cell lung cancer | 93 | 1.6934 | 3.5432 | 0.29028 |
| hsa00514 | Other types of O-glycan biosynthesis | 22 | 0.40059 | 7.489 | 0.29028 |
| hsa05231 | Choline metabolism in cancer | 99 | 1.8027 | 3.3284 | 0.33521 |
| hsa05212 | Pancreatic cancer | 75 | 1.3656 | 3.6613 | 0.36504 |
| si*Scr* Vehicle vs si*CBLL1* Vehicle cells – SE events | | | | | |
| **All DSGs** | **Description** | **Size** | **Expect** | **Ratio** | **FDR** |
| hsa03460 | Fanconi anaemia pathway | 54 | 2.0967 | 3.8156 | 0.17118 |
| hsa04920 | Adipocytokine signalling pathway | 69 | 2.6791 | 3.3594 | 0.17118 |
| hsa04922 | Glucagon signalling pathway | 103 | 3.9992 | 2.7506 | 0.17118 |
| hsa01100 | Metabolic pathways | 1305 | 50.669 | 1.3815 | 0.17118 |
| hsa04140 | Autophagy | 128 | 4.9699 | 2.4145 | 0.20959 |
| hsa03440 | Homologous recombination | 41 | 1.5919 | 3.769 | 0.20959 |
| hsa04141 | Protein processing in endoplasmic reticulum | 165 | 6.4065 | 2.1853 | 0.20959 |
| hsa04919 | Thyroid hormone signalling pathway | 116 | 4.5039 | 2.4423 | 0.20959 |
| hsa04120 | Ubiquitin mediated proteolysis | 137 | 5.3193 | 2.2559 | 0.20959 |
| hsa04910 | Insulin signalling pathway | 137 | 5.3193 | 2.2559 | 0.20959 |

| si*Scr* Vehicle vs si*CBLL1* Vehicle cells – MXE events | | | | | |
|---|---|---|---|---|---|
| **All DSGs** | **Description** | **Size** | **Expect** | **Ratio** | **FDR** |
| hsa01100 | Metabolic pathways | 1305 | 20.093 | 1.5926 | 0.63362 |
| hsa05212 | Pancreatic cancer | 75 | 1.1548 | 4.3299 | 0.63362 |
| hsa04725 | Cholinergic synapse | 112 | 1.7245 | 3.4793 | 0.63362 |
| hsa01200 | Carbon metabolism | 116 | 1.786 | 3.3594 | 0.63362 |
| hsa00630 | Glyoxylate and dicarboxylate metabolism | 30 | 0.46191 | 6.4948 | 0.63362 |
| hsa04611 | Platelet activation | 123 | 1.8938 | 3.1682 | 0.63362 |
| hsa00051 | Fructose and mannose metabolism | 33 | 0.5081 | 5.9043 | 0.65173 |
| hsa04068 | FoxO signalling pathway | 132 | 2.0324 | 2.9522 | 0.65549 |
| hsa04066 | HIF-1 signalling pathway | 100 | 1.5397 | 3.2474 | 0.68547 |
| hsa03440 | Homologous recombination | 41 | 0.63128 | 4.7523 | 0.6957 |
| si*Scr* Vehicle vs si*CBLL1* Vehicle cells – RI events | | | | | |
| **All DSGs** | **Description** | **Size** | **Expect** | **Ratio** | **FDR** |
| hsa00520 | Amino sugar and nucleotide sugar metabolism | 48 | 0.63623 | 7.8588 | 0.11421 |
| hsa00052 | Galactose metabolism | 31 | 0.4109 | 9.7348 | 0.11421 |
| hsa03040 | Spliceosome | 134 | 1.7761 | 3.9411 | 0.21199 |
| hsa04142 | Lysosome | 123 | 1.6303 | 3.6802 | 0.46776 |
| hsa04216 | Ferroptosis | 40 | 0.53019 | 5.6583 | 0.8416 |
| hsa00604 | Glycosphingolipid biosynthesis | 15 | 0.19882 | 10.059 | 0.8416 |
| hsa04962 | Vasopressin-regulated water reabsorption | 44 | 0.58321 | 5.1439 | 0.8416 |
| hsa03018 | RNA degradation | 79 | 1.0471 | 3.82 | 0.8416 |
| hsa00511 | Other glycan degradation | 18 | 0.23859 | 8.3827 | 0.84506 |
| hsa00531 | Glycosaminoglycan degradation | 19 | 0.25184 | 7.9415 | 0.84506 |
| si*Scr* Vehicle vs si*CBLL1* Vehicle cells – A3SS events | | | | | |
| **All DSGs** | **Description** | **Size** | **Expect** | **Ratio** | **FDR** |
| hsa00310 | Lysine degradation | 59 | 0.85313 | 8.2051 | **0.006573** |
| hsa03410 | Base excision repair | 33 | 0.47717 | 8.3827 | 0.2015 |
| hsa04142 | Lysosome | 123 | 1.7786 | 3.9358 | 0.2141 |
| hsa05165 | Human papillomavirus infection | 339 | 4.9019 | 2.448 | 0.28473 |
| hsa03013 | RNA transport | 171 | 2.4726 | 2.831 | 0.7715 |
| hsa00511 | Other glycan degradation | 18 | 0.26028 | 7.6842 | 1 |
| hsa04512 | ECM-receptor interaction | 82 | 1.1857 | 3.3735 | 1 |
| hsa00520 | Amino sugar and nucleotide sugar metabolism | 48 | 0.69407 | 4.3223 | 1 |
| hsa01212 | Fatty acid metabolism | 48 | 0.69407 | 4.3223 | 1 |
| hsa03015 | mRNA surveillance pathway | 91 | 1.3158 | 3.0399 | 1 |

# Appendix 16 Nottingham BCa TMA patient database

## Table xvii Patient demographics and clinicopathological parameters examined in Nottingham BCa TMA with CBLL1 staining.

The Nottingham BCa TMA used for CBLL1 staining comprised tissue cores from 1499 patients acquired following surgical removal of their tumour. The number of patients in each parameter group is given. NPI = Nottingham Prognostic Index; NST = invasive breast cancer of no special type; ILC = invasive lobular carcinoma; ER = estrogen receptor; PR = progesterone receptor; HER2 = human epidermal growth factor receptor 2; TNBC = triple negative breast cancer; NPI = Nottingham Prognostic Index.

| Clinicopathological parameter | Patient frequency n (%) |
|---|---|
| **Tumour grade** | |
| 1 | 187 (12.5%) |
| 2 | 500 (33.3%) |
| 3 | 812 (54.2%) |
| **Tubular differentiation** | |
| T1 | 81 (5.4%) |
| T2 | 449 (30.0%) |
| T3 | 969 (64.6%) |
| **Nuclear pleiomorphism** | |
| P1 | 32 (2.1%) |
| P2 | 421 (28.1%) |
| P3 | 1046 (69.8%) |
| **Mitotic count** | |
| M1 | 518 (34.5%) |
| M2 | 295 (19.7%) |
| M3 | 686 (45.8%) |
| **Lymph node status** | |
| Negative | 899 (60.0%) |
| Positive | 600 (40.0%) |
| **Lymph node stage** | |
| 1 | 899 (60.0%) |
| 2 | 457 (30.5%) |
| 3 | 143 (9.5%) |
| **Tumour size** | |
| <2cm | 784 (52.3%) |
| ≥2cm | 715 (49.7%) |
| **NPI Category** | |
| Good prognostic group | 418 (27.9%) |
| Moderate prognostic group | 790 (52.7%) |
| Poor prognostic group | 291 (19.4%) |
| **Molecular class** | |
| Luminal A | 409 (31.4%) |
| HER2 enriched | 98 (7.5%) |
| Triple negative | 302 (23.2%) |
| Luminal B | 493 (37.9%) |

| Clinicopathological parameter | Patient frequency n (%) |
|---|---|
| **Histological tumour type** | |
| NST | 1038 (69.2%) |
| ILC | 99 (6.6%) |
| Metaplastic carcinoma | 6 (0.4%) |
| Pure special tumour type | 50 (3.4%) |
| Mixed NST & other tumour type | 306 (20.4%) |
| **Vascular invasion** | |
| Absent | 987 (65.8%) |
| Present | 512 (34.2%) |
| **Ki67 index group** | |
| Low | 479 (40.7%) |
| High | 699 (59.3%) |
| **ER status** | |
| Negative | 428 (28.7%) |
| Positive | 1065 (71.3%) |
| **PR status** | |
| Negative | 666 (45.3%) |
| Positive | 805 (54.7%) |
| **HER2 status** | |
| Negative | 1242 (84.7%) |
| Positive | 225 (15.3%) |
| **Triple negative status** | |
| Non-TN | 1163 (79.4%) |
| TN | 302 (20.6%) |
| **Age** | |
| ≤49 years | 542 (36.2%) |
| ≥50 years | 957 (63.8%) |
| **Menopausal status** | |
| Pre | 604 (40.3%) |
| Post | 895 (59.7%) |

# Appendix 17 Nottingham BCa TMA patient database and clinical correlations with CBLL1 expression

## Table xviii Correlation of CBLL1 staining with clinicopathological parameters in Nottingham cohort.

CBLL1 nuclear and cytoplasmic staining was correlated with relevant clinicopathological patient parameters. NST = invasive breast cancer of no special type; ILC = invasive lobular carcinoma; ER = estrogen receptor; PR = progesterone receptor; HER2 = human epidermal growth factor receptor 2; TN = triple negative. Statistical p-values determined by χ2-test and p≤0.05 highlighted in bold.

| Clinicopathological criteria | Nuclear CBLL1 expression (%) | | χ² (p value) | Cytoplasmic CBLL1 expression (%) | | χ² (p value) |
|---|---|---|---|---|---|---|
| | Low (≤70) | High (≥71) | | Low (≤70) | High (≥71) | |
| **Tumour grade** | | | | | | |
| 1 | 80 (42.8%) | 107 (57.2%) | **76.901 (<0.0001)****** | 102 (54.5%) | 85 (45.5%) | **8.504 (0.014)*** |
| 2 | 223 (44.6%) | 277 (55.4%) | | 289 (57.8%) | 211 (42.2%) | |
| 3 | 541 (66.6%) | 271 (33.4%) | | 403 (49.6%) | 409 (50.4%) | |
| **Tubular differentiation** | | | | | | |
| T1 | 36 (44.4%) | 45 (55.6%) | **25.930 (<0.0001)****** | 45 (55.6%) | 36 (44.4%) | 3.649 (0.161) |
| T2 | 216 (48.1%) | 233 (51.9%) | | 221 (49.2%) | 228 (50.8%) | |
| T3 | 592 (61.1%) | 377 (38.9%) | | 528 (54.5%) | 441 (45.5%) | |
| **Nuclear pleiomorphism** | | | | | | |
| P1 | 18 (56.3%) | 14 (43.8%) | **20.643 (<0.0001)****** | 20 (62.5%) | 12 (37.5%) | **11.585 (0.003)**** |
| P2 | 198 (47.0%) | 223 (53.0%) | | 250 (59.4%) | 171 (40.6%) | |
| P3 | 628 (60.0%) | 418 (40.0%) | | 524 (50.1%) | 522 (49.9%) | |
| **Mitotic count** | | | | | | |
| M1 | 206 (39.8%) | 312 (60.2%) | **113.301 (<0.0001)****** | 301 (58.1%) | 217 (41.9%) | **10.640 (0.005)**** |
| M2 | 156 (52.9%) | 139 (47.1%) | | 159 (53.9%) | 136 (46.1%) | |
| M3 | 482 (70.3%) | 204 (29.7%) | | 334 (48.7%) | 352 (51.3%) | |
| **Lymph node status** | | | | | | |
| Negative | 510 (56.7%) | 389 (43.3%) | 0.165 (0.684) | 480 (53.4%) | 419 (46.6%) | 0.162 (0.687) |
| Positive | 334 (55.7%) | 266 (44.3%) | | 314 (52.3%) | 286 (47.7%) | |
| **Lymph node stage** | | | | | | |
| 1 | 510 (56.7%) | 389 (43.3%) | 0.261 (0.878) | 480 (53.4%) | 419 (46.6%) | 0.212 (0.899) |
| 2 | 256 (56.0%) | 201 (44.0%) | | 238 (52.1%) | 219 (47.9%) | |
| 3 | 78 (54.5%) | 65 (45.5%) | | 76 (53.1%) | 67 (46.9%) | |
| **Tumour size** | | | | | | |
| <2cm | 405 (51.7%) | 379 (48.3%) | **14.421 (<0.0001)****** | 422 (53.8%) | 362 (46.2%) | 0.486 (0.486) |
| ≥2cm | 439 (61.4%) | 276 (38.6%) | | 372 (52.0%) | 343 (48.0%) | |
| **Nottingham Prognostic Index Category** | | | | | | |
| Good prognostic group | 190 (45.5%) | 228 (54.5%) | **28.940 (<0.0001)****** | 249 (59.6%) | 169 (40.4%) | **10.665 (0.005)**** |
| Moderate prognostic group | 470 (59.5%) | 320 (40.5%) | | 393 (49.7%) | 397 (50.3%) | |
| Poor prognostic group | 184 (63.2%) | 107 (36.8%) | | 152 (52.2%) | 139 (47.8%) | |
| **Molecular class** | | | | | | |
| Luminal A | 157 (38.4%) | 252 (61.6%) | **89.427 (<0.0001)****** | 229 (56.0%) | 180 (44.0%) | 5.114 (0.164) |
| HER2 enriched | 67 (68.4%) | 31 (31.6%) | | 53 (54.1%) | 45 (45.9%) | |
| Triple negative | 214 (70.9%) | 88 (29.1%) | | 144 (47.7%) | 158 (52.3%) | |
| Luminal B | 300 (60.9%) | 193 (39.1%) | | 266 (54.0%) | 227 (46.0%) | |

Table continued on next page

| Clinicopathological criteria | Nuclear CBLL1 expression (%) | | $\chi^2$ (p value) | Cytoplasmic CBLL1 expression (%) | | $\chi^2$ (p value) |
|---|---|---|---|---|---|---|
| | Low (≤70) | High (≥71) | | Low (≤70) | High (≥71) | |
| **Histological tumour type** | | | | | | |
| NST | 629 (60.6%) | 409 (39.4%) | **33.558 (<0.0001)****** | 523 (50.4%) | 515 (49.6%) | **22.718 (<0.0001)****** |
| ILC | 41 (41.4%) | 58 (58.6%) | | 74 (74.7%) | 25 (25.3%) | |
| Metaplastic carcinoma | 6 (100.0%) | 0 (0.0%) | | 4 (66.7%) | 2 (33.3%) | |
| Pure special tumour type | 25 (50.0%) | 25 (50.0%) | | 25 (50.0%) | 25 (50.0%) | |
| Mixed NST & other tumour type | 143 (46.7%) | 163 (53.3%) | | 168 (54.9%) | 138 (45.1%) | |
| **Vascular invasion** | | | | | | |
| Absent | 547 (55.4%) | 440 (44.6%) | 0.917 (0.338) | 531 (53.8%) | 456 (46.2%) | 0.801 (0.371) |
| Present | 297 (58.0%) | 215 (42.0%) | | 263 (51.4%) | 249 (48.6%) | |
| **Ki67 index group** | | | | | | |
| Low | 203 (42.4%) | 276 (57.6%) | **54.930 (<0.0001)****** | 266 (55.5%) | 213 (44.5%) | 2.126 (0.145) |
| High | 449 (64.2%) | 250 (35.8%) | | 358 (51.2%) | 341 (48.8%) | |
| **ER status** | | | | | | |
| Negative | 301 (70.3%) | 127 (29.7%) | **48.232 (<0.0001)****** | 209 (48.8%) | 219 (51.2%) | 4.146 (0.042)* |
| Positive | 539 (50.6%) | 526 (49.4%) | | 582 (54.6%) | 483 (45.4%) | |
| **PR status** | | | | | | |
| Negative | 434 (65.2%) | 232 (34.8%) | **38.395 (<0.0001)****** | 360 (54.1%) | 306 (45.9%) | 0.333 (0.564) |
| Positive | 395 (49.1%) | 410 (50.9%) | | 423 (52.5%) | 382 (47.5%) | |
| **HER2 status** | | | | | | |
| Negative | 674 (54.3%) | 568 (45.7%) | **12.768 (<0.0001)****** | 654 (52.7%) | 588 (47.3%) | 0.096 (0.757) |
| Positive | 151 (67.1%) | 74 (32.9%) | | 121 (53.8%) | 104 (46.2%) | |
| **Triple negative status** | | | | | | |
| Non-TN | 606 (52.1%) | 557 (47.9%) | **34.218 (<0.0001)****** | 635 (54.6%) | 528 (45.4%) | **4.608 (0.032)*** |
| TN | 214 (70.9%) | 88 (29.1%) | | 144 (47.7%) | 158 (52.3%) | |
| **Age** | | | | | | |
| ≤49 years | 311 (57.4%) | 231 (42.6%) | 0.399 (0.527) | 260 (48.0%) | 282 (52.0%) | **8.513 (0.004)**** |
| ≥50 years | 533 (55.7%) | 424 (44.3%) | | 534 (55.8%) | 423 (44.2%) | |
| **Menopausal status** | | | | | | |
| Pre | 335 (55.5%) | 269 (44.5%) | 0.291 (0.590) | 285 (47.2%) | 319 (52.8%) | **13.582 (<0.0001)****** |
| Post | 509 (56.9%) | 386 (43.1%) | | 509 (56.9%) | 386 (43.1%) | |

# Appendix 18 Representative images of E-cadherin IHC staining of Nottingham cohort TMA of BCa tissue

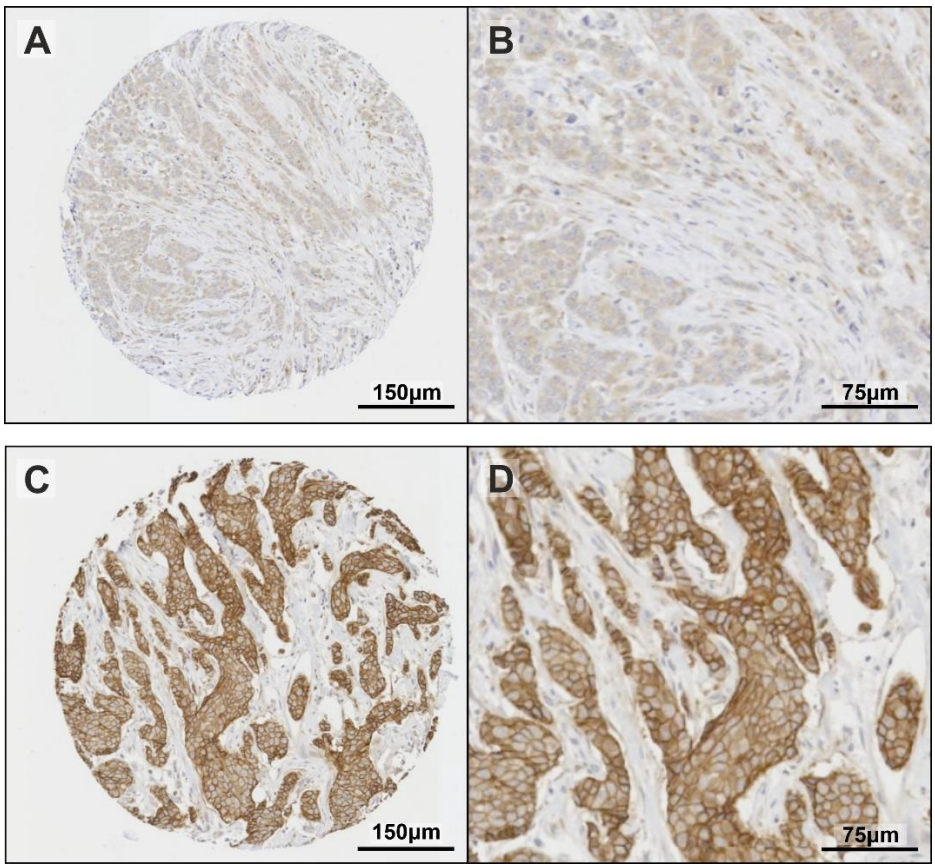


**Figure xiv Representative images of E-cadherin IHC staining of Nottingham cohort TMA of breast cancer tissue**

IHC staining of breast cancer patient tissue samples was carried out to determine the membrane expression of E-cadherin. (**A** and **B**) Representative images of low level E-cadherin expression. (**C** and **D**) Representative images of high level E-cadherin expression.

# Appendix 19 Nottingham BCa TMA patient database

### Table xix Patient demographics and clinicopathological parameters examined in Nottingham BCa TMA with E-cadherin staining.

The Nottingham BCa TMA used for E-cadherin staining comprised tissue cores from 2126 patients acquired following surgical removal of their tumour. The number of patients in each parameter group is given. NPI = Nottingham Prognostic Index; NST = invasive breast cancer of no special type; ILC = invasive lobular carcinoma; ER = estrogen receptor; PR = progesterone receptor; HER2 = human epidermal growth factor receptor 2; TNBC = triple negative breast cancer; NPI = Nottingham Prognostic Index.

| Clinicopathological parameter | Patient frequency n (%) |
|---|---|
| **Tumour grade** | |
| 1 | 311 (14.6%) |
| 2 | 749 (35.2%) |
| 3 | 1066 (50.2%) |
| **Tubular differentiation** | |
| T1 | 130 (6.1%) |
| T2 | 635 (29.9%) |
| T3 | 1361 (64.0%) |
| **Nuclear pleiomorphism** | |
| P1 | 44 (2.1%) |
| P2 | 629 (29.6%) |
| P3 | 1453 (68.3%) |
| **Mitotic count** | |
| M1 | 861 (40.4%) |
| M2 | 416 (19.6%) |
| M3 | 849 (40.0%) |
| **Lymph node status** | |
| Negative | 1284 (60.4%) |
| Positive | 1361 (39.6%) |
| **Lymph node stage** | |
| 1 | 1284 (60.4%) |
| 2 | 639 (30.1%) |
| 3 | 203 (9.5%) |
| **Tumour size** | |
| <2cm | 1175 (55.3%) |
| ≥2cm | 951 (44.7%) |
| **NPI Category** | |
| Good prognostic group | 652 (30.7%) |
| Moderate prognostic group | 1104 (51.9%) |
| Poor prognostic group | 370 (17.4%) |
| **Molecular class** | |
| Luminal A | 690 (37.2%) |
| HER2 enriched | 117 (6.3%) |
| Triple negative | 361 (19.5%) |
| Luminal B | 688 (37.0%) |

| Clinicopathological parameter | Patient frequency n (%) |
|---|---|
| **Histological tumour type** | |
| NST | 1411 (66.4%) |
| ILC | 171 (8.0%) |
| Metaplastic carcinoma | 8 (0.4%) |
| Pure special tumour type | 73 (3.4%) |
| Mixed NST & other tumour type | 463 (21.8%) |
| **Vascular invasion** | |
| Absent | 1411 (68.6%) |
| Present | 667 (31.4%) |
| **Ki67 index group** | |
| Low | 770 (46.1%) |
| High | 899 (53.9%) |
| **ER status** | |
| Negative | 508 (23.9%) |
| Positive | 1615 (76.1%) |
| **PR status** | |
| Negative | 877 (41.5%) |
| Positive | 1238 (58.5%) |
| **HER2 status** | |
| Negative | 1824 (86.6%) |
| Positive | 283 (13.4%) |
| **Triple negative status** | |
| Non-TN | 1732 (82.8%) |
| TN | 361 (17.2%) |
| **Age** | |
| ≤49 years | 712 (33.5%) |
| ≥50 years | 1414 (66.5%) |
| **Menopausal status** | |
| Pre | 804 (37.8%) |
| Post | 1332 (62.2%) |

# Appendix 20 Nottingham BCa TMA patient database and clinical correlations with E-cadherin expression

## Table xx Correlation of E-cadherin staining with clinicopathological parameters in Nottingham cohort.

CBLL1 nuclear and cytoplasmic staining was correlated with relevant clinicopathological patient parameters. NST = invasive breast cancer of no special type; ILC = invasive lobular carcinoma; ER = estrogen receptor; PR = progesterone receptor; HER2 = human epidermal growth factor receptor 2; TN = triple negative. Statistical p-values determined by $\chi 2$-test and $p \leq 0.05$ highlighted in bold.

| Clinicopathological criteria | Membrane E-cadherin expression (%) | | $\chi^2$ (p value) |
|---|---|---|---|
| | Low (≤130) | High (≥131) | |
| **Tumour grade** | | | |
| 1 | 135 (43.4%) | 176 (56.6%) | 15.199 (0.001)*** |
| 2 | 376 (50.2%) | 373 (49.8%) | |
| 3 | 591 (55.4%) | 475 (44.6%) | |
| **Tubular differentiation** | | | |
| T1 | 55 (42.3%) | 75 (57.7%) | 40.695 (<0.0001)**** |
| T2 | 271 (42.7%) | 364 (57.3%) | |
| T3 | 776 (57.0%) | 585 (43.0%) | |
| **Nuclear pleiomorphism** | | | |
| P1 | 26 (59.1%) | 18 (40.9%) | 5.334 (0.069) |
| P2 | 347 (55.2%) | 282 (44.8%) | |
| P3 | 729 (50.2%) | 724 (49.8%) | |
| **Mitotic count** | | | |
| M1 | 415 (48.2%) | 446 (51.8%) | 12.265 (0.002)** |
| M2 | 208 (50.0%) | 208 (50.0%) | |
| M3 | 479 (56.4%) | 370 (43.6%) | |
| **Lymph node status** | | | |
| Negative | 690 (53.7%) | 594 (46.3%) | 4.707 (0.030)* |
| Positive | 412 (48.9%) | 430 (51.1%) | |
| **Lymph node stage** | | | |
| 1 | 690 (53.7%) | 594 (46.3%) | 7.667 (0.022)* |
| 2 | 302 (47.3%) | 337 (52.7%) | |
| 3 | 110 (54.2%) | 93 (45.8%) | |
| **Tumour size** | | | |
| <2cm | 578 (49.2%) | 597 (50.8%) | 7.349 (0.007)** |
| ≥2cm | 524 (55.1%) | 427 (44.9%) | |
| **Nottingham Prognostic Index Category** | | | |
| Good prognostic group | 319 (48.9%) | 333 (51.1%) | 3.805 (0.149) |
| Moderate prognostic group | 593 (53.7%) | 511 (46.3%) | |
| Poor prognostic group | 190 (51.4%) | 180 (48.6%) | |
| **Molecular class** | | | |
| Luminal A | 332 (48.1%) | 358 (51.9%) | 26.364 (<0.0001)**** |
| HER2 enriched | 63 (53.8%) | 54 (46.2%) | |
| Triple negative | 231 (64.0%) | 130 (36.0%) | |
| Luminal B | 343 (49.9%) | 345 (50.1%) | |

Table continued from previous page

| Clinicopathological criteria | Membrane E-cadherin protein expression (%) | | $\chi^2$ (p value) |
|---|---|---|---|
| | Low (≤130) | High (≥131) | |
| **Histological tumour type** | | | |
| NST | 703 (49.8%) | 708 (50.2%) | 94.374 (<0.0001)**** |
| ILC | 147 (86.0%) | 24 (14.0%) | |
| Metaplastic carcinoma | 7 (87.5%) | 1 (12.5%) | |
| Pure special tumour type | 35 (47.9%) | 38 (52.1%) | |
| Mixed NST & other tumour type | 210 (45.4%) | 253 (54.6%) | |
| **Vascular invasion** | | | |
| Absent | 792 (54.3%) | 667 (45.7%) | 11.175 (0.001)*** |
| Present | 310 (46.5%) | 357 (53.5%) | |
| **Ki67 index group** | | | |
| Low | 377 (49.0%) | 393 (51.0%) | 4.319 (0.038)* |
| High | 486 (54.1%) | 413 (45.9%) | |
| **ER status** | | | |
| Negative | 311 (61.2%) | 197 (38.8%) | 23.669 (<0.0001)**** |
| Positive | 789 (48.9%) | 826 (51.1%) | |
| **PR status** | | | |
| Negative | 491 (56.0%) | 386 (44.0%) | 10.415 (0.001)*** |
| Positive | 605 (48.9%) | 633 (51.1%) | |
| **HER2 status** | | | |
| Negative | 947 (51.9%) | 877 (48.1%) | 0.105 (0.746) |
| Positive | 144 (50.9%) | 139 (49.1%) | |
| **Triple negative status** | | | |
| Non-TN | 852 (49.2%) | 880 (50.8%) | 26.196 (<0.0001)**** |
| TN | 231 (64.0%) | 130 (36.0%) | |
| **Age** | | | |
| <=49 years | 370 (52.0%) | 342 (48.0%) | 0.007 (0.931) |
| >=50 years | 732 (51.8%) | 682 (48.2%) | |
| **Menopausal status** | | | |
| Pre | 409 (50.9%) | 395 (49.1%) | 0.481 (0.488) |
| Post | 693 (49.8%) | 629 (47.6%) | |

# Appendix 21 Analysis of KEGG pathways related to differentially expressed genes upon $\beta E_2$ treatment in MCF7 scrambled control cells

**Table xxi Analysis of significantly enriched KEGG pathways associated with differentially expressed genes (DEGs) upon $\beta E_2$ treatment in MCF7 scrambled control cells (si*Scr* Vehicle vs si*Scr* $\beta E_2$) (FDR<0.05).**

| All DEGs | Description | Size | Expect | Ratio | FDR |
|---|---|---|---|---|---|
| hsa03030 | DNA replication | 36 | 10.011 | 2.5971 | 7.32E-06 |
| hsa04360 | Axon guidance | 175 | 48.664 | 1.685 | 7.32E-06 |
| hsa04110 | Cell cycle | 124 | 34.482 | 1.711 | 0.0002 |
| hsa04514 | Cell adhesion molecules (CAMs) | 144 | 40.044 | 1.6482 | 0.0002 |
| hsa05200 | Pathways in cancer | 526 | 146.27 | 1.3126 | 0.000273 |
| hsa04510 | Focal adhesion | 199 | 55.338 | 1.4818 | 0.001404 |
| hsa05414 | Dilated cardiomyopathy (DCM) | 90 | 25.027 | 1.7181 | 0.001883 |
| hsa05412 | Arrhythmogenic right ventricular cardiomyopathy (ARVC) | 72 | 20.022 | 1.798 | 0.002074 |
| hsa04261 | Adrenergic signalling in cardiomyocytes | 144 | 40.044 | 1.5233 | 0.003756 |
| hsa04914 | Progesterone-mediated oocyte maturation | 99 | 27.53 | 1.6346 | 0.003756 |
| hsa03440 | Homologous recombination | 41 | 11.401 | 2.0173 | 0.003756 |
| hsa04010 | MAPK signalling pathway | 295 | 82.034 | 1.3409 | 0.005064 |
| hsa03430 | Mismatch repair | 23 | 6.3959 | 2.3453 | 0.005064 |
| hsa04934 | Cushing syndrome | 154 | 42.825 | 1.4711 | 0.006435 |
| hsa05032 | Morphine addiction | 91 | 25.306 | 1.6202 | 0.006457 |
| hsa04915 | Estrogen signalling pathway | 137 | 38.097 | 1.4962 | 0.006457 |
| hsa05410 | Hypertrophic cardiomyopathy (HCM) | 83 | 23.081 | 1.6464 | 0.006457 |
| hsa04218 | Cellular senescence | 160 | 44.493 | 1.4384 | 0.009345 |
| hsa04015 | Rap1 signalling pathway | 206 | 57.285 | 1.3791 | 0.009891 |
| hsa05205 | Proteoglycans in cancer | 201 | 55.895 | 1.3776 | 0.011385 |
| hsa04024 | cAMP signalling pathway | 199 | 55.338 | 1.3734 | 0.012291 |
| hsa04971 | Gastric acid secretion | 75 | 20.856 | 1.6302 | 0.012291 |
| hsa05166 | Human T-cell leukaemia virus 1 infection | 255 | 70.911 | 1.3256 | 0.012291 |
| hsa05418 | Fluid shear stress and atherosclerosis | 139 | 38.654 | 1.4488 | 0.012488 |
| hsa04921 | Oxytocin signalling pathway | 152 | 42.269 | 1.4195 | 0.014324 |
| hsa03460 | Fanconi anaemia pathway | 54 | 15.016 | 1.7314 | 0.014324 |
| hsa03320 | PPAR signalling pathway | 74 | 20.578 | 1.6036 | 0.017132 |
| hsa04670 | Leukocyte transendothelial migration | 112 | 31.145 | 1.4769 | 0.017979 |
| hsa04725 | Cholinergic synapse | 112 | 31.145 | 1.4769 | 0.017979 |
| hsa04926 | Relaxin signalling pathway | 130 | 36.151 | 1.4384 | 0.018076 |
| hsa04916 | Melanogenesis | 101 | 28.086 | 1.4954 | 0.019862 |
| hsa04728 | Dopaminergic synapse | 131 | 36.429 | 1.4274 | 0.020648 |
| hsa00230 | Purine metabolism | 174 | 48.386 | 1.364 | 0.021543 |
| hsa04713 | Circadian entrainment | 96 | 26.696 | 1.4984 | 0.021989 |

Table continued from previous page

| All DEGs | Description | Size | Expect | Ratio | FDR |
|---|---|---|---|---|---|
| hsa04512 | ECM-receptor interaction | 82 | 22.803 | 1.5349 | 0.024058 |
| hsa04022 | cGMP-PKG signalling pathway | 163 | 45.327 | 1.3678 | 0.024058 |
| hsa04540 | Gap junction | 88 | 24.471 | 1.512 | 0.024058 |
| hsa05217 | Basal cell carcinoma | 63 | 17.519 | 1.5982 | 0.028305 |
| hsa04020 | Calcium signalling pathway | 183 | 50.889 | 1.3362 | 0.028305 |
| hsa05034 | Alcoholism | 180 | 50.055 | 1.3385 | 0.028305 |
| hsa02010 | ABC transporters | 44 | 12.236 | 1.7163 | 0.029585 |

# Appendix 22 Analysis of KEGG pathways related to differentially expressed genes upon $\beta E_2$ treatment in MCF7 *CBLL1* knockdown cells

**Table xxii Analysis of KEGG pathways associated with differentially expressed genes upon $\beta E_2$ treatment in MCF7 *CBLL1* knockdown cells (si*CBLL1* Vehicle vs si*CBLL1* $\beta E_2$) (FDR<0.05).**

| All DEGs | Description | Size | Expect | Ratio | FDR |
|---|---|---|---|---|---|
| hsa04110 | Cell cycle | 124 | 30.896 | 2.0391 | 1.20E-07 |
| hsa03030 | DNA replication | 36 | 8.9699 | 2.8986 | 5.00E-07 |
| hsa04360 | Axon guidance | 175 | 43.604 | 1.7888 | 8.78E-07 |
| hsa04218 | Cellular senescence | 160 | 39.866 | 1.6555 | 0.000277 |
| hsa05200 | Pathways in cancer | 526 | 131.06 | 1.3353 | 0.00033 |
| hsa03460 | Fanconi anaemia pathway | 54 | 13.455 | 2.081 | 0.00099 |
| hsa04010 | MAPK signalling pathway | 295 | 73.503 | 1.4149 | 0.001611 |
| hsa03430 | Mismatch repair | 23 | 5.7308 | 2.6175 | 0.002094 |
| hsa04914 | Progesterone-mediated oocyte maturation | 99 | 24.667 | 1.7027 | 0.002998 |
| hsa05414 | Dilated cardiomyopathy (DCM) | 90 | 22.425 | 1.7392 | 0.002998 |
| hsa04114 | Oocyte meiosis | 124 | 30.896 | 1.6183 | 0.002998 |
| hsa05166 | Human T-cell leukaemia virus 1 infection | 255 | 63.537 | 1.4165 | 0.002998 |
| hsa00230 | Purine metabolism | 174 | 43.354 | 1.4762 | 0.007371 |
| hsa00100 | Steroid biosynthesis | 19 | 4.7341 | 2.5348 | 0.010852 |
| hsa04115 | p53 signalling pathway | 72 | 17.94 | 1.728 | 0.01206 |
| hsa05032 | Morphine addiction | 91 | 22.674 | 1.6318 | 0.01228 |
| hsa04540 | Gap junction | 88 | 21.926 | 1.6419 | 0.01228 |
| hsa04510 | Focal adhesion | 199 | 49.583 | 1.4118 | 0.01228 |
| hsa04015 | Rap1 signalling pathway | 206 | 51.328 | 1.4028 | 0.01228 |
| hsa00240 | Pyrimidine metabolism | 101 | 25.165 | 1.5895 | 0.01228 |
| hsa03440 | Homologous recombination | 41 | 10.216 | 1.9578 | 0.012437 |
| hsa05210 | Colorectal cancer | 86 | 21.428 | 1.6334 | 0.013149 |
| hsa04390 | Hippo signalling pathway | 154 | 38.371 | 1.4594 | 0.013378 |
| hsa00480 | Glutathione metabolism | 56 | 13.953 | 1.7917 | 0.01342 |
| hsa04068 | FoxO signalling pathway | 132 | 32.89 | 1.4898 | 0.01468 |
| hsa04350 | TGF-beta signalling pathway | 84 | 20.93 | 1.6245 | 0.01468 |
| hsa05418 | Fluid shear stress and atherosclerosis | 139 | 34.634 | 1.4726 | 0.015034 |
| hsa04926 | Relaxin signalling pathway | 130 | 32.391 | 1.4819 | 0.01706 |
| hsa01524 | Platinum drug resistance | 73 | 18.189 | 1.6494 | 0.018905 |
| hsa05410 | Hypertrophic cardiomyopathy (HCM) | 83 | 20.681 | 1.5957 | 0.021293 |
| hsa04928 | Parathyroid hormone synthesis, secretion and action | 106 | 26.411 | 1.5145 | 0.023367 |
| hsa04142 | Lysosome | 123 | 30.647 | 1.4683 | 0.025505 |
| hsa04915 | Estrogen signalling pathway | 137 | 34.135 | 1.4355 | 0.02801 |
| hsa05225 | Hepatocellular carcinoma | 168 | 41.859 | 1.3856 | 0.029922 |
| hsa00670 | One carbon pool by folate | 20 | 4.9833 | 2.2074 | 0.03496 |
| hsa04750 | Inflammatory mediator regulation of TRP channels | 99 | 24.667 | 1.5 | 0.03496 |
| hsa04713 | Circadian entrainment | 96 | 23.92 | 1.505 | 0.035593 |
| hsa05205 | Proteoglycans in cancer | 201 | 50.082 | 1.3378 | 0.035593 |
| hsa05222 | Small cell lung cancer | 93 | 23.172 | 1.5104 | 0.03579 |
| hsa04728 | Dopaminergic synapse | 131 | 32.64 | 1.4093 | 0.04549 |
| hsa02010 | ABC transporters | 44 | 10.963 | 1.7331 | 0.046088 |
| hsa05226 | Gastric cancer | 149 | 37.125 | 1.3737 | 0.048158 |

**N.B. No significantly over-represented pathways were identified in either MCF7 si*Scr* Vehicle vs si*CBLL1* Vehicle or in MCF7 si*Scr* +$\beta E_2$ vs si*CBLL1* +$\beta E_2$.**

# Appendix 23 Summary of KEGG pathways related to differentially expressed genes in MCF7 cells grouped by $\beta E_2$ treatment and *CBLL1* knockdown

**Table xxiii Summary of KEGG pathways associated with differentially expressed genes in MCF7 cells grouped by $\beta E_2$ treatment and *CBLL1* knockdown (FDR<0.05).**

| KEGG pathways unique to si*Scr* Vehicle vs si*Scr* $\beta E_2$ | KEGG pathways common to si*Scr* Vehicle vs si*Scr* $\beta E_2$ & si*CBLL1* Vehicle vs si*CBLL1* $\beta E_2$ | KEGG pathways unique to si*CBLL1* Vehicle vs si*CBLL1* $\beta E_2$ |
|---|---|---|
| Cell adhesion molecules (CAMs) | DNA replication | Oocyte meiosis |
| Arrhythmogenic right ventricular cardiomyopathy (ARVC) | Axon guidance | Steroid biosynthesis |
| Adrenergic signalling in cardiomyocytes | Cell cycle | p53 signalling pathway |
| Cushing syndrome | Pathways in cancer | Pyrimidine metabolism |
| cAMP signalling pathway | Focal adhesion | Colorectal cancer |
| Gastric acid secretion | Dilated cardiomyopathy (DCM) | Hippo signalling pathway |
| Oxytocin signalling pathway | Progesterone-mediated oocyte maturation | Glutathione metabolism |
| PPAR signalling pathway | Homologous recombination | FoxO signalling pathway |
| Leukocyte transendothelial migration | MAPK signalling pathway | TGF-beta signalling pathway |
| Cholinergic synapse | Mismatch repair | Platinum drug resistance |
| Melanogenesis | Morphine addiction | Parathyroid hormone synthesis, secretion and action |
| ECM-receptor interaction | Estrogen signalling pathway | Lysosome |
| cGMP-PKG signalling pathway | Hypertrophic cardiomyopathy (HCM) | Hepatocellular carcinoma |
| Basal cell carcinoma | Cellular senescence | One carbon pool by folate |
| Calcium signalling pathway | Rap1 signalling pathway | Inflammatory mediator regulation of TRP channels |
| Alcoholism | Proteoglycans in cancer | Small cell lung cancer |
| | Human T-cell leukaemia virus 1 infection | Gastric cancer |
| | Fluid shear stress and atherosclerosis | |
| | Fanconi anaemia pathway | |
| | Relaxin signalling pathway | |
| | Dopaminergic synapse | |
| | Purine metabolism | |
| | Circadian entrainment | |
| | Gap junction | |
| | ABC transporters | |

# Appendix 24 Analysis of KEGG pathways related to differentially expressed genes upon $\beta E_2$ treatment in T-47D scrambled control cells

**Table xxiv Analysis of KEGG pathways associated with differentially expressed genes upon $\beta E_2$ treatment in T-47D scrambled control cells (si*Scr* Vehicle vs si*Scr* $\beta E_2$) (FDR<0.05).**

| All DEGs | Description | Size | Expect | Ratio | FDR |
|---|---|---|---|---|---|
| hsa03030 | DNA replication | 36 | 6.0201 | 3.9867 | 9.99E-09 |
| hsa04110 | Cell cycle | 124 | 20.736 | 2.2666 | 1.65E-06 |
| hsa04360 | Axon guidance | 175 | 29.264 | 1.7769 | 0.001235 |
| hsa04010 | MAPK signalling pathway | 295 | 49.331 | 1.5203 | 0.005766 |
| hsa03440 | Homologous recombination | 41 | 6.8562 | 2.4795 | 0.008424 |
| hsa04115 | p53 signalling pathway | 72 | 12.04 | 2.0764 | 0.008424 |
| hsa03410 | Base excision repair | 33 | 5.5184 | 2.537 | 0.020473 |
| hsa04724 | Glutamatergic synapse | 114 | 19.064 | 1.731 | 0.023663 |
| hsa03460 | Fanconi anaemia pathway | 54 | 9.0301 | 2.1041 | 0.023663 |
| hsa04530 | Tight junction | 170 | 28.428 | 1.5829 | 0.023663 |
| hsa00240 | Pyrimidine metabolism | 101 | 16.89 | 1.7762 | 0.023663 |
| hsa05200 | Pathways in cancer | 526 | 87.96 | 1.296 | 0.036144 |

# Appendix 25 Analysis of KEGG pathways related to differentially expressed genes upon $\beta E_2$ treatment in T-47D *CBLL1* knockdown cells

**Table xxv Analysis of KEGG pathways related to differentially expressed genes upon $\beta E_2$ treatment in T-47D *CBLL1* knockdown cells (si*CBLL1* Vehicle vs si*CBLL1* $\beta E_2$) (FDR<0.05).**

| All DEGs | Description | Size | Expect | Ratio | FDR |
|---|---|---|---|---|---|
| hsa03030 | DNA replication | 36 | 6.2032 | 4.1914 | 1.60E-10 |
| hsa04110 | Cell cycle | 124 | 21.367 | 2.5273 | 7.56E-10 |
| hsa03460 | Fanconi anaemia pathway | 54 | 9.3049 | 2.4718 | 0.001152 |
| hsa05200 | Pathways in cancer | 526 | 90.636 | 1.3902 | 0.001862 |
| hsa04115 | p53 signalling pathway | 72 | 12.406 | 2.1763 | 0.001862 |
| hsa03410 | Base excision repair | 33 | 5.6863 | 2.8138 | 0.001862 |
| hsa05166 | Human T-cell leukaemia virus 1 infection | 255 | 43.94 | 1.5476 | 0.003822 |
| hsa05205 | Proteoglycans in cancer | 201 | 34.635 | 1.588 | 0.006903 |
| hsa04010 | MAPK signalling pathway | 295 | 50.832 | 1.4754 | 0.006903 |
| hsa03440 | Homologous recombination | 41 | 7.0648 | 2.4063 | 0.007279 |
| hsa00240 | Pyrimidine metabolism | 101 | 17.404 | 1.7812 | 0.017744 |
| hsa03430 | Mismatch repair | 23 | 3.9632 | 2.7755 | 0.018717 |
| hsa04360 | Axon guidance | 175 | 30.155 | 1.5586 | 0.021196 |
| hsa05222 | Small cell lung cancer | 93 | 16.025 | 1.7473 | 0.034961 |

**N.B. No significantly over-represented pathways were identified in either T-47D si*Scr* Vehicle vs si*CBLL1* Vehicle or in T-47D si*Scr* +$\beta E_2$ vs si*CBLL1* +$\beta E_2$.**

# Appendix 26 Summary of KEGG pathways related to differentially expressed genes in T-47D cells grouped by $\beta E_2$ treatment and *CBLL1* knockdown

**Table xxvi Summary of KEGG pathways related to differentially expressed genes in T-47D cells grouped by $\beta E_2$ treatment and *CBLL1* knockdown (FDR<0.05).**

| **KEGG pathways unique to si*Scr* Vehicle vs si*Scr* $\beta E_2$** | **KEGG pathways common to si*Scr* Vehicle vs si*Scr* $\beta E_2$ & si*CBLL1* Vehicle vs si*CBLL1* $\beta E_2$** | **KEGG pathways unique to si*CBLL1* Vehicle vs si*CBLL1* $\beta E_2$** |
|---|---|---|
| Glutamatergic synapse<br>Tight junction | DNA replication<br>Cell cycle<br>Axon guidance<br>MAPK signalling pathway<br>Homologous recombination<br>p53 signalling pathway<br>Base excision repair<br>Fanconi anaemia pathway<br>Pyrimidine metabolism<br>Pathways in cancer | Human T-cell leukaemia virus-1 infection<br>Proteoglycans in cancer<br>Mismatch repair<br>Small cell lung cancer |

# Appendix 27 Summary of overlapping KEGG pathways related to differentially expressed genes in MCF7 and T-47D cells grouped by $\beta E_2$ treatment and *CBLL1* knockdown

**Summary of overlapping KEGG pathways related to differentially expressed genes in MCF7 and T-47D cells grouped by $\beta E_2$ treatment and *CBLL1* knockdown (FDR<0.05) created using Venny 2.1.0 (https://bioinfogp.cnb.csic.es/tools/venny/).**

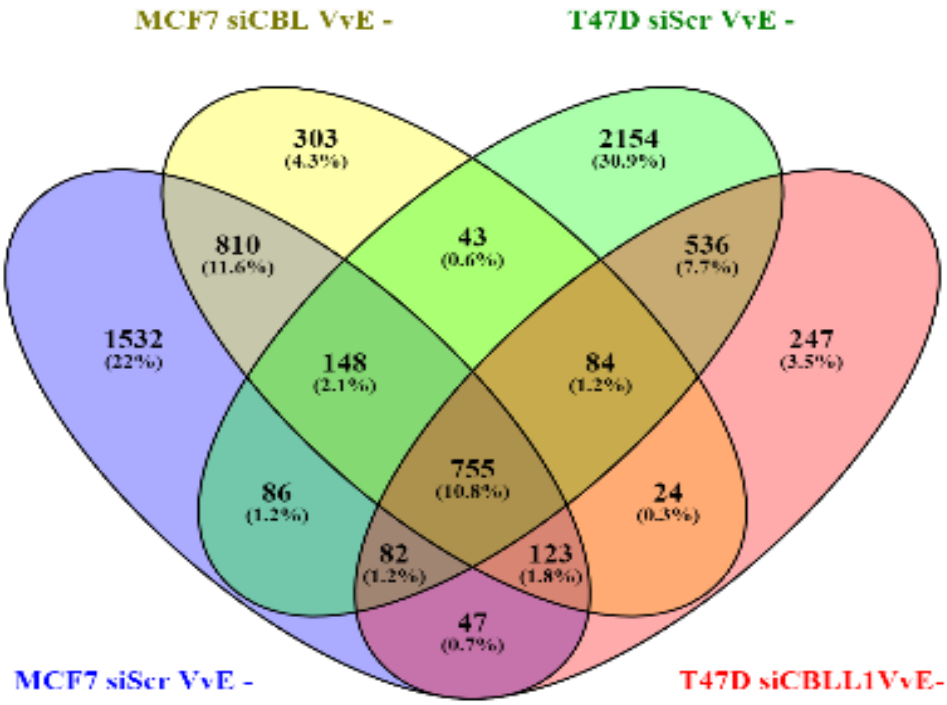


**Figure ixv Venn diagram of overlapping KEGG pathways related to differentially expressed genes in MCF7 and T-47D cells grouped by $\beta E_2$ treatment and *CBLL1* knockdown**

# Appendix 28 Analysis of KEGG pathways related to differentially spliced genes in MCF7 cells

**Table xxvii Analysis of KEGG pathways associated with differentially spliced genes in MCF7 cells (dPSI ≥5%, FDR<0.05).**

| si*Scr* Vehicle vs si*Scr* $\beta E_2$ cells – SE events | | | | | |
|---|---|---|---|---|---|
| **All DSGs** | **Description** | **Size** | **Expect** | **Ratio** | **FDR** |
| hsa05230 | Central carbon metabolism in cancer | 65 | 4.2208 | 3.3169 | 5.54E-05 |
| hsa04810 | Regulation of actin cytoskeleton | 213 | 13.831 | 2.0967 | 0.000106 |
| hsa04666 | Fc gamma R-mediated phagocytosis | 91 | 5.9091 | 2.7077 | 0.000216 |
| hsa05131 | Shigellosis | 65 | 4.2208 | 3.08 | 0.000225 |
| hsa01230 | Biosynthesis of amino acids | 75 | 4.8701 | 2.8747 | 0.00028 |
| hsa04520 | Adherens junction | 72 | 4.6753 | 2.7806 | 0.00064 |
| hsa00562 | Inositol phosphate metabolism | 74 | 4.8052 | 2.7054 | 0.000839 |

| si*Scr* Vehicle vs si*CBLL1* Vehicle cells – A5SS events | | | | | |
|---|---|---|---|---|---|
| **All DSGs** | **Description** | **Size** | **Expect** | **Ratio** | **FDR** |
| hsa03010 | Ribosome | 153 | 1.7617 | 5.1088 | 6.01E-05 |

| si*CBLL1* Vehicle vs si*CBLL1* $\beta E_2$ cells – A5SS events | | | | | |
|---|---|---|---|---|---|
| **All DSGs** | **Description** | **Size** | **Expect** | **Ratio** | **FDR** |
| hsa03010 | Ribosome | 153 | 3.339 | 4.7919 | 1.83E-07 |
| si*CBLL1* Vehicle vs si*CBLL1* $\beta E_2$ cells – SE events | | | | | |
| **All DSGs** | **Description** | **Size** | **Expect** | **Ratio** | **FDR** |
| hsa05100 | Bacterial invasion of epithelial cells | 74 | 6.6678 | 2.9995 | 5.18E-06 |
| hsa04360 | Axon guidance | 175 | 15.769 | 1.9659 | 0.000177 |
| hsa04120 | Ubiquitin mediated proteolysis | 137 | 12.344 | 2.0252 | 0.000462 |
| hsa01100 | Metabolic pathways | 1305 | 117.59 | 1.2671 | 0.00067 |
| hsa03440 | Homologous recombination | 41 | 3.6943 | 2.9775 | 0.000747 |
| si*CBLL1* Vehicle vs si*CBLL1* $\beta E_2$ cells – RI events | | | | | |
| **All DSGs** | **Description** | **Size** | **Expect** | **Ratio** | **FDR** |
| hsa03013 | RNA transport | 171 | 3.5029 | 3.7112 | 4.45E-05 |

**N.B. No significantly over-represented pathways were identified in MCF7 si*Scr* +$\beta E_2$ vs si*CBLL1* +$\beta E_2$.**

# Appendix 29 Analysis of KEGG pathways related to differentially spliced genes in T-47D cells

**Table xxviii Analysis of KEGG pathways associated with differentially spliced genes in T-47D cells (dPSI ≥5%, FDR<0.05).**

| si*CBLL1* Vehicle vs si*CBLL1* $\beta E_2$ cells – MXE events | | | | | |
|---|---|---|---|---|---|
| **All DSGs** | **Description** | **Size** | **Expect** | **Ratio** | **FDR** |
| hsa04014 | Ras signalling pathway | 232 | 3.7274 | 3.756 | 1.89E-05 |
| hsa04071 | Sphingolipid signalling pathway | 118 | 1.8958 | 4.7472 | 0.000109 |
| hsa04810 | Regulation of actin cytoskeleton | 213 | 3.4221 | 3.5066 | 0.000149 |
| hsa04510 | Focal adhesion | 199 | 3.1972 | 3.4405 | 0.000335 |
| hsa04670 | Leukocyte transendothelial migration | 112 | 1.7994 | 4.4458 | 0.000415 |
| hsa05170 | Human immunodeficiency virus 1 infection | 212 | 3.4061 | 3.2295 | 0.000573 |
| hsa04137 | Mitophagy | 65 | 1.0443 | 5.7454 | 0.000578 |
| hsa05131 | Shigellosis | 65 | 1.0443 | 5.7454 | 0.000578 |
| hsa04664 | Fc epsilon RI signalling pathway | 68 | 1.0925 | 5.4919 | 0.000737 |
| hsa05211 | Renal cell carcinoma | 69 | 1.1086 | 5.4123 | 0.000797 |
| hsa04140 | Autophagy | 128 | 2.0565 | 3.8901 | 0.001008 |
| hsa05100 | Bacterial invasion of epithelial cells | 74 | 1.1889 | 5.0466 | 0.001154 |
| hsa05212 | Pancreatic cancer | 75 | 1.205 | 4.9793 | 0.001238 |
| hsa04024 | cAMP signalling pathway | 199 | 3.1972 | 3.1277 | 0.001308 |
| hsa05205 | Proteoglycans in cancer | 201 | 3.2293 | 3.0966 | 0.00141 |
| hsa04015 | Rap1 signalling pathway | 206 | 3.3097 | 3.0214 | 0.001695 |
| hsa04012 | ErbB signalling pathway | 85 | 1.3656 | 4.3935 | 0.002361 |
| hsa04370 | VEGF signalling pathway | 59 | 0.94792 | 5.2747 | 0.002467 |
| hsa05210 | Colorectal cancer | 86 | 1.3817 | 4.3424 | 0.002506 |
| si*CBLL1* Vehicle vs si*CBLL1* $\beta E_2$ cells – RI events | | | | | |
| **All DSGs** | **Description** | **Size** | **Expect** | **Ratio** | **FDR** |
| hsa03040 | Spliceosome | 134 | 1.8479 | 4.8704 | 8.87E-05 |

**N.B. No significantly over-represented pathways were identified in either T-47D si*Scr* Vehicle vs si*Scr* +$\beta E_2$, T-47D si*Scr* Vehicle vs si*CBLL1* Vehicle, or T-47D si*Scr* Vehicle +$\beta E_2$ vs si*CBLL1* +$\beta E_2$.**